

# **Risk Analysis of Ground Water Contamination Detection Networks, Using Stochastic Modeling and Decision Theory**

PhD Thesis submitted by

**Konstantinos Papapetridis**

Advisor:

**Assoc.Prof. Dr Evan Paleologos**

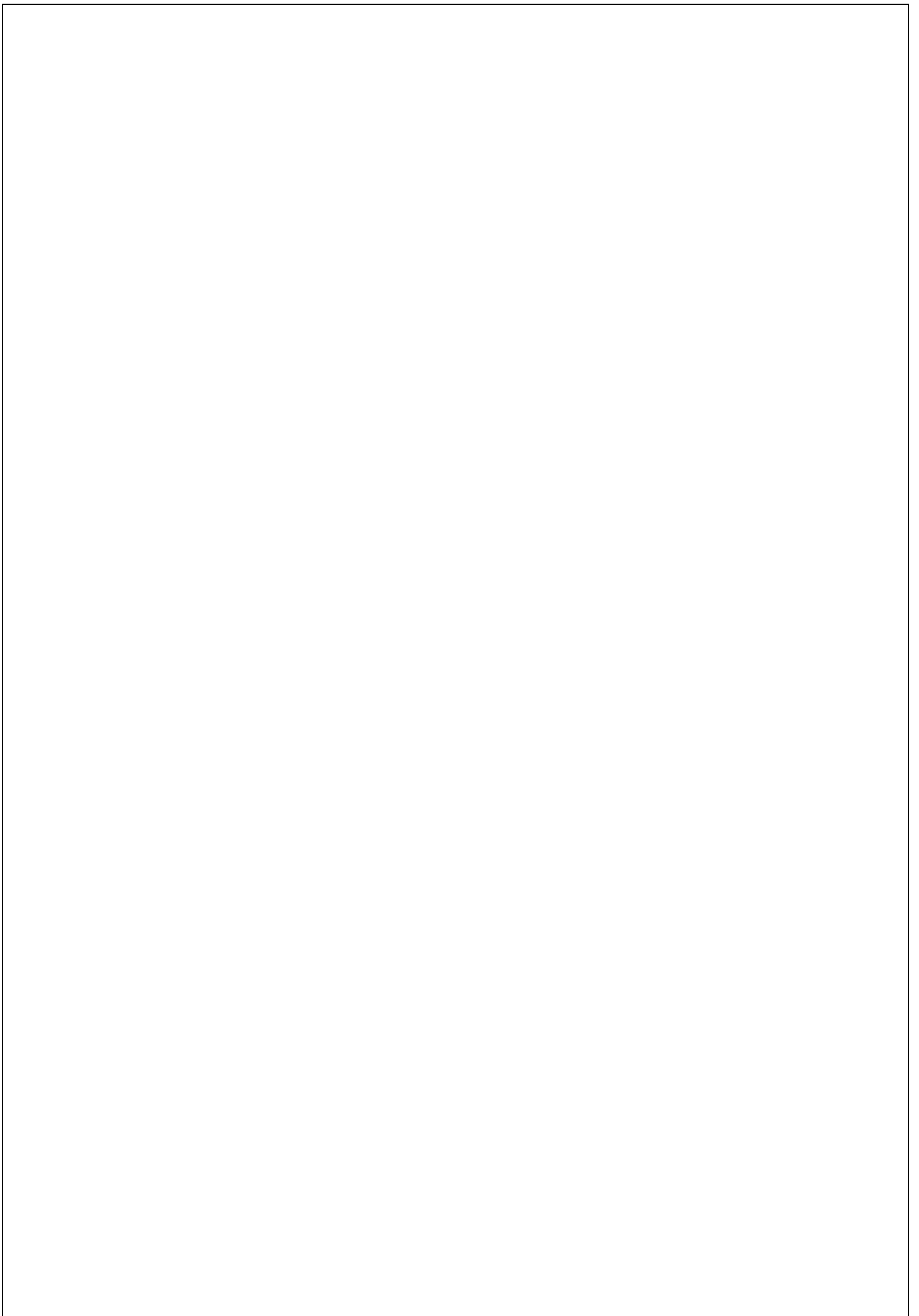
In Partial Fulfillment of the  
Requirements for the degree of  
Philosophy Diploma



Technical University of Crete  
School of Environmental  
Engineering  
Chania, Crete  
20 August 2013

©[PhD Thesis  
Konstantinos Papapetridis  
All Rights Reserved

to Argyro and to Aella



# Acknowledgements

---

I wish to thank my advisor, Associate Professor Dr Evan Paleologos, for giving me the opportunity to start a PhD in the field of Hydrology. I appreciate his faith in me, as he has never failed to provide me with the moral, professional and financial support necessary during this PhD. Although very busy, he has always found time to discuss the research results and offer his valuable advice.

I would also like to thank Professor Dr George Karatzas and Professor Dr Nikolaos Nikolaidis, members of my PhD Committee, for their guidance and their useful comments throughout my research.

Moreover, I am grateful to Professor Dr Aristotelis Mantoglou for providing me with the 2-D Spectral Turning Bands source code used in the computational model of my research.

I would like to extend my gratitude to the Technical University of Crete, as it supported me with a research grant.

Furthermore, I would like to thank Ms Georgia Poniridou, secretary of the Environmental Engineering Department of the Technical University of Crete, for all the procedural help she provided during my research, making my life a little bit easier.

I would also like to thank my family for always encouraging and supporting me, especially my wife, Argyro Arampatzoglou, for all the editing work and her valuable linguistic corrections in the text.

# TABLE OF CONTENTS

Acknowledgements .....	v
Table of Contents.....	vi
Table of Figures .....	10
Table of Tables .....	14
<b>SUMMARY</b> .....	18
<b>ΠΕΡΙΛΗΨΗ</b> .....	24
<b>CHAPTER 1: Introduction</b>	
1.1 Groundwater Pollution .....	31
1.2 Groundwater Protection.....	35
1.3 Landfills and Leachate .....	36
1.4 Problem Definition .....	38
1.5 Research Objectives .....	42
1.6 Thesis Outline.....	43
<b>CHAPTER 2: Two-dimensions model structure</b>	
2.1 Introduction .....	45
2.2 Stochastic Approach.....	46
2.3 Simulating Random Fields: Turning Bands .....	47
2.3.1 TBM Theoretical Background.....	49
2.3.2 Establishment of the One-dimensional Linear Process .....	50
2.3.3 Number and Distribution of Turning Bands.....	51
2.3.4 Spectral Discretization and Random Fields Generation.....	51
2.4 Flow Equation .....	52
2.5 Velocity Field.....	56
2.6 Conservation Hypothesis and Diffusion – Dispersion Equation .....	57

2.7	Random Walk Tracking Particle .....	58
2.8	Problem Uncertainties and Model Structure.....	64
2.9	Simulation Model .....	65
2.9.1	Model Structure .....	65
<b>CHAPTER 3: Instantaneous groundwater pollution detection probability in heterogeneous aquifers</b>		
3.1	Introduction .....	71
3.2	Model Description .....	73
3.3	Number of Simulations and Tracking Particles.....	77
3.4	Results and Discussion .....	82
3.4.1	Effect of Number and Distance of Wells on Detection Probability .....	82
3.4.2	Effect of Field's Heterogeneity and Dispersion .....	84
3.4.3	Effect of Sampling Frequency .....	84
3.5	Remedial Action Response Delay .....	87
3.6	Conclusions .....	91
<b>CHAPTER 4: Sampling frequency of groundwater monitoring system and remediation delay at contaminated sites</b>		
4.1	Introduction .....	94
4.2	Model Description .....	96
4.3	Sampling Frequency of Groundwater Monitoring .....	98
4.4	Remediation Delay .....	108
4.5	Conclusions .....	111
<b>CHAPTER 5: Parameters on stochastic simulation of contaminant detection probability</b>		
5.1	Introduction .....	113
5.2	Model description and simulation results .....	114
5.2.1	Control Area Size.....	115
5.2.2	Multiple Point Sources.....	117
5.2.3	Quantity of Pollution .....	121

5.3	Conclusions .....	124
<b>CHAPTER 6: Modeling of aquifer pollution detection probability triggered by precipitation</b>		
6.1	Introduction .....	126
6.2	Model Description .....	129
6.3	Simulation Results.....	133
6.3.1	Number of Wells .....	133
6.3.2	Field Heterogeneity .....	134
6.3.3	Dispersion.....	136
6.3.4	Sampling Frequency .....	139
6.3.5	Time of detection and contaminated area.....	142
6.3.6	Remediation delay .....	146
6.4	Conclusions .....	149
<b>CHAPTER 7: Conclusions</b>		
7.1	Instantaneous groundwater pollution detection probability in heterogeneous aquifers .....	152
7.2	Sampling frequency of groundwater monitoring system and remediation delay at contaminated sites .....	154
7.3	Parameters on stochastic simulation of contaminant detection probability...	155
7.4	Aquifer pollution detection probability triggered by precipitation .....	155
<b>Appendix A</b>		
2-D	Source Code .....	158
A-1	Instantaneous Pollution .....	159
A-2	Precipitation Event Pollution Source Code .....	181
A-3	Flow Numerical Solution .....	203
A-4	Flow Numerical Solution and STUBA Subroutine .....	207
<b>Appendix B</b>		
Tables of	Simulation Results .....	239
B.1	Instantaneous Pollution .....	240

B.2	Precipitation Trigered Pollution .....	263
References	.....	277

# Table of Figures

---

<b>Figure 1.1:</b> Main landfill characteristics and leachate escape into saturated zone .....	38
<b>Figure 2.1:</b> Turning Bands Mechanism (Mantoglou and Wilson,1982).....	48
<b>Figure 2.2:</b> A 2-D hydraulic conductivity field generated by STUBA, where $\mu_K = 2.3$ , $\sigma_{\ln K}^2 = 2.0$ and $\lambda = 20m$ . .....	52
<b>Figure 2.3:</b> 3-D Field Discretization .....	55
<b>Figure 2.4:</b> Operating principle of Monte Carlo method .....	66
<b>Figure 2.5:</b> Instantaneous case pollution Monte Carlo simulation process diagram .....	67
<b>Figure 2.6:</b> Precipitation triggered pollution case Monte Carlo simulation process diagram .....	69
<b>Figure 3.1 :</b> Section of simulated flow field with a rectangular landfill $W \times L$ , a 2000 particles plume, and a magnified well-detection area.....	76
<b>Figure 3.2:</b> Detection probability $P_d$ versus number of Monte Carlo simulations for 3 cases of well arrangement, heterogeneity, and dispersion .....	79
<b>Figure 3.3:</b> Comparison between numerical and theoretical $P_d$ versus $\log_{10}$ of number of tracking particles $N$ , $N=500, 1,000, 2,000, 4,000, 8,000, 16,000, 32,000, 64,000, 128,000, 256,000$ , and $512,000$ .....	81
<b>Figure 3.4:</b> Optimum detection distance for 3, 6, and 12 wells. Top: Heterogeneous ( $\sigma_{\ln K}^2=2.00$ , $\alpha_T=0.20m$ ) flow field. Bottom: homogeneous flow field with $\alpha_T=0.001m$ .....	83
<b>Figure 3.5:</b> Dependence of the probability of detection on sampling frequency (5a: homogeneous, $\alpha_T=0.01m$ , and 5b: heterogeneous aquifer, $\sigma_{\ln K}^2=1.0$ , $\alpha_T=0.20m$ ).....	86
<b>Figure 3.6:</b> Effect of remedial action response: Corrected detection probability $P_d^{cor}$ for six monitoring wells, sampling once a day, in a homogeneous field (a: $\alpha_T=0.01m$ , and b: $\alpha_T=0.10m$ ), as a function of remedial action delay.....	89
<b>Figure 3.7:</b> Corrected detection probability $P_d^{cor}$ for a heterogeneous field $\sigma_{\ln K}^2=1.5$ , $\alpha_T=0.05m$ for twelve monitoring wells as a function of remedial action delay and sampling frequency...	91
<b>Figure 4.1:</b> Half section of simulated flow field illustrating the rectangular CPSA, an 8000 particles plume evolved for 10 years, and a magnified well-detection area (wells are deliberately placed further away for illustration purposes) .....	97

<b>Figure 4.2:</b> Percent detection change between daily and annual sampling for different well arrangements and types of soil .....	101
<b>Figure 4.3:</b> 12 monitoring wells: $P_d/P_{d(D)}$ versus $\log_{10}(\alpha T)$ for homogeneous soils $\sigma_{lnK2} = 0.0$ .....	103
<b>Figure 4.4:</b> $P_d/P_{d(D)}$ versus $\sigma_{lnK2}$ : (a) $\alpha T = 0.20m$ , and (b) $\alpha T = 0.50m$ for 12 monitoring wells .....	105
<b>Figure 4.5:</b> $\langle T_{obs} \rangle / \langle T_{ar} \rangle$ versus sampling frequency for an 8-well monitoring arrangement in different hydrogeological environments .....	106
<b>Figure 4.6:</b> $\langle A_{obs} \rangle / \langle A_{ar} \rangle$ versus sampling frequency for an 8-well monitoring arrangement in different hydrogeological environments .....	108
<b>Figure 4.7:</b> $AtAt + dt$ versus $\log(\alpha T)$ for 6 monitoring wells and different Remedial Action Delay Times (RADTi): (a) homogeneous, and (b) heterogeneous soils with $\sigma Y2 = 1.0$ .....	110
<b>Figure 4.8:</b> $AtAt + dt$ versus heterogeneity $\sigma Y2$ for fixed dispersion $\alpha T = 0.02 m$ for different Remedial Action Delay Times (RADTi) and 3 monitoring wells.....	111
<b>Figure 5.1:</b> Detection Probability $P_d$ change in relation to control area relative size, in a homogeneous low (a) and high (b) dispersion field, and in a heterogeneous low (c) and high (d) dispersion field.....	116
<b>Figure 5.2:</b> Detection probability $P_d$ change shown as monitoring wells density in relation to control area width is kept constant and equal to 0.05. ....	117
<b>Figure 5.3:</b> Change in detection probability $P_d$ for a single source (dashed lines) and dual source (solid lines) pollution, as the number of wells is increased, for homogeneous ( $\sigma_{lnK}^2 = 0$ ) and heterogeneous ( $\sigma_{lnK}^2 = 1, \sigma_{lnK}^2 = 2$ ) cases, considering four dispersion cases, $a_T = 0.01m$ (a) , $a_T = 0.01m$ (b), $a_T = 0.01m$ (c) and $a_T = 0.01m$ (d) . ....	118
<b>Figure 5.4:</b> Detection probability $P_d$ relative percentage difference between a dual and a single pollution source case in two different transverse dispersion coefficient cases. ....	119
<b>Figure 5.5:</b> Change of detection probability $P_d$ for a single source (dashed lines) and dual source (solid lines) pollution, as sampling frequency changes from daily (ED), monthly (1M), bimonthly (2M), quarterly (3M), every four months (4M), biannually (6M) and annually (12M).....	121
<b>Figure 5.6:</b> Change of detection probability $P_d$ of different monitoring wells installations, as the initial concentration of a single source instantaneous pollution increases at a homogeneous $\sigma_{lnK}^2 = 0.0$ aquifer .....	122

- Figure 5.7:** Change of detection probability  $P_d$  for different monitoring wells installations, as the initial concentration of a single source instantaneous pollution increases at a heterogeneous  $\sigma_{\ln K}^2 = 1.0$  aquifer ..... 123
- Figure 5.8:** Change of detection probability  $P_d$  for different monitoring wells installations, as the initial concentration of a single source instantaneous pollution increases at a heterogeneous  $\sigma_{\ln K}^2 = 2.0$  aquifer ..... 124
- Figure 6.1:** Plot of Groundwater Monitoring Data Indicating High COD and Cl Levels after a landfill leak case repair has taken place (vertical line), where the spikes are due to rain episodes on the area (Collucci et al., 1999). ..... 128
- Figure 6.2:**  $P_d$  change as the number of monitoring wells increases from 1 – 20, as well as comparison between an instantaneous case of pollution and a precipitation coupled case for a medium dispersion homogeneous field (a:  $\sigma^2(\log K)=0.0$ ,  $\alpha_T=0.10m$ ) and a low dispersion heterogeneous field, (b:  $\sigma^2(\log K)=2.0$ ,  $\alpha_T=0.010m$ ). ..... 134
- Figure 6.3:** Groundwater pollution detection probability  $P_d$  of a 3-well arrangement in relation to the field's heterogeneity as this is reflected through variance of the natural logarithm of hydraulic conductivity ( $\sigma_{\ln K}^2$ ). Dashed lines are the precipitation triggered pollution (Precip.) and solid lines are for instantaneous cases (Instant.). ..... 134
- Figure 6.4:** Groundwater pollution detection probability  $P_d$  of a 12-well arrangement in relation to the field's heterogeneity as this is reflected through variance of the natural logarithm of hydraulic conductivity ( $\sigma_{\ln K}^2$ ). Dashed lines are the precipitation triggered pollution (Precip.) and solid lines are for instantaneous cases (Instant.). ..... 135
- Figure 6.5:** Pollution dispersion and deformation as it is transported during a 30-year time span into aquifers, where on the vertical axis heterogeneity increases and on the horizontal axis transverse dispersion coefficient increases. .... 137
- Figure 6.6:**  $P_d$  change of a 3-well arrangement, in relation with transverse dispersion coefficient  $\alpha_T$  increase, in three different heterogeneity cases, as well as comparison between precipitation related pollution cases (dashed lines) and instantaneous pollution cases (solid lines) ..... 138
- Figure 6.7:** Percentage change of  $P_d$  as sampling frequency changes for a 4-well monitoring installation among daily (D), monthly (1 M), bimonthly (2 M), quarterly (3 M), every 4 months (4 M), biannual (6 M) and annual (A) sampling. The first column of the graphs reflects the results of an instantaneous case of pollution and the second column reflects a

precipitation event related pollution, while horizontally heterogeneity changes, as is reflected through the variance of the  $\ln K$ . ..... 140

**Figure 6.8:** Change of ratio between average time of pollution arrival on monitoring installation ( $\langle T_{ar} \rangle$ ) and time of actual pollution observation ( $\langle T_{obs} \rangle$ ) in relation to sampling frequency for a 3-well monitoring arrangement. .... 144

**Figure 6.9:** Change of ratio of the average polluted area  $\langle A_{pol} \rangle$  to the area  $L$  of the contaminant potential source area in relation to the logarithm of transverse dispersion coefficient  $a_T$  for three different cases of field heterogeneity. .... 145

**Figure 6.10:** Change of ratio between the average polluted area  $\langle A_{obs} \rangle$  at the plume's actual detection by an 8-well monitoring arrangement and the average polluted area  $\langle A_{obs} \rangle$  when the plume is actually observed upon its arrival at the monitoring installation in relation to sampling frequency. .... 146

**Figure 6.11:** At  $At + dt$  versus  $\log(\alpha T)$  for 6 monitoring wells and different Remedial Action Delay Times (RADTi): (a) homogeneous, (b) heterogeneous soils with  $\sigma Y2 = 1.0$  and (c) heterogeneous soils with  $\sigma Y2 = 2.0$ . .... 148

# Table of Tables

---

<b>Table 3.1:</b> Corrected detection probability $P_d^{cor}$ for two aquifers with $\sigma_{lnK}^2=0.0$ and $\sigma_{lnK}^2=1.0$ , and two different sampling frequencies, once a day and biannually .....	90
<b>Table 4.1:</b> Detection Probability $P_d$ (%) .....	99
<b>Table 4.2:</b> Detection Probability $P_d$ (%) .....	100
<b>Table B.1:</b> Detection probability in case of $\sigma_{lnK}^2 = 0.0$ and $\sigma_{lnK}^2 = 0.5$ , for different sampling frequencies .....	240
<b>Table B.2:</b> Detection probability in case of $\sigma_{lnK}^2 = 1.0$ and $\sigma_{lnK}^2 = 1.5$ , for different sampling frequencies .....	241
<b>Table B.3:</b> Detection probability in case of $\sigma_{lnK}^2 = 2.0$ , for different sampling frequencies .....	242
<b>Table B.4:</b> Detection probability, average detection time, contaminated area in case of detection failure and relative contaminated area to control area $L$ for various RADTi in case of $\sigma_{lnK}^2 = 0.0$ assuming daily (ED) and monthly (1M) sampling frequencies .....	243
<b>Table B.5:</b> Detection probability, average detection time, contaminated area in case of detection failure and relative contaminated area to control area $L$ for various RADTi in case of $\sigma_{lnK}^2 = 0.0$ assuming bimonthly (2M) and quarterly (3M) sampling frequencies .....	244
<b>Table B.6:</b> Detection probability, average detection time, contaminated area in case of detection failure and relative contaminated area to control area $L$ for various RADTi in case of $\sigma_{lnK}^2 = 0.0$ assuming every 4 months (4M) and biannually (6M) sampling frequencies....	245
<b>Table B.7:</b> Detection probability, average detection time, contaminated area in case of detection failure and relative contaminated area to control area $L$ for various RADTi in case of $\sigma_{lnK}^2 = 0.0$ assuming annually (12M) sampling frequency .....	246
<b>Table B.8:</b> Detection probability, average detection time, contaminated area in case of detection failure and relative contaminated area to control area for various RARDTi in case of $\sigma_{lnK}^2 = 0.5$ assuming daily (ED) and monthly (1M) sampling frequencies .....	247
<b>Table B.9:</b> Detection probability, average detection time, contaminated area in case of detection failure and relative contaminated area to control area for various RADTi in case of $\sigma_{lnK}^2 = 0.5$ assuming bimonthly (2M) and quarterly (3M) sampling frequencies .....	248

**Table B.10:** Detection probability, average detection time, contaminated area in case of detection failure and relative contaminated area to control area  $L$  for various RADTi in case of  $\sigma_{\ln K}^2 = 0.5$  assuming every 4 months (4M) and biannually (6M) sampling frequencies.... 249

**Table B.11:** Detection probability, average detection time, contaminated area in case of detection failure and relative contaminated area to control area  $L$  for various RADTi in case of  $\sigma_{\ln K}^2 = 0.5$  assuming annually sampling frequency..... 250

**Table B.12:** Detection probability, average detection time, contaminated area in case of detection failure and relative contaminated area to control area for various RADTi in case of  $\sigma_{\ln K}^2 = 1.0$  assuming daily (ED) and monthly (1M) sampling frequencies ..... 251

**Table B.13:** Detection probability, average detection time, contaminated area in case of detection failure and relative contaminated area to control area for various RADTi in case of  $\sigma_{\ln K}^2 = 1.0$  assuming bimonthly (2M) and quarterly (3M) sampling frequencies ..... 252

**Table B.14:** Detection probability, average detection time, contaminated area in case of detection failure and relative contaminated area to control area  $L$  for various RADTi in case of  $\sigma_{\ln K}^2 = 1.0$  assuming every 4 months (4M) and biannually (6M) sampling frequencies... 253

**Table B.15:** Detection probability, average detection time, contaminated area in case of detection failure and relative contaminated area to control area  $L$  for various RADTi in case of  $\sigma_{\ln K}^2 = 1.0$  assuming annually sampling frequency ..... 254

**Table B.16:** Detection probability, average detection time, contaminated area in case of detection failure and relative contaminated area to control area for various RADTi in case of  $\sigma_{\ln K}^2 = 1.5$  assuming daily (ED) and monthly (1M) sampling frequencies ..... 255

**Table B.17:** Detection probability, average detection time, contaminated area in case of detection failure and relative contaminated area to control area for various RADTi in case of  $\sigma_{\ln K}^2 = 1.5$  assuming bimonthly (2M) and quarterly (3M) sampling frequencies ..... 256

**Table B.18:** Detection probability, average detection time, contaminated area in case of detection failure and relative contaminated area to control area  $L$  for various RADTi in case of  $\sigma_{\ln K}^2 = 1.5$  assuming every 4 months (4M) and biannually (6M) sampling frequencies... 257

**Table B.19:** Detection probability, average detection time, contaminated area in case of detection failure and relative contaminated area to control area  $L$  for various RADTi in case of  $\sigma_{\ln K}^2 = 1.5$  assuming annually sampling frequency ..... 258

**Table B.20:** Detection probability, average detection time, contaminated area in case of detection failure and relative contaminated area to control area for various RADTi in case of  $\sigma_{\ln K}^2 = 2.0$  assuming daily (ED) and monthly (1M) sampling frequencies.....259

**Table B.21:** Detection probability, average detection time, contaminated area in case of detection failure and relative contaminated area to control area for various RADTi in case of  $\sigma_{\ln K}^2 = 2.0$  assuming bimonthly (2M) and quarterly (3M) sampling frequencies.....260

**Table B.22:** Detection probability, average detection time, contaminated area in case of detection failure and relative contaminated area to control area  $L$  for various RADTi in case of  $\sigma_{\ln K}^2 = 2.0$  assuming every 4 months (4M) and biannually (6M) sampling frequencies ..261

**Table B.23:** Detection probability, average detection time, contaminated area in case of detection failure and relative contaminated area to control area  $L$  for various RADTi in case of  $\sigma_{\ln K}^2 = 2.0$  assuming annually sampling frequency.....262

**Table B.24:** Detection probability in case of  $\sigma_{\ln K}^2 = 0.0$ ,  $\sigma_{\ln K}^2 = 1.0$  and  $\sigma_{\ln K}^2 = 2.0$ , for different transverse coefficients and sampling frequencies.....263

**Table B.25:** Precipitation triggered pollution detection probability, average detection time, contaminated area in case of detection failure and relative contaminated area to control area for various RADTi in case of  $\sigma_{\ln K}^2 = 0.0$  assuming daily (ED) and monthly (1M) sampling frequencies.....264

**Table B.26:** Precipitation triggered pollution detection probability, average detection time, contaminated area in case of detection failure and relative contaminated area to control area for various RADTi in case of  $\sigma_{\ln K}^2 = 0.0$  assuming bimonthly (2M) and quarterly (3M) sampling frequencies.....265

**Table B.27:** Precipitation triggered pollution detection probability, average detection time, contaminated area in case of detection failure and relative contaminated area to control area for various RADTi in case of  $\sigma_{\ln K}^2 = 0.0$  assuming every 4 months (4M) and biannually (6M) sampling frequencies.....266

**Table B.28:** Precipitation triggered pollution detection probability, average detection time, contaminated area in case of detection failure and relative contaminated area to control area for various RADTi in case of  $\sigma_{\ln K}^2 = 0.0$  assuming annually sampling frequency.....267

**Table B.29:** Precipitation triggered pollution detection probability, average detection time, contaminated area in case of detection failure and relative contaminated area to control

area for various RADTi in case of  $\sigma_{\ln K}^2 = 1.0$  assuming daily (ED) and monthly (1M) sampling frequencies.....268

**Table B.30:** Precipitation triggered pollution detection probability, average detection time, contaminated area in case of detection failure and relative contaminated area to control area for various RADTi in case of  $\sigma_{\ln K}^2 = 1.0$  assuming bimonthly (2M) and quarterly (3M) sampling frequencies.....269

**Table B.31:** Precipitation triggered pollution detection probability, average detection time, contaminated area in case of detection failure and relative contaminated area to control area for various RADTi in case of  $\sigma_{\ln K}^2 = 1.0$  assuming every 4 months (4M) and biannually (6M) sampling frequencies .....270

**Table B.32:** Precipitation triggered pollution detection probability, average detection time, contaminated area in case of detection failure and relative contaminated area to control area for various RADTi in case of  $\sigma_{\ln K}^2 = 1.0$  assuming annually sampling frequency .....271

**Table B.33:** Precipitation triggered pollution detection probability, average detection time, contaminated area in case of detection failure and relative contaminated area to control area for various RADTi in case of  $\sigma_{\ln K}^2 = 2.0$  assuming daily (ED) and monthly (1M) sampling frequencies.....272

**Table B.34:** Precipitation triggered pollution detection probability, average detection time, contaminated area in case of detection failure and relative contaminated area to control area for various RADTi in case of  $\sigma_{\ln K}^2 = 2.0$  assuming bimonthly (2M) and quarterly (3M) sampling frequencies.....273

**Table B.35:** Precipitation triggered pollution detection probability, average detection time, contaminated area in case of detection failure and relative contaminated area to control area for various RADTi in case of  $\sigma_{\ln K}^2 = 2.0$  assuming every 4 months (4M) and biannually (6M) sampling frequencies .....274

**Table B.36:** Precipitation triggered pollution detection probability, average detection time, contaminated area in case of detection failure and relative contaminated area to control area for various RADTi in case of  $\sigma_{\ln K}^2 = 2.0$  assuming annually sampling frequency .....275

# SUMMARY

Groundwater is an important freshwater natural resource. People used to believe that natural filtering resulting from water working its way through the subsurface was enough to provide sufficient protection from contamination to allow untreated water to be delivered for domestic or agricultural uses. Then dramatic incidents in the 70s (e.g. Love Canal case) made everybody realize that groundwater had been contaminated from hundreds of thousands of leaking underground storage tanks, industrial waste pits, home septic systems, municipal and industrial landfills, accidental chemical spills, careless use of solvents, illegal dumping, as well as widespread use of agricultural chemicals. Groundwater contamination became the environmental issue of the 80s.

Once contaminated, groundwater is difficult to restore. Restoration of groundwater contaminated by releases of anthropogenic chemicals to a condition allowing for unrestricted use and unlimited exposure remains a significant technical and institutional challenge. Moreover, one dominant attribute on subsurface remediation efforts has been lengthy delays between discovery of the problem and its solution. Some reasons for these extended timeframes are ineffective subsurface investigations, difficulties in characterizing the nature and extent of the problem in highly heterogeneous subsurface environments, remedial technologies, and a variety of administrative, policy and political factors.

It is evident that, in order to control groundwater contamination by means of immediate alert and minimize remediation cost, an alarm system is required to constantly monitor subsoil water quality. A reliable and efficient monitoring system design is of great importance to the overall design of a facility that may pose a groundwater pollution threat. In the case of monitoring groundwater contamination pollution detection for sanitary landfills, EU regulations commonly require one background (upstream) well and two downgradient wells. The position, number (more than the minimum requirement) and depth of the monitoring wells are proposed by the facility's operator and/or by local authorities. In most cases, a quarterly sampling is undertaken.

Subsurface water pollution due to landfill leaks has become an important issue during the last three decades. While sanitary landfills constitute the most widely used management approach for the disposal of solid waste because of their simplicity and cost effectiveness, historical records indicate that landfills exhibit a high failure rate in terms of groundwater contamination. Subsurface heterogeneity and lack of information about the exact location and duration of a leak render it extremely difficult to predict and detect subsurface water pollution before it has already spread and become evident. Monitoring aquifer contamination via wells is influenced by many uncertain factors, where the heterogeneity of the geologic environment, the quantity and nature of the contaminants, the number and location of the monitoring wells, and the frequency of sampling are factors affecting successful detection. However, there is no recognition of uncertainty factors in regulations.

Successful detection of an underground pollutant transported into an aquifer is directly dependent on the possibility of calculating the movement and dispersion of the pollutant in an environment, about which very few things are actually known. This lack of information is caused by the difficulties of experimentally measuring, at any of its points, the various hydraulic properties of a geological field (hydraulic conductivity, hydraulic head, porosity etc.) so as to predict, or even approximate, the way a plume can propagate into the aquifer. Additional uncertainty factors of the problem are lack of information about the point from which pollution originates in a landfill waste, the duration of the leak and the extent of the plume, typically dependent on the nature of the polluting substance. Thus, it is impossible to know with certainty how the pollutant concentrations in the subsoil change, which means that we cannot directly predict the likelihood of successful detection of groundwater pollution into heterogeneous aquifers from a specific arrangement of monitoring wells.

In the present thesis a stochastic two-dimensional numerical model was developed and utilized to address the problem of evaluating the effectiveness of contaminant detection in heterogeneous aquifers by linear arrangements of monitoring wells. Although it can be said that the two-dimensional approach is not the most realistic description of the actual situation, it actually simplifies the computational problem, losing only the vertical information about the movement and the detection of plumes. Moreover, when the horizontal dimensions of an aquifer are much greater than its thickness, which is our case, then the results of two dimensions provide a good approximation of reality. In numerical experiments based on the Monte Carlo framework, geological heterogeneity was simulated by the Spectral Turning Bands method and groundwater pollution transportation and dispersion was simulated by the Random Walk Tracking Particle method. Simulations were conducted to determine the detection probabilities and areas of groundwater contamination assuming different levels of geologic heterogeneity as well as pollutant dispersion, and to evaluate the effectiveness of

various monitoring wells sampling frequencies. Two different cases were examined, as far as duration of pollution is concerned, assuming instantaneous and precipitation triggered pollution, where pollution diffuses into the aquifer proportionally to rain height during the monitoring period of time.

This work introduces a new perspective for the correction of risk analysis. Contemporary risk analysis considers the cost of alternative remediation procedures by assuming that the contamination area to be remediated coincides with the area calculated at the time of detection. However, there is always a considerable lag between the time that a plume is detected and the time when remediation commences. This time lag constitutes a random variable that depends on available resources and technologies, as well as efficiency of administrative decision-making. A new risk analysis framework is proposed that corrects estimated costs due to remediation delays.

Initially, the objective of this work was to numerically estimate in two dimensions the probability of groundwater pollution detection, originating instantly from a point source inside the physical boundaries of a landfill cell, achieved by a linear arrangement of varying number monitoring wells. The monitoring installation was considered in different cases to be located in various distances from the landfill facility and perpendicular to the flow field. Sensitivity analysis was performed to define what is the minimum number of Monte Carlo realizations where stochastically calculated detection probability is stabilized. Results were compared with theoretical values that were analytically calculated in the case of a homogeneous field. Having determined a high resolution simulation scheme, the distances of monitoring wells from the landfill cell trailing edge were examined in order to define, for every hydro-geological case simulated, the maximum detection probability a monitoring setting may achieve.

Probabilities of detection and contaminated groundwater areas were calculated for different arrangements of monitoring wells. It was shown that detection decreased as heterogeneity increased. Monitoring with 20 wells provided high detection, while 3 wells resulted in four out of five contamination cases remaining undetected. For fixed heterogeneity, for each well arrangement, detection probability increased up to a certain value, with increasing transverse dispersion coefficient, and then it decreased. The impact of sampling frequency of wells on groundwater contamination detection was studied. The frequency of sampling was a critical factor in heterogeneous aquifers. It appeared that a minimum sampling should take place twice a year, with the monthly sampling being the optimum choice, considering the effort involved and the improvement in detection. In heterogeneous aquifers a large number of monitoring wells sampled infrequently did not perform better in terms of detection than a lower number of wells sampled regularly. Finally,

remediation action delay time was introduced as an expression that accounted for the delay between detection and remedial action, in order to provide a correction to decision analysis that evaluated the economic worth of well monitoring. This expression illustrated the fact that delays longer than 3 years were equivalent to reducing the economic performance of 12 wells to that of a lower number of wells, meaning that higher failure costs should be considered than those assumed in current risk analysis.

Afterwards, high-resolution numerical Monte Carlo realizations were utilized to study the impact of sampling frequency on detection probability at contaminated sites located in heterogeneous subsurface environments, in conjunction with different hydro-geological parameters. For all types of soils detection probability was seen to decrease as sampling became less frequent. Irrespective of the density of a monitoring network at highly dispersive subsurface environments, a very rigorous sampling schedule had to be maintained in order to retain the detection performance of the network. Highly heterogeneous soils through the presence of low permeability zones appeared to impede the spread of the contaminants and, hence, restrict the effects of dispersion. Analysis of the time lag, between the time that contaminants first appeared at monitoring locations and the time they were actually observed, as well as of the increase of the plume area that resulted from this time lag, led to the conclusion that monthly sampling was required for a wide range of hydro-geological environments. Moreover, sampling frequency impact on remedial action delay was studied. It was demonstrated that in highly dispersive environments the remediation response must be of the order of a few months if one does not wish the contaminated areas and remediation costs to grow significantly.

Then, it was numerically studied how the number of point pollution sources, the size of the controlled area (landfill) and the quantity of an instantaneous aquifer injection pollution event affected detection probability by a linear monitoring well arrangement. For this purpose a two-dimensional high resolution Monte Carlo stochastic model was utilized. In each examined parameter it was considered that the rest of the factors affecting detection probability estimation remained constant. Simulations were performed in the context of uncertainty factors deriving from the environment itself, where the pollution was propagating, and the lack of information about certain parameters, concerning the initial conditions of the leak.

It was numerically verified in the cases examined that as the size of the control area became larger, while the number of wells remained constant, detection probability decreased. Consequently, if the width of a control area was increased, so should the number of monitoring wells, so that the same well density would be maintained. In all simulated cases, the general observation was that when two similar groundwater pollution sources were

present, then contamination detection was easier as the average detection probability increased between 35% – 55%. The same trend in detection probability increase relative to single source cases was observed, regardless of the sampling frequency.

The simulation results indicated that when the initial concentration of pollution was below 1,000 mgr/lit, its detection was very hard, regardless of the aquifer's hydro-geological parameters. The efficiency of monitoring wells in low to medium dispersion aquifers reached a maximum, which was independent of the initial mass of pollution intruding the aquifer. The turning point of the concentration of the initial pollution was  $C = 8,000 \text{mgr} / \text{lit}$ , which was the value where detection probability reached a plateau. It was also observed that only in high dispersion environments increase of pollution resulted in higher detection probability. In every case lower concentrations were harder to be detected, dictating that in order for monitoring setting to be sensitive at least simulation level, even in small amounts of pollution, a minimum of 12 wells must be used.

Finally, considering a different way groundwater pollution in the context of triggering it according to local precipitation events, it was assumed that there was a point pollution source inside a controlled area of specific dimensions (landfill, industrial installation, military base), which injected a quantity of pollutant inside the aquifer, each time rain occurred. The quantity of the pollutant that diffused into groundwater was considered linearly proportional to the recorded daily average precipitation height. Data from a thirty-year time series of daily average rainfall from Macedonia airport was used and linearly coupled with the pollutant mass diffused directly into the aquifer, assuming that no recharge occurred. The two-dimensional area was downstream monitored by a linear arrangement of wells network, consisting of different numbers of drilling wells in each studied case. The ability of the monitoring installation was evaluated through the probability of successful pollution detection. The effects on successful pollution detection of the aquifer's hydro-geological parameters, as they were reflected in the field's hydraulic conductivity variance and dispersion coefficients, have been studied too. Moreover, the influences of the aquifer sampling frequency and of the remedial actions delay time were examined into detection probability that a monitoring wells arrangement can achieve. Results were directly compared to those of instantaneous pollution simulated cases, considering the rest of the computational parameters common.

It was shown that detection probability of a monitoring arrangement increased faster, as the number of wells increased, in precipitation related pollution than in instantaneous cases. In all simulations the main hydro-geological parameter affecting detection probability, average detection time and average contaminated area, was the dispersion of the field. In the case of precipitation triggered heterogeneous aquifer pollution, sampling frequency

practically did not seem to affect detection probability of the monitoring network. In any simulated case, remedial action delay time was essential in estimating the risk concerning the detection ability of a groundwater monitoring installation, as it was a hidden parameter that might give a very big offset in risk calculation.

# ΠΕΡΙΛΗΨΗ

Τα υπόγεια νερά αποτελούν σημαντική φυσική πηγή πόσιμου νερού. Οι άνθρωποι παλιά πίστευαν ότι το φυσικό φιλτράρισμα του νερού ως αποτέλεσμα της υπόγειας ροής του ήταν αρκετό για να παρέχει ικανή προστασία από μολύνσεις, έτσι ώστε χωρίς καμία επεξεργασία το νερό να μπορεί να διατεθεί για οικιακή και αγροτική χρήση. Τότε, δραματικά γεγονότα τη δεκαετία του 1970 (π.χ. η περίπτωση του Love Canal) έκαναν τους πάντες να συνειδητοποιήσουν ότι τα υπόγεια νερά είχαν μολυνθεί από εκατοντάδες χιλιάδες υπόγειες δεξαμενές αποθήκευσης που είχαν διαρροές, δεξαμενές βιομηχανικών αποβλήτων, οικιακά σηπτικά συστήματα, αστικούς και βιομηχανικούς χώρους ταφής απορριμμάτων, τυχαίες χημικές διαρροές, απρόσεκτη χρήση διαλυτών, παράνομη απόρριψη αποβλήτων, καθώς επίσης και από εκτεταμένη χρήση γεωργικών χημικών. Η μόλυνση των υπογείων υδάτων έγινε το σημαντικότερο περιβαλλοντικό ζήτημα της δεκαετίας του 1980.

Από τη στιγμή που θα μολυνθούν τα υπόγεια ύδατα, είναι δύσκολο να αποκατασταθούν. Η αποκατάσταση των υπογείων υδάτων που έχουν μολυνθεί από διάθεση ανθρωπογενών χημικών, σε τέτοιο βαθμό ώστε να επιτρέπεται η απεριόριστη χρήση αυτών των υδάτων και η έκθεση σ' αυτά, παραμένει σημαντική τεχνική και θεσμική πρόκληση. Επιπλέον, ένα κυρίαρχο χαρακτηριστικό των προσπαθειών υπόγειας αποκατάστασης υδάτων αποτελούν οι χρονοβόρες καθυστερήσεις από τη στιγμή της ανακάλυψης του προβλήματος ως την επίλυσή του. Ορισμένες αιτίες γι' αυτά τα εκτεταμένα χρονοδιαγράμματα περιλαμβάνουν τις αναποτελεσματικές υπόγειες έρευνες, τις δυσκολίες χαρακτηρισμού της φύσης και του μεγέθους του προβλήματος σε πολύ ετερογενή υπόγεια περιβάλλοντα, τις τεχνολογίες αποκατάστασης και μία πλειάδα διοικητικών, στρατηγικών και πολιτικών παραγόντων.

Είναι εμφανές ότι, για να ελεγχθεί η μόλυνση των υπογείων υδάτων μέσω ενός συστήματος άμεσης ειδοποίησης και να ελαχιστοποιηθεί το κόστος αποκατάστασης, απαιτείται ένα σύστημα συναγερμού που θα παρακολουθεί σε σταθερή βάση την ποιότητα των υπογείων υδάτων. Ο σχεδιασμός ενός αξιόπιστου και αποτελεσματικού συστήματος παρακολούθησης είναι εξαιρετικά σημαντικός για τον συνολικό σχεδιασμό μιας

εγκατάστασης που ίσως δημιουργήσει απειλή μόλυνσης σε υπόγεια ύδατα. Στην περίπτωση παρακολούθησης της ανίχνευσης μόλυνσης υπογείων υδάτων για χώρους υγειονομικής ταφής απορριμμάτων, οι κανονισμοί της Ε.Ε. συνήθως απαιτούν ένα πηγάδι υποβάθρου (ανάντη) και δύο πηγάδια κατάντη. Η θέση, ο αριθμός (πέραν της ελάχιστης απαίτησης) και το βάθος των πηγαδιών ελέγχου καθορίζονται από τον διαχειριστή της εγκατάστασης και/ή από τις τοπικές αρχές. Στις περισσότερες περιπτώσεις, διενεργείται τριμηνιαία δειγματοληψία.

Η υπόγεια ρύπανση υδάτων λόγω διαρροών σε χώρους ταφής απορριμμάτων αποτελεί ένα σημαντικό θέμα τις τρεις τελευταίες δεκαετίες. Ενώ οι χώροι υγειονομικής ταφής απορριμμάτων αποτελούν την πιο διαδεδομένη προσέγγιση διαχείρισης της τελικής διάθεσης στερεών αποβλήτων εξαιτίας της απλότητας στην κατασκευή και του χαμηλού κόστους λειτουργίας, τα ιστορικά δεδομένα μας δείχνουν ότι οι χώροι αυτοί παρουσιάζουν υψηλό βαθμό αστοχίας όσον αφορά στη μόλυνση υπογείων υδάτων. Η ετερογένεια του υπεδάφους και η έλλειψη πληροφορίας σχετικά με την ακριβή θέση και διάρκεια μιας διαρροής καθιστούν εξαιρετικά δύσκολη την πρόβλεψη και ανίχνευση υπόγειας μόλυνσης του νερού πριν αυτή εξαπλωθεί και γίνει εμφανής. Η παρακολούθηση της μόλυνσης του υδροφόρου ορίζοντα μέσω πηγαδιών ελέγχου επηρεάζεται από πολλούς παράγοντες αβεβαιότητας, όπως την ετερογένεια του γεωλογικού περιβάλλοντος, την ποσότητα και τη φύση των μολυσματικών ουσιών, τον αριθμό και τη θέση των πηγαδιών ελέγχου και τη συχνότητα δειγματοληψίας. Παρ' όλα αυτά, δεν υπάρχει αναγνώριση των παραγόντων αβεβαιότητας σε θεσμικό επίπεδο.

Η επιτυχής ανίχνευση μιας μόλυνσης των υπογείων νερών που μεταφέρεται στον υδροφόρο ορίζοντα εξαρτάται άμεσα από την πιθανότητα υπολογισμού της κίνησης και της διασποράς του μολυσματικού παράγοντα στο περιβάλλον, κάτι για το οποίο ουσιαστικά πολύ λίγα πράγματα γνωρίζουμε. Αυτή η έλλειψη πληροφοριών προκαλείται από τις δυσκολίες πειραματικών μετρήσεων, σε οποιοδήποτε από τα σημεία του, των διαφόρων υδραυλικών ιδιοτήτων ενός γεωλογικού πεδίου (υδραυλική αγωγιμότητα, υδραυλικό μέτωπο, διαπερατότητα κτλ) για να προβλέψουμε, ή έστω να προσεγγίσουμε, τον τρόπο με τον οποίο ένα πλούμιο μπορεί να διαδοθεί στον υδροφόρο ορίζοντα. Επιπρόσθετοι παράγοντες αβεβαιότητας του προβλήματος είναι η έλλειψη πληροφοριών σχετικά με το σημείο από το οποίο ξεκινά η μόλυνση σε έναν χώρο ταφής απορριμμάτων, η διάρκεια της διαρροής και η έκταση του πλουμίου, τα οποία συνήθως εξαρτώνται από τη φύση του ρυπαντή. Κατά συνέπεια, είναι αδύνατο να ξέρουμε με βεβαιότητα πώς μεταβάλλονται οι συγκεντρώσεις του ρυπαντή στο υπέδαφος, κάτι που σημαίνει ότι δεν μπορούμε άμεσα να προβλέψουμε την πιθανότητα επιτυχούς ανίχνευσης μόλυνσης υπογείων υδάτων μέσα σε ετερογενείς υδροφόρους ορίζοντες από μία συγκεκριμένη διάταξη πηγαδιών ελέγχου.

Στην παρούσα διατριβή αναπτύχθηκε και χρησιμοποιήθηκε ένα στοχαστικό δισδιάστατο αριθμητικό μοντέλο για να αντιμετωπιστεί το πρόβλημα αξιολόγησης της αποτελεσματικότητας της ανίχνευσης υπόγειας ρύπανσης σε ετερογενείς υδροφόρους ορίζοντες μέσω γραμμικών διατάξεων πηγαδιών παρακολούθησης. Παρόλο που μπορεί να υποστηριχθεί ότι η δισδιάστατη προσέγγιση δεν είναι και η πιο ρεαλιστική περιγραφή της πραγματικής κατάστασης, στην ουσία απλοποιεί το υπολογιστικό πρόβλημα γιατί χάνει μόνο την κάθετη πληροφορία σχετικά με την κίνηση και την ανίχνευση των πλουμίων. Επιπλέον, όταν οι οριζόντιες διαστάσεις ενός υδροφόρου ορίζοντα υπερβαίνουν κατά πολύ το πάχος του, όπως στην περίπτωση μας, τότε τα αποτελέσματα στις δύο διαστάσεις παρέχουν μία καλή προσέγγιση της πραγματικότητας. Στα αριθμητικά πειράματα που βασίζονται στην τεχνική Monte Carlo, η γεωλογική ετερογένεια προσομοιώθηκε με τη μέθοδο Spectral Turning Bands και η υπόγεια μεταφορά και διασπορά της ρύπανσης με τη μέθοδο Random Walk Tracking Particle. Οι προσομοιώσεις διεξήχθησαν για να προσδιοριστούν οι πιθανότητες ανίχνευσης και οι περιοχές μόλυνσης υπογείων υδάτων, προϋποθέτοντας διαφορετικά επίπεδα γεωλογικής ετερογένειας και διασποράς ρυπαντή, και να εκτιμηθεί η αποτελεσματικότητα διαφόρων συχνοτήτων δειγματοληψίας πηγαδιών παρακολούθησης. Δύο διαφορετικές περιπτώσεις εξετάστηκαν, όσον αφορά στη διάρκεια της ρύπανσης, υποθέτοντας στιγμιαία ρύπανση και ρύπανση λόγω βροχόπτωσης, όπου η ρύπανση διαχέεται στον υδροφόρο ορίζοντα κατ' αναλογία με το ύψος βροχόπτωσης την περίοδο παρακολούθησης.

Η παρούσα εργασία αναπτύσσει μία νέα οπτική για τη διόρθωση της ανάλυσης ρίσκου. Η σύγχρονη ανάλυση ρίσκου εξετάζει το κόστος εναλλακτικών διαδικασιών αποκατάστασης προϋποθέτοντας ότι η μολυσμένη περιοχή προς αποκατάσταση συμπίπτει με την περιοχή που υπολογίστηκε τη χρονική περίοδο της ανίχνευσης. Εν τούτοις, υπάρχει πάντοτε μια σημαντική καθυστέρηση μεταξύ της περιόδου που ένα πλούμιο ανιχνευθεί και της περιόδου που θα αρχίσει η αποκατάστασή του. Αυτή η χρονική καθυστέρηση αποτελεί τυχαία μεταβλητή που εξαρτάται από τους διαθέσιμους πόρους και τεχνολογίες, καθώς επίσης και από την αποτελεσματικότητα της διοικητικής λήψης αποφάσεων. Προτείνεται ένα νέο πλαίσιο ανάλυσης ρίσκου που διορθώνει το εκτιμώμενο κόστος λόγω καθυστερήσεων αποκατάστασης.

Αρχικά, ο στόχος της παρούσας εργασίας ήταν ο αριθμητικός υπολογισμός σε δύο διαστάσεις της πιθανότητας ανίχνευσης ρύπανσης υπογείων υδάτων, η οποία ξεκινά στιγμιαία από μία σημειακή πηγή εντός των φυσικών ορίων ενός χώρου απόθεσης απορριμμάτων και επιτυγχάνεται από μία γραμμική διάταξη πηγαδιών παρακολούθησης που αποτελείται κάθε φορά από διαφορετικούς αριθμούς πηγαδιών. Θεωρήθηκε ότι η εγκατάσταση παρακολούθησης, σε διαφορετικές περιπτώσεις, βρίσκεται σε διαφορετικές

αποστάσεις από την εγκατάσταση του χώρου απόθεσης απορριμμάτων και κάθετα στο πεδίο ροής. Πραγματοποιήθηκε έλεγχος ευαισθησίας του μοντέλου για να προσδιοριστεί ο ελάχιστος αριθμός επαναλήψεων Monte Carlo όπου η στοχαστικά υπολογιζόμενη πιθανότητα ανίχνευσης σταθεροποιείται. Έγινε σύγκριση των αριθμητικών αποτελεσμάτων με τις θεωρητικές τιμές οι οποίες υπολογίζονται αναλυτικά στην περίπτωση ενός ομογενούς πεδίου. Έχοντας προσδιορίσει ένα υψηλής διακριτότητας σχήμα προσομοιώσεων, οι αποστάσεις των πηγαδιών παρακολούθησης από το χείλος εκφυγής του χώρου απόθεσης απορριμμάτων εξετάστηκαν με σκοπό να προσδιοριστεί, για κάθε υδρο-γεωλογική περίπτωση που προσομοιώθηκε, η μέγιστη πιθανότητα ανίχνευσης που μπορεί να επιτευχθεί από μία διάταξη παρακολούθησης.

Οι πιθανότητες ανίχνευσης και οι μολυσμένες περιοχές των υπογείων υδάτων υπολογίστηκαν για διαφορετικές διατάξεις πηγαδιών παρακολούθησης. Φάνηκε ότι η ανίχνευση μειωνόταν όσο η ετερογένεια αυξανόταν. Η παρακολούθηση με 20 πηγάδια παρείχε υψηλή ανιχνευσιμότητα, ενώ η ανίχνευση με 3 πηγάδια είχε ως αποτέλεσμα τη μη ανίχνευση τεσσάρων στις πέντε περιπτώσεις μόλυνσης. Θεωρώντας σταθερή την ετερογένεια του πεδίου, για κάθε διάταξη πηγαδιών, η πιθανότητα ανίχνευσης αυξήθηκε μέχρι μία συγκεκριμένη τιμή, καθώς αυξανόταν ο συντελεστής εγκάρσιας διασποράς, και μετά μειώθηκε. Μελετήθηκε η επίδραση της συχνότητας δειγματοληψίας των πηγαδιών στην ανίχνευση ρύπανσης υπογείων υδάτων. Η συχνότητα δειγματοληψίας ήταν κρίσιμος παράγοντας σε ετερογενείς υδροφορείς. Φάνηκε ότι η ελάχιστη δειγματοληψία θα έπρεπε να γίνεται δύο φορές ανά έτος, ενώ η μηνιαία δειγματοληψία φάνηκε ως η βέλτιστη λύση λαμβάνοντας υπ' όψη την απαιτούμενη διαδικασία και τη βελτίωση ανίχνευσης. Σε ετερογενείς υδροφόρους ορίζοντες, μεγάλος αριθμός πηγαδιών παρακολούθησης από τα οποία δεν γινόταν συχνή δειγματοληψία δεν απέδωσαν καλύτερα σε όρους ανίχνευσης απ' ό,τι μικρότερος αριθμός πηγαδιών από τα οποία γινόταν τακτική δειγματοληψία. Τέλος, ο χρόνος καθυστέρησης της ενέργειας αποκατάστασης εισήχθη ως έκφραση που αντιπροσώπευε την καθυστέρηση μεταξύ της ανίχνευσης και της ενέργειας αποκατάστασης, προκειμένου να εισάγει μία διόρθωση στην ανάλυση απόφασης η οποία αξιολογούσε οικονομικά τα πηγάδια παρακολούθησης. Αυτή η έκφραση κατέδειξε το γεγονός ότι καθυστερήσεις πέραν των 3 ετών ισοδυναμούσαν με μείωση της οικονομικής απόδοσης 12 πηγαδιών στα επίπεδα διατάξεων με μικρότερο αριθμό πηγαδιών, δηλαδή θα έπρεπε να ληφθεί υπ' όψη μεγαλύτερο κόστος αστοχίας από αυτό που συνήθως θεωρείται στην ανάλυση ρίσκου.

Στη συνέχεια, χρησιμοποιήθηκαν υψηλής διακριτότητας αριθμητικές επαναλήψεις Monte Carlo για να μελετηθεί η επίδραση της συχνότητας δειγματοληψίας στην πιθανότητα ανίχνευσης, σε μολυσμένες περιοχές που εντοπίζονταν σε ετερογενή υπόγεια περιβάλλοντα,

σε συνδυασμό με διαφορετικές υδρο-γεωλογικές παραμέτρους. Για όλους τους τύπους των εδαφών παρατηρήθηκε ότι η πιθανότητα ανίχνευσης μειωνόταν όσο η δειγματοληψία γινόταν λιγότερο συχνά. Ανεξάρτητα από την πυκνότητα του δικτύου παρακολούθησης σε υπόγεια περιβάλλοντα υψηλής διασποράς, έπρεπε να τηρηθεί ένα πολύ αυστηρό πρόγραμμα δειγματοληψίας έτσι ώστε να διατηρηθεί η απόδοση ανίχνευσης του δικτύου. Εδάφη υψηλής ετερογένειας, εξαιτίας της παρουσίας ζωνών χαμηλής διαπερατότητας, φάνηκε ότι εμπόδιζαν την εξάπλωση των ρυπαντών και, κατά συνέπεια, περιόριζαν την επίδραση της διασποράς. Η ανάλυση της καθυστέρησης μεταξύ του χρόνου πρώτης εμφάνισης των ρυπαντών στα σημεία παρακολούθησης και του χρόνου που πραγματικά παρατηρήθηκαν, καθώς επίσης και η αύξηση στην περιοχή του πλουμίου που προέκυψε από αυτή τη χρονική καθυστέρηση, οδήγησαν στο συμπέρασμα ότι απαιτούνταν μηνιαία δειγματοληψία για ένα μεγάλο εύρος υδρο-γεωλογικών παραμέτρων. Επιπλέον, μελετήθηκε η επίδραση της συχνότητας δειγματοληψίας στην καθυστέρηση ενέργειας αποκατάστασης. Φάνηκε ότι σε περιβάλλοντα υψηλής διασποράς η αντίδραση αποκατάστασης πρέπει να είναι της τάξης μερικών μηνών αν κάποιος δεν επιθυμεί σημαντική αύξηση των μολυσμένων περιοχών και του κόστους αποκατάστασης.

Έπειτα, μελετήθηκε αριθμητικά ο τρόπος με τον οποίον ο αριθμός των σημειακών πηγών ρύπανσης, το μέγεθος της περιοχής ελέγχου (χώρος απόθεσης αποβλήτων) και η ποσότητα μιας στιγμιαίας έγχυσης ρύπανσης στον υδροφόρο ορίζοντα επηρεάζουν την πιθανότητα ανίχνευσης μόλυνσης από μία γραμμική διάταξη πηγαδιών παρακολούθησης. Γι' αυτόν τον σκοπό χρησιμοποιήθηκε ένα δισδιάστατο, υψηλής διακριτότητας, στοχαστικό μοντέλο Monte Carlo. Σε κάθε εξεταζόμενη παράμετρο θεωρήθηκε ότι οι υπόλοιποι παράγοντες που επηρεάζουν τον υπολογισμό της πιθανότητας ανίχνευσης παρέμεναν σταθεροί. Οι προσομοιώσεις πραγματοποιήθηκαν στα πλαίσια παραγόντων αβεβαιότητας που προκύπτουν από το ίδιο το περιβάλλον, όπου η ρύπανση μεταφέρεται, και από την έλλειψη πληροφοριών συγκεκριμένων παραμέτρων, που αφορούν στις αρχικές συνθήκες της διαρροής.

Επιβεβαιώθηκε αριθμητικά στις περιπτώσεις που εξετάστηκαν ότι καθώς αυξανόταν το μέγεθος της περιοχής ελέγχου, ενώ ο αριθμός των πηγαδιών παρέμενε σταθερός, μειωνόταν η πιθανότητα ανίχνευσης. Συνεπώς, αν αυξανόταν το πλάτος μιας περιοχής ελέγχου, το ίδιο θα έπρεπε να συμβεί και με τον αριθμό των πηγαδιών παρακολούθησης, έτσι ώστε να διατηρούνταν η πυκνότητά τους. Σε όλες τις περιπτώσεις που προσομοιώθηκαν, η γενική παρατήρηση ήταν ότι όταν υπήρχαν δύο παρόμοιες πηγές υπόγειας ρύπανσης τότε η ανίχνευση της μόλυνσης ήταν ευκολότερη, καθώς η μέση αύξηση της πιθανότητας ανίχνευσης ήταν μεταξύ 35% - 55%. Παρατηρήθηκε η ίδια αυξητική τάση στην πιθανότητα

ανίχνευσης σε σχέση με τις περιπτώσεις μίας πηγής ρύπανσης, ανεξάρτητα από τη συχνότητα δειγματοληψίας.

Τα αποτελέσματα των προσομοιώσεων δείχνουν ότι όταν η αρχική συγκέντρωση της ρύπανσης ήταν κάτω από 1.000 mg/l, η ανίχνευσή της ήταν πολύ δύσκολη, ανεξάρτητα από τις υδρο-γεωλογικές παραμέτρους του υδροφορέα. Η αποτελεσματικότητα των πηγαδιών παρακολούθησης σε υδροφορείς με χαμηλή ως μέτρια διασπορά έφτασαν σε μία μέγιστη τιμή, ανεξάρτητη από την αρχική μάζα της ρύπανσης που διείσδυσε στον υδροφόρο ορίζοντα. Το σημείο καμπής της συγκέντρωσης της αρχικής ρύπανσης ήταν  $C = 8,000 \text{ mg/l}$ , η οποία ήταν η τιμή στην οποία η πιθανότητα ανίχνευσης έφτασε σε σημείο πλατώ. Παρατηρήθηκε επίσης ότι μόνο σε περιβάλλοντα υψηλής διασποράς η αύξηση της μόλυνσης είχε ως αποτέλεσμα υψηλότερη πιθανότητα ανίχνευσης. Σε κάθε περίπτωση, ήταν δύσκολο να ανιχνευθούν χαμηλές τιμές συγκέντρωσης, υποδεικνύοντας ότι προκειμένου μία διάταξη παρακολούθησης να είναι ευαίσθητη, τουλάχιστο κατά την προσομοίωσή της, ακόμη και για μικρές ποσότητες ρύπανσης, απαιτείται η χρήση ενός ελάχιστου αριθμού 12 πηγαδιών.

Τέλος, μελετώντας έναν διαφορετικό τρόπο ρύπανσης υπόγειων υδάτων στα πλαίσια της πρόκλησής της σύμφωνα την τοπική βροχόπτωση, υποθέσαμε ότι υπήρχε μία σημειακή πηγή ρύπανσης μέσα σε ελεγχόμενη περιοχή συγκεκριμένων διαστάσεων (χώροι απόθεσης αποβλήτων, βιομηχανικές εγκαταστάσεις, στρατιωτικές βάσεις) η οποία διοχέτευε μια ποσότητα ρύπανσης εντός του υδροφόρου ορίζοντα σε κάθε βροχόπτωση. Η ποσότητα του ρυπαντή που διαχεόταν στα υπόγεια ύδατα θεωρήθηκε γραμμικά ανάλογη ως προς την ημερήσια καταγραφή του μέσου ύψους βροχόπτωσης. Χρησιμοποιήθηκαν δεδομένα από μία χρονοσειρά 30 ετών μέσης ημερήσιας βροχόπτωσης στο αεροδρόμιο «Μακεδονία» και συσχετίστηκαν γραμμικά με τη μάζα του ρυπαντή που διαχεόταν απευθείας στον υδροφόρο ορίζοντα, υποθέτοντας ότι δεν είχαμε επαναφόρτισή του. Η δισδιάστατη περιοχή επιτηρούνταν κατάντη από γραμμική διάταξη δικτύου πηγαδιών, το οποίο αποτελούνταν από διαφορετικό αριθμό γεωτρήσεων-πηγαδιών σε κάθε περίπτωση που μελετήθηκε. Μελετήθηκαν επίσης οι επιδράσεις των υδρο-γεωλογικών παραμέτρων του υδροφορέα στην επιτυχή ανίχνευση της ρύπανσης, όπως εκφράστηκαν στη διακύμανση υδραυλικής αγωγιμότητας του πεδίου και στους συντελεστές διασποράς. Επιπλέον, εξετάστηκαν οι επιδράσεις της συχνότητας δειγματοληψίας του υδροφόρου ορίζοντα και του χρόνου καθυστέρησης ενεργειών αποκατάστασης στην πιθανότητα ανίχνευσης που μπορεί να πετύχει μια διάταξη πηγαδιών παρακολούθησης. Τα αποτελέσματα συγκρίθηκαν άμεσα με αυτά των προσομοιωμένων περιπτώσεων στιγμιαίας ρύπανσης, θεωρώντας ότι οι υπόλοιπες υπολογιστικές παράμετροι ήταν κοινές.

Φάνηκε ότι η πιθανότητα ανίχνευσης μίας διάταξης παρακολούθησης αυξανόταν γρηγορότερα, όταν αυξανόταν κι ο αριθμός των πηγαδιών, σε ρύπανση σχετιζόμενη με

βροχόπτωση απ' ότι στις περιπτώσεις στιγμιαίας ρύπανσης. Σε όλες τις προσομοιώσεις η κύρια υδρο-γεωλογική παράμετρος που επηρέαζε την πιθανότητα ανίχνευσης, τον μέσο χρόνο ανίχνευσης και τη μέση μολυσμένη περιοχή ήταν η διασπορά του πεδίου. Στην περίπτωση πρόκλησης από βροχόπτωση ρύπανσης ετερογενούς υδροφορέα, η συχνότητα δειγματοληψίας πρακτικά δεν φάνηκε να επηρεάζει την πιθανότητα ανίχνευσης ενός δικτύου παρακολούθησης. Σε κάθε περίπτωση που προσομοιώθηκε, η καθυστέρηση των ενεργειών αποκατάστασης ήταν ουσιώδης για τον υπολογισμό του ρίσκου που αφορούσε στην ικανότητα ανίχνευσης μίας εγκατάστασης παρακολούθησης υπογείων υδάτων, καθώς αποτελούσε κρυφή παράμετρο που θα μπορούσε να προκαλέσει μεγάλη απόκλιση στον υπολογισμό του ρίσκου.

# CHAPTER 1

## Introduction

---

### 1.1 Groundwater Pollution

Safe drinking water is essential to human and other life form survival. Actually, it is the special physical and chemical properties of water which render it a significant factor for the existence of life on Earth; at least in the form we know it. Yet, not all of this water is suitable for humans to use. In fact, only 2.5% of the Earth's water is freshwater. Less than 0.3% of all freshwater is found in rivers, lakes and the atmosphere, whereas an even smaller amount (0.003%) is contained within biological bodies and manufactured products (Gleick, 1993). This natural resource is becoming scarcer in certain places, and its availability is a major social and economic concern. Water, however, is not a finite resource, but rather recirculates during the Earth's water cycle, where it moves continually through evaporation and transpiration (evapo-transpiration), condensation, precipitation and surface runoff, usually reaching the sea. Some runoff infiltrates the ground and goes into aquifers. This groundwater later flows back to the surface from springs and ends up recharging rivers or flowing directly into the sea. Groundwater storage is important since clean freshwater is essential to the survival of humans and other land-based life.

Groundwater, which is thought of as liquid water flowing through shallow aquifers, is a natural resource which constitutes the largest reservoir of freshwater in the world, accounting for over 97% of all freshwaters available on earth (EU/Groundwater-Directive, 2008). Technically, groundwater can also include soil moisture, permafrost, immobile water in very low permeability bedrock and deep geothermal or oil formation water. Until recently, focus on groundwater has mainly concerned its use as drinking water (e.g. about 75% of European Union (EU) residents depend on groundwater for their water supply), and groundwater has

also been recognized as an important resource for industry (e.g. cooling waters) and agriculture (irrigation). It has, however, become increasingly obvious that groundwater should not only be viewed as a water supply reservoir, but should also be protected because of its environmental value (EU/Groundwater-Directive, 2008).

Most concern over groundwater contamination has focused on pollution associated with human activities. Human groundwater contamination can either be directly related to waste disposal (private sewage disposal systems, land disposal of solid waste, municipal wastewater, wastewater impoundments, land spreading of sludge, brine disposal from the petroleum industry, mine waste, deep-well disposal of liquid waste, animal feedlot waste, radioactive waste) or not (accidents, military operations, certain agricultural activities, mining, highway de-icing, acid rain, improper well construction and maintenance, road salt) (LENNTECH, 2013). Since groundwater moves slowly through the subsurface, the impact of anthropogenic activities may last for a long time. This means that pollution which occurred some decades ago — originating from agriculture, industry or other human activities — may still be threatening groundwater quality today and, in some cases, will continue to do so for several generations to come.

Large quantities of organic compounds are manufactured and used by industries, agriculture and municipalities. Recent reports show that pollution from domestic, agricultural and industrial sources is still a major concern, despite the progress in some fields, either directly through discharges (effluents) or indirectly through the spread of nitrogen fertilizers and pesticides, as well as leaching from old contaminated industrial or waste disposal sites (e.g. landfills, mines, heavy manufacturing industry etc.). While point sources have caused most of the pollution identified to date, there is evidence that diffuse sources are having an increasing impact on groundwater. For example, nitrate concentrations currently exceed the nitrate guideline values in approximately one third of groundwater bodies in Europe (EU/Groundwater-Directive, 2008).

These man-made organic compounds are of most concern. In many locations groundwater has been contaminated by chemicals for many decades, though this form of pollution was not recognized as a serious environmental problem until the 1980s. According to *Lenntech* website, contamination sources may be:

Natural: groundwater contains some impurities, even if it is unaffected by human activities.

The types and concentrations of natural impurities depend on the nature of the geological material through which groundwater moves and the quality of the recharge water. Groundwater moving through sedimentary rocks and soils may pick up a wide range of compounds such as magnesium, calcium and chlorides. Some aquifers have

a high natural concentration of dissolved constituents such as arsenic, boron, selenium and chromium. The effects of these natural sources of contamination of groundwater quality depend on the type of contaminant and its concentrations.

Agricultural: Pesticides, fertilizers, herbicides and animal waste are agricultural sources of groundwater contamination. Their manifestations are varied and numerous: spillage of fertilizers and pesticides during handling, runoff from the loading and washing of pesticide sprayers or other application equipment, use of chemicals uphill from or within a few hundred feet of a well, storage of agricultural chemicals near conduits to groundwater, such as open and abandoned wells, sink holes, or surface depressions where ponded water is likely to accumulate. Contamination may also occur when chemicals are stored in uncovered areas, unprotected from wind and rain, or are stored in locations where groundwater flows from the direction of the chemical storage to the well.

Industrial: Manufacturing and service industries have high demands for cooling water, processing water and water for cleaning purposes. Groundwater pollution occurs when used water is returned to the hydrological cycle. Modern economic activity requires transportation and storage of material used in manufacturing, processing, and construction. Along the way, some of this material can be lost through spillage, leakage or improper handling. The disposal of waste associated with the above activities contributes to yet another source of groundwater contamination. Some businesses, usually without access to sewer systems, rely on shallow underground disposal. They use cesspools or dry holes, or send the wastewater into septic tanks. Any of these forms of disposal can lead to contamination of underground sources of drinking water. Dry holes and cesspools introduce waste directly into the ground, whereas septic systems cannot treat industrial waste. Wastewater disposal practices of certain types of businesses, such as automobile service stations, dry cleaners, electrical component or machine manufacturers, photo processors and metal fabricators, are of particular concern because the waste they generate is likely to contain toxic chemicals. Other industrial sources of contamination include cleaning off holding tanks, spraying equipment on the open ground, waste disposal in septic systems or dry wells and storage of hazardous materials in uncovered areas or in areas that do not have pads with drains or catchment basins. Moreover, underground and above ground storage tanks holding petroleum products, acids, solvents and chemicals can develop leaks from corrosion, defects, improper installation or mechanical failure of the pipes and fittings. Furthermore, mining of fuel and non-fuel minerals can create many opportunities for groundwater contamination. The problems

stem from the mining process itself, the disposal of waste and the processing of the ores and the waste they create.

Military: operations and maintenance of military systems, such as fighter aircrafts, ships and vehicles, are activities similar to industrial ones, producing a great amount of pollutants. Even if national regulations are applied to all of these military activities concerning waste handling, there are cases on the battlefield during military operations where environmental issues are not the first priority. In addition, usage of weapons that cause infrastructure damage may create uncontrolled groundwater pollution, as storage facilities or industrial resources destruction can release chemicals into the ground, which will infiltrate the aquifer or may be transported away from the theatre of operations, affecting people and polluting communities not invoked in the confrontation.

Residential: Residential wastewater systems can be a source of many categories of contaminants, including bacteria, viruses, nitrates from human waste, as well as organic compounds. Injection wells used for domestic wastewater disposal (septic systems, cesspools, drainage wells for storm water runoff, groundwater recharge wells) are of particular concern to groundwater quality if located close to drinking water wells. Improper storage or disposal of household chemicals such as paints, synthetic detergents, solvents, oils, medicines, disinfectants, pool chemicals, pesticides, batteries, gasoline and diesel fuel can also lead to groundwater contamination. When these chemicals are stored in garages or basements with floor drains, spills and flooding may introduce them as contaminants into the groundwater. When thrown in the household trash, these products will eventually be carried into groundwater because community landfills are not equipped to handle hazardous materials. Similarly, waste dumped or buried in the ground can contaminate the soil and leach into groundwater.

Once contaminated, groundwater is difficult to restore. A study by the United States of America National Research Council (U.S.N.R.C., 2012) indicated that there are at least 126,000 groundwater sites that may have contaminated soil or groundwater, requiring some form of remediation. Almost 10 percent of these sites are considered "complex," meaning restoration is unlikely to be achieved in the next 50 to 100 years due to technological limitations. The same report adds that the estimated cost of complete cleanup at these sites ranges from \$110 billion to \$127 billion, but the figures for both the number of sites and the costs are likely underestimations.

One dominant attribute of subsurface remediation efforts has been the lengthy delays between discovery of the problem and its solution (U.S.N.R.C., 2012). The reasons for these extended timeframes are now well-known: ineffective subsurface investigations, difficulties in characterizing the nature and extent of the problem in highly heterogeneous subsurface environments, remedial technologies incapable of achieving restoration in many geological settings, continued improvements in analytical detection limits leading to discovery of additional chemicals of concern, evolution of more stringent drinking water standards, and the realization that other exposure pathways, such as vapor intrusion, pose unacceptable health risks. A variety of administrative and policy factors also result in extensive delays, including, but not limited to, high regulatory personnel turnover, the difficulty in determining cost-effective remedies to meet cleanup goals and allocation of responsibility at multiparty sites.

## **1.2 Groundwater Protection**

Groundwater protection describes the management processes by which groundwater quality and resources are protected against pollution and over-exploitation. This can mainly be achieved by three interwoven factors: environmental legislation, ethics and education. Each of these plays its part in influencing national-level environmental decisions and personal-level environmental values and behaviors. For environmental and, consequently, groundwater protection to become a reality, it is important for societies to develop each of these areas that, together, will inform and drive environmental decisions (Solomon, 2010). In the present study, only the component of environmental legislation will be of immediate concern and will be used as a reference system, as this factor sets liability limits on the way various human activities are controlled.

A policy establishment on groundwater protection expresses a political willingness towards that direction and the way this policy will be applied is by setting regulations. In the case of EU, laws designed to protect groundwater against pollution and deterioration are part of a larger regulatory framework that can be traced back to the 1990s. The concept of groundwater protection as tackled by different pieces of legislation is now fully integrated into the basic measures of the EU Water Framework Directive.

There are specific basic regulatory measures of direct relevance to groundwater protection. One in particular, the Landfill Directive, is of immediate concern in the present study, as its limits have been applied to compare with simulation results. The Landfill Directive seeks to prevent or reduce the negative effects of landfill waste on the environment, including groundwater. It establishes provisions for issuing permits based on a range of conditions, including impact assessment studies. For each site, groundwater, geological, and

hydrogeological conditions in the area must be identified. The sites must be designed so as to prevent groundwater from entering landfill waste, so as to collect and treat contaminated water and leachate, as well as prevent the pollution of soils, groundwater or surface water by using the appropriate technical precautions, such as geological barriers and bottom liners. The Landfill Directive also sets a minimum requirement on groundwater quality monitoring. It establishes criteria for waste testing and acceptance, taking into consideration the protection of the surrounding environment, including groundwater.

Regarding municipal landfills, an initial sampling must be carried out in at least three locations before the filling operations, in order to establish reference values for future sampling. Having started the operation of the facility, a groundwater pollution detection monitoring program must be established, which must consist of at least one up-gradient background well and two down-gradient wells (EU, 1999/31/EC). The purpose of detection monitoring is early detection of a release to groundwater based on comparison of down-gradient well data to background data for a limited number of water quality parameters. The number of monitoring wells can be increased on the basis of a specific hydro-geological survey and the need of the operator to control the risk and the liabilities in case of groundwater pollution. Regulation compliance of monitoring samples for an expanded suite of hazardous constituents requires establishment of concentration limits (compliance or cleanup standards), should any of these constituents be detected. Down-gradient well data is compared to concentration limits for each well on a periodic basis. The purpose of compliance monitoring is to determine if the release to groundwater is significant enough to warrant corrective action. Corrective action typically requires leachate leak source location identification and control, as well as groundwater remedial measures. The issues of a monitoring system design for detection, along with a sampling policy and timely remedial action compliance, are addressed in this thesis.

### **1.3 Landfills and Leachate**

Increasingly affluent lifestyles and the continuing industrial and commercial growth in many countries around the world in the past decade have been accompanied by rapid increases in both municipal and industrial solid waste production. The sanitary landfill method for the ultimate disposal of solid waste material continues to be widely accepted and used due to its economic advantages (Renou et al., 2008). A municipal solid waste landfill system is an engineered deposit of waste onto or into the ground in such a way that pollution to the environment is prevented (ISWA, 1992). Alternatively a sanitary landfill, as defined in Article 2 of the European Directive 1999/31/EC, is any area onto or into the ground used for

at least a year for the disposal of solid waste. The critical components of a sanitary landfill are a natural element, the hydro-geological setting, and four engineered ones: the bottom liner, the cover, the leachate collection system and the monitoring system for the detection of a potential contamination leak (Paleologos, 2008). The bottom liner and the leachate collection system are complementary elements. The bottom liner constitutes the barrier to the environment for liquid and gas leaks from a landfill, and the leachate collection system, which is placed immediately below the waste, collects the leachate before it reaches the bottom liner. If collection of the leachate were to fail, the hydraulic load would make the liquid waste penetrate the bottom liner and be released in the environment (Figure 1.1). The basic operation of the cover is to prevent the infiltration of water into a landfill and the monitoring system checks the total operation of a landfill and its impact on the environment.

The main objective of landfilling is to provide a place for the final storage of waste in a way that does not impair human health and the surrounding environment. This objective can be reached by isolating the waste disposed of from the environment, so that emissions from the disposal site can be collected and treated prior to their release to the environment (Munawar & Fellner, 2013). Globally, more than 70% of municipal waste generated is disposed of in landfills (Zacarias-Farah & Geyer-Allely, 2003).

The main landfill emissions are biogas, airborne particulates and leachate. Biogas is produced during the biodegradation of the organic matter inside the waste bulk, while airborne particulates are generated during waste mechanical compression. Leachate is defined as the aqueous effluent generated as a consequence of rainwater percolation through waste, in conjunction with the biochemical processes in waste cells and the inherent water content of the waste (Renou et al., 2008). During landfill operation, leachates are produced mainly due to infiltration of rainwater through the refuse tips (Tatsi & Zouboulis, 2002). Leachate may contain large amounts of organic matter (biodegradable, but also refractory to biodegradation), where humic-type constituents consist an important group, as well as ammonia-nitrogen, heavy metals and chlorinated organic or inorganic salts. The composition of landfill leachates varies greatly depending on the age of the facility (Lema et al., 1988).

While landfills in many countries are currently designed and manufactured to minimize releases through the use of leachate barrier systems, capping of the site, leachate removal for treatment and barrier failure or degradation over time make groundwater pollution possible, while low rates of leachate removal in comparison to inflow to leachate treatment plants, for instance due to a rainfall, can result in seepage to both surface and groundwater (Slack et al., 2007). Despite all counter measures aiming at eliminating the chance of barrier leakage, the risk of leachate groundwater contamination cannot be completely eliminated or even, in some cases, controlled. The impact of landfill leachates on underlying aquifers has prompted a great

number of studies (Apgar & Langmuir, 1971; Miller & Mishra, 1989b, 1989a; Kjeldsen, 1993; Kaczmarek et al., 1997; Gau & Chow, 1998; Riediker, 2000; De Cortázar et al., 2002; Tatsi & Zouboulis, 2002; Slack et al., 2007; Renou et al., 2008). It is estimated by the U.S. Environmental Protection Agency that all landfills, irrespectively of the type of bottom liner, may present contamination leaks with time, and at least 40% of the operating landfills in the United States exhibit “some type of leak” (ITRC, 2003).

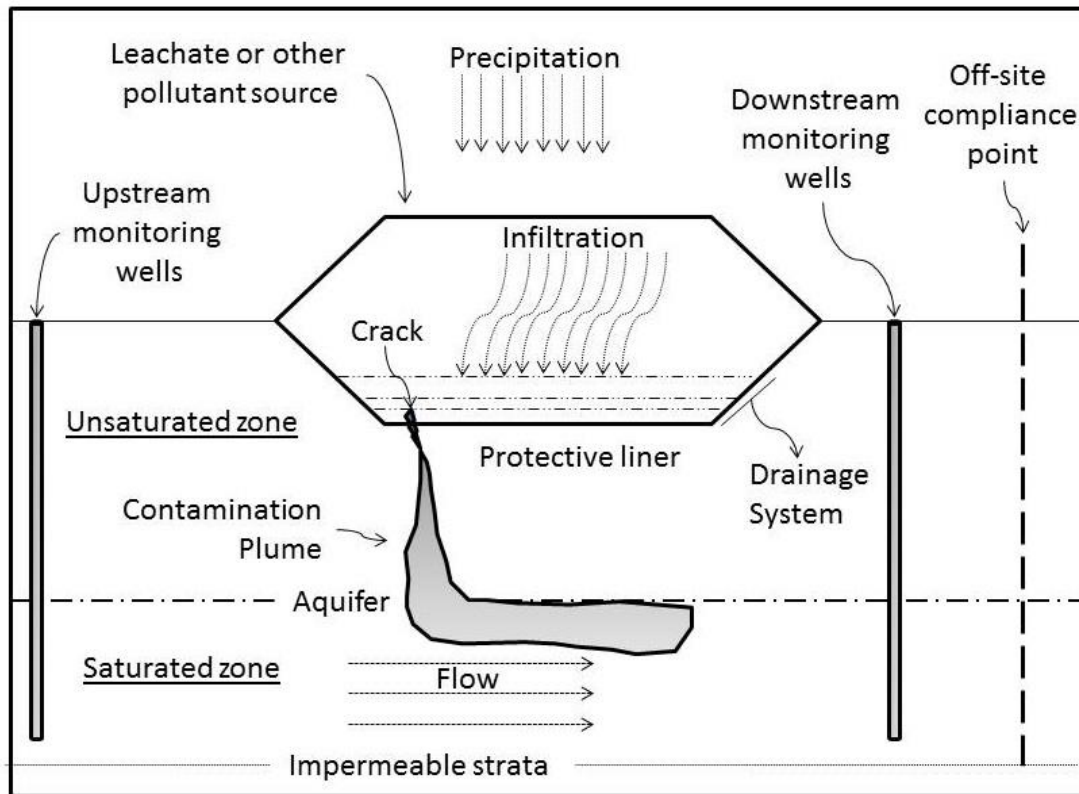


**Figure 1.1:** Main landfill characteristics and leachate escape into saturated zone

## 1.4 Problem Definition

Leachate production and management is now recognized as one of the greatest problems associated with the environmentally sound operation of sanitary landfills, because this liquid waste can cause considerable pollution problems by contacting the surrounding soil, ground or surface waters, and therefore it is considered a major pollution hazard unless precautionary measures are implemented (Baccini et al., 1987). The leachate problem is made worse by the fact that many landfill sites are operating without an appropriate impermeable bottom liner or an effective collection and subsequent treatment system (Lema et al., 1988), meaning that after the facility closes it is highly probable for pollution to escape into

groundwater. Moreover, in abandoned landfills there is rarely any leachate collection and removal system available. Thus, leachate gravitationally drains through the waste mass and eventually develops a hydraulic head on the base of the facility (or liner, if one is present). Either leakage is accelerated due to this increased head or the head continues to build in the waste mass, creating groundwater pollution threat (Koerner & Soong, 2000).

In order for aquifer leachate contamination to be discovered, regulations impose the use of a groundwater monitoring system. The objective of a monitoring network is to gather information to be used for such purposes as characterization of ambient conditions, detection of the existence or location of undesirable conditions, and verification of compliance with regulations (Loaiciga et al., 1992). Therefore, the design of a reliable and efficient groundwater monitoring system is of great importance for groundwater protection policy, as it helps to determine the likelihood and severity of contamination problems. In addition, an early warning would minimize the landfill operator's liabilities.

However, because of the numerous and significant uncertainties involved, often it is difficult to ensure that a specific monitoring system will perform as initially expected. Uncertainty stems from the fact that we do not know exactly when and where the pollution will originate and how it is going to evolve into underground environment for which very few things are known. It is not possible to know beforehand when a containment installation or a protective barrier will fail, allowing pollutants to intrude into groundwater, as long-term durability of synthetic lining systems is in doubt (Allen, 2001; Zhao et al., 2007). Consequently, the best thing to do is set an "alarm" mechanism in case of failure and aquifer contamination.

Even though identifying leaks in landfill liners is an essential part of waste management and there are leak detection tools, such as electro-chemical sensing (Rumer & Mitchell, 1995; Laine et al., 1997), that can be installed to identify them soon after they occur, legislation does not oblige facility operators to install such a tool. Because leak detection tools are costly to install initially, landfill operators detect contaminant plumes caused by leaks in the landfill liner by collecting groundwater samples and analyzing them. One limitation of this method is that it does not prevent groundwater from becoming contaminated. Another limitation is the expense of comprehensive monitoring for all groundwater which comes in contact with a landfill.

Because the majority of landfills are lined with geo-membranes, most leaks are point sources, not widespread (Giroud & Bonaparte, 1989; Rumer & Mitchell, 1995). This is mainly due to the fact that usually leaks are developed at the bottom of the protective barriers, underneath great quantities of waste, where there is no access to perform a direct inspection.

Either due to a functional failure (material or leachate removal failure) or due to an accidental event (liner tear or puncture) the footprint of the contamination source is usually very small. If there is no monitoring well in the path of a plume, it is possible for the front of the plume to pass by the line of wells at the point of compliance without being detected. This could also happen in case sampling intervals of monitoring wells allow contamination to pass over undetected. 99/31/ EU Directive states that the sampling frequency must be based on possibility for remedial actions between two samplings if a trigger level is reached. In general, groundwater should be monitored quarterly, biannually or annually, depending on the type of waste, size and design of the landfill, along with aquifer material. In most cases a quarterly monitoring is required. However, annual monitoring can be undertaken for small landfills located in remote places far away from any groundwater use source. Installing enough monitoring wells to be sure of intercepting a narrow plume in any position can be prohibitively expensive (Godfrey et al., 1987). In addition, a very rigorous sampling policy in order to detect small plume pollution briefly injected into groundwater may increase a landfill's operating cost too much. Consequently, it is rather impossible to predict the exact location of the failure and the source of pollution. Potentially, every point inside a landfill's vicinity may be a contamination source.

As soon as pollution enters the saturated zone, it is very difficult to determine the exact path of its propagation. Spreading of solutes in transport through geological formations (aquifers, petroleum reservoirs) is governed by the large-scale spatial variability of permeability (Dagan, 1994). Geological formations that act as flow conduits are often characterized by highly variable three-dimensional structures consisting of layers, lenses and, perhaps, fractures in various materials, ranging from sand and gravel to clay or rocks. Corresponding to these material fluctuations is a similar variability in the characteristic hydraulic parameters used for the description of both flow and transport in porous media scale balance equations (Tompson et al., 1987a). Because of the seemingly erratic spatial variation of hydraulic conductivity  $K$  and the scarcity of field data, it is very difficult, if not impossible, to deterministically define the path of plume contamination. Field uncertainty is an important factor in hydrological applications (unlike controlled laboratory experiments), where there is usually large uncertainty in characterizing even the statistical structure of  $K$  (Fiori et al., 2006).

Finally, another factor of uncertainty stems from the fact that there is no exact time provision in pollution control and in environmental restoration after contamination has been discovered. Even if regulations prompt landfill operators to apply an emergency plan so as for pollution to be controlled, additional remediation actions must be taken in order for environmental damage to be restored and further pollution danger to be eliminated. In real

life, though, immediate remediation actions are not the case. Even the EU 99/31 Directive on landfill operation states that when a monitoring well sample analysis indicates evidence of groundwater pollution, another sample must be taken and, if pollution is verified again, then measures are to be taken. However, as time passes plume contamination areal coverage gets bigger. Time between groundwater pollution detection and the line of action that someone is willing to follow as soon as it is successfully discovered defines the worthiness of the detection information. Thus, holistic consideration of leachate groundwater contamination detection entails uncertainty as to restoration time.

A reliable groundwater detection monitoring system entails various challenges due to the nature of the problem. The performance of a landfill's monitoring wells for leachate polluted groundwater has prompted a great number of studies (Morisawa & Inoue, 1991; Hudak & Loaiciga, 1992; Loaiciga et al., 1992; Meyer et al., 1994; Hudak, 2001; Kim & Lee, 2007) mainly focusing on the optimization of pollution detection probability in relation to the number and location of the wells. Additional research has been done in order to determine how hydro-geological or monitoring installation parameters affect successful groundwater pollution (Hudak, 1998; Warrick et al., 1998; Hudak, 2005; Yenigül et al., 2005; Yenigül et al., 2011), as well as studies have been done to develop methods to reduce the costs associated with long term monitoring of sites groundwater contamination (Reed et al., 2000; Wu et al., 2005).

However, landfills are not the only groundwater pollution sources. For many industrial activities, such as those taking place at oil refineries and chemical plants, it is almost impossible to prevent pollution. If shallow groundwater is present, it is likely that the industrial site will become polluted somewhere in the future or has been polluted at some point in the past. It is of vital importance to human health and the public acceptance of these activities that groundwater pollution is detected before it crosses the terrain boundary of the refinery or plant (Bierkens, 2006). This way it can be hydrologically contained or cleaned up. Hence, many refineries and plants have a monitoring network at the boundary of their sites to detect plumes of polluted groundwater.

Much of the literature on optimizing monitoring networks for groundwater quality is concerned with mapping contaminant plumes from landfills (Loaiciga, 1989; Loaiciga et al., 1992; McLaughlin et al., 1993; Yenigul et al., 2006). In case of larger sites with industrial activities, the plumes themselves are usually not of interest. Interest is focused on detecting the plumes before they leave the site at some distance from the boundary (Bierkens, 2006). Although the present study started mainly by examining municipal waste sanitary landfill cases, results were expanded in every facility where groundwater monitoring is legally

implemented or simply advised, in order for aquifer pollution to be detected and liabilities to be avoided.

## 1.5 Research Objectives

The purpose of this research is to numerically investigate groundwater contamination detection probability achieved by a linear monitoring arrangement of wells and to provide a novel framework that modifies traditional risk analyses by supplying a corrected detection probability that accounts for delays in remedial actions. A stochastic 2-D model has been developed that performs high resolution Monte Carlo simulation, which accounts for uncertainties stemming from:

- i. Geological heterogeneity, as reflected to hydraulic conductivity  $K$
- ii. Dispersion of pollution, as described by longitudinal and transverse dispersion coefficients  $a_L, a_T$
- iii. Size of a landfill or a controlled area where groundwater pollution may occur
- iv. Location of contamination source
- v. Number of contamination sources
- vi. Quantity of pollution that infiltrates groundwater
- vii. Duration of leak
- viii. Sampling frequency
- ix. Delays in remediation actions

The numerical experiment results of the present thesis are used to acquire an insight on the way field heterogeneity, pollution source location, duration and quantity in relation to sampling frequency as well as remediation delay affect the efficiency of an established monitoring network of groundwater pollution and its operating policy. Even if numerical simulations are not equivalent to field experiments, results are adequate to provide a quick and affordable first estimation on what to expect from such a running monitoring system or from one under consideration.

First estimation is defined as the preliminary calculation of detection probability that a specific monitoring installation may provide, without performing any field measures but only using an expert's views and observations on assigning values at mean hydraulic conductivity, at heterogeneity, as this is reflected into hydraulic conductivity variations, and at dispersion coefficient. By applying all these parameters at the present work model, in conjunction with sampling policy and an estimation of possible pollution control or remediation delay, the

outcome probabilities can help an engineer perform risk analysis in terms of cost for a specific monitoring installation easily and decide what would be the best tradeoff choice among the number of monitoring wells, an adopted sampling policy and a possible pollution detection failure. Moreover, additional costs originating from remediation delay, depending on available resources and technologies, as well as efficiency of administration decision-making, are also introduced as decision parameters.

## 1.6 Thesis Outline

This thesis comprises seven chapters, which describe the objectives and results obtained in this study. *Chapter 2* provides an outline of the basic simulation schemes that are used and describes the numerical techniques of the computational model that simulates transportation and dispersion of contaminant plumes originating from a groundwater pollution controlled area leakage, such as a landfill. The numerical methods of the solution of governing flow and contaminant transport equations are described in this chapter. A brief introduction is made on subsurface heterogeneity simulation using the Spectral Turning Bands method, as well as pollution advection and dispersion simulation using Random Walking Particles method. At the end of *Chapter 2* the model's structure is analyzed and a brief description of the source code is referenced.

In *Chapter 3*, a high resolution Monte Carlo stochastic model is developed to simulate contaminant transport from an instantaneous source into heterogeneous two-dimensional aquifers. The effect of a representative number of particles on the plume's description is studied and compared with its theoretical detection probability in case of a homogeneous aquifer. Probabilities of detection  $P_d$  and contaminated groundwater areas are calculated for different arrangements of monitoring wells. An expression is proposed that accounts for the delay between detection and remedial action in order to provide a correction to decision analyses that evaluate the economic worth of well monitoring. *Chapter 3* has been adapted from *Papapetridis K., Paleologos EK., (2012), "Sampling Frequency of Groundwater Monitoring and Remediation Delay at Contaminated Sites", Water Resources Management 26(9), pp.2673-2688, doi: 10.1007/s11269-012-0039-8.*

*Chapter 4* examines the monitoring wells frequency of sampling at contaminated sites located in two-dimensional heterogeneous subsurface environments. Aquifer heterogeneity and the pollution dispersion effect on detection probability, in conjunction with the sampling policy adopted, are examined. The impact of delays in remedial response is also investigated in terms of the growth that such delays incur on contaminated areas and remediation costs. High-resolution numerical Monte Carlo realizations are utilized to simulate contaminant

movement in heterogeneous two-dimensional aquifers and to calculate the probabilities of detection  $P_d$  attained by various monitoring well arrangements. *Chapter 4* has been adapted from *Papapetridis K., Paleologos EK., (2011), "Contaminant detection probability in heterogeneous aquifers and corrected risk analysis for remedial response delay"*, *Water Resources Research* 47(10), doi:10.1029/2011WR010652.

*Chapter 5* studies how the number of point sources, the size of the controlled area (landfill) and the quantity of an instantaneous aquifer injection pollution event affect detection of an instantaneous pollution into a two-dimensional aquifer by a monitoring network of wells. A two-dimensional stochastic model is utilized to perform numerical experiments. In each examined parameter it is considered that the rest of the factors affecting detection probability estimation remain constant. Simulations are performed in the context of uncertainty factors deriving from the environment itself, where the pollution is propagating, and the lack of information about certain parameters concerning the initial conditions of the leak.

In *Chapter 6* a two-dimensional stochastic model is developed in order to study, in terms of detection probability, the efficiency of linear groundwater pollution monitoring well networks, as pollution originates from a random point source inside a controlled area and is triggered by precipitation events. A thirty-year time series of daily average rain data has been used and linearly coupled with the pollutant mass diffused directly into the aquifer. The effects on successful pollution detection of the aquifer's hydro-geological parameters, as reflected in the field's hydraulic conductivity variance and dispersion coefficients, have been studied. In addition, the influence of the aquifer's sampling frequency and remedial action delay time is examined, referring to the detection probability that a monitoring well arrangement can succeed from the moment a successful detection has been recorded. Results are directly compared with these of instantaneous pollution simulated cases, as they have been studied in previous Chapters, considering the rest of the computational parameters common.

*Chapter 7* concludes the thesis with a summary of the main results and some recommendations for practical application and future research are proposed.

Thesis concludes with two Appendixes. In *Appendix A* the FORTRAN source code is listed for both cases of pollution duration that have been studied. In addition, STUBA listing is provided along with flow equations arithmetic solution subroutine. Finally, in *Appendix B* all the simulation numerical results are presented.

# CHAPTER 2

## Two-dimensions model structure

---

### 2.1 Introduction

Geological field observations at various scales have shown that both physical and chemical properties exhibit high spatial variability or, otherwise, heterogeneity. This is due to the fact that many of the characteristics of geological formations - such as cracks and voids containing the horizontal and vertical stratification, or the type and age of the rocks exhibit also great variability in space. Experimentally, for example, it has been found that the hydraulic conductivity of a geological field can vary between several orders of magnitude, with a discontinuous manner, thereby making its description in a deterministic way almost impossible (Gelhar et al., 1992).

Contaminant transport depends on the nature of the contaminant and the hydro-geological parameters that form an aquifer's flow field. In a steady flow, flow stream lines remain constant over time, while otherwise in transient cases they change, making the study of the problem much more difficult both on a physical level, in understanding the evolution of the same phenomenon, and for the computational requirements in order to achieve a numerical description of the flow. The aim, however, of this work is not the general study of heterogeneous aquifer transport phenomena, but the study of groundwater pollution detection probability by a monitoring wells network under conditions of uncertainty regarding environmental and operating parameters. For this reason, in order to simplify our problem, a steady flow will be considered.

Although in the present study two-dimensional (2-D) fields are utilized to simulate a plume's evolution and its detection, during the following paragraphs the case of three-dimensional (3-D) geological field equations are developed, in order for the presentation of

the equations in space to be considered complete. Although it can be said that the two-dimensional approach is not the most realistic description of the actual situation, it simplifies the computational problem, losing only the vertical information about the movement and the detection of plumes. Moreover, when the horizontal dimensions of an aquifer are much greater than its thickness, which is our case, then the results of two dimensions provide a good approximation of reality (Dagan, 1986; Dagan et al., 2009). On the other hand, running simulations in 2-D saves computational time. The reduction of the 3-D equations to 2-D is simply done by ignoring the factors of the third component.

## **2.2 Stochastic Approach**

Natural heterogeneity of aquifer materials provides the direct motivation to approach many groundwater problems in a probabilistic framework. As a consequence of the variable processes involved in the genesis of permeable earth materials, it seems that such complex heterogeneity will be omnipresent. The fundamental problem is how to deal with this heterogeneous reality as we attempt to develop quantitative descriptions of flow in large-scale aquifer systems. More specifically, engineers would like to know how to find appropriate average parameters which can be applied to large-scale flow models and, at the same time, how to be able to evaluate the influence of modeled heterogeneity on the quality of predictions from such models.

One approach to deal with the complex heterogeneity of natural aquifer materials would be to construct a detailed deterministic model which represents the actual heterogeneity of the aquifer. However, for realistic field problems, this degree of spatial resolution would require enormous computational resources and, more importantly, would be impractical in terms of the amount of data required to specify the actual complex three-dimensional heterogeneity. Furthermore, this level of detail in the output would be excessive in relation to predictive requirements for many applications.

Alternatively, the heterogeneity can be represented in terms of random hydraulic parameters characterized by a limited number of statistical parameters. These random parameters will then appear as coefficients in partial differential equations which express our classical laboratory-based physical understanding of the flow processes. Consequently, the resulting predictions are represented through probability distributions or, more realistically, in terms of statistical moments (Gelhar, 1986).

In a stochastic approach we attempt to gain useful information about the behavior of naturally heterogeneous systems by treating them as if the hydraulic parameters were random. More specifically, to represent the spatial structure, parameters such as hydraulic conductivity

$K$  can be viewed as random processes or spatial random fields. The spatial persistence of the random field of the hydraulic conductivity natural logarithm can be characterized in terms of the second moment, that is, the covariance between two different locations.

Carefully designed natural gradient field-scale tracer experiments have been conducted to study the movement of contaminants in heterogeneous aquifers with a high sampling resolution in space and time, from which stochastic theories have been partially validated at the Borden (Freyberg, 1986; Mackay et al., 1986; Woodbury & Sudicky, 1991; Farrell et al., 1994) and Cape Cod (LeBlanc et al., 1991; Hess et al., 1992) aquifers. These two aquifers are relatively homogeneous ( $\sigma_{\ln K}^2 \approx 0.2$ ) and the successful application of stochastic theories at these sites does not establish their validity in more heterogeneous aquifers (Fernández-García et al., 2005). The MADE (Boggs et al., 1992) field-scale tracer test was conducted in a substantially more heterogeneous aquifer ( $\sigma_{\ln K}^2 \approx 2.7$ ) but a spatial trend in hydraulic conductivity and nonuniform flows prevented the macrodispersivity from approaching a constant value (Adams & Gelhar, 1992). Thus the basic predictions of stochastic theories (effective conductivity and dispersion) could not be directly verified at the MADE site (Fernández-García et al., 2005).

The ergodic hypothesis which underlies the treatment of aquifer flows in a probabilistic sense is a fundamental admission. In simple terms, the ergodic hypothesis presumes that the behavior of a spatially averaged property of an aquifer is represented probabilistically by the ensemble average over a large number of realizations of aquifers having the same underlying statistical properties. For the spatial averaging process to be meaningful, the heterogeneities must be relatively small in terms of their spatial scale, as compared with the overall scale of observation. If there is this disparity in the scales, it should be possible to view larger-scale variations as deterministic trends around which there are more localized variations which can be viewed as stationary. The requirement for the result to be applicable is that the mean hydraulic gradient does not change significantly over a distance corresponding to the correlation scale of the head process (Gelhar, 1986).

### **2.3 Simulating Random Fields: Turning Bands**

The Turning Bands method is a simulation technique which was developed to create stationary, correlated, multi-dimensional Gaussian fields from a normal distribution with mean zero (0) and a specific covariance function. This method was first developed and applied by *Journel* (1974) and developed for the general case of the 2-D field by *Mantoglou*

and Wilson (1982) as Spectral Turning Bands method (STUBA), because of the use of a spectral method for line generation.

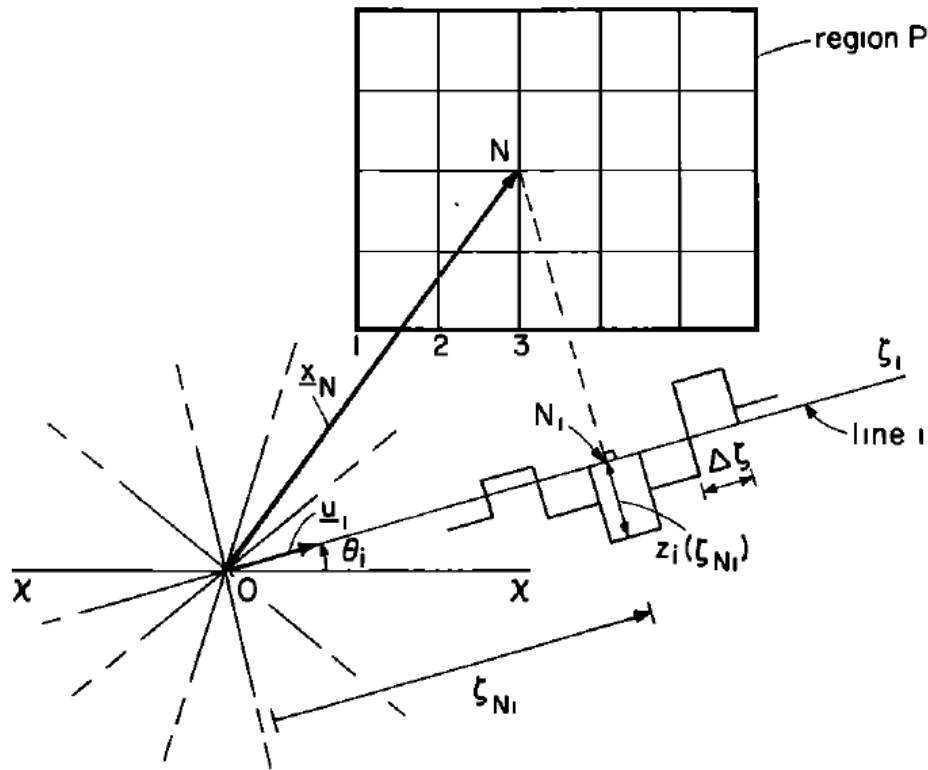


**Figure 2.1:** Turning Bands Mechanism (Mantoglou and Wilson,1982)

The Turning Bands method is based on the theory of multivariate stochastic processes. The basic idea of the method is converted into a multi-dimensional simulation of a sum of equivalent dimensional simulations. The operation of the algorithm is, in short, to create 2-D and 3-D fields by successively promoting and combining the values derived from the simulations of random numbers with a certain autocorrelation function along lines which are launched by a random point in space outside the scope. This technique has the effect of creating output random fields, which can simulate a hydraulic capacity of the studied, as is hydraulic conductivity. Although the random field was generated by specifying geostatistical parameters, estimates of these parameters from single realizations of the generated field are variable (Shafer & Varljen, 1990; Rehfeldt et al., 1992).

STUBA is an iterative method of two main steps. First, it creates a reflective process (random numbers) along a line given covariance function and mean value zero (0). Then, it creates an orthogonal projection of this line on each point of the simulated field matching, at this point, the value of the linear stochastic process. We consider a large number of lines which, however, have a common starting point, leading to the above procedure being repeated

several times (Figure 2.1). Visually this can be represented as areas that revolve around their common center. The final result for each point, which is the random number of stochastic processes implemented, is the weighted average of these projections.

Today there are two main ways for the production of one-dimensional stochastic processes along the lines. The first concerns the approximation of spatial areas (Space Domain) and can handle functions only with specific covariance. The second approach relates to the spectral region (Spectral Domain) and can handle a larger number of 2-D processes.

### 2.3.1 TBM Theoretical Background

We consider  $Z_i(u) = 1, 2, \dots, N$  a set of  $N$  independent implementations of a one-dimensional second order stationary stochastic process along a line, with autocorrelation function  $\rho_l(u_0)$ , where  $u_0$  is the spatial hysteresis on the line. The values we get from the relationship are:

$$Z_s(x, y, z) = \frac{1}{\sqrt{N}} \sum_{i=1}^N Z_i(u) \quad (2.1)$$

This is essentially the simulation of the random field, which is indicated by the index  $s$  (simulated). The field generated by this equation has a mean value equal to zero (0). The relationship between the autocorrelation function of the linear process  $\rho_l(u_0)$  and that of the three dimensional random field  $\rho(u_0)$  is given by *Mantoglou and Wilson* (1982), and *Mantoglou* (1987):

$$\rho_l(u_0) = \frac{d}{du_0} [u_0 \rho(u_0)] \quad (2.2)$$

while for a two-dimensional random field the relationship becomes:

$$\int_0^s \frac{\rho_l du_0}{\sqrt{(s^2 - u_0^2)}} = \frac{\pi}{2} \rho(s) \quad (2.3)$$

where  $s$  is spatial hysteresis. From Eq.(2.3) it is not easy to extract  $\rho_l(u_0)$  directly as a function of  $\rho(s)$ . For this reason, a spectral method has been created by *Mantoglou and Wilson* (1982) which extracts the autocorrelation function of the process along the lines of various autocorrelation functions of a two-dimensional field.

To create 2-D random fields it is required to solve the integral Eq. (2.3), which cannot readily be expressed as  $\rho_l = f(\rho(s))$ . To overcome this difficulty, an expression is created

that connects the spectral density function of the one-dimension process with the function of radial spectral density of the two-dimensional process used. This expression in Fourier space is given by:

$$S_i(\omega) = \frac{\sigma_Z^2}{2} S(\omega) \quad (2.4)$$

and connects  $S_i(\omega)$  with the product of  $S(\omega)$  over half of the variation of the two-dimensional process. The steps followed in the implementation of SSTUBA are outlined below.

### 2.3.2 Establishment of the One-dimensional Linear Process

There are two main techniques for the creation of the process lines. The first is the Fourier transformation (Fast Fourier Transformation), which can be used to give us the complex process,  $X(u) = Z(u) + iY(u)$ , which is given by *Tompson et al.* (1989) as:

$$X(u) = \int_{all\omega} e^{i\omega u} dW(\omega) \approx \sum_{all\omega} e^{i\omega_j u} dW(\omega_j) \quad (2.5)$$

where  $X$  is the sum of sinusoidal functions of complex sequences with different wavelengths, where each increases by a random complex of average size equal to zero (0). The second technique is called Normal Integration by Fourier (Standard Fourier Integration). According to this method, the real part of the complex process  $X(u)$  is given by:

$$\text{Re } X(u) = Z(u) = \int_{all\omega} |dW(\omega)| \cos(\omega u + \phi_\omega) \quad (2.6)$$

and can be directly used to create distinct approaches using positive frequencies:

$$Z_i(u) = \sum_{j=1}^M |dW(\omega_j)| \cos(\omega_j u + \phi_j) \quad (2.7)$$

where  $\phi_j$  are independent random angles with uniform distribution between 0 and  $2\pi$ ,  $M$  is the number of harmonics used in the simulation,  $\omega_j = (j - 0.5)\Delta\omega$ ,  $j = 1, 2, \dots, M$ ,  $\Delta\omega$  is the discretized frequency which is given by  $\omega_{\max}/M$ , and  $\omega_{\max}$  is the maximum frequency used in all calculations.  $|dW(\omega_j)|$  is calculated deterministically from the spectrum range as

$$|dW(\omega_j)| = [4S_i(\omega_j)\Delta\omega]^{1/2} \quad (2.8)$$

where  $S_i(\omega_j)$  is the spectral density function of the actual process  $Z(u)$  on the lines.

$S_i(\omega_j)$  is considered negligible outside the region  $[-\omega_{\max}, +\omega_{\max}]$ . Substituting (2.8) in (2.7) we obtain the generator function of the one-dimensional process on each line  $i$  as (Shinozuka & Jan, 1972):

$$Z_i(u) = 2 \sum_{j=1}^M \left[ S_i(\omega_j) \Delta\omega \right]^{1/2} \cos(\omega'_j u + \phi_j) \quad (2.9)$$

where  $\omega'_j = \omega_j + \delta\omega$ . Frequency  $\delta\omega$  is a small frequency range, uniformly distributed between  $-\Delta\omega'/2$  and  $\Delta\omega'/2$ , where  $\Delta\omega' = \Delta\omega/20$ , which is added in order for periodic phenomena to be avoided.

The approach of this methodology results in a discrete frequency  $\Delta\omega$  as the maximum cutoff frequency is  $\omega_{\max} = M\Delta\omega$ . This method requires more computational time than the FFT, but is much more flexible in the choice of parameter values  $M, \Delta\omega, \Delta u, \omega_{\max}$  and  $u_{\max}$  (Tompson et al., 1989).

### 2.3.3 Number and Distribution of Turning Bands

The theory of STUBA is based on the approach that we have an infinite number of rotating lines. Let us assume that the lines have random orientations, as resulting from a uniform distribution of a unit circle or sphere of a unit for the case of 2-D or 3-D fields, respectively. It has been shown (Mantoglou & Wilson, 1982) that if the lines are selected on the unit circle or on the unit sphere, with equal angles between them and with predetermined directions, then the autocorrelation function of the random field we try to simulate converges faster towards the theoretical form. Usually, a number of lines between eight (8) to sixteen (16) is a good choice for an isotropic autocorrelated function. In case an anisotropic situation is dealt with, it is necessary to select a larger number of lines.

### 2.3.4 Spectral Discretization and Random Fields Generation

The implementation process  $Z_i(u_n)$  on line  $i$  at the point  $n$  is done by integrating a series of discretized random components coming from the whole spectral range. Discretization factor of frequency  $\Delta\omega$  must be small enough to achieve an adequate degree of precision, while the number of harmonics  $M$  must be large enough to be counted as contributions of spectral edges at  $\omega_{\max} = M\Delta\omega$ . *Mantoglou and Wilson (1982)* have calculated that the values can vary between 50 and 100, while  $\omega_{\max}$  in each case was 40 times larger than the correlation length.

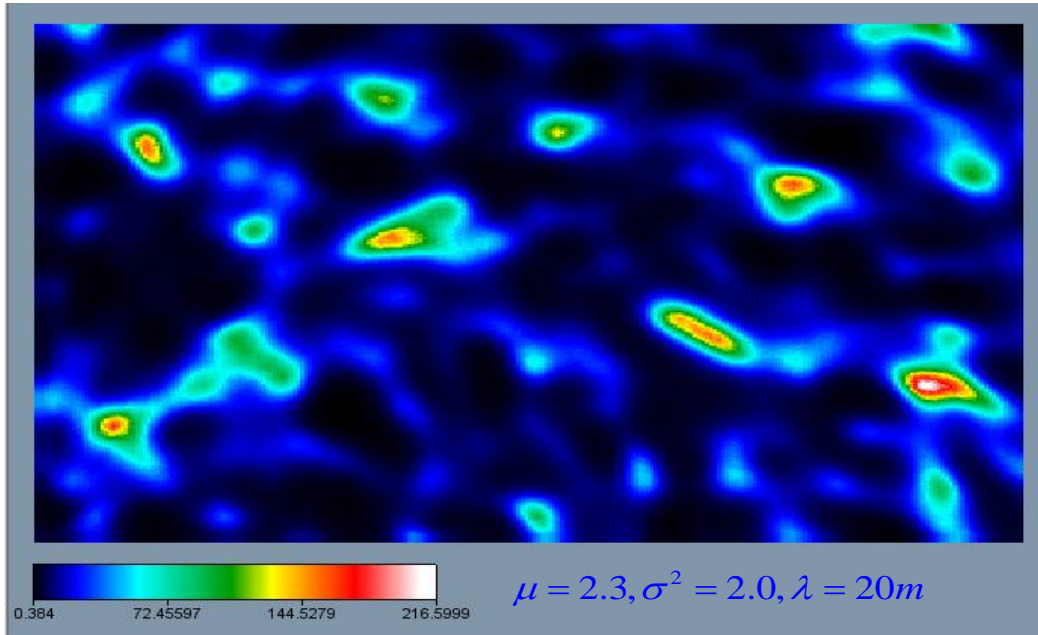


**Figure 2.2:** A 2-D hydraulic conductivity field generated by STUBA, where  $\mu_K = 2.3$ ,  $\sigma_{\ln K}^2 = 2.0$  and  $\lambda = 20m$ .

The length of the discretization  $\Delta u$  used on the lines should be chosen smaller than the respective lengths  $\Delta x, \Delta y$  of the simulated field. This is a more general rule that should be applied to avoid arithmetical errors during calculations (Mantoglou & Wilson, 1982). Additionally, the minimum length of the lines is defined by their orientation and the size of the field that we wish to simulate.

Generation of random fields  $Z_s(x, y, z)$  will ultimately derive from the entire selection of a finite number of lines  $L$  and their specified orientation, from the discretization of the single dimensional process  $Z_i(u)$  by assigning a random value on each discrete point  $n$  of each line, from the following orthogonal projection of these values on points  $x$  of the simulated field and, finally, by dividing the sum of the projections at each point by the factor  $L^{1/2}$  to obtain the final value (Elfeki, 1996) (

Figure 2.2).

## 2.4 Flow Equation

The equations which describe the flow of a permanent incompressible fluid through a porous material are the continuity equation of the mass:

$$\nabla \cdot \mathbf{q}(\mathbf{x}) = 0 \quad (2.10)$$

and Darcy Law:

$$q(\mathbf{x}) = -K(\mathbf{x})\nabla h \quad (2.11)$$

where  $x \in \mathbb{R}^3$ , where  $h[L]$  is hydraulic front,  $K(\mathbf{x}) [L/T]$  is hydraulic conductivity and  $B[L]$  is the aquifer's depth. Combining the above equations we get,

$$\nabla \cdot (K(\mathbf{x})\nabla h) = 0 \quad (2.12)$$

which in  $\mathbb{R}^3$  is written,

$$\frac{\partial}{\partial x} \left( K(\mathbf{x}) \frac{\partial h}{\partial x} \right) + \frac{\partial}{\partial y} \left( K(\mathbf{x}) \frac{\partial h}{\partial y} \right) + \frac{\partial}{\partial z} \left( K(\mathbf{x}) \frac{\partial h}{\partial z} \right) = 0 \quad (2.13)$$

The above partial differential equation describes the permanent groundwater flow in 3-D within the saturated zone of an isotropic, heterogeneous, porous material with a constant depth aquifer (Bear & Buchlin, 1987). The resolution, in conjunction with the boundary conditions specified for the particular model, gives values of the hydraulic front as distinct change in space within the heterogeneous saturated control volume.

We assume a 3-D dimensional elementary parallelepiped volume of dimensions  $L_x$ ,  $L_y$  and  $L_z$  which it simulates a heterogeneous, saturated aquifer (Figure 2.3). The reference axes of the system are oriented so that they coincide with the flow direction. The flow field is described by uniform hydraulic head difference in perpendicular planes to  $x$ -axis, which are applied at the boundaries 0 and  $L_x$  of the volume control. This results in the coincidence of the hydraulic gradient direction with that of the average flow. The boundary condition of zero flow is applied to the two remaining directions, i.e.  $\partial h / \partial y = 0$  and  $\partial h / \partial z = 0$ .

At the volume control that has been defined the flow equation is solved numerically, considering the hydraulic conductivity as a second order random function. The method used in this work is that of finite differences calculated at seven (7) adjacent points (Desbarats, 1992; Sarris, 1999), defined in the center of the elementary cubes of the lattice in which the parallelepiped is discretized. If, for example, the point  $(i, j, k)$  is considered, then that function value on it is calculated according to points  $(i+1, j, k)$ ,  $(i-1, j, k)$ ,  $(i, j+1, k)$ ,  $(i, j-1, k)$ ,  $(i, j, k+1)$  and  $(i, j, k-1)$ . The central scheme of the hydraulic head calculation was used in order the same volume to correspond to the hydraulic conductivity parameters, so

as each of them to acquire the same weight into arithmetic calculation of the differential flow equation.

The flow equation discretization into the centers of the elementary volumes, which are also called nodes of the grid, with dimensions  $D_x$ ,  $D_y$  and  $D_z$  is made by approaching the second and first derivatives with the differences of the hydraulic heads. By analyzing each term of the equation flow separately, it is for the direction of the  $x$  - axis ,

$$K \frac{\partial h}{\partial x} \approx K \left( i + \frac{1}{2}, j, k \right) \left[ \frac{h(i+1, j, k) - h(i, j, k)}{\Delta x} \right] \quad (2.14)$$

where  $K(i+1/2, j, k)$  is the value of hydraulic conductivity in the mid-space between nodes  $(i, j, k)$  and  $(i+1, j, k)$ , which is approximated with the harmonic mean of the two adjacent nodes in  $X$  direction and is given by,

$$K \left( i + \frac{1}{2}, j, k \right) = \frac{2K(i+1, j, k)K(i, j, k)}{K(i, j, k) + K(i+1, j, k)} \quad (2.15)$$

Similarly, we have for directions  $Y$  and  $Z$ ,

$$K \frac{\partial h}{\partial y} \approx K \left( i, j + \frac{1}{2}, k \right) \left[ \frac{h(i, j+1, k) - h(i, j, k)}{\Delta y} \right] \quad (2.16)$$

$$K \frac{\partial h}{\partial z} \approx K \left( i, j, k + \frac{1}{2} \right) \left[ \frac{h(i, j, k+1) - h(i, j, k)}{\Delta z} \right] \quad (2.17)$$

where  $K \left( i, j + \frac{1}{2}, k \right) = 2K(i, j+1, k)K(i, j, k) / K(i, j, k) + K(i, j+1, k)$  and

$$K \left( i, j, k + \frac{1}{2} \right) = 2K(i, j, k+1)K(i, j, k) / K(i, j, k) + K(i, j, k+1).$$

The above equation is discretized to

$$\begin{aligned}
& \frac{K\left(i+\frac{1}{2}, j, k\right)\left[\frac{h(i+1, j, k)-h(i, j, k)}{\Delta x}\right]-K\left(i-\frac{1}{2}, j, k\right)\left[\frac{h(i, j, k)-h(i-1, j, k)}{\Delta x}\right]}{\Delta x} + \\
& \frac{K\left(i, j+\frac{1}{2}, k\right)\left[\frac{h(i, j+1, k)-h(i, j, k)}{\Delta y}\right]-K\left(i, j-\frac{1}{2}, k\right)\left[\frac{h(i, j, k)-h(i, j-1, k)}{\Delta y}\right]}{\Delta y} + \\
& \frac{K\left(i, j, k+\frac{1}{2}\right)\left[\frac{h(i, j, k+1)-h(i, j, k)}{\Delta z}\right]-K\left(i, j, k-\frac{1}{2}\right)\left[\frac{h(i, j, k)-h(i, j, k-1)}{\Delta z}\right]}{\Delta z} = 0
\end{aligned} \tag{2.18}$$

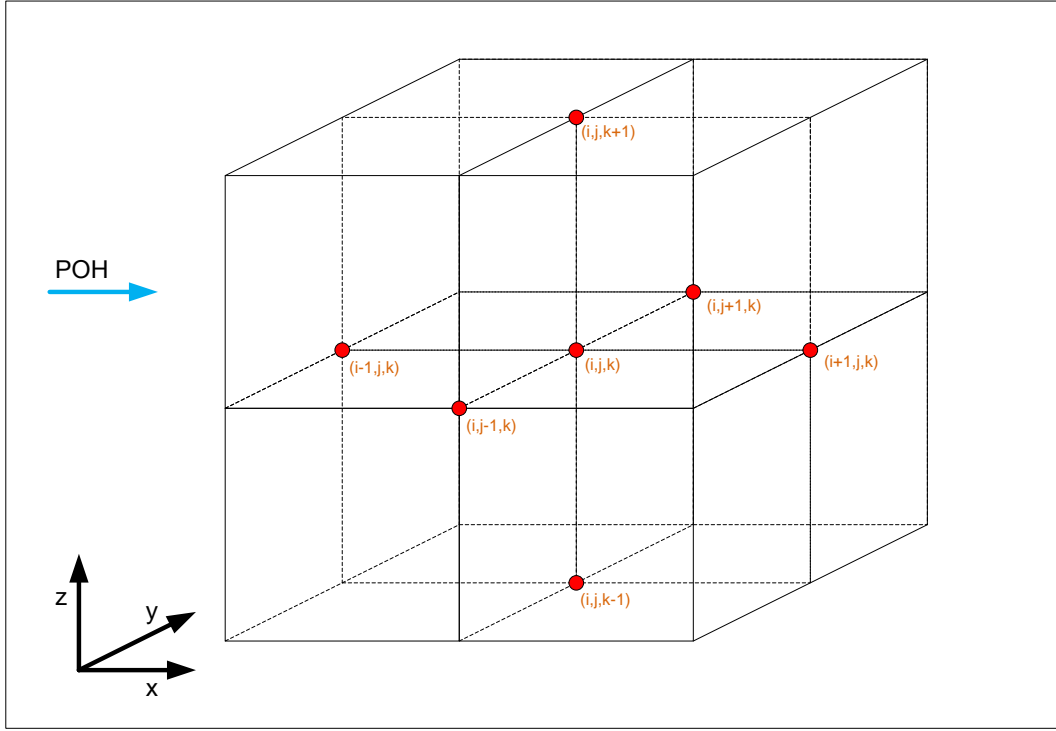


**Figure 2.3:** 3-D Field Discretization

We are forming and calculating, using the known values of hydraulic conductivity on each node, the terms below,

$$A(i, j, k) = K\left(i + \frac{1}{2}, j, k\right) / \Delta x^2 \quad (2.19)$$

$$B(i, j, k) = K\left(i, j + \frac{1}{2}, k\right) / \Delta y^2 \quad (2.20)$$

$$C(i, j, k) = K\left(i, j, k + \frac{1}{2}\right) / \Delta z^2 \quad (2.21)$$

$$D(i, j, k) = K\left(i - \frac{1}{2}, j, k\right) / \Delta x^2 \quad (2.22)$$

$$E(i, j, k) = K\left(i, j - \frac{1}{2}, k\right) / \Delta y^2 \quad (2.23)$$

$$F(i, j, k) = K\left(i, j, k - \frac{1}{2}\right) / \Delta z^2 \quad (2.24)$$

$$G(i, j, k) = A(i, j, k) + B(i, j, k) + C(i, j, k) + D(i, j, k) + E(i, j, k) + F(i, j, k) \quad (2.25)$$

Consequently, the three-dimensional approximation using the finite differences scheme of the flow equation is written as

$$\begin{aligned}
G(i, j, k)h(i, j, k) &= A(i, j, k)h\left(i + \frac{1}{2}, j, k\right) + B(i, j, k)h\left(i, j + \frac{1}{2}, k\right) + \\
C(i, j, k)h\left(i, j, k + \frac{1}{2}\right) &+ D(i, j, k)h\left(i - \frac{1}{2}, j, k\right) + E(i, j, k)h\left(i, j - \frac{1}{2}, k\right) + \\
+F(i, j, k)h\left(i, j, k - \frac{1}{2}\right) & \quad (2.26)
\end{aligned}$$

To solve the above equation we consider Dirichlet boundary conditions on X-axis, where we assume known values of hydraulic front at  $X=0$  and  $X=L_x$ . On Y-axis and Z-axis we consider Neumann boundary conditions, assuming no flow at the boundaries of  $Y=0$ ,  $Y=L_y$ ,  $Z=0$  and  $Z=L_z$ . Algebraic equations along with their boundary conditions are computationally solved, using the iterative scheme of Line Successive Over Relaxation Method (LSORM) (Young, 1954), whose source code was developed by *Desbarats* (1992) and adopted directly by the work of *Sarris* (1999). According to this arithmetic method, hydraulic head values on grid nodes are continuously updated until the difference between the last two successive values becomes less than a predefined limit, which in this case was set equal to  $10^{-5}$ . The final results of this computational process are hydraulic heads on every node  $h(i, j, k)$  of the simulated area's grid.

## 2.5 Velocity Field

Using Darcy's law velocity field components were calculated on each grid node. Velocities were calculated according to

$$\mathbf{u} = \frac{K_{xx}}{\varepsilon} \frac{\partial h(x, y, z)}{\partial x} \hat{u} + \frac{K_{yy}}{\varepsilon} \frac{\partial h(x, y, z)}{\partial y} \hat{v} + \frac{K_{zz}}{\varepsilon} \frac{\partial h(x, y, z)}{\partial z} \hat{k} \quad (2.27)$$

where  $\varepsilon$  is the field's effective porosity. Due to isotropy, it is  $K = K_{xx} = K_{yy} = K_{zz}$  and every component is calculated as

$$u_x = \frac{K}{\varepsilon} \frac{\partial h(x, y, z)}{\partial x}, \quad u_y = \frac{K}{\varepsilon} \frac{\partial h(x, y, z)}{\partial y} \quad \text{and} \quad u_z = \frac{K}{\varepsilon} \frac{\partial h(x, y, z)}{\partial z} \quad (2.28)$$

The partial derivative on each node  $i, j, k$  is given by the three-point approximation where

$$\frac{\partial h(x, y, z)}{\partial x} = \frac{h(x_{i+1}, y, z) - h(x_{i-1}, y, z)}{2\Delta x} \quad (2.29)$$

$$\frac{\partial h(x, y, z)}{\partial y} = \frac{h(x, y_{j+1}, z) - h(x, y_{j-1}, z)}{2\Delta y} \quad (2.30)$$

$$\frac{\partial h(x, y, z)}{\partial z} = \frac{h(x, y, z_{k+1}) - h(x, y, z_{k-1})}{2\Delta z} \quad (2.31)$$

where -1 and +1 indexes indicate hydraulic head on nodes before and after the node whose velocity components we want to calculate. At boundaries of the simulated area, where  $(x = 0, x = L_x)$  and  $(y = 0, y = L_y)$ , the difference between two adjacent nodes was used.

## 2.6 Conservation Hypothesis and Diffusion – Dispersion Equation

A basic assumption in this work is that pollution is caused by a single substance, which is chemically inert in the environment. In addition, no sorption occurs. This means that groundwater plume transportation and dispersion depend only on the speed of the flow field and the heterogeneity of the subsoil. Although this assumption is not realistic, it allows us to study the phenomenon of pollution transportation and monitoring system performance, only as a function of the heterogeneity of the subsoil. In fact, various pollutants during groundwater transportation are suffering biological processes (biodegradation) as well as chemical changes which, as a rule, slow down the flow of plumes without necessarily reducing their toxic effects (Rowe, 1995; Fatta et al., 1999; Renou et al., 2008). In the case of 3-D steady flow, the transport-diffusion can be written (Bear, 1988)

$$\begin{aligned} & \frac{\partial C}{\partial t} + v_x \frac{\partial C}{\partial x} + v_y \frac{\partial C}{\partial y} + v_z \frac{\partial C}{\partial z} - \frac{\partial}{\partial x} \left[ D_{xx} \frac{\partial C}{\partial x} + D_{xy} \frac{\partial C}{\partial y} + D_{xz} \frac{\partial C}{\partial z} \right] - \\ & - \frac{\partial}{\partial y} \left[ D_{yx} \frac{\partial C}{\partial x} + D_{yy} \frac{\partial C}{\partial y} + D_{yz} \frac{\partial C}{\partial z} \right] - \frac{\partial}{\partial z} \left[ D_{zx} \frac{\partial C}{\partial x} + D_{zy} \frac{\partial C}{\partial y} + D_{zz} \frac{\partial C}{\partial z} \right] = 0 \end{aligned} \quad (2.32)$$

where  $C$  is pollution concentration at time  $t$  at position  $(x, y, z)$ , and  $v_x, v_y, v_z$  are the measures of flow velocity components at directions  $x, y, z$  respectively. Factors  $D_{ij}$ , where  $i, j = 1, 2, 3$ , are components of the hydro – dispersion tensor and are given by (Bear, 1988; Feyen et al., 1998)

$$D_{i,j} = (a_T |v| + D_m) \delta_{ij} + (a_L - a_T) \frac{v_i v_j}{|v|} \quad (2.33)$$

where  $\delta_{ij}$  is Kronecker's operator,  $a_L [L]$  is the longitudinal dispersion coefficient,  $a_T [L]$  is the transverse dispersion coefficient,  $D_m$  the molecular diffusion coefficient and

$|v| = \sqrt{v_x^2 + v_y^2 + v_z^2}$  is the measure of groundwater flow velocity. Concentration  $C$  boundary conditions of the 2-D simulation is  $\partial C/\partial y(x,0,t) = 0$ ,  $\partial C/\partial y(x,L_y,t) = 0$  for every  $t \geq 0$  and  $C(x,y,0) = 0$  when  $0 \leq x \leq L_x, 0 \leq y \leq L_y$ .

## 2.7 Random Walk Tracking Particle

The Random Walk Tracking Particle (RWTP) method treats the transport of a solute mass via a large number of particles. It moves each particle through the porous medium using the velocity field obtained from the solution of the flow equation to simulate advection and adds a random displacement to simulate dispersion. This approach avoids solving the transport equation directly and therefore is virtually free of numerical dispersion and artificial oscillations (Salamon et al., 2006b).

RWTP is a method from Statistical Physics which has been used in the analysis of dispersion and diffusion processes in porous media. It was observed that particles accumulate in low permeability zones, resulting in unrealistic concentrations (Kinzelbach, 1987). This is due to the fact that a slight dissimilarity between the random walk equation, better known as the Fokker-Planck equation, and the advection-dispersion equation exists. In mildly heterogeneous systems, where groundwater flow velocity changes only slightly, this difference is negligible. However, in aquifers with a high variability in groundwater flow velocity, i.e. very heterogeneous hydraulic conductivity fields or areas with strong sink/source conditions, this difference gains importance, and a correction term to retrieve the advection-dispersion equation has to be included.

Mathematical formulation of RWTP begins with the transport equation of a conservative solute in an aquifer, which at the representative elemental volume scale is given by the following equation

$$\frac{\partial c}{\partial t} + \nabla \cdot (\mathbf{u}c) = \nabla \cdot (\mathbf{D}\nabla c) \quad (2.34)$$

where  $D$  is the dispersion coefficient tensor, usually denoted as

$$\mathbf{D} = (a_r |\mathbf{u}| + D_m) \mathbf{I} + (a_L - a_r) \frac{\mathbf{u}\mathbf{u}^t}{|\mathbf{u}|} \quad (2.35)$$

$c$  is the dissolved concentration,  $t$  is the time,  $a_L$  and  $a_r$  are the longitudinal and transverse dispersivity respectively,  $D_m$  is the molecular diffusion coefficient,  $u$  is the velocity vector obtained from the solution of the steady-state flow equation, and  $|u|$  is the magnitude of the

velocity vector. Here, porosity is assumed constant and velocity fluctuations are mainly attributed to a spatially varying hydraulic conductivity. This represents a second-order partial differential equation, which can be solved using an Eulerian approach by standard finite difference or finite element methods.

RWTP simulates solute transport by partitioning the solute mass into a large number of representative particles. The evolution of a particle in time is driven by a drift term that relates to the advective movement and a superposed Brownian motion responsible for dispersion. The displacement of a particle is written in its traditional form, given by the Itô -Taylor integration scheme (Gardiner, 1990)

$$\mathbf{X}_p(t + \Delta t) = \mathbf{X}_p(t) + \mathbf{A}(\mathbf{X}_p, t)\Delta t + \mathbf{B}(\mathbf{X}_p, t) \cdot \xi(t)\sqrt{\Delta t} \quad (2.36)$$

where  $\Delta t$  is the time step,  $\mathbf{X}_p(t)$  is the position of a particle at time  $t$ ,  $\mathbf{A}$  is a drift vector, the displacement matrix  $\mathbf{B}$  is a tensor defining the strength of dispersion and  $\xi(t)$  is a vector of independent, normally distributed random variables with zero mean and unit variance.

It has been demonstrated by Itô (1951) that the particle density distribution  $f(\mathbf{X}_p, t)$ , defined as the probability of finding a particle within a given interval  $[\mathbf{X}_p, \mathbf{X}_p + d\mathbf{X}_p]$  at a given time  $t$  and obtained from Eq.(2.36) fulfills, in the limit of large particle numbers and an infinitesimally small step size, the Fokker-Planck equation, which describes the motion of the particle density distribution  $f$ , and is given by

$$\frac{\partial f}{\partial t} + \nabla \cdot (\mathbf{u}f) = \nabla \nabla : (\mathbf{D}f) \quad (2.37)$$

where the colon refers to the outer product for multiplying two tensors and thus

$$\nabla \nabla : (\mathbf{D}f) \equiv \sum_{i=1}^n \sum_{j=1}^n \frac{\partial^2 D_{ij}}{\partial x_i \partial x_j} f \quad (2.38)$$

where  $n$  denotes the dimensions number.

Both the advection-dispersion and the Fokker-Planck equation are similar to each other as both are composed of an advection-drift term and a dispersion-diffusion term. In order, though, for an analogy to be established between them, Eq. (2.34) has to be modified as (Kinzelbach, 1987):

$$\frac{\partial c}{\partial t} + \nabla \cdot (\mathbf{u}c) + \nabla \cdot (c\nabla \cdot \mathbf{D}) = \nabla \nabla : (\mathbf{D}c) \quad (2.39)$$

Using a modified velocity term where

$$\mathbf{u}^* = \mathbf{u} + \nabla \cdot \mathbf{D} \quad (2.40)$$

it can be shown that the solute transport equation for heterogeneous porous media can be transformed into an equivalent of the Fokker-Planck equation (Itô's interpretation)

$$\frac{\partial c}{\partial t} + \nabla \cdot (\mathbf{u}^* c) = \nabla \nabla : (\mathbf{D} c) \quad (2.41)$$

Substituting the drift vector  $\mathbf{A}$  in Eq.(2.36), the RWTP final scheme is obtained,

$$\mathbf{X}_p(t + \Delta t) = \mathbf{X}_p(t) + (\mathbf{u}(\mathbf{X}_p, t) + \nabla \cdot \mathbf{D}(\mathbf{X}_p, t))\Delta t + \mathbf{B}(\mathbf{X}_p, t) \cdot \boldsymbol{\xi}(t)\sqrt{\Delta t} \quad (2.42)$$

where the displacement matrix  $\mathbf{B}$  is related to the dispersion tensor according to the relationship

$$2\mathbf{D} = \mathbf{B} \cdot \mathbf{B}^T \quad (2.43)$$

It must be noted that  $\mathbf{D}$  is defined in terms of  $u$  and not of  $u^*$ . For isotropic porous media the three-dimensional form of the displacement matrix  $\mathbf{B}$ , ignoring the molecular diffusion coefficient, can be expressed as (Tompson et al., 1987a)

$$\mathbf{B} = \begin{pmatrix} \frac{u_x}{|u|} \sqrt{2a_L |u|} & -\frac{u_x u_z}{|u| \sqrt{u_x^2 + u_y^2}} \sqrt{2a_T |u|} & -\frac{u_y}{\sqrt{u_x^2 + u_y^2}} \sqrt{2a_T |u|} \\ \frac{u_y}{|u|} \sqrt{2a_L |u|} & -\frac{u_y u_z}{|u| \sqrt{u_x^2 + u_y^2}} \sqrt{2a_T |u|} & \frac{u_x}{\sqrt{u_x^2 + u_y^2}} \sqrt{2a_T |u|} \\ \frac{u_z}{|u|} \sqrt{2a_L |u|} & \frac{\sqrt{u_x^2 + u_y^2}}{|u|} \sqrt{2a_T |u|} & 0 \end{pmatrix} \quad (2.44)$$

or in two dimensions

$$\mathbf{B} = \begin{pmatrix} \frac{u_x}{|u|} \sqrt{2a_L |u|} & -\frac{u_y}{\sqrt{u_x^2 + u_y^2}} \sqrt{2a_T |u|} \\ \frac{u_y}{|u|} \sqrt{2a_L |u|} & \frac{u_x}{\sqrt{u_x^2 + u_y^2}} \sqrt{2a_T |u|} \end{pmatrix} \quad (2.45)$$

The components  $\partial D_{ij} / \partial X_j$  can be evaluated using the general expression for  $D_{ij}$  (Uffink, 1990),

$$D_{i,j} = a_T |v| \delta_{ij} + (a_L - a_T) \frac{v_i v_j}{|v|} \quad (2.46)$$

which in matrix form in three dimensions is

$$D = \begin{pmatrix} a_T |u| + (a_L - a_T) \frac{u_x^2}{|u|} & (a_L - a_T) \frac{u_x u_y}{|u|} & (a_L - a_T) \frac{u_x u_z}{|u|} \\ (a_L - a_T) \frac{u_y u_x}{|u|} & a_T |u| + (a_L - a_T) \frac{u_y^2}{|u|} & (a_L - a_T) \frac{u_y u_z}{|u|} \\ (a_L - a_T) \frac{u_z u_x}{|u|} & (a_L - a_T) \frac{u_z u_y}{|u|} & a_T |u| + (a_L - a_T) \frac{u_z^2}{|u|} \end{pmatrix} \quad (2.47)$$

and its gradient is

$$\nabla \cdot \mathbf{D}(\mathbf{X}_p, t) = \begin{pmatrix} \frac{\partial D_{xx}}{\partial x} & \frac{\partial D_{xy}}{\partial x} & \frac{\partial D_{xz}}{\partial x} \\ \frac{\partial D_{yx}}{\partial y} & \frac{\partial D_{yy}}{\partial y} & \frac{\partial D_{yz}}{\partial y} \\ \frac{\partial D_{zx}}{\partial z} & \frac{\partial D_{zy}}{\partial z} & \frac{\partial D_{zz}}{\partial z} \end{pmatrix} \quad (2.48)$$

where every single component is written

$$\begin{aligned} \frac{\partial D_{xx}}{\partial x} &= \frac{(a_L u_x^3 + 2a_L u_x u_y^2 + 2a_L u_x u_z^2 - a_T u_x u_y^2 - a_T u_x u_z^2)}{|u|^3} \frac{\partial u_x}{\partial x} + \\ &\quad \frac{(2a_T u_x^2 u_y + a_T u_y^3 + a_T u_y u_z^2 - a_L u_x^2 u_y)}{|u|^3} \frac{\partial u_y}{\partial x} + \\ &\quad \frac{(2a_T u_x^2 u_z + a_T u_y^2 u_z + a_T u_z^3 - a_L u_x^2 u_z)}{|u|^3} \frac{\partial u_z}{\partial x} \end{aligned} \quad (2.49)$$

$$\begin{aligned} \frac{\partial D_{xy}}{\partial x} &= \frac{(a_L - a_T)(1 - u_x^2) u_y}{|u|^3} \frac{\partial u_x}{\partial x} + \frac{(a_L - a_T)(1 - u_y^2) u_x}{|u|^3} \frac{\partial u_y}{\partial x} - \\ &\quad \frac{(a_L - a_T) u_x u_y u_z}{|u|^3} \frac{\partial u_z}{\partial x} \end{aligned} \quad (2.50)$$

$$\begin{aligned} \frac{\partial D_{xz}}{\partial x} &= \frac{(a_L - a_T)(1 - u_x^2) u_z}{|u|^3} \frac{\partial u_x}{\partial x} - \frac{(a_L - a_T) u_x u_y u_z}{|u|^3} \frac{\partial u_y}{\partial x} + \\ &\quad \frac{(a_L - a_T)(1 - u_z^2) u_x}{|u|^3} \frac{\partial u_z}{\partial x} \end{aligned} \quad (2.51)$$

$$\begin{aligned} \frac{\partial D_{yx}}{\partial y} &= \frac{(a_L - a_T)(1 - u_x^2)u_y}{|u|^3} \frac{\partial u_x}{\partial y} + \frac{(a_L - a_T)(1 - u_y^2)u_x}{|u|^3} \frac{\partial u_y}{\partial y} - \\ &\quad \frac{(a_L - a_T)u_x u_y u_z}{|u|^3} \frac{\partial u_z}{\partial y} \end{aligned} \quad (2.52)$$

$$\begin{aligned} \frac{\partial D_{yy}}{\partial y} &= \frac{(a_T u_x^3 + 2a_T u_x u_y^2 + a_T u_x u_z^2 - a_L u_x u_y^2)}{|u|^3} \frac{\partial u_x}{\partial y} + \\ &\quad \frac{(2a_L u_x^2 u_y + a_L u_y^3 + 2a_L u_y u_z^2 - a_T u_x^2 u_y - a_T u_y u_z^2)}{|u|^3} \frac{\partial u_y}{\partial y} + \\ &\quad \frac{(a_T u_x^2 u_z + 2a_T u_y^2 u_z + a_T u_z^3 - a_L u_y^2 u_z)}{|u|^3} \frac{\partial u_z}{\partial y} \end{aligned} \quad (2.53)$$

$$\begin{aligned} \frac{\partial D_{yz}}{\partial y} &= -\frac{(a_L - a_T)u_x u_y u_z}{|u|^3} \frac{\partial u_x}{\partial y} + \frac{(a_L - a_T)(1 - u_y^2)u_z}{|u|^3} \frac{\partial u_y}{\partial y} + \\ &\quad \frac{(a_L - a_T)(1 - u_z^2)u_y}{|u|^3} \frac{\partial u_z}{\partial y} \end{aligned} \quad (2.54)$$

$$\begin{aligned} \frac{\partial D_{zx}}{\partial z} &= \frac{(a_L - a_T)(1 - u_x^2)u_z}{|u|^3} \frac{\partial u_x}{\partial z} - \frac{(a_L - a_T)u_x u_y u_z}{|u|^3} \frac{\partial u_y}{\partial z} + \\ &\quad \frac{(a_L - a_T)(1 - u_z^2)u_x}{|u|^3} \frac{\partial u_z}{\partial z} \end{aligned} \quad (2.55)$$

$$\begin{aligned} \frac{\partial D_{zy}}{\partial z} &= -\frac{(a_L - a_T)u_x u_y u_z}{|u|^3} \frac{\partial u_x}{\partial z} + \frac{(a_L - a_T)(1 - u_y^2)u_z}{|u|^3} \frac{\partial u_y}{\partial z} + \\ &\quad \frac{(a_L - a_T)(1 - u_z^2)u_y}{|u|^3} \frac{\partial u_z}{\partial z} \end{aligned} \quad (2.56)$$

$$\begin{aligned}
\frac{\partial D_{zz}}{\partial z} = & \frac{(a_T u_x^3 + a_T u_x u_y + 2a_T u_x u_z^2 - a_L u_x u_z^2)}{|u|^3} \frac{\partial u_x}{\partial z} + \\
& \frac{(a_T u_x^2 u_y + a_T u_y^3 + 2a_T u_y u_z^2 - a_L u_y u_z^2)}{|u|^3} \frac{\partial u_y}{\partial z} + \\
& \frac{(2a_L u_x^2 u_z + 2a_L u_y^2 u_z + a_L u_z^3 - a_T u_y^2 u_z - a_T u_x^2 u_z)}{|u|^3} \frac{\partial u_z}{\partial z}
\end{aligned} \tag{2.57}$$

Accordingly in two dimensions it is

$$D = \begin{pmatrix} a_T |u| + (a_L - a_T) \frac{u_x^2}{|u|} & (a_L - a_T) \frac{u_x u_y}{|u|} \\ (a_L - a_T) \frac{u_y u_x}{|u|} & a_T |u| + (a_L - a_T) \frac{u_y^2}{|u|} \end{pmatrix} \tag{2.58}$$

and its gradient is

$$\nabla \cdot \mathbf{D}(\mathbf{X}_p, t) = \begin{pmatrix} \frac{\partial D_{xx}}{\partial x} & \frac{\partial D_{xy}}{\partial x} \\ \frac{\partial D_{yx}}{\partial y} & \frac{\partial D_{yy}}{\partial y} \end{pmatrix} \tag{2.59}$$

where,

$$\frac{\partial D_{xx}}{\partial x} = \frac{(a_L u_x^3 + 2a_L u_x u_y^2 - a_T u_x u_y^2)}{|u|^3} \frac{\partial u_x}{\partial x} + \frac{(2a_T u_x^2 u_y + a_T u_y^3 - a_L u_x^2 u_y)}{|u|^3} \frac{\partial u_y}{\partial x} \tag{2.60}$$

$$\frac{\partial D_{xy}}{\partial x} = \frac{(a_L - a_T)(1 - u_x^2)u_y}{|u|^3} \frac{\partial u_x}{\partial x} + \frac{(a_L - a_T)(1 - u_y^2)u_x}{|u|^3} \frac{\partial u_y}{\partial x} \tag{2.61}$$

$$\frac{\partial D_{yx}}{\partial y} = \frac{(a_L - a_T)(1 - u_x^2)u_y}{|u|^3} \frac{\partial u_x}{\partial y} + \frac{(a_L - a_T)(1 - u_y^2)u_x}{|u|^3} \frac{\partial u_y}{\partial y} \tag{2.62}$$

$$\frac{\partial D_{yy}}{\partial y} = \frac{(a_T u_x^3 + 2a_T u_x u_y^2 - a_L u_x u_y^2)}{|u|^3} \frac{\partial u_x}{\partial y} + \frac{(2a_L u_x^2 u_y + a_L u_y^3 - a_T u_x^2 u_y)}{|u|^3} \frac{\partial u_y}{\partial y} \tag{2.63}$$

An extensive review of the method can be found in the work of *Tompson et al.* (1989), *Salamon et al.* (2006b), and *Delay et al.*(2005).

Numerical implementation of the random walk equations is relatively simple with one exception. When solving the flow equation using numerical methods, the resulting hydraulic heads and the associated velocity field are usually given as discrete point information. Yet,

simulation of solute transport by the random walk methodology requires continuous information of the velocity field. Therefore, a map of velocities from this discrete information has to be generated. This velocity map should fulfill the local fluid mass balance at any location and the local solute mass conservation at any grid-cell interface. In practice, this means that there is a need for a velocity interpolation scheme. The velocity interpolation approach addresses the problem of discontinuities in the dispersion tensor.

During the present study the bilinear interpolation scheme was used. In this approach the velocities are first linearly interpolated in one direction and then in the orthogonal direction using their neighboring grid-cells, so that velocities are obtained for each corner of the cell. The velocity at any point can then be calculated as a weighed average of these four velocities as is shown in Eq.(2.64) and Eq.(2.65). Approaching the cell interface of cells  $(i, j)$  and  $(i, j + 1)$  from either side, it results in a smooth transition of the velocity  $u_x$  and thus in an equal dispersive solute mass flux from either side,

$$u_x = (\Delta x - F_x)(\Delta_y - F_y)u_{x,(i-1/2,j-1/2)} + F_x(\Delta_y - F_y)u_{x,(i+1/2,j-1/2)} + (\Delta x - F_x)F_y u_{x,(i+1/2,j-1/2)} + F_x F_y u_{x,(i+1/2,j+1/2)} \quad (2.64)$$

$$u_y = (\Delta x - F_x)(\Delta_y - F_y)u_{y,(i-1/2,j-1/2)} + F_x(\Delta_y - F_y)u_{y,(i+1/2,j-1/2)} + (\Delta x - F_x)F_y u_{y,(i+1/2,j-1/2)} + F_x F_y u_{y,(i+1/2,j+1/2)} \quad (2.65)$$

## 2.8 Problem Uncertainties and Model Structure

The problem involves essentially five different factors of uncertainty: the natural variability of the geological field, the dispersion of pollution, the initiation point of pollution, the size of the source and the duration of the leak. Each of these factors will be addressed during simulations, either within a stochastic framework or a deterministic one, setting a baseline which will remain constant during each different study.

Hydraulic conductivity is one of the major uncertainties of the model (Gelhar, 1986; Gómez-Hernández & Gorelick, 1989; Gelhar et al., 1992; Harvey & Gorelick, 1995)(Yenigul, 2005). Available experimental evidence from studies in different geological areas has shown that hydraulic conductivity can be simulated by a stochastic process (Freeze, 1975; Gutjahr et al., 1978), which means that this parameter can be simulated by a random variable which, however, follows a specific probability distribution. Consequently, neighboring hydraulic conductivity values are statistically correlated. It has been seen in former surveys (Freeze, 1975; Gelhar, 1986; Sudicky, 1986) that hydraulic conductivity is better simulated as a function of logarithmic normal distribution (log-normal). Although there are several ways to

create random geological fields, such as the Sequential Gaussian simulation (Dimitrakopoulos & Luo, 2004) and geo-statistical technics such as kriging (Hoeksema & Kitanidis, 1985), the Spectral Turning Bands Method (STUBA), which is very fast computationally, was used to simulate the two-dimensional geological field.

Upon the time the pollutant enters the aquifer's flow field, it starts to move along the streamlines. In addition to this movement, there is another velocity component which comes from the diffusion and the dispersion of the pollutant inside the medium. There are a number of possible numerical approaches for solving the transport problem and simulating this kind of movement. In this study the Particle Tracking method based upon 'Random Walk' approach (Tompson et al., 1987a; Uffink, 1990; Yenigül et al., 2005; Salamon et al., 2006b; Salamon et al., 2006a; Yenigül et al., 2011) has been utilized. This choice is based on the algorithm's ease of implementation, its mass conservative nature and its computational effort economy, since it is independent from the control area we want to simulate. Sensitivity analysis to the number of the tracking particles used was conducted in order to better describe the contaminated plume transportation.

It is assumed that the start of a leak comes from a single point in the area of control and that all the quantity of leachate enters instantly into the aquifer's field of flow. This assumption holds true either for the instantaneous or for the precipitation triggered pollution case. It is also assumed that the only possibility of detection of underground contamination is through the wells of the monitoring system installation.

During each simulation a different, equally-probable point of the control area is selected, within its natural boundaries, as a starting point of pollution. In this way, the uncertainty of the starting point of pollution is simulated, as every point within a controlled area has the same potential, as any other point, to be the one where the pollution starts. It is considered that at the beginning of the simulation or, in the case precipitation triggered pollution, at the beginning of every simulated day the total concentration of the pollutant is injected into the flow field of the aquifer's saturated zone and thereafter starts to move and disperse.

## **2.9 Simulation Model**

### **2.9.1 Model Structure**

The basic assumption of the Monte Carlo simulation framework is that the hydraulic conductivity of a geological field can be simulated by random numbers, which have specific statistical moments (Freeze 1975). According to this method, a random number generator

function produces, via a particular process, hypothetical values of hydraulic conductivity of each point of the geological field that is to be simulated and which is required to be used in further calculations. These values are derived from a function with a given probability density, resulting in a certain distribution with a known mean and other statistical moments. By doing so, a geological field is created which simulates the real field about which hydraulic conductivity and its change are known in detail. The variogram of the field that is constructed, which captures the correlation of a point of the field with its neighbors according to the distance between them, is close to that of the real field. With this mechanism it is possible to "know" the heterogeneity of the hydro-geological environment. This process is repeated several times and each time it creates a different but equally probable geological field simulation. In each of these realizations the classical differential equations describing the respective problem can be solved to compute, for example, the flow field of a pollutant in the subsoil. From the total realization of the equally probable flux fields the statistical measures of the parameters of interest can be calculated, such as the hydraulic front, the speed of pollutants or the size and geometry of the created plumes. An illustrative way of how the Monte Carlo method works is depicted in Figure 2.4.

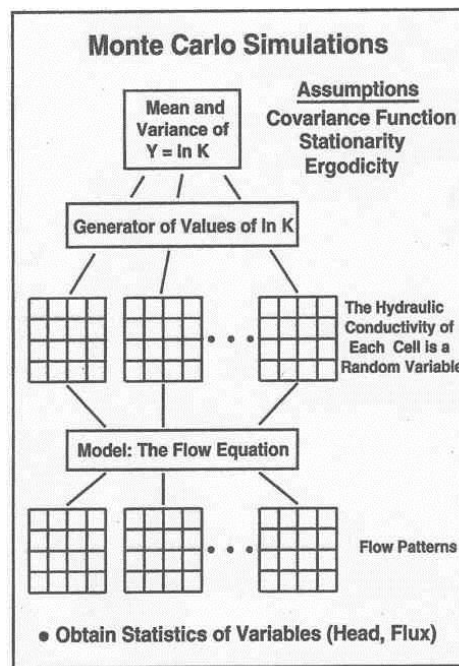


**Figure 2.4:** Operating principle of Monte Carlo method

This approach has the major advantage that it is relatively simple and easily applicable even to complex problems of three-dimensional hydro-geological environments. The only requirement is computing power. Of course, the rationale on which the operation of Monte Carlo stochastic modeling is established is that of ergodicity, which is axiomatically accepted. This enables us to assume that true values of the parameters of the geological field are

approximated, as they are statistically calculated using numerous fantastic realizations of the random fields.

According to this framework, a number of outputs of hydraulic conductivity fields is derived and the plume's detection from the specific arrangement of wells is evaluated separately in each of these realizations. The steps that the model follows are:

**Step 1:** A 2-D random hydraulic conductivity field is created using the STUBA. The field is 1000 m  $L_x$  long and 400 m  $L_y$  wide. Heterogeneity is expressed through the variance of hydraulic conductivity  $\sigma_{\ln K}^2$ , which varies between 0.0 (homogeneous field) and 2.0 (highly heterogeneous field), depending on the cases studied. Hydraulic conductivity logarithmic mean is constant and equal to 2.3 in all cases. Moreover, the correlation length  $\lambda$  of the field is considered to be equal to 20 m for both directions x and y (isotropic medium).

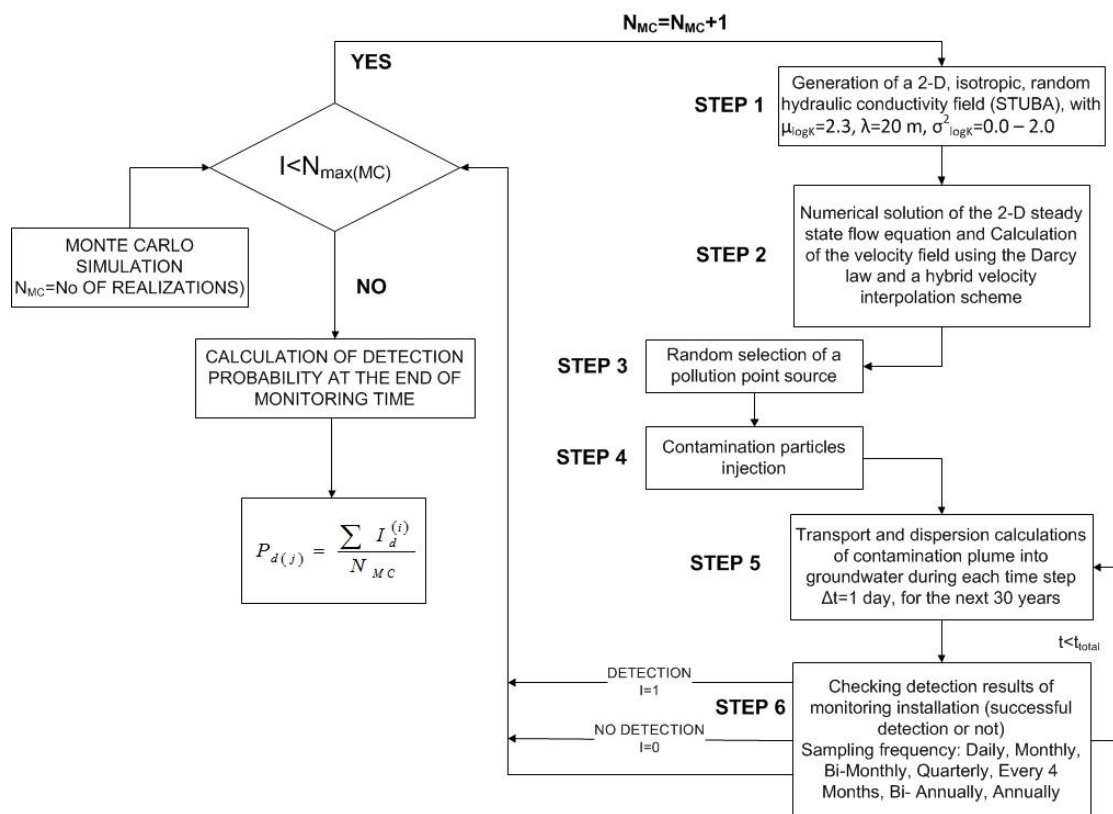


**Figure 2.5:** Instantaneous case pollution Monte Carlo simulation process diagram

**Step 2:** The hydraulic head field is calculated, numerically solving the partial differential equation describing the steady state flow of groundwater in two dimensions within the saturated zone of an isotropic, heterogeneous, porous medium with a fixed depth of aquifer Eq.(2.13) (Bear, 1988). The boundary conditions set for the model are constant

hydraulic pressure equal to 0.001 m between nodes perpendicular to the direction of flow and no-flow conditions at the lower and upper boundaries of the control area. The region was discretized setting  $\Delta x = \Delta y = 2m$ . Eq.(2.13) is numerically solved on each grid's node according to the method of seven point finite differences, using an algorithm that has been developed by *Desbarats* (1992). The calculation of velocity field on each node of the control area takes place using Darcy's law.

**Step 3:** A point is randomly selected inside the boundaries of the control area, which may be considered as a landfill cell, where the pollution is thought to have started. The landfill facility is assumed to be located between 50m and 100m in  $x - axis$  direction and 140m and 260m in  $y - axis$  direction.

**Step 4:** At instantaneous cases, the total mass of the pollutant injected into the aquifer is 1000gr, and the initial concentration of the contaminant is calculated equal to 4000 mgr/l, assuming effective porosity equal to 0.25. Threshold  $C_{TH}$  concentration that is detectable from monitoring wells is set to 0.35% (or 28 particles per cell) of the initial concentration. At the precipitation triggered pollution case, it was considered that if during a simulation time step a rainfall took place, then a certain quantity of pollution, proportional to the total rain height, would have been injected into the aquifer and diffused into the flow very rapidly, without disturbing groundwater flow. Threshold detection limit was also set at  $C_{Th} = 14\text{mgr/l}$ , which indicates the presence of chemicals into groundwater in such a degree that remediation actions should take place.

**Step 5:** Evolution of the contaminant plume is obtained by employing the Random Walk Particle algorithm, where several individual random movements of particles form a dispersing particle cloud characterizing the contaminant's mass distribution. Eq. (2.42) in two dimensions provides the displacement of each particle in every time step  $\Delta t$ . In all simulations at this survey the values of longitude and transverse dispersion coefficients,  $\alpha_L, \alpha_T$ , are interrelated through the  $\alpha_T = \alpha_L / 10$ . Different cases of dispersion have been studied, where  $\alpha_T$  varies between 0.001m for low dispersion subsoil and 0.50m for high dispersion cases.

**Step 6:** The contaminant's concentration has been monitored at each well, whether it is equal to or greater than the threshold concentration of detection. Because the solution of advection-dispersion transport equation by the Random Walk method provides discrete displacement of particles and not the concentration values themselves, a new grid similar to the one used for the solution of groundwater flow equations is

superimposed onto the control area, so as for particle density in each grid to be converted into concentrations. The average concentration in a grid cell  $(i, j)$ , with dimensions  $\Delta x$  and  $\Delta y$  in  $x$ -axis and  $y$ -axis directions respectively, is given by:

$$C_{ij}(t) = \frac{M_0 n_{ij}(t)}{Nnb\Delta x\Delta y} \quad (2.66)$$

where  $C_{ij}(t)$  is the volume average concentration in grid cell  $(i, j)$  at time  $t$ ,  $M_0$  is the total initial mass of the particles,  $n_{ij}(t)$  is the number of particles in grid cell  $(i, j)$ ,  $N$  is the total number of particles,  $n$  is effective porosity and  $b$  is the depth of the aquifer, considered equal to one. If contamination in any of the wells' configuration is

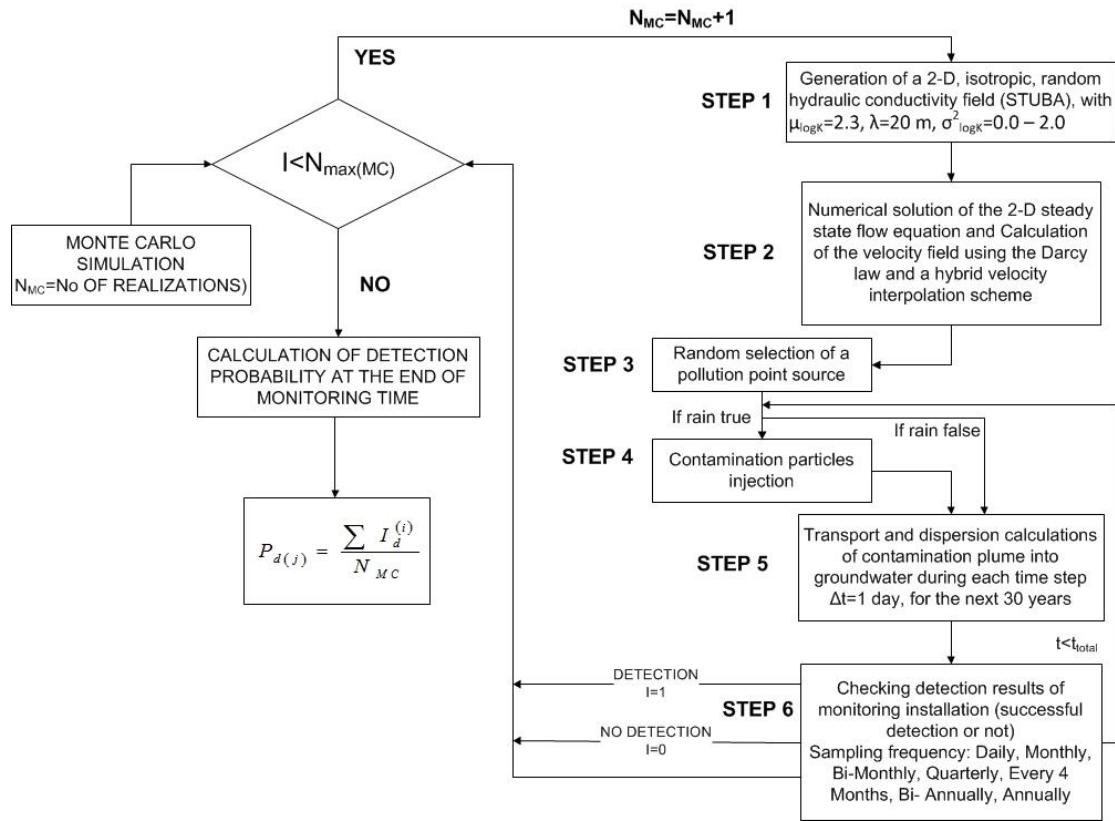


**Figure 2.6:** Precipitation triggered pollution case Monte Carlo simulation process diagram

detected at any time step during monitoring time, which is set to 30 years, a successful detection is logged as a unit value (1). If the total running time is less than the monitoring period and the examined case concerns the instantaneous pollution case, the process goes to STEP 5 (Figure 2.5). If it is the precipitation triggered pollution case examined and the total running time is less than the monitoring period, the process goes before STEP 4, where pollution is added if there is rainfall recorded

(Figure 2.6). If the total running time is equal to the monitoring period (30 years=10,950 days) and the number of total realizations is less than 3,000, the process goes to STEP 1 and restarts. Before that, if there is a successful detection, then its time is recorded and the total contaminated area is calculated. At the end of the 3,000 simulations, the average time of detection and the average contaminated area are calculated if daily (ED) sampling is assumed. Moreover, the average contaminated area is also calculated assuming different sampling frequencies, namely monthly (1 M), bimonthly (2 M), quarterly (3 M), every 4 months, biannual (6 M) and annual (A). The polluted area is additionally calculated every 3 months, every 6 months, once a year, every 2 years and every 3 years after successful detection, in order for remedial action delay time to be evaluated. If, on the other hand, there hasn't been any contamination detection, then at the end of the monitoring time a zero value (0) is logged and the process begins once more from Step 1. The average contaminated area is calculated in case of failure. The detection probability of the specific arrangement of monitoring wells is calculated by the ratio of simulations in which we have successfully detected the pollution to the total number of simulations, which is:

$$P_d = \frac{1}{N_{MC}} \sum_{i=1}^{N_{MC}} I_d^{(i)} \quad (2.67)$$

# CHAPTER 3

## **Instantaneous groundwater pollution detection probability in heterogeneous aquifers**

---

### **3.1 Introduction**

Successful detection of aquifer contamination via monitoring wells is a complicated problem with many factors, such as the heterogeneity of the geologic environment, the quantity and nature of the contaminants, the number and location of the monitoring wells, and the frequency of sampling, all contributing to the uncertainty of early detection. Detection of contaminants, of course, is of value if remedial actions follow as soon as possible, so that the volume of contaminated groundwater to be treated is minimized. The current article addresses these issues by investigating the case of instantaneous leakage from a landfill facility into a heterogeneous aquifer.

There are several factors that influence the likelihood of early detection of an aquifer's contamination by a landfill leak. Dispersion of the contaminants in heterogeneous geologic formations determines the spread and evolution of a plume. The stochastic Monte Carlo framework has been used to address the problem of optimizing the number and location of monitoring wells in heterogeneous aquifers (Hudak & Loaiciga, 1992; McLaughlin et al., 1993; Meyer et al., 1994; Storck et al., 1997; Bierkens, 2006; Salamon et al., 2006a) in order to determine the maximum detection probability or minimum contaminated area.

A second source of uncertainty arises from lack of knowledge about the leak itself. The location of the source, the quantities and chemical composition of the contaminants, and the time when a leak originated are questions with significant uncertainties involved. Simulation

studies (Meyer et al., 1994; Storck et al., 1997; Yenigül et al., 2005; Bierkens, 2006; Yenigul et al., 2006; Yenigül et al., 2011) usually assume conservative contaminants, with continuous or instantaneous leakages, and with the source's location randomly selected within a landfill's area.

The frequency of a sampling program that is implemented at a monitoring well system is another component that defines the likelihood or not of detecting contaminant concentrations above regulatory threshold values. The EU Directive 1999/31/EU on “the landfill of waste” states that sampling for monitoring purposes should be conducted “...*At a frequency to be determined by the competent authority and in any event at least once a year...*” The dependence of the probability of detection on the sampling frequency can be explained if one considers the sub-region of the plume characterized by concentrations, which are above the threshold regulatory limits. This sub-region changes, continually, in space and time, as a result of its advective and dispersive movement, and hence infrequent sampling may result in obtaining samples at wells that are used as regulatory check points when this critical part of the plume has already travelled elsewhere. Our article investigates the dependence of contaminant detection probabilities on aquifer heterogeneity and dispersion, as well as of the interaction between sampling frequency and monitoring well-arrangement.

Yet contaminant detection is of value if followed by quick remedial response. Indeed, most risk cost-analysis studies (Freeze et al., 1990; Bierkens, 2006; Yenigul et al., 2006), when analyzing the economic performance of different monitoring well systems assume that remedial actions are instantaneous, i.e., remediation activities commence exactly when detection is attained. According to this risk framework the contaminated groundwater volume at detection time is estimated; multiplied by the remediation cost per unit volume, and then this total remediation cost enters a decision analysis.

A different probabilistic risk analysis framework in subsurface contamination is proposed by (Tartakovsky, 2007), and (Bolster et al., 2009) where the probability of aquifer contamination is based on a rare event approximation and it depends on the probabilities of the system's constitutive parts (natural attenuation and remediation) failing.

Practically, there is always a time lag between contaminant detection and remedial action response. The EU directive 1999/31/EU on “*the landfill of waste,*” for example, states that landfill operators should notify competent authorities first of any significant adverse environmental effects revealed by the monitoring procedures, and then follow the authorities' decision on the nature and timing of the corrective measures. Considering the time needed for administrative decisions and for arrangements with local contractors in order to initiate remedial procedures introduces a time lag between detection and remediation time. During

this time lag a plume continues to move into an aquifer contaminating larger groundwater volumes.

The effect of this time lag, named as remedial action response delay by us, on the outcome of decision analyses is investigated in this study. Our article provides a novel framework to modify traditional risk analyses by supplying corrected detection probabilities that account for delays in remedial actions. In our approach the weights that detection probabilities provide onto remediation costs in traditional decision analyses are downgraded the further away a remedial response has moved from the time of detection. Correspondingly, the weights applied on failure costs are increased, effectively penalizing delayed remedial actions.

### **3.2 Model Description**

Our study involved the stochastic simulation of groundwater flow and contaminant transport in heterogeneous aquifers of horizontal dimensions much greater than their thickness (Meyer et al., 1994; Yenigül et al., 2005; Yenigül et al., 2011). The wells were assumed to fully penetrate the aquifer resulting in vertically-averaged concentration measurements.

The physical problem at hand involves five sources of uncertainty: The heterogeneity of the two-dimensional geologic field, the dispersion of the contaminant, and the initiation point, size, and duration of a leak. The contaminant was assumed to be conservative, and fully water soluble.

The heterogeneity of the geologic environment was addressed through the hydraulic conductivity, which was simulated as a log-normal, stationary, second order, isotropic stochastic process (Gelhar, 1986; Sudicky, 1986; Elfeki, 1996) using the Spectral Turning Bands Method (STUBA) (Mantoglou & Wilson, 1982; Brooker, 1985; Mantoglou, 1987; Tompson et al., 1987a). The second source of uncertainty arises from the way a pollutant is transported into the subsurface heterogeneous environment. Upon entering an aquifer's flow field, a pollutant starts not only to move along the streamlines, but in addition to diffuse and disperse into the geologic medium. The particle tracking method based on the 'random walk' approach (Ahlstrom et al., 1977; Prickett et al., 1981; Kinzelbach, 1987; Tompson et al., 1987b; Tompson & Gelhar, 1990b; Uffink, 1990; Zimmermann et al., 2001; Hassan & Mohamed, 2003; Delay et al., 2005b; Salamon et al., 2006b; Salamon et al., 2006a) was adopted to simulate a plume's advective and dispersive movement. Our choice of algorithm was based on its ease of implementation, its mass conservative nature, its numerical dispersion-free characteristic and its computational economy.

The contaminant was assumed to be conservative and water soluble. While, some contaminants are conservative (e.g. chloride), (Fatta et al., 1999), the majority are prone to biological and chemical transformations that tend to alter the transport rate and lead to concentration reduction (Renou et al., 2008). Although a plume's evolution is determined by the contaminants' chemical characteristics and the site-specific physical, chemical, and biological conditions - for example, the existence of low permeability zones that may lead to fingering and the creation of diffusion-dominated 'hot spots' (*National Academies*, 1994), or the development of geochemical conditions that may activate natural source contaminant production (for example, chromium from ophiolites) (Izbicki et al., 2008), etc. - the assumption of a conservative contaminant is useful in order isolate the impact on the detection probability of sampling frequency and remedial action delay in heterogeneous subsurface environments.

Other sources of uncertainty relate to the location and areal extent of a leak, together with the quantity and duration of contaminant release. In this study it is assumed that any point in the landfill can be a potential source of leakage, taking place once, and resulting in an instantaneous ejection of contaminants into an aquifer.

Initial leakage from a landfill is usually due to holes and tears in geo-membranes because of poor waste deposition or membrane ageing, and resulting in embrittlement, stress cracking, and chemical erosion near welded seams (Lee & Jones-Lee, 1994; Allen, 2001). Most of these failures are distinct and usually of very small dimensions leading to one or multiple point sources of contamination. Thus, (Collucci et al., 1999) have reported that two holes, each 5cm×3cm, and a crack of 63cm×31cm were the source of leachate leakage from a municipal solid waste landfill in northern Italy, whereas (Laine et al., 1997) reported, through an electrical leak imaging method (ELIM), leakage from two 80mm-long cuts at an active landfill. In addition, at several waste disposal facilities with natural clay bottom barriers, leakages may be caused by deposition of fluid containers over cracks or failure zones of small areal extent. Consequently, we have assumed that the size of the leakage source is a single point inside the landfill area, representing a worst case scenario in terms of detection because the plume to be formed will be very narrow and difficult to detect (Meyer et al., 1994; Allen, 2001; Hudak, 2005).

The case of an instantaneous leak refers physically to a sudden discharge of leachate into the aquifer as a result of high hydraulic head, which might have built up on the liner due to continuous or localized leachate presence (Koerner & Soong, 2000), in conjunction with the development of a crack or tear at a weak area of the bottom liner. A high hydraulic head may develop due to clogging of the leachate collection and drainage pipeline system (Koerner & Koerner, 1995), or due to large precipitation fluctuations, which in turn may cause

excessive water percolation through the wastes (Collucci et al., 1999; Fatta et al., 1999; Tatsi & Zouboulis, 2002). Numerically, instantaneous ejections can be considered leaks whose duration is less than the modeling time step  $\Delta t$  that is used in the transport of contaminants, set here equal to one day.

The contribution of the unsaturated zone in the contaminant's movement and dispersion was neglected. In the unsaturated zone, flows are gravity driven and thus are primarily vertical, with the saturated-zone transport presenting perhaps the greatest opportunity for a contaminant to travel large distances (Academies, 1994). Cases where ignoring the influence of the unsaturated zone may be a valid approximation include those when the water table is relatively close to the bottom of the facility and contaminants move vertically towards the aquifer (Meyer et al., 1994; Çelik et al., 2009); when there is a highly permeable vadose zone or non-stratified deposits between a point source and the aquifer (Hudak, 2005), or when there is fingered flow, which significantly increases the vertical pore water velocity leading to rapid discharge of contaminant into the saturated zone (Selker et al., 1996).

Seven linear configurations of monitoring installations were examined consisting of 1, 2, 3, 4, 6, 12 and 20 wells, equally spaced from each other. Wells that were located at the ends of each arrangement were placed half the distance from the landfill's top and bottom edges so that the efficiency of the monitoring system would be maximized (Yenigül et al., 2005). The distance,  $d$ , of the monitoring installations from the landfill's trailing edge was normalized with respect to the landfill's width,  $L$ .

The procedure for the Monte Carlo simulations was as follows:

2-D random hydraulic conductivity fields were created by STUBA (Mantoglou & Wilson, 1982) for a flow field 1,000m long and 400m wide. The variance of the log hydraulic conductivity varied from 0.0 (homogeneous aquifer) to 2.0 (strongly heterogeneous aquifer), while the mean of the log hydraulic conductivity was taken to be equal to 2.3. The correlation length,  $\lambda$ , was considered constant and equal to 20 m for both directions  $X$  and  $Y$  (isotropic medium).

Numerical calculations of steady state two-dimensional groundwater flow were based on a finite difference 7-point scheme (Sarris & Paleologos, 2004), with the velocity on each grid node calculated by Darcy's law. Continuous velocity values inside the domain were calculated using a bilinear interpolation scheme (Salamon et al., 2006b).

A rectangular landfill facility was located between  $x$ -coordinates of 10m and 60m, and  $y$ -coordinates of 140m and 260m (Figure 3.1). A point was selected randomly inside the

landfill as the starting point of pollution. The total pollutant mass was equal to 1,000gr, simulated by 2,000 or 8,000 discrete particles (depending on the case investigated). The initial concentration of the point source,  $C_0 = M_0 / (nV_0)$ , was 4,000mgr/lt, where  $M_0$  the initial mass,  $n = 0.25$  the effective porosity, and  $V_0 = 1\text{m}^3$ . The threshold concentration  $C_{TH}$ , which was detectable from the monitoring wells, was set at 0.35% of the initial concentration. This corresponds to a level of critical contamination from nitrate, cyclohexanon, or diethyleneglycol, which would require remedial procedures (Yenigül et al., 2005).

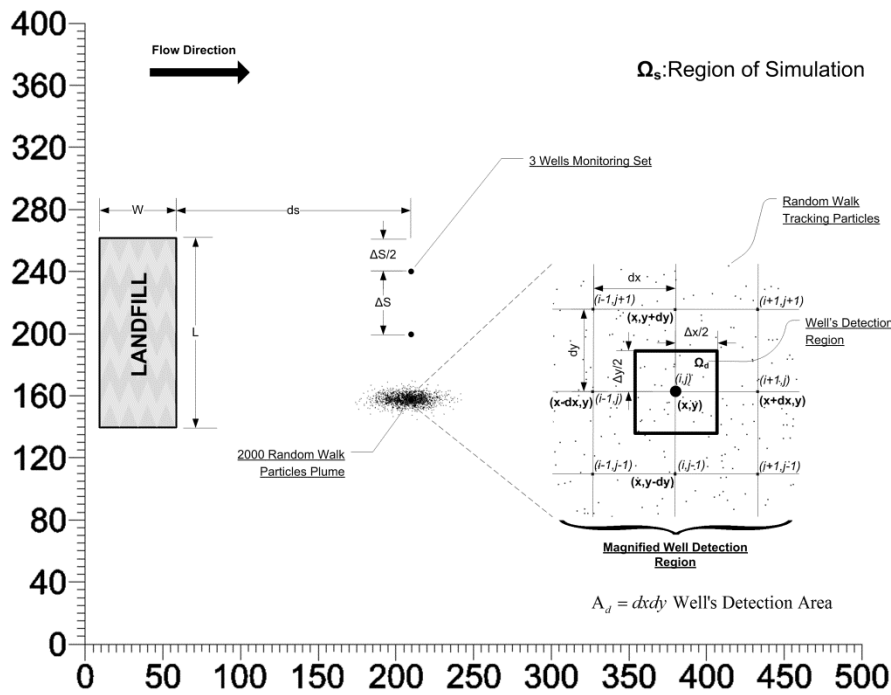


**Figure 3.1** : Section of simulated flow field with a rectangular landfill  $W \times L$ , a 2000 particles plume, and a magnified well-detection area

Evolution of the plume was simulated via the random walk particle tracking algorithm. A brief overview of particle displacement equations can be found in the work of (Salamon et al., 2006b) and in the more extensive work of (Tompson et al., 1987a). For each geologic field reproduced by STUBA different transverse dispersion coefficients,  $a_T$ , were examined, varying between  $0.001m$  and  $0.5m$ . The longitudinal dispersion coefficient,  $a_L$ , was calculated by the relation  $a_L = 10a_T$  (Spitz & Moreno, 1996; Cirpka & Kitanidis, 2001).

For each dispersion case different linear arrangements of monitoring wells were examined, each time step utilizing various frequency sampling policies: on-line (every day), once every two, three, four, six and twelve months. If the contaminant's concentration at any monitoring well of a specific well arrangement was found equal to, or greater than the

threshold concentration, then detection was considered to have been achieved. Because the random walk particle method provides discrete particle displacements and not the concentration values themselves, the particle density found in each computational cell was converted to a concentration value with the use of a mesh similar to the one used for the solution of groundwater flow equation. The average concentration in a grid cell  $(i, j)$  with dimensions  $\Delta x = \Delta y = 2$  m in the  $x$ - and  $y$ -directions, respectively, is given by

$$C_{ij}(t) = \frac{M_0 n_{ij}(t)}{Nnb\Delta x\Delta y} \quad (3.1)$$

Here  $C_{ij}(t)$  is the volume averaged concentration in a grid cell  $(i, j)$  at time  $t$ ,  $M_0$  is the total initial mass of the contaminants,  $n_{ij}(t)$  is the number of particles found inside a cell  $(i, j)$ ,  $N$  is the total number of particles,  $n$  is the porosity, and  $b$  is the depth of the aquifer taken equal to unit. If a value of concentration was found, in any one of the wells of a specific arrangement, to equal or exceed the threshold value  $C_{TH}$  at any time step, during the 30-year monitoring period, then, successful detection was considered to have been attained and was given in any simulation  $i$  the value  $I_{det}^{(i)} = 1$ , otherwise it took the value of 0.

The detection probability of a specific arrangement of monitoring wells was calculated as the ratio of simulations where successful detection was attained over the total number of simulations,  $N_{MC}$ , and was expressed as

$$P_d = \frac{1}{N_{MC}} \sum_{i=1}^{N_{MC}} I_{det}^{(i)} \quad (3.2)$$

If contamination was detected, then the total polluted area was calculated at the moment of detection. This calculation was repeated again 3, 6, 12, 24 and 36 months after the initial detection, in order to record the evolution of the plume. In case where no successful detection was accomplished the total contaminated area was calculated at the end of the 30-year monitoring period.

### 3.3 Number of Simulations and Tracking Particles

One of the computational shortcomings of Monte Carlo stochastic simulations is that the accuracy of the results depends on the number of realizations utilized. Although many stochastic numerical studies have shown (Storck et al., 1997; Sarris & Paleologos, 2004; Yenigül et al., 2005) that, in many cases, approximately 500 simulations may be sufficient for

results to converge to a constant value, the calculations to estimate detection probabilities of monitoring systems have practical use as entries in decision-making analyses. There, the detection probability is multiplied by remediation costs, and hence an error in the value of  $P_d$ , from the constant value that is attained at a higher number of simulations, may affect the outcome of a decision.

Figure 3.2 plots the dependence of the detection probability on the number of Monte Carlo simulations for three different cases of well arrangements, levels of heterogeneity, and dispersion of the plume. This figure indicates that convergence of  $P_d$  is attained at about 3,000 simulations, with the average difference from the value of  $P_d$  returned from 500 simulations being approximately 4%. In all subsequent calculations of our study the number of 3,000 realizations was used for all cases of hydro-geologic investigation. Alternatively, one could consider that the flow and transport calculations could be performed with a smaller number of simulations and at the decision level a sensitivity analysis could be conducted on the effect on the results by small perturbations of the value of the detection probability.

Our study investigated numerically the effect of the number of particles, used to simulate a plume of total mass  $M$ , on the detection probability. The particle tracking method assigns the solute mass of the contaminants to a group of  $N$  particles having identical, unchanging amounts of mass, and free to move independently in time. A particle in each time step is displaced in two ways: the first motion involves movement along a streamline, while the second is a random displacement, whose direction and magnitude are chosen so that the overall distribution of the cloud of particles reproduces the desired concentration. Because of the need to use a large number of particles in order to obtain consistent and reliable results of contaminant concentration there exists a strong dependence of the calculated values of  $P_d$  on the total number of particles used in the simulations. On the other hand, the computational effort, per time step, is proportional to the number of particles used, making the optimization of  $N$  necessary.

Contaminant concentration by the method of particle tracking is calculated by measuring the number of particles found in each grid cell of area  $A_d$  (Figure 3.1) and applying Equation (3.1). Consequently, contrary to the space-and-time continuous concentrations that are provided by analytical methods, the particle tracking method provides discrete values of concentrations  $C(A_d t)$  - in the form of step functions - to adjacent grid cells. The discrepancy between the concentration distribution obtained via the random walk tracking particle and the analytical solution, averaged over cell area  $A_d$ , can be quantified

through the total square error of the concentration over the flow domain  $\Omega_s$  (Figure 3.1), given by (Ahlstrom et al., 1977; Kinzelbach, 1987; Tompson et al., 1987a)

$$\varepsilon^2 = \frac{(M/n)^2}{NA_d} \quad (3.3)$$

This result is a global measure of the error in concentration over  $\Omega_s$  and shows that a factor of two reduction in the global error can be accomplished either by a four-fold increase in the number of particles  $N$  or an equivalent increase in the sampling region  $\Omega_d$  from which concentrations are estimated (Tompson et al., 1987a). Since in our case  $\Omega_d$  was set equal to  $A_d$  (Figure 3.1), which was derived from the finite difference mesh, improvement in  $\varepsilon^2$  is conditioned on an increase in the number of tracking particles. (Kinzelbach, 1987) has reported that in his numerical experiments an increase in the number of particle  $N$  did not lead to an improvement in  $\varepsilon^2$  as described by Eq. (3.3).

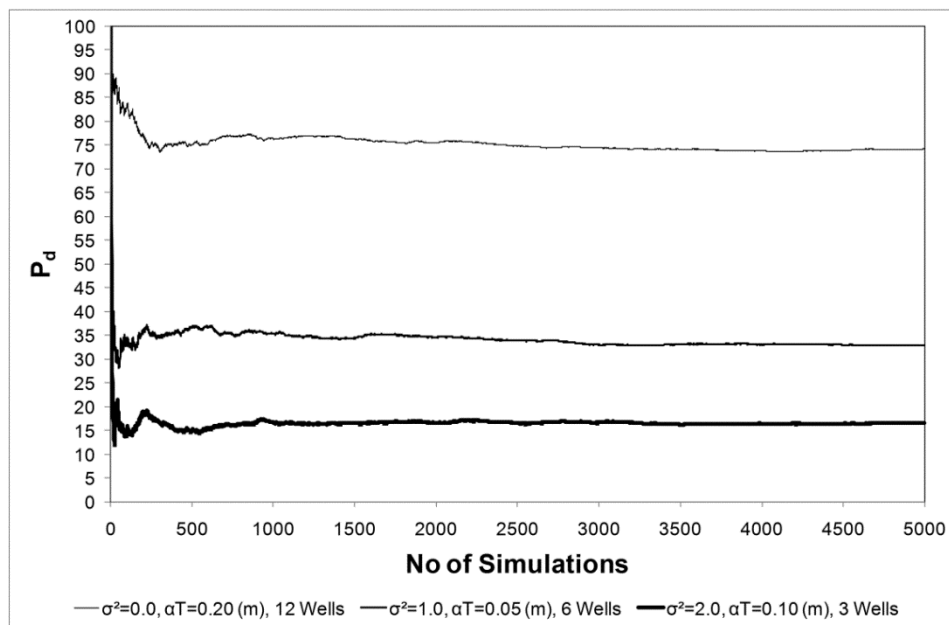


**Figure 3.2:** Detection probability  $P_d$  versus number of Monte Carlo simulations for 3 cases of well arrangement, heterogeneity, and dispersion

*Yenigül et al.* (2011) defined the theoretical detection probability  $P_{d(TH)}$  for a single well, in a homogeneous medium and for an instantaneous release, as the ratio of the maximum width  $2l$  of the plume at time  $t$  to the width of a landfill  $L$ . These authors found that,

$$P_{d(TH)} = \frac{2l}{L}, \text{ when } y_w - l > y_c - \frac{L}{2} \text{ or } y_w + l < y_c + \frac{L}{2}, \quad (3.4)$$

where  $y_c$  is the  $y$ -coordinate of the landfill's center line, and  $y_w$  is the  $y$ -coordinate of the well. When the well is close to the upper or lower boundary of the landfill  $P_{d(TH)}$  is given by

$$P_{d(TH)} = \frac{l + L/2 - y_w + y_c}{L}, \text{ if } y_w + l > y_c + \frac{L}{2}, \quad (3.5)$$

or

$$P_{d(TH)} = \frac{l + L/2 - y_c + y_w}{L}, \text{ if } y_w - l < y_c - \frac{L}{2} \quad (3.6)$$

respectively.

Based on the above equations the total  $P_{d(TH)}$  for the case of multiple, equally spaced, wells, arranged linearly was formulated by us as the sum of the detection probability of each individual well. When the maximum width of the plume extended over more than half the distance  $d$  between the wells the total width of the landfill was covered, yielding  $P_{d(TH)} = 1$ .

In every other case ( $2l < d$ )  $P_{d(TH)}$  was calculated to be

$$P_{d(TH)} = n \frac{2l}{L} \quad (3.7)$$

Figure 3.3 depicts the theoretical  $P_{d(TH)}$  and the numerical  $P_d$  for five different wells arrangements (1, 3, 6, 12 and 20 wells) against the  $\log_{10} N$ , where the number of tracking particles  $N$  took the values of 500, 1000, 2000, 4000, 8000, 16000, 32000, 64000, 128000, 256000, and 512000. The results were obtained for a homogeneous field with  $a_r = 0.10a_L$ ; the monitoring set was located at a distance  $d = 0.125L = 15$  m (where maximum detection was attained), and the maximum plume's half width was calculated to be  $l = 3.085$  m (Yenigül et al., 2011). The threshold number of particles inside a well, in order to attain detection, was adjusted so that the detection concentration limit remained constant at  $0.35\% \cdot C_0$ . Figure 3.3 indicates that as the number of particles increases, the numerical detection probability  $P_d$  converges to the theoretical value  $P_{d(TH)}$ , with  $P_d$  becoming almost equal to the theoretical value when 64,000 or more particles are used. When only one well is considered then even 8,000 particles appear to be sufficient for  $P_d$  to converge to  $P_{d(TH)}$ .

Yenigul *et al.* (2011) performed a sensitivity analysis of the approximation provided by particles ranging from 500 to 8,000 to the analytical plume's concentrations in a homogeneous and heterogeneous field. This author concluded that 2,000 particles provide a satisfactory tradeoff between accuracy and computational cost for the calculation of concentration in these flow fields. For the detection probability, however, she concluded that this number of particles resulted in values greater than the analytical ones.

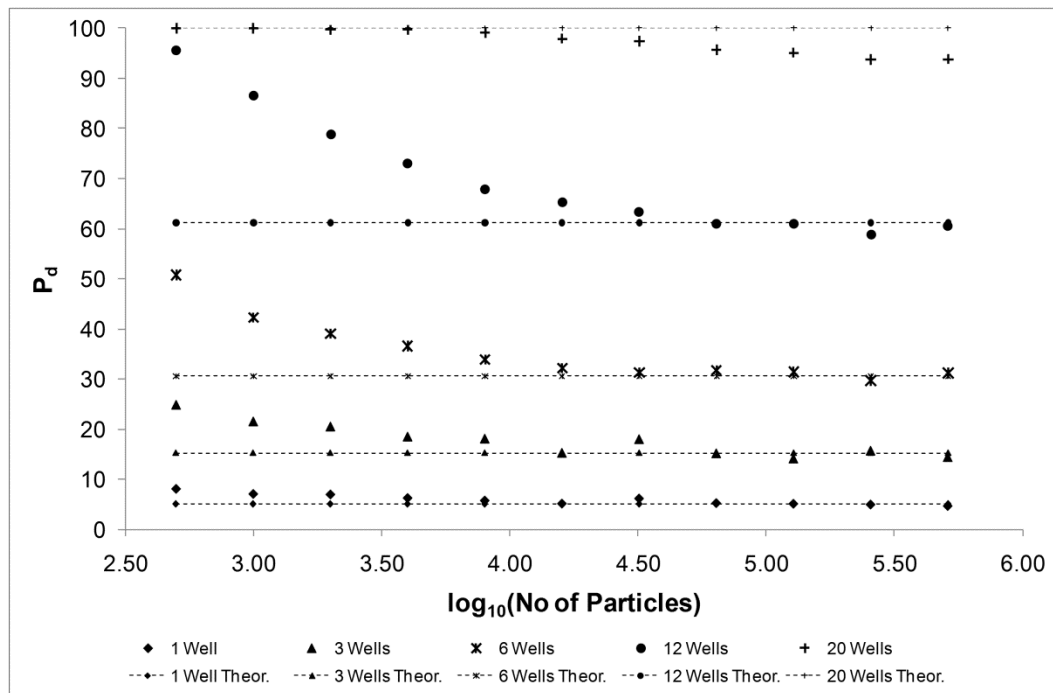


**Figure 3.3:** Comparison between numerical and theoretical  $P_d$  versus  $\log_{10}$  of number of tracking particles  $N$ ,  $N=500, 1,000, 2,000, 4,000, 8,000, 16,000, 32,000, 64,000, 128,000, 256,000,$  and  $512,000$

It is apparent from Figure 3.3 that, independently from the number of monitoring wells, the detection probability decreases as the number of particles increases. This occurs because an increase in the number of tracking particles would make the concentration variations between sequential cells smoother, since a larger number of smaller particles are distributed into various cells. As a result the contamination plume is described better, reducing some erroneous detection cases, which occur when the concentration at a monitoring numerical cell is found to be marginally above or below the detection threshold limit. This may explain the discrepancy between analytical and numerical results for the detection probability, which was observed by Yenigul *et al.* (2006) by using 2,000 particles for calculations.

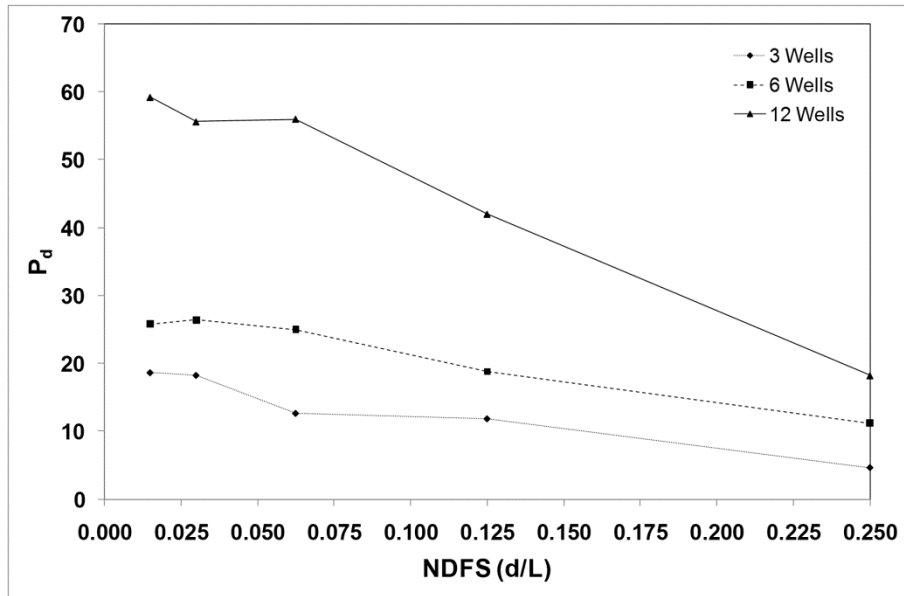
## 3.4 Results and Discussion

### 3.4.1 Effect of Number and Distance of Wells on Detection Probability

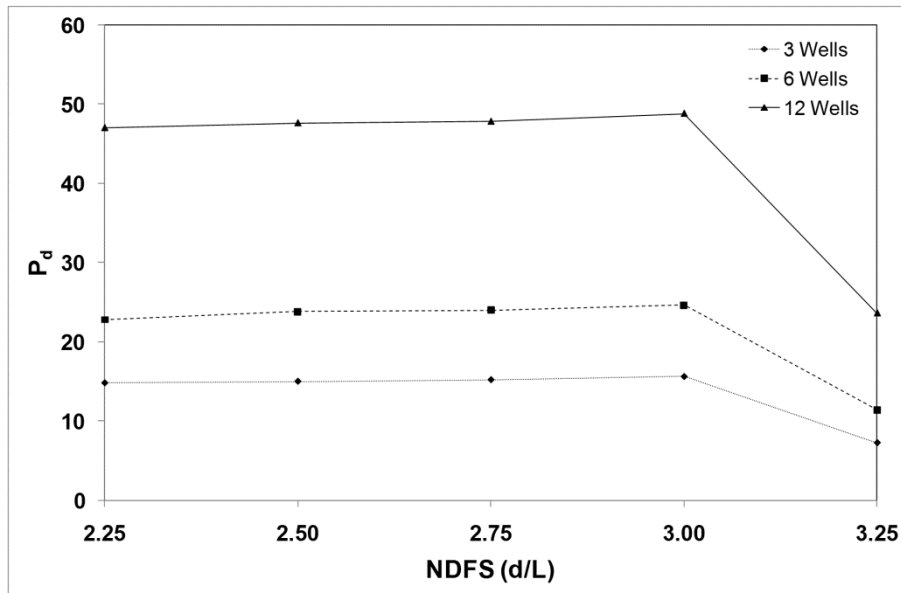
The number of wells that are used in a monitoring arrangement has a great influence on the likelihood of detecting or not potential contamination events from a landfill facility. Table 1 presents the results of our simulations for different levels of heterogeneity, values of transverse dispersion coefficients  $\alpha_T = 0.001, 0.01, 0.02, 0.05, 0.1, 0.2, 0.5\text{m}$  or different number of monitoring wells, NOW=1, 2, 3, 4, 6, 12, and 20, and for two cases, the first utilizing 500 hydrogeological realizations and 2,000 tracking particles, and the second utilizing 3,000 realizations and 8,000 tracking particles. The detection probabilities shown in this table refer to the optimum distance  $d$  from the contamination source, normalized by the width  $L$  of the landfill. The normalized optimum distance is designated as NDFS, and it refers to that distance from the landfill where the maximum detection probability was observed for each arrangement of wells.

Our numerical experiments showed that, in most cases, different monitoring wells, under the same conditions of heterogeneity and dispersion, perform better at slightly different distances. For example, Figure 3.4(b), 6 wells attain the maximum  $P_d$  at a normalized distance of 0.03, while 3 and 12 wells attain the maximum  $P_d$  at NDFS=0.015. On the other hand Figure 3.4(a) indicates that all 3, 6, and 12 wells attain their maximum  $P_d$  at the same distance. Because of the computational effort it was chosen that the values of  $P_d$ , shown in Table 4.1, would be calculated (in each  $\alpha_T$  case) at the same NDFS for all arrangement of wells, with NDFS selected as the distance where the performance of the majority of the well arrangements was maximized.

The first observation from Table 4.1 refers to the variability of the values of  $P_d$  obtained by the numerical scheme utilizing 500 realizations and 2,000 particles, and that which uses 3,000 realizations and 8,000 particles. This is to be expected since Figure 2 indicates that at 500 Monte Carlo realizations  $P_d$  is well within the zone where significant fluctuations around its asymptotic value still occur, and in particular that depending on  $\sigma_Y^2$  and  $\alpha_T$  the value of  $P_d$  obtained by 500 realizations, for the case of 3 wells, may underestimate the asymptotic value obtained by 3,000 realizations, while for 6 and 12 wells the opposite result may hold true. This variability in  $P_d$  from the two numerical schemes becomes more pronounced when the number of wells exceeds 3, in agreement with the results of Figure 3.3, which indicate that the choice of the number of tracking particles influences  $P_d$  more when the number of wells increases.



(a)



(b)

**Figure 3.4:** Optimum detection distance for 3, 6, and 12 wells. Top: Heterogeneous ( $\sigma^2_{lnK}=2.00$ ,  $a_T=0.20m$ ) flow field. Bottom: homogeneous flow field with  $a_T=0.001m$ .

It is evident from the results at Table 4.1 that in all cases of hydrogeological heterogeneity and dispersion the more wells utilized for detection purposes the greater the detection probability. It is notable that the use of 20 monitoring wells provides extremely high detection probabilities, which in some cases, at least at the numerical level, may reach full detection. In terms of the minimum requirement of the 3 monitoring wells stipulated in the 1999/31/EU directive “on the landfill of waste” we found that, in agreement with (Yenigül et

al., 2005), the detection probability from this well arrangement remained very low, not exceeding 19%. The implication of this result is that approximately four out of five cases of leakage from a landfill will remain undetected if such a well arrangement is to be used.

### 3.4.2 Effect of Field's Heterogeneity and Dispersion

For a given geologic field the dispersion coefficient determines the form that a contaminant's plume takes (Meyer et al., 1994; Yenigül et al., 2005). The longitudinal dispersion causes elongation of the plume in the direction of groundwater flow, while the transverse dispersion causes it to widen. This means that the farther a plume travels, the more it spreads and dilutes into the aquifer.

The dispersion of pollutants as they travel into an aquifer results in two opposing situations with regards to monitoring. As the plume evolves the contaminated area increases, making it more likely for a plume to be detected by a monitoring system. On the other hand though, as the plume evolves the concentration drops, making it more difficult to obtain high concentration samples, and hence to detect at a distance from the source. For a fixed heterogeneity level Table 4.1 shows that for each specific arrangement of wells the maximum detection probability increases with increasing dispersion coefficient up to a certain value of  $\alpha_T$  and then  $P_d$  decreases. For the homogenous case this saddle point occurs at about the value of  $\alpha_T = 0.1m$  to  $0.2m$ , while the effect of increasing heterogeneity appears to be the appearance of the saddle point at lower  $\alpha_T$  values.

The heterogeneity of the subsurface environment also influences the detection probability of a particular installation of monitoring wells. Analysis of the results in Table 4.1 shows that in general the efficiency of contaminant detection from a specific well arrangement decreases as the variance of  $Y = \ln K$  increases. This conclusion holds consistently for the system of 6, 12, and 20 wells, but it appears to be more tentative for the lower number of wells. This may be attributed to the fact that arrangements of 1, 2, 3, and 4 wells return relative small detection probabilities and hence numerical errors from the limited number of realizations and tracking particles have the potential to make this trend less apparent. Indeed, the greater the heterogeneity the closer the monitoring wells must be to the contaminant source in order for detection to occur.

### 3.4.3 Effect of Sampling Frequency

According to the EU directive 1999/31/EU on “*the landfill of waste*” sampling for monitoring purposes should be conducted “...*At a frequency to be determined by the competent authority, and in any event at least once a year...*” Annex III of the same directive

specifies that for the protection of groundwater, monitoring of its chemical composition should follow a site-specific sampling frequency, which would be based on the velocity of groundwater flow, in order to allow for the “...possibility for remedial actions between two samplings if a trigger level is reached...”

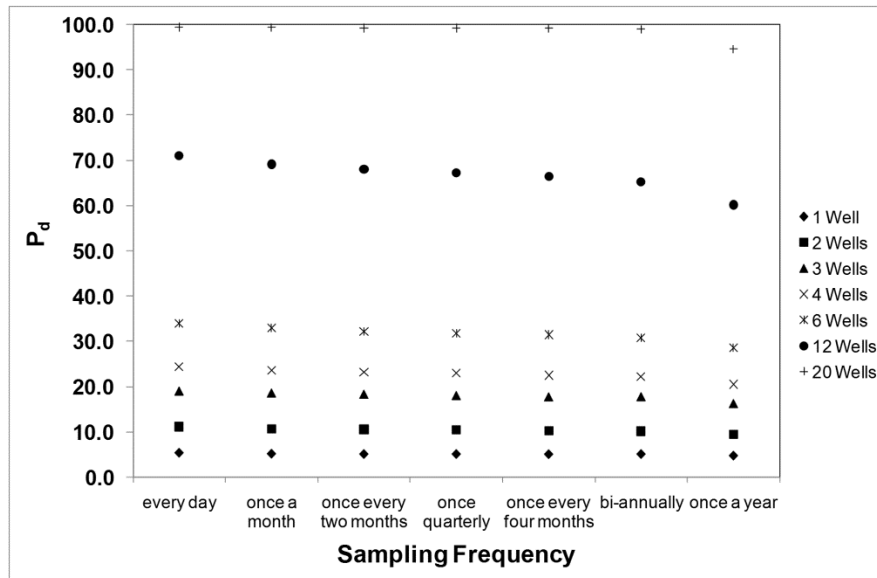
Yenigul *et al.* (2006) examined the way that sampling frequency affects the detection probability of a contaminant plume, which emanates from a continuous leak of constant flow rate. These authors concluded that in the continuous leak case the detection probability of all the monitoring systems they considered remained insensitive to the sampling frequency, in contrast to the contaminated area, which increased as the sampling frequency decreased.

In the present study the dependence of the detection probability on the sampling frequency was investigated for the case where the contaminant's mass got released instantaneously into an aquifer. Figure 3.5 shows the results of our numerical experiments (3,000 realizations and 8,000 tracking particles) for two cases: the first is a homogeneous aquifer with  $a_T = 0.01$  m, and the second is a heterogeneous one with  $\sigma_Y^2 = 1.0$  and  $a_T = 0.20$  m. For both cases the sampling frequencies considered were: once a day, once a month, once every two months, once quarterly, once every four months, bi-annually, and once a year.

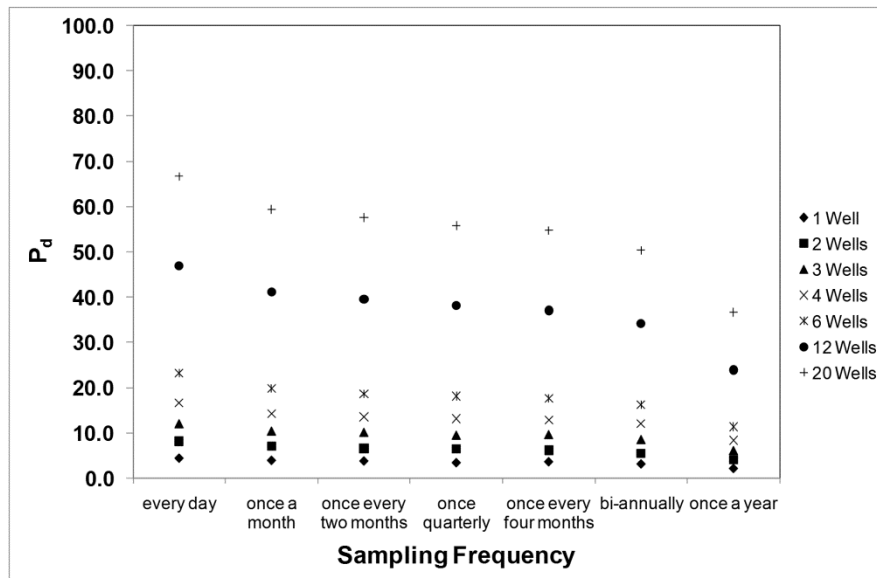
Figure 3.5(a) indicates that for the case of instantaneous release, if monitoring of a homogeneous and of low dispersion aquifer is performed with up to three wells, no higher detection of the contamination is obtained by sampling done more frequently than once a year. If 4, 6, or 12 monitoring wells are used then conducting bi-annual sampling increases the probability of detection by about 8% and sampling once a month improves  $P_d$  by 15% relative to the detection obtained if sampling is done annually. The case of 20 monitoring wells indicates that full detection can be accomplished with this arrangement if bi-annual sampling takes place.

The effect of sampling frequency on the detection probability is more pronounced when the aquifer is heterogeneous and dispersion is increased (Figure 3.5(b)). When 3 wells are used it is worth to proceed to bi-annual sampling, which will provide a 40% improvement on the detection probability, or else proceed directly to daily sampling that will improve detection by over 90%, relative to the  $P_d$  determined by annual sampling. For the cases of 4 and 6 monitoring wells bi-annual sampling improves  $P_d$  by 43%, and once a month increases  $P_d$  about 70%, again relative to the  $P_d$  determined by annual sampling. Finally, 12 and 20 monitoring wells show a substantial improvement in the  $P_d$  which approaches 40% simply

by sampling twice instead of once a year, and much higher improvements if a more frequent sampling schedule is performed.



(a)



(b)

**Figure 3.5:** Dependence of the probability of detection on sampling frequency (5a: homogeneous,  $a_T=0.01m$ , and 5b: heterogeneous aquifer,  $\sigma_{\ln K}^2=1.0$ ,  $a_T=0.20m$ )

As a general rule it appears that under all conditions at least bi-annual sampling should occur at a monitoring system. If one wants a higher detection probability then sampling at a frequency of once a month appears to be the optimum choice for most well arrangements,

considering both the effort involved if one were to proceed with a much more intense sampling and the improvements on detection attained at this level. It is interesting to note that in heterogeneous aquifers a large number of monitoring wells (such as the case of 12 wells considered here) if sampled infrequently (for example, once a year) does not perform much better in terms of detection than arrangements having a lower number of wells, but which are sampled more regularly.

### 3.5 Remedial Action Response Delay

Decision analyses that evaluate the economic worth of different arrangements of monitoring wells are performed by defining a risk term  $R$ , which is associated with the probability of detection  $P_d$  (and the probability of failure to detect,  $P_f = 1 - P_d$ ), and the associated cost of remediating the detected volume of contaminated groundwater,  $C_d$  (correspondingly, of the remediation cost  $C_f$  of a much larger contaminated volume, due to a plume's failure to be detected by a monitoring system, and becoming apparent only by reaching, for example, the drinking wells of a community). This risk term  $R$  is defined for every monitoring system, whose economic worth is investigated, as (Bedford & Cooke, 2003; Yenigul et al., 2006):

$$R = P_d C_d + P_f C_f \quad (3.8)$$

The remediation costs in both cases can be obtained by multiplying the contaminated volume, which is evaluated during the stochastic groundwater flow and contaminant transport numerical analysis, by the remediation cost per unit contaminated water volume. The decision analysis then proceeds by determining that particular well arrangement that optimizes the risk factor  $R$ , i.e., determining this monitoring system that maximizes the detection probability while minimizing the contaminated area, or equivalently minimizing the remediation cost.

Implicit in the decision analysis framework described above is the assumption that remediation takes place immediately after detection occurs, in other words that the contaminated groundwater volume (contaminated area, equivalently, in our case of two-dimensional investigation), which is remediated, is the same with the volume observed and calculated at the time of detection. In reality, there is always a delay in the response, from the time when the exceedance of a threshold value of a chemical is observed until the time when remediation measures commence. This remedial action delay has as a result the increase of the contaminated volume, as the plume continues to evolve in time, and an increase of the

remediation cost compared to that which would be calculated if the contaminated volume at detection were to be used.

One way to address this issue is to use the ratio of  $A_t/A_{t+dt}$ , where  $A_t$  is the contaminated area in the two-dimensional case (correspondingly, contaminated volume in 3-D) at time  $t$  of detection, and  $A_{t+dt}$  is the contaminated area at time  $t + dt$  when remediation might take place, to correct for this remedial action delay. Of course the time interval  $dt$  between detection and remediation is not known a priori, and a sensitivity analysis can be performed, as is done here, to determine the influence of  $dt$  on the risk factor  $R$ . Multiplying this ratio by  $P_d$  results in a reduced detection probability  $P_d^{cor}$ , i.e., an increased delay in the response to remediate can be considered, in terms of economic outcome, as equivalent to a monitoring arrangement with a decreased efficiency to detect. While  $P_d$  contains information about the degree of our knowledge of the event detection,  $P_d^{cor}$  can be considered as a measure of the degree  $P_d$  is utilized. For example, if 20 monitoring wells were used and full detection were to take place,  $P_d=1.0$ , then Equation (3.8) would calculate  $R$  considering the second (failure) term equal to zero, irrespectively of the fact that in some cases remediation might take place only when the plume has reached a critical stage, for example threatening community drinking wells. Therefore,  $P_d^{cor}$  is a way to measure the economic impact of different remedial action delays as a divergence, from the maximum economic outcome (which takes place at detection) occurs for a specific monitoring installation.

This approach provides also a corrected probability of failure  $P_f^{cor}$ , which will increase as the time to respond increases resulting in an increase of the weighted cost of failure that enters into expression (3.8) of the risk factor  $R$ . In essence the above procedure downgrades the importance of the first term in  $R$ , which provides the weighted remediation cost due to detection, and upgrades the significance of the second term, which provides the weighted cost due to failure to detect, in order to account in the calculation of  $R$  for a delay in the remedial response after detection. This procedure is summarized in the following equation yielding a corrected risk  $R^{cor}$  that accounts for the remedial action response delay,

$$R^{cor} = P_d^{cor} C_d + P_f^{cor} C_f \quad (3.9)$$

where

$$P_d^{cor} = P_d \left( \frac{A_t}{A_{t+dt}} \right), \text{ and } P_f^{cor} = 1 - P_d^{cor} \quad (3.10)$$

In our model it is assumed that the pollutant is conservative, and that a particle found within a grid cell at particular time step, classifies the cell as contaminated, even if the concentration is below the regulatory limit.

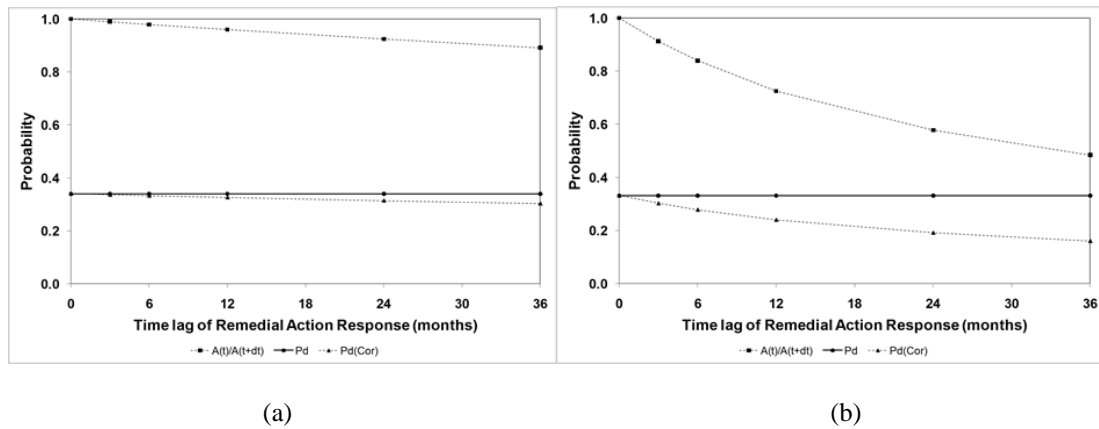


**Figure 3.6:** Effect of remedial action response: Corrected detection probability  $P_d^{cor}$  for six monitoring wells, sampling once a day, in a homogeneous field (a:  $a_T=0.01m$ , and b:  $a_T=0.10m$ ), as a function of remedial action delay

Table 4.2 provides the results for  $P_d^{cor}$  for 3, 6, 12 and 20 monitoring wells, in two cases of aquifer heterogeneity ( $\sigma_Y^2 = 0.0$  and  $\sigma_Y^2 = 1.0$ ), and for two sampling frequencies, every day and once every six months. The ratio  $A_t/A_{t+dt}$  was evaluated numerically through Monte Carlo simulations, with  $A_{t+dt}$  calculate at time lags of 3, 6, 12, 24, and 36 months beyond the detection time. Figure 3.6a shows that for six monitoring wells in a homogeneous field of low transverse dispersion, and hence of contaminant transport taking place at a slow rate, the use of expression (3.8) for the risk factor  $R$  provides a good approximation to an optimum decision. A delay in the deliberations on planning, cost, and technology application will not affect critically the contaminated groundwater volume and hence the remediation cost. On the other hand, if contamination takes place in a homogeneous environment, but of high dispersion, then (Figure 3.6b) indicates that the contaminated groundwater area will increase fast with time, and so any remediation delays of the order of 3 years and above beyond the time of detection, would be almost equivalent to a monitoring system providing detection with half its number of wells.

Figure 3.7 summarizes the results for the effect of remedial action delay in a heterogeneous field of  $\sigma_Y^2 = 1.5$  and  $a_T = 0.05m$ , for twelve monitoring wells as a function of the sampling frequency as well. When sampling is performed every day a remediation delay of 36 months is equivalent to reducing the detection probability from 59% to 22%, or increasing the failure probability from 41% to 78%. This means that the larger of the two costs, the failure cost, which enters into expression (3.8) increases by 90% as a result of the delay. If sampling is performed every 6 months then  $P_d$  is reduced from 42% to 19%.



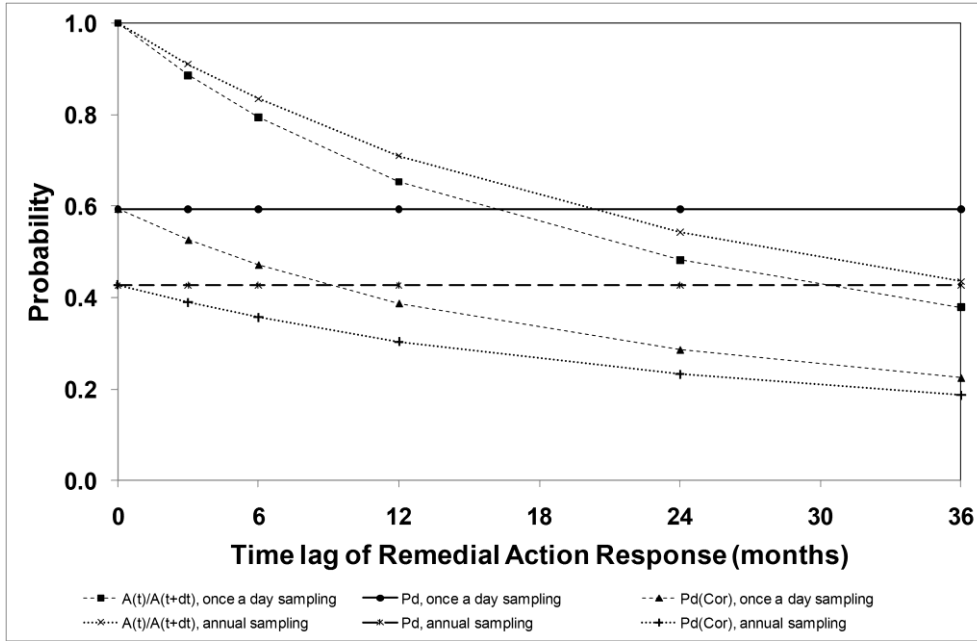


**Figure 3.7:** Corrected detection probability  $P_d^{cor}$  for a heterogeneous field  $\sigma_{lnK}^2=1.5$ ,  $\alpha_T=0.05m$  for twelve monitoring wells as a function of remedial action delay and sampling frequency

### 3.6 Conclusions

A Monte Carlo stochastic model was developed to simulate contaminant transport into heterogeneous, two-dimensional aquifers. Pollution originated from a random, instantaneous point source within a landfill facility. Different arrangements and distances of monitoring wells from a landfill were considered, and the corresponding detection probabilities  $P_d$  and contaminated groundwater areas, at different time periods, were calculated. The following major conclusions can be drawn from the current study.

1. Convergence of the probability of detection  $P_d$  to a constant value was attained at about 3,000 Monte Carlo simulations, with the average difference, from all cases, from the value of  $P_d$  returned by 500 simulations being approximately 4%. The number of tracking particles used to simulate contaminant transport had a strong influence on the values of  $P_d$  calculated through numerical experiments. For arrangements of 12 and 20 wells convergence of the  $P_d$  to a stable value was attained at very high particle numbers. Cases of 1, 2, 3, 4, and 6 wells require at least 8,000 tracking particles in order to define a stable probability of detection.

2. Our results showed that in all cases of hydrogeological heterogeneity and dispersion the more wells utilized for detection purposes the greater the  $P_d$ . The use of 20 monitoring wells provides extremely high detection probabilities, which in some cases, at least at the numerical level, reach full detection. In terms of the minimum requirement of the 3 monitoring wells stipulated in the 1999/31/EU directive “*on the landfill of waste*” it was found, in agreement with (Yenigül et al., 2005), that the detection probability from this well arrangement remained very low, not exceeding 19%. The implication of this result is that approximately four out of five cases of leakage from a landfill will remain undetected if only 3 monitoring wells are used.
3. For a fixed heterogeneity level, for each specific arrangement of wells, the maximum detection probability increases with increasing dispersion coefficient up to a certain value of  $\alpha_T$  and then  $P_d$  decreases. For the homogenous case this saddle point occurs at about the value of  $\alpha_T = 0.1$  to  $0.2m$ , while the effect of increasing heterogeneity appears to be the appearance of the saddle point at lower  $\alpha_T$  values. For transverse dispersion greater than  $0.2m$  maximum detection is attained very close to the trailing edge of landfill. As a general rule the efficiency of contaminant detection from a specific well arrangement decreases as the variance of  $Y$  increases.
4. The frequency of sampling is critical in heterogeneous aquifers of high dispersion. Bi-annual sampling improves the detection probability, for almost all well arrangements, by about 40%, whereas once a month sampling improves  $P_d$  by about 70%, relative to the detection determined by annual sampling. As a general rule it appears that under all conditions at least bi-annual sampling should occur at a monitoring system. If one wants a higher detection probability then sampling at a frequency of once a month appears to be the optimum choice for most well arrangements, considering both the effort involved, if one were to proceed with a much more intense sampling, and the improvements on detection attained at this level. It is interesting to note that in heterogeneous aquifers a large number of monitoring wells if sampled infrequently does not perform much better in terms of detection than arrangements having a lower number of wells, but which are sampled more regularly.
5. Finally, decision-making analyses that evaluate the economic worth of different arrangements of wells calculate remediation costs based on contaminated

groundwater volumes that are estimated at the time of detection. In practice there is always a remedial action response delay, and contaminated volumes and hence remedial costs surpass those calculated at detection time. To correct for this situation we propose here an expression for a corrected risk factor  $R^{cor}$  that accounts for remedial action response delay,

$$R^{cor} = P_d^{cor} C_d + P_f^{cor} C_f \quad (3.11)$$

$$P_d^{cor} = P_d \left( \frac{A_t}{A_{t+dt}} \right), \text{ and } P_f^{cor} = 1 - P_d^{cor} \quad (3.12)$$

$A_t$  corresponds to the contaminated area (volume) at detection time  $t$ , and  $A_{t+dt}$  is the contaminated area (volume) at a later time due to delays in remediation procedures. Our approach can be viewed as a way to downgrade the importance of early detection, if not followed by quick remedial response, in risk analysis calculations.

Our expression allows us to estimate for a heterogeneous field, where twelve monitoring wells are operating and sampled every day, that a remediation delay of 36 months is equivalent to reducing the detection probability from 59% to 22%, or increasing the failure probability from 41% to 78%, almost doubling the failure cost entering risk calculations. If sampling is performed every 6 months then  $P_d$  is reduced from 42% to 19%, i.e., a delay of 36 months is equivalent to reducing the performance of 12 wells to that of only 3 wells.

# CHAPTER 4

## **Sampling frequency of groundwater monitoring system and remediation delay at contaminated sites**

---

### **4.1 Introduction**

Geologic disposal of municipal wastes has been the dominant waste disposal practice and still remains the most profitable option in terms of exploitation and capital costs (Renou et al., 2008). On the other hand, disposal sites, whether old abandoned dumping grounds or sanitary landfills, have been responsible for soil and groundwater contamination as the aqueous effluent generated from rainwater, percolating through the wastes, or from biochemical processes, has leaked into the subsurface environment (Collucci et al., 1999; Koerner & Soong, 2000; Tsanis, 2006). Hence, early detection of aquifer contamination from a pollution source and quick remedial response is critical for plume minimization, reduction of remedial and legal costs, and decrease of the environmental and health impacts.

The duration of a leak may vary from a sudden to a continuous discharge of steady or variable rate. Sudden discharges into an aquifer can occur as high hydraulic head may develop as a result of continuous or localized leachate presence on the soil surface, or the bottom liner of unlined or lined landfills, respectively (Koerner & Soong, 2000); precipitation fluctuations leading to excessive percolation through the wastes (Fatta et al., 1999; Tatsi & Zouboulis, 2002), or, in the case of a landfill, clogging of the leachate collection and drainage pipeline system (Koerner & Koerner, 1995).

Even in lined landfills leakages can occur due to tears and holes in the geo-membranes caused by poor waste disposal practices and/or failure near welded membrane seams (Lee &

Jones-Lee, 1994; Allen, 2001). Synthetic materials used as bottom liners are prone to failure due to ageing, embrittlement, stress cracking, chemical corrosion, from extended leachate exposure, and elevated temperatures, from exothermic processes taking place in a landfill (Allen, 2001). Most locations of failure are of small dimension in relation to a landfill's cell area, constituting point sources of contamination (Collucci et al., 1999). Similar failure concerns refer to landfills with clay bottom barriers, where fracturing, due to differential waste deposition, chemical degradation, or ageing, can lead to contaminant leaks into the subsurface environment.

In practice it is very difficult to distinguish between instantaneous and continuous releases of contaminants. Instantaneous contaminant releases are more difficult to detect because they translate to narrow plumes and hence the characteristics of the geologic environment, the density of the monitoring well network, and the frequency of sampling become determining factors on whether detection can be achieved. Furthermore, instantaneous contamination releases may be followed by continuous leaks as landfill failure zones become more generalized. Continuous leaks are more probable to detect as the area with contaminant concentrations greater than the threshold detection limits increases, but in that case the effect of the initial instantaneous release becomes difficult to differentiate.

Detection of aquifer contamination is performed with the use of monitoring wells that are sampled according to a frequency schedule. Effective monitoring, and hence early remediation action, constitutes a complicated problem with many uncertainties involved, arising from the heterogeneity of the geologic medium, the aquifer's depth and the hydraulic gradient, the quantity and nature of the contaminants, all affecting the number, location, and frequency of sampling of a monitoring network.

*Yenigül et al.*, (2005) conducted numerical experiments of the influence of aquifer heterogeneity and dispersion, and well density on the probability of plume detection,  $P_d$ , resulting from landfill contaminant releases. These authors concluded that the number of wells and aquifer dispersion are the dominant factors affecting detection probability. (Papapetridis & Paleologos, 2011a) demonstrated that the frequency of sampling is critical in heterogeneous aquifers, with bi-annual or monthly sampling improving  $P_d$  by 40 %, and 70 %, respectively, relative to that by annual sampling. They recommended that sampling should take place twice a year, at a minimum, with once-in-a-month appearing the optimum choice, considering the effort involved and the improvements in detection. These authors also introduced the notion of remedial action delay and provided a correction to decision analyses to account for the cost of delays in remedial actions.

The present study utilizes the stochastic Monte Carlo framework to investigate contaminant transport in heterogeneous aquifers (Hudak & Loaiciga, 1992; Meyer et al., 1994; Storck et al., 1997; Yenigül et al., 2005; Bierkens, 2006; Yenigul et al., 2006; Papapetridis & Paleologos, 2011a, 2011b; Yenigül et al., 2011) in order to evaluate the effect of sampling frequency on the detection probability of a linear monitoring arrangement of wells. Although our study considers for illustration purposes that an instantaneous contaminant release has emanated from a random point within a landfill's area, our analysis is also relevant for other cases as well, such as when contamination can be considered to have emanated from a small area of waste deposition, and from an unknown point of contamination within that area (Højberg et al., 2007). The change in  $P_d$  for various sampling schedules, degree of heterogeneity and dispersion is quantified, together with the average time needed for detection depending on the sampling performed. In addition, the concept of the remedial action delay is further expounded for specific well arrangements and sampling schedules in geologic environments of differing heterogeneity and dispersion. Our study aims to define the critical factors that determine an optimal groundwater monitoring sampling strategy and to quantify how the contaminated area, and hence the cost of remediation is affected by delays in remedial actions.

## 4.2 Model Description

Our study employed the Monte Carlo numerical framework to simulate groundwater flow and contaminant transport in 2-D heterogeneous aquifers with the use of the Spectral Turning Bands Method (STUBA) (Tompson et al., 1987a; Ababou et al., 1989; McLaughlin et al., 1993; Elfeki, 1996; Paleologos & Sarris, 2011). The range of the log hydraulic conductivity variance varied from 0.0 (homogeneous aquifer) to 2.0 (strongly heterogeneous aquifer), and the mean of the log hydraulic conductivity was set equal to 2.3. The correlation length,  $\lambda$ , was considered constant and equal to 20m for both  $x$ - and  $y$ - directions. Contaminant transport into the subsurface heterogeneous environment was simulated using the particle tracking method based on the 'random walk' approach (Ahlstrom et al., 1977; Prickett et al., 1981; Tompson & Gelhar, 1990a; Uffink, 1990; Zimmermann et al., 2001; Hassan & Mohamed, 2003; Delay et al., 2005b; Yenigül et al., 2005; Salamon et al., 2006b; Yenigül et al., 2011). For each case of heterogeneous field 3,000 Monte Carlo realizations and 8,000 particles were utilized to calculate the groundwater velocity and the contaminant's movement into the subsurface environment. Transverse dispersion coefficients,  $\alpha_T$ , were set equal to  $\alpha_T = 0.01, 0.02, 0.05, 0.10, 0.20, 0.50\text{m}$ , corresponding to values observed in field

experiments (Gelhar, 1986), and the longitudinal dispersion coefficient,  $\alpha_L$ , was calculated by the relation  $a_L = 0.10a_T$ .

Steady state groundwater flow in an isotropic, heterogeneous porous medium, with a fixed depth of aquifer was considered with a constant hydraulic gradient of 0.001m, between the nodes lying perpendicular to the direction of flow, and no-flow conditions at the lower and upper boundaries of the flow domain. Although hydraulic gradient variations or other hydrogeological considerations, such as the existence of fast pathways or of “hot” spots, where contaminants may be sorbed and slowly released at a later time have been seen to occur, our analysis did not extend on these aspects that are difficult to address, without detailed field investigations (Mahar & Datta, 2000). The simulated region was 1,000 m long and 400 m wide (Figure 4.1), and it was discretized in cells of area  $dx \cdot dy = 2 \cdot 2 \text{ m}^2$ , creating a  $500 \times 200$  grid. A rectangular area simulating a contaminant potential source area (CPSA), for example a section of a landfill, or the area of a waste storage facility, was situated between  $x$ -coordinates 10m and 60m, and  $y$ -coordinates of 140m and 260m (Figure 4.1). At a random

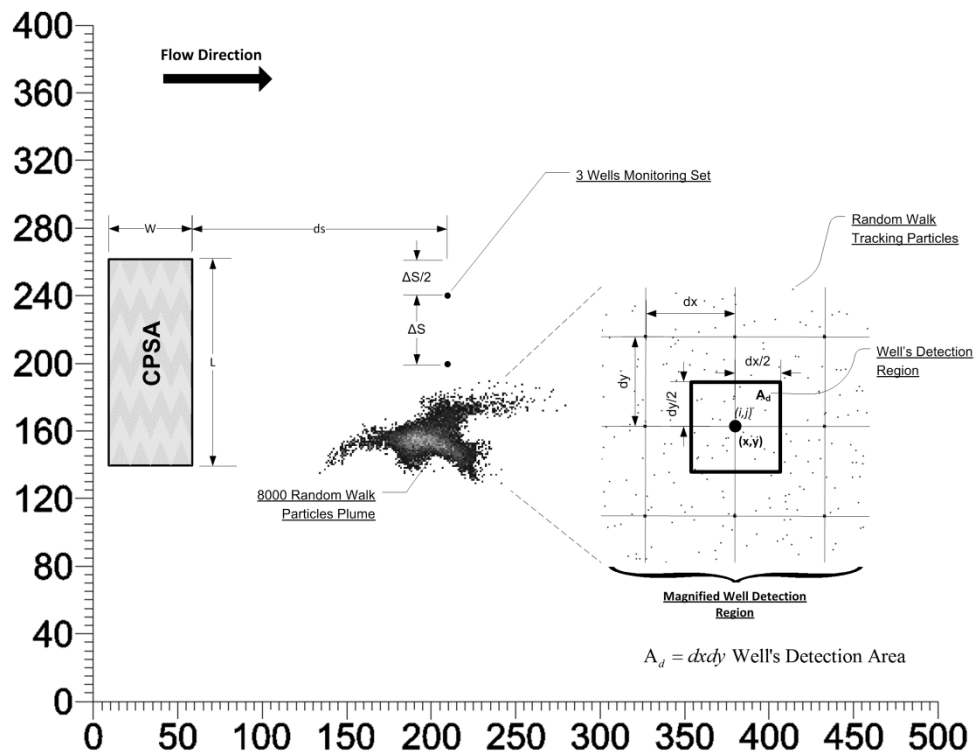


**Figure 4.1:** Half section of simulated flow field illustrating the rectangular CPSA, an 8000 particles plume evolved for 10 years, and a magnified well-detection area (wells are deliberately placed further away for illustration purposes)

point within these boundaries a contamination event was initiated that polluted the aquifer. The total contaminant mass was equal to 1,000 gr, and was assumed conservative and fully water soluble. The initial concentration of the point source,  $C_0 = M_0 / (nV_0)$ , was 4,000mgr/lt, where  $M_0$  the initial mass,  $n=0.25$  the effective porosity, and the volume  $V_0 = 1\text{m}^3$ . The threshold concentration  $C_{TH}$ , detectable by the monitoring wells was set at 0.35 % of the initial concentration, corresponding to  $C_{TH} = 14\text{mgr/lt}$  or 112 particles in a single cell. The uncertainty regarding the potential location within a cell of a landfill, where a leak might have developed, stems from the lack of information on potential failure locations at a landfill's bottom liner. In case pollution from a different facility is assumed, such as from an industrial plant or a military facility, uncertainty about the contamination's point source may stem from our inability to detect leaks from waste carrying pipelines, or underground storage areas of liquid waste, or even accidental spills during operations. In either case, it was assumed that any point within the rectangular CPSA is an equal-probable source of leakage, taking place once as a single failure event at zero time (when the simulation begun) and resulting in an instantaneous ejection of contaminants into the aquifer. Monitoring wells were assumed to fully penetrate the aquifer resulting in vertically-averaged concentration measurements. Six linear configurations were examined consisting of 1, 3, 6, 8, 12 and 20 wells, equally spaced from each other. Wells that were located at the ends of each arrangement were placed half the distance from the cell's top and bottom edges so that the efficiency of the monitoring system would be maximized (Yenigül et al., 2005). Monitoring of the aquifer and plume evolution was simulated for a 30-year period.

### 4.3 Sampling Frequency of Groundwater Monitoring

Table 4.1 and Table 4.2 present the results for the detection probability  $P_d$  (%) achieved for different number of wells (NOW), where NOW=1, 3, 6, 8, 12, 20, for various levels of heterogeneity,  $\sigma_{lnK}^2 = 0.0, 0.5, 1.0, 2.0$  and values of transverse dispersion coefficients,  $a_T = 0.01, 0.02, 0.05, 0.10, 0.20, 0.50\text{m}$ . The values for the detection probability are given at NDFS, which was the distance from the trailing edge of the CPSA where  $P_d$  was maximized, normalized by the width ( $L_o = 120\text{m}$ ) of the facility. (Papapetridis & Paleologos, 2011a) have shown that, in most cases, different monitoring wells, under the same conditions of heterogeneity and dispersion, performed better, in terms of  $P_d$ , at slightly different distances. However, because of the computational effort it was chosen that the values of  $P_d$ , shown in Table 4.1 and Table 4.2, would be calculated (in each  $a_T$  case) at the same NDFS for all

**Table 4.1:** Detection Probability  $P_d$  (%)

NOW	$\sigma^2_{\ln K}=0.0$								$\sigma^2_{\ln K}=0.5$							
	NDFS	D	1M	2M	3M	4M	6M	A	NDFS	D	1M	2M	3M	4M	6M	A
	<b><math>a_T=0.01</math> m</b>								<b><math>a_T=0.01</math> m</b>							
<b>1</b>	<b>2.25</b>	6.0	5.7	5.6	5.5	5.4	5.4	4.9	<b>1.50</b>	5.4	5.2	5.2	5.2	5.1	5.0	4.5
<b>3</b>	<b>2.25</b>	18.9	18.2	17.8	17.5	17.1	16.9	15.9	<b>1.50</b>	15.1	14.5	14.3	14.1	13.9	13.6	11.8
<b>6</b>	<b>2.25</b>	35.4	34.3	33.6	33.4	32.7	32.3	29.8	<b>1.50</b>	30.7	29.5	29.0	28.6	28.2	27.5	24.1
<b>8</b>	<b>2.25</b>	47.2	45.5	44.8	44.2	43.3	42.8	39.9	<b>1.50</b>	41.5	39.7	38.9	38.3	37.9	37.1	32.7
<b>12</b>	<b>2.25</b>	70.5	68.5	67.4	66.7	65.8	64.8	59.5	<b>1.50</b>	57.0	55.5	54.5	53.5	53.1	51.8	46.7
<b>20</b>	<b>2.25</b>	99.6	99.5	99.4	99.4	99.3	99.3	95.1	<b>1.50</b>	77.2	75.9	75.0	74.2	73.5	72.7	66.8
	<b><math>a_T=0.02</math> m</b>								<b><math>a_T=0.02</math> m</b>							
<b>1</b>	<b>1.50</b>	5.8	5.6	5.5	5.4	5.3	5.2	4.5	<b>0.50</b>	5.9	5.9	5.9	5.7	5.7	5.6	4.5
<b>3</b>	<b>1.50</b>	18.2	17.5	17.0	16.7	16.3	15.9	14.0	<b>0.50</b>	16.9	16.6	16.4	15.9	16.0	15.5	12.8
<b>6</b>	<b>1.50</b>	34.6	32.9	31.8	31.2	31.0	30.2	27.4	<b>0.50</b>	33.2	32.4	32.0	31.7	31.2	30.8	25.8
<b>8</b>	<b>1.50</b>	46.3	43.9	43.0	42.1	41.5	40.2	36.5	<b>0.50</b>	43.6	42.0	41.5	40.9	40.7	39.5	33.8
<b>12</b>	<b>1.50</b>	69.0	65.6	64.5	63.2	62.4	60.3	55.0	<b>0.50</b>	61.9	60.0	59.2	58.7	58.0	57.0	48.6
<b>20</b>	<b>1.50</b>	99.4	99.3	99.0	98.7	98.5	97.1	89.4	<b>0.50</b>	84.4	83.0	82.2	81.9	81.6	80.8	71.8
	<b><math>a_T=0.05</math> m</b>								<b><math>a_T=0.05</math> m</b>							
<b>1</b>	<b>0.50</b>	5.8	5.5	5.2	5.3	5.1	4.9	4.4	<b>0.50</b>	5.6	5.0	4.7	4.5	4.2	4.0	3.0
<b>3</b>	<b>0.50</b>	18.2	17.3	16.7	16.3	16.3	15.6	13.9	<b>0.50</b>	14.9	13.6	12.9	12.6	12.0	11.5	8.9
<b>6</b>	<b>0.50</b>	34.1	31.9	31.0	30.6	30.2	29.0	25.3	<b>0.50</b>	29.9	27.0	25.5	24.7	24.0	22.8	17.0
<b>8</b>	<b>0.50</b>	45.8	43.2	42.2	41.3	40.5	39.4	34.7	<b>0.50</b>	39.1	35.1	33.7	33.0	31.5	29.7	23.4
<b>12</b>	<b>0.50</b>	69.0	65.1	63.0	61.9	60.7	59.0	52.3	<b>0.50</b>	55.7	50.2	48.0	46.2	44.4	41.8	33.2
<b>20</b>	<b>0.50</b>	99.4	98.9	98.1	97.4	96.5	94.9	84.7	<b>0.50</b>	78.2	73.4	70.9	69.2	67.4	64.5	51.7
	<b><math>a_T=0.10</math> m</b>								<b><math>a_T=0.10</math> m</b>							
<b>1</b>	<b>0.125</b>	5.7	5.3	5.1	4.9	5.0	4.7	4.4	<b>0.125</b>	6.4	5.9	5.6	5.3	5.2	4.8	4.0
<b>3</b>	<b>0.125</b>	18.1	16.9	16.4	15.9	16.0	15.3	13.9	<b>0.125</b>	16.2	14.9	14.4	13.9	13.5	12.9	10.3
<b>6</b>	<b>0.125</b>	33.9	31.8	30.9	30.0	29.5	28.6	25.1	<b>0.125</b>	30.3	28.0	27.1	26.0	25.7	24.3	19.9
<b>8</b>	<b>0.125</b>	45.8	42.6	41.4	40.7	39.9	38.8	34.1	<b>0.125</b>	42.2	38.4	37.1	35.9	36.0	33.8	27.6
<b>12</b>	<b>0.125</b>	67.9	63.7	62.0	60.5	59.8	57.5	51.1	<b>0.125</b>	62.2	56.4	54.6	52.3	51.8	48.7	39.8
<b>20</b>	<b>0.125</b>	99.1	97.3	96.0	95.1	93.9	92.3	83.6	<b>0.125</b>	87.0	81.9	79.9	77.9	76.5	73.2	60.7
	<b><math>a_T=0.20</math> m</b>								<b><math>a_T=0.20</math> m</b>							
<b>1</b>	<b>0.030</b>	4.7	4.1	3.8	3.6	3.6	3.3	2.7	<b>0.030</b>	4.8	4.2	4.1	4.0	3.9	3.7	2.7
<b>3</b>	<b>0.030</b>	14.3	12.3	11.6	10.9	11.0	10.1	8.1	<b>0.030</b>	12.9	11.2	10.9	10.6	10.4	9.8	7.2
<b>6</b>	<b>0.030</b>	26.1	22.5	21.2	20.5	19.5	19.2	14.6	<b>0.030</b>	24.1	20.2	19.2	18.6	17.9	16.7	11.7
<b>8</b>	<b>0.030</b>	36.1	30.7	29.1	27.9	27.5	26.1	20.0	<b>0.030</b>	32.5	28.5	27.1	25.9	25.4	23.2	16.2
<b>12</b>	<b>0.030</b>	53.9	46.0	44.3	42.1	42.0	39.1	30.2	<b>0.030</b>	48.3	42.3	40.5	39.2	37.9	35.9	25.3
<b>20</b>	<b>0.030</b>	80.8	70.9	68.2	65.9	64.8	62.1	47.7	<b>0.030</b>	69.6	61.7	59.7	58.0	56.6	53.3	37.4
	<b><math>a_T=0.50</math> m</b>								<b><math>a_T=0.50</math> m</b>							
<b>1</b>	<b>0.015</b>	2.4	2.2	1.9	1.9	1.9	1.7	0.1	<b>0.015</b>	3.0	2.6	2.4	2.2	2.1	1.8	0.9
<b>3</b>	<b>0.015</b>	7.3	6.2	5.8	5.6	5.5	5.0	0.4	<b>0.015</b>	7.8	6.9	6.6	6.2	5.9	4.9	1.8
<b>6</b>	<b>0.015</b>	13.7	11.5	11.1	10.7	10.5	9.8	0.8	<b>0.015</b>	13.5	10.9	10.5	10.0	9.3	7.8	2.8
<b>8</b>	<b>0.015</b>	18.2	15.1	14.4	13.7	13.5	12.5	1.3	<b>0.015</b>	18.0	15.1	14.4	13.7	13.0	10.6	3.4
<b>12</b>	<b>0.015</b>	27.6	23.9	22.5	22.2	21.3	19.8	2.4	<b>0.015</b>	27.5	22.6	21.3	20.5	19.5	16.1	5.6
<b>20</b>	<b>0.015</b>	40.5	36.7	35.0	34.2	33.4	31.0	3.1	<b>0.015</b>	38.2	34.0	32.8	31.7	30.0	25.4	8.7

NOW: No of Wells, NDFS: Normalized Distance from Source, D: Daily, 1M: Every Month, 2M: Once every two months, 3M: Once every three months, 4M: Once every four months, 6M: Bi-Annually, A: Annually

**Table 4.2:** Detection Probability  $P_d$  (%)

NOW	$\sigma^2_{\ln K}=1.0$								$\sigma^2_{\ln K}=2.0$							
	NDFS	D	1M	2M	3M	4M	6M	A	NDFS	D	1M	2M	3M	4M	6M	A
	<b><math>a_T=0.01</math> m</b>								<b><math>a_T=0.01</math> m</b>							
<b>1</b>	<b>1.25</b>	5.7	5.3	5.2	5.2	5.1	5.0	4.0	<b>0.50</b>	5.3	5.1	5.1	5.1	4.8	4.7	3.3
<b>3</b>	<b>1.25</b>	14.7	14.0	13.6	13.4	13.2	12.8	10.4	<b>0.50</b>	14.2	13.9	13.8	13.6	13.1	12.4	9.7
<b>6</b>	<b>1.25</b>	27.4	26.3	25.6	25.0	24.5	23.8	19.9	<b>0.50</b>	23.8	23.2	22.7	22.5	22.1	20.9	16.9
<b>8</b>	<b>1.25</b>	35.7	34.4	33.6	32.9	32.6	31.3	25.6	<b>0.50</b>	32.3	31.6	31.1	30.7	30.0	28.4	22.8
<b>12</b>	<b>1.25</b>	50.4	48.4	47.8	46.7	46.2	45.2	37.5	<b>0.50</b>	46.8	45.8	45.2	44.4	43.6	40.9	33.6
<b>20</b>	<b>1.25</b>	68.8	66.7	65.7	64.7	64.3	62.4	53.6	<b>0.50</b>	64.7	63.4	62.7	62.1	61.1	58.2	47.5
	<b><math>a_T=0.02</math> m</b>								<b><math>a_T=0.02</math> m</b>							
<b>1</b>	<b>0.50</b>	6.3	5.9	5.7	5.7	5.6	5.3	4.5	<b>0.25</b>	5.0	4.9	4.8	4.7	4.7	4.6	3.8
<b>3</b>	<b>0.50</b>	17.0	16.2	15.9	15.7	15.5	14.8	12.0	<b>0.25</b>	13.5	13.0	12.9	12.7	12.4	12.0	9.7
<b>6</b>	<b>0.50</b>	28.5	27.5	26.9	26.6	26.0	25.0	20.7	<b>0.25</b>	28.0	27.1	26.7	26.0	25.7	24.4	19.8
<b>8</b>	<b>0.50</b>	42.1	40.8	39.9	39.3	38.6	37.0	29.9	<b>0.25</b>	36.7	35.3	34.5	34.3	33.3	31.6	25.4
<b>12</b>	<b>0.50</b>	57.5	55.6	54.7	53.9	53.5	52.2	44.1	<b>0.25</b>	50.6	49.1	48.1	47.6	46.2	44.0	35.5
<b>20</b>	<b>0.50</b>	77.0	75.5	74.6	74.2	73.5	72.0	61.9	<b>0.25</b>	71.7	70.2	69.0	68.6	67.0	64.6	54.4
	<b><math>a_T=0.05</math> m</b>								<b><math>a_T=0.05</math> m</b>							
<b>1</b>	<b>0.125</b>	5.7	5.6	5.5	5.4	5.1	5.0	3.7	<b>0.125</b>	5.1	4.9	4.7	4.6	4.4	4.1	3.0
<b>3</b>	<b>0.125</b>	17.0	16.5	16.2	16.0	15.4	14.8	11.9	<b>0.125</b>	14.0	13.4	13.0	12.6	12.4	11.5	9.0
<b>6</b>	<b>0.125</b>	33.3	31.9	31.2	30.8	30.2	29.2	23.7	<b>0.125</b>	29.8	28.3	27.8	27.0	26.5	24.7	20.3
<b>8</b>	<b>0.125</b>	43.5	42.1	41.5	40.9	40.3	39.0	32.7	<b>0.125</b>	40.4	38.3	37.5	37.1	36.1	34.3	27.0
<b>12</b>	<b>0.125</b>	61.8	59.7	59.1	58.3	57.5	55.8	47.1	<b>0.125</b>	56.4	54.2	53.1	52.2	51.2	48.2	39.1
<b>20</b>	<b>0.125</b>	86.3	84.7	84.2	83.1	82.9	80.6	68.7	<b>0.125</b>	76.9	74.8	73.9	73.1	71.7	68.9	56.9
	<b><math>a_T=0.10</math> m</b>								<b><math>a_T=0.10</math> m</b>							
<b>1</b>	<b>0.0625</b>	5.4	5.1	5.1	4.8	4.8	4.6	3.7	<b>0.0625</b>	4.9	4.6	4.4	4.1	4.1	3.9	3.1
<b>3</b>	<b>0.0625</b>	17.1	15.9	15.8	15.2	14.9	14.1	10.9	<b>0.0625</b>	14.7	13.7	13.0	12.4	12.2	11.5	8.4
<b>6</b>	<b>0.0625</b>	31.6	29.4	28.5	27.6	27.1	25.5	19.7	<b>0.0625</b>	28.9	26.6	25.7	25.0	24.0	22.7	17.2
<b>8</b>	<b>0.0625</b>	43.2	40.0	38.6	37.8	36.8	34.8	27.6	<b>0.0625</b>	37.5	34.7	33.2	32.4	31.2	29.2	22.7
<b>12</b>	<b>0.0625</b>	60.8	56.5	54.8	53.7	52.5	49.5	38.8	<b>0.0625</b>	54.5	50.4	48.9	47.1	45.6	42.7	32.5
<b>20</b>	<b>0.0625</b>	86.2	82.7	81.0	79.5	78.5	74.9	59.3	<b>0.0625</b>	74.7	71.1	69.4	67.8	65.9	61.9	47.9
	<b><math>a_T=0.20</math> m</b>								<b><math>a_T=0.20</math> m</b>							
<b>1</b>	<b>0.030</b>	4.0	3.4	3.2	3.0	3.0	2.7	1.7	<b>0.015</b>	3.8	3.5	3.4	3.2	3.0	2.7	1.9
<b>3</b>	<b>0.030</b>	12.8	11.2	10.6	10.3	10.0	9.2	5.9	<b>0.015</b>	12.2	10.4	10.0	9.4	8.9	7.9	5.1
<b>6</b>	<b>0.030</b>	22.0	19.2	18.0	17.8	16.7	15.6	10.0	<b>0.015</b>	22.0	19.0	17.8	16.6	15.8	14.3	9.7
<b>8</b>	<b>0.030</b>	31.1	26.6	25.3	24.5	23.2	21.3	14.7	<b>0.015</b>	29.2	24.8	23.4	22.2	21.2	18.6	12.6
<b>12</b>	<b>0.030</b>	44.7	38.6	37.0	35.8	34.3	31.7	21.0	<b>0.015</b>	44.0	38.2	36.2	34.8	33.0	29.4	18.6
<b>20</b>	<b>0.030</b>	64.6	57.8	55.6	53.6	52.7	48.0	32.8	<b>0.015</b>	62.3	55.6	53.0	50.9	48.6	43.4	29.9
	<b><math>a_T=0.50</math> m</b>								<b><math>a_T=0.50</math> m</b>							
<b>1</b>	<b>0.015</b>	2.2	2.0	1.9	1.6	1.5	1.2	0.4	<b>0.015</b>	2.1	1.8	1.7	1.5	1.4	1.0	0.7
<b>3</b>	<b>0.015</b>	7.7	6.7	6.4	5.8	5.4	4.1	1.6	<b>0.015</b>	6.8	5.4	4.9	4.4	4.0	3.1	1.8
<b>6</b>	<b>0.015</b>	12.7	10.9	10.4	9.7	9.3	7.2	2.7	<b>0.015</b>	12.0	10.0	8.9	8.0	7.3	5.6	3.4
<b>8</b>	<b>0.015</b>	18.1	15.6	14.4	13.4	12.2	9.5	4.0	<b>0.015</b>	16.6	13.9	12.5	11.8	10.6	8.4	4.6
<b>12</b>	<b>0.015</b>	25.3	21.6	20.5	19.0	17.8	14.0	5.7	<b>0.015</b>	25.4	22.1	20.5	19.2	17.5	13.5	6.0
<b>20</b>	<b>0.015</b>	36.9	32.9	31.5	29.8	28.0	22.3	9.2	<b>0.015</b>	34.7	30.6	28.9	26.8	24.6	19.3	9.9

NOW: No of Wells, NDFS: Normalized Distance from Source, D: Daily, 1M: Every Month, 2M: Once every two months, 3M: Once every three months, 4M: Once every four months, 6M: Bi-Annually, A: Annually

arrangement of wells, with NDFS selected as the distance where the performance of the majority of the wells was maximized. (Mahar & Datta, 2000) have concluded that, with the exception of low transverse dispersive subsurface environments, observation wells should be located downstream, in close proximity to contamination sources. All numerical experiments were based on 3,000 Monte Carlo flow simulations and 8,000 tracking particles. Sampling frequencies that were considered were as follows: daily (D), once every month (1 M), once every 2 months (2 M), once every 3 months (3 M), once every 4 months (4 M), bi-annually (6 M), and annually (A).

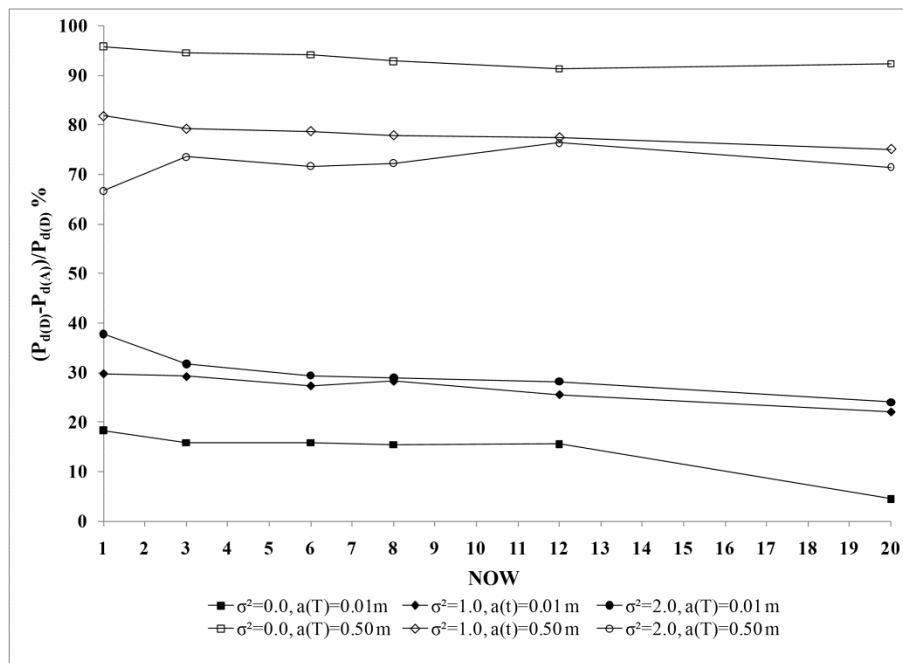


**Figure 4.2:** Percent detection change between daily and annual sampling for different well arrangements and types of soil

Several conclusions can be drawn from these tables. Monitoring networks with up to 6 wells have, at best, a 35% chance to detect subsurface contamination, which quickly deteriorates even further if sampling becomes less frequent than once-a-day and the geologic environment departs from ideal homogeneous conditions. The addition of two more wells, i.e., a network of 8 wells with sampling only twice per year performs practically at least as well, for all types of soils considered here, with 6 wells, where samples are collected and analyzed every day. It appears therefore that networks of 6 wells do not accomplish the goal of successful monitoring, considering both their low probability of detection and the fact that an intense, daily, sampling effort, and corresponding expenditure, is required in order to maintain such low performance. Furthermore, for all types of soils and dispersions analyzed, networks of 8 wells, even if sampled daily, have a maximum detection probability that does

not exceed 50%. This means that under the best conditions, at least at the numerical level, one out of two contamination events would remain undetected, if monitored by 8 wells. If a higher confidence is needed in the performance of a monitoring network to detect contaminant plumes then 20 wells are required in order to at least, with a monthly sampling, in the majority of situations ( $a_T \leq 0.20$  m) have a probability of detection that is greater than the probability of failure to detect.

Figure 4.2 plots the percent change of  $P_d$  between daily and annual sampling for all combinations of monitoring wells and different types of soils. When the subsurface environment is homogeneous and of low dispersion ( $\alpha_T=0.01$  m) arrangements that consist of up to 12 wells have a deterioration of about 20% in their respective  $P_d$ , whereas 20 wells have a decrease in detection of about 5%. A potential explanation of this result, in conjunction with the values in Table 1 that show almost full detection for 20 wells, is that in homogeneous media of low dispersion a large number of wells, such as 20 wells, provide such a dense coverage of the area downstream a landfill that a plume cannot remain undetected and even a single observation is sufficient to verify a contamination event. In contrast homogeneous soils of high dispersion ( $a_T=0.5$ m) indicate an almost doubling of the detection capability if sampling is performed daily compared to that of annually. This result indicates that, irrespective of the density of the monitoring network, because contaminants disperse strongly concentrations at the monitoring points can quickly drop below the threshold detection limits, and hence the detection capability of a monitoring network in such an environment can become extremely low, unless a rigorous sampling schedule is followed. A similar situation holds for heterogeneous soils of high dispersion, with the heterogeneity appearing to ameliorate slightly the dispersion effects, but not sufficiently, in practical terms in order to alter our conclusion about the criticality of the sampling schedule. Finally, heterogeneous soils of low dispersion appear to increase the discrepancy between the sampling schedules with most notable the influence on 20-well arrangements. In this type of soils full detection is no longer possible with 20 wells and only the combination of a dense network and frequent sampling can retain a credibly high level of detection (Table 4.1 and Table 4.2).

The effect of dispersion on the detection probability attained through various sampling frequencies is illustrated in Figure 4.3. This figure utilizes 12 wells and plots the ratio of  $P_d/P_{d(D)}$  as a function of the  $\log_{10}(a_T)$  for homogeneous soils ( $\sigma_{\ln k}^2 = 0.0$ ). Here  $P_d$  corresponds to the detection probability of a sampling schedule, and  $P_{d(D)}$  to that of daily sampling. For a homogeneous field as transverse dispersion increases the ratio of  $P_d/P_{d(D)}$  decreases. For all sampling schedules (with the exception of annual sampling) it appears that

for  $a_T$  in the range of 0.01m to 0.10m the departure of detection achieved by any sampling frequency to that by daily sampling,  $P_{d(D)}$ , appears to remain approximately constant and smaller than 10%. At  $a_T = 0.20\text{m}$  an additional 10% decline in detection is observed relative to that at  $a_T = 0.10\text{m}$ , and subsequently the ratio  $P_d/P_{d(D)}$  remained constant, until  $a_T = 0.50\text{m}$ . If annual sampling is considered then the ratio  $P_d/P_{d(D)}$  continuously declines, and when  $a_T > 0.10\text{m}$  the rate of decline becomes very sharp. This figure in conjunction with Table 4.1 indicate that in homogeneous soils and for dispersions up to  $a_T \leq 0.20\text{m}$  monthly sampling at 12 wells retains a probability of detection that is greater than 60%, which in practical terms does not differ significantly from that attained by daily sampling. For greater dispersion coefficients this particular well arrangement returns a probability of detection that is equal to or lower to the probability of failure to detect, deteriorating very rapidly the moment sampling departs from a daily schedule. For 12 wells in heterogeneous soils a similar analysis did not provide any additional insight to the pattern of behavior observed in Figure 4.3 and Figure 4.4.

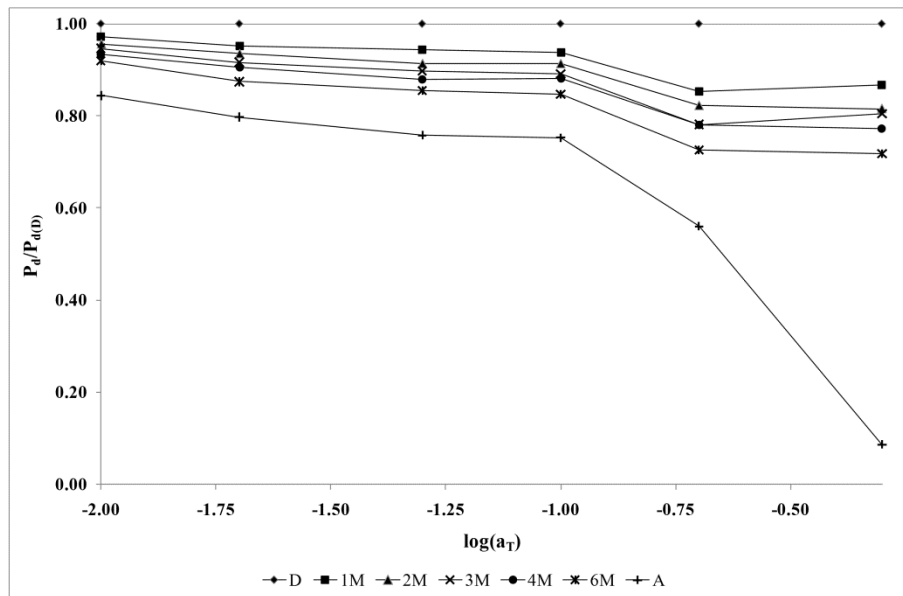


**Figure 4.3:** 12 monitoring wells:  $P_d/P_{d(D)}$  versus  $\log_{10}(a_T)$  for homogeneous soils ( $\sigma_{lnK}^2 = 0.0$ )

Field heterogeneity did not appear to affect contaminant detection probability as strongly as transverse dispersion did. Figure 4a indicates that when the transverse dispersion coefficient was equal to or less than 0.20m and for sampling performed at least three times a

year the ratio  $P_d/P_{d(D)}$  remained approximately constant (with minor fluctuations, which are on the average less than 2%) as the variance of  $\ln K$ ,  $\sigma_{\ln K}^2$ , increased. If sampling became more sparse then a decrease of  $P_d/P_{d(D)}$  on the average of 5%, and 20% for the bi-annual and annual schedules, respectively, relative to daily sampling was observed.

When the transverse dispersion coefficient  $a_T$  equaled 0.50m it appeared that in certain situations an increase in the heterogeneity ameliorated the effects of large transverse dispersion. This can be seen in Figure 4.4(b) for all types of sampling, up to bi-annual, where initially, the detection probability declined by approximately 6%, relative to that by daily sampling, as the field became mildly heterogeneous ( $\sigma_{\ln K}^2 = 0.5$ ), and then increased by the same amount when  $\sigma_{\ln K}^2 = 1.0$  to remain constant and equal to the detection achieved by daily sampling, for higher heterogeneities. For bi-annual sampling the initial decrease in  $P_d/P_{d(D)}$  was 18% at  $\sigma_{\ln K}^2 = 0.5$  and continued to decrease by an additional 10% as heterogeneity increased. In contrast when sampling took place only once a year the ratio  $P_d/P_{d(D)}$  improved with increased field heterogeneity. This improvement was of the order of 120% from  $\sigma_{\ln K}^2 = 0.0$  to  $\sigma_{\ln K}^2 = 0.5$ , and by another 20% as  $\sigma_{\ln K}^2$  reached the value of 2.0.

An explanation for this behavior may be that while high transverse dispersion leads to greater dilution and lower concentrations at set monitoring points after a time interval, which would not be possible to detect if sampling is not frequent, high heterogeneity through the presence of low permeability regions may impede the lateral spread of contaminants, thus counteracting the effects of transverse dispersion. Irrespective of the above, at this level of dispersion the use of 12 wells achieved a maximum detection of 27% (Table 4.1), if sampled daily and any other sampling schedule corresponded to a monitoring of plume migration of an even lower efficiency. The frequency of sampling is of interest in order to minimize the time lag between the time that concentrations above a threshold limit first appear at the locations of a monitoring network and the time that these concentrations are actually observed through sampling. The effort of course is to identify the extent of the contaminated area as soon as contaminants become observable and to initiate remediation efforts as soon as possible.

In order to investigate these aspects in each Monte Carlo realization, for each  $\sigma_{\ln K}^2$  and  $a_T$  hydrogeological case analyzed, the time of contaminant release from the landfill facility was set to zero. The time step of our numerical calculations was 1 day and the number of days ( $T_{ar}$ ) required for concentrations above a threshold limit to arrive at an, at least, one well of

an 8-well arrangement was recorded for each realization. Then, if one were to utilize, for example, a monthly monitoring schedule the concentrations at the well monitoring locations would be checked 30-days after the initial contaminant release to observe whether they exceeded or not the threshold limit. If no exceedance of the limit was detected then the next checking period at the wells would be 30-days later and so on. The number of days ( $T_{obs}$ ) for observation of contamination to be achieved at the monitoring points, based on a specific sampling schedule, would be recorded. The ratio of average observation time,  $\langle T_{obs} \rangle$ , to average arrival time of contaminants at the monitoring points,  $\langle T_{ar} \rangle$ , over 3,000 simulations for each  $\sigma_{lnK}^2$  and  $a_T$  case is plotted on the  $y$ -axis of Figure 4.5. Of course a daily sampling with our numerical time step set equal to 1 day would return a ratio equal to unity for all hydrogeological cases.

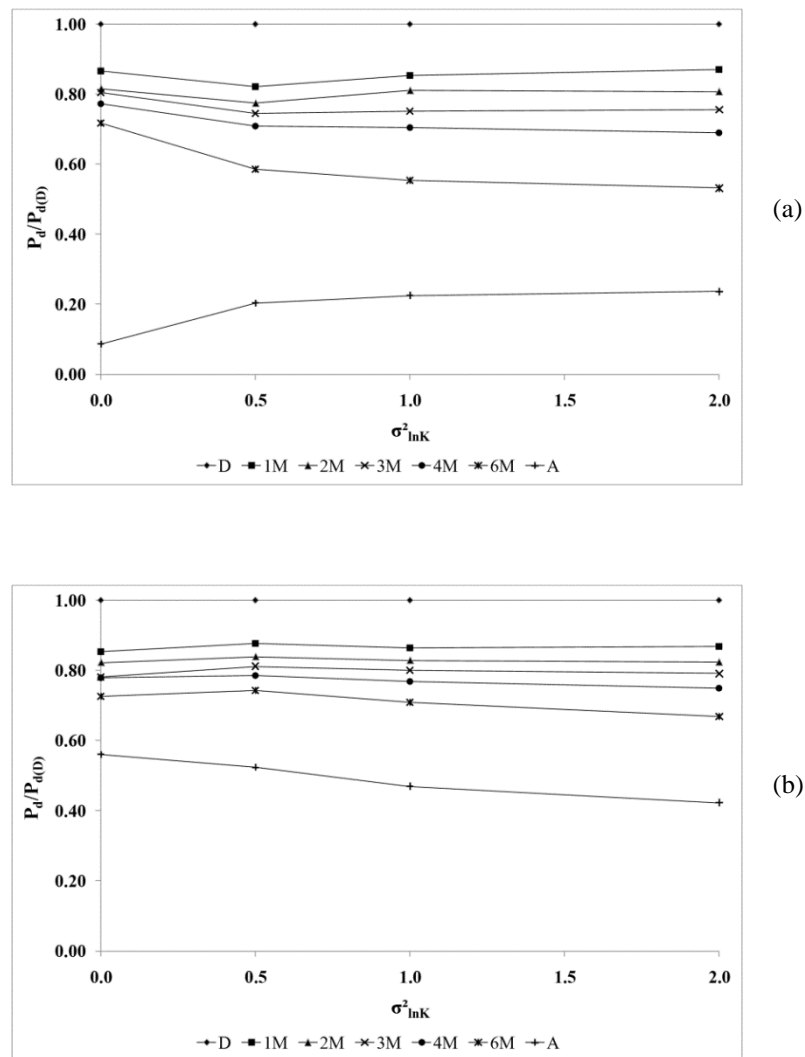
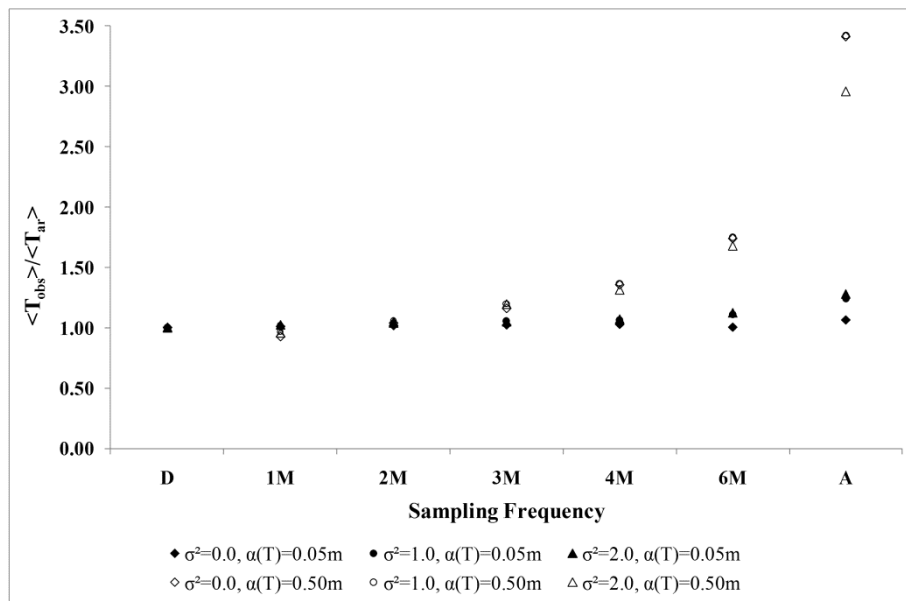


Figure 4.4:  $P_d / P_{d(D)}$  versus  $\sigma_{lnK}^2$ : (a)  $\alpha_T = 0.20m$ , and (b)  $\alpha_T = 0.50m$  for 12 monitoring wells

Figure 4.5 shows that when dispersion is low ( $a_T = 0.05\text{m}$ ) the average observation time does not differ from the average arrival time if groundwater is sampled no later than every 4 months. The frequency of sampling starts to affect the ratio  $\langle T_{obs} \rangle / \langle T_{ar} \rangle$  only when the variance of  $\ln K$  becomes greater than one and sampling is performed bi-annually or annually. When  $a_T = 0.05\text{m}$  and  $\sigma_{\ln K}^2 = 2.0$  then annual sampling returned a  $\langle T_{obs} \rangle$  that is 20% higher than  $\langle T_{ar} \rangle$ .



**Figure 4.5:**  $\langle T_{obs} \rangle / \langle T_{ar} \rangle$  versus sampling frequency for an 8-well monitoring arrangement in different hydrogeological environments

The average observation time starts to diverge from the average arrival time when dispersion is high ( $a_T = 0.50\text{m}$ ) and sampling is performed less frequent than every 3 months. Then there is a 25% difference between the times of observation and first arrival of the contaminants at the monitoring locations, which increases to 240% in the case of annual sampling. Therefore, it appears that if one wishes, under the specific conditions of the hydraulic gradient considered in this study, to detect contaminants as soon as they reach monitoring check-points collection of samples every 2 months appears to be a safe sampling strategy for a wide range of hydrogeological environments. When the hydraulic gradient is one order of magnitude smaller than the one considered here it was calculated through numerical experiments that the average  $P_d$  differs by about 15% from that of our base hydraulic gradient case, leading to approximately the same sampling strategy. On the other hand, when the hydraulic gradient is one order of magnitude greater than our base hydraulic

gradient case the average  $P_d$  from all monitoring cases differs by about 60% from the results presented here, and the sampling strategy to be developed would differ from that of the base case discussed here.

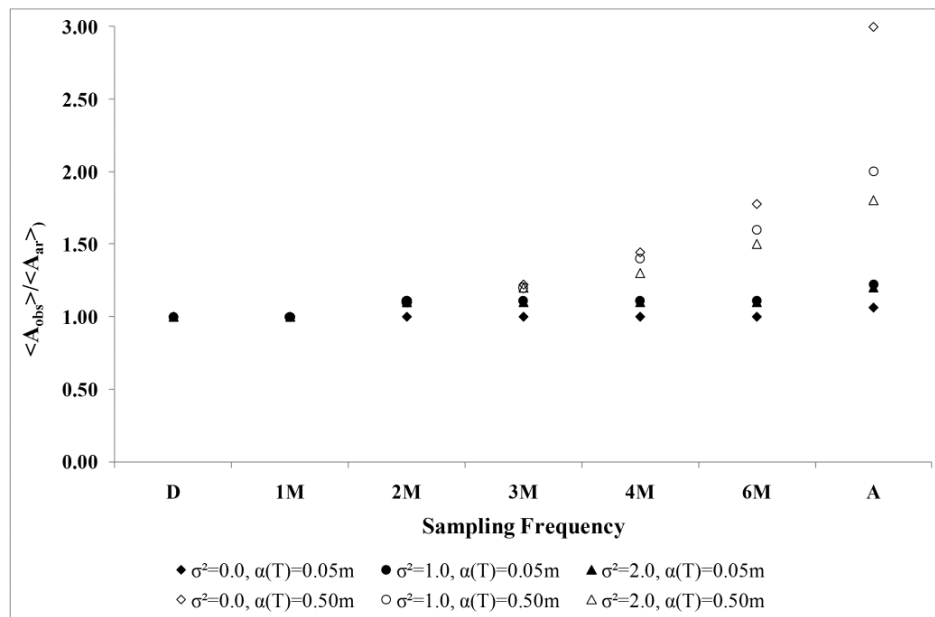
The discrepancy between average observation and arrival times translates into differences between the average area of the plume that exists when the first above-the-threshold concentrations have reached the monitoring points,  $\langle A_{ar} \rangle$ , and the extent of that area when observation of the subsurface contamination is made,  $\langle A_{obs} \rangle$ . The extent to which a contaminated area has grown as a result of infrequent observation has of course consequences in the volume of groundwater needed to be treated, and correspondingly, in the cost of remediation.

Figure 4.6 shows that when groundwater samples are obtained at least once a month, then no change in the contaminated area occurs as a result of the monthly delay in sampling compared to that by a daily schedule, irrespective of hydrogeological conditions. When dispersion is low ( $a_T = 0.05\text{m}$ ) it appears that the movement of contaminants in the subsurface environment is so slow that the contaminated area does not increase by more than 10% from the area that an optimum daily sampling would discern. In this case even sparse information on the state of groundwater, even of the order of once a year, would not lead to significantly more costly remediation efforts.

For high dispersion ( $a_T = 0.50\text{m}$ ) an initial observation from Figure 4.6 is that with the exception of monthly sampling all other less frequent sampling schedules result in significant delays in detecting contaminant concentrations at the monitoring points, which allow the plume area to enlarge and hence result in more costly remediation efforts. The less frequent the sampling the more the plume has time to enlarge, with for example, in the case of sampling that is performed every 4 months, the plume to have grown, in some subsurface environments, by at least 50% relative to its size at the time of the plume's first arrival at the monitoring wells. The second observation is that when dispersion is high, stronger heterogeneities (the existence of high and low permeability zones) appear to mitigate a plume's evolution and not allowing it to spread as much as in environments of low heterogeneity.

Thus, Figure 4.6 shows that for all sampling schedules in high dispersion environments strong heterogeneities  $\sigma_{\ln K}^2 \geq 1.0$  result in smaller  $\langle A_{obs} \rangle / \langle A_{ar} \rangle$  ratios than those that correspond to  $\sigma_{\ln K}^2 \leq 0.5$ . The fact that infrequent sampling in strongly heterogeneous environments provides plume areas that do not diverge as strongly, from the plume areas existing at the time of monitoring-point arrival, as in mild or homogeneous environments

seems to support the notion that the existence of high and low permeability zones appear to impede a plume's spread and the effects of high dispersion.



**Figure 4.6:**  $\langle A_{obs} \rangle / \langle A_{ar} \rangle$  versus sampling frequency for an 8-well monitoring arrangement in different hydrogeological environments

#### 4.4 Remediation Delay

Decision analyses of remediation actions define a risk term  $R$ , which associates the cost of remediation of a contaminated volume of groundwater,  $C_d$ , and the cost  $C_f$  of a much larger volume, due to failure of the monitoring system to detect with the probability of detection  $P_d$ , and the probability of failure  $P_f = 1 - P_d$ . Thus,  $R$  measures the performance of various monitoring systems via the impact that different levels of detection have on remediation costs (Freeze et al., 1990; Yenigul et al., 2006):

$$R = P_d C_d + P_f C_f \quad (4.1)$$

This description assumes that remediation takes place immediately after detection, i.e., that the groundwater volume to be remediated coincides with the contaminated volume at detection time. (Papapetridis & Paleologos, 2011a) provided a correction for the delay in response, which results in an increase of the contaminated volume, as the plume continues to evolve, and correspondingly to an increase of the remediation cost compared to that if the contaminated volume at detection were to be used. *Papapetridis and Paleologos (2011a)*

(Papapetridis & Paleologos, 2011a) defined a corrected risk  $R^{cor}$  that accounts for the remedial action response delay as follows:

$$R^{cor} = P_d^{cor} C_d + P_f^{cor} C_f \quad (4.2)$$

where

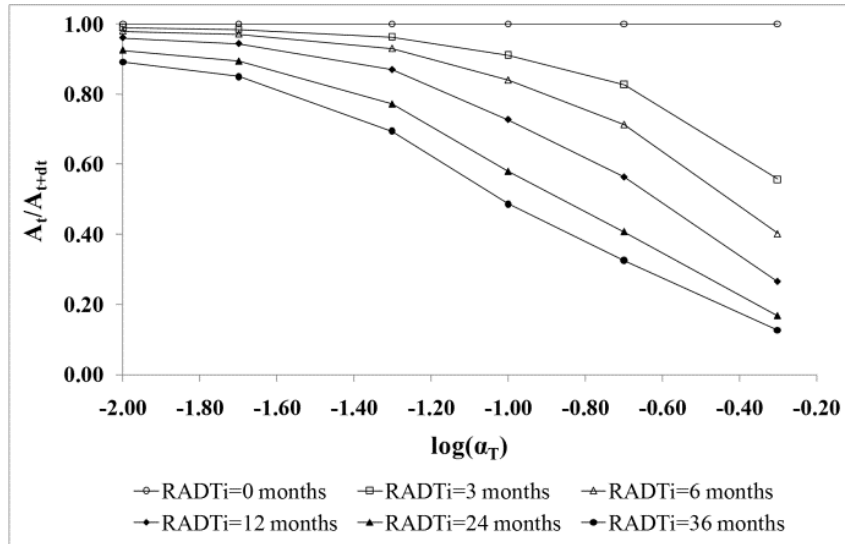
$$P_d^{cor} = P_d \left( \frac{A_t}{A_{t+dt}} \right) \quad (4.3)$$

and

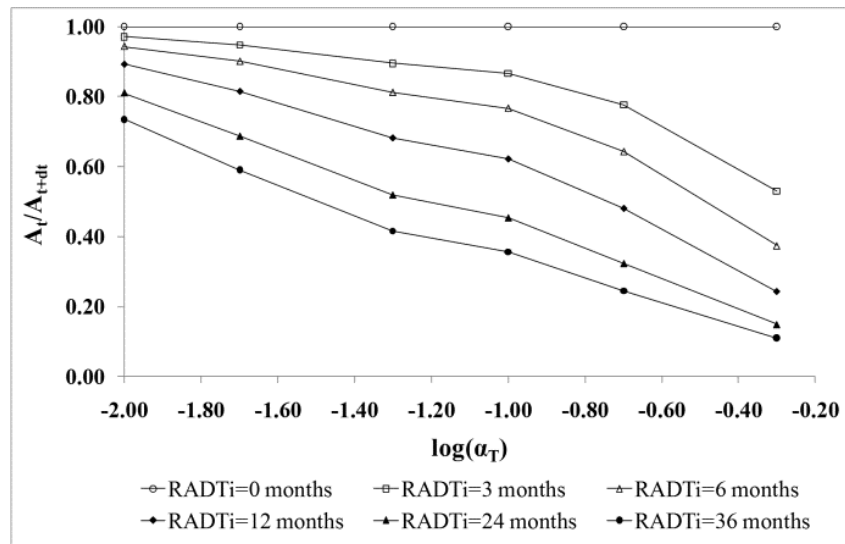
$$P_f^{cor} = 1 - P_d^{cor} \quad (4.4)$$

The corrected detection probability  $P_d^{cor}$  is a measure of the economic impact of a remedial action delay, when the contaminated area has extended to  $A_{t+dt}$ , as a divergence from the maximum economic outcome that would take place at detection time, when the contaminated area is  $A_t$ . This procedure results in increasing the failure probability and weighted cost of failure in the calculation of the risk factor as the time interval  $dt$  increases. Sensitivity analyses can then illustrate to decision-makers the influence of remedial delays on the cost of remediation.

Figure 4. demonstrates the influence of dispersion on the first term, the weighted cost due to detection, and correspondingly, the increase of the much larger failure term in Equation (4.1), through the ratio  $A_t/A_{t+dt}$ , in homogeneous and heterogeneous soils for different Remedial Action Delay Times (RADTi). In homogeneous soils (Figure 4.a) delays of even 6 months at  $a_r = 0.10\text{m}$  result in a 20% downgrading of the first term of equation (4.1), and at  $a_r = 0.50\text{m}$  this reduction reaches about 60%. At 2 or 3-year time delays for  $a_r = 0.10\text{m}$  an almost 45% reduction of the weight of the first term in the calculation of the risk has occurred, which for highly dispersive environments of  $a_r = 0.50\text{m}$  this reaches almost 80%. The difference between homogeneous and heterogeneous soils (Figure 4.b) is that in heterogeneous soils the impact of consecutive delays on the ratio  $A_t/A_{t+dt}$  tends to be greater than that in homogeneous soils of similar dispersion. It appears that in highly dispersive environments not only sampling must be very frequent, in order not to allow the contaminated area to grow as a result of lack of observation, but in addition the remediation response must be of the order of a few months if one does not wish the remediation costs to grow significantly.



(a)



(b)

**Figure 4.7:**  $A_t/A_{t+dt}$  versus  $\log(\alpha_T)$  for 6 monitoring wells and different Remedial Action Delay Times (RADTi): (a) homogeneous, and (b) heterogeneous soils with  $\sigma_Y^2 = 1.0$

The heterogeneity of the subsurface environment influences the ratio  $A_t/A_{t+dt}$  but not to the same extent as dispersion. Figure 4.8 illustrates that in low dispersion environments ( $a_T = 0.02\text{m}$ ) delays of up to 6 months would decrease the ratio  $A_t/A_{t+dt}$  by less than 20% in highly heterogeneous soils, an equivalent result to that obtained previously for  $a_T = 0.10\text{m}$  and homogeneous soils. A five-fold increase in the dispersion coefficient produces an

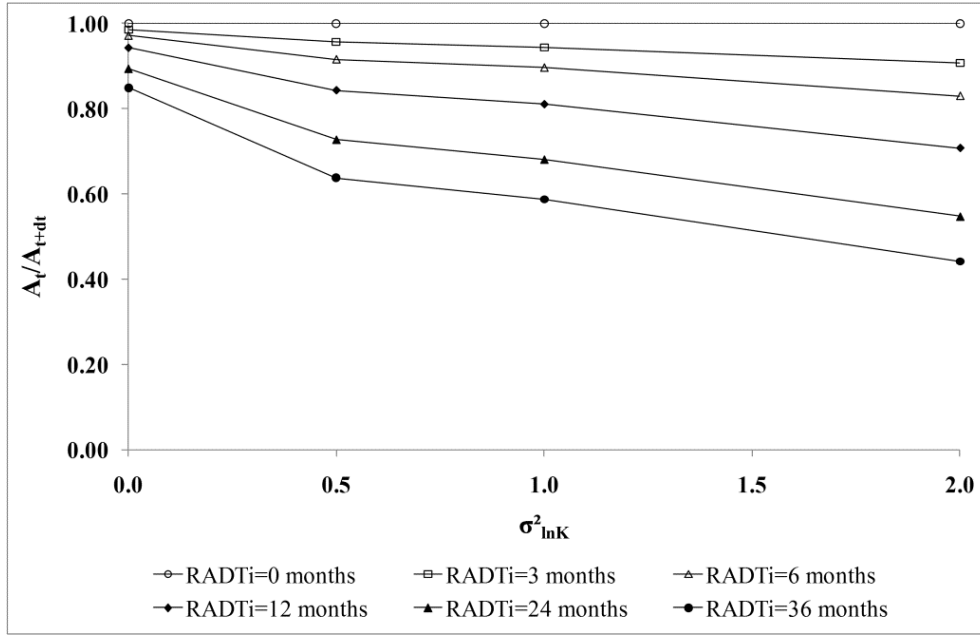


**Figure 4.8:**  $A_t/A_{t+dt}$  versus heterogeneity  $\sigma_Y^2$  for fixed dispersion  $\alpha_T = 0.02 \text{ m}$  for different Remedial Action Delay Times (RADTi) and 3 monitoring wells

equivalent spread in the contamination to that by several orders of magnitude increase in the heterogeneity of a field. At 2 or 3-year time delays again for ( $a_T = 0.02\text{m}$  an almost 45% reduction of the weight of the first term in the calculation of the risk has occurred at  $\sigma_{\ln K}^2 = 2.0$ , an equivalent result to that of homogeneous soils with a five times higher dispersion. Results in high dispersion environments ( $a_T = 0.20\text{m}$ ) exhibited a similar pattern to that of Figure 4. with the main difference being that the impact of consecutive delays on the ratio  $A_t/A_{t+dt}$  tended to be greater at the same  $\sigma_{\ln K}^2$  than that presented in this figure. Both Figure 4. and Figure 4.8 calculate the areas  $A_t$  considering immediate detection, i.e., of sampling that is performed daily.

## 4.5 Conclusions

This work investigates the impact of sampling frequency on the probability to detect groundwater contamination in various subsurface environments, as well as the effects that sampling schedules and remediation delays have on the growth of contaminated subsurface areas and remediation costs. High-resolution numerical Monte Carlo realizations were utilized to simulate contaminant movement in heterogeneous, two-dimensional aquifers and to calculate the probabilities of detection  $P_d$ , and contaminated areas by various monitoring well arrangements. Networks of 8 wells, even if sampled daily, had a maximum detection probability that under the best conditions allowed one out of two contamination events to

remain undetected. If a higher confidence in the performance of a monitoring network was needed then 20 wells sampled monthly returned a probability of detection greater than the probability of failure even in highly dispersive environments. In homogeneous media of low dispersion a large number of wells provide such density of coverage of the area downstream a landfill that a plume cannot remain undetected even with few observations. In contrast in homogeneous soils of high dispersion, irrespective of the density of monitoring network, because contaminants disperse strongly and concentrations at the monitoring points drop below the threshold limits quickly a rigorous sampling schedule must be followed in order to retain a network's performance. A similar situation holds for heterogeneous soils of high dispersion, with the existence of low permeability zones appearing to ameliorate the dispersion effects, but not sufficiently in order to alter our conclusion about the criticality of the sampling schedule. The frequency of sampling is also of interest in order to minimize the time lag between the time that concentrations above a threshold limit first appear at monitoring locations and the time that these concentrations get to be observed through sampling. The objective of course is to delineate the extent of the contaminated area and to initiate remediation efforts as soon as possible. Analysis of the lag between the time that contaminants appeared at monitoring sites and the time they got to be observed led to the conclusion that, in terms of time delay, sampling every 2 months constitutes a safe strategy for a wide range of hydrogeological environments. In the case of aquifers that exhibit fast pathways of contaminant transport, through the existence of high permeability zones, farther investigation is required. However, in terms of growth of contaminated area with the exception of monthly sampling all other less frequent schedules resulted in significant enlargement of plume areas, thus leading to more costly remediation.

Traditional decision analyses assume that remediation takes place immediately after detection that is that the groundwater volume to be remediated coincides with the contaminated volume at detection time. Based on a correction presented by (Papapetridis & Paleologos, 2011a) for remedial response delays, which result in an increase of the contaminated volume as the plume continues to evolve, the current study demonstrates that in highly dispersive environments the remediation response must be of the order of a few months if one does not wish the contaminated areas and remediation costs to grow significantly.

# CHAPTER 5

## Parameters on stochastic simulation of contaminant detection probability

---

### 5.1 Introduction

Groundwater contamination plume detection is an important aspect of environmental protection, during landfill operation and after closure time. Groundwater monitoring network design and operation has become a subject of major concern mainly in the last three decades (Nunes et al., 2007). Successful detection of an underground pollutant transported into an aquifer is directly dependent on the information of a possible protective barrier failure and the possibility of calculating the movement and dispersion of the pollutant in an environment about which very few things are actually known. This lack of information is caused by the fact that there are difficulties of experimentally measuring, at any point in the geological field, its various hydraulic properties (hydraulic conductivity, hydraulic head, porosity etc.) so as to predict, or even approximate, the way a plume can propagate into the aquifer. Additional uncertainty factors of the problem are lack of information about the geometry and the number of sources from which pollution originates in a landfill waste, the quantity of pollution intruding into the aquifer as well as the duration of the leak.

In order to simulate hydro-geological as well as epistemic uncertainties, the latter arising through lack of knowledge of the landfill and monitoring installation system parameters, a stochastic model in a Monte Carlo context has been utilized. *Yenigul et al.* (2006) performed simulations studying in two dimensions the effect of a field's heterogeneity and dispersion on detection probability of groundwater pollution by a linear arrangement of a landfill's downgradient monitoring wells, originating from a random, single point source inside the vicinity of the installation. The effect of the number of wells, their distance from the landfill and the size of the source were studied too. *Papapetridis and Paleologos* (2011a) performed high resolution Monte Carlo numerical experiments studying more hydro-geological cases, in addition to the effect of monitoring wells sampling frequency.

In the present study we examine how the number of point sources, the size of the controlled area (landfill) and the quantity of an instantaneous aquifer injection pollution event affect groundwater pollution detection probability of a monitoring installation. For this purpose a two-dimensional stochastic model is utilized to perform numerical experiments. The monitoring installation was considered in different cases to be located in various distances from the landfill facility and perpendicular to the flow field. This work extends that of *Papapetridis and Paleologos (2011a)*, thoroughly investigating additional uncertainty aspects of detecting instantaneous aquifer pollution. In each examined parameter it is considered that the rest of the factors affecting detection probability estimation remain constant. Simulations are performed in the context of uncertainty factors deriving from the environment itself, where the pollution is propagating, and from the lack of information about certain parameters, concerning the initial conditions of the leak.

## 5.2 Model description and simulation results

A 2-D steady groundwater flow in a heterogeneous, isotropic and confined aquifer was considered in this study. Our study employed the Monte Carlo numerical framework to simulate groundwater flow and contaminant transport in 2-D heterogeneous aquifers with the use of the Spectral Turning Bands Method (STUBA) (Mantoglou & Wilson, 1982) to stochastically simulate hydro-geological heterogeneity and the Random Walk Tracking Particles algorithm (Tompson et al., 1987a; Salamon et al., 2006b) to simulate the advection and dispersion of the pollution into the aquifer.

Hydro-geological heterogeneity was expressed through the natural logarithm of hydraulic conductivity variance  $\sigma_{\ln K}^2$ , which varied among 0.0 (homogeneous aquifer), 1.0 (medium heterogeneity) and 2.0 (strongly heterogeneous aquifer). The mean of the log hydraulic conductivity was set equal to 2.3. The correlation length,  $\lambda$ , was considered constant and equal to 20 m for both directions  $x$  and  $y$ . Transverse dispersion coefficients,  $\alpha_T$ , were set equal to  $\alpha_T = 0.01, 0.05, 0.10, 0.50$  m, corresponding to values observed in field experiments, and the longitudinal dispersion coefficient,  $\alpha_L$ , was calculated by the relation  $\alpha_L = 10\alpha_T$ . Contaminant transport into the subsurface heterogeneous environment was simulated using the Particle Tracking method based on the ‘Random Walk’ approach.

The simulated region was 1000m long and 400m wide, discretized by  $\Delta x = \Delta y = 2 \times 2m^2$  cells, creating a  $500 \times 200$  grid. 3,000 Monte Carlo realizations were performed in order to calculate groundwater pollution detection probability by a linear arrangement of monitoring wells. Six linear configurations were examined, consisting of 1, 3,

4, 6, 8, 12 and 20 wells, equally spaced from one another. Wells that were located at the ends of each arrangement were placed half the distance from the cell's top and bottom edges, so that the efficiency of the monitoring system would be maximized. Monitoring of the aquifer and plume evolution was simulated for a 30-year period.

The simulation parameters of the control area where simulation originated, the quantity of pollution that entered the aquifer instantaneously at  $t = 0$  and the number of sources were customized accordingly, so that their effect on monitoring efficiency could be examined. More details on the simulation model development are referred at *Papapetridis and Paleologos (2012a)*.

### 5.2.1 Control Area Size

A rectangular control area of  $120 \times 50 m^2$  – a landfill cell or other installation capable of causing groundwater pollution – was used as reference area  $L$ , situated between x-coordinates of 10 m and 60 m, and y-coordinates of 140 m and 260 m. This specific size was chosen in order to concur with the dimensions of the area used at the study of *Papapetridis and Paleologos (2012a)*. Control area cases that were numerically studied were equal to  $0.3L$ ,  $2L/3$ ,  $L$ ,  $4L/3$ ,  $5L/3$  and  $2L$ . It was assumed that any point within a cell of the control area was an equally-probable source of leakage, taking place once as a single failure event at zero time (when the simulation began) and resulting in an instantaneous ejection of contaminants into the aquifer. The total contaminant mass was equal to 1,000 gr, and was assumed conservative and fully water soluble. The initial concentration of the point source,  $C_0 = M_0 / (nV_0)$  was 4,000 mgr/lt, where  $M_0$  the initial pollution mass,  $n = 0.25$  the effective porosity, and  $V_0 = 1.0 m^3$  the volume. The threshold concentration  $C_{TH}$ , detectable by the monitoring wells, was set at 0.35% of the initial concentration, corresponding to  $C_{TH} = 14 mgr / lt$ .

Simulation results showed that when the size of the control area became larger than  $L$ , then detection probability  $P_d$  diminished. On the other hand, when the size became smaller than  $L$ , detection probability  $P_d$  increased or, if it had already achieved maximum value, it remained the same. At Figure 5.1 it is observed that in case of a homogeneous, low dispersion field (Figure 5.1.a)  $P_d$  drops fast as the control area is increased. Between reference sizes  $L$  and  $2L$  there is a 60% reduction in  $P_d$  when 20 monitoring wells are used, while in the case of a dispersive homogeneous field (Figure 5.1b) the same reduction is only 43%. At monitoring installations with a smaller number of wells this reduction is even bigger, as in case of 3 wells, for example, where  $P_d$  reduction is 84%. When the control area becomes less

that the reference area, then in the first case (Figure 5.1.a) we observe that  $P_d$  remains the same, as it has reached maximum, while at the dispersive case (Figure 5.1.b)  $P_d$  continues to increase as the monitored area goes from  $L$  to  $0.3L$ .

When a heterogeneous field is considered, the same change in  $P_d$  occurs. The difference in  $P_d$  between the control area reference size  $L$  and  $2L$  is 58%, in case of 20 monitoring wells in a low dispersion field (Figure 5.1c), and 54% when a higher dispersion field is simulated (Figure 5.1d). If an installation is made up of 3 wells,  $P_d$  percentage reduction is 85% and 84% respectively.

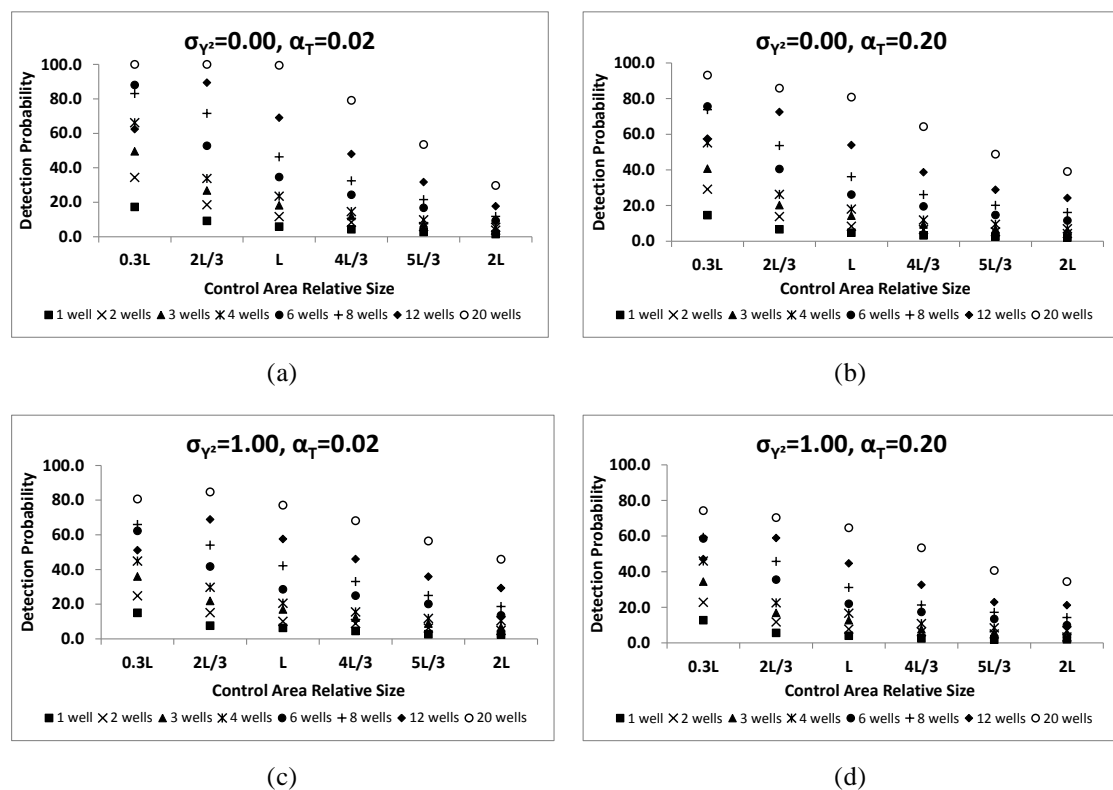


**Figure 5.1:** Detection Probability  $P_d$  change in relation to control area relative size, in a homogeneous low (a) and high (b) dispersion field, and in a heterogeneous low (c) and high (d) dispersion field.

At the heterogeneous case it is observed, though, that when the control area becomes smaller than the reference size  $L$ , then  $P_d$  increases. In a heterogeneous, low dispersion field a dropdown in  $P_d$  (Figure 5.1c) occurs when the control area becomes smaller than  $2L/3$  and at least 12 wells are used, and this fact results from the way monitoring wells are located by the model itself on the grid nodes. During simulation the trailing edge of the control area is divided by the number of wells to be used. The integer part of the outcome is used as the space between two successive wells. In addition, the integer part of half the previous outcome

is used as the starting point for No1 well. In cases where 12 and 20 wells are used, the starting point of the placement of the wells is at the beginning of the control area's trailing edge, leading to a portion of the trailing edge at the top end, equal to the distance between two wells, being unattended. This is why in these cases detection probability seems falsely to be reducing. When dispersion becomes higher, then the effect of monitoring wells placement faints, due to the fact that in higher dispersion aquifers pollution originating from an unattended portion of the control area can still be detected as it covers a larger area while it is transported. In conclusion, it can be said that as the control area's size becomes larger, detection probability  $P_d$  decreases. It has been numerically verified that the fewer the monitoring wells, the less the detection probability. When the control area becomes smaller,  $P_d$  increases until it reaches a maximum point.

Examining the case where monitoring wells density remains constant as the control area changes, then it has been observed (Figure 5.2) that detection probability changes very little. In Figure 5.2, as control area width increases from  $0.3L$  (40 m) to  $2L$  (240 m), the number of wells increases from 2 to 12, providing this way a constant density of wells equal to 0.005. Besides the case of low dispersion homogeneous field, where a  $P_d$  dropdown of 50% is observed between sizes  $4L/3$  and  $2L$ , in the rest of the cases detection probability  $P_d$  changes less than 15%, meaning that monitoring installation efficiency practically remains the same. Consequently, if the width of a control area where possible groundwater pollution may originate is to be increased, so should the number of monitoring wells, maintaining at least the same density as for the initial size.

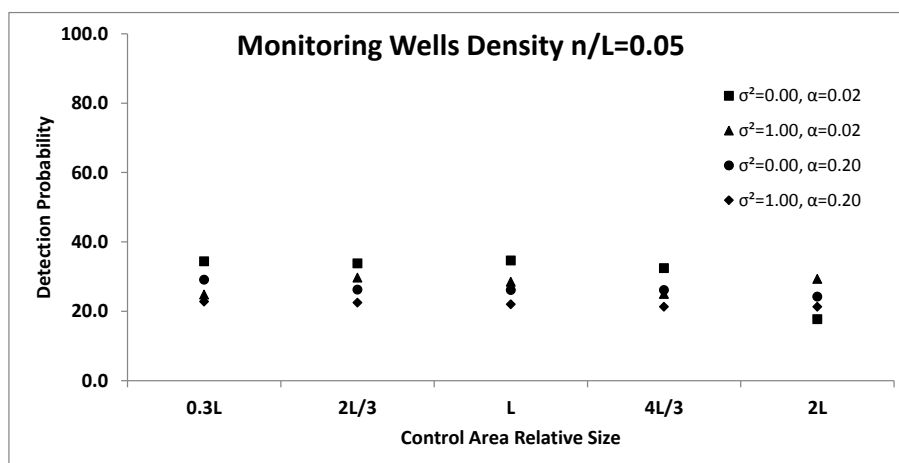
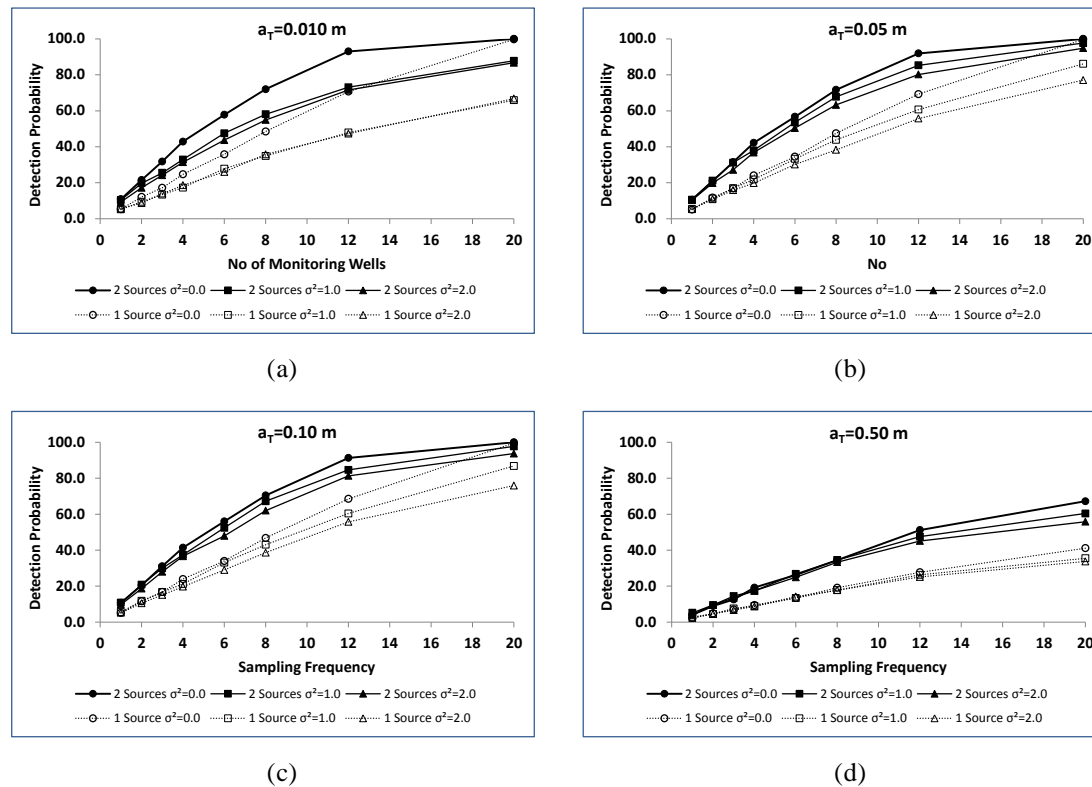


Figure 5.2: Detection probability  $P_d$  change shown as monitoring wells density in relation to control area width is kept constant and equal to 0.05.

## 5.2.2 Multiple Point Sources

Uncertainty regarding the potential location of a leak within a cell of a landfill stems from the lack of information on potential failure locations at a landfill's bottom liner. In all stochastic modeling so far, single pollution source has been the common case. It is not impossible, though, to have more than one pollution source at the same region, caused by the same or different reasons. At least in one case (Collucci et al., 1999), two different tears at a landfill's protective liner have been documented, providing this way two groundwater pollution sources charging the aquifer at the same time.



**Figure 5.3:** Change in detection probability  $P_d$  for a single source (dashed lines) and dual source (solid lines) pollution, as the number of wells is increased, for homogeneous ( $\sigma_{\ln K}^2 = 0$ ) and heterogeneous ( $\sigma_{\ln K}^2 = 1, \sigma_{\ln K}^2 = 2$ ) cases, considering four dispersion cases,  $a_T = 0.010$  m (a),  $a_T = 0.05$  m (b),  $a_T = 0.10$  m (c) and  $a_T = 0.50$  m (d).

In the present study it was assumed that two point pollution sources act at the same time. Both of them inject the same quantity of pollution into the aquifer at, providing an initial concentration at the point of injection. Both plumes are transported independently, without any other interaction between them. Both sources are inside the control area vicinity (equal to reference size) and in each computational realization different sources are independently selected with equal probability. The objective is to study how dual pollution sources affect detection probability achieved by a groundwater linear monitoring arrangement

If pollution plumes originate from adjacent sources, they may be transported very closely, crossing each other, providing this way greater pollutant concentration at grid cells. On the other hand, it is possible for them to move to completely different regions, increasing the detection probability as there is more areal coverage. Simulation results showed that groundwater detection probability is increased when two sources are the case (Figure 5.3). In all cases of heterogeneity and transverse dispersion coefficient, it is observed (Figure 5.3a,b,c,d – Figure 5.4) that, as the number of monitoring wells is increased, the difference between  $P_d$  tends to decrease. More specifically, when dispersion is among  $a_T = 0.01 - 0.10\text{m}$ , the average relative percentage difference between dual and single sources is 37% , while in the case of higher dispersion, where  $a_T = 0.50\text{m}$ , the same difference is 47%. In the case of a low dispersion homogeneous field there is no difference in  $P_d$ , something that results from the fact that 100% detection had already been achieved in the single source case.

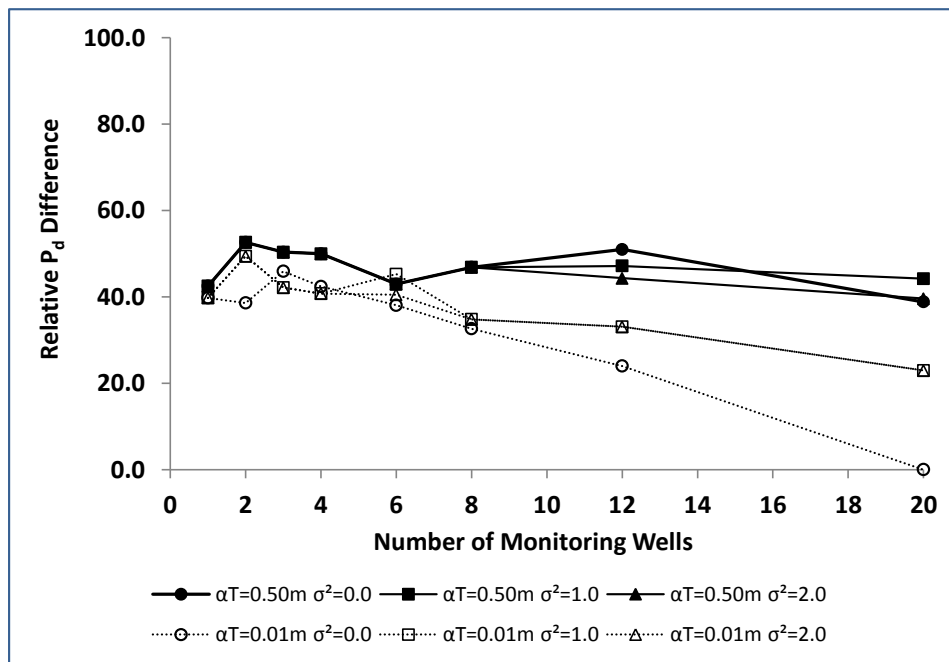
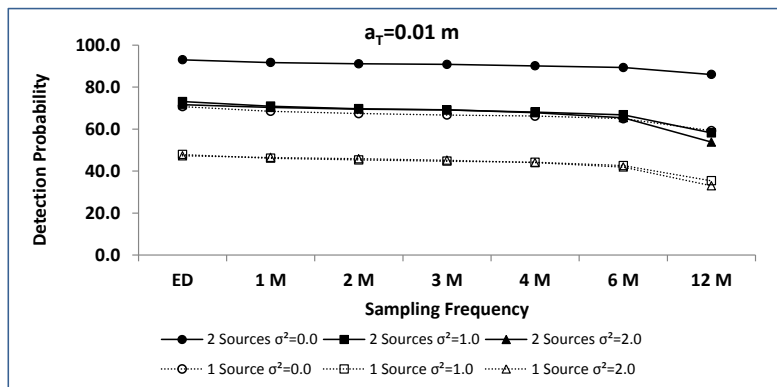


**Figure 5.4:** Detection probability  $P_d$  relative percentage difference between a dual and a single pollution source case in two different transverse dispersion coefficient cases.

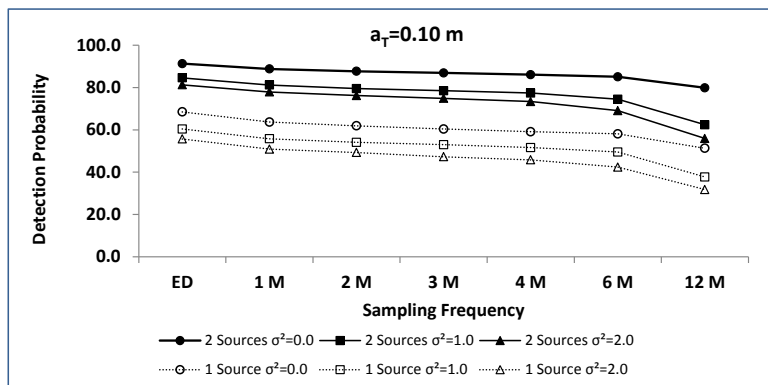
In all simulated cases, the general observation (Figure 5.3) is that when two equivalent groundwater pollution sources are present their detection is easier, as the average  $P_d$  increase is among 35% – 55%, but for the cases where detection was already 100% successful due to the presence of a dense monitoring network (20 wells). It is obvious that if there were more than two instantaneous sources, injecting the same initial pollution concentration, as in the

cases at hand, would make the  $P_d$  difference even greater, as it seems that plume superposition results in an average detection probability increase of 45%. This means that in any single pollution case where  $P_d$  is at least 50%, an average increase of 90% would be expected if at least three pollution sources were present, setting monitoring wells detection capabilities to a maximum of 100%.

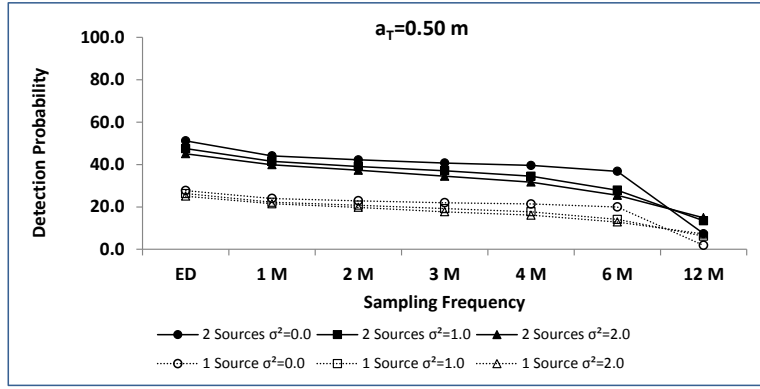
Different sampling frequencies were studied in the case of two pollution sources. It was assumed that sampling was performed at the same time at every monitoring well. Time intervals were assumed to be daily (ED), monthly (1M), bimonthly (2M), quarterly (3M), every four months (4M), biannually (6M) and annually (12M). Studying  $P_d$  change in relation to sampling frequency in the case of two sources, the same trend is observed (Figure 5.5a,b,c) in every numerically studied case of field heterogeneity and pollutant dispersion coefficient. The same  $P_d$  increase relative to single source cases is observed, independently of the sampling frequency. Consequently, aquifer sampling more often does not alter monitoring efficiency in terms of the presence of more pollution sources.



(a)



(b)



(c)

**Figure 5.5:** Change of detection probability  $P_d$  for a single source (dashed lines) and dual source (solid lines) pollution, as sampling frequency changes from daily (ED), monthly (1M), bimonthly (2M), quarterly (3M), every four months (4M), biannually (6M) and annually (12M)

### 5.2.3 Quantity of Pollution

The sensitivity of groundwater pollution detection probability  $P_d$  to pollutant quantity, instantaneously injected into a 2-D aquifer through a randomly selected single point source, was examined during numerical experiments. A rectangular reference control area  $L$  was, in all simulations, the region where pollution could originate. Three heterogeneity cases were studied, as reflected in  $\sigma_{\ln K}^2$  of hydraulic conductivity  $K$ , where  $\sigma_{\ln K}^2 = 0.0$  was the homogeneous one,  $\sigma_{\ln K}^2 = 1.0$  was the medium heterogeneous one and  $\sigma_{\ln K}^2 = 2.0$  was the strong heterogeneous one. Four different pollution dispersion cases were examined, corresponding to  $a_T = 0.01m, 0.05m, 0.10m$  and  $0.50m$ .

Eight different initial pollution quantities were numerically studied, among 125gr, 250gr, 500gr, 1,000gr, 1,500gr, 2,000gr, 2,500gr, and 3,000gr, providing an initial pollution concentration  $C_0$  of 500mgr/lit, 1,000 mgr/lit, 2,000mgr/lit, 4,000mgr/lit, 6,000mgr/lit, 8,000mgr/lit, 10,000mgr/lit, and 12,000mgr/lit respectively. Detection threshold concentration was set equal to  $C_{TH} = 14mgr/lit$  in all cases. Each different initial pollution quantity was simulated in all hydro-geological cases, as previously described.

Simulation results indicated that when the initial concentration of pollution is below 1,000mgr/lit then its detection is very hard, as  $P_d$  is below 20% even for a 20-well setting, in every hydro-geological configuration (Figure 5.6:, Figure 5.7, Figure 5.8:). As the initial concentration of pollution is increased, so does detection probability. In the case of a homogenous field, when initial concentration is bigger than 4000mgr/lit, there is little change in  $P_d$  achieved by every monitoring configuration when dispersion is less than  $a_T = 0.50m$

(Figure 5.6:a,b,c). In the case dispersion is as large as  $a_T = 0.50m$ , it is observed (Figure 5.6:) that as  $C$  is increased so does  $P_d$ . For example, when  $C = 6,000mgr/lt$ , detection probability of a 12-well installation is  $P_d = 42.4\%$ , while when  $C = 12,000mgr/lt$  probability is  $P_d = 81.8\%$  respectively, which is almost twice as big as the pollution concentration.

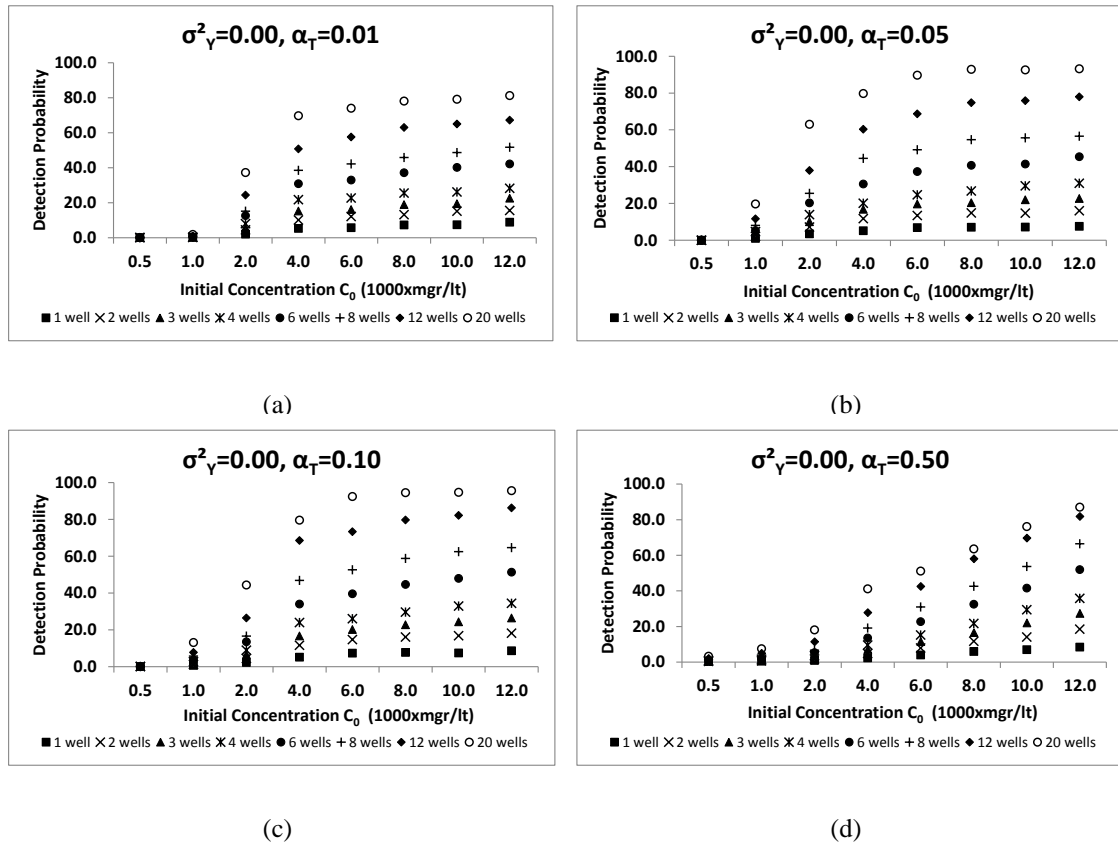


**Figure 5.6:** Change of detection probability  $P_d$  of different monitoring wells installations, as the initial concentration of a single source instantaneous pollution increases at a homogeneous  $\sigma_{lnK}^2 = 0.0$  aquifer

Another interesting observation is the fact that in high dispersion value (Figure 5.6:)  $P_d$  differences between different monitoring wells settings tend to decrease as the initial concentration of pollution increases. This effect is observed in all heterogeneity cases when transverse dispersion coefficient is as high as  $a_T = 0.50m$  (Figure 5.6:, Figure 5.7d, Figure 5.8:). In all other lower dispersion cases it is observed that, as soon as initial concentration overcomes  $C = 4,000mgr/lt$ , then  $P_d$  changes very little (less than 5%), regardless of the number of wells, which means that further pollution injection into groundwater does not make its detection easier. This is very interesting, as it indicates that actually in low to medium dispersion aquifers monitoring wells efficiency reaches a maximum, which is independent of

the initial mass of pollution intruding into groundwater (Figure 5.6: Figure 5.7a,b,c, Figure 5.8:). Only in high dispersion environment increase of pollution reflects to higher detection probability. The turning point for the concentration of initial pollution is  $C = 8,000mgr / lt$ , which is the value where  $P_d$  starts to stabilize. Lower concentrations were harder to detect, dictating that in order for a monitoring setting to be sensitive, at least at simulation level, even in small amounts of pollution a large number of wells must be used.

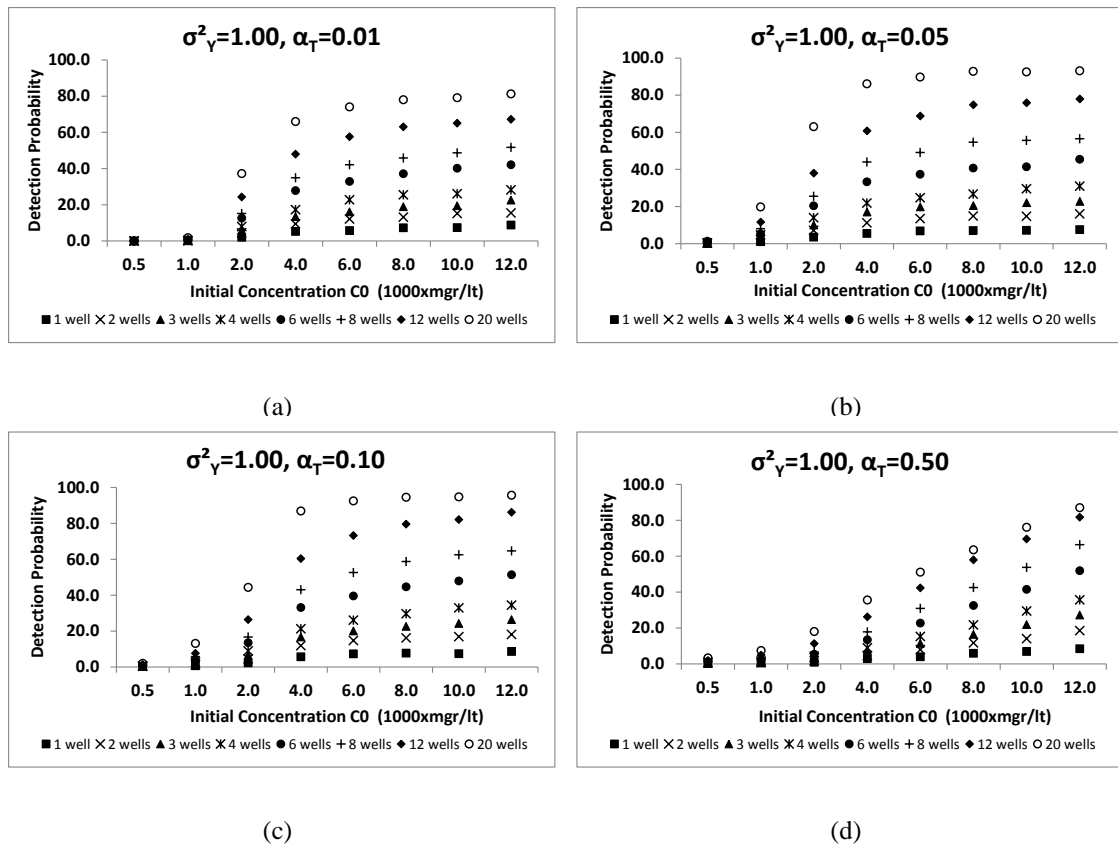


**Figure 5.7:** Change of detection probability  $P_d$  for different monitoring wells installations, as the initial concentration of a single source instantaneous pollution increases at a heterogeneous  $\sigma_{inK}^2 = 1.0$  aquifer

Simulations indicated that dispersion is the main hydro-geological parameter that affects plume detection in relation to the initial concentration of pollution. When dispersion increases as high as  $\alpha_T = 0.50m$ ,  $P_d$  increases almost linearly to initial concentration, because pollution disperses faster in a larger area and, in conjunction with the fact that a larger pollutant mass reserves greater detectable areal coverage, plume is detected more easily. On the contrary, in lower dispersion fields smaller plumes are produced and, even if a larger pollution mass is injected into groundwater, it leads to polluted regions of greater concentration and not in greater areal coverage, which is the main geometric attribute for a

plume to be more easily detected (Yenigul et al., 2006; Papapetridis & Paleologos, 2011a, 2012), resulting in a  $P_d$  plateau.

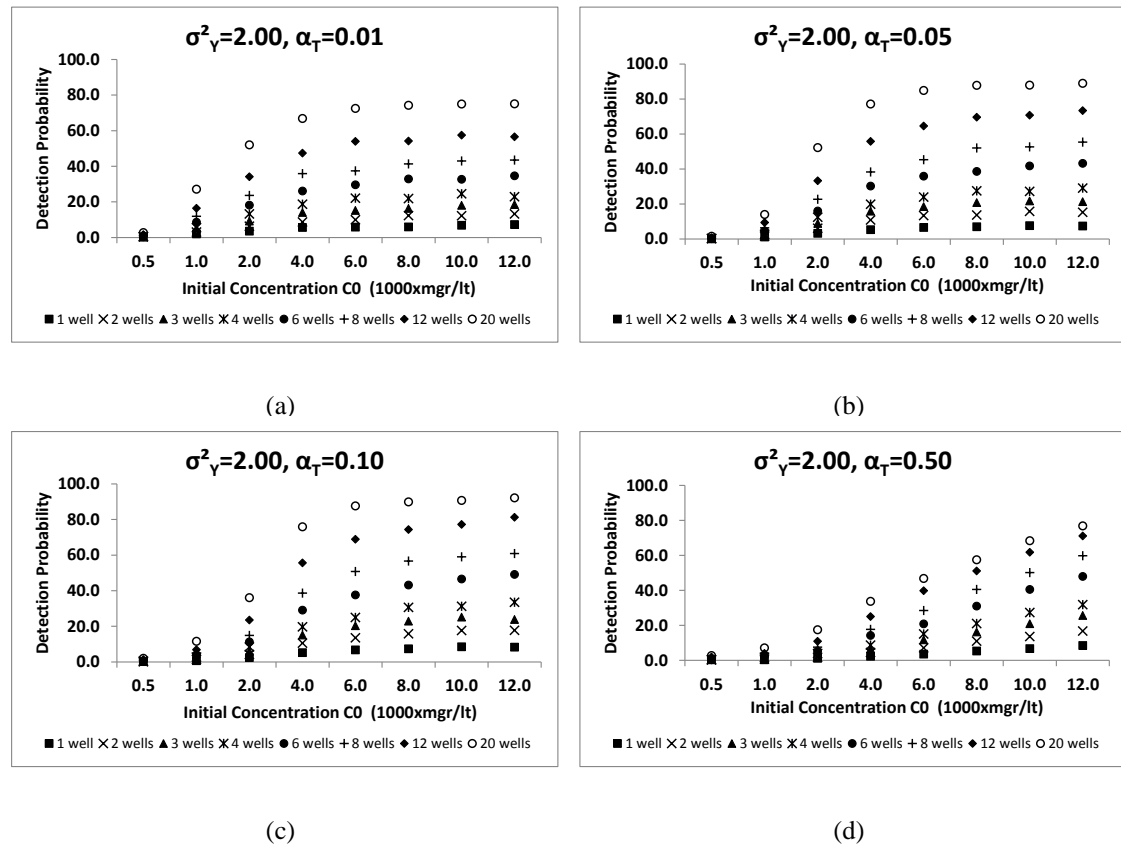


**Figure 5.8:** Change of detection probability  $P_d$  for different monitoring wells installations, as the initial concentration of a single source instantaneous pollution increases at a heterogeneous  $\sigma_{\ln K}^2 = 2.0$  aquifer

### 5.3 Conclusions

In the present work a Monte Carlo approach of a stochastic model was used, simulating hydro-geological and epistemic uncertainties in groundwater pollution transport and detection by monitoring wells in order to study how the number of point sources, the size of the controlled area (e.g. a landfill facility) and the quantity of an instantaneous injected pollution affect plume detection. In each examined parameter it was considered that the rest of the factors affecting  $P_d$  estimation remain constant. Simulations were performed in the context of uncertainty factors deriving from the environment itself, reflected onto hydraulic conductivity  $K$  parameter and the lack of information about the initial conditions of a leak.

It was numerically verified in the cases examined in this work that as the size of the control area became larger and the number of wells remained constant, detection probability  $P_d$  decreased. In addition, the fewer the monitoring wells, the smaller the detection

probability. However, when the control area became smaller, then  $P_d$  increased, until it reached the maximum value of 100% detection. Consequently, if the width of a control area was to be increased, so should the number of monitoring wells, maintaining at least the same density as that of the initial case.

In all simulated cases, the general observation is that when two equivalent groundwater pollution sources are present, then their detection is easier as the average  $P_d$  increase is among 35% – 55%, except for the cases where detection was already 100% successful due to the presence of a dense monitoring network (20 wells). The same trend in  $P_d$  increase relative to a single source case is observed, regardless of the sampling frequency. More frequent aquifer sampling does not alter monitoring efficiency in terms of the presence of more pollution sources.

Simulation results indicated that when the initial pollution concentration was below 1,000 mgr/lit , its detection was very hard, regardless of the aquifer's hydro-geological parameters. The efficiency of low to medium dispersion aquifers monitoring wells reaches a maximum, which is independent of the initial mass of pollution intruding into the aquifer. The turning point of the initial pollution concentration was  $C = 8,000 \text{mgr} / \text{lit}$  , which was the value where  $P_d$  reached a plateau. It has been observed, too, that only in high dispersion environment, where  $a_T = 0.50m$  , increase of pollution reflects higher detection probability. In every case, lower concentrations were harder to detect, dictating that in order for a monitoring setting to be sensitive, at least at simulation level, even in small amounts of pollution at least 12 wells must be used.

# CHAPTER 6

## **Modeling of aquifer pollution detection probability triggered by precipitation**

---

### **6.1 Introduction**

Groundwater pollution is mainly caused by the presence of chemical compounds in concentrations for which, according to National and International regulations, water is considered harmful and unusable not only for human and animal consumption but even for irrigating purposes. Most of these substances, produced during various human activities, should be treated and disposed appropriately as soon as they are considered wastes by the end user, so as not to pose a threat on the environment and to public health.

There are some occasions, though, where these chemicals intrude into the aquifer accidentally, by reckless handling or even due to the lack of any administration provision. Cracks on underground petroleum tanks, chemical transportation accidents and uncontrolled waste disposal are some possible pollution sources. The current legislation system states that the polluter, whether proven to have polluted on purpose or by accident, pays not only for the damage caused to other properties but for the restoration of the environmental damage too. However, in the case of water pollution there is an accountable loss on its value, as *Paleologos* (2008) showed, through water's quality degradation after restoration, because Water Regulations state that initially potable water must be restored to that condition where it can be used at least for irrigation.

Aquifer pollution can be the result of an undiscovered condition, where infrastructure damage or failure may lead to uncontrolled liquid wastes disposal, first into the vadose zone and finally into the groundwater flow. Landfills may be an example of the situation described,

as leachate concentrate at the lower level of the installation are pumped out using perforated tubing systems. There are cases, however, where leachate penetrate protective liner and clay barriers, usually through small cracks and holes (Laine et al., 1997; Collucci et al., 1999; Tatsi & Zouboulis, 2002; El-Zein, 2008), causing groundwater pollution. It is speculated that in the United States alone a 40% of active sanitary landfills suffer from leachate leakage problems (Paleologos, 2008). This is the main reason for installing downstream aquifer pollution monitoring wells, so that a case of leachate leak into groundwater can be detected and appropriate countermeasures can be taken.

Groundwater quality monitoring wells are also used at industrial sites (Bierkens, 2006), as it is possible for certain quantities of dangerous chemical compounds to escape and contaminate the aquifer due to waste handling or storage failure. The main objective is to detect pollution originating from the facility, at some distance from it, so that it can be cleaned up or controlled before contaminated groundwater reaches areas outside the site. In this case a bigger number of wells can be utilized, according to the magnitude of the facility and the danger that its waste may pose to public health.

Moreover, illegally dumped municipal or industrial wastes are another uncontrolled source of groundwater pollution. Waste may initially contain various dangerous chemical compounds, which may pose serious threats to local communities and ecosystems if they escape into the environment and especially into groundwater. Long term air exposure of organic matter contained into waste, as well as biological decay processes may cause toxic substances production (Fatta et al., 1999). These dangerous substances dissolve into, mix with or chemically react with precipitation water during raining periods, producing solutes which flow and finally infiltrate groundwater, where pollution is uncontrollably transported by the flow.

Waste dumps can be considered as point pollution sources triggered each time by precipitation to deliver pollutants into the aquifer. Although it is natural to assume that the chemical footprint of pollutants will not possibly be the same as time passes (Kulikowska & Klimiuk, 2008; Renou et al., 2008), that organic matter decomposes or other chemical processes take place, that concentrations will not remain constant as rainfall varies and that the quantity of the pollutant is not the same, precipitation is a mean that may cause or amplify the effects of a point pollution source. Pollutants mass transfer takes place by dissolving them into precipitation water, thus increasing their mobility, leading in protective barrier overflow or rapid infiltration into groundwater. Leachate flow rate from sanitary landfill sites varies both from site to site and seasonally at each site. In relatively warm climates the increase in leachate production after precipitation is quite rapid (Shinozuka & Jan, 1972). At least in one case it has been documented that, during a raining incident, groundwater's pollutant

concentrations (COD, Cl, NH<sub>40</sub>) originating from a small liner crack in the landfill increased temporarily and repeatedly according to the local precipitation event (Collucci et al., 1999) (Figure 6.1). As a first approximation, the quantity of leachate produced may be regarded as proportional to the volume of water percolating through waste (Shinozuka & Jan, 1972).

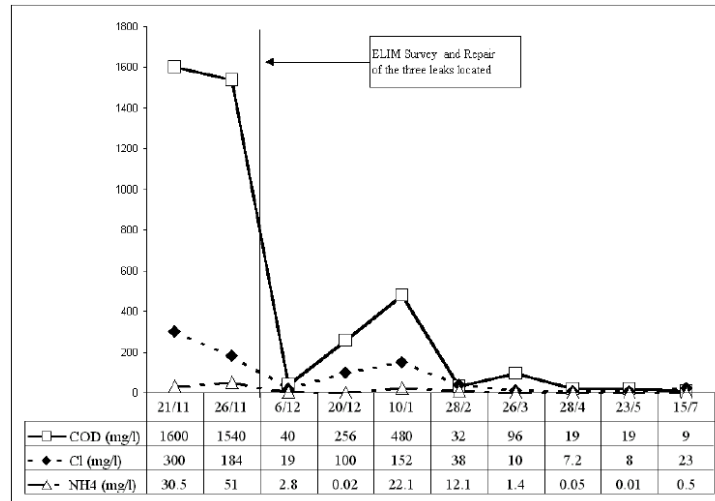


**Figure 6.1:** Plot of Groundwater Monitoring Data Indicating High COD and Cl Levels after a landfill leak case repair has taken place (vertical line), where the spikes are due to rain episodes on the area (Collucci et al., 1999).

In the real world however, there are many different ways for a pollution to happen. It may be spotted in a very small region or it may cover a large area. It may take place in a short period of time, as it usually happens during an accident, or it may be continuous if there is a permanent undiscovered leak, for example in a hydrocarbon pipeline transfer system. Moreover, it may be triggered by some other random event, such as rupture in a high pressure fuel transfer pipeline system or a precipitation event which augments solute infiltration into an aquifer. This means that not only does the event of pollution affect the way groundwater is contaminated, but also spatial and time characteristics contribute to the evolution and consequences of this event.

Considering a different way of a groundwater pollution incident in the context of triggering it according to local precipitation events, in the present study we have assumed that there is a point pollution source inside a controlled area of specific dimensions which injects a quantity of pollutant inside the aquifer, each time rain occurs. It can be assumed that this is a municipal waste sanitary landfill cell where a local liner failure has occurred or an area where uncontrolled industrial waste dumping has taken place and a local leak has commenced, causing pollutant exposure, flow and concentration at the lowest point of the area. Furthermore, it has now been recognized that the dominant mechanism of contaminant migration may be diffusion through the protective liner and not advection (Tompson et al.,

1989; Allen, 2001; El-Zein, 2008). The pollutant has been assumed to dissolve into rainwater percolating through wastes, concentrating at the bottom of the facility, where the developed hydraulic head causes pollutant intrusion into groundwater. The quantity of the pollutant that infiltrates is considered linearly analogous to the recorded daily average precipitation height, for a specific location. While there are computational models to simulate or to forecast precipitation intensity as well as time events (Moustris et al., 2011), a 30-year time series rain data from Macedonia Airport in Thessaloniki was used in order to save computational time. The area, which in our study was simulated in two dimensions (2-D), is downstream controlled by a linearly arranged monitoring network, consisting of a different number of drilling wells arrangements in each study case. The ability of the monitoring installation is evaluated through the probability of successful pollution detection, and its performance is evaluated in different hydro-geological environments.

The pulsing ejection of different quantities of pollution into groundwater during every time step, represents a different concept of time dependence between the time of ejection and the quantity that is ejected, as it is different from the instantaneous or the continuous cases with a steady inflow rate. While in the case of instantaneous ejection of pollution a certain number of particles enters the aquifer at the beginning of the simulation (Yenigül et al., 2005; Papapetridis & Paleologos, 2011a) or in the case of continuous pollution a certain number of particles is ejected during each time step (Yenigul et al., 2006), in the case of pulsing pollution a relation between a natural phenomenon that augments pollution transportation and pollution quantity is established.

## 6.2 Model Description

Heterogeneous aquifer structural properties, such as size, position and amount of clay lenses, sand and gravel layers, as well as the resulting distribution of hydraulic conductivity, porosity and hydro-geochemical parameters significantly control groundwater flow and spread of solutes (Dagan, 1989; Ptak et al., 2004). In order to study the effects of pollution transport and dispersion into a heterogeneous subsurface environment in relation to its detection probability  $P_d$  by a monitoring wells network, the Monte Carlo numerical framework was used. Uncertainty due to contaminant subsurface heterogeneity is reflected by the spatial variability of hydraulic conductivity. Hence, hydraulic conductivity is treated as a random space function. The natural logarithm of the isotropic hydraulic conductivity [ $Y = \ln(K)$ ] is modeled as a stationary Gaussian field with a geometric mean value of 2.30m/day. Variance ranged among 0.0 (homogeneous aquifer), 1.0 (medium heterogeneous aquifer) and

2.0 (strongly heterogeneous aquifer) and the isotropic covariance of  $Y$  is chosen to be of exponential form with correlation length  $\lambda = 20m$ .

In each different hydro-geological case that was examined, the Monte Carlo scheme consisted of 2,000 simulations. Heterogeneous aquifers in the model were simulated using the 2-D Spectral Turning Bands method (STUBA) (Mantoglou & Wilson, 1982; Ababou et al., 1989; Tompson & Gelhar, 1990a; McLaughlin et al., 1993; Emery, 2008; Paleologos & Sarris, 2011). The aquifer is assumed to be confined, with a given hydraulic head at its left and right boundaries, resulting in a macroscopically constant hydraulic gradient of 0.001m. Source location uncertainty was envisaged considering equally probable different points of pollution origin during each different simulation which belongs inside the control area.

Contaminant advection and dispersion were simulated using the Random Walk Tracking Particle approach, as described by *Tompson et al.* (1987b) and comprehensively reviewed by *Salomon et al.* (2006b). This choice is based on the algorithm's ease of implementation, its mass conservative nature and its computational effort economy, since it is independent of the control area we want to simulate. In each of the 2,000 Monte Carlo heterogeneous field realizations, pollution was simulated by a certain number of equal mass particles, which were ejected into the aquifer. In our study we considered that the number of particles entering the streamline flow of groundwater was related linearly with the total daily precipitation height at the simulation region. Precipitation events triggered pollution infiltration, resulting in a pulsing ejection, each time with different quantities, of pollution. In fact, precipitation increased pollution mobility, either by dissolving pollutants into the water or by simply mixing them with it and, in some cases, where chemical processes occurred, caused the increase of the pollutant quantity. Either way, this ended up with larger quantities of pollution that were transported along with rainwater through the vadose zone into the aquifer.

In this study we assumed that pollution enters directly into groundwater flow, neglecting transportation effects into the unsaturated zone. Even if the thickness of the vadose zone significantly affects the leakage of an installation's protective barrier, resulting in a substantial overestimation up to a factor of about 3.5 (Çelik et al., 2009), this holds true if the aquifer is very near at the source of pollution or if a fingering effect favors a specific direct path of pollution propagation into groundwater flow (Selker et al., 1996). In addition, the coupling of precipitation and pollution events focuses only on the pollution quantity infiltrated into the flow, considering mainly a mass diffusion transfer mechanism (Tsanis, 2006), and not on the recharge of the aquifer with polluted water due to precipitation. As a result, a steady state flow of groundwater without a free surface recharge is assumed. Even if aquifer recharge is not taken in mind, meaning that flow equation still satisfies Laplace

equation (Harr, 1962; Bear & Buchlin, 1987), this computational simplification isolates and excels the effects on pollution dispersion and detection of a pulsing pollution source, which is related with an actual phenomenon.

It was considered that if during a simulation time step, equal to  $dt = 1$  day, a precipitation event took place, then a certain quantity of pollution, proportional to the total rain height, would have infiltrated the aquifer and diffused into the flow, without disturbing groundwater flow. A proportionality factor between the total daily precipitation height and pollution mass infiltration was set in, so as to provide a detectable concentration of pollution at the point (cell) and time of ejection. Considering that the lowest recorded precipitation height data was 1mm, it was assumed that this quantity would provide detectable pollution. Threshold detection limit was set at  $C_{Th} = 14\text{mgr/l}$ , which indicates the presence of chemicals into groundwater in such a degree that remediation actions should take place. This level of pollution is typical for chemicals such as nitrate, cyclohexanon and diethynglycol (Yenigül et al., 2005). The threshold detection limit of pollution concentration in a  $2 \times 2$  m cell (the depth is considered to be equal to 1m for unit consistency) is produced by 28 particles, which provide enough resolution to describe the plume's transportation and detection by monitoring wells (Yenigül et al., 2005; Papapetridis & Paleologos, 2010). Given that concentration in a cell equals  $C = M/(nV)$ , where  $n=0.25$  is the effective porosity constant during all simulations, the pollution mass representing the detectable limit equals 14,000mgr or 500mgr per particle.

A thirty-year time series of daily average precipitation data from Macedonia airport in Thessaloniki was used. A total precipitation height for this period of time was recorded equal to 13,291.06mm. Considering that a 1mm precipitation height ejected pollution into the aquifer is represented by 28 particles, the total number of particles utilized to simulate the pollutant's advection and dispersion into the subsurface environment, at the end of the 30-year simulation, was 372,150. During each simulation time step, total precipitation height for that day was taken into account and linearly transformed into a number of pollutant particles. Then, this number of particles was added, through the same point source, to the total number of particles that were already transported into the aquifer. As a result of this kind of pollution inflow, a continuous plume of pollution was formed. If its concentration was larger than the threshold limit at the time of sampling at the grid cells where monitoring wells were located, then a successful detection was recorded. In every simulated case studied, detection time was recorded and the total contaminated area was calculated. In order for a  $2 \times 2$  m cell to be considered polluted, concentration must be at least equal to  $C_{Th}$ , meaning that at least 28 particles must exist inside the grid's cell at the moment of sampling. At the end of the 2,000

simulations the average time of detection and the average contaminated area are calculated if daily (ED) sampling is assumed. Moreover, the average contaminated area is also calculated assuming different sampling frequencies, namely monthly (1 M), bimonthly (2 M), quarterly (3 M), every 4 months, biannual (6 M) and annual (A). The polluted area was additionally calculated 3 months, 6 months, 1 year, 2 years and 3 years after successful detection in order to evaluate the remedial action delay time (RADTi) as this was introduced by *Papapetridis and Paleologos (2011a)*.

A computational model developed by *Papapetridis and Paleologos (2011b)* was used in order to perform the Monte Carlo simulations. The model was initially developed in order to simulate an instantaneous case of heterogeneous aquifer pollution. The practical meaning of instantaneous pollution is that the event itself takes place in a very short period of time in relation to the 1-day time step which the simulation uses. Consequently, a pressurized tank or a pipe system that is suddenly relieved due to some localized structural failure, an industrial accident or a landfill leak may potentially produce such kind of pollution. In order for the model to facilitate multiple pollution injections into the aquifer originating from the same point, during the 30-year monitoring period, certain modifications were made. Even if in the scenario of pulsing pollution the computational time needed was significantly increased, a contemporary workstation was able to provide results in a reasonable time span.

Five different cases of transverse dispersion coefficients,  $\alpha_T$ , were investigated. These values varied among  $\alpha_T = 0.001, 0.01, 0.05, 0.10,$  and  $0.50\text{m}$ , corresponding to values observed in field experiments (Gelhar, 1986) which describe soils of low, medium and high dispersion. In each simulation, dispersion was considered to remain constant and the longitudinal dispersion coefficient,  $\alpha_L$ , was calculated by the relation  $\alpha_L = 0.10\alpha_T$  (Spitz & Moreno, 1996).

The simulated region was 1,000 m long, 400 m wide and, assuming a discretization of the area in cells of  $dx \cdot dy = 2 \times 2 \text{ m}^2$ , a  $500 \times 200$  grid was created. A rectangular area simulating a contaminant potential source area (CPSA), for example a section of a landfill, or the area of a waste storage facility, was situated between  $x$ -coordinates 10m and 60m, and  $y$ -coordinates of 140m and 260m. At a random point within these boundaries a contamination event was initiated, which polluted the aquifer every time a precipitation event occurred.

The contaminant mass was assumed conservative and fully water soluble. The uncertainty, regarding the potential location within a cell of a landfill where a leak might have developed, stems from the lack of information on potential failure locations at a landfill's bottom liner. In case pollution from a different facility is assumed, such as from an industrial

plant or a military facility, uncertainty about the contamination's point source may stem from our inability to detect leaks from waste carrying pipelines, underground storage areas of liquid waste, or even accidental spills during operations. In either case, it was assumed that any point within the rectangular CPSA there was an equally probable source of leakage, taking place once as a single failure event at zero time (when the simulation began) and resulting in an instantaneous ejection of contaminants into the aquifer. Monitoring wells were assumed to fully penetrate the aquifer, resulting in vertically-averaged concentration measurements. Eight linear configurations were examined, consisting of 1, 2, 3, 4, 6, 8, 12 and 20 wells, equally spaced from one another. Wells that were located at the ends of each arrangement were placed half the distance from the cell's top and bottom edges so that the efficiency of the monitoring system would be maximized (Yenigül *et al.*, 2005). Monitoring of the aquifer and plume evolution was simulated for a 30-year period.

## 6.3 Simulation Results

### 6.3.1 Number of Wells

Considering the number of wells of the monitoring and detection arrangement of the installation, simulation results showed that even one of the smallest monitoring networks, that of 4 wells, in case of a homogeneous medium dispersive field, is capable of providing a 100% successful detection of pollution (Figure 6.2a). Even in a highly heterogeneity field where  $\sigma_{\log K}^2 = 2.0$  with as low dispersion as  $a_T = 0.01m$ , 4 wells will detect groundwater pollution half the time (Figure 6.2b). Comparing simulation results in relation to detection probability  $P_d$  between instantaneous pollution of the aquifer with a small quantity of pollution (1 kgr of a conservative pollutant, providing a 4,000mgr/l initial concentration) and precipitation initiative pollution, for the latter it is clearly seen that  $P_d$  rapidly increases as the number of monitoring wells is increased, reaching a maximum of 100% detection when more than 3 wells are utilized, while for the former  $P_d$  presents an almost linear increment, succeeding maximum detection only with a dense monitoring arrangement. In case of a strongly heterogeneous field,  $P_d$  is always significantly less than the precipitation initiative case. In the precipitation initiative pollution case even a 3-well installation, which according to EU legislation is the minimum requirement for groundwater monitoring of an operational landfill, can detect aquifer pollution in more than 50%, depending on the field's hydrogeological properties.

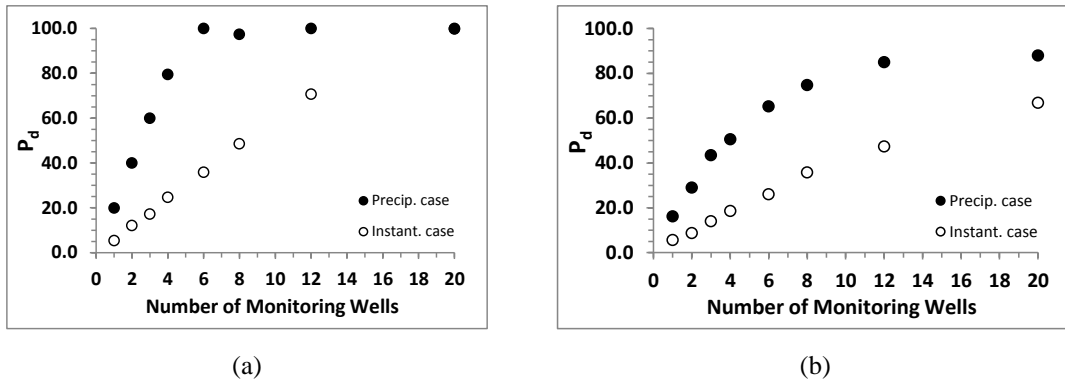


**Figure 6.2:**  $P_d$  change as the number of monitoring wells increases from 1 – 20, as well as comparison between an instantaneous case of pollution and a precipitation coupled case for a medium dispersion homogeneous field (a:  $\sigma^2(\log K)=0.0$ ,  $\alpha_T=0.10m$ ) and a low dispersion heterogeneous field, (b:  $\sigma^2(\log K)=2.0$ ,  $\alpha_T=0.010m$ ).

### 6.3.2 Field Heterogeneity

Subsurface heterogeneity, which in this study is reflected by the spatial variability of the hydraulic conductivity, has been examined for three different cases. When a small number of wells is used, as shown in Figure 6.3 where 3 wells are considered, at very low dispersion fields,  $P_d$  decreases by 23% when heterogeneity increases from 0.0 to 2.0. At low dispersion environment a 27% decrease is observed between homogeneous and strongly heterogeneous cases. At higher dispersion value,  $P_d$  remains practically constant as heterogeneity increases.

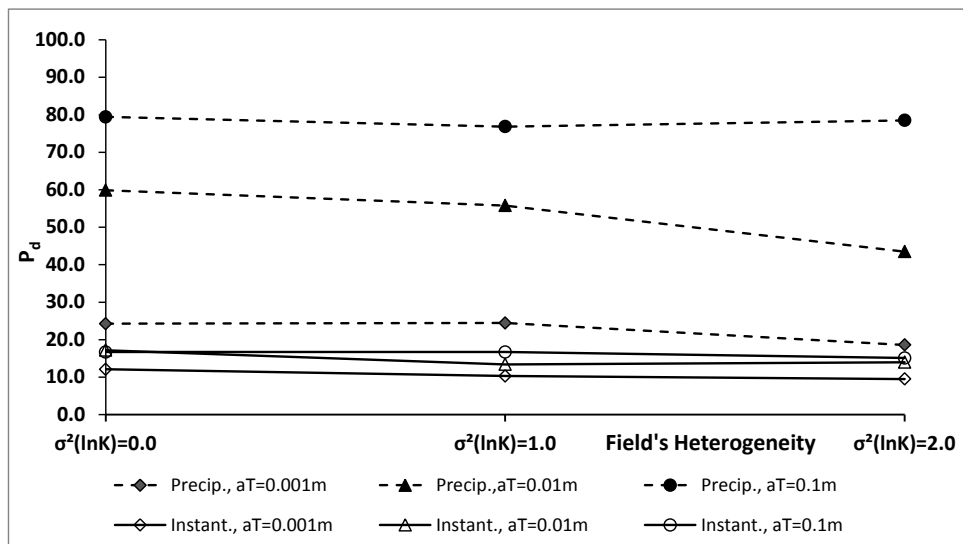


**Figure 6.3:** Groundwater pollution detection probability  $P_d$  of a 3-well arrangement in relation to the field's heterogeneity as this is reflected through variance of the natural logarithm of hydraulic conductivity ( $\sigma^2_{\ln K}$ ). Dashed lines are the precipitation triggered pollution (Precip.) and solid lines are for instantaneous cases (Instant.).

Examining an arrangement consisting of 12 wells (Figure 6.4), it is seen more patently that, as dispersion is increased, the effect of heterogeneity increase on  $P_d$  is languished. More specifically, at a very low dispersion field, where the transverse dispersion coefficient equals  $a_T = 0.001m$ , there is a significant 33.5% dropdown at the  $P_d$  between the homogeneous and the strong heterogeneous cases, while at  $a_T = 0.01m$  the dropdown is 15%. At greater dispersion values, it is observed at the simulation results that there is no difference in detection probability, as it is 100% for every heterogeneous case that has been studied.

If an instantaneous pollution case is considered (Figure 6.4), then it is noted that  $P_d$  is decreased as heterogeneity is increased. At transverse dispersion coefficient  $a_T = 0.001m$  a 29% decrease is observed, while at  $a_T = 0.01m$  and at  $a_T = 0.1m$  the decrease is 31% and 19% decrease respectively. Similarly, as the dispersion is increased, the effect of field heterogeneity on detection is lessened. This pattern holds true in both simulation scenarios, either instantaneous or precipitation caused pollution is computationally examined.

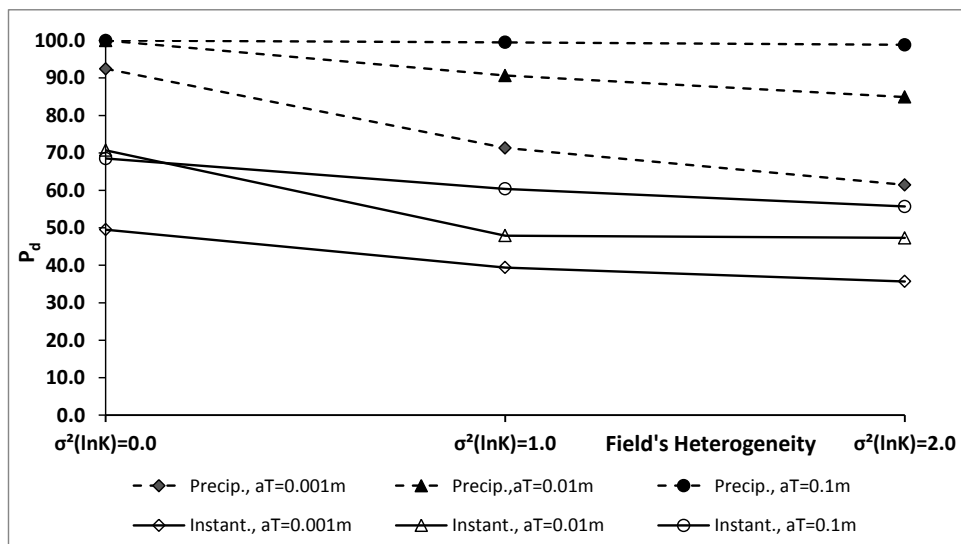


**Figure 6.4:** Groundwater pollution detection probability  $P_d$  of a 12-well arrangement in relation to the field's heterogeneity as this is reflected through variance of the natural logarithm of hydraulic conductivity ( $\sigma_{\ln K}^2$ ). Dashed lines are the precipitation triggered pollution (Precip.) and solid lines are for instantaneous cases (Instant.).

Hydraulic conductivity variation highly affects pollution plume propagation into the aquifer, as several tracer field experiments have shown (Freyberg, 1986; LeBlanc et al., 1991; Boggs et al., 1992). A solute plume in a given realization can be pictured as diffusing slowly, owing to local scale dispersion, and winding like a meandering stream because of large-scale regional heterogeneity (Dagan, 1984) (Figure 6.5). This solute behavior sometimes tends to separate a plume's formation into more than one branches, resulting in regions of smaller

pollutant concentration and flow paths that bypass the monitoring arrangements. While in the case of instantaneous pollution fast deformation of pollution plume due to hydraulic conductivity variations may lead to areas of lower concentration than that of the detection threshold limit, which will result into a no detection situation, in the case of precipitation initiated pollution, because the pollutant keeps being added into the flow, it is more logical to assume that detectable preferential flow paths are formed through highly hydraulic conductivity paths, allowing for a significant portion of plume to escape detection (Figure 6.5).

However, as dispersion is increased, pollution dilutes faster and in a greater area (Figure 6.5). Considering the fact that a variable amount of pollutant mass is added throughout time, greater areal coverage is possible where concentration is above a detectable limit. This means that dilution of the plume below the detection limit, due to deformation along the propagation path, is not observed. The effect of plume deformation along with higher dispersion alleviates the influence of heterogeneity on  $P_d$ . The fact that the average  $P_d$  decrease is 16% in case of 12 wells, when at the same configuration for the instantaneous case the average decrease is 26%, indicates that preferential flow is possibly the main mechanism responsible for  $P_d$  decrease as the field gets more heterogeneous and dilution of the plume is hindered by pollutant injection

### 6.3.3 Dispersion

For a given structure of the simulated geological field, subsurface heterogeneity and dispersion are the main factors that directly determine the form that the developed contaminant plume will have. In the case of an instantaneous pollution event the longitudinal dispersion causes the elongation of pollution in the direction of movement of groundwater flow and is proportional to the total underground travel time of the pollutant and its speed in the subsoil. On the other hand, the transverse dispersion causes the widening of the plume and also depends on the total time running and the flow rate. This means that the farther a plume travels, the more it spreads and dilutes into the ground, rendering it non-detectable (Papapetridis & Paleologos, 2010). This behavior is reflected by the fact that as dispersion is increased (in this study all comparisons refer to different transverse dispersion coefficients) among  $a_T = 0.05 - 0.10m$ , as demonstrated in Figure 6.6, depending on heterogeneity and assuming all other parameters remain the same, detection probability of groundwater pollution  $P_d$  initially increases to a maximum, because of the plume dispersion leading to a larger area coverage where pollutant concentration is bigger than the threshold limit, resulting in more detectable cases. However, as dispersion continues to increase, it is observed that  $P_d$

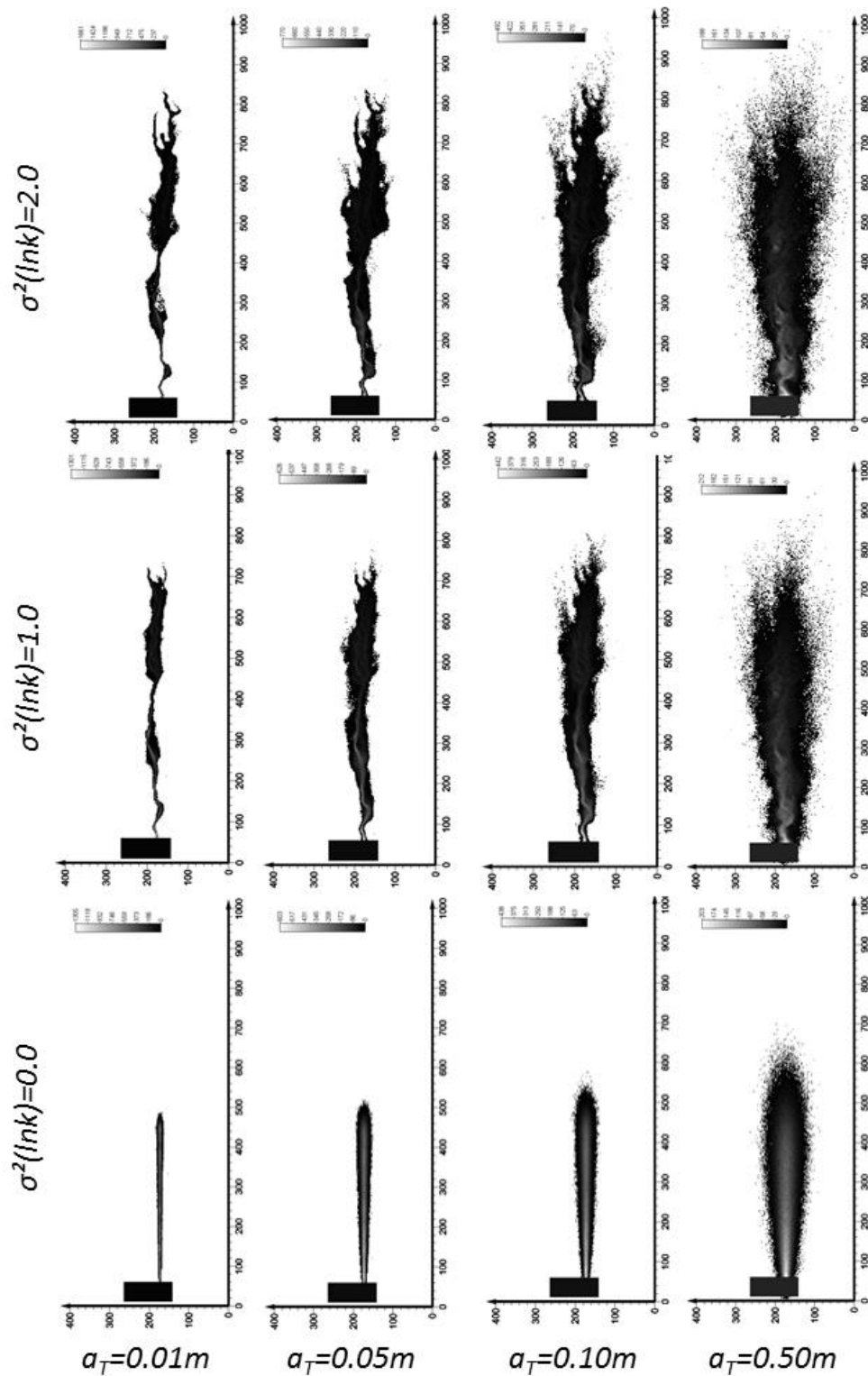


**Figure 6.5 :** Pollution dispersion and deformation as it is transported during a 30-year time span into aquifers, where on the vertical axis heterogeneity increases and on the horizontal axis transverse dispersion coefficient increases.

decreases again, reaching as low as 40% of the maximum value achieved (Figure 6.6). This happens because pollution dissolves so fast into groundwater that the concentration drops

rapidly below the detectable limit, causing the plume's detection escape. This behavior is the same for every well configuration.

On the other hand, examining the results of precipitation related pollution, we notice that detection probability  $P_d$  tends to increase as the field's dispersion is increased. In case of a 3-well installation (Figure 6.6) the average difference between  $a_T = 0.001m$  and  $a_T = 0.50m$  is 78%, in all three cases of heterogeneity studied. It is noteworthy that even this configuration, which constitutes the least demand of monitoring for a sanitary landfill, may succeed detection in every case when dispersion is equal to or higher than  $a_T = 0.50m$ , while in the case of medium heterogeneity a successful detection of over 50% can be achieved in as low a dispersion as  $a_T = 0.01m$ . Of course, these results refer to the specific computational model and all of its initial assumptions made during the Monte Carlo simulations. Nevertheless, a behavior of the monitoring system is indicated, even if different assumptions may lead to different numbers.

It can also be seen that there is a small difference in  $P_d$  as field heterogeneity is increased. In homogeneous and low heterogeneity cases  $P_d$  at  $a_T = 0.001m$  is 24%, while in the case of  $\sigma_{\ln K}^2 = 2.0$  the  $P_d = 18.6\%$ .  $P_d$  increases almost linearly and when dispersion gets larger than  $a_T = 0.10m$  heterogeneity does not seem to affect the effectiveness of the monitoring network.

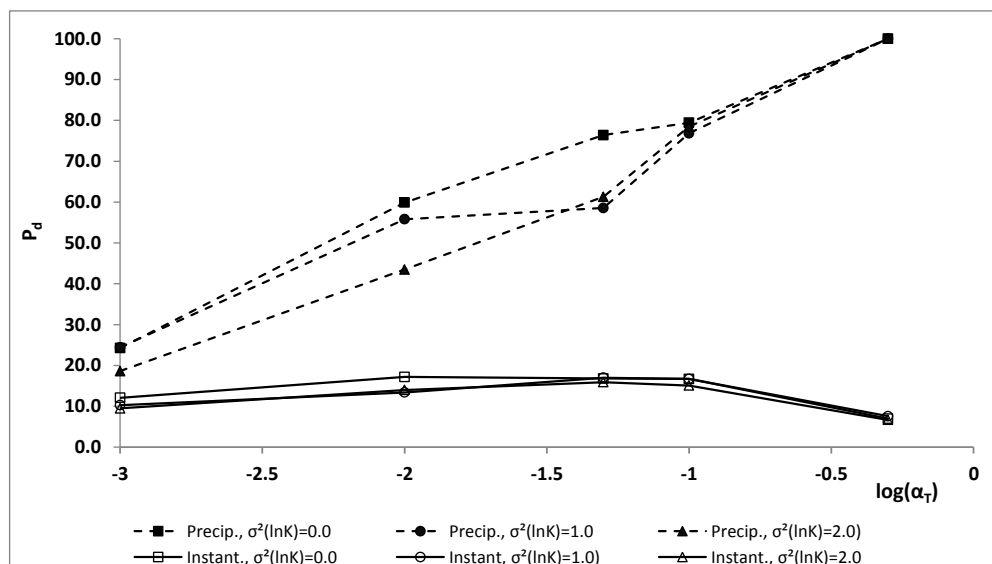


**Figure 6.6:**  $P_d$  change of a 3-well arrangement, in relation with transverse dispersion coefficient  $\alpha_T$  increase, in three different heterogeneity cases, as well as comparison between precipitation related pollution cases (dashed lines) and instantaneous pollution cases (solid lines)

This behavior is mainly the result of the way heterogeneity and dispersion of the field affect the geometry of the plume and the areal coverage as plume is transported in groundwater. As it was explained in the previous paragraph, the plume's deformation due to heterogeneity causes a  $P_d$  decrease as  $\sigma_{\ln K}^2$  is increased. This happens until a specific point of dispersion, as further dispersion increase results in no heterogeneity effect on the detection outcome (Figure 6.5). Contrary to instantaneous pollution, the fact that pollutant mass is constantly added to the aquifer, driven by precipitation through a mass diffusion mechanism, provides enough pollutant to larger portions of the plume's area, resulting in possible detection. This means that when pollution is added, thus preventing the plume's dissolution into the aquifer below a detectable limit, dispersion is the main factor that affects its detectability.

#### 6.3.4 Sampling Frequency

Sampling frequency is an important factor that may significantly affect the effectiveness of a monitoring installation. For example, according to European Council Directive 1999/31/EC of 26 April 1999 on the landfill of waste it is stated that "The frequency of (groundwater) sampling could be adapted on the basis of the morphology of the landfill waste. This has to be specified in the permit." In addition, a landfill operator is obliged to report all monitoring results to the competent authorities once a year. This obligation poses a maximum boundary on sampling frequency. Moreover, it is also stated that "the frequency must be based on possibility for remedial actions between two samplings if a trigger is reached". This dictates a minimum sampling strategy on groundwater sampling frequency, assuming that there is adequate knowledge of the hydro-geological environment, of the chemical footprint for all possible pollutants and, of course, of the fact that remedial actions should commence the moment the trigger event has occurred, which could be the detection of groundwater pollution by a monitoring well. In most of the cases, groundwater sampling frequency is determined by partial knowledge of the velocity of groundwater flow and the cost of the applied sampling policy.

Detection probability dependence on sampling frequency was investigated by *Papapetridis and Paleologos* (2011a, 2011b) in the case of an instantaneous pollution originating from a landfill. In that study it was assumed that the starting point of a leak comes from a single point in the control area and that all of the leachate's quantity enters instantly into the aquifer's field of flow. This type of failure is very difficult to detect, since the trace of the source is very small, as opposed to massive, multiple or continues leaks, where the trace is often large enough to be directly detected (*Papapetridis & Paleologos, 2010*). Seven different sampling frequencies were applied, which assumed sampling from every monitoring well of

the installation at the same time daily (D), monthly (1 M), bimonthly (2 M), quarterly (3 M), every four months (4 M), biannually (6 M) and annually (A).

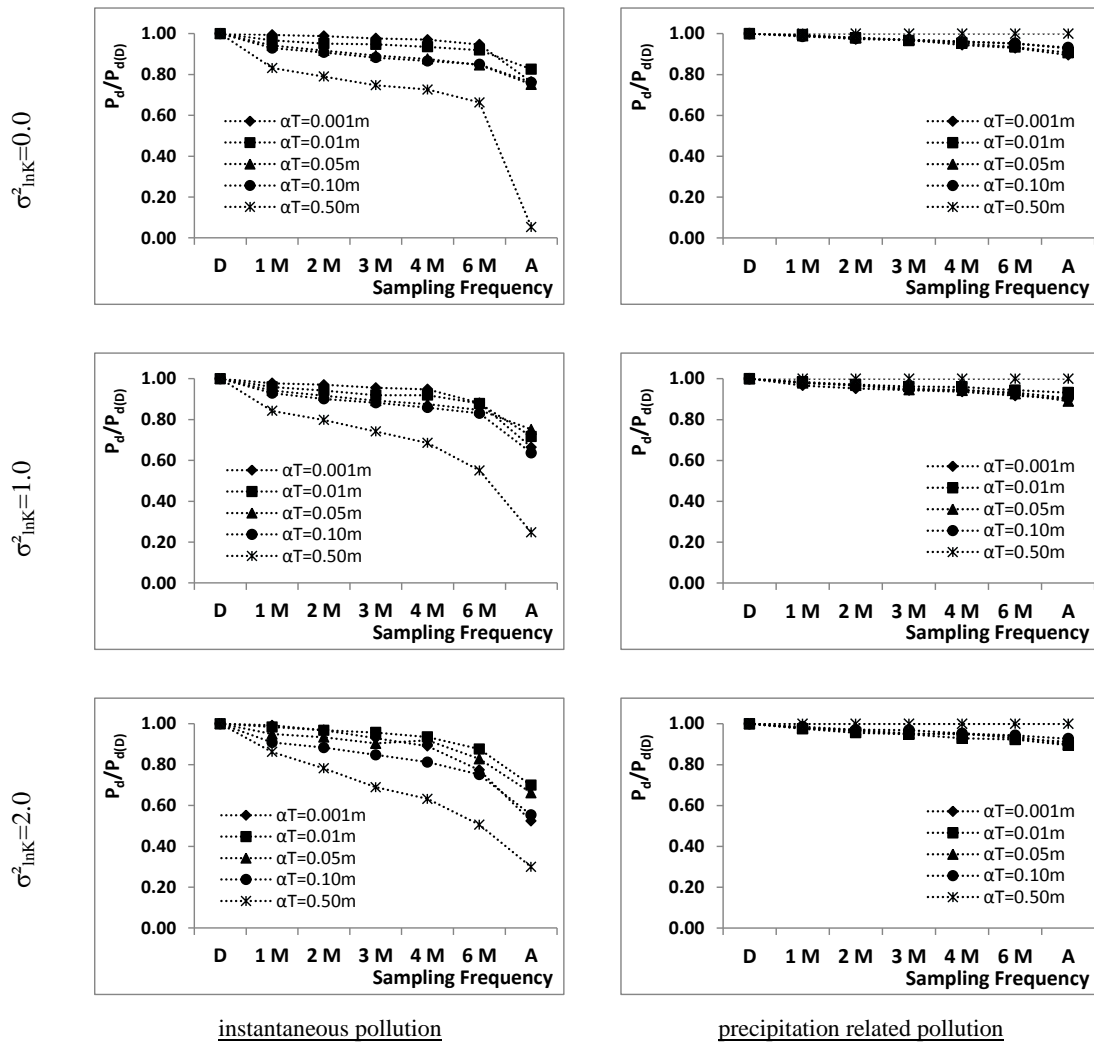


**Figure 6.7:** Percentage change of  $P_d$  as sampling frequency changes for a 4-well monitoring installation among daily (D), monthly (1 M), bimonthly (2 M), quarterly (3 M), every 4 months (4 M), biannual (6 M) and annual (A) sampling. The first column of the graphs reflects the results of an instantaneous case of pollution and the second column reflects a precipitation event related pollution, while horizontally heterogeneity changes, as is reflected through the variance of the  $\ln K$ .

Simulation results by *Papapetridis and Paleologos* (2011b) showed that in case of instantaneous release, the effect of sampling frequency on detection probability is more pronounced when dispersion of pollution into the aquifer is increased. In the case of a 4-well installation (first column in Figure 6.7) it can be observed that when a homogeneous field is considered the decrease of detection probability  $P_d$  is almost 100%, which means that the monitoring installation is actually cancelled, as it is entirely ineffective. As heterogeneity is increased, from  $\sigma_{\ln K}^2 = 0.0$  to  $\sigma_{\ln K}^2 = 2.0$ , the average improvement of  $P_d$  regarding a 4-well network, between biannual (6 M) and daily (D) sampling, excluding the case of high

dispersion ( $a_r = 0.50m$ ), is 17% while the same gain of  $P_d$  between annual (A) and sampling daily (D) is 46%. If we consider the improvement between biannual (6 M) or annual (A) and monthly (1 M) sampling, then the  $P_d$  gain is 12% and 40% respectively.

It can be seen by simulation results that there is a significant difference when sampling once a year and once every 6 months. This difference becomes even bigger if a high dispersion geological environment is considered. As a general rule, it appears that under all conditions at least biannual sampling should occur at a monitoring system (Papapetridis & Paleologos, 2011b), which complies with EU Directive in case of a waste sanitary landfill. If one wants higher detection probability, then monthly sampling appears to be the optimum choice for most well arrangements, considering both the effort involved if one were to proceed with a much more intense sampling and the improvements on detection attained at this level. It is noteworthy that in heterogeneous aquifers a large number of monitoring wells (a setting larger than 8 wells) does not perform much better in terms of detection if sampled infrequently (for example, once a year) than arrangements having a lower number of wells but are sampled more regularly.

Detection probability  $P_d$  in relation to sampling frequency in case of a pulsing pollution triggered by a precipitation event presents a totally different behavior, as it is depicted in the second column of Figure 6.7, where  $P_d$  changes in relation to applicable sampling frequency. The striking observation is that pollution dispersion amplifies the effectiveness of the monitoring wells arrangement. Even in the case of 4 wells it can be seen that despite the field's heterogeneity a 100% detection is achieved at every sampling frequency applied, when transverse dispersion is as high as  $a_r = 0.50m$ . Even in lower dispersion fields it can be seen that there is practically no gain in detection if groundwater is sampled more frequently than once every three months, as the average gain in  $P_d$  is less than 3%. When sampling is performed biannually then the average improvement in relation to monthly sampling, regardless of the geological heterogeneity, is 5% and if we consider annual sampling then the improvement to monthly sampling is 8%. It can also be noted that as dispersion increases the importance of sampling frequency is diminished, which is the opposite in the case of an instantaneous ejection of pollution into the aquifer.

The fact that pollution infiltrates the aquifer due to precipitation triggered events and that groundwater is recharged with pollutant mass result in retaining a plume's pollutant concentration above a detectable limit in a larger area. In heterogeneous fields, as field experiments have shown (Boggs et al., 1992), pollution is transported in paths where hydraulic conductivity is higher in relation to the adjacent areas. As dispersion causes greater

areal coverage by the plume, which in addition maintains detectable concentration values, detection is easier even if sampling is scarcer, as the paths of the plume remain basically the same, depending on hydraulic conductivity values.

It can be stated that in order for the operator of a controlled facility to succeed sufficient levels of possible groundwater pollution detection, they must focus on the problems that may come up from an instantaneous ejection rather than from a precipitation related one. It could safely be assumed that in the case of a continuous leak of pollutant into the aquifer the same results concerning sampling frequency policy would apply.

### 6.3.5 Time of detection and contaminated area

The average time needed until pollution is actually discovered from the monitoring was studied and compared to cases of instantaneous pollution. Assuming that  $\langle T_{obs} \rangle$  is the average number of days over 2,000 Monte Carlo simulations, in order for observation of contamination to be achieved at the monitoring points, based on a specific sampling schedule, and  $\langle T_{ar} \rangle$  being the average time for the pollution to arrive at the detection network, then in Figure 6.8 the ratio of  $\langle T_{obs} \rangle / \langle T_{ar} \rangle$  is plotted on the y-axis in relation to sampling frequency. Six different diagrams depict how time ratio changes for each three studied heterogeneities  $\sigma_{lnK}^2$  and two cases of transverse dispersion  $a_T$ , where the solid line describes the precipitation coupled pollution (PCP) events and the dashed line the instantaneous one (IP). A daily sampling with a 1-day numerical time step gives a ratio equal to one for all hydro-geological cases.

Diagrams depict, once more, that dispersion is the main contributing factor which influences the average detection time of groundwater pollution. The same behavior is observed in both cases of pollution origination, precipitation event started or instantaneous. In the case of a low dispersion environment, where  $a_T = 0.01m$  or less (Figure 6.8, first column),  $\langle T_{obs} \rangle / \langle T_{ar} \rangle$  ratio does not practically change when a homogeneous field is considered, while in the case of a heterogeneity field there is an average 10% increase in detection time ratio between daily and annual sampling, independently from the magnitude of heterogeneity, when pollution is coupled with precipitation, while in the case of instantaneous pollution the same difference is 8%. Practically, it can be said that there is no difference between instantaneous and pulsing pollution when the transverse dispersion coefficient is as low as  $a_T = 0.05m$  or lower.

In cases of higher values of dispersion where  $a_T = 0.1m$  or more (Figure 6.8, second column),  $\langle T_{obs} \rangle / \langle T_{ar} \rangle$  ratio actually increases as heterogeneity is increased. Pollution

dispersion functions as a background field attribute, which augments the influence of geological heterogeneity on the average time needed in order for pollution to be detected. It can be seen that in the case of PCP, when hydraulic conductivity variation is  $\sigma_{\ln K}^2 = 1.0$ , then the  $\langle T_{obs} \rangle / \langle T_{ar} \rangle$  ratio changes 15.5% between the monthly and bi-annual sampling and 22% between the monthly and annual sampling frequency, while for  $\sigma_{\ln K}^2 = 2.0$  the differences are 11% and 27% respectively. The same trend is observed in the cases of IP, but the time ratio difference in the case of  $\sigma_{\ln K}^2 = 1.0$  is 7% between the monthly and bi-annual sampling and 13% between the monthly and annual sampling frequency. In the case of  $\sigma_{\ln K}^2 = 2.0$  the difference is 5% and 18% respectively. Either way, heterogeneity increase in a high dispersion geological environment causes delayed pollution detection by the same monitoring wells network. As heterogeneity increases, differences in the average detection time between different sampling frequencies tend to decrease when sampling is performed at least twice a year or more. However, when sampling is performed once a year and heterogeneity increases, then the average needed detection time is increased, dictating that pollution is transported and dispersed for more time into the aquifer in order for detection to be accomplished.

It is also observed that when  $\sigma_{\ln K}^2 = 2.0$ , the average change of the time ratio  $\langle T_{obs} \rangle / \langle T_{ar} \rangle$  between bimonthly and every 4 months sampling frequency is less than 4%, while in the case of IP there is no practical difference even when the aquifer is sampled once every 4 months. In the corresponding diagram (Figure 6.8,  $\sigma_{\ln K}^2 = 2.0$ ,  $a_T = 0.05m$ )  $\langle T_{obs} \rangle / \langle T_{ar} \rangle$  drops below one, meaning that groundwater detection is accomplished 1% faster when sampling is performed fewer times a year than daily. This is artificial due to numerical approximations during computational procedure.

However, it is a fact that, as far as the presented simulation results are concerned, under the same hydro-geological parameters and adopting the same sampling frequency, IP event of groundwater pollution seems to be detected faster than the PCP. Moreover, it is noted that as heterogeneity increases the influence of different sampling intervals on detection time ratio  $\langle T_{obs} \rangle / \langle T_{ar} \rangle$  is more pronounced between precipitation events coupled pollution and instantaneous cases, as the average difference between them for the same sampling frequency is 8% in case of  $\sigma_{\ln K}^2 = 1.0$  and 12% in case of  $\sigma_{\ln K}^2 = 2.0$ . Aquifer pulsing pollution is detected later because more time is needed until the necessary pollutant mass accumulates into the aquifer, so that the plume's concentration exceeds concentration detection threshold limit. As heterogeneity is increased and plume is distorted and separated into smaller regions

(Figure 6.5), more mass diffusion is required to reach a detectable limit, meaning more precipitation events and, consequently, delayed pollution detection.

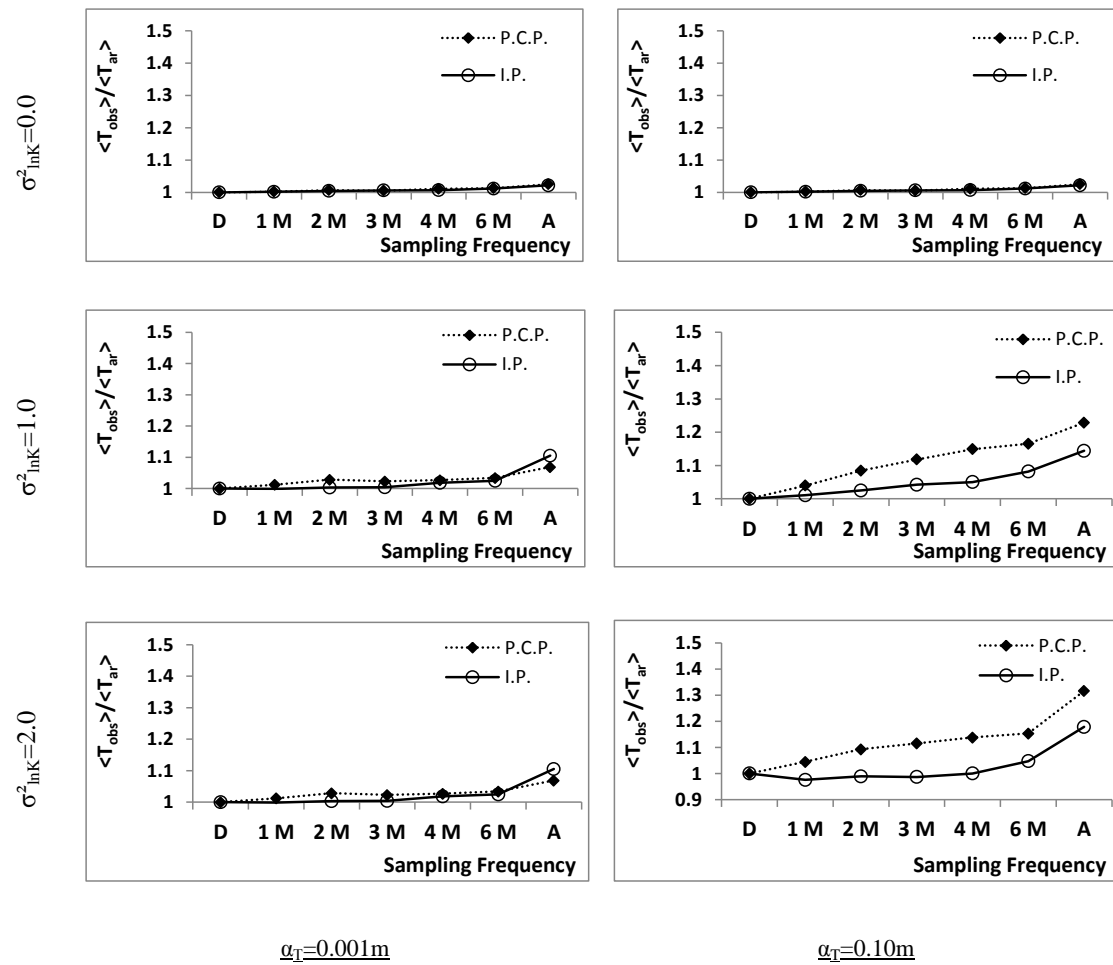


**Figure 6.8:** Change of ratio between average time of pollution arrival on monitoring installation ( $\langle T_{ar} \rangle$ ) and time of actual pollution observation ( $\langle T_{obs} \rangle$ ) in relation to sampling frequency for a 3-well monitoring arrangement.

An immediate result of late detection is the fact that the polluted area is growing larger. Pollution dispersion is again the main mechanism that multiplies the polluted area as this is increased. Figure 6.9 depicts the ratio of average polluted area  $\langle A_{pol} \rangle$  when groundwater pollution is actually detected by an 8-well monitoring network, to the control area  $L$  in relation to the logarithm of transverse dispersion coefficient. The striking feature of the diagram (Figure 6.9) is that for dispersion values above  $a_T = 0.10m$  the relative polluted area is almost 3 times bigger than when dispersion coefficient is  $a_T = 0.10m$ . This means that there is an upper limit beyond which the contaminated area increases very fast, making a possible remediation decision really expensive. It is noteworthy that this behavior is practically independent of the field's heterogeneity.

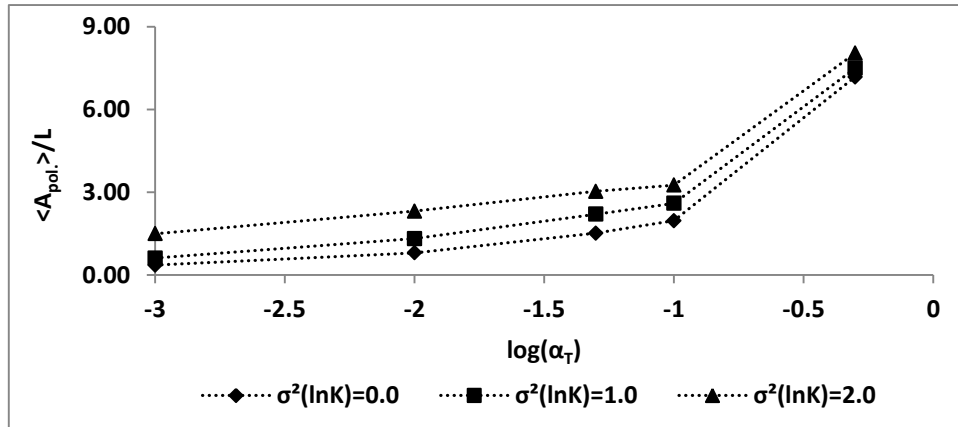


**Figure 6.9:** Change of ratio of the average polluted area  $\langle A_{pol.} \rangle$  to the area  $L$  of the contaminant potential source area in relation to the logarithm of transverse dispersion coefficient  $\alpha_T$  for three different cases of field heterogeneity.

Comparing average detection in relation to sampling frequency, we verified for the cases simulated that if sampling is performed at least twice a year in a low dispersion environment then average detection time is not practically affected. If again we assume that  $\langle A_{ar} \rangle$  is the average polluted area as soon as the plume actually arrives at and is detected by the monitoring wells arrangement, it is noticed that at a low dispersion field the average polluted area ratio changes less than 20% if groundwater is sampled at least 3 times a year, despite heterogeneity. In a homogeneous field the average change in area ratio is 7% if the aquifer is sampled at least twice a year, while in heterogeneous cases the difference in ratio is 19% if  $\sigma_{\ln K}^2 = 1.0$  and 29% if  $\sigma_{\ln K}^2 = 2.0$  respectively. In case sampling policy dictates annual sampling, then in highly heterogeneous aquifers the average polluted area is increased by 75%. Consequently, it is noticed that even if there is a 10% increase at detection time at low dispersion fields, when sampled annually the polluted area is dramatically increased, creating this way an expensive remediation background.

Examining greater dispersion value where  $\alpha_T = 0.50m$ , it can be seen that the effect of sampling frequency is more pronounced on  $\langle A_{obs} \rangle / \langle A_{ar} \rangle$  ratio. There is an almost linear increase of the polluted area as sampling is performed more scarcely, until the biannual frequency is reached, where the contaminated area is two times larger than the one at the time of the plume's actual arrival at the monitoring installation. At the point where sampling is performed once a year, the contaminated area becomes 2.7 times larger than the  $\langle A_{ar} \rangle$ , considering the heterogeneous cases, and 3.5 at the homogeneous case. In heterogeneous cases the effect of groundwater sampling frequency is less than in the homogeneous one, something which is due to the fact that aquifer heterogeneity causes plume deformations leading to creation of multiple pollution branches that may be transported in different

directions from the main bulk of contamination and, in conjunction with high dispersion of multiple ejected pollutant, may provide larger detectable areas, easier to find even if sampling is performed annually.

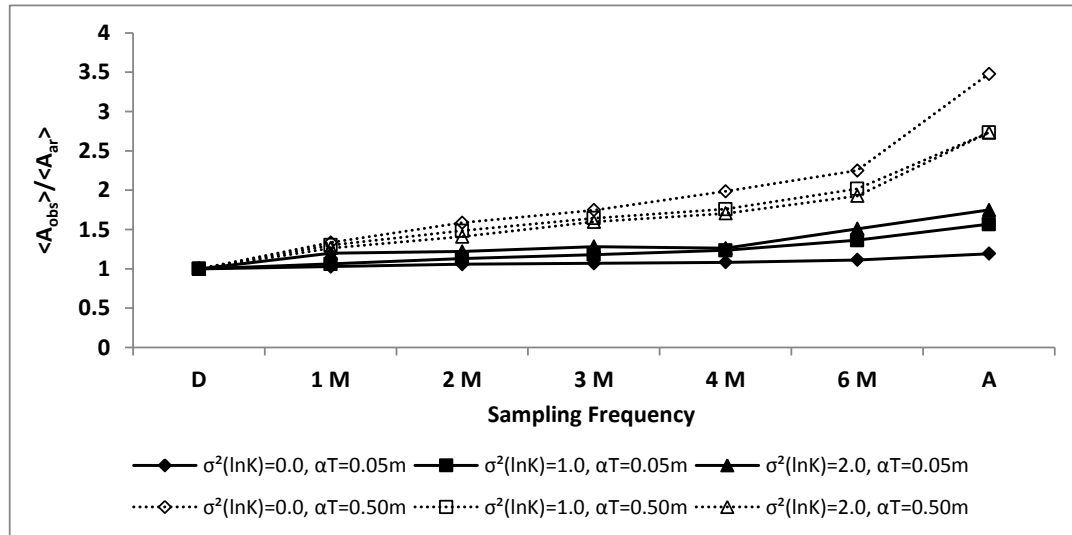


**Figure 6.10:** Change of ratio between the average polluted area  $\langle A_{obs} \rangle$  at the plume's actual detection by an 8-well monitoring arrangement and the average polluted area  $\langle A_{obs} \rangle$  when the plume is actually observed upon its arrival at the monitoring installation in relation to sampling frequency.

### 6.3.6 Remediation delay

*Papapetridis and Paleologos* (2011a) defined a corrected risk  $R^{cor}$  that accounts for the remedial action delay time (RADTi) as follows:

$$R^{cor} = P_d^{cor} C_d + P_f^{cor} C_f \quad (6.1)$$

where

$$P_d^{cor} = P_d \left( \frac{A_t}{A_{t+dt}} \right) \quad (6.2)$$

and

$$P_f^{cor} = 1 - P_d^{cor} \quad (6.3)$$

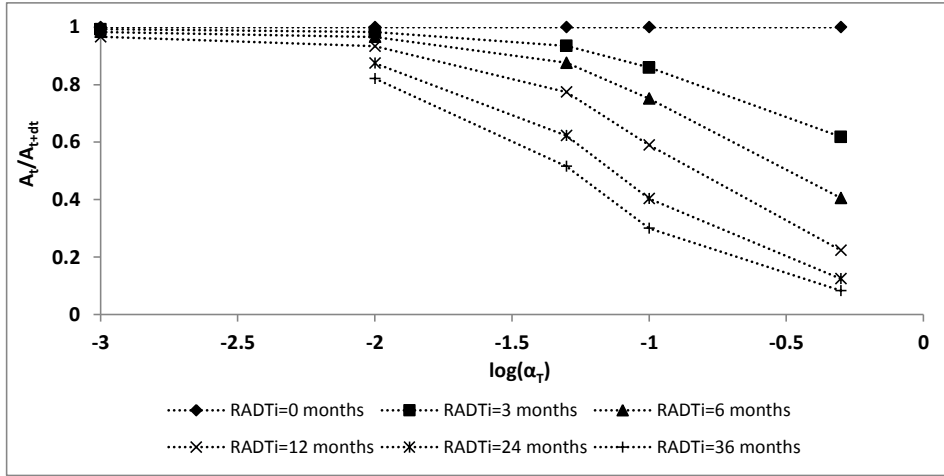
The corrected detection probability  $P_d^{cor}$  has been proposed as a measure of the economic impact of a remedial action delay, when the contaminated area has extended to  $A_{t+dt}$ , dictating a divergence from the maximum economic outcome that would take place at detection time, when the contaminated area is  $A_t$ . This procedure results in increasing the

failure probability and weighed cost of failure in the calculation of the risk factor as the time interval  $dt$  increases. Sensitivity analysis can then illustrate to decision-makers the influence of delays on the cost of remediation, as risk analysis can be sub-optimal when it has high costs, low probability of success, or inconclusive results (Lund, 2008). An extensive study in case of instantaneous aquifer pollution can be found in the work of *Papapetridis and Paleologos* (2012).

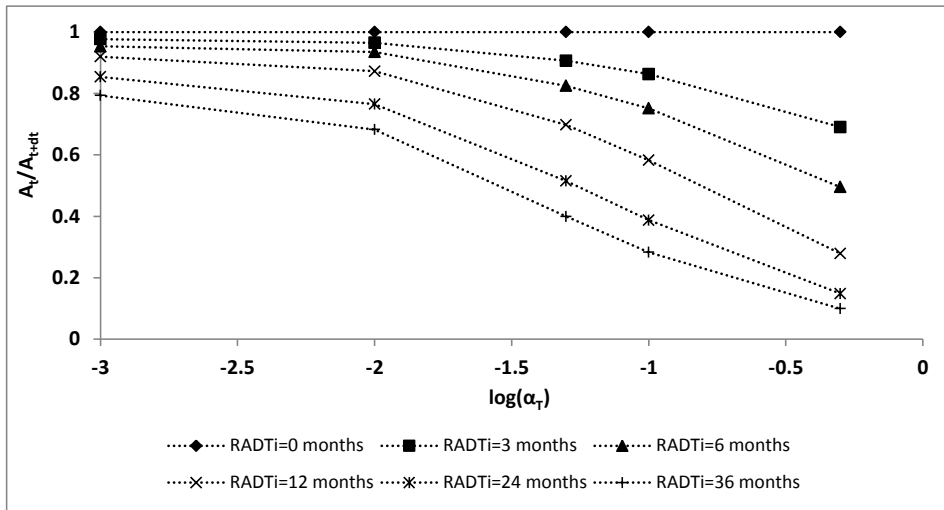
In order to study the effect of RADTi when PCP event takes place, the change of  $A_t/A_{t+dt}$  ratio, achieved by 6 monitoring wells, in relation to aquifer dispersion is demonstrated in Figure 6.11 (a)-(c), for each of the three heterogeneous cases that have been computationally studied. A common feature in all three diagrams is the fact that the more remediation actions are delayed, the more the contaminated area increases, causing the degradation of the initial probability's  $P_d$  value, according to Equation (6.2). In Figure 6.11(a) data referring to 24 and 36 months RADTi was not able to be calculated because the time of detection was already long enough. Therefore, adding more time to monitor the evolution of the plume overran the total 30-year simulation time.

In the only case heterogeneity does not practically affect  $P_d$  is when the aquifer is homogeneous and the dispersion of the pollution is as low as  $a_T = 0.001m$ . As heterogeneity increases, even at this low level of dispersion, the  $A_t/A_{t+dt}$  ratio decreases. In the case of a 6-well configuration at  $\sigma_{\ln K}^2 = 2.0$  and RADTi equal to 12 months, the polluted area ratio is 0.86, altering the initial detection probability  $P_d$  from 49% to 42.5% and for RADTi equal to 36 months to 32%. When dispersion is increased beyond  $a_T = 0.01m$ , the effect of RADTi is more pronounced, degrading probability  $P_d$  to 10% of its initial value, irrespectively of the aquifer's heterogeneity.

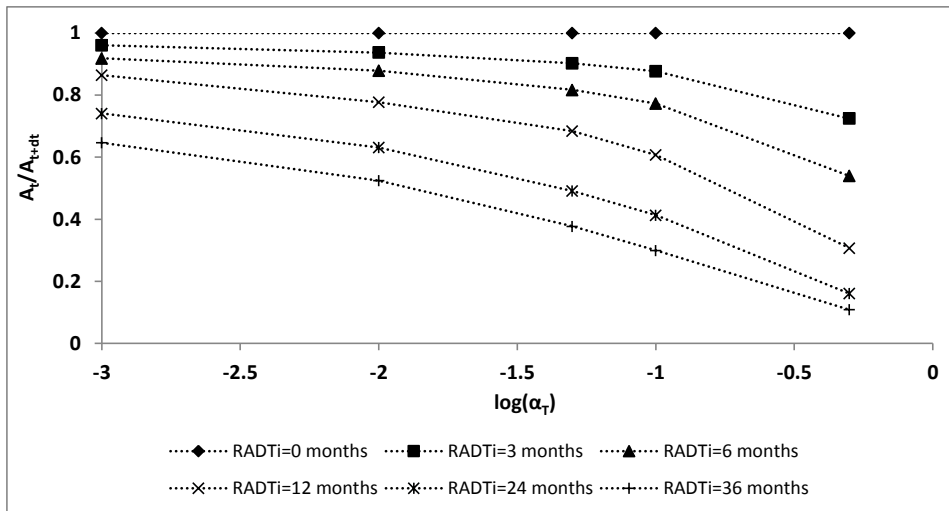
In the case of landfill originating groundwater pollution 99/31/ EU Directive states that the sampling frequency must be based on possibility for remedial actions between two samplings if a trigger level is reached. This may be interpreted in RADTi occurring in less than the sampling frequency, which should be at least once a year for a landfill installation, according to the same Directive. But, if this is the case, then assuming an aquifer where transverse dispersion coefficient is at least  $a_T = 0.10m$  and is sampled annually, the corrective detection probability will be 70% of its initial value of 96%, providing a  $P_d^{cor}$  equal to 67%. This is the detection probability that 3 monitoring wells may achieve if sampled annually, which is increased only by 10% when 2 wells are sampled daily.



(a)



(b)



(c)

**Figure 6.11:**  $A_t/A_{t+dt}$  versus  $\log(\alpha_T)$  for 6 monitoring wells and different Remedial Action Delay Times (RADTi): (a) homogeneous, (b) heterogeneous soils with  $\sigma_\gamma^2 = 1.0$  and (c) heterogeneous soils with  $\sigma_\gamma^2 = 2.0$

Instantaneous pollution cases that have been simulated in the authors' previous works (Papapetridis & Paleologos, 2011a, 2011b, 2012), presented a similar to precipitation triggered pollution behavior. In former studies, though, it was considered that an area specified inside a grid cell was contaminated even if there was the smallest amount of pollution inside it, and not necessarily a detectable pollutant concentration above the threshold limit. This was assumed to demonstrate the immediate effect of RADTi, otherwise due to pollution dilution into the aquifer there would be a false increase of detection probability, originating by the fact that the contaminated area above the threshold limit would actually be diminished. However, the above hypothesis can stand true if the chemical footprint of the pollutant is of such nature that the overall quality degradation of groundwater renders it unusable for desired uses, such as potable water, even in small concentrations. So, even if there is a similarity in RADTi between instantaneous and precipitation related pollution cases, it is a fact that the absolute polluted area in the latter case is larger, rendering it more expensive in terms of remediation.

## 6.4 Conclusions

In this study groundwater pollution triggered by local precipitation events was investigated in relation to its detection probability by various linear arrangements of monitoring wells, and how this probability is affected by the number of wells, hydro-geological parameters, sampling frequency and remediation action delay time. Moreover, comparisons were made with instantaneous cases of groundwater pollution, assuming the same hydro-geological conditions.

It was shown in this set of simulations that detection probability of a monitoring arrangement increases faster in precipitation event related pollution than in instantaneous cases, as the number of wells increases. In fact, a small number of monitoring wells, even less than 6, may achieve a 100% detection, in case of a homogeneous and of a medium dispersion aquifer. Moreover, a 3-well installation can detect groundwater pollution more than 50% of the time, depending on the field's hydro-geological properties.

Dispersion and heterogeneity are the hydro-geological parameters that directly affect the efficiency of the monitoring network. Preferential flow due to heterogeneity deformation and scattering of the plume is rather the main mechanism responsible for  $P_d$  decrease as the field gets more heterogeneous, and dilution of plume is hindered by pollutant mass pulsing injection. In any heterogeneity case dispersion amplifies the effectiveness of the monitoring wells. In fact, detection probability augmentation is so strong that even 3 wells computationally succeed 100% detection in a very high dispersion aquifer, where

$a_T = 0.50m$ . On the contrary, at instantaneous pollution cases dispersion initially increases  $P_d$ , but after a maximum has been reached detection probability diminishes due to fast dilution of pollution.

In the case of precipitation event triggered heterogeneous aquifer pollution, sampling frequency practically does not seem to affect detection probability of the monitoring network. Even if sampling is performed annually the improvement of  $P_d$  in relation to monthly sampling is 8%, while the effort made is 12 times bigger. On the other side, if instantaneous pollution is assumed it appears that under all conditions at least biannual sampling should occur and, moreover, if one wants higher detection probability then monthly sampling is the optimum choice for most well arrangements. In order for sufficient levels of monitoring groundwater pollution to be achieved, one must focus on the problems arising from an instantaneous ejection rather than a precipitation related one.

The average detection time of groundwater pollution in the case of precipitation triggered events does not practically change as sampling frequency increases up to biannual sampling and the simulated aquifer presents as low a transverse dispersion as  $a_T = 0.001m$ . However, as dispersion increases to  $a_T = 0.10m$  and, at the same, a heterogeneous aquifer of hydraulic conductivity variation  $\sigma_{lnK}^2 = 1.0$  is assumed, simulations showed that the ratio  $\langle T_{obs} \rangle / \langle T_{ar} \rangle$  increases up to 22% between monthly and annual sampling. Either way, heterogeneity increase in a high dispersion geological environment causes delayed pollution detection by the same monitoring wells network. Results showed that as heterogeneity increases, differences in average detection time between different sampling frequencies tend to decrease when sampling is performed at least twice a year or more. Time ratio  $\langle T_{obs} \rangle / \langle T_{ar} \rangle$  concerning detection of instantaneous pollution cases changes in relation to sampling frequency, similarly to precipitation triggered cases. However, when dispersion and heterogeneity are increased their effects are less acute when it comes to detection time.

Average polluted area ratio  $\langle A_{obs} \rangle / \langle A_{ar} \rangle$  in a low dispersion environment changes less than 20% if groundwater is sampled at least 3 times a year, despite heterogeneity. However, if annual sampling is adapted, then in highly heterogeneous aquifers the average polluted area is increased by 75%. This means that even if there is a 10% increase at detection time at low dispersion fields, the polluted area is dramatically increased when sampled annually. When dispersion is  $a_T = 0.50m$ , it is seen that the effect of sampling frequency is more pronounced on  $\langle A_{obs} \rangle / \langle A_{ar} \rangle$  ratio. The polluted area is almost linearly increased as sampling is performed more scarcely until the biannual frequency is reached, when the contaminated area is twice as large as the one at the time of the plume's actual arrival at the

monitoring installation. When annual sampling is assumed, the contaminated area becomes 2.7 times larger than the  $\langle A_{ar} \rangle$  in the heterogeneous cases and 3.5 in the homogeneous case.

In all simulations the main hydro-geological parameter was the field's dispersion, affecting detection probability, average detection time and the contaminated area, all in relation to sampling frequency. In conjunction with the fact that pollutant mass is constantly added when precipitation occurs, even in different quantities and in random time, depending on rain events, dispersion causes greater detectable areal coverage. Consequently, when it increases it creates a favorable background in terms of pollution detection and renders the effectiveness of monitoring wells arrangements tolerable in scarce sampling frequency, when it is performed at least twice a year.

On the other hand, when RADTi is increased, dispersion results on the detection probability corrective factor in Equation (2) are more pronounced. In a high dispersion aquifer  $P_d^{cor}$  rapidly deteriorates even if RADTi is 6 months or less. Heterogeneity seems to affect RADTi when dispersion is equal or less than  $\alpha_r = 0.01m$ , causing less than 7% decrease at the initial detection probability in case of a 12-month delay and assuming a homogeneous aquifer. Similarly, when the hydraulic conductivity variance is  $\sigma_{\ln K}^2 = 1.0$ , the respective decrease is 13% and when  $\sigma_{\ln K}^2 = 2.0$  the decrease is 23%.

In any case RADTi is essential in estimating the risk concerning the ability of a groundwater monitoring installation to detect pollution, as it is a hidden parameter that may give a very big offset in risk calculations. Even if, according to current legislation, remedial actions should take place as soon as a trigger event occurs, this is not always the case, as locating and controlling a groundwater source is usually a set of many actions, performed by different collaborating groups of people (installation operator, local contractors). This kind of collaborations, among people of different interests and disciplines, in conjunction with funding problems, may lead in longer RADTi and, consequently, in bigger and more complicated environmental issues.

# CHAPTER 7

## Conclusions

---

The objective of this research was to numerically investigate groundwater contamination detection probability achieved by a linear monitoring arrangement of wells and to provide a novel framework that modifies traditional risk analysis by supplying a corrected detection probability that accounts for delays in remedial actions. A stochastic two-dimensional model was developed that performed high resolution Monte Carlo simulations, coupling a finite difference flow model and a Random Walk Particle Tracking algorithm that simulated contamination plume advection and dispersion. Uncertainty stemming from the subsurface field itself was simulated with the Spectral Turning Bands method.

Pollution source was assumed to be a randomly selected point inside the controlled area boundaries where the pollution is considered to have started. Two major cases concerning duration of the pollution were examined. The instantaneous case, whose duration of pollution is less than the modeling time step  $\Delta t$  which was set equal to one day, and the precipitation triggered pollution, where it was assumed that each time rain occurred a quantity of pollution, proportional to the daily average precipitation height, injected into the aquifer. Conclusions are summarized at the next paragraphs.

### **7.1 Instantaneous groundwater pollution detection probability in heterogeneous aquifers**

Pollution originated instantaneously from a random point source within a landfill facility. Different arrangements and distances of monitoring wells from a landfill were

considered, and the corresponding detection probabilities  $P_d$  and contaminated groundwater areas, at different time periods, were calculated.

It was observed that convergence of the probability of detection  $P_d$  to a constant value was attained, for all monitoring configurations, at about 3,000 Monte Carlo simulations. The number of tracking particles used to simulate contaminant transport had a strong influence on the values of  $P_d$  calculated through numerical experiments. For all monitoring arrangements convergence of the  $P_d$  to a stable value was attained at 8,000 tracking particles.

In all cases of hydro-geological heterogeneity and dispersion, the more wells utilized for detection purposes the greater the  $P_d$ . For a fixed heterogeneity level, for each specific arrangement of wells, the maximum detection probability increases, along with dispersion coefficient up to a certain value of  $\alpha_T$ , and then decreases. For transverse dispersion greater than  $0.2m$ , maximum detection is attained very close to the trailing edge of the landfill. As a general rule, the efficiency of contaminant detection from a specific well arrangement decreases as the variance of  $\ln K$  increases.

The frequency of sampling is critical in heterogeneous aquifers of high dispersion. In generally, it appears that under all conditions at least biannual sampling should occur at a monitoring system. If one wants a higher detection probability, then sampling at a monthly frequency appears to be the optimum choice for most well arrangements, considering both the effort involved, if one were to proceed with a much more intense sampling, and the improvements on detection attained at this level. It is interesting to note that in heterogeneous aquifers if a large number of monitoring wells is sampled infrequently, they do not perform much better in terms of detection than arrangements having a lower number of wells but which are sampled more regularly.

Decision-making analysis that evaluates the economic worth of different arrangements of wells calculates remediation costs based on contaminated groundwater volumes that are estimated at the time of detection. In practice there is always a remedial action response delay and hence remedial costs surpass those calculated at detection time. To correct this situation an expression is proposed for a corrected risk factor  $R^{cor}$  that accounts for remedial action response delay,

$$R^{cor} = P_d^{cor} C_d + P_f^{cor} C_f \quad (6.4)$$

$$P_d^{cor} = P_d \left( \frac{A_t}{A_{t+dt}} \right), \text{ and } P_f^{cor} = 1 - P_d^{cor} \quad (6.5)$$

$A_t$  corresponds to the contaminated area (volume) at detection time  $t$ , and  $A_{t+dt}$  is the contaminated area (volume) at a later time, due to delays in remediation procedures. Our approach can be viewed as a way to downgrade the importance of early detection, if not followed by quick remedial response, in risk analysis calculations. This expression estimates, for example, in a heterogeneous field where twelve monitoring wells operate and are sampled every day, that a remediation delay of 36 months almost doubles the failure cost which enters risk calculations.

## **7.2 Sampling frequency of groundwater monitoring system and remediation delay at contaminated sites**

Using high-resolution numerical Monte Carlo two-dimensional simulations, the impact of sampling frequency on the probability of detecting groundwater contamination in various subsurface environments was investigated, as well as the effects that sampling schedules and remediation delays have on the growth of contaminated subsurface areas and remediation costs. In homogeneous media of low dispersion, a large number of wells provide such density of coverage of the area downstream a landfill that a plume cannot remain undetected, even with few observations. On the other hand, in homogeneous soils of high dispersion, irrespective of the density of the monitoring network, because contaminants disperse strongly and concentrations at the monitoring points drop below the threshold limits quickly, a rigorous sampling schedule must be followed in order to retain a network's performance.

A similar situation holds for heterogeneous soils of high dispersion, with the existence of low permeability zones appearing to ameliorate the dispersion effects, but not sufficiently enough in order to alter the conclusion about the criticality of the sampling schedule. The frequency of sampling is also of interest in order to minimize the time lag between the time that concentrations above a threshold limit first appear at monitoring locations and the time that these concentrations are observed through sampling. The objective, of course, is to delineate the extent of the contaminated area and to initiate remediation efforts as soon as possible. Analysis of the lag between the time that contaminants appeared at monitoring sites and the time they were observed led to the conclusion that, in terms of time delay, bimonthly sampling constitutes a safe strategy for a wide range of hydro-geological environments. In the case of aquifers that exhibit fast pathways of contaminant transport, through the existence of high permeability zones, further investigation is required. However, in terms of the growth of

the contaminated are, with the exception of monthly sampling, all other less frequent schedules resulted in significant enlargement of plume areas, thus leading to more costly remediation. Moreover, it was demonstrated that remedial response delays in highly dispersive environments must be of the order of a few months if one does not wish the contaminated areas and remediation costs to grow significantly.

### **7.3 Parameters on stochastic simulation of contaminant detection probability**

It was studied how the number of point sources, the size of the controlled area (e.g. a landfill facility) and the quantity of an instantaneous injected pollution affect plume detection of a monitoring well setting. In each examined parameter it was considered that the rest of the factors affecting estimation remain constant. Simulations were performed in the context of uncertainty factors deriving from the environment itself, reflected on the parameter of hydraulic conductivity and the lack of information about the initial conditions of a leak.

It was numerically verified, in the cases examined, that as the size of the control area becomes larger and the number of wells remains constant, then detection probability decreases. If the width of a control area is to be increased, so must the number of monitoring wells, maintaining at least the same density as in the initial size.

In all simulated cases, the general observation is that when two equivalent groundwater pollution sources are present their detection is easier. More often aquifer sampling does not alter monitoring efficiency in terms of the presence of more pollution sources.

Simulation results indicated that when the initial concentration of pollution is very low (below 1,000 mgr/lit) then its detection is very hard, regardless of the aquifer's hydro-geological parameters. The monitoring wells efficiency of low to medium dispersion aquifers reaches a maximum, which is independent of the initial mass of pollution intruding the aquifer. The turning point of initial pollution concentration is  $C = 8,000 \text{mgr} / \text{lit}$ , which is the value where  $P_d$  reaches a plateau. In every case, lower concentrations were harder to detect, dictating that in order for a monitoring setting to be sensitive, at least at simulation level, even for small amounts of pollution at least 12 wells must be used.

### **7.4 Modeling of aquifer pollution detection probability triggered by precipitation**

Groundwater pollution triggered by local precipitation events was investigated in relation to its detection probability by various linear arrangements of monitoring wells. Also,

the way this probability is affected by the number of wells, hydro-geological parameters, sampling frequency and remediation action delay time was examined. Moreover, comparisons were made with instantaneous cases of groundwater pollution, assuming the same hydro-geological conditions.

It was shown that detection probability of a monitoring arrangement increases faster in precipitation event related pollution than in instantaneous cases, as the number of wells increases. In fact, a small number of monitoring wells, even less than 6, may achieve a 100% detection, in the case of a homogeneous medium dispersion aquifer. Moreover, a 3-well installation can detect groundwater pollution more than 50% of the time, depending on the field's hydro-geological properties.

Dispersion and heterogeneity are the hydro-geological parameters that directly affect the efficiency of the monitoring network. Preferential flow due to heterogeneity deformation and scattering of the plume is possibly the main mechanism responsible for  $P_d$  decrease, as the field gets more heterogeneous and dilution of plume is hindered by pollutant mass pulsing injection. In any heterogeneity case, dispersion amplifies the effectiveness of the monitoring wells. On the contrary, at instantaneous pollution cases, dispersion initially increases  $P_d$  but, after a maximum has been reached, detection probability diminishes due to fast dilution of pollution.

In the case of precipitation event triggered heterogeneous aquifer pollution, sampling frequency practically does not seem to affect detection probability of the monitoring network. On the other hand, if instantaneous pollution is assumed, it appears that under all conditions at least biannual sampling should occur and, moreover, if one wants higher detection probability, monthly sampling is the optimum choice for most well arrangements. In order for sufficient levels of monitoring groundwater pollution to be achieved, one must focus on the problems arising from an instantaneous ejection rather than a precipitation related one.

The average detection time of groundwater pollution in the case of precipitation triggered events does not practically change as sampling frequency increases up to biannual sampling and the simulated aquifer presents very low transverse dispersion ( $a_T = 0.001m$ ). Heterogeneity increase in a high dispersion geological environment causes delayed pollution detection from the same monitoring wells network. Time ratio  $\langle T_{obs} \rangle / \langle T_{ar} \rangle$  concerning detection of instantaneous pollution cases changes in relation to sampling frequency similar to those of precipitation triggered cases. However, when dispersion and heterogeneity are increased, their effects are less acute when it comes to detection time.

The average polluted area ratio  $\langle A_{obs} \rangle / \langle A_{ar} \rangle$  increases as field dispersion increases. When dispersion is very high ( $a_r = 0.50m$ ) the polluted area is almost linearly increased, as sampling is performed more scarcely until the biannual frequency is reached.

In all simulations the main hydro-geological parameter was the field's dispersion, affecting detection probability, average detection time and the contaminated area, all in relation to sampling frequency. In conjunction with the fact that pollutant mass is constantly added when precipitation occurs, even in different quantities and in random time, depending on rain events, dispersion causes greater detectable areal coverage. Consequently, when it increases it creates a favorable background in terms of pollution detection and renders the effectiveness of monitoring wells arrangements tolerable in scarce sampling frequency, when it is performed at least twice a year.

When RADTi is increased, dispersion results are more pronounced for the detection probability corrective factor. In a high dispersion aquifer  $P_d^{cor}$  rapidly deteriorates even if RADTi is 6 months or less. As heterogeneity increases, it seems that RADTi affects less  $P_d$  assuming the same pollution dispersion. In any case, RADTi is essential to estimate the risk concerning the ability of a groundwater monitoring installation to detect pollution, as it is a hidden parameter that may give a very big offset in risk calculations.

# APPENDIX A

## 2-D Source Code

---

Source code for all cases that have been numerically simulated is provided. In Section 1 source code for the instantaneous case of pollution is provided. In Section 2 code modeling pollution related to precipitation events is provided. Because of the fact that subroutines that solve steady flow equations numerically and Spectral Turning Bands that produce random fields are common between them, they are referred at Section 3 and 4 respectively. It must be noted that Turning Bands algorithm in 2-D is different from that in 3-D. In order TUBA subroutine to run it needs a complementary file named “tuba211d.inc”, which must be located in the folder where compilation is to take place. The listing for this file is:

```
C      INCLUDE FILE FOR TUBA VERSION 2.11d
C-----
--
      COMMON /TBAPAR/ ICOVF, IPAA, LINES, FMAX, NHAR, NMAX, UN, FX, FY,
1  XO, YO, TBMX, KS, IP, NX, NY, XMAX, YMAX, DX, DY, NXY,  AM, AN, AV, CLX, CLY,
1  IDFP, IURN,  DS, UD, KD, NR, CK, FM, FA,  A1, A3, A5, KT, DT, SG, B0, B1, B2,
1  NF, IPF, ISAJ, IULP, MSK, IMSEX
```

In order a 2-D model simulation to take place, source code of Section 1 or 2 along with code of Section 3 and 4 must be combined and compiled together. All source code is programmed in FORTRAN 77 and has been compiled using the freeware editor and compiler FORCE 2.0. All runs performed in a workstation equipped with two quad core Xeon microprocessors and 12 GB of RAM memory.

## A-1 Instantaneous Pollution

```
1      PROGRAM TBRW
2      C
3      C      TBRW CODE HAS BEEN DEVELOPED BY PAPANETRIDIS KONSTANTINOS
4      C      TUBA HAS BEEN DEVELOPED BY DR A.MANTOGLOU
5      C      FLOW HAS BEEN DEVELOPED BY DR A.J.DESBARATS
6      C
7      C-----
8      C      MONTE CARLO STOCHASTIC SCHEME SIMULATING 2-D POLLUTION FLOW
9      C      INTO A HETEROGENEOUS AQUIFERS. HETEROGENEOUS AQUIFERS IN THE
10     C      MODEL WERE SIMULATED USING THE 2-D SPECTRAL TURNING BANDS
11     C      METHOD(STUBA) (ABABOU ET AL., 1989; MANTOGLOU AND WILSON, 1982;
12     C      MCLAUGHLIN ET AL., 1993; PALEOLOGOS AND SARRIS, 2011; TOMPSON
13     C      AND GELHAR, 1990B). THE AQUIFER IS ASSUMED TO BE CONFINED,
14     C      WITH GIVEN HYDRAULIC HEAD AT LEFT AND RIGHT BOUNDARIES,
15     C      RESULTING IN A MACROSCOPICALLY CONSTANT HYDRAULIC GRADIENT OF
16     C      0.001. SOURCE LOCATION UNCERTAINTY WAS ENVISAGED CONSIDERING
17     C      EQUALLY PROBABLE DIFFERENT POINT OF POLLUTION ORIGIN DURING
18     C      EACH DIFFERENT SIMULATION, WHICH BELONGS INSIDE THE CONTROL AREA
19     C
20     C      LOGNORMAL MEDIA
21     C      CORRELATED CONDUCTIVITY FIELD
22     C      2-D TURNING BANDS METHOD (TUBA)
23     C      DOUBLE PRECISION USED
24     C      HYBRID INTERPOLATION VELOCITY SCHEME
25     C
26     C      PARAMETER IDENTIFICATION:
27     C      IMEM= 1024000 MAX PARTICLES
28     C      KW=8 MONITORING WELLS ARRANGEMENT (1,2,3,4,6,8,12,20)
29     C      KSA=7 SAMPLING FREQUENCIES (1,30,60,90,120,180,360 DAYS)
30     C      MDS=7 DISPERSION CASES (0.001,0.01,0.02,0.05,0.10,0.20,0.50 M)
31     C
32     C      ONE INPUT FILE IS REQUIRED: TUBA211.INC
33     C      THIS FILE IS PROVIDED BY TUBA DEVELOPER
34     C
35     C-----
36     C
37     C      IMPLICIT DOUBLE PRECISION (A-H,O-Z)
38     C
39     C      KW:No OF WELLS, KSA:SAMPLING INTERVALS, MDS:TRANSVERSE DISPERSION
40     C      PARAMETER (IMEM=1024000)
41     C      PARAMETER (KW=8,KSA=7,MDS=7)
42     C      DOUBLE PRECISION P (IMEM),VELX (IMEM),VELY (IMEM),VELZ (IMEM),RK (IMEM)
43     C      DOUBLE PRECISION TATOD(MDS,0:KSA-1,KW),ATOD(0:KSA-1,KW),
44     C      & TDCM(MDS)
45     C      DOUBLE PRECISION NCAR(0:KSA-1,KW),CAR1(0:KSA-1,KW),
46     C      & CAR3(0:KSA-1,KW),CAR6(0:KSA-1,KW),CAR12(0:KSA-1,KW),
47     C      & CAR24(0:KSA-1,KW),CAR36(0:KSA-1,KW),TNCAR(MDS,0:KSA-1,KW),
48     C      & TCAR1(MDS,0:KSA-1,KW),TCAR3(MDS,0:KSA-1,KW),TCAR6(MDS,0:KSA-1,
49     C      & KW),TCAR12(MDS,0:KSA-1,KW),TCAR24(MDS,0:KSA-1,KW),
50     C      & TCAR36(MDS,0:KSA-1,KW)
51     C      INTEGER TS,TEND,TPRD,SNSIM,TVC,TDET(MDS,0:KSA-1,KW),FDET(MDS,
52     C      & 0:KSA-1,KW),NOW(KW),ISA(0:KSA-1),ORPOSO,PX,PY,PZ,LFC(100000)
53     C      LOGICAL DET(0:KSA-1,KW),MONITOR
54     C      CHARACTER SDATE_R*8,DATE_R*8,T_R*10,ST_R*10
55     C
56     C      COMMON /PARAM/ P0,P1,EP,DX,DY,DZ,NX,NY,NZ,NSEED
57     C      COMMON /SOLVE/ OMEGA,TOL,TOL1,MITER,SNSIM
58     C      COMMON /VELOCITY/ VELX,VELY,VELZ
59     C      COMMON /PARTICLE/ PM,TVC,NPAR
```

```

60      COMMON /LANDFILL/ LFXI, LFXE, LFYI, LFYE, LFAR, LFC
61      COMMON /MONITORING/ SIGMA, MONITOR, NOW, ISA
62      COMMON /TIME/ TS, TEND, TPRD, NSIM
63      COMMON /WAREA/ NCAR, CAR1, CAR3, CAR6, CAR12, CAR24, CAR36
64      C
65      C-----
66      C-   GRID SPACING FOR TURNING BAND SIMULATIONS IN X
67      C-   DIFFERENT FROM ABOVE SO AS TO CREATE ANISOTROPY. NOTE
68      C-   THAT TURNING BAND ROUTINE CAN ONLY SIMULATE ISOTROPIC
69      C-   FIELDS AND THAT, TO GENERATE ANISOTROPIC FIELDS, YOU HAVE
70      C-   TO TRANSFORM THE GRID SPACING....
71      C-----
72      C
73      C-----HETEROGENEITY OF THE FIELD -----
74      C
75      SIGMA=1.00D0
76      C
77      C-----PARAMETER INITIALIZATION-----
78      C
79      NSIM=3000           !NUMBER OF SIMULATIONS
80      C
81      TEND=10950         !TIME MONITOR ENDS (30 YEARS)
82      TPRD=1            !PERIOD OF TIME THAT LEAK OCCURS
83      TS=1              !TIME STEP (DAYS)
84      C
85      LNDFX=1000        !LENGHT OF SIMULATION AREA (METERS)
86      LNDFY=400         !WIDTH OF SIMULATION AREA (METERS)
87      LNDFZ=1          !DEPTH OF SIMULATION AREA (METERS)
88      DX=2              !DX STEP ON X AXIS (METERS)
89      DY=2              !DY STEP ON Y AXIS (METERS)
90      DZ=1              !DZ STEP ON X AXIS (METERS)
91      NX=INT(LNDFX/DX)  !NODES IN X-DIRECTION (DIMENSIONLESS)
92      NY=INT(LNDFY/DY)  !NODES IN Y-DIRECTION (DIMENSIONLESS)
93      NZ=INT(LNDFZ/DZ)  !NODES IN Z-DIRECTION (DIMENSIONLESS)
94      C
95      DL=0.D0           !TB BLOCK DIMENSION
96      DC=0.D0           !TB BLOCK DIMENSION
97      DN=0.D0           !TB BLOCK DIMENSION
98      C
99      A=20.D0           !CORELLATION COEFFICIENT (METERS)
100     A=(-1.D0)*ABS(A)
101     HEADG=0.001D0
102     P0=0.D0           !STARTING HYDRAULIC HEAD
103     P1=NX*DX*HEADG    !ENDING HYDRAULIC HEAD
104     EP=0.25D0         !EFFECTIVE POROSITY
105     ALPHA=2.3D0       !MEAN lnK
106     C
107     NPAR=8000         !TOTAL PARTICLES TO BE EJECTED
108     PM=1              !PARTICLE'S MASS
109     TVC=112           !THRESHOLD VOLUMETRIC CONCENTRATION
110     C
111     MONITOR=. TRUE.   !PARAMETER THAT CONTROLS IF WE MONITOR OR NOT
112     C
113     C   RANDOM NUMBER SEEDS
114     DSEED=2147811051.D0 !seed number for RNG`
115     NSEED=1236547896  !15.8
116     C
117     C
118     C   BETA FOR NOW ON IS THE STANDARD DEVIATION NOT THE VARIANCE
119     BETA=SQRT(SIGMA)
120     C
121     TOL=0.00001D0
122     TOL1=0.00005D0
123     MITER=2000
124     SNSIM=0           ! NUMBER OF SIMULATIONS WITH FLOW FIELD
125     SOLUTION
126     NNNN=NX*NY*NZ
127     NXNY=NX*NY

```

```

128      DSEED=DSEED*NXNY*NY*BETA*DX/ (NSIM*NSIM)
129      SSXEN=0.D0
130      RKPOIN21=0.D0
131      RKPOIN22=0.D0
132      RKPOINT1=0.D0
133      RKPOINT2=0.D0
134      SSX2EN=0.D0
135      C
136      DO 22 K=1,MDS
137          DO 22 J=0,KSA-1
138              DO 22 I=1,KW
139                  TDET(K,J,I)=0
140                  FDET(K,J,I)=0
141                  TATOD(K,J,I)=0.D0
142      22 CONTINUE
143      C
144      C      FLOW EQUATIONS RELAXATION FACTOR
145      C      - DEPEDENCE HAS BEEN OBSERVED. BEST RESULTS ARE ACCOMPLISHED
146      C      WHEN RELAXATION FACTOR IS THE HIGHER POSSIBLE (INITIAL WAS 1.85)
147      C      OMEGA0=1.85D0
148      C
149      C      IF(nnnn.GE.180000) OMEGA0=1.88D0
150      C      IF(nnnn.GE.240000) OMEGA0=1.91D0
151      C      IF(nnnn.GE.390000) OMEGA0=1.92D0
152      C      IF(nnnn.GE.490000) OMEGA0=1.95D0
153      C      IF(nnnn.GE.700000) OMEGA0=1.97D0
154      C      IF(nnnn.GE.850000) OMEGA0=1.98D0
155      C      IF(nnnn.GE.850000) TOL=0.0001D0
156      C      IF(nnnn.GE.850000) TOL1=0.0005D0
157      C
158      C
159      C      PRINTING ON SCREEN THE STARTING TIME
160      C      CALL DATE_AND_TIME (SDATE_R,ST_R)
161      C
162      C      3-D TB INPUT DATA (BLOCK DIMENSIONS)
163      C      IF(DL.EQ.0.0) DL=DX
164      C      IF(DC.EQ.0.0) DC=DY
165      C      IF(DN.EQ.0.0) DN=DZ
166      C
167      C
168      C -----PRINTING INITIAL INFORMATION-----
169      C
170      C      PRINT*, 'THIS IS THE TOTAL PLUME TRANSPORT SIMULATION!'
171      C      PRINT*, 'NUMBER OF REALIZATIONS : ', NSIM
172      C      PRINT 715, NX, NY, NZ
173      C      PRINT 716, DX, DY, DZ
174      C      PRINT 717, DL, DC, DN
175      C
176      C      715 FORMAT(' GRID SIZE : ', I3, 'X', I3, 'X', I3)
177      C      716 FORMAT(' BLOCK DIMENSIONS : ', F5.2, ' X', F5.2, ' X', F5.2)
178      C      717 FORMAT(' TB BLOCK DIMENSIONS : ', F5.2, ' X', F5.2, ' X', F5.2)
179      C
180      C      PRINT*, 'CORRELATION RANGE (LENGTH UNITS) : ', A
181      C      PRINT*, ' & VARIANCE : ', BETA*BETA
182      C      PRINT*
183      C      PRINT*, ' ***** STARTING SIMULATIONS *****'
184      C      PRINT*
185      C
186      C
187      C-----ESTABLISHING MONITOR SYSTEM AND SAMPLING POLICY-----
188      C      LANDFILL'S GEOMETRY
189      C      CALL LANDF
190      C
191      C      NUMBER OF WELLS
192      C      DO IW=1, KW
193      C          IF(IW.LE.4) NOW(IW)=IW
194      C          IF(IW.EQ.5) NOW(IW)=6
195      C          IF(IW.EQ.6) NOW(IW)=8

```

```

196         IF(IW.EQ.7) NOW(IW)=12
197         IF(IW.EQ.8) NOW(IW)=20
198     ENDDO
199 C
200 C     SAMPLING INTERVALS
201     DO JS=0,KSA-1
202         IF(JS.GE.1.AND.JS.LE.4) ISA(JS)=JS*30
203         IF(JS.EQ.0) ISA(JS)=1
204         IF(JS.EQ.5) ISA(JS)=180
205         IF(JS.EQ.6) ISA(JS)=365
206     ENDDO
207 C
208 C     DISPERSIVITY FACTOR
209     DO MTDC=1,MDS
210         IF(MTDC.EQ.1) TDCM(MTDC)=0.001D0
211         IF(MTDC.EQ.2) TDCM(MTDC)=0.01D0
212         IF(MTDC.EQ.3) TDCM(MTDC)=0.02D0
213         IF(MTDC.EQ.4) TDCM(MTDC)=0.05D0
214         IF(MTDC.EQ.5) TDCM(MTDC)=0.10D0
215         IF(MTDC.EQ.6) TDCM(MTDC)=0.20D0
216         IF(MTDC.EQ.7) TDCM(MTDC)=0.50D0
217     ENDDO
218 C
219 C     INITIALISING AVERAGE CONTAMINATED CELL AREA
220     DO 28 MTDC=1,MDS
221         DO 28 JS=0,KSA-1
222             DO 28 IW=1,KW
223                 TNCAR(MTDC,JS,IW)=0.D0
224                 TCAR1(MTDC,JS,IW)=0.D0
225                 TCAR3(MTDC,JS,IW)=0.D0
226                 TCAR6(MTDC,JS,IW)=0.D0
227                 TCAR12(MTDC,JS,IW)=0.D0
228                 TCAR24(MTDC,JS,IW)=0.D0
229                 TCAR36(MTDC,JS,IW)=0.D0
230     28 CONTINUE
231 C
232 C
233 C -----CREATING REPORT FILES -----
234     OPEN(9,FILE='ERROR.TXT',STATUS='REPLACE')
235 C     OPEN(11,FILE='RESULTS.TXT',STATUS='REPLACE')
236 C     OPEN(14,FILE='K_EXAMPLE.TXT',STATUS='UNKNOWN')
237 C     OPEN(22,FILE='VELOCITIES_EXAMPLE.TXT',STATUS='UNKNOWN')
238 C     OPEN(23,FILE='HEADS_EXAMPLE.TXT',STATUS='UNKNOWN')
239     OPEN(48,FILE='PROBABILITIES.TXT',STATUS='UNKNOWN')
240     OPEN(39,FILE='SOURCE.TXT',STATUS='UNKNOWN')
241     OPEN(50,FILE='RWREPORT.TXT',STATUS='UNKNOWN')
242 C
243     SNSIMOLD=0          ! PARAMETER THAT CONTROLS PROBABILITIES FILE OUTPUT
244 C
245 C
246 C*****
247 C-----LOOP ON THE NUMBER OF SIMULATIONS-----
248 C
249     IS=0
250     DOWHILE(SNSIM.LT.NSIM)          ! BASIC SIMULATION LOOP BEGINS
251 C
252     IS=IS+1          !SIMULATION COUNTER
253 C
254     CALL DATE_AND_TIME (DATE_R,T_R)
255 C
256     WRITE(9,719) IS,NSIM,t_r(1:2),t_r(3:4),t_r(5:6)
257     PRINT 718,IS,INT(SNSIM)+1,NSIM,SNSIM*100./NSIM,T_R(1:2),
258     & T_R(3:4),T_R(5:6)
259 C
260     718 FORMAT('TOT.SIM.No:',I4,2X,' SIM.No:',I4,' OF ',I4,3X,
261     + F4.1,1X,'% COMPLETED ',' START TIME: ',A2,':',A2,':',A2)
262     719 FORMAT('SIM #',I4,'/',I4,3X,'START TIME: ',A2,':',A2,':',A2)
263 C

```

```

264 C
265 C-----SIMULATE STANDARD NORMAL DEVIATES BY TURNING BANDS-----
266 C
267 C
268 PRINT*
269 PRINT*, ' STARTING TURNING BANDS ALGORITHM ... '
270 CALL TUBA (NX, NY, DX, DY, ALPHA, BETA, -A, RK)
271 C
272 C
273 C-----CALCULATING MEAN ENSAMBLE MEAN AND VARIANCE-----
274 C
275 SUM=0.D0
276 SSX=0.D0
277 SSX2=0.D0
278 RKPOINT1=RKPOINT1+BETA*RK (432)
279 RKPOINT2=RKPOINT2+BETA*RK (845)
280 RKPOIN21=RKPOIN21+BETA*BETA*RK (432) *RK (432)
281 RKPOIN22=RKPOIN22+BETA*BETA*RK (845) *RK (845)
282 DO 12 K=1, NZ
283 DO 12 J=1, NY
284 DO 12 I=1, NX
285 IP= (K-1) *NXNY+ (J-1) *NX+I
286 C TEMP=ALPHA+BETA*RK (IP)
287 TEMP=RK (IP)
288 SSX=SSX+TEMP
289 SSX2=SSX2+TEMP*TEMP
290 TEMP=EXP (TEMP)
291 RK (IP) =TEMP
292 SUM=SUM+TEMP
293 P (IP) =P0+ (P1-P0) * (I-0.5D0) /NX
294 12 CONTINUE
295 C
296 SSX=SSX/NNNN
297 SSXEN=SSXEN+SSX
298 SSX2EN=SSX2EN+ (SSX2/NNNN)
299 SSX2=SSX2/NNNN-SSX*SSX
300 C
301 C
302 C-----SOLVE FLOW EQUATION-----
303 C
304 PRINT*, ' STARTING TO SOLVE THE FLOW PROBLEM ... '
305 C
306 OMEGA=OMEGA0
307 CHECKSNSIM=SNSIM ! KEEPING OLD VALUE OF SOLVED CASES
308 C
309 CALL FLOW3D (RK, P, ICON, DMAX)
310 C
311 C
312 C !!! PROCEED ONLY IF THERE IS A SOLUTION OF THE FLOW PROBLEM !!!
313 IF (SNSIM.GT.CHECKSNSIM) THEN ! CHECKING
314 C
315 C-----CALCULATING THE VELOCITY FIELD FOR EACH REALISATION-----
316 C
317 PRINT*, ' STARTING TO CALCULATE THE VELOCITY FIELD ... '
318 C
319 CALL VEL (RK, P, VELX, VELY, VELZ)
320 PRINT*, ' Velocity Field Calculated!'
321 PRINT*
322 C
323 C
324 C-----OUTPUT VALUES FOR VELOCITIES, K AND H FOR VISUALIZATION PURPOSES--
325 C IF (SNSIM.EQ.NSIM) THEN
326 C
327 DO 221 K=1, NZ
328 DO 221 J=1, NY
329 DO 221 I=1, NX
330 C IP= (K-1) *NXNY+ (J-1) *NX+I
331 C WRITE (14, 667) I, J, K, RK (IP)

```

```

332 C          WRITE (22,668) I,J,K,VELX(IP),VELY(IP),VELZ(IP)
333 C          WRITE (23,667) I,J,K,P(IP)
334 C 221 CONTINUE
335 C      ENDIF
336 C
337 C 667  FORMAT (3(I4,1X),F10.4)
338 C 668  FORMAT (3(I4,1X),3(F9.6,1X))
339 C
340 C
341 C-----CREATING AND MONITOR POLLUTION-----
342 C      IF(MONITOR.EQV..TRUE.) THEN
343 C          PRINT*, '    CREATING AND MONITOR POLLUTION ...    '
344 C      ELSE
345 C          PRINT*, '    CREATING POLLUTION ...    '
346 C      ENDIF
347 C
348 C      CALL RANDORIGIN(XO,YO,ORPOSO) ! DERMING POLLUTION ORIGIN
349 C          PX=INT(XO)
350 C          PY=INT(YO)
351 C          PZ=1
352 C          IF(YO-PY.GE.0.5) PY=PY+1          !COUNTS ON CENTRAL Y
353 C          IF(XO-PX.GE.0.5) PX=PX+1          !COUNTS ON CENTRAL X
354 C          PRINT*
355 C          PRINT 900,PX,PY,PZ
356 C
357 C      DO 115 MTDC=1,MDS          ! LOOP OVER DIRPERSION FACTOR
358 C          TDC=TDCM(MTDC)
359 C          WRITE(50,*) 'TDC=',TDC
360 C          CALL RANDOMWALK(IS,TDC,XO,YO,ORPOSO,DET,ATOD)
361 C
362 C      DO 125 JS=0,KSA-1
363 C          DO 130 IW=1,KW          ! MULTI-WELL LOOP
364 C              IF(DET(JS,IW).EQV..TRUE.) THEN
365 C                  TDET(MTDC,JS,IW)=TDET(MTDC,JS,IW)+1
366 C              ELSEIF(DET(JS,IW).EQV..FALSE.) THEN
367 C                  FDET(MTDC,JS,IW)=FDET(MTDC,JS,IW)+1
368 C              ENDIF
369 C
370 C      CALCULATING CONTAMINATED AREA
371 C      TNCAR(MTDC,JS,IW)=TNCAR(MTDC,JS,IW)+NCAR(JS,IW)
372 C      TCAR1(MTDC,JS,IW)=TCAR1(MTDC,JS,IW)+CAR1(JS,IW)
373 C      TCAR3(MTDC,JS,IW)=TCAR3(MTDC,JS,IW)+CAR3(JS,IW)
374 C      TCAR6(MTDC,JS,IW)=TCAR6(MTDC,JS,IW)+CAR6(JS,IW)
375 C      TCAR12(MTDC,JS,IW)=TCAR12(MTDC,JS,IW)+CAR12(JS,IW)
376 C      TCAR24(MTDC,JS,IW)=TCAR24(MTDC,JS,IW)+CAR24(JS,IW)
377 C      TCAR36(MTDC,JS,IW)=TCAR36(MTDC,JS,IW)+CAR36(JS,IW)
378 C
379 C      CALCULATING AVERAGE TIME OF DETECTION
380 C      TATOD(MTDC,JS,IW)=TATOD(MTDC,JS,IW)+ATOD(JS,IW)
381 C
382 C
383 C      IF(IW.EQ.7.AND.MTDC.EQ.5.AND.JS.EQ.0.AND.(SNSIM.EQ.1.OR.SNSIM
384 C      & .NE.SNSIMOLD)) THEN
385 C          WRITE(48,*) SNSIM,NOW(IW),1.*TDET(MTDC,JS,IW)/SNSIM
386 C          SNSIMOLD=SNSIM
387 C          PRINT*, 'HI',NOW(IW)
388 C      ENDIF
389 C
390 C 130 CONTINUE          ! CLOSING MULTI-WELL LOOP
391 C
392 C 125 CONTINUE          ! CLOSING SAMPLING LOOP
393 C      WRITE(50,*) '*****'
394 C      WRITE(50,*) '*****'
395 C      WRITE(50,*) '*****'
396 C      WRITE(50,*)
397 C
398 C      IF(JS.EQ.KSA.AND.IW.EQ.KW) GOTO 115
399 C      PRINT*, '-----'

```

```

400 C
401 115 CONTINUE ! DISPERSION LOOP
402 C
403 ENDIF ! CHECKING IF
404 C
405 PRINT*, '*****'
406 &*****'
407 PRINT*, '*****'
408 &*****'
409 PRINT*
410 PRINT*
411 ENDDO ! CLOSING SIMULATION LOOP
412 C
413 C*****
414 C
415 C
416 C-----CALCULATE THE ENSEMBLE STATISTICS AND WRITE THE RESULTS-----
417 C
418 ALLREP=1.D0*IS
419 RKPOINT1=RKPOINT1/ALLREP
420 RKPOIN21=RKPOIN21/ALLREP-RKPOINT1*RKPOINT1
421 RKPOINT2=RKPOINT2/ALLREP
422 RKPOIN22=RKPOIN22/ALLREP-RKPOINT2*RKPOINT2
423 SSXEN=SSXEN/ALLREP
424 SSX2EN=SSX2EN/ALLREP-SSXEN*SSXEN
425 C
426 C CONTAMINATED AREA RELATIVE TO LANDFILL'S AREA FOR EACH PERIOD
427 DO 510 MTDC=1,MDS
428 DO 510 JS=0,KSA-1
429 DO 510 IW=1,KW
430 IF(FDET(MTDC,JS,IW).NE.0) TNCAR(MTDC,JS,IW)=(TNCAR(MTDC,JS,IW)/
431 & FDET(MTDC,JS,IW))/LFAR
432 IF(TDET(MTDC,JS,IW).NE.0) THEN
433 TCAR1(MTDC,JS,IW)=(TCAR1(MTDC,JS,IW)/TDET(MTDC,JS,IW))/LFAR
434 TCAR3(MTDC,JS,IW)=(TCAR3(MTDC,JS,IW)/TDET(MTDC,JS,IW))/LFAR
435 TCAR6(MTDC,JS,IW)=(TCAR6(MTDC,JS,IW)/TDET(MTDC,JS,IW))/LFAR
436 TCAR12(MTDC,JS,IW)=(TCAR12(MTDC,JS,IW)/TDET(MTDC,JS,IW))/LFAR
437 TCAR24(MTDC,JS,IW)=(TCAR24(MTDC,JS,IW)/TDET(MTDC,JS,IW))/LFAR
438 TCAR36(MTDC,JS,IW)=(TCAR36(MTDC,JS,IW)/TDET(MTDC,JS,IW))/LFAR
439 C
440 C AVERAGE TIME OF DETECTION
441 TATOD(MTDC,JS,IW)=TATOD(MTDC,JS,IW)/TDET(MTDC,JS,IW)
442 C
443 ENDIF
444 510 CONTINUE
445 C
446 C-----WRITING OUTPUT-----
447 OPEN(16,FILE='FINAL_REPORT.TXT',STATUS='UNKNOWN')
448 OPEN(17,FILE='Pd_EXCEL.TXT',STATUS='UNKNOWN')
449 OPEN(18,FILE='TOTAL_EXCEL.TXT',STATUS='UNKNOWN')
450 C
451 PRINT*
452 WRITE(*,*) 'TOTAL FIELD SIMULATIONS: ',NSIM
453 WRITE(*,*) 'NUMBER THAT FLOW FIELD WAS SIMULATED: ',SNSIM
454 C
455 CALL DATE_AND_TIME (DATE_R,T_R)
456 C
457 WRITE(16,*) 'THIS IS THE FINAL REPORT:'
458 WRITE(16,*)
459 WRITE(16,*) 'TOTAL FIELD SIMULATIONS: ',NSIM
460 WRITE(16,*) 'NUMBER THAT FLOW FIELD WAS SIMULATED: ',SNSIM
461 WRITE(16,*)
462 WRITE(16,*) 'START TIME : ',ST_R(1:2),':',ST_R(3:4),':',ST_R(5:6),
463 + ' AT ',SDATE_R(5:6), '/',SDATE_R(7:8), '/',SDATE_R(3:4)
464 WRITE(16,*) 'END TIME : ',T_R(1:2),':',T_R(3:4),':',T_R(5:6),
465 + ' AT ',DATE_R(5:6), '/',DATE_R(7:8), '/',DATE_R(3:4)
466 WRITE(16,811)NX,NY,NZ
467 WRITE(16,812)DX,DY,DZ

```

```

468      WRITE(16,813) DL,DC, DN
469      WRITE(16,*)
470  C
471      PRINT*
472      PRINT*
473      WRITE(16,*) 'START TIME : ',ST_R(1:2),':',ST_R(3:4),':',ST_R(5:6),
474 + ' AT ',SDATE_R(5:6), '/',SDATE_R(7:8), '/',SDATE_R(3:4)
475      PRINT*, 'END TIME : ',T_R(1:2),':',T_R(3:4),':',T_R(5:6),
476 + ' AT ',DATE_R(5:6), '/',DATE_R(7:8), '/',DATE_R(3:4)
477      PRINT 811,NX,NY,NZ
478      PRINT 812,DX,DY,DZ
479      PRINT 813,DL,DC, DN
480  C
481  811  FORMAT(' GRID SIZE : ',I3,'X',I3,'X',I3)
482  812  FORMAT(' BLOCK DIMENSIONS      : ',F5.2,'X',F5.2,'X',F5.2)
483  813  FORMAT(' TB BLOCK DIMENSIONS : ',F5.2,'X',F5.2,'X',F5.2)
484  900  FORMAT('STARTING POINT OF POLLUTION: ', 'PX=',I3,2X,'PY=',I3,
485 & 2X,'PZ=',I3)
486  C
487      WRITE(16,*)
488      WRITE(16,*) 'THE ENS.MEAN IS:',SSXEN,' AND THE ENS.VAR IS:',SSX2EN
489      WRITE(16,*) 'THE ENS.MEAN IN TWO POINTS IS : ',RKPOINT1,RKPOINT2
490      WRITE(16,*) ' AND THE ENS. VARIANCE IS : ',RKPOIN21,RKPOIN22
491      WRITE(16,*)
492      WRITE(16,*) 'CORRELATION SCALE = ',A,' WITH ',SNSIM,' SIMULATIONS'
493      WRITE(16,*) 'INITIAL HEAD: ',HEADG
494      WRITE(16,*) 'No OF PARTICLES:',NPAR
495      WRITE(16,*) 'TVC:',TVC,' PARTICLES'
496      WRITE(16,*) 'VARIANCE : ',BETA*BETA
497      WRITE(16,*)
498  C
499  C      DETECTION REPORT FILE
500      WRITE(16,*)
501      WRITE(16,*) 'No OF SIMULATION=',SNSIM
502      WRITE(16,*) 'TOTAL MONITOR TIME=',TEND
503      WRITE(16,*)
504      DO MTDC=1,MDS
505      WRITE(16,*) 'DISPERSION FACTOR:',TDCM(MTDC)
506      DO 512 JS=0,KSA-1
507      WRITE(16,*) '*****'
508      WRITE(16,*) 'SAMPLING TIME INTERVALS (DAYS): ',ISA(JS)
509      WRITE(16,*) '          -----'
510      DO 512 IW=1,KW
511      WRITE(16,*) 'NUMBER OF MONITOR WELLS : ',NOW(IW)
512      WRITE(16,*) 'NORMALIZED DISTANCE AMONG WELLS: ',1./NOW(IW)
513      WRITE(16,*) 'DETECTED POLLUTION=',TDET(MTDC,JS,IW)
514      WRITE(16,*) 'NOT DETECTED POLLUTION=',FDET(MTDC,JS,IW)
515      WRITE(16,*) 'PROBABILITY OF DETECTION=',100.*TDET(MTDC,JS,IW) /
516 & SNSIM,'% '
517      WRITE(16,*) 'PROBABILITY OF FAILURE=',100.*FDET(MTDC,JS,IW) /
518 & SNSIM,'% '
519      WRITE(16,*)
520      WRITE(16,*) 'AVERAGE TIME OF CONTAMINATION DETECTION=',
521 & TATOD(MTDC,JS,IW)
522      WRITE(16,*)
523      WRITE(16,*) 'AVERAGE POLLUTED VOLUME ON FAILURE=',
524 & TNCAR(MTDC,JS,IW)
525      WRITE(16,*) 'AVERAGE POLLUTED VOLUME ON DETECTION=',
526 & TCAR1(MTDC,JS,IW)
527      WRITE(16,*) 'AVERAGE POLLUTED VOLUME 3 MONTHS LATER=',
528 & TCAR3(MTDC,JS,IW)
529      WRITE(16,*) 'AVERAGE POLLUTED VOLUME 6 MONTHS LATER=',
530 & TCAR6(MTDC,JS,IW)
531      WRITE(16,*) 'AVERAGE POLLUTED VOLUME 12 MONTHS LATER=',
532 & TCAR12(MTDC,JS,IW)
533      WRITE(16,*) 'AVERAGE POLLUTED VOLUME 24 MONTHS LATER=',
534 & TCAR24(MTDC,JS,IW)
535      WRITE(16,*) 'AVERAGE POLLUTED VOLUME 36 MONTHS LATER=',

```

```

536      &      TCAR36 (MTDC, JS, IW)
537      WRITE (16, *)
538  512  CONTINUE
539      WRITE (16, *) '*****'
540      WRITE (16, *) '*****'
541  ENDDO
542  C
543  C      REPORTING DATA FOR EXCEL USE
544      DO K=1, MDS
545          DO I=1, KW
546              WRITE (17, 540) (100.0*TDET (K, J, I) /SNSIM, J=0, KSA-1)
547              WRITE (18, 560) ( 100.0*TDET (K, J, I) /SNSIM, INT (TATOD (K, J, I)),
548      &      TNCAR (K, J, I), TCAR1 (K, J, I), TCAR3 (K, J, I), TCAR6 (K, J, I),
549      &      TCAR12 (K, J, I), TCAR24 (K, J, I), TCAR36 (K, J, I), J=0, KSA-1)
550          ENDDO
551      ENDDO
552  C
553      540  FORMAT (7 (F5.1, 1X))
554      560  FORMAT (7 (F5.1, 1X, I4, 1X, 7 (F6.4, 1X)))
555  C
556  C
557      PRINT*, 'THE ENS.MEAN IS:', SSXEN, ' AND THE ENS.VAR IS:', SSX2EN
558      PRINT*, 'THE ENS.MEAN IN TWO POINTS IS : ', RKPOINT1, RKPOINT2
559      PRINT*, ' AND THE ENS. VARIANCE IS : ', RKPOIN21, RKPOIN22
560      PRINT*
561      PRINT*, 'CORRELATION SCALE = ', A, ' WITH ', SNSIM, ' SIMULATIONS'
562      PRINT*, 'INITIAL HEAD: ', HEADG
563      PRINT*, 'No OF PARTICLES:', NPAR
564      PRINT*, 'VARIANCE : ', SIGMA
565      PRINT*
566      PRINT*
567      PRINT*, 'DONE ..... '
568  C
569      STOP
570      END          !END OF MAIN PROGRAM
571  C
572  C
573  C
574  C-*****SUBROUTINES*****SUBROUTINES*****SUBROUTINES*****
575  C
576  C
577  C*****
578  C***** SUBROUTINE RANDOMWALK (DET, TDETECTED, POLVOL) *****
579  C*****
580  C
581  C      The random walk particle tracking (RWPT) method treats the transport
582  C      of a solute mass via a large number of particles. It moves each
583  C      particle through the porous medium using the velocity field obtained
584  C      from the solution of the flow equation to simulate advection and
585  C      adds a random displacement to simulate dispersion
586  C
587  C
588      SUBROUTINE RANDOMWALK (IS, TDC, RPX, RPY, ORPOS, DET, TOD)
589  C
590      IMPLICIT DOUBLE PRECISION (A-H, O-Z)
591      PARAMETER (IMEM=1024000)
592      PARAMETER (KW=8, KSA=7)
593  C
594      DOUBLE PRECISION X (IMEM), Y (IMEM), Z (IMEM), XPR (IMEM), YPR (IMEM),
595      & ZPR (IMEM), LDC, NDFS, TOD (0:KSA-1, KW)
596      DOUBLE PRECISION NCAR (0:KSA-1, KW), CAR1 (0:KSA-1, KW),
597      & CAR3 (0:KSA-1, KW), CAR6 (0:KSA-1, KW), CAR12 (0:KSA-1, KW),
598      & CAR24 (0:KSA-1, KW), CAR36 (0:KSA-1, KW)
599      DIMENSION C (IMEM), PRPOS (IMEM), LFC (100000)
600      DIMENSION RLOCLAND (IMEM), CC (20), NW (20), MWX (20), MWY (20)
601      INTEGER C, POS, PX, PY, PZ, PAR, PRPOS, ORPOS, PART, CC, TVC
602      INTEGER TEND, TPRD, TS, TTL, PRSMTTL (0:KSA-1, KW), NOW (KW), ISA (0:KSA-1)
603      LOGICAL MW (0:KSA-1, KW, 20), MONITOR, DET (0:KSA-1, KW)

```

```

604 C
605 COMMON /PARAM/ P0, P1, EP, DX, DY, DZ, NX, NY, NZ, NSEED
606 COMMON /PARTICLE/ PM, TVC, NPAR
607 COMMON /POLLUTION/ C, OOB
608 COMMON /LANDFILL/ LFXI, LFXE, LFYI, LFYE, LFAR, LFC
609 COMMON /MONITORING/ SIGMA, MONITOR, NOW, ISA
610 COMMON /TIME/ TS, TEND, TPRD, NSIM
611 COMMON /WAREA/ NCAR, CAR1, CAR3, CAR6, CAR12, CAR24, CAR36
612 C
613 C OPEN(30, FILE='C_ANALYTICALLY.TXT', STATUS='UNKNOWN')
614 C
615 C-----INITIALIZATION OF MATRICES AND PARAMETERS-----
616 NXNY=NX*NY ! LEVEL NODES
617 OOB=0 ! PARTICLES OUT OF BOUNDARIES
618 TOTALPART=0 ! TOTAL PARTICLE COUNTER
619 LDC=10*TDC ! LONGITUDAL DISPERSION
620 C
621 C COORDINATES OF POLLUTION ORIGIN
622 PX=INT(RPX)
623 PY=INT(RPY)
624 PZ=1
625 IF(RPY-PY.GE.0.5) PY=PY+1 ! COUNTS ON CENTRAL Y
626 IF(RPX-PX.GE.0.5) PX=PX+1 ! COUNTS ON CENTRAL X
627 C
628 DO JS=0, KSA-1
629 DO IW=1, KW
630 DO K=1, NOW(IW)
631 MW(JS, IW, K) = .FALSE. ! MONITOR WELL INITIAL DETECTION VALUE
632 ENDDO
633 ENDDO
634 ENDDO
635 C
636 DO JS=0, KSA-1
637 DO IW=1, KW
638 DET(JS, IW) = .FALSE. ! DETECTION PARAMETER (IF PLUME IS
639 DETECTED THEN TRUE)
640 TOD(JS, IW) = 0.D0 ! AVERAGE TIME OF DETECTION
641 PRSMTTL(JS, IW) = 0 ! INITIAL TIME OF SAMPLING
642 C
643 C INITIALISING CONTAMINATED CELL AREA
644 NCAR(JS, IW) = 0.D0
645 CAR1(JS, IW) = 0.D0
646 CAR3(JS, IW) = 0.D0
647 CAR6(JS, IW) = 0.D0
648 CAR12(JS, IW) = 0.D0
649 CAR24(JS, IW) = 0.D0
650 CAR36(JS, IW) = 0.D0
651 ENDDO
652 ENDDO
653 C
654 DO I=1, IMEM
655 X(I) = 0.D0
656 Y(I) = 0.D0
657 Z(I) = 0.D0
658 XPR(I) = 0.D0
659 YPR(I) = 0.D0
660 ZPR(I) = 0.D0
661 C(I) = 0
662 ENDDO
663 C
664 CALL WNDIFS(SIGMA, TDC, NDFS)
665 C
666 C DIMENSION RESTORATION FACTORS
667 DISTLENGT=DX
668 DISTTIME=TS
669 C DISTVEL=DX/TS
670 C
671 C REMOVING DIMENSIONS

```

```

672         LDC=LDC/DX
673         TDC=TDC/DY
674         DX=DX/DX
675         DY=DY/DY
676         DZ=DZ/DZ
677         TEND=TEND/TS
678         TPRD=TPRD/TS
679         TS=TS/TS
680     C
681     C
682     C *****RANDOM WALK PARTICLE TRACKING ALGORITHM*****
683     C
684     C -----TIME PROGRESSION-----
685     C
686         DO 20 TTL=1, TEND, TS
687     C
688     C     NUMBER OF PARTICLES TO BE RELEASED EACH TIME
689     C     INSTANT LEAK (TPRD=1) - CONTINUOUS LEAK (TPRD>1)
690     C     IF (TTL .LE. TPRD) THEN
691         PART=NPAR+NPAR* (TTL-1)
692         TOTALPART=PART
693         C (ORPOS) =C (ORPOS) +NPAR
694         DO PAR=PART-NPAR+1, PART
695             PRPOS (PAR) =ORPOS
696             X (PAR) =RPX
697             Y (PAR) =RPY
698             Z (PAR) =PZ
699             XPR (PAR) =X (PAR)
700             YPR (PAR) =Y (PAR)
701             ZPR (PAR) =Z (PAR)
702         ENDDO
703     C     ENDIF
704     C
705     C -----PARTICLE'S PROGRESSION ALGORITHM-----
706     C
707         DO 10 PAR=1, PART
708     C
709     C     CHECKING IF PARTICLE WAS INSIDE BOUNDARIES, THEN
710     C     EXECUTE THE NEXT POSITION ALGORITHM
711     C     IF (XPR (PAR) .GE. 1 .AND. XPR (PAR) .LE. NX-1 .AND. YPR (PAR) .LE. NY-1 .AND.
712     C     & YPR (PAR) .GE. 1 .AND. ZPR (PAR) .GT. 0 .AND. ZPR (PAR) .LE. NZ) THEN
713     C
714     C     DETERMINING 3 RANDOM NUMBERS
715         R1=RVNORMAL (NSEED)
716         R2=RVNORMAL (NSEED)
717     C         R3=RVNORMAL (NSEED)
718     C
719     C     CALCULATING PARTICLE'S VELOCITY
720         CALL VCL (X (PAR) , Y (PAR) , Z (PAR) , VLX, VLY, VLZ)
721         CALL VCB (X (PAR) , Y (PAR) , Z (PAR) , VBX, VBY, VBZ)
722     C
723         VB=SQRT (VBX**2+VBY**2+VBZ**2)
724     C
725     C     CALCULATING VELOCITY DERIVATIVES (BETWEEN CELL BOUNDARIES)
726         XIP=INT (X (PAR) )
727         YIP=INT (Y (PAR) )
728         CALL VCL (X (PAR) , YIP, Z (PAR) , VLXD, VLYD, VLZ)
729         CALL VCL (X (PAR) , YIP+1, Z (PAR) , VLXU, VLYU, VLZ)
730         CALL VCL (XIP, Y (PAR) , Z (PAR) , VLXL, VLYL, VLZ)
731         CALL VCL (XIP+1, Y (PAR) , Z (PAR) , VLXR, VLYR, VLZ)
732     C
733         UXUVX=(VLXL-VLXR) /DX
734         UYUVY=(VLYU-VLYD) /DY
735         UYUVX=(VLXU-VLXD) /DY
736         UXUVY=(VLYL-VLYR) /DX
737     C
738     C     CALCULATING FOKKER-PLANCK EQUATION ADDITIONAL TERM
739         DLT=LDC-TDC

```

```

740 C
741 UXUDYX=(DLT/VB**3) * ((VBY**3) *UXUVX+ (VBX**3) *UXUVY)
742 C
743 UYUDYY=(2.D0*TDC*VBX*VB**2-TDC*VBX**3-LDC*VBX*VBY**2) *
744 & UYUVX/VB**3+ (2.D0*LDC*VBY*VB**2-TDC*VBY*VBX**2-
745 & LDC*VBY**3) *UYUVY/VB**3
746 C
747 C Y COMPONENT FOKKER-PLANK STAGNATION TERM
748 FPTY=UXUDYX+UYUDYY
749 C
750 C
751 UXUDXX=(2.D0*LDC*VBX*VB**2-LDC*VBX**3-TDC*VBX*VBY**2) *
752 & UXUVX/VB**3+ (2.D0*TDC*VBY*VB**2-LDC*VBY*VBX**2-
753 & TDC*VBY**3) *UXUVY/VB**3
754 C
755 UYUDXY=(DLT/VB**3) * ((VBY**3) *UYUVX+ (VBX**3) *UYUVY)
756 C
757 C X COMPONENT FOKKER-PLANK STAGNATION TERM
758 FPTX=UXUDXX+UYUDXY
759 C
760 C DETERMINING THE NEW POSITION
761 FLDC=R1*SQRT(2.D0*LDC*VB*TS)
762 FTDC=R2*SQRT(2.D0*TDC*VB*TS)
763 C
764 X(PAR)=XPR(PAR)+VLX*TS+(VBX/VB)*FLDC-(VBY/VB)*FTDC+FPTX*TS
765 Y(PAR)=YPR(PAR)+VLY*TS+(VBY/VB)*FLDC+(VBX/VB)*FTDC+FPTY*TS
766 C
767 C CHECKING IF BOYNDARIES HAVE BEEN REACHED
768 C CHECKING X END BOUNDARY
769 IF(X(PAR) .LT.1 .OR. X(PAR) .GT.NX-1) THEN
770 C (PRPOS(PAR))=C (PRPOS(PAR))-1
771 XPR(PAR)=X(PAR)
772 OOB=OOB+1
773 GOTO 10
774 ENDIF
775 C CHECKING Y END BOUNDARY
776 IF(Y(PAR) .GT.NY-1 .OR. Y(PAR) .LT.1) THEN
777 C (PRPOS(PAR))=C (PRPOS(PAR))-1
778 YPR(PAR)=Y(PAR)
779 OOB=OOB+1
780 GOTO 10
781 ENDIF
782 C CHECKING Z DOWN END BOUNDARY
783 IF(Z(PAR) .LT.0) THEN
784 C (PRPOS(PAR))=C (PRPOS(PAR))-1
785 ZPR(PAR)=Z(PAR)
786 OOB=OOB+1
787 GOTO 10
788 ENDIF
789 C CHECKING Z TOP END BOUNDARY.IF EQUAL NZ ASSIGN PREVIOUS VALUE
790 C PLUME IS FORCED INSIDE THE VOLUME. THIS POLICY MAY BE ALTERED
791 IF(Z(PAR) .GT.NZ) Z(PAR)=NZ
792 C
793 C KEEPING POSITIONS
794 XPR(PAR)=X(PAR)
795 YPR(PAR)=Y(PAR)
796 ZPR(PAR)=Z(PAR)
797 C
798 C -----CALCULATING CONCENTRATIONS-----
799 C
800 C WELLS ARE LOCATED ON GRID'S NODES
801 MCLX=INT(X(PAR))
802 MCLY=INT(Y(PAR))
803 C
804 DIFX=X(PAR)-MCLX
805 DIFY=Y(PAR)-MCLY
806 C
807 IF(DIFX .GE.0.5) MCLX=MCLX+1

```

```

808      IF(DIFY.GE.0.5) MCLY=MCLY+1
809      C
810      POS=(MCLY-1)*NX+MCLX
811      C
812      C (POS)=C (POS)+1
813      C (PRPOS (PAR))=C (PRPOS (PAR))-1
814      PRPOS (PAR)=POS
815      C
816      C
817      ENDIF      ! INSIDE BOUNDARIES IF
818      C
819      C
820      10      CONTINUE
821      C
822      C -----MONITOR-----
823      IF(MONITOR.EQV..TRUE.) THEN
824      C      ESTABLISHING A SAMPLING POLICY (INVSM=INTERVAL OF SAMPLING)
825      DO 90 JS=0,KSA-1
826      C
827      C      MONITOR WELLS
828      DO 95 IW=1,KW
829      IF(INT(TTL-PRSMTTL(JS,IW)).EQ.ISA(JS)) THEN
830      PRSMTTL(JS,IW)=TTL      ! KEEPING TIME OF PREVIOUS STEP
831      DO KK=1,NOW(IW)
832      BW=(LFYE-LFYI)/NOW(IW)
833      IBW=INT(BW/2)
834      MWX(KK)=INT(LFXE+(LFYE-LFYI)*NDFS)      ! X DIMENSION OF MONITOR
835      WELL
836      MWY(KK)=INT(LFYI+(IBW+(KK-1)*BW))      ! Y DIMENSION OF MONITOR
837      WELL
838      ENDDO
839      C
840      C      MONITORING WELLS 1 - NOW(IW) (NUMBER OF WELLS)
841      DO 70 K=1,NOW(IW)
842      CC(K)=0
843      C      DEPTH OF WELLS (NZ=1 EQV 2-D)
844      DO 80 IZ=1,NZ
845      NW(K)=(IZ-1)*NXNY+(MWY(K)-1)*NX+MWX(K)
846      CC(K)=CC(K)+C(NW(K))
847      IF(CC(K)*PM.GE.TVC) THEN
848      IF(DET(JS,IW).EQV..FALSE.) THEN
849      MW(JS,IW,K)=TRUE.
850      DET(JS,IW)=TRUE.
851      TOD(JS,IW)=TTL
852      ENDIF
853      ENDIF
854      80      CONTINUE
855      C
856      70      CONTINUE      ! CLOSING MONITOR LOOP
857      ENDIF      ! SAMPLING POLICY IF
858      C
859      IF(DET(JS,IW).EQV..TRUE.) THEN
860      IF(TTL.EQ.TOD(JS,IW)) CALL POLVOL(CAR1(JS,IW))
861      IF(TTL.EQ.TOD(JS,IW)+90) CALL POLVOL(CAR3(JS,IW))
862      IF(TTL.EQ.TOD(JS,IW)+180) CALL POLVOL(CAR6(JS,IW))
863      IF(TTL.EQ.TOD(JS,IW)+365) CALL POLVOL(CAR12(JS,IW))
864      IF(TTL.EQ.TOD(JS,IW)+730) CALL POLVOL(CAR24(JS,IW))
865      IF(TTL.EQ.TOD(JS,IW)+1095) CALL POLVOL(CAR36(JS,IW))
866      ENDIF
867      C
868      C
869      95      CONTINUE      ! CLOSING WELL LOOP
870      90      CONTINUE      ! CLOSING SAMPLING LOOP
871      C
872      ENDIF      ! MONITOR IF
873      C
874      20      CONTINUE
875      C

```

```

876 C
877 DO JS=0,KSA-1
878 DO IW=1,KW
879 IF (DET(JS,IW) .EQV. .FALSE.) CALL POLVOL(NCAR(JS,IW))
880 ENDDO
881 ENDDO
882 C
883 C -----EXPORTING CONCENTRATIONS ON A SELECTED REALISATION -----
884 C IF (IS.EQ.NSIM) THEN
885 OPEN(32,FILE='CONCENTRATION.TXT',STATUS='UNKNOWN')
886 QWVAL=20
887 LVAL=10
888 DO 40 K=1,NZ
889 DO 40 J=1,NY
890 DO 40 I=1,NX
891 IP=(K-1)*NXNY+(J-1)*NX+I
892 RLOCLAND(IP)=C(IP)
893 C VISUALIZATION OF LANDFILL'S LOCATION ON THE FIELD LATTICE AND
894 C ITS MONITOR WELLS
895 DO KK=1,NOW(IW)
896 IF (I.EQ.MWX(KK) .AND. J.EQ.MWY(KK)) RLOCLAND(IP)=QWVAL
897 ENDDO
898 C
899 IF (K.EQ.NZ .AND. J.GE.LFYI .AND. J.LE.LFYE .AND.
900 $ I.GE.LFXI .AND. I.LT.LFXE) RLOCLAND(IP)=LVAL
901 C
902 WRITE(32,*) I,J,K,RLOCLAND(IP)
903 C
904 40 CONTINUE
905 C
906 CLOSE(32)
907 C
908 C -----CHECKING HOW MANY PARTICLES WERE COUNTED AND IF WE HAD C<0 -----
909 NP=0
910 E0=0
911 DO 45 K=1,NZ
912 DO 45 J=1,NY
913 DO 45 I=1,NX
914 IP=(K-1)*NXNY+(J-1)*NX+I
915 IF (C(IP) .LT.0) THEN
916 E0=E0+1
917 PRINT 145,C(IP),I,J
918 WRITE(50,145)C(IP),I,J
919 ENDIF
920 NP=NP+C(IP)
921 45 CONTINUE
922 145 FORMAT('ATTENTION:NEGATIVE VALUE OF CONCENTRATION C',I5,
923 &' , AT POSITION X=',I4,' AND Y=',I4)
924 C
925 C RESTORING DIMENSIONS
926 LDC=LDC*DISTLENGT
927 TDC=TDC*DISTLENGT
928 DX=DX*DISTLENGT
929 DY=DY*DISTLENGT
930 DZ=DZ
931 TEND=TEND*DISTTIME
932 TPRD=TPRD*DISTTIME
933 TS=TS*DISTTIME
934 C
935 C
936 C REPORTING VALUES
937 WRITE(50,*) IS,'/',NSIM
938 WRITE(50,800)NX,NY,NZ
939 WRITE(50,900)PX,PY,PZ
940 WRITE(50,*)
941 WRITE(50,*) 'TIME STEP: ',TS
942 WRITE(50,*) 'TOTAL PARTICLES INJECTED: ',TOTALPART
943 WRITE(50,*) 'PARTICLES TRACKED: ',NP

```

```

944      WRITE(50,*) 'PARTICLES MISSED: ',OOB
945      WRITE(50,*) 'TOTAL TRACKED & MISSED= ',NP+OOB
946      WRITE(50,*)
947  C
948      DO JS=0,KSA-1
949          WRITE(50,*) '*****'
950          DO IW=1,KW
951  C      WRITE(50,*) 'LOCATION OF WELLS : ',
952  C      & ('WELL:',K,' (' ,MWX(K) ,',',MWY(K) ,') ', ' - ',K=1,NOW(IW))
953          WRITE(50,*) 'SAMPLING INTERVAL (DAYS):',ISA(JS)
954          IF(DET(JS,IW) .EQV. .TRUE.) THEN
955              DO K=1,NOW(IW)
956                  IF(MW(JS,IW,K) .EQV. .TRUE.) THEN
957                      WRITE(50,*)NOW(IW) , '-WELLS, MONITORING WELL:',K,
958                      & ' HAS DETECTED POLLUTION'
959                      WRITE(50,*) 'DETECTION TIME= ',TOD(JS,IW) , ' OF ',TEND
960                  ENDIF
961              ENDDO
962          ELSEIF(DET(JS,IW) .EQV. .FALSE.) THEN
963              WRITE(50,*) 'NO DETECTION SUCCEEDED BY ',NOW(IW) ,
964              & ' MONITORING WELLS '
965          ENDIF
966  C
967          WRITE(50,*)
968          WRITE(50,*) 'POLLUTED VOLUME ON FAILURE=',NCAR(JS,IW)/LFAR
969          WRITE(50,*) 'POLLUTED VOLUME ON DETECTION=',CAR1(JS,IW)/LFAR
970          WRITE(50,*) 'POLLUTED VOLUME 3 MONTHS LATER=',CAR3(JS,IW)/LFAR
971          WRITE(50,*) 'POLLUTED VOLUME 6 MONTHS LATER=',CAR6(JS,IW)/LFAR
972          WRITE(50,*) 'POLLUTED VOLUME 12 MONTHS LATER=',CAR12(JS,IW)/LFAR
973          WRITE(50,*) 'POLLUTED VOLUME 24 MONTHS LATER=',CAR24(JS,IW)/LFAR
974          WRITE(50,*) 'POLLUTED VOLUME 36 MONTHS LATER=',CAR36(JS,IW)/LFAR
975          WRITE(50,*) '-----'
976          WRITE(50,*)
977      ENDDO
978  ENDDO
979  C
980  C      PRINTING ON SCREEN
981      PRINT*
982      PRINT*, 'TDC: ',TDC
983      PRINT*, 'TOT INJ:',TOTALPART, ' / TRACKED:',NP, ' / MISSED:',OOB,
984      & ' / TOT TRACKED & MISSED= ',NP+OOB
985      PRINT*
986  C
987  C
988      800 FORMAT('X=',I4,2X,'Y=',I4,2X,'Z=',I4)
989      900 FORMAT('STARTING POINT OF POLLUTION: ', 'PX=',I3,2X,'PY=',I3,
990      & 2X,'PZ=',I3)
991  C
992      RETURN
993      END
994  C
995  C
996  C-----
997  C      NORMAL RANDOM NUMBER FUNCTION GENERATOR
998  C-----
999  C
1000      FUNCTION RVNORMAL(SEED)
1001          IMPLICIT DOUBLE PRECISION (A-H,O-Z)
1002          DATA S,T / 0.449871,-0.386595 /
1003          DATA A,B / 0.19600,0.25472 /
1004          INTEGER SEED
1005  C
1006      100  U=RANM(SEED)
1007          V=RANM(SEED)
1008          V=1.7156D0*(V-0.5D0)
1009          X=U-S
1010          Y=ABS(V)-T
1011          Q=X*X+Y*(A*Y-B*X)

```

```

1012 C
1013 IF(V**2.GT.-4*LOG(U)*U**2) GOTO 100
1014 IF(Q.GT.0.27846) GOTO 100
1015 IF(Q.LT.0.27597) RVNORMAL=V/U
1016 RETURN
1017 END
1018 C
1019 C
1020 C-----
1021 C RANDOM NUMBER FUNCTION (0-1 EQUAL PROBABLE)
1022 C-----
1023 C
1024 FUNCTION RANDM(IDUM)
1025 INTEGER IDUM, IM1, IM2, IMM1, IA1, IQ1, IQ2, IR1, NTAB, NDIV
1026 DOUBLE PRECISION RANDM, AM, EPS, RNMX
1027 PARAMETER (IM1=2147483563, IM2=2147483399, AM=1.D0/IM1, IMM1=IM1-1,
1028 * IA1=40014, IA2=40692, IQ1=53668, IQ2=52774, IR1=12211,
1029 * NTAB=32, NDIV=1+IMM1/NTAB, EPS=1.2E-7, RNMX=1.D0-EPS)
1030 INTEGER IDUM2, J, K, IV(NTAB), IY
1031 SAVE IV, IY, IDUM2
1032 DATA IDUM2/123456789/, IV/NTAB*0/, IY/0/
1033 IF (IDUM.LE.0) THEN
1034 IDUM=MAX(-IDUM, 1)
1035 IDUM2=IDUM
1036 DO 11 J=NTAB+8, 1, -1
1037 K=IDUM/IQ1
1038 IDUM=IA1*(IDUM-K*IQ1)-K*IR1
1039 IF (IDUM.LT.0) IDUM=IDUM+IM1
1040 IF (J.LE.NTAB) IV(J)=IDUM
1041 11 CONTINUE
1042 IY=IV(1)
1043 ENDIF
1044 K=IDUM/IQ1
1045 IDUM=IA1*(IDUM-K*IQ1)-K*IR1
1046 IF (IDUM.LT.0) IDUM=IDUM+IM1
1047 K=IDUM2/IQ2
1048 IDUM2=IA2*(IDUM2-K*IQ2)
1049 IF (IDUM2.LT.0) IDUM2=IDUM+IM2
1050 J=1+IY/NDIV
1051 IY=IV(J)-IDUM2
1052 IV(J)=IDUM
1053 IF (IY.LT.1) IY=IY+IMM1
1054 RANDM=MIN(AM*IY, RNMX)
1055 RETURN
1056 END
1057 C
1058 C
1059 C
1060 C*****
1061 C SUBROUTINE LANDFL: LANDFILL'S SHAPE AND BOUNDARIES
1062 C*****
1063 C
1064 SUBROUTINE LANDF
1065 IMPLICIT DOUBLE PRECISION (A-H, O-Z)
1066 COMMON /PARAM/ P0, P1, EP, DX, DY, DZ, NX, NY, NZ, NSEED
1067 COMMON /LANDFILL/ LFXI, LFXE, LFYI, LFYE, LFAR, LFC
1068 INTEGER LFC(100000)
1069 C
1070 NN=NX*NY
1071 C
1072 DO I=1, NN
1073 LFC(I)=0
1074 ENDDO
1075 C
1076 C --> RECTAGULAR LANDFILL <--
1077 C LANDFILL (COORDINATIONS IN METERS/D TO GET DIMENSIONLESS NUMBERS)
1078 LFXI=INT(10/DX) !LANDFILL'S X INITIAL BOUNDARY LIMIT
1079 LFXE=INT(60/DX) !LANDFILL'S X ENDING BOUNDARY LIMIT

```

```

1080         LFYI=INT(140/DY)           !LANDFILL'S Y INITIAL BOUNDARY LIMIT
1081         LFYE=INT(260/DY)           !LANDFILL'S Y ENDING BOUNDARY LIMIT
1082         LFAR=(LFXE-LFXI-1)*(LFYE-LFYI-1) !LF'S DIMENSIONLESS AREA (No OF
1083 CELLS)
1084         C
1085         DO J=1,NY
1086             DO I=1,NX
1087                 IP=(J-1)*NX+I
1088                 IF(J.GE.LFYI.AND.J.LE.LFYE.AND.I.GE.LFXI.AND.I.LT.LFXE) THEN
1089                     LFC(IP)=1
1090                 ENDIF
1091             ENDDO
1092         ENDDO
1093         C
1094         RETURN
1095         END
1096         C
1097         C
1098         C
1099         C*****
1100         C     SUBROUTINE RANDORIGIN: CREATING RANDOM ORIGIN POINT OF POLLUTION
1101         C*****
1102         C
1103         SUBROUTINE RANDORIGIN(RPX,RPY,ORPOS)
1104         IMPLICIT DOUBLE PRECISION (A-H,O-Z)
1105         COMMON /PARAM/ P0,P1,EP,DX,DY,DZ,NX,NY,NZ,NSEED
1106         COMMON /LANDFILL/ LFXI,LFXE,LFYI,LFYE,LFAR,LFC
1107         INTEGER ORPOS,LFC(100000)
1108         C
1109         XL=ABS(LFXE-LFXI)
1110         YL=ABS(LFYE-LFYI)
1111         RPX=XL*RANDM(NSEED)+LFXI
1112         RPY=YL*RANDM(NSEED)+LFYI
1113         PX=INT(RPX)
1114         PY=INT(RPY)
1115         PZ=1
1116         IF(RPY-PY.GE.0.5) PY=PY+1           !COUNTS ON CENTRAL Y
1117         IF(RPX-PX.GE.0.5) PX=PX+1           !COUNTS ON CENTRAL X
1118         C
1119         ORPOS=(PY-1)*NX+PX   ! INITIAL CUBIC ELEMENT POSITION OF PARTICLES
1120         C
1121         WRITE(39,*) PX,PY
1122         C
1123         RETURN
1124         END
1125         C
1126         C
1127         C
1128         C*****
1129         C     SUBROUTINE WNDFS: WELLS' DISTANCE FROM SOURCE (NORMALIZED)
1130         C*****
1131         C
1132         SUBROUTINE WNDFS(SIGMA,AT,DFS)
1133         IMPLICIT DOUBLE PRECISION (A-H,O-Z)
1134         C
1135         IF(SIGMA.EQ.0.D0) THEN
1136             IF(AT.EQ.0.001D0) DFS=3.0D0
1137             IF(AT.EQ.0.01D0) DFS=2.25D0
1138             IF(AT.EQ.0.02D0) DFS=1.50D0
1139             IF(AT.EQ.0.05D0) DFS=0.50D0
1140             IF(AT.EQ.0.1D0) DFS=0.125D0
1141             IF(AT.EQ.0.2D0) DFS=0.030D0
1142             IF(AT.EQ.0.5D0) DFS=0.015D0
1143         ENDIF
1144         C
1145         IF(SIGMA.EQ.0.25D0) THEN
1146             IF(AT.EQ.0.001D0) DFS=1.75D0
1147             IF(AT.EQ.0.01D0) DFS=1.50D0

```

```

1148         IF(AT.EQ.0.02D0) DFS=1.00D0
1149         IF(AT.EQ.0.05D0) DFS=0.50D0
1150         IF(AT.EQ.0.1D0) DFS=0.125D0
1151         IF(AT.EQ.0.2D0) DFS=0.30D0
1152         IF(AT.EQ.0.5D0) DFS=0.015D0
1153     ENDIF
1154 C
1155     IF(SIGMA.EQ.0.50D0) THEN
1156         IF(AT.EQ.0.001D0) DFS=1.75D0
1157         IF(AT.EQ.0.01D0) DFS=1.50D0
1158         IF(AT.EQ.0.02D0) DFS=0.50D0
1159         IF(AT.EQ.0.05D0) DFS=0.50D0
1160         IF(AT.EQ.0.1D0) DFS=0.125D0
1161         IF(AT.EQ.0.2D0) DFS=0.030D0
1162         IF(AT.EQ.0.5D0) DFS=0.015D0
1163     ENDIF
1164 C
1165     IF(SIGMA.EQ.0.75D0) THEN
1166         IF(AT.EQ.0.001D0) DFS=1.75D0
1167         IF(AT.EQ.0.01D0) DFS=1.25D0
1168         IF(AT.EQ.0.02D0) DFS=0.50D0
1169         IF(AT.EQ.0.05D0) DFS=0.25D0
1170         IF(AT.EQ.0.1D0) DFS=0.125D0
1171         IF(AT.EQ.0.2D0) DFS=0.030D0
1172         IF(AT.EQ.0.5D0) DFS=0.015D0
1173     ENDIF
1174 C
1175     IF(SIGMA.EQ.1.D0) THEN
1176         IF(AT.EQ.0.001D0) DFS=1.75D0
1177         IF(AT.EQ.0.01D0) DFS=1.25D0
1178         IF(AT.EQ.0.02D0) DFS=0.50D0
1179         IF(AT.EQ.0.05D0) DFS=0.125D0
1180         IF(AT.EQ.0.1D0) DFS=0.0625D0
1181         IF(AT.EQ.0.2D0) DFS=0.030D0
1182         IF(AT.EQ.0.5D0) DFS=0.015D0
1183     ENDIF
1184 C
1185     IF(SIGMA.EQ.1.5D0) THEN
1186         IF(AT.EQ.0.001D0) DFS=1.25D0
1187         IF(AT.EQ.0.01D0) DFS=1.00D0
1188         IF(AT.EQ.0.02D0) DFS=0.50D0
1189         IF(AT.EQ.0.05D0) DFS=0.125D0
1190         IF(AT.EQ.0.1D0) DFS=0.0625D0
1191         IF(AT.EQ.0.2D0) DFS=0.015D0
1192         IF(AT.EQ.0.5D0) DFS=0.015D0
1193     ENDIF
1194 C
1195     IF(SIGMA.EQ.2.0D0) THEN
1196         IF(AT.EQ.0.001D0) DFS=0.75D0
1197         IF(AT.EQ.0.01D0) DFS=0.50D0
1198         IF(AT.EQ.0.02D0) DFS=0.25D0
1199         IF(AT.EQ.0.05D0) DFS=0.125D0
1200         IF(AT.EQ.0.1D0) DFS=0.0625D0
1201         IF(AT.EQ.0.2D0) DFS=0.015D0
1202         IF(AT.EQ.0.5D0) DFS=0.015D0
1203     ENDIF
1204 C
1205     RETURN
1206     END
1207 C
1208 C
1209 C
1210 C*****
1211 C    SUBROUTINE POLVOL: ESTIMATING THE POLLUTED VOLUME
1212 C*****
1213     SUBROUTINE POLVOL(VOL)
1214     IMPLICIT DOUBLE PRECISION (A-H,O-Z)
1215 C

```

```

1216      PARAMETER (IMEM=1024000)
1217      COMMON /PARAM/ P0, P1, EP, DX, DY, DZ, NX, NY, NZ, NSEED
1218      COMMON /POLLUTION/ C, OOB
1219      INTEGER C (IMEM)
1220  C
1221      NXNY=NX*NY
1222      VOL=0
1223      DO 50 K=1, NZ
1224          DO 50 J=1, NY
1225              DO 50 I=1, NX
1226                  IP=(K-1)*NXNY+(J-1)*NX+I
1227                  IF(C(IP) .GT. 0) VOL=VOL+1
1228      50 CONTINUE
1229  C
1230      VOL=VOL+OOB      !PARTICLES OUT OF BOUNDARIES INCLUDED (1 CELL/PAR)
1231  C
1232      RETURN
1233      END
1234  C
1235  C
1236  C*****
1237  C      CALCULATING THE VELOCITY FIELD
1238  C*****
1239  C
1240      SUBROUTINE VEL (RK, P, VELX, VELY, VELZ)
1241  C
1242  C      VELOCITIES ARE CALCULATED IN A SHIFTED GRID, EQUAL TO 1/2 IN RELATION
1243  C      TO THE INITIAL GRID WHERE K AND H ARE CALCULATED. THIS MEANS THAT
1244  C      VX(I+1/2, J, K), VY(I, J+1/2, K), VZ(I, J, K+1/2). CALCULATIONS OF VELOCITY
1245  C      ONTO OTHER POINTS OF SIMULATION AREA MUST ACCOUNT FOR THIS SHIFT.
1246  C      VELOCITIES ON INITIAL GRID NODES ARE LINEARLY INTERPOLATED,
1247  C      BETWEEN I+1, I AND J+1, J.
1248  C      IMPLICIT DOUBLE PRECISION (A-H, O-Z)
1249  C      PARAMETER (IMEM=1024000)
1250  C      DOUBLE PRECISION P (IMEM), RK (IMEM), VELX (IMEM), VELY (IMEM), VELZ (IMEM)
1251  C      DOUBLE PRECISION VELXI (IMEM), VELYI (IMEM), VELZI (IMEM)
1252  C      INTEGER TS, TEND, TPRD
1253  C      COMMON /PARAM/ P0, P1, EP, DX, DY, DZ, NX, NY, NZ, NSEED
1254  C      COMMON /TIME/ TS, TEND, TPRD, NSIM
1255  C
1256  C      INITIALIZATION OF MATRICES AND PARAMETERS
1257  C      DO I=1, IMEM
1258  C          VELXI (I)=0. DO
1259  C          VELYI (I)=0. DO
1260  C          VELZI (I)=0. DO
1261  C          VELX (I)=0. DO
1262  C          VELY (I)=0. DO
1263  C          VELZ (I)=0. DO
1264  C      ENDDO
1265  C
1266  C      NXNY=NX*NY
1267  C
1268  C      CALCULATING
1269  C      DO 810 K=1, NZ
1270  C          DO 810 J=1, NY
1271  C              DO 810 I=1, NX
1272  C                  IP=(K-1)*NXNY+(J-1)*NX+I
1273  C
1274  C      VELOCITY ON X AXIS (I+1/2)
1275  C      IF(I .GE. 1 .AND. I .LE. NX-1) THEN      ! CALCULATING grad(H)
1276  C          GRADHX=(P (IP+1)-P (IP)) /DX
1277  C          RKPX=2. DO*RK (IP+1) *RK (IP) / (RK (IP+1)+RK (IP))
1278  C          VELXI (IP)=RKPX*GRADHX/EP      ! CALCULATING VELOCITY
1279  C      ENDIF
1280  C
1281  C      IF(I .EQ. NX) VELXI (IP)=VELXI ((K-1)*NXNY+(J-1)*NX+NX-1)
1282  C
1283  C      VELOCITY ON Y AXIS (J+1/2)

```

```

1284      IF(J.GE.1.AND.J.LE.NY-1) THEN                                ! CALCULATING grad(H)
1285          GRADHY=(P(IP+NX)-P(IP))/DY
1286          RKPY=2.DO*RK(IP+NX)*RK(IP)/(RK(IP+NX)+RK(IP))
1287          VELYI(IP)=RKPY*GRADHY/EP                                     ! CALCULATING VELOCITY
1288      ENDIF
1289  C
1290      IF(J.EQ.NY) VELYI(IP)=VELYI((K-1)*NXNY+(J-1-1)*NX+I)
1291  C
1292  C      VELOCITY ON Z AXIS (K+1/2)
1293      IF(K.GT.1.AND.K.LT.NZ) THEN                                ! CALCULATING grad(H)
1294          GRADHZ=(P(IP+NXNY)-P(IP))/DZ
1295          RKPZ=2.DO*RK(IP+NXNY)*RK(IP)/(RK(IP+NXNY)+RK(IP))
1296          VELZI(IP)=RKPZ*GRADHZ/EP                                     ! CALCULATING VELOCITY
1297      ENDIF
1298  C
1299      IF(K.EQ.NZ) VELZI(IP)=VELZ((K-1-1)*NXNY+(J-1)*NX+I)
1300  C
1301      810 CONTINUE
1302  C
1303  C      LINEARLY INTERPOLATING VELOCITIES ON (I,J)
1304  C      VELOCITY ON X AXIS [(I+1/2)+(I-1/2)]/2
1305      DO 820 K=1,NZ
1306          DO 820 J=1,NY
1307              DO 820 I=2,NX-1
1308                  IP=(K-1)*NXNY+(J-1)*NX+I
1309                  IB=(K-1)*NXNY+(J-1)*NX+I-1
1310                  VELX(IP)=(VELXI(IP)+VELXI(IB))/2.DO
1311      820 CONTINUE
1312  C
1313  C      VELOCITY ON Y AXIS [(J+1/2)+(J-1/2)]/2
1314      DO 830 K=1,NZ
1315          DO 830 J=2,NY-1
1316              DO 830 I=1,NX
1317                  IP=(K-1)*NXNY+(J-1)*NX+I
1318                  IB=(K-1)*NXNY+(J-1-1)*NX+I
1319                  VELY(IP)=(VELYI(IP)+VELYI(IB))/2.DO
1320      830 CONTINUE
1321  C
1322  C      VELOCITY ON (NX,J) SIDE
1323      DO J=1,NY
1324          IP=(J-1)*NX+1
1325          IE=(J-1)*NX+NX
1326          VELX(IP)=VELXI(IP)
1327          VELX(IE)=VELXI(IE)
1328      ENDDO
1329  C
1330  C      VELOCITY ON (I,NY) SIDE
1331      DO I=1,NX
1332          IE=(NY-1)*NX+I
1333          VELY(I)=VELYI(I)
1334          VELX(IE)=VELXI(IE)
1335      ENDDO
1336  C
1337  C
1338  C      REMOVING DIMENSIONS (VELOCITY IN DX/TS M/DAY UNITS)
1339      DO 850 K=1,NZ
1340          DO 850 J=1,NY
1341              DO 850 I=1,NX
1342                  IP=(K-1)*NXNY+(J-1)*NX+I
1343                  VELX(IP)=VELX(IP)/(DX/TS)
1344                  VELY(IP)=VELY(IP)/(DY/TS)
1345                  VELZ(IP)=VELZ(IP)/(DZ/TS)
1346      850 CONTINUE
1347  C
1348  C
1349      RETURN
1350      END
1351  C

```

```

1352 C
1353 C*****
1354 C      3D HYBRID VELOCITY INTERPOLATION SCHEME SUBROUTINES
1355 C*****
1356 C
1357 C
1358 C      SUBROUTINE VCL (XPR, YPR, ZPR, VLX, VLY, VLZ)
1359 C
1360 C*****
1361 C      LINEAR VELOCITY INTERPOLATION
1362 C
1363 C      IMPLICIT DOUBLE PRECISION (A-H,O-Z)
1364 C      PARAMETER (IMEM=1024000)
1365 C
1366 C      DOUBLE PRECISION VELX (IMEM) ,VELY (IMEM) ,VELZ (IMEM)
1367 C
1368 C      COMMON /VELOCITY/ VELX,VELY,VELZ
1369 C      COMMON /PARAM/ P0,P1,EP,DX,DY,DZ,NX,NY,NZ,NSEED
1370 C
1371 C
1372 C      NXNY=NX*NY
1373 C      VLX=0.D0
1374 C      VLY=0.D0
1375 C      VLZ=0.D0
1376 C      I=INT (XPR)
1377 C      J=INT (YPR)
1378 C      K=INT (ZPR)
1379 C
1380 C      FX=XPR-INT (XPR)
1381 C      FY=YPR-INT (YPR)
1382 C
1383 C      ----- X-AXIS -----
1384 C      IF (INT (XPR) .GE. 1 .AND. INT (XPR) .LE. NX-1) THEN
1385 C          VLX= (DX-FX) *VELX ( (K-1) *NXNY+ (J-1) *NX+I) +
1386 C      &      FX*VELX ( (K-1) *NXNY+ (J-1) *NX+I+1)
1387 C      ENDIF
1388 C
1389 C      IF (INT (XPR) .EQ. NX) VLX=VELX ( (K-1) *NXNY+ (J-1) *NX+NX)
1390 C
1391 C
1392 C      ----- Y-AXIS -----
1393 C      IF (INT (YPR) .GE. 1 .AND. INT (YPR) .LE. NY-1) THEN
1394 C          VLY= (DY-FY) *VELY ( (K-1) *NXNY+ (J-1) *NX+I) +
1395 C      &      FY*VELY ( (K-1) *NXNY+ (J-1+1) *NX+I)
1396 C      ENDIF
1397 C
1398 C      IF (INT (YPR) .EQ. NY) VLY=VELY ( (K-1) *NXNY+ (NY-1) *NX+I)
1399 C      RETURN
1400 C      END
1401 C
1402 C
1403 C
1404 C*****
1405 C
1406 C      SUBROUTINE VCB (XPR, YPR, ZPR, VBX, VBY, VBZ)
1407 C
1408 C*****
1409 C      BILINEAR VELOCITY INTERPOLATION
1410 C
1411 C
1412 C      IMPLICIT DOUBLE PRECISION (A-H,O-Z)
1413 C      PARAMETER (IMEM=1024000)
1414 C
1415 C      DOUBLE PRECISION VELX (IMEM) ,VELY (IMEM) ,VELZ (IMEM)
1416 C
1417 C      COMMON /VELOCITY/ VELX,VELY,VELZ
1418 C      COMMON /PARAM/ P0,P1,EP,DX,DY,DZ,NX,NY,NZ,NSEED
1419 C

```

```

1420 C
1421 NXNY=NX*NY
1422 VBX=0.D0
1423 VBY=0.D0
1424 VBZ=0.D0
1425 I=INT(XPR)
1426 J=INT(YPR)
1427 K=INT(ZPR)
1428 C
1429 FX=XPR-INT(XPR)
1430 FY=YPR-INT(YPR)
1431 C
1432 C ----- X-AXIS -----
1433 IF(INT(XPR) .GE.1 .AND. INT(XPR) .LE. NX-1 .AND. INT(YPR) .LE. NY-1) THEN
1434     BVX1=(DX-FX) * (DY-FY) *VELX((K-1)*NXNY+(J-1)*NX+I)
1435     BVX2=FX*(DY-FY) *VELX((K-1)*NXNY+(J-1)*NX+I+1)
1436     BVX3=(DX-FX) *FY*VELX((K-1)*NXNY+(J-1+1)*NX+I)
1437     BVX4=FX*FY*VELX((K-1)*NXNY+(J-1+1)*NX+I+1)
1438     VBX=BVX1+BVX2+BVX3+BVX4
1439 ENDIF
1440 C
1441 IF(INT(XPR) .EQ. NX) VBX=VELX((K-1)*NXNY+(J-1)*NX+NX)
1442 C
1443 C ----- Y-AXIS -----
1444 IF(INT(YPR) .GE.1 .AND. INT(YPR) .LE. NY-1 .AND. INT(XPR) .LE. NX-1) THEN
1445     BVY1=(DX-FX) * (DY-FY) *VELY((K-1)*NXNY+(J-1)*NX+I)
1446     BVY2=FX*(DY-FY) *VELY((K-1)*NXNY+(J-1)*NX+I+1)
1447     BVY3=(DX-FX) *FY*VELY((K-1)*NXNY+(J-1+1)*NX+I)
1448     BVY4=FX*FY*VELY((K-1)*NXNY+(J-1+1)*NX+I+1)
1449     VBY=BVY1+BVY2+BVY3+BVY4
1450 ENDIF
1451 C
1452 IF(INT(YPR) .EQ. NY) VBY=VELX((K-1)*NXNY+(NY-1)*NX+I)
1453 RETURN
1454 END

```

## A-2 Precipitation Event Pollution Source Code

```

1      PROGRAM TBRW
2      C
3      C      Last change: 28 FEB 2012
4      C      CASES RAIN DATA INPUT
5      C      LANDFILL RECTAGULAR
6      C      ONE INPUT FILE IS REQUIRED: TUBA211.INC
7      C
8      C-----
9      C      FLOW MODELLING
10     C      LOGNORMAL MEDIA
11     C      CORRELATED CONDUCTIVITY FIELD
12     C      2-D TURNING BANDS METHOD (TUBA)
13     C      DOUBLE PRECISION USED
14     C      HYBRID INTERPOLATION VELOCITY SCHEME
15     C
16     C      PARAMETER IDENTIFICATION:
17     C      IMEM= 1024000 MAX PARTICLES
18     C      KW=8 MONITORING WELLS ARRANGEMENT (1,2,3,4,6,8,12,20)
19     C      KSA=7 SAMPLING FREQUENCIES (1,30,60,90,120,180,360 DAYS)
20     C      MDS=7 DISPERSION CASES (0.001,0.01,0.02,0.05,0.10,0.20,0.50 M)
21     C
22     C-----
23     C
24     C      IMPLICIT DOUBLE PRECISION (A-H,O-Z)
25     C
26     C      MUST CHANGE IN FLOW3D,VELOCITY,RANDOMWALK,INTERVEL SUBROUTINES TOO
27     C      PARAMETER (IMEM=1024000)
28     C      PARAMETER (KW=8,KSA=7,MDS=5)
29     C      KW:No OF WELLS, KSA:SAMPLING INTERVALS, MDS:TRANSVERSE DISPERSION
30     C
31     C      DIMENSION RVARIO(300),GAM(300)
32     C      DOUBLE PRECISION P (IMEM),VELX (IMEM),VELY (IMEM),VELZ (IMEM),RK (IMEM)
33     C      DOUBLE PRECISION TATOD(MDS,0:KSA-1,KW),ATOD(0:KSA-1,KW),
34     C      & TDCM(MDS)
35     C      DOUBLE PRECISION NCAR(0:KSA-1,KW),CAR1(0:KSA-1,KW),
36     C      & CAR3(0:KSA-1,KW),CAR6(0:KSA-1,KW),CAR12(0:KSA-1,KW),
37     C      & CAR24(0:KSA-1,KW),CAR36(0:KSA-1,KW),TNCAR(MDS,0:KSA-1,KW),
38     C      & TCAR1(MDS,0:KSA-1,KW),TCAR3(MDS,0:KSA-1,KW),TCAR6(MDS,0:KSA-1,
39     C      & KW),TCAR12(MDS,0:KSA-1,KW),TCAR24(MDS,0:KSA-1,KW),
40     C      & TCAR36(MDS,0:KSA-1,KW),RAIN(10950)
41     C      INTEGER TS,TEND,TPRD,SNSIM,TVC,TDET(MDS,0:KSA-1,KW),FDET(MDS,
42     C      & 0:KSA-1,KW),NOW(KW),ISA(0:KSA-1),ORPOSO,PX,PY,PZ,LFC(100000),
43     C      & NPAR(10950)
44     C      LOGICAL DET(0:KSA-1,KW),MONITOR
45     C      CHARACTER SDATE_R*8,DATE_R*8,T_R*10,ST_R*10
46     C
47     C      COMMON /PARAM/ P0,P1,EP,DX,DY,DZ,NX,NY,NZ,NSEED
48     C      COMMON /SOLVE/ OMEGA,TOL,TOL1,MITER,SNSIM
49     C      COMMON /VELOCITY/ VELX,VELY,VELZ
50     C      COMMON /PARTICLE/ PM,TVC,NPAR
51     C      COMMON /LANDFILL/ LFXI,LFXE,LFYI,LFYE,LFAR,LFC
52     C      COMMON /MONITORING/ SIGMA,MONITOR,NOW,ISA
53     C      COMMON /TIME/ TS,TEND,TPRD,NSIM
54     C      COMMON /WAREA/ NCAR,CAR1,CAR3,CAR6,CAR12,CAR24,CAR36
55     C
56     C-----
57     C-      GRID SPACING FOR TURNING BAND SIMULATIONS IN X
58     C-      DIFFERENT FROM ABOVE SO AS TO CREATE ANISOTROPY. NOTE
59     C-      THAT TURNING BAND ROUTINE CAN ONLY SIMULATE ISOTROPIC
60     C-      FIELDS AND THAT, TO GENERATE ANISOTROPIC FIELDS, YOU HAVE
61     C-      TO TRANSFORM THE GRID SPACING....
62     C-----
63     C
64     C-----HETEROGENITY OF THE FIELD -----
65     C

```

```

66      SIGMA=1.00D0
67      C
68      C-----PARAMETER INITIALIZATION-----
69      C
70      NSIM=50              !NUMBER OF SIMULATIONS
71      C
72      TEND=10950          !TIME MONITOR ENDS (30 YEARS)
73      TPRD=10950         !PERIOD OF TIME THAT LEAK OCCURS
74      TS=1                !TIME STEP (DAYS)
75      C
76      LNDFX=1000         !LENGHT OF SIMULATION AREA (METERS)
77      LNDFY=400          !WIDTH OF SIMULATION AREA (METERS)
78      LNDFZ=1            !DEPTH OF SIMULATION AREA (METERS)
79      DX=2                !DX STEP ON X AXIS (METERS)
80      DY=2                !DY STEP ON Y AXIS (METERS)
81      DZ=1                !DZ STEP ON X AXIS (METERS)
82      NX=INT(LNDFX/DX)   !NODES IN X-DIRECTION (DIMENSIONLESS)
83      NY=INT(LNDFY/DY)   !NODES IN Y-DIRECTION (DIMENSIONLESS)
84      NZ=INT(LNDFZ/DZ)   !NODES IN Z-DIRECTION (DIMENSIONLESS)
85      C
86      DL=0.D0             !TB BLOCK DIMENSION
87      DC=0.D0             !TB BLOCK DIMENSION
88      DN=0.D0             !TB BLOCK DIMENSION
89      C
90      A=20.D0             !CORELLATION COEFFICIENT (METERS)
91      A=(-1.D0)*ABS(A)
92      HEADG=0.001D0
93      P0=0.D0             !STARTING HYDRAULIC HEAD
94      P1=NX*DX*HEADG     !ENDING HYDRAULIC HEAD
95      EP=0.25D0          !EFFECTIVE POROSITY
96      ALPHA=2.3D0        !MEAN lnK
97      C
98      C CONTAMINATION PARTICLES CALCULATION
99      PM=28                !PARTICLE'S MASS
100     TVC=28               !THRESHOLD VOLUMETRIC CONCENTRATION
101     NTPART=0
102     C
103     C READING RAIN HEIGHT (mm) DATA
104     OPEN(20, FILE='RAIN30.TXT', STATUS='OLD')
105     DO I=1, TPRD
106         READ(20, *) RAIN(I)
107         NPAR(I)=INT(RAIN(I)*PM)
108         NTPART=NTPART+NPAR(I)
109     C     PRINT*, I, NPAR(I), NTPART
110     ENDDO
111     CLOSE(20)
112     C
113     C
114     MONITOR=.TRUE.       !PARAMETER THAT CONTROLS IF WE MONITOR OR NOT
115     C
116     C RANDOM NUMBER SEEDS
117     DSEED=2147811051.D0  !seed number for RNG`
118     NSEED=1236541350    !15.8
119     C
120     C
121     C- BETA FOR NOW ON IS THE STANDARD DEVIATION NOT THE VARIANCE
122     BETA=SQRT(SIGMA)
123     C
124     TOL=0.00001D0
125     TOL1=0.00005D0
126     MITER=2000
127     SNSIM=0              ! NUMBER OF SIMULATIONS WITH FLOW FIELD
128     SOLUTION
129     NNNN=NX*NY*NZ
130     NXNY=NX*NY
131     DSEED=DSEED*NXNY*NY*BETA*DX/(NSIM*NSIM)
132     SSXEN=0.D0
133     RKPOIN21=0.D0

```

```

134      RKPOIN22=0.D0
135      RKPOINT1=0.D0
136      RKPOINT2=0.D0
137      SSSX2EN=0.D0
138  C
139      DO 22 K=1,MDS
140          DO 22 J=0,KSA-1
141              DO 22 I=1,KW
142                  TDET(K,J,I)=0
143                  FDET(K,J,I)=0
144                  TATOD(K,J,I)=0.D0
145      22 CONTINUE
146  C
147  C      FLOW EQUATIONS RELAXATION FACTOR
148  C      - DEPEDENCE HAS BEEN OBSERVED. BEST RESULTS (?) ARE ACCOMPLISHED
149  C      WHEN RELAXATION FACTOR IS THE HIGHER POSSIBLE (INITIAL WAS 1.85)
150      OMEGA0=1.85D0
151  C
152      IF(nnnn.GE.180000) OMEGA0=1.88D0
153      IF(nnnn.GE.240000) OMEGA0=1.91D0
154      IF(nnnn.GE.390000) OMEGA0=1.92D0
155      IF(nnnn.GE.490000) OMEGA0=1.95D0
156      IF(nnnn.GE.700000) OMEGA0=1.97D0
157      IF(nnnn.GE.850000) OMEGA0=1.98D0
158      IF(nnnn.GE.850000) TOL=0.0001D0
159      IF(nnnn.GE.850000) TOL1=0.0005D0
160  C
161  C
162  C      PRINTING ON SCREEN THE STARTING TIME
163      CALL DATE_AND_TIME (SDATE_R,ST_R)
164  C
165  C      3-D TB INPUT DATA (BLOCK DIMENSIONS)
166      IF(DL.EQ.0.0) DL=DX
167      IF(DC.EQ.0.0) DC=DY
168      IF(DN.EQ.0.0) DN=DZ
169  C
170  C
171  C -----PRINTING INITIAL INFORMATION-----
172  C
173      PRINT*, 'THIS IS THE TOTAL PLUME TRANSPORT SIMULATION!'
174      PRINT*, 'NUMBER OF REALIZATIONS : ',NSIM
175      PRINT 715,NX,NY,NZ
176      PRINT 716,DX,DY,DZ
177      PRINT 717,DL,DC,DN
178  C
179      715 FORMAT(' GRID SIZE : ',I3,'X',I3,'X',I3)
180      716 FORMAT(' BLOCK DIMENSIONS : ',F5.2,' X',F5.2,' X',F5.2)
181      717 FORMAT(' TB BLOCK DIMENSIONS : ',F5.2,' X',F5.2,' X',F5.2)
182  C
183      PRINT*, 'CORRELATION RANGE (LENGTH UNITS) : ',A
184      PRINT*, ' & VARIANCE : ',BETA*BETA
185      PRINT*
186      PRINT*, ' ***** STARTING SIMULATIONS *****'
187      PRINT*
188  C
189  C
190  C-----ESTABLISHING MONITOR SYSTEM AND SAMPLING POLICY-----
191  C      LANDFILL'S GEOMETRY
192      CALL LANDF
193  C
194  C      NUMBER OF WELLS
195      DO IW=1,KW
196          IF(IW.LE.4) NOW(IW)=IW
197          IF(IW.EQ.5) NOW(IW)=6
198          IF(IW.EQ.6) NOW(IW)=8
199          IF(IW.EQ.7) NOW(IW)=12
200          IF(IW.EQ.8) NOW(IW)=20
201      ENDDO

```

```

202 C
203 C SAMPLING INTERVALS
204 DO JS=0, KSA-1
205 IF(JS.GE.1.AND.JS.LE.4) ISA(JS)=JS*30
206 IF(JS.EQ.0) ISA(JS)=1
207 IF(JS.EQ.5) ISA(JS)=180
208 IF(JS.EQ.6) ISA(JS)=365
209 ENDDO
210 C
211 C DISPERSIVITY FACTOR
212 DO MTDC=1, MDS
213 IF(MTDC.EQ.1) TDCM(MTDC)=0.001D0
214 IF(MTDC.EQ.2) TDCM(MTDC)=0.01D0
215 C IF(MTDC.EQ.3) TDCM(MTDC)=0.02D0
216 IF(MTDC.EQ.3) TDCM(MTDC)=0.05D0
217 IF(MTDC.EQ.4) TDCM(MTDC)=0.10D0
218 C IF(MTDC.EQ.6) TDCM(MTDC)=0.20D0
219 IF(MTDC.EQ.5) TDCM(MTDC)=0.50D0
220 ENDDO
221 C
222 C INITIALISING AVERAGE CONTAMINATED CELL AREA
223 DO 28 MTDC=1, MDS
224 DO 28 JS=0, KSA-1
225 DO 28 IW=1, KW
226 TNCAR(MTDC, JS, IW)=0.D0
227 TCAR1(MTDC, JS, IW)=0.D0
228 TCAR3(MTDC, JS, IW)=0.D0
229 TCAR6(MTDC, JS, IW)=0.D0
230 TCAR12(MTDC, JS, IW)=0.D0
231 TCAR24(MTDC, JS, IW)=0.D0
232 TCAR36(MTDC, JS, IW)=0.D0
233 28 CONTINUE
234 C
235 C
236 C -----CREATING REPORT FILES -----
237 OPEN(9, FILE='ERROR.TXT', STATUS='REPLACE')
238 C OPEN(11, FILE='RESULTS.TXT', STATUS='REPLACE')
239 C OPEN(14, FILE='K_EXAMPLE.TXT', STATUS='UNKNOWN')
240 C OPEN(22, FILE='VELOCITIES_EXAMPLE.TXT', STATUS='UNKNOWN')
241 C OPEN(23, FILE='HEADS_EXAMPLE.TXT', STATUS='UNKNOWN')
242 OPEN(48, FILE='PROBABILITIES.TXT', STATUS='UNKNOWN')
243 OPEN(39, FILE='SOURCE.TXT', STATUS='UNKNOWN')
244 OPEN(50, FILE='RWREPORT.TXT', STATUS='UNKNOWN')
245 C
246 SNSIMOLD=0 ! PARAMETER THAT CONTROLS PROBABILITIES FILE OUTPUT
247 C
248 C
249 C*****
250 C-----LOOP ON THE NUMBER OF SIMULATIONS-----
251 C
252 IS=0
253 DOWHILE(SNSIM.LT.NSIM) ! BASIC SIMULATION LOOP BEGINS
254 C
255 IS=IS+1 !SIMULATION COUNTER
256 C
257 CALL DATE_AND_TIME (DATE_R, T_R)
258 C
259 WRITE(9, 719) IS, NSIM, t_r(1:2), t_r(3:4), t_r(5:6)
260 PRINT 718, IS, INT(SNSIM)+1, NSIM, SNSIM*100./NSIM, T_R(1:2),
261 & T_R(3:4), T_R(5:6)
262 C
263 718 FORMAT('TOT.SIM.No:', I4, 2X, ' SIM.No:', I4, ' OF ', I4, 3X,
264 + F4.1, 1X, '% COMPLETED ', ' START TIME: ', A2, ':', A2, ':', A2)
265 719 FORMAT('SIM #', I4, '/', I4, 3X, 'START TIME: ', A2, ':', A2, ':', A2)
266 C
267 C
268 C-----SIMULATE STANDARD NORMAL DEVIATES BY TURNING BANDS-----
269 C-

```

```

270 C
271 PRINT*
272 PRINT*, ' STARTING TURNING BANDS ALGORITHM ... '
273 CALL TUBA (NX, NY, DX, DY, ALPHA, BETA, -A, RK)
274 C
275 C
276 C-----CALCULATING MEAN ENSAMBLE MEAN AND VARIANCE-----
277 C
278 SUM=0.D0
279 SSX=0.D0
280 SSX2=0.D0
281 RKPOINT1=RKPOINT1+BETA*RK (432)
282 RKPOINT2=RKPOINT2+BETA*RK (845)
283 RKPOIN21=RKPOIN21+BETA*BETA*RK (432) *RK (432)
284 RKPOIN22=RKPOIN22+BETA*BETA*RK (845) *RK (845)
285 DO 12 K=1, NZ
286 DO 12 J=1, NY
287 DO 12 I=1, NX
288 IP= (K-1) *NXNY+ (J-1) *NX+I
289 C TEMP=ALPHA+BETA*RK (IP)
290 TEMP=RK (IP)
291 SSX=SSX+TEMP
292 SSX2=SSX2+TEMP*TEMP
293 TEMP=EXP (TEMP)
294 RK (IP) =TEMP
295 SUM=SUM+TEMP
296 P (IP) =P0+ (P1-P0) * (I-0.5D0) /NX
297 12 CONTINUE
298 C
299 SSX=SSX/NNNN
300 SSXEN=SSXEN+SSX
301 SSX2EN=SSX2EN+ (SSX2/NNNN)
302 SSX2=SSX2/NNNN-SSX*SSX
303 C
304 C
305 C-----SOLVE FLOW EQUATION-----
306 C
307 PRINT*, ' STARTING TO SOLVE THE FLOW PROBLEM ... '
308 C
309 OMEGA=OMEGA0
310 CHECKSNSIM=SNSIM ! KEEPING OLD VALUE OF SOLVED CASES
311 C
312 CALL FLOW3D (RK, P, ICON, DMAX)
313 C
314 C
315 C !!! PROCEED ONLY IF THERE IS A SOLUTION OF THE FLOW PROBLEM !!!
316 IF (SNSIM.GT.CHECKSNSIM) THEN ! CHECKING
317 C
318 C-----CALCULATING THE VELOCITY FIELD FOR EACH REALISATION-----
319 C
320 PRINT*, ' STARTING TO CALCULATE THE VELOCITY FIELD ... '
321 C
322 CALL VEL (RK, P, VELX, VELY, VELZ)
323 PRINT*, ' Velocity Field Calculated!'
324 PRINT*
325 C
326 C
327 C-----OUTPUT VALUES FOR VELOCITIES, K AND H FOR VISUALIZATION PURPOSES--
328 C IF (SNSIM.EQ.NSIM) THEN
329 C
330 C DO 221 K=1, NZ
331 C DO 221 J=1, NY
332 C DO 221 I=1, NX
333 C IP= (K-1) *NXNY+ (J-1) *NX+I
334 C WRITE (14, 667) I, J, K, RK (IP)
335 C WRITE (22, 668) I, J, K, VELX (IP), VELY (IP), VELZ (IP)
336 C WRITE (23, 667) I, J, K, P (IP)
337 C 221 CONTINUE

```

```

338 C      ENDIF
339 C
340 C 667  FORMAT(3(I4,1X),F10.4)
341 C 668  FORMAT(3(I4,1X),3(F9.6,1X))
342 C
343 C
344 C-----CREATING AND MONITOR POLLUTION-----
345 C      IF(MONITOR.EQV. .TRUE.) THEN
346 C          PRINT*, '    CREATING AND MONITOR POLLUTION ...      '
347 C      ELSE
348 C          PRINT*, '    CREATING POLLUTION ...      '
349 C      ENDIF
350 C
351 C      CALL RANDORIGIN(XO,YO,ORPOSO) ! DERMING POLLUTION ORIGIN
352 C          PX=INT(XO)
353 C          PY=INT(YO)
354 C          PZ=1
355 C          IF(YO-PY.GE.0.5) PY=PY+1          !COUNTS ON CENTRAL Y
356 C          IF(XO-PX.GE.0.5) PX=PX+1          !COUNTS ON CENTRAL X
357 C          PRINT*
358 C          PRINT 900, PX, PY, PZ
359 C
360 C      DO 115 MTDC=1,MDS          ! LOOP OVER DIRPERSION FACTOR
361 C          TDC=TDCM(MTDC)
362 C          WRITE(50,*) 'TDC=', TDC
363 C          CALL RANDOMWALK(IS,TDC,XO,YO,ORPOSO,DET,ATOD)
364 C
365 C          DO 125 JS=0,KSA-1
366 C              DO 130 IW=1,KW          ! MULTI-WELL LOOP
367 C                  IF(DET(JS,IW) .EQV. .TRUE.) THEN
368 C                      TDET(MTDC,JS,IW)=TDET(MTDC,JS,IW)+1
369 C                  ELSEIF(DET(JS,IW) .EQV. .FALSE.) THEN
370 C                      FDET(MTDC,JS,IW)=FDET(MTDC,JS,IW)+1
371 C                  ENDIF
372 C
373 C      CALCULATING CONTAMINATED AREA
374 C          TNCAR(MTDC,JS,IW)=TNCAR(MTDC,JS,IW)+NCAR(JS,IW)
375 C          TCAR1(MTDC,JS,IW)=TCAR1(MTDC,JS,IW)+CAR1(JS,IW)
376 C          TCAR3(MTDC,JS,IW)=TCAR3(MTDC,JS,IW)+CAR3(JS,IW)
377 C          TCAR6(MTDC,JS,IW)=TCAR6(MTDC,JS,IW)+CAR6(JS,IW)
378 C          TCAR12(MTDC,JS,IW)=TCAR12(MTDC,JS,IW)+CAR12(JS,IW)
379 C          TCAR24(MTDC,JS,IW)=TCAR24(MTDC,JS,IW)+CAR24(JS,IW)
380 C          TCAR36(MTDC,JS,IW)=TCAR36(MTDC,JS,IW)+CAR36(JS,IW)
381 C
382 C      CALCULATING AVERAGE TIME OF DETECTION
383 C          TATOD(MTDC,JS,IW)=TATOD(MTDC,JS,IW)+ATOD(JS,IW)
384 C
385 C
386 C      IF(IW.EQ.7 .AND. MTDC.EQ.5 .AND. JS.EQ.0 .AND. (SNSIM.EQ.1 .OR. SNSIM
387 C      & .NE. SNSIMOLD)) THEN
388 C          WRITE(48,*) SNSIM,NOW(IW),1.*TDET(MTDC,JS,IW)/SNSIM
389 C          SNSIMOLD=SNSIM
390 C          PRINT*, 'HI',NOW(IW)
391 C      ENDIF
392 C
393 C      130  CONTINUE          ! CLOSING MULTI-WELL LOOP
394 C
395 C      125  CONTINUE          ! CLOSING SAMPLING LOOP
396 C          WRITE(50,*) '*****'
397 C          WRITE(50,*) '*****'
398 C          WRITE(50,*) '*****'
399 C          WRITE(50,*)
400 C
401 C          IF(JS.EQ.KSA .AND. IW.EQ.KW) GOTO 115
402 C          PRINT*, '-----'
403 C
404 C      115  CONTINUE          ! DISPERSION LOOP
405 C

```

```

406      ENDIF                                ! CHECKING IF
407  C
408      PRINT*, '*****'
409      &'*****'
410      PRINT*, '*****'
411      &'*****'
412      PRINT*
413      PRINT*
414      ENDDO                                ! CLOSING SIMULATION LOOP
415  C
416  C*****
417  C
418  C
419  C-----CALCULATE THE ENSEMBLE STATISTICS AND WRITE THE RESULTS-----
420  C-
421      ALLREP=1.D0*IS
422      RKPOINT1=RKPOINT1/ALLREP
423      RKPOIN21=RKPOIN21/ALLREP-RKPOINT1*RKPOINT1
424      RKPOINT2=RKPOINT2/ALLREP
425      RKPOIN22=RKPOIN22/ALLREP-RKPOINT2*RKPOINT2
426      SSXEN=SSXEN/ALLREP
427      SSX2EN=SSX2EN/ALLREP-SSXEN*SSXEN
428  C
429  C      CONTAMINATED AREA RELATIVE TO LANDFILL'S AREA FOR EACH PERIOD
430  DO 510 MTDC=1,MDS
431      DO 510 JS=0,KSA-1
432          DO 510 IW=1,KW
433              IF(FDET(MTDC,JS,IW).NE.0) TNCAR(MTDC,JS,IW)=(TNCAR(MTDC,JS,IW)/
434      & FDET(MTDC,JS,IW))/LFAR
435              IF(TDET(MTDC,JS,IW).NE.0) THEN
436                  TCAR1(MTDC,JS,IW)=(TCAR1(MTDC,JS,IW)/TDET(MTDC,JS,IW))/LFAR
437                  TCAR3(MTDC,JS,IW)=(TCAR3(MTDC,JS,IW)/TDET(MTDC,JS,IW))/LFAR
438                  TCAR6(MTDC,JS,IW)=(TCAR6(MTDC,JS,IW)/TDET(MTDC,JS,IW))/LFAR
439                  TCAR12(MTDC,JS,IW)=(TCAR12(MTDC,JS,IW)/TDET(MTDC,JS,IW))/LFAR
440                  TCAR24(MTDC,JS,IW)=(TCAR24(MTDC,JS,IW)/TDET(MTDC,JS,IW))/LFAR
441                  TCAR36(MTDC,JS,IW)=(TCAR36(MTDC,JS,IW)/TDET(MTDC,JS,IW))/LFAR
442  C
443  C      AVERAGE TIME OF DETECTION
444      TATOD(MTDC,JS,IW)=TATOD(MTDC,JS,IW)/TDET(MTDC,JS,IW)
445  C
446      ENDIF
447  510 CONTINUE
448  C
449  C-----WRITING OUTPUT-----
450      OPEN(16,FILE='FINAL_REPORT.TXT',STATUS='UNKNOWN')
451      OPEN(17,FILE='Pd_EXCEL.TXT',STATUS='UNKNOWN')
452      OPEN(18,FILE='TOTAL_EXCEL.TXT',STATUS='UNKNOWN')
453  C
454      PRINT*
455      WRITE(*,*) 'TOTAL FIELD SIMULATIONS: ',NSIM
456      WRITE(*,*) 'NUMBER THAT FLOW FIELD WAS SIMULATED: ',SNSIM
457  C
458      CALL DATE_AND_TIME (DATE_R,T_R)
459  C
460      WRITE(16,*) 'THIS IS THE FINAL REPORT:'
461      WRITE(16,*)
462      WRITE(16,*) 'TOTAL FIELD SIMULATIONS: ',NSIM
463      WRITE(16,*) 'NUMBER THAT FLOW FIELD WAS SIMULATED: ',SNSIM
464      WRITE(16,*)
465      WRITE(16,*) 'START TIME : ',ST_R(1:2),':',ST_R(3:4),':',ST_R(5:6),
466      + ' AT ',SDATE_R(5:6), '/',SDATE_R(7:8), '/',SDATE_R(3:4)
467      WRITE(16,*) 'END TIME : ',T_R(1:2),':',T_R(3:4),':',T_R(5:6),
468      + ' AT ',DATE_R(5:6), '/',DATE_R(7:8), '/',DATE_R(3:4)
469      WRITE(16,811)NX,NY,NZ
470      WRITE(16,812)DX,DY,DZ
471      WRITE(16,813)DL,DC,DN
472      WRITE(16,*)
473  C

```

```

474      PRINT*
475      PRINT*
476      WRITE(16,*) 'START TIME : ', ST_R(1:2), ':', ST_R(3:4), ':', ST_R(5:6),
477 + ' AT ', SDATE_R(5:6), '/', SDATE_R(7:8), '/', SDATE_R(3:4)
478      PRINT*, 'END TIME : ', T_R(1:2), ':', T_R(3:4), ':', T_R(5:6),
479 + ' AT ', DATE_R(5:6), '/', DATE_R(7:8), '/', DATE_R(3:4)
480      PRINT 811, NX, NY, NZ
481      PRINT 812, DX, DY, DZ
482      PRINT 813, DL, DC, DN
483
484      C
485      811  FORMAT(' GRID SIZE : ', I3, 'X', I3, 'X', I3)
486      812  FORMAT(' BLOCK DIMENSIONS      : ', F5.2, 'X', F5.2, 'X', F5.2)
487      813  FORMAT(' TB BLOCK DIMENSIONS : ', F5.2, 'X', F5.2, 'X', F5.2)
488      900  FORMAT('STARTING POINT OF POLLUTION: ', 'PX=', I3, 2X, 'PY=', I3,
489 & 2X, 'PZ=', I3)
490
491      C
492      WRITE(16,*)
493      WRITE(16,*) 'THE ENS.MEAN IS:', SSXEN, ' AND THE ENS.VAR IS:', SSX2EN
494      WRITE(16,*) 'THE ENS.MEAN IN TWO POINTS IS : ', RKPOINT1, RKPOINT2
495      WRITE(16,*) ' AND THE ENS. VARIANCE IS : ', RKPOIN21, RKPOIN22
496      WRITE(16,*)
497      WRITE(16,*) 'CORRELATION SCALE = ', A, ' WITH ', SNSIM, ' SIMULATIONS'
498      WRITE(16,*) 'INITIAL HEAD: ', HEADG
499      WRITE(16,*) 'No OF PARTICLES:', TOTALPART
500      WRITE(16,*) 'TVC:', TVC, ' PARTICLES'
501      WRITE(16,*) 'VARIANCE : ', BETA*BETA
502      WRITE(16,*)
503
504      C
505      C
506      DETECTION REPORT FILE
507      WRITE(16,*)
508      WRITE(16,*) 'No OF SIMULATION=', SNSIM
509      WRITE(16,*) 'TOTAL MONITOR TIME=', TEND
510      WRITE(16,*)
511      DO MTDC=1, MDS
512      WRITE(16,*) 'DISPERSION FACTOR:', TDCM(MTDC)
513      DO 512 JS=0, KSA-1
514      WRITE(16,*) '*****'
515      WRITE(16,*) 'SAMPLING TIME INTERVALS (DAYS): ', ISA(JS)
516      WRITE(16,*) '-----'
517      DO 512 IW=1, KW
518      WRITE(16,*) 'NUMBER OF MONITOR WELLS : ', NOW(IW)
519      WRITE(16,*) 'NORMALIZED DISTANCE AMONG WELLS: ', 1./NOW(IW)
520      WRITE(16,*) 'DETECTED POLLUTION=', TDET(MTDC, JS, IW)
521      WRITE(16,*) 'NOT DETECTED POLLUTION=', FDET(MTDC, JS, IW)
522      WRITE(16,*) 'PROBABILITY OF DETECTION=', 100.*TDET(MTDC, JS, IW) /
523 & SNSIM, '%'
524      WRITE(16,*) 'PROBABILITY OF FAILURE=', 100.*FDET(MTDC, JS, IW) /
525 & SNSIM, '%'
526      WRITE(16,*)
527      WRITE(16,*) 'AVERAGE TIME OF CONTAMINATION DETECTION=',
528 & TATOD(MTDC, JS, IW)
529      WRITE(16,*)
530      WRITE(16,*) 'AVERAGE POLLUTED VOLUME ON FAILURE=',
531 & TNCAR(MTDC, JS, IW)
532      WRITE(16,*) 'AVERAGE POLLUTED VOLUME ON DETECTION=',
533 & TCAR1(MTDC, JS, IW)
534      WRITE(16,*) 'AVERAGE POLLUTED VOLUME 3 MONTHS LATER=',
535 & TCAR3(MTDC, JS, IW)
536      WRITE(16,*) 'AVERAGE POLLUTED VOLUME 6 MONTHS LATER=',
537 & TCAR6(MTDC, JS, IW)
538      WRITE(16,*) 'AVERAGE POLLUTED VOLUME 12 MONTHS LATER=',
539 & TCAR12(MTDC, JS, IW)
540      WRITE(16,*) 'AVERAGE POLLUTED VOLUME 24 MONTHS LATER=',
541 & TCAR24(MTDC, JS, IW)
542      WRITE(16,*) 'AVERAGE POLLUTED VOLUME 36 MONTHS LATER=',
543 & TCAR36(MTDC, JS, IW)
544      WRITE(16,*)
545
546      512  CONTINUE

```

```

542      WRITE(16,*) '*****'
543      WRITE(16,*) '*****'
544      ENDDO
545      C
546      C      REPORTING DATA FOR EXCEL USE
547      DO K=1,MDS
548          DO I=1,KW
549              WRITE(17,540) (100.0*TDET(K,J,I)/SNSIM,J=0,KSA-1)
550              WRITE(18,560) ( 100.0*TDET(K,J,I)/SNSIM,INT(TATOD(K,J,I)),
551          &      TNCAR(K,J,I),TCAR1(K,J,I),TCAR3(K,J,I),TCAR6(K,J,I),
552          &      TCAR12(K,J,I),TCAR24(K,J,I),TCAR36(K,J,I),J=0,KSA-1)
553          ENDDO
554      ENDDO
555      C
556      540  FORMAT(7(F5.1,1X))
557      560  FORMAT(7(F5.1,1X,I4,1X,7(F6.4,1X)))
558      C
559      C
560      PRINT*, 'THE ENS.MEAN IS:',SSXEN,' AND THE ENS.VAR IS:',SSX2EN
561      PRINT*, 'THE ENS.MEAN IN TWO POINTS IS : ',RKPOINT1,RKPOINT2
562      PRINT*, ' AND THE ENS. VARIANCE IS : ',RKPOIN21,RKPOIN22
563      PRINT*
564      PRINT*, 'CORRELATION SCALE = ',A,' WITH ',SNSIM,' SIMULATIONS'
565      PRINT*, 'INITIAL HEAD: ',HEADG
566      PRINT*, 'No OF PARTICLES:',NTPART
567      PRINT*, 'VARIANCE : ',SIGMA
568      PRINT*
569      PRINT*
570      PRINT*, 'DONE ..... '
571      C
572      C      PAUSE
573      STOP
574      END          !END OF MAIN PROGRAM
575      C
576      C
577      C
578      C
579      C-*****SUBROUTINES*****SUBROUTINES*****SUBROUTINES*****
580      C
581      C
582      C*****
583      C***** SUBROUTINE RANDOMWALK(DET,TDETECTED,POLVOL) *****
584      C*****
585      C
586      SUBROUTINE RANDOMWALK(IS,TDC,RPX,RPY,ORPOS,DET,TOD)
587      C
588      IMPLICIT DOUBLE PRECISION (A-H,O-Z)
589      PARAMETER (IMEM=1024000)
590      PARAMETER (KW=8,KSA=7)
591      C
592      DOUBLE PRECISION X(IMEM),Y(IMEM),Z(IMEM),XPR(IMEM),YPR(IMEM),
593      & ZPR(IMEM),LDC,NDFS,TOD(0:KSA-1,KW)
594      DOUBLE PRECISION NCAR(0:KSA-1,KW),CAR1(0:KSA-1,KW),
595      & CAR3(0:KSA-1,KW),CAR6(0:KSA-1,KW),CAR12(0:KSA-1,KW),
596      & CAR24(0:KSA-1,KW),CAR36(0:KSA-1,KW)
597      DIMENSION C(IMEM),PRPOS(IMEM),LFC(100000)
598      DIMENSION RLOCLAND(IMEM),CC(20),NW(20),MWX(20),MWY(20)
599      INTEGER C,POS,PX,PY,PZ,PAR,PRPOS,ORPOS,PART,CC,TVC,NPAR(10950)
600      INTEGER TEND,TPRD,TS,TTL,PRSMTTL(0:KSA-1,KW),NOW(KW),ISA(0:KSA-1)
601      LOGICAL MW(0:KSA-1,KW,20),MONITOR,DET(0:KSA-1,KW)
602      C
603      COMMON /PARAM/ P0,P1,EP,DX,DY,DZ,NX,NY,NZ,NSEED
604      COMMON /PARTICLE/ PM,TVC,NPAR
605      COMMON /POLLUTION/ C,OOB
606      COMMON /LANDFILL/ LFXI,LFXE,LFYI,LFYE,LFAR,LFC
607      COMMON /MONITORING/ SIGMA,MONITOR,NOW,ISA
608      COMMON /TIME/ TS,TEND,TPRD,NSIM
609      COMMON /WAREA/ NCAR,CAR1,CAR3,CAR6,CAR12,CAR24,CAR36

```

```

610 C
611 C      OPEN(30,FILE='C_ANALYTICALLY.TXT',STATUS='UNKNOWN')
612 C
613 C-----INITIALIZATION OF MATRICES AND PARAMETERS-----
614      NXNY=NX*NY          ! LEVEL NODES
615      OOB=0              ! PARTICLES OUT OF BOUNDARIES
616      TOTALPART=0       ! TOTAL PARTICLE COUNTER
617      LDC=10*TDC        !LONGITUDAL DISPERSSION
618      PART=0            !INITIAL PARTICLE COUNTER
619 C
620 C      COORDINATES OF POLLUTION ORIGIN
621      PX=INT(RPX)
622      PY=INT(RPY)
623      PZ=1
624      IF(RPY-PY.GE.0.5) PY=PY+1      !COUNTS ON CENTRAL Y
625      IF(RPX-PX.GE.0.5) PX=PX+1      !COUNTS ON CENTRAL X
626 C
627      DO JS=0, KSA-1
628          DO IW=1, KW
629              DO K=1, NOW(IW)
630                  MW(JS, IW, K) = .FALSE.      ! MONITOR WELL INITIAL DETECTION VALUE
631              ENDDO
632          ENDDO
633      ENDDO
634 C
635      DO JS=0, KSA-1
636          DO IW=1, KW
637              DET(JS, IW) = .FALSE.      ! DETECTION PARAMETER (IF PLUME IS
638      DETECTED THEN TRUE)
639              TOD(JS, IW) = 0.D0      ! AVERAGE TIME OF DETECTION
640              PRSMTTL(JS, IW) = 0      ! INITIAL TIME OF SAMPLING
641 C
642 C      INITIALISING CONTAMINATED CELL AREA
643      NCAR(JS, IW) = 0.D0
644      CAR1(JS, IW) = 0.D0
645      CAR3(JS, IW) = 0.D0
646      CAR6(JS, IW) = 0.D0
647      CAR12(JS, IW) = 0.D0
648      CAR24(JS, IW) = 0.D0
649      CAR36(JS, IW) = 0.D0
650      ENDDO
651      ENDDO
652 C
653      DO I=1, IMEM
654          X(I) = 0.D0
655          Y(I) = 0.D0
656          Z(I) = 0.D0
657          XPR(I) = 0.D0
658          YPR(I) = 0.D0
659          ZPR(I) = 0.D0
660          C(I) = 0
661      ENDDO
662 C
663      CALL WNDIFS(SIGMA, TDC, NDFS)
664 C
665 C      DIMENSION RESTORATION FACTORS
666      DISTLENGT=DX
667      DISTTIME=TS
668 C      DISTVEL=DX/TS
669 C
670 C      REMOVING DIMENSIONS
671      LDC=LDC/DX
672      TDC=TDC/DY
673      DX=DX/DX
674      DY=DY/DY
675      DZ=DZ/DZ
676      TEND=TEND/TS
677      TPRD=TPRD/TS

```

```

678          TS=TS/TS
679      C
680      C
681      C *****RANDOM WALK PARTICLE TRACKING ALGORITHM*****
682      C
683      C -----TIME PROGRESSION-----
684      C
685          DO 20 TTL=1, TEND, TS
686      C
687      C      NUMBER OF PARTICLES TO BE RELEASED EACH TIME
688      C      INSTANT LEAK (TPRD=1) - CONTINUOUS LEAK (TPRD>1)
689      C      IF(TTL .LE. TPRD) THEN
690          PART=PART+NPAR(TTL)
691      C      PRINT*, TTL, NPAR(TTL), PART
692          TOTALPART=PART
693          C(ORPOS)=C(ORPOS)+NPAR(TTL)
694          DO PAR=PART-NPAR(TTL)+1, PART
695              PRPOS(PAR)=ORPOS
696              X(PAR)=RPX
697              Y(PAR)=RPY
698              Z(PAR)=PZ
699              XPR(PAR)=X(PAR)
700              YPR(PAR)=Y(PAR)
701              ZPR(PAR)=Z(PAR)
702          ENDDO
703      C      ENDIF
704      C
705      C -----PARTICLE'S PROGRESSION ALGORITHM-----
706      C
707          DO 10 PAR=1, PART
708      C
709      C      CHECKING IF PARTICLE WAS INSIDE BOUNDARIES, THEN
710      C      EXECUTE THE NEXT POSITION ALGORITHM
711      C      IF(XPR(PAR) .GE. 1 .AND. XPR(PAR) .LE. NX-1 .AND. YPR(PAR) .LE. NY-1 .AND.
712      C      & YPR(PAR) .GE. 1 .AND. ZPR(PAR) .GT. 0 .AND. ZPR(PAR) .LE. NZ) THEN
713      C
714      C      DETERMINING 3 RANDOM NUMBERS
715          R1=RVNORMAL(NSEED)
716          R2=RVNORMAL(NSEED)
717      C      R3=RVNORMAL(NSEED)
718      C
719      C      CALCULATING PARTICLE'S VELOCITY
720          CALL VCL(X(PAR), Y(PAR), Z(PAR), VLX, VLY, VLZ)
721          CALL VCB(X(PAR), Y(PAR), Z(PAR), VBX, VBY, VBZ)
722      C
723          VB=SQRT(VBX**2+VBY**2+VBZ**2)
724      C
725      C      CALCULATING VELOCITY DERIVATIVES (BETWEEN CELL BOUNDARIES)
726          XIP=INT(X(PAR))
727          YIP=INT(Y(PAR))
728          CALL VCL(X(PAR), YIP, Z(PAR), VLXD, VLYD, VLZ)
729          CALL VCL(X(PAR), YIP+1, Z(PAR), VLXU, VLYU, VLZ)
730          CALL VCL(XIP, Y(PAR), Z(PAR), VLXL, VLYL, VLZ)
731          CALL VCL(XIP+1, Y(PAR), Z(PAR), VLXR, VLYR, VLZ)
732      C
733          UXUVX=(VLXL-VLXR)/DX
734          UYUVY=(VLYU-VLYD)/DY
735          UYUVX=(VLXU-VLXD)/DY
736          UXUVY=(VLYL-VLYR)/DX
737      C
738      C      CALCULATING FOKKER-PLANCK EQUATION ADDITIONAL TERM
739          DLT=LDC-TDC
740      C
741          UXUDYX=(DLT/VB**3)*((VBY**3)*UXUVX+(VBX**3)*UXUVY)
742      C
743          UYUDYY=(2.00*TDC*VBX*VB**2-TDC*VBX**3-LDC*VBX*VBY**2)*
744      C      & UYUVX/VB**3+(2.00*LDC*VBY*VB**2-TDC*VBY*VBX**2-
745      C      & LDC*VBY**3)*UYUVY/VB**3

```

```

746 C
747 C      Y COMPONENT FOKKER-PLANK STAGNATION TERM
748 C      FPTY=UXUDYX+UYUDYY
749 C
750 C
751 C      UXUDXX=(2.D0*LDC*VBX*VB**2-LDC*VBX**3-TDC*VBX*VBY**2)*
752 &      UXUVX/VB**3+(2.D0*TDC*VBY*VB**2-LDC*VBY*VBX**2-
753 &      TDC*VBY**3)*UXUVY/VB**3
754 C
755 C      UYUDXY=(DLT/VB**3)*((VBY**3)*UYUVX+(VBX**3)*UYUVY)
756 C
757 C      X COMPONENT FOKKER-PLANK STAGNATION TERM
758 C      FPTX=UXUDXX+UYUDXY
759 C
760 C      DETERMINING THE NEW POSITION
761 C      FLDC=R1*SQRT(2.D0*LDC*VB*TS)
762 C      FTDC=R2*SQRT(2.D0*TDC*VB*TS)
763 C
764 C      X(PAR)=XPR(PAR)+VLX*TS+(VBX/VB)*FLDC-(VBY/VB)*FTDC+FPTX*TS
765 C      Y(PAR)=YPR(PAR)+VLY*TS+(VBY/VB)*FLDC+(VBX/VB)*FTDC+FPTY*TS
766 C
767 C      CHECKING IF BOYNDARIES HAVE BEEN REACHED
768 C      CHECKING X END BOUNDARY
769 C      IF(X(PAR).LT.1.OR.X(PAR).GT.NX-1) THEN
770 C          C(PRPOS(PAR))=C(PRPOS(PAR))-1
771 C          XPR(PAR)=X(PAR)
772 C          OOB=OOB+1
773 C          GOTO 10
774 C      ENDIF
775 C      CHECKING Y END BOUNDARY
776 C      IF(Y(PAR).GT.NY-1.OR.Y(PAR).LT.1) THEN
777 C          C(PRPOS(PAR))=C(PRPOS(PAR))-1
778 C          YPR(PAR)=Y(PAR)
779 C          OOB=OOB+1
780 C          GOTO 10
781 C      ENDIF
782 C      CHECKING Z DOWN END BOUNDARY
783 C      IF(Z(PAR).LT.0) THEN
784 C          C(PRPOS(PAR))=C(PRPOS(PAR))-1
785 C          ZPR(PAR)=Z(PAR)
786 C          OOB=OOB+1
787 C          GOTO 10
788 C      ENDIF
789 C      CHECKING Z TOP END BOUNDARY.IF EQUAL NZ ASSIGN PREVIOUS VALUE
790 C      PLUME IS FORCED INSIDE THE VOLUME. THIS POLICY MAY BE ALTERED
791 C      IF(Z(PAR).GT.NZ) Z(PAR)=NZ
792 C
793 C      KEEPING POSITIONS
794 C      XPR(PAR)=X(PAR)
795 C      YPR(PAR)=Y(PAR)
796 C      ZPR(PAR)=Z(PAR)
797 C
798 C -----CALCULATING CONCENTRATIONS-----
799 C
800 C      WELLS ARE LOCATED ON GRID'S NODES
801 C      MCLX=INT(X(PAR))
802 C      MCLY=INT(Y(PAR))
803 C
804 C      DIFX=X(PAR)-MCLX
805 C      DIFY=Y(PAR)-MCLY
806 C
807 C      IF(DIFX.GE.0.5) MCLX=MCLX+1
808 C      IF(DIFY.GE.0.5) MCLY=MCLY+1
809 C
810 C      POS=(MCLY-1)*NX+MCLX
811 C
812 C      C(POS)=C(POS)+1
813 C      C(PRPOS(PAR))=C(PRPOS(PAR))-1

```

```

814          PRPOS (PAR) =POS
815      C
816      C
817      ENDIF      ! INSIDE BOUNDARIES IF
818      C
819      C
820      10      CONTINUE
821      C
822      C -----MONITOR-----
823      IF(MONITOR.EQV..TRUE.) THEN
824      C      ESTABLISHING A SAMPLING POLICY (INVSM=INTERVAL OF SAMPLING)
825      DO 90 JS=0,KSA-1
826      C
827      C      MONITOR WELLS
828      DO 95 IW=1,KW
829      IF(INT(TTL-PRSMTTL(JS,IW)) .EQ. ISA(JS)) THEN
830      PRSMTTL(JS,IW)=TTL      ! KEEPING TIME OF PREVIOUS STEP
831      DO KK=1,NOW(IW)
832      BW=(LFYE-LFYI)/NOW(IW)
833      IBW=INT(BW/2)
834      MWX(KK)=INT(LFXE+(LFYE-LFYI)*NDFS)      !X DIMENSION OF MONITOR
835      WELL
836      MWY(KK)=INT(LFYI+(IBW+(KK-1)*BW))      !Y DIMENSION OF MONITOR
837      WELL
838      ENDDO
839      C
840      C      MONITORING WELLS 1 - NOW(IW) (NUMBER OF WELLS)
841      DO 70 K=1,NOW(IW)
842      CC(K)=0
843      C      DEPTH OF WELLS (NZ=1 EQV 2-D)
844      DO 80 IZ=1,NZ
845      NW(K)=(IZ-1)*NXNY+(MWY(K)-1)*NX+MWX(K)
846      CC(K)=CC(K)+C(NW(K))
847      IF(CC(K)*PM.GE.TVC) THEN
848      IF(DET(JS,IW) .EQV..FALSE.) THEN
849      MW(JS,IW,K)=.TRUE.
850      DET(JS,IW)=.TRUE.
851      TOD(JS,IW)=TTL
852      ENDIF
853      ENDIF
854      80      CONTINUE
855      C
856      70      CONTINUE      ! CLOSING MONITOR LOOP
857      ENDIF      ! SAMPLING POLICY IF
858      C
859      IF(DET(JS,IW) .EQV..TRUE.) THEN
860      IF(TTL.EQ.TOD(JS,IW)) CALL POLVOL(CAR1(JS,IW))
861      IF(TTL.EQ.TOD(JS,IW)+90) CALL POLVOL(CAR3(JS,IW))
862      IF(TTL.EQ.TOD(JS,IW)+180) CALL POLVOL(CAR6(JS,IW))
863      IF(TTL.EQ.TOD(JS,IW)+365) CALL POLVOL(CAR12(JS,IW))
864      IF(TTL.EQ.TOD(JS,IW)+730) CALL POLVOL(CAR24(JS,IW))
865      IF(TTL.EQ.TOD(JS,IW)+1095) CALL POLVOL(CAR36(JS,IW))
866      ENDIF
867      C
868      C
869      95      CONTINUE      ! CLOSING WELL LOOP
870      90      CONTINUE      ! CLOSING SAMPLING LOOP
871      C
872      ENDIF      ! MONITOR IF
873      C
874      20      CONTINUE
875      C
876      C
877      DO JS=0,KSA-1
878      DO IW=1,KW
879      IF(DET(JS,IW) .EQV..FALSE.) CALL POLVOL(NCAR(JS,IW))
880      ENDDO
881      ENDDO

```

```

882 C
883 C -----EXPORTING CONCENTRATIONS ON A SELECTED REALISATION -----
884 C IF (IS.EQ.NSIM) THEN
885 OPEN(32, FILE='CONCENTRATION.TXT', STATUS='UNKNOWN')
886 QWVAL=20
887 LVAL=10
888 DO 40 K=1, NZ
889 DO 40 J=1, NY
890 DO 40 I=1, NX
891 IP=(K-1)*NXNY+(J-1)*NX+I
892 RLOCLAND(IP)=C(IP)
893 C VISUALIZATION OF LANDFILL'S LOCATION ON THE FIELD LATTICE AND
894 C ITS MONITOR WELLS
895 DO KK=1, NOW(IW)
896 IF (I.EQ.MWX(KK) .AND. J.EQ.MWY(KK)) RLOCLAND(IP)=QWVAL
897 ENDDO
898 C
899 IF (K.EQ.NZ .AND. J.GE.LFYI .AND. J.LE.LFYE .AND.
900 $ I.GE.LFXI .AND. I.LT.LFXE) RLOCLAND(IP)=LVAL
901 C
902 WRITE(32, *) I, J, K, RLOCLAND(IP)
903 C
904 40 CONTINUE
905 C
906 CLOSE(32)
907 C
908 C -----CHECKING HOW MANY PARTICLES WERE COUNTED AND IF WE HAD C<0 -----
909 NP=0
910 E0=0
911 DO 45 K=1, NZ
912 DO 45 J=1, NY
913 DO 45 I=1, NX
914 IP=(K-1)*NXNY+(J-1)*NX+I
915 IF (C(IP) .LT.0) THEN
916 E0=E0+1
917 PRINT 145, C(IP), I, J
918 WRITE(50, 145) C(IP), I, J
919 ENDIF
920 NP=NP+C(IP)
921 45 CONTINUE
922 145 FORMAT('ATTENTION:NEGATIVE VALUE OF CONCENTRATION C', I5,
923 &', AT POSITION X=', I4, ' AND Y=', I4)
924 C
925 C RESTORING DIMENSIONS
926 LDC=LDC*DISTLENGT
927 TDC=TDC*DISTLENGT
928 DX=DX*DISTLENGT
929 DY=DY*DISTLENGT
930 DZ=DZ
931 TEND=TEND*DISTTIME
932 TPRD=TPRD*DISTTIME
933 TS=TS*DISTTIME
934 C
935 C
936 C REPORTING VALUES
937 WRITE(50, *) IS, '/', NSIM
938 WRITE(50, 800) NX, NY, NZ
939 WRITE(50, 900) PX, PY, PZ
940 WRITE(50, *)
941 WRITE(50, *) 'TIME STEP: ', TS
942 WRITE(50, *) 'TOTAL PARTICLES INJECTED: ', TOTALPART
943 WRITE(50, *) 'PARTICLES TRACKED: ', NP
944 WRITE(50, *) 'PARTICLES MISSED: ', OOB
945 WRITE(50, *) 'TOTAL TRACKED & MISSED= ', NP+OOB
946 WRITE(50, *)
947 C
948 DO JS=0, KSA-1
949 WRITE(50, *) '*****'

```

```

950      DO IW=1,KW
951      C      WRITE(50,*)'LOCATION OF WELLS : ',
952      C      & ('WELL:',K,' (' ,MWX(K) , ' , ,MWY(K) , ' ) ' , ' - ' ,K=1,NOW(IW))
953      WRITE(50,*)'SAMPLING INTERVAL (DAYS):',ISA(JS)
954      IF(DET(JS,IW).EQV..TRUE.) THEN
955          DO K=1,NOW(IW)
956          IF(MW(JS,IW,K).EQV..TRUE.) THEN
957              WRITE(50,*)NOW(IW),'-WELLS, MONITORING WELL:',K,
958              & ' HAS DETECTED POLLUTION'
959              WRITE(50,*)'DETECTION TIME= ',TOD(JS,IW),' OF ',TEND
960          ENDIF
961          ENDDO
962          ELSEIF(DET(JS,IW).EQV..FALSE.) THEN
963              WRITE(50,*)'NO DETECTION SUCCEEDED BY ',NOW(IW),
964              & ' MONITORING WELLS '
965          ENDIF
966      C
967      WRITE(50,*)
968      WRITE(50,*)'POLLUTED VOLUME ON FAILURE=',NCAR(JS,IW)/LFAR
969      WRITE(50,*)'POLLUTED VOLUME ON DETECTION=',CAR1(JS,IW)/LFAR
970      WRITE(50,*)'POLLUTED VOLUME 3 MONTHS LATER=',CAR3(JS,IW)/LFAR
971      WRITE(50,*)'POLLUTED VOLUME 6 MONTHS LATER=',CAR6(JS,IW)/LFAR
972      WRITE(50,*)'POLLUTED VOLUME 12 MONTHS LATER=',CAR12(JS,IW)/LFAR
973      WRITE(50,*)'POLLUTED VOLUME 24 MONTHS LATER=',CAR24(JS,IW)/LFAR
974      WRITE(50,*)'POLLUTED VOLUME 36 MONTHS LATER=',CAR36(JS,IW)/LFAR
975      WRITE(50,*)'-----'
976      WRITE(50,*)
977      ENDDO
978      ENDDO
979      C
980      C      PRINTING ON SCREEN
981      PRINT*
982      PRINT*,'TDC: ',TDC
983      PRINT*,'TOT INJ:',TOTALPART,' / TRACKED:',NP,' / MISSED:',OOB,
984      & ' / TOT TRACKED & MISSED=',NP+OOB
985      PRINT*
986      C
987      C
988      800 FORMAT('X=',I4,2X,'Y=',I4,2X,'Z=',I4)
989      900 FORMAT('STARTING POINT OF POLLUTION: ', 'PX=',I3,2X,'PY=',I3,
990      & 2X,'PZ=',I3)
991      C
992      RETURN
993      END
994      C
995      C
996      C-----
997      C      NORMAL RANDOM NUMBER FUNCTION GENERATOR
998      C-----
999      C
1000     FUNCTION RVNORMAL(SEED)
1001     IMPLICIT DOUBLE PRECISION (A-H,O-Z)
1002     DATA S,T / 0.449871,-0.386595 /
1003     DATA A,B / 0.19600,0.25472 /
1004     INTEGER SEED
1005     C
1006     100  U=RANM(SEED)
1007     V=RANM(SEED)
1008     V=1.7156D0*(V-0.5D0)
1009     X=U-S
1010     Y=ABS(V)-T
1011     Q=X*X+Y*(A*Y-B*X)
1012     C
1013     IF(V**2.GT.-4*LOG(U)*U**2) GOTO 100
1014     IF(Q.GT.0.27846) GOTO 100
1015     IF(Q.LT.0.27597) RVNORMAL=V/U
1016     RETURN
1017     END

```

```

1018 C
1019 C
1020 C-----
1021 C   RANDOM NUMBER FUNCTION (0-1 EQUAL PROBABLE)
1022 C-----
1023 C
1024 C   FUNCTION RANDM(IDUM)
1025 C   INTEGER IDUM, IM1, IM2, IMM1, IA1, IQ1, IQ2, IR1, NTAB, NDIV
1026 C   DOUBLE PRECISION RANDM, AM, EPS, RNMX
1027 C   PARAMETER (IM1=2147483563, IM2=2147483399, AM=1.D0/IM1, IMM1=IM1-1,
1028 C   *   IA1=40014, IA2=40692, IQ1=53668, IQ2=52774, IR1=12211,
1029 C   *   NTAB=32, NDIV=1+IMM1/NTAB, EPS=1.2E-7, RNMX=1.D0-EPS)
1030 C   INTEGER IDUM2, J, K, IV(NTAB), IY
1031 C   SAVE IV, IY, IDUM2
1032 C   DATA IDUM2/123456789/, IV/NTAB*0/, IY/0/
1033 C   IF (IDUM.LE.0) THEN
1034 C       IDUM=MAX(-IDUM, 1)
1035 C       IDUM2=IDUM
1036 C   DO 11 J=NTAB+8, 1, -1
1037 C       K=IDUM/IQ1
1038 C       IDUM=IA1*(IDUM-K*IQ1)-K*IR1
1039 C       IF (IDUM.LT.0) IDUM=IDUM+IM1
1040 C       IF (J.LE.NTAB) IV(J)=IDUM
1041 C 11 CONTINUE
1042 C   IY=IV(1)
1043 C   ENDIF
1044 C   K=IDUM/IQ1
1045 C   IDUM=IA1*(IDUM-K*IQ1)-K*IR1
1046 C   IF (IDUM.LT.0) IDUM=IDUM+IM1
1047 C   K=IDUM2/IQ2
1048 C   IDUM2=IA2*(IDUM2-K*IQ2)
1049 C   IF (IDUM2.LT.0) IDUM2=IDUM+IM2
1050 C   J=1+IY/NDIV
1051 C   IY=IV(J)-IDUM2
1052 C   IV(J)=IDUM
1053 C   IF (IY.LT.1) IY=IY+IMM1
1054 C   RANDM=MIN(AM*IY, RNMX)
1055 C   RETURN
1056 C   END
1057 C
1058 C
1059 C
1060 C*****
1061 C   SUBROUTINE LANDFL: LANDFILL'S SHAPE AND BOUNDARIES
1062 C*****
1063 C
1064 C   SUBROUTINE LANDF
1065 C   IMPLICIT DOUBLE PRECISION (A-H,O-Z)
1066 C   COMMON /PARAM/ P0, P1, EP, DX, DY, DZ, NX, NY, NZ, NSEED
1067 C   COMMON /LANDFILL/ LFXI, LFXE, LFYI, LFYE, LFAR, LFC
1068 C   INTEGER LFC(100000)
1069 C
1070 C   NN=NX*NY
1071 C
1072 C   DO I=1, NN
1073 C       LFC(I)=0
1074 C   ENDDO
1075 C
1076 C   --> RECTAGULAR LANDFILL <--
1077 C   LANDFILL (COORDINATIONS IN METERS/D TO GET DIMENSIONLESS NUMBERS)
1078 C   LFXI=INT(10/DX)           !LANDFILL'S X INITIAL BOUNDARY LIMIT
1079 C   LFXE=INT(60/DX)           !LANDFILL'S X ENDING BOUNDARY LIMIT
1080 C   LFYI=INT(140/DY)          !LANDFILL'S Y INITIAL BOUNDARY LIMIT
1081 C   LFYE=INT(260/DY)          !LANDFILL'S Y ENDING BOUNDARY LIMIT
1082 C   LFAR=(LFXE-LFXI-1)*(LFYE-LFYI-1) !LF'S DIMENSIONLESS AREA (No OF
1083 C   CELLS)
1084 C
1085 C   DO J=1, NY

```

```

1086         DO I=1,NX
1087             IP=(J-1)*NX+I
1088             IF(J.GE.LFYI.AND.J.LE.LFYE.AND.I.GE.LFXI.AND.I.LT.LFXE) THEN
1089                 LFC(IP)=1
1090             ENDIF
1091         ENDDO
1092     ENDDO
1093 C
1094     RETURN
1095 END
1096 C
1097 C
1098 C*****
1099 C    SUBROUTINE RANDORIGIN: CREATING RANDOM ORIGIN POINT OF POLLUTION
1100 C*****
1101 C
1102     SUBROUTINE RANDORIGIN(RPX,RPY,ORPOS)
1103     IMPLICIT DOUBLE PRECISION (A-H,O-Z)
1104     COMMON /PARAM/ P0,P1,EP,DX,DY,DZ,NX,NY,NZ,NSEED
1105     COMMON /LANDFILL/ LFXI,LFXE,LFYI,LFYE,LFAR,LFC
1106     INTEGER ORPOS,LFC(100000)
1107 C
1108     XL=ABS(LFXE-LFXI)
1109     YL=ABS(LFYE-LFYI)
1110     RPX=XL*RANDM(NSEED)+LFXI
1111     RPY=YL*RANDM(NSEED)+LFYI
1112     PX=INT(RPX)
1113     PY=INT(RPY)
1114     PZ=1
1115     IF(RPY-PY.GE.0.5) PY=PY+1           !COUNTS ON CENTRAL Y
1116     IF(RPX-PX.GE.0.5) PX=PX+1         !COUNTS ON CENTRAL X
1117 C
1118     ORPOS=(PY-1)*NX+PX    ! INITIAL CUBIC ELEMENT POSITION OF PARTICLES
1119 C
1120     WRITE(39,*) PX,PY
1121 C
1122     RETURN
1123 END
1124 C
1125 C
1126 C
1127 C*****
1128 C    SUBROUTINE WNDFS: WELLS' DISTANCE FROM SOURCE (NORMALIZED)
1129 C*****
1130 C
1131     SUBROUTINE WNDFS(SIGMA,AT,DFS)
1132     IMPLICIT DOUBLE PRECISION (A-H,O-Z)
1133 C
1134     IF(SIGMA.EQ.0.D0) THEN
1135         IF(AT.EQ.0.001D0) DFS=3.0D0
1136         IF(AT.EQ.0.01D0) DFS=2.25D0
1137         IF(AT.EQ.0.02D0) DFS=1.50D0
1138         IF(AT.EQ.0.05D0) DFS=0.50D0
1139         IF(AT.EQ.0.1D0) DFS=0.125D0
1140         IF(AT.EQ.0.2D0) DFS=0.030D0
1141         IF(AT.EQ.0.5D0) DFS=0.015D0
1142     ENDIF
1143 C
1144     IF(SIGMA.EQ.0.25D0) THEN
1145         IF(AT.EQ.0.001D0) DFS=1.75D0
1146         IF(AT.EQ.0.01D0) DFS=1.50D0
1147         IF(AT.EQ.0.02D0) DFS=1.00D0
1148         IF(AT.EQ.0.05D0) DFS=0.50D0
1149         IF(AT.EQ.0.1D0) DFS=0.125D0
1150         IF(AT.EQ.0.2D0) DFS=0.30D0
1151         IF(AT.EQ.0.5D0) DFS=0.015D0
1152     ENDIF
1153 C

```

```

1154      IF(SIGMA.EQ.0.50D0) THEN
1155          IF(AT.EQ.0.001D0) DFS=1.75D0
1156          IF(AT.EQ.0.01D0) DFS=1.50D0
1157          IF(AT.EQ.0.02D0) DFS=0.50D0
1158          IF(AT.EQ.0.05D0) DFS=0.50D0
1159          IF(AT.EQ.0.1D0) DFS=0.125D0
1160          IF(AT.EQ.0.2D0) DFS=0.030D0
1161          IF(AT.EQ.0.5D0) DFS=0.015D0
1162      ENDIF
1163  C
1164      IF(SIGMA.EQ.0.75D0) THEN
1165          IF(AT.EQ.0.001D0) DFS=1.75D0
1166          IF(AT.EQ.0.01D0) DFS=1.25D0
1167          IF(AT.EQ.0.02D0) DFS=0.50D0
1168          IF(AT.EQ.0.05D0) DFS=0.25D0
1169          IF(AT.EQ.0.1D0) DFS=0.125D0
1170          IF(AT.EQ.0.2D0) DFS=0.030D0
1171          IF(AT.EQ.0.5D0) DFS=0.015D0
1172      ENDIF
1173  C
1174      IF(SIGMA.EQ.1.D0) THEN
1175          IF(AT.EQ.0.001D0) DFS=1.75D0
1176          IF(AT.EQ.0.01D0) DFS=1.25D0
1177          IF(AT.EQ.0.02D0) DFS=0.50D0
1178          IF(AT.EQ.0.05D0) DFS=0.125D0
1179          IF(AT.EQ.0.1D0) DFS=0.0625D0
1180          IF(AT.EQ.0.2D0) DFS=0.030D0
1181          IF(AT.EQ.0.5D0) DFS=0.015D0
1182      ENDIF
1183  C
1184      IF(SIGMA.EQ.1.5D0) THEN
1185          IF(AT.EQ.0.001D0) DFS=1.25D0
1186          IF(AT.EQ.0.01D0) DFS=1.00D0
1187          IF(AT.EQ.0.02D0) DFS=0.50D0
1188          IF(AT.EQ.0.05D0) DFS=0.125D0
1189          IF(AT.EQ.0.1D0) DFS=0.0625D0
1190          IF(AT.EQ.0.2D0) DFS=0.015D0
1191          IF(AT.EQ.0.5D0) DFS=0.015D0
1192      ENDIF
1193  C
1194      IF(SIGMA.EQ.2.0D0) THEN
1195          IF(AT.EQ.0.001D0) DFS=0.75D0
1196          IF(AT.EQ.0.01D0) DFS=0.50D0
1197          IF(AT.EQ.0.02D0) DFS=0.25D0
1198          IF(AT.EQ.0.05D0) DFS=0.125D0
1199          IF(AT.EQ.0.1D0) DFS=0.0625D0
1200          IF(AT.EQ.0.2D0) DFS=0.015D0
1201          IF(AT.EQ.0.5D0) DFS=0.015D0
1202      ENDIF
1203  C
1204      RETURN
1205      END
1206  C
1207  C
1208  C
1209  C*****
1210  C  SUBROUTINE POLVOL: ESTIMATING THE POLLUTED VOLUME
1211  C*****
1212      SUBROUTINE POLVOL(VOL)
1213      IMPLICIT DOUBLE PRECISION (A-H,O-Z)
1214  C
1215      PARAMETER (IMEM=1024000)
1216      COMMON /PARAM/ P0,P1,EP,DX,DY,DZ,NX,NY,NZ,NSEED
1217      COMMON /POLLUTION/ C,OOB
1218      INTEGER C(IMEM)
1219  C
1220      NXNY=NX*NY
1221      VOL=0

```

```

1222      DO 50 K=1,NZ
1223          DO 50 J=1,NY
1224              DO 50 I=1,NX
1225                  IP=(K-1)*NXNY+(J-1)*NX+I
1226                  IF(C(IP).GT.28)VOL=VOL+1
1227      50 CONTINUE
1228      C
1229      VOL=VOL+OOB      !PARTICLES OUT OF BOUNDARIES INCLUDED (1 CELL/PAR)
1230      C
1231      RETURN
1232      END
1233      C
1234      C
1235      C
1236      C*****
1237      C      CALCULATING THE VELOCITY FIELD
1238      C*****
1239      C
1240      SUBROUTINE VEL(RK,P,VELX,VELY,VELZ)
1241      C
1242      C      VELOCITIES ARE CALCULATED IN A SHIFTED GRID, EQUAL TO 1/2 IN RELATION
1243      C      TO THE INITIAL GRID WHERE K AND H ARE CALCULATED. THIS MEANS THAT
1244      C      VX(I+1/2,J,K), VY(I,J+1/2,K), VZ(I,J,K+1/2). CALCULATIONS OF VELOCITY
1245      C      ONTO OTHER POINTS OF SIMULATION AREA MUST ACCOUNT FOR THIS SHIFT.
1246      C      VELOCITIES ON INITIAL GRID NODES ARE LINEARLY INTERPOLATED,
1247      C      BETWEEN I+1,I AND J+1,J.
1248      C
1249      IMPLICIT DOUBLE PRECISION (A-H,O-Z)
1250      PARAMETER (IMEM=1024000)
1251      C
1252      DOUBLE PRECISION P(IMEM),RK(IMEM),VELX(IMEM),VELY(IMEM),VELZ(IMEM)
1253      DOUBLE PRECISION VELXI(IMEM),VELYI(IMEM),VELZI(IMEM)
1254      INTEGER TS,TEND,TPRD
1255      C
1256      COMMON /PARAM/ P0,P1,EP,DX,DY,DZ,NX,NY,NZ,NSEED
1257      COMMON /TIME/ TS,TEND,TPRD,NSIM
1258      C
1259      C      INITIALIZATION OF MATRICES AND PARAMETERS
1260      DO I=1,IMEM
1261      VELXI(I)=0.DO
1262      VELYI(I)=0.DO
1263      VELZI(I)=0.DO
1264      VELX(I)=0.DO
1265      VELY(I)=0.DO
1266      VELZ(I)=0.DO
1267      ENDDO
1268      C
1269      NXNY=NX*NY
1270      C
1271      C      CALCULATING
1272      DO 810 K=1,NZ
1273      DO 810 J=1,NY
1274      DO 810 I=1,NX
1275      IP=(K-1)*NXNY+(J-1)*NX+I
1276      C
1277      C      VELOCITY ON X AXIS (I+1/2)
1278      IF(I.GE.1.AND.I.LE.NX-1) THEN      ! CALCULATING grad(H)
1279      GRADHX=(P(IP+1)-P(IP))/DX
1280      RKPX=2.DO*RK(IP+1)*RK(IP)/(RK(IP+1)+RK(IP))
1281      VELXI(IP)=RKPX*GRADHX/EP      ! CALCULATING VELOCITY
1282      ENDIF
1283      C
1284      IF(I.EQ.NX) VELXI(IP)=VELXI((K-1)*NXNY+(J-1)*NX+NX-1)
1285      C
1286      C      VELOCITY ON Y AXIS (J+1/2)
1287      IF(J.GE.1.AND.J.LE.NY-1) THEN      ! CALCULATING grad(H)
1288      GRADHY=(P(IP+NX)-P(IP))/DY
1289      RKPX=2.DO*RK(IP+NX)*RK(IP)/(RK(IP+NX)+RK(IP))

```

```

1290      VELYI (IP) = RKPY * GRADHY / EP                ! CALCULATING VELOCITY
1291      ENDIF
1292      C
1293      IF (J.EQ.NY) VELYI (IP) = VELYI ((K-1) * NXNY + (J-1-1) * NX + I)
1294      C
1295      C      VELOCITY ON Z AXIS (K+1/2)
1296      IF (K.GT.1 .AND. K.LT.NZ) THEN                ! CALCULATING grad(H)
1297          GRADHZ = (P (IP + NXNY) - P (IP)) / DZ
1298          RKPZ = 2.00 * RK (IP + NXNY) * RK (IP) / (RK (IP + NXNY) + RK (IP))
1299          VELZI (IP) = RKPZ * GRADHZ / EP            ! CALCULATING VELOCITY
1300      ENDIF
1301      C
1302      IF (K.EQ.NZ) VELZI (IP) = VELZ ((K-1-1) * NXNY + (J-1) * NX + I)
1303      C
1304      810 CONTINUE
1305      C
1306      C      LINEARLY INTERPOLATING VELOCITIES ON (I,J)
1307      C      VELOCITY ON X AXIS [(I+1/2)+(I-1/2)]/2
1308      DO 820 K=1,NZ
1309          DO 820 J=1,NY
1310              DO 820 I=2,NX-1
1311                  IP = (K-1) * NXNY + (J-1) * NX + I
1312                  IB = (K-1) * NXNY + (J-1) * NX + I - 1
1313                  VELX (IP) = (VELXI (IP) + VELXI (IB)) / 2.00
1314      820 CONTINUE
1315      C
1316      C      VELOCITY ON Y AXIS [(J+1/2)+(J-1/2)]/2
1317      DO 830 K=1,NZ
1318          DO 830 J=2,NY-1
1319              DO 830 I=1,NX
1320                  IP = (K-1) * NXNY + (J-1) * NX + I
1321                  IB = (K-1) * NXNY + (J-1-1) * NX + I
1322                  VELY (IP) = (VELYI (IP) + VELYI (IB)) / 2.00
1323      830 CONTINUE
1324      C
1325      C      VELOCITY ON (NX,J) SIDE
1326      DO J=1,NY
1327          IP = (J-1) * NX + 1
1328          IE = (J-1) * NX + NX
1329          VELX (IP) = VELXI (IP)
1330          VELX (IE) = VELXI (IE)
1331      ENDDO
1332      C
1333      C      VELOCITY ON (I,NY) SIDE
1334      DO I=1,NX
1335          IE = (NY-1) * NX + I
1336          VELY (I) = VELYI (I)
1337          VELY (IE) = VELYI (IE)
1338      ENDDO
1339      C
1340      C
1341      C      REMOVING DIMENSIONS (VELOCITY IN DX/TS M/DAY UNITS)
1342      DO 850 K=1,NZ
1343          DO 850 J=1,NY
1344              DO 850 I=1,NX
1345                  IP = (K-1) * NXNY + (J-1) * NX + I
1346                  VELX (IP) = VELX (IP) / (DX/TS)
1347                  VELY (IP) = VELY (IP) / (DY/TS)
1348                  VELZ (IP) = VELZ (IP) / (DZ/TS)
1349      850 CONTINUE
1350      C
1351      C
1352      RETURN
1353      END
1354      C
1355      C
1356      C
1357      C

```

```

1358 C*****
1359 C      3D HYBRID VELOCITY INTERPOLATION SCHEME SUBROUTINES
1360 C*****
1361 C
1362 C
1363 C      SUBROUTINE VCL (XPR, YPR, ZPR, VLX, VLY, VLZ)
1364 C
1365 C*****
1366 C      LINEAR VELOCITY INTERPOLATION
1367 C
1368 C      IMPLICIT DOUBLE PRECISION (A-H,O-Z)
1369 C      PARAMETER (IMEM=1024000)
1370 C
1371 C      DOUBLE PRECISION VELX (IMEM) , VELY (IMEM) , VELZ (IMEM)
1372 C
1373 C      COMMON /VELOCITY/ VELX, VELY, VELZ
1374 C      COMMON /PARAM/ P0, P1, EP, DX, DY, DZ, NX, NY, NZ, NSEED
1375 C
1376 C
1377 C      NXNY=NX*NY
1378 C      VLX=0.D0
1379 C      VLY=0.D0
1380 C      VLZ=0.D0
1381 C      I=INT (XPR)
1382 C      J=INT (YPR)
1383 C      K=INT (ZPR)
1384 C
1385 C      FX=XPR-INT (XPR)
1386 C      FY=YPR-INT (YPR)
1387 C
1388 C      ----- X-AXIS -----
1389 C      IF (INT (XPR) .GE. 1 .AND. INT (XPR) .LE. NX-1) THEN
1390 C          VLX= (DX-FX) *VELX ( (K-1) *NXNY+ (J-1) *NX+I) +
1391 C      &          FX*VELX ( (K-1) *NXNY+ (J-1) *NX+I+1)
1392 C      ENDIF
1393 C
1394 C      IF (INT (XPR) .EQ. NX) VLX=VELX ( (K-1) *NXNY+ (J-1) *NX+NX)
1395 C
1396 C
1397 C      ----- Y-AXIS -----
1398 C      IF (INT (YPR) .GE. 1 .AND. INT (YPR) .LE. NY-1) THEN
1399 C          VLY= (DY-FY) *VELY ( (K-1) *NXNY+ (J-1) *NX+I) +
1400 C      &          FY*VELY ( (K-1) *NXNY+ (J-1+1) *NX+I)
1401 C      ENDIF
1402 C
1403 C      IF (INT (YPR) .EQ. NY) VLY=VELY ( (K-1) *NXNY+ (NY-1) *NX+I)
1404 C
1405 C
1406 C      RETURN
1407 C      END
1408 C
1409 C
1410 C
1411 C*****
1412 C
1413 C      SUBROUTINE VCB (XPR, YPR, ZPR, VBX, VBY, VBZ)
1414 C
1415 C*****
1416 C      BILINEAR VELOCITY INTERPOLATION
1417 C
1418 C
1419 C      IMPLICIT DOUBLE PRECISION (A-H,O-Z)
1420 C      PARAMETER (IMEM=1024000)
1421 C
1422 C      DOUBLE PRECISION VELX (IMEM) , VELY (IMEM) , VELZ (IMEM)
1423 C
1424 C      COMMON /VELOCITY/ VELX, VELY, VELZ
1425 C      COMMON /PARAM/ P0, P1, EP, DX, DY, DZ, NX, NY, NZ, NSEED

```

```

1426 C
1427 C
1428 NXNY=NX*NY
1429 VBX=0.D0
1430 VBY=0.D0
1431 VBZ=0.D0
1432 I=INT(XPR)
1433 J=INT(YPR)
1434 K=INT(ZPR)
1435 C
1436 FX=XPR-INT(XPR)
1437 FY=YPR-INT(YPR)
1438 C
1439 C
1440 C ----- X-AXIS -----
1441 IF(INT(XPR) .GE. 1 .AND. INT(XPR) .LE. NX-1 .AND. INT(YPR) .LE. NY-1) THEN
1442     BVX1=(DX-FX)*(DY-FY)*VELX((K-1)*NXNY+(J-1)*NX+I)
1443     BVX2=FX*(DY-FY)*VELX((K-1)*NXNY+(J-1)*NX+I+1)
1444     BVX3=(DX-FX)*FY*VELX((K-1)*NXNY+(J-1+1)*NX+I)
1445     BVX4=FX*FY*VELX((K-1)*NXNY+(J-1+1)*NX+I+1)
1446     VBX=BVX1+BVX2+BVX3+BVX4
1447 ENDIF
1448 C
1449 IF(INT(XPR) .EQ. NX) VBX=VELX((K-1)*NXNY+(J-1)*NX+NX)
1450 C
1451 C ----- Y-AXIS -----
1452 IF(INT(YPR) .GE. 1 .AND. INT(YPR) .LE. NY-1 .AND. INT(XPR) .LE. NX-1) THEN
1453     BVY1=(DX-FX)*(DY-FY)*VELY((K-1)*NXNY+(J-1)*NX+I)
1454     BVY2=FX*(DY-FY)*VELY((K-1)*NXNY+(J-1)*NX+I+1)
1455     BVY3=(DX-FX)*FY*VELY((K-1)*NXNY+(J-1+1)*NX+I)
1456     BVY4=FX*FY*VELY((K-1)*NXNY+(J-1+1)*NX+I+1)
1457     VBY=BVY1+BVY2+BVY3+BVY4
1458 ENDIF
1459 C
1460 IF(INT(YPR) .EQ. NY) VBY=VELY((K-1)*NXNY+(NY-1)*NX+I)
1461 C
1462 C
1463 RETURN
1464 END
1465
1466
1467

```

## A-3 Flow Numerical Solution

(T.Sarris, personal communication, developed by A.J. Desbarats)

```

1  C*****
2  C   SOLVING THE FLOW PROBLEM
3  C*****
4  C
5  C   SUBROUTINE FLOW3D(RK, P, ICON, DMAX)
6  C
7  C   IMPLICIT DOUBLE PRECISION (A-H,O-Z)
8  C   PARAMETER (IMEM=1024000)
9  C   DOUBLE PRECISION P (IMEM), B (IMEM), F (IMEM), S (IMEM), A (IMEM), D (IMEM),
10 C   &           RK (IMEM)
11 C
12 C   COMMON /PARAM/ P0, P1, EP, DX, DY, DZ, NX, NY, NZ, NSEED
13 C
14 C-----
15 C   SET CONSTANTS AND INITIALIZE VECTORS
16 C-----
17     NNNN=NX*NY*NZ
18     NXNY=NX*NY
19     TX=2.D0*DZ*(DY/DX)
20     TY=2.D0*DZ*(DX/DY)
21     TZ=2.D0*DX*(DY/DZ)
22     DO 5 I=1, NNNN
23     A(I)=0.D0
24     B(I)=0.D0
25     F(I)=0.D0
26     S(I)=0.D0
27     D(I)=0.D0
28     5 CONTINUE
29 C
30 C-----
31 C   SET UP DIAGONAL VECTORS FOR K+1 AND K-1
32 C-----
33     IF(NZ.EQ.1) GO TO 14
34     NZ1=NZ-1
35     DO 10 IK=1, NZ1
36     DO 10 IJ=1, NY
37     DO 10 II=1, NX
38     IP=(IK-1)*NXNY+(IJ-1)*NX+II
39     S(IP)=-1.D0*TZ*RK(IP)*RK(IP+NXNY)/(RK(IP)+RK(IP+NXNY))
40     10 CONTINUE
41 C
42 C-----
43 C   SET UP DIAGONAL VECTORS FOR J+1 AND J-1
44 C-----
45     14 IF(NY.EQ.1) GO TO 19
46     NY1=NY-1
47     DO 15 IK=1, NZ
48     DO 15 IJ=1, NY1
49     DO 15 II=1, NX
50     IP=(IK-1)*NXNY+(IJ-1)*NX+II
51     F(IP)=-1.D0*TY*RK(IP)*RK(IP+NX)/(RK(IP)+RK(IP+NX))
52     15 CONTINUE
53 C
54 C-----
55 C   SET UP DIAGONAL VECTORS FOR I+1 AND I-1
56 C-----
57     19 NX1=NX-1
58     DO 20 IK=1, NZ
59     DO 20 IJ=1, NY
60     DO 20 II=1, NX1

```

```

61      IP=(IK-1)*NXNY+(IJ-1)*NX+II
62      B(IP)=-1.D0*TX*RK(IP)*RK(IP+1)/(RK(IP)+RK(IP+1))
63      20  CONTINUE
64      C
65      C-----
66      C      SET UP MAIN DIAGONAL AND RHS VECTOR
67      C-----
68      DO 25 IK=1,NZ
69      DO 25 IJ=1,NY
70      IP=(IK-1)*NXNY+(IJ-1)*NX+1
71      TBOUND=TX*RK(IP)
72      PBOUND=P0
73      A(IP)=TBOUND
74      D(IP)=TBOUND*PBOUND
75      DO 26 II=1,NX
76      IP=(IK-1)*NXNY+(IJ-1)*NX+II
77      ZIP=0.D0
78      GIP=0.D0
79      CIP=0.D0
80      IF(IP.GT.NXNY) ZIP=S(IP-NXNY)
81      IF(IP.GT.NX) GIP=F(IP-NX)
82      IF(IP.GT.1) CIP=B(IP-1)
83      A(IP)=A(IP)-S(IP)-ZIP-F(IP)-GIP-CIP-B(IP)
84      26  CONTINUE
85      TBOUND=TX*RK(IP)
86      PBOUND=P1
87      A(IP)=A(IP)+TBOUND
88      D(IP)=TBOUND*PBOUND
89      25  CONTINUE
90      C
91      C      SOLVE HEPTADIAGONAL LINEAR SYSTEM OF EQUATIONS
92      C      USING A LINE SUCCESSIVE OVER RELAXATION (LSOR) METHOD.
93      C
94      CALL LSOR(A,B,F,S,D,P,ICON,DMAX)
95      C
96      RETURN
97      END
98      C
99      C
100     C
101     C*****
102     SUBROUTINE LSOR(A,B,F,S,D,P,ICON,DMAX)
103     C*****
104     C
105     IMPLICIT DOUBLE PRECISION (A-H,O-Z)
106     DOUBLE PRECISION AZL(500),BZL(500),CZL(500),DZL(500),UZL(500),
107     & UM(500),A(1),B(1),F(1),S(1),D(1),P(1)
108     INTEGER SNSIM
109     C
110     COMMON /SOLVE/ OMEGA,TOL,TOL1,MITER,SNSIM
111     COMMON /PARAM/ P0,P1,EP,DX,DY,DZ,NX,NY,NZ,NSEED
112     C
113     NXNY=NX*NY
114     IDEBUG=1
115     IOCODE=9
116     ICON=0
117     NITER=0
118     MFLAG=MITER-50
119     DMAX=1.D0
120     RHO1=0.D0
121     THETA=0.D0
122     C
123     C-----
124     C      ITERATE ON SOLUTION
125     C-----
126     C
127     11  CONTINUE
128     C

```

```

129      TW=1.D0-OMEGA
130      DMAX0=DMAX
131      THETA0=THETA
132      IOCODE=9
133      IF(NITER.GE.MITER) THEN
134          WRITE(IOCODE,3000)NITER,TOL,DMAX
135          PRINT 3000,NITER,TOL,DMAX
136          PRINT*, '*****'
137      &*****'
138          PRINT*
139          PRINT*
140          RETURN
141      ENDIF
142      C
143      NITER=NITER+1
144      DMAX=0.D0
145      C
146      DO 20 K=1,NZ
147      DO 20 J=1,NY
148      C
149      C-----
150      C      SOLVE TRIDIAGONAL SYSTEM FOR BLOCK (J,K)
151      C-----
152      DO 15 I=1,NX
153      IP=(K-1)*NXNY+(J-1)*NX+I
154      UM(I)=P(IP)
155      AZL(I)=A(IP)
156      DZL(I)=D(IP)
157      BZL(I)=B(IP)
158      CIP=0.D0
159      IF(IP.GT.1)CIP=B(IP-1)
160      CZL(I)=CIP
161      IF(NY.EQ.1) GO TO 14
162      JM=J-1
163      JP=J+1
164      IF(J.EQ.1) JM=1
165      IF(J.EQ.NY) JP=NY
166      IPM=(K-1)*NXNY+(JM-1)*NX+I
167      IPP=(K-1)*NXNY+(JP-1)*NX+I
168      GIP=0.D0
169      IF(IP.GT.NX)GIP=F(IP-NX)
170      DZL(I)=DZL(I)-GIP*P(IPM)-F(IP)*P(IPP)
171      14 IF(NZ.EQ.1) GO TO 15
172      KM=K-1
173      KP=K+1
174      IF(K.EQ.1) KM=1
175      IF(K.EQ.NZ) KP=NZ
176      IPM=(KM-1)*NXNY+(J-1)*NX+I
177      IPP=(KP-1)*NXNY+(J-1)*NX+I
178      ZIP=0.D0
179      IF(IP.GT.NXNY) ZIP=S(IP-NXNY)
180      DZL(I)=DZL(I)-ZIP*P(IPM)-S(IP)*P(IPP)
181      15 CONTINUE
182      C
183      C-----
184      C      CALL TRIDIAGONAL SYSTEM SOLVER
185      C-----
186      CALL THOMAS(AZL,BZL,CZL,DZL,UZL,NX)
187      C
188      C-----
189      C      UPDATE SOLUTION
190      C-----
191      DO 16 I=1,NX
192      GZLSOR=UZL(I)
193      IPX=(K-1)*NXNY+(J-1)*NX+I
194      P(IPX)=TW*UM(I)+OMEGA*GZLSOR
195      ARG=P(IPX)-UM(I)
196      DM=ABS(ARG)

```

```

197      IF(DM.GT.DMAX) DMAX=DM
198      16  CONTINUE
199      C
200      20  CONTINUE
201      C
202      C-----
203      C      UPDATE ACCELERATION PARAMETER OMEGA
204      C-----
205      IF(TOL1.EQ.0.D0) GO TO 25
206      THETA=DMAX/DMAX0
207      DELTA=THETA-THETA0
208      ARG=DELTA
209      ARG=ABS(ARG)
210      IF(ARG.GT.TOL1) GO TO 25
211      OM=OMEGA-1.D0
212      RHO1=(THETA+OM) * (THETA+OM) / (THETA*OMEGA*OMEGA)
213      IF(RHO1.GE.1.D0) GO TO 25
214      ARG=1.D0-RHO1
215      OMEGA=2.D0 / (1.D0+SQRT(ARG))
216      IF(NITER.GE.MFLAG) OMEGA=0.5D0
217      C
218      C-----
219      C      TEST FOR CONVERGENCE
220      C-----
221      25  IF(DMAX.GT.TOL) GO TO 11
222      IF(IDEBUG.NE.1) GO TO 300
223      WRITE(IICODE,4000)NITER,OMEGA,DMAX,THETA,RHO1
224      PRINT*, '      Flow Field Solved!!!'
225      PRINT*
226      300  CONTINUE
227      ICON=1
228      C
229      C      COUNTER : NUMBER OF FLOW FIELD SOLUTION
230      SNSIM=SNSIM+1
231      C
232      4000 FORMAT(T5,'CONVERGENCE (LSOR) REACHED AFTER ',I4,
233      + ' ITERATIONS',5X,'OMEGA = ',F6.3/
234      +T5,'DMAX = ',F10.6,5X,'THETA = ',F10.6,5X,'RHO1 = ',F10.6/)
235      3000 FORMAT(T15,'Convergence (LSOR) was NOT reached IN',I5,
236      + ' ITERATIONS'/T15,'TOL= ',F10.7,10X,'DMAX = ',F15.7)
237      C
238      RETURN
239      END
240      C
241      C
242      C*****
243      SUBROUTINE THOMAS(A,B,C,D,X,N)
244      C*****
245      C
246      IMPLICIT DOUBLE PRECISION (A-H,O-Z)
247      DOUBLE PRECISION A(1),B(1),C(1),D(1),X(1),Q(500),G(500)
248      C
249      WI=A(1)
250      G(1)=D(1)/WI
251      DO 10 I=2,N
252      Q(I-1)=B(I-1)/WI
253      WI=A(I)-C(I)*Q(I-1)
254      G(I)=(D(I)-C(I)*G(I-1))/WI
255      10  CONTINUE
256      X(N)=G(N)
257      DO 20 I=2,N
258      J=N-I+1
259      X(J)=G(J)-Q(J)*X(J+1)
260      20  CONTINUE
261      RETURN
262      END
263

```

## A-4 Flow Numerical Solution and STUBA Subroutine

(A.Mantoglou, personal communication)

```
1 C*****
2 C-   TURNING BANDS FIELD GENERATOR
3 C*****
4 C
5 C   SUBROUTINE TUBA (NXDIM, NYDIM, DXX, DYY, FKM, FKV, CRL, TUBARK)
6 C-----
7 C
8 C   Main program module for TUBA, Version 2.11d
9 C
10 C-----
11 C
12 C   INCLUDE FILE FOR TUBA VERSION 2.11d
13 C
14 C   COMMON /TBAPAR/ ICOVF, IPAA, LINES, FMAX, NHAR, NMAX, UN, FX, FY,
15 C
16 C   1 XO, YO, TBMX, KS, IP, NX, NY, XMAX, YMAX, DX, DY, NXY, AM, AN, AV, CLX, CLY,
17 C
18 C   1 IDFP, IURN, DS, UD, KD, NR, CK, FM, FA, A1, A3, A5, KT, DT, SG, B0, B1, B2,
19 C
20 C   1 NF, IPF, SAJ, IULP, MSK, IMSEX
21 C
22 C-----
23 C
24 C   LOGICAL UNIT IDENTIFIERS
25 C
26 C   IN = standard input - terminal ( generally, this will be unit 5 )
27 C
28 C   IT = standard output - terminal ( generally, this will be unit 6 )
29 C
30 C   IL = listing file unit
31 C
32 C   IO = output data unit
33 C
34 C   L1 = used for reading (x,y) points, mask file data, then for storing
35 C
36 C   the (x,y) generation points in direct access file for gridded fields
37 C
38 C   L2 = used for areal average processes - stores line process data for
39 C
40 C   each line in direct access file (to reduce memory requirements)
41 C
42 C-----
43 C
44 C   PARAMETER (IN=5, IT=6, IL=77, IO=20, L1=21, L2=22, LGTH=1000000)
45 C   COMPLEX C (LGTH/2)
46 C   DOUBLE PRECISION TUBARK (1000000), DXX, DYY, FKM, FKV, CRL
47 C   REAL A (LGTH), TBKK (1000000)
48 C   INTEGER XDIM, YDIM
49 C   EQUIVALENCE (A, C)
50 C   INCLUDE 'tuba211d.inc'
51 C   COMMON /KFIELD/ TBKK
52 C   COMMON /PGPARS/ PCL, IPG
53 C   COMMON /ADRSES/ LXI, LPP, LPA, LZ1, LZZ, LZM, LSS, LCC, LFF, LTT, LDZ,
54 C   1 LS1, LS2, LC1, LC2
55 C
56 C   XMAX=DXX*NXDIM
57 C   YMAX=DYY*NYDIM
58 C   NX=NXDIM
```

```

59      NY=NYDIM
60      AM=FKM
61      AN=0.0
62      AV=FKV*FKV
63      CLX=CRL
64      CLY=CRL
65
66      KS=2
67      IP=2
68      LINES=160
69  C
70  C      READ INPUT AND OUTPUT PARAMETERS
71  C      CALL RDINPT (IN, IT, IL, L1, A(1), A(1), MODEL, NLINE, NSIM)
72  C
73  C      CALCULATE INTERNAL PARAMETERS
74  C      CALL INTPAR (A(1))
75  C
76  C      CREATE THE <NAME>.INP CARD FILE
77  C      CALL LSTINP (IL)
78  C
79  C      CALCULATE "ADDRESSES" OF ARRAY POINTERS
80  C      CALL ADDRES (IT, IL, LGTH)
81  C
82  C      CALCULATE (X,Y) POINT PROJECTIONS ONTO THE TBM LINES
83  C      CALL CALXYP (IT, L1, A(LXY), A(LZM), A(LSS), A(LCC), A(LPP))
84  C
85  C      CALCULATION OF LINE PROCESS ARRAY DATA
86  C      CALL CALINP (IT, L2, A(LPA), A(LSS), A(LCC), A(LS1), A(LC1), A(LFF))
87  C
88  C      BEGIN SIMULATING THE RANDOM FIELD(S)
89  C      DO 20 ISIM=1, NSIM
90  C          WRITE (IT, *)
91  C          IF (NSIM.GT.1) CALL PROGSS (' SIMULATION NUMBER ...',
92  C          1              IT, ISIM, NSIM, 5)
93  C          PCLSAV = PCL
94  C          IPGSAV = IPG
95  C          CALL RESEED (ISIM, NUSEED)
96  C          DO 10 L=1, NLINE
97  C              IF (MODEL.LE.3) CALL SPCTRL (L, L2, A(LPA), A(LZ1), C(LDZ/2+1),
98  C              1              A(LS1), A(LC1), A(LS2), A(LC2))
99  C              IF (MODEL.EQ.4) CALL MOVAVG (A(LTT), A(LZ1), A(LFF))
100  C              IF (MODEL.EQ.5) CALL WNRLVY (A(LZ1))
101  C              CALL PROJCT (L, IT, L1, A(LXY), A(LPP), A(LSS), A(LCC), A(LZZ),
102  C              1              A(LZM), A(LZ1))
103  C          10 CONTINUE
104  C          CALL OUTPUT (IT, IL, IO, ISIM, NSIM, A(LXY), A(LZZ), A(LZM), NUSEED)
105  C          PCL = PCLSAV
106  C          20 CONTINUE
107  C
108  C          OPEN (34, FILE='TBKK.TXT', STATUS='UNKNOWN')
109  C          DO 30 J=1, NY
110  C              DO 30 I=1, NX
111  C                  IP=(J-1)*NX+I
112  C                  TUBARK(IP)=TBKK(IP)
113  C          30 CONTINUE
114  C
115  C          CLOSE (77)
116  C
117  C          RETURN
118  C          END
119  C
120  C
121  C      BLOCK DATA
122  C-----
123  C-
124  C      INITIALIZE DATA FOR VARIABLES IN LABELED COMMON STATEMENTS
125  C
126  C      INCLUDE 'tuba211d.inc'

```

```

127 C
128 Comt COMMON /SEEDS/ needed by URNITMB
129 COMMON /SEEDS/ ML,MM,MK,L,M,K
130 C
131 Comt COMMON /ADRSES/ needed by ADDRES, MAIN
132 COMMON /ADRSES/LXY,LPP,LPA,LZ1,LZZ,LZM,LSS,LCC,LFF,LTT,LDZ,
133 1 LS1,LS2,LC1,LC2
134 C
135 Comt COMMON /IRSGRD/ needed by DEFPAR, FLDPAR
136 COMMON /IRSGRD/ GXMIN,GYMIN
137 C
138 Comt DATA L, M, K and ML, MM, MK needed by URNITMB
139 DATA L, M, K /089347405, 301467177, 240420681/
140 DATA ML,MM,MK /65539, 33554433, 36243609/
141 C
142 Comt DATA LS1,LS2 ... needed by ADRSES
143 DATA LS1,LS2,LC1,LC2 /1,1,1,1/, MSK /0/
144 C
145 Comt DATA FM,FA,AM .. needed by INTPAR
146 DATA FM,FA,AM,AN,AV,CLX,CLY /1.0, 0.0, 0.0, 0.0, 1.0, 1.0, 1.0/
147 C
148 Comt DATA GXMIN,GYMIN needed by FLDPAR
149 DATA GXMIN,GYMIN /1.E+15,1.E+15/
150 C
151 END
152 C
153 C
154 SUBROUTINE ADDRES(IT,IL,LGTH)
155 -----
156 -
157 C CALCULATE ADDRESSES OF ARRAY POINTERS
158 C
159 C LXY,LPP,LPA, ETC. ARE THE "ADDRESSES" OF THE XY,PP,PA ARRAYS IN
160 C THE ONE DIMENSIONAL ARRAY A. IF SIMULATING AT ARBITRARY (X,Y)
161 C LOCATIONS (KS=1), THESE COORDINATES (NXY OF THEM) ARE STORED
162 C AT THE BEGINNING OF ARRAY A. IF A MASK FILE IS USED, IT IS ALSO
163 C (MUTUALLY EXCLUSIVE OPTIONS) STORED AT THE BEGINNING OF ARRAY A.
164 C
165 INCLUDE 'tuba211d.inc'
166 CHARACTER BITES*10
167 COMMON /ADRSES/LXY,LPP,LPA,LZ1,LZZ,LZM,LSS,LCC,LFF,LTT,LDZ,
168 1 LS1,LS2,LC1,LC2
169 Comt SEE BLOCK DATA MODULE
170 Comt DATA LS1,LS2,LC1,LC2 /1,1,1,1/
171 C
172 IGS = 0
173 KSS = MIN(2,KS)
174 IF(KS.GT.1) NXY = NX*NY
175 IF(KS.EQ.3) IGS = NX+NY
176 LXY = 1
177 LZM = 1 + IGS
178 LPP = (2-KSS)*(2*NXY) + 1 + MIN(MSK,1)*NXY + IGS
179 LPA = LPP + 2*(KSS-1)*NX
180 LZ1 = LPA + NHAR
181 LZZ = LZ1 + MAX(NMAX,NHAR)
182 LSS = LZZ + NXY
183 LCC = LSS + LINES
184 LFF = LCC + LINES
185 LTT = LFF + KD
186 LDZ = LTT + NR
187 LRQ = LDZ + 2*NHAR
188 C
189 C THESE ARRAYS ARE FOR SHINOZUKA AND JAN METHOD
190 IF(ICOVF.LE.3 .AND. ISAJ.EQ.1) THEN
191 LS1 = LTT + NR
192 LC1 = LS1 + NHAR
193 LS2 = LC1 + NHAR
194 LC2 = LS2 + NHAR

```

```

195      LRQ = LC2 + NHAR
196      END IF
197  C
198  C  DIRECT ACCESS FILES USE AN ADDITIONAL 8 BYTES PER RECORD
199  C  BXY = BYTES FOR (X,Y) DATA; BAA = BYTES FOR AREAL AVERAGE DATA
200  BXY = ( 4*(2*NXY) + 8*NY )
201  BAA = ( 4*NHAR*LINES + 8*LINES ) * (IPAA-1)
202  FDS = ( BXY + BAA ) * 1.E-06
203  BITES = ' Megabytes'
204  IF(FDS.LT.1) THEN
205      BITES = ' Kilobytes'
206      FDS = 1000 * FDS
207  END IF
208  C  WRITE(IT,10) LGTH,LRQ, LGTH-LRQ, FDS, BITES
209  WRITE(IL,10) LGTH,LRQ, LGTH-LRQ, FDS, BITES
210  10  FORMAT(/' Number Of Elements Allocated In A Array =',I9,
211  1  /' Total Storage Required For Computations =',I9,
212  1  /' No Of Elements In Excess of Requirements =',I9,/' Free',
213  1  ' Disk Space Needed For Computations =',F9.3,A,/)
214  C
215  IF(LRQ.LT.0 .AND. IDFP.EQ.2) WRITE(IT,15)
216  15  FORMAT(' ***** err, integer overflow - you may be specifying',
217  1  /' the Turning Band line parameters improperly.',
218  2  /' Recheck Turning Band parameter input values')
219  C
220  C  The following should NEVER occur
221  IF(LRQ.LT.0 .AND. IDFP.EQ.1) WRITE(IT,16)
222  16  FORMAT(' ***** err, integer overflow - contact code author',
223  1  /' send email message to: dazimme@somnet.sandia.gov')
224  C
225  IF(LRQ.GT.LGTH) WRITE(IT,20)
226  20  FORMAT(' ***** err, Insufficient Storage (Dimension of A Array)',
227  1  /' Increase Parameter LGTH in main program')
228  C
229  IF(LRQ.GT.LGTH) STOP
230  C
231  RETURN
232  END
233  C
234  C
235  SUBROUTINE CALINP(IT,L2,PA,SS,CC,S1,C1,FF)
236  -----
237  --
238  C  CALCULATION OF ARRAY DATA NEEDED FOR LINE PROCESS GENERATION
239  C
240  REAL PA(*), SS(*), CC(*), S1(*), C1(*), FF(*)
241  INCLUDE 'tuba211d.inc'
242  COMMON /PGPARS/ PCL,IPG
243  CHARACTER LPMA*47,LPSM*43,LPTB*43,LPSP*47
244  DATA LPMA /' Calculating Line Process Data ... (MA Process)'/
245  DATA LPSM /' Calculating Line Process Data ... Harmonic'/
246  DATA LPTB /' Calculating Line Process Data ... Line No'/
247  DATA LPSP /' Calculating Line Process Data ... ( Spectral )'/
248
249  C  NO ARRAY DATA NEEDED FOR NON-STATIONARY GENERALIZED COVARIANCE MODELS
250  C  GC MODEL LINE PROCESS PARAMETERS CALCULATED IN SUBROUTINE INTPAR
251  IF(ICOVF.EQ.5) RETURN
252  Comt WRITE(IT,*) 'Calculating Line Process Data ... (GC Models)'
253
254  C  MOVING AVERAGE GENERATION OF THE LINE PROCESS
255  IF(IULP.EQ.2) THEN
256  C  USER-DEFINED MOVING AVERAGE ALGORITHM GOES HERE
257  C  THE FF ARRAY CONTAINS THE MOVING AVERAGE WEIGHTS
258  C  SEE SECTIONS 2.4 AND 5.4 OF THE USER'S MANUAL
259  Comt WRITE(IT,*) ' Calculating Line Process Data ... (MA Process)'
260  IF(IPF.GE.2) WRITE(IT,'(A)') LPMA
261  CK = 1.0
262  RETURN

```

```

263      END IF
264
265 C      MOVING AVERAGE GENERATION OF THE LINE PROCESS (TELIS COVARIANCE)
266      IF(ICOVF.EQ.4) THEN
267 Comt   WRITE(IT,*)' Calculating Line Process Data ... (MA Process) '
268       IF(IPF.GE.2) WRITE(IT,'(A)') LPMA
269       DO 10 K=1,KD
270         XT = DS*FLOAT(K-1)
271         FF(K) = (1.-XT)*EXP(-XT)
272 10      CONTINUE
273         CX = 1.-EXP(-2.*DS)
274         CK = SQRT(12.*CX*CX/(CX-DS*EXP(-2.*DS)))
275         RETURN
276      END IF
277
278 C      SPECTRAL GENERATION OF THE LINE PROCESS (SAJ AND FFT METHODS)
279      AX = FX/CLX
280      AY = FY/CLY
281      DOM = FMAX/FLOAT(NHAR)
282      DLM = 0.1*DOM
283 C      IF(IPF.EQ.1) WRITE(IT,'(A)') LPSP
284      IF(IPAA.EQ.2) GO TO 33
285
286 C      line generation for POINT processes ...
287      DO 20 M=1,NHAR
288 Comt   CALL PROGSS(' Calculating Line Process Data ... Harmonic',
289       IF(IPF.GE.2) CALL PROGSS(LPSM,IT,M,NHAR,20)
290       OM = (FLOAT(M)-0.5)*DOM
291       SPEC = SPDF(OM,ICOVF)*DOM
292 C      This if block pertains only to the Shinozuka and Jan method
293       IF(ISAJ.EQ.1) THEN
294         OMM = OM + URN55()*DLM
295         C1(M) = COS(OMM*UN)
296         S1(M) = SIN(OMM*UN)
297         SPEC = 2.0*SQRT(SPEC)
298       END IF
299       PA(M) = SPEC
300 20     CONTINUE
301       RETURN
302
303 C      line generation for AREAL AVERAGE processes ...
304 33     LREC = 4*NHAR
305       OPEN(UNIT=L2,STATUS='SCRATCH',ACCESS='DIRECT',RECL=LREC,
306 1      FORM='UNFORMATTED')
307       DO 40 L=1,LINES
308         IF(IPF.GE.2) CALL PROGSS(LPTB,IT,L,LINES,10)
309 C         IF(IPF.EQ.2) CALL PROGSS(LPTB,IT,L,LINES,10)
310 comt   IF(IPF.EQ.3) CALL PROGSS(' Turning Band Line ...',IT,L,LINES,10)
311 comt   PCLSAV = PCL
312 comt   IPGSAV = IPG
313       DO 30 M=1,NHAR
314 Comt   CALL PROGSS(' Calculating Line Process Data ... Harmonic',
315 comt   IF(IPF*IPGSAV.EQ.3) CALL PROGSS(LPSM,IT,M,NHAR,20)
316       OM = (FLOAT(M)-0.5)*DOM
317       SPEC = SPDF(OM,ICOVF)*DOM
318 C      This if block pertains only to the Shinozuka and Jan method
319       IF(ISAJ.EQ.1) THEN
320         OMM = OM + URN55()*DLM
321         C1(M) = COS(OMM*UN)
322         S1(M) = SIN(OMM*UN)
323         SPEC = 2.0*SQRT(SPEC)
324       END IF
325       AC = CC(L)
326       AS = SS(L)
327       IF(ICOVF.EQ.0) AASD = WTUSR(OM,AC,AS,AX,AY)*SPEC
328       IF(ICOVF.EQ.1) AASD = WTEXP(OM,AC,AS,AX,AY)*SPEC
329       IF(ISAJ.EQ.1) AASD = 2.*SQRT(AASD)
330       PA(M) = AASD

```

```

331 30      CONTINUE
332      WRITE (UNIT=L2,REC=L) (PA(M),M=1,NHAR)
333 comt    PCL = PCLSAV
334 40      CONTINUE
335
336      RETURN
337      END
338
339
340
341      SUBROUTINE CALXYC(K,GS,X,Y)
342 C-----
343 --
344 C      CALCULATE (x,y) COORDINATES FOR GRIDDED OUTPUT
345
346      REAL    GS(*)
347      INCLUDE 'tuba211d.inc'
348
349 C      KS = 1  OUTPUT AT SPECIFIED (X,Y) LOCATIONS
350 C      KS = 2  OUTPUT ONTO A BLOCK OR POINT CENTERED REGULARLY SPACED GRID
351 C      KS = 3  OUTPUT ONTO A BLOCK OR POINT CENTERED IRREGULARLY SPACED GRID
352 C      IP = 1  POINT CENTERED GRID,   IP = 2  BLOCK CENTERED GRID
353
354 C      DECODE I AND J INDICES FROM SINGLE INDEX REFERENCE
355      J = K/NX + 1
356      IF(MOD(K,NX).EQ.0) J = J - 1
357      I = K - (J-1)*NX
358      V = 1.0/FLOAT(IP)
359      IF(KS.EQ.2) X = (I-V)*DX
360      IF(KS.EQ.2) Y = (J-V)*DY
361      IF(KS.EQ.3) THEN
362          X = 0
363          Y = 0
364      DO 10 II=1,I-1
365 10      X = X + GS(II)
366          X = X + (1-V)*GS(I)
367      DO 20 JJ=1,J-1
368 20      Y = Y + GS(NX+JJ)
369          Y = Y + (1-V)*GS(NX+J)
370      END IF
371
372      RETURN
373      END
374
375
376
377      SUBROUTINE CALXYP(IT,IU,GS,ZM,SS,CC,PP)
378 C-----
379 --
380 C      CALCULATE (X,Y) POINT PROJECTIONS ONTO THE TBM LINES
381
382      PARAMETER (PI=3.1415926)
383      REAL    CC(*), SS(*), GS(*), ZM(*), PP(2,*)
384      INCLUDE 'tuba211d.inc'
385      CHARACTER PPCS*43
386      DATA    PPCS /' Calculating Projection Points ... Point No'/
387
388 C      CALCULATE SINES AND COSINES OF TBM LINE ANGLES
389      DTHA = PI/FLOAT(LINES)
390      TNOT = URN55() * 2.0*PI
391      DO 10 L=1,LINES
392          THETA = FLOAT(L)*DTHA + TNOT
393          CC(L) = COS(THETA)
394          SS(L) = SIN(THETA)
395 10      CONTINUE
396
397 C      NORMALIZED PROJECTON POINTS FOR KS=1 OBTAINED IN SUBROUTINE PROJCT
398      IF(KS.EQ.1) THEN

```

```

399      WRITE(IT,*)'Projection Points Not Calculated -> Read as Input'
400      WRITE(IT,*)'Projection Points = (x,y) Field Generation Points'
401      IF(IULP.EQ.2 .OR. ICOVF.GE.4) WRITE(IT,*)
402      RETURN
403  END IF
404
405  C      CALCULATE AND STORE THE NORMALIZED (X,Y) PROJECTION POINTS FOR GRIDS
406      LREC = 2*(4*NX)
407      OPEN(UNIT=IU,STATUS='SCRATCH',ACCESS='DIRECT',RECL=LREC,
408      1  FORM='UNFORMATTED')
409  C      IF(IPF.EQ.1) WRITE(IT,*)'Calculating Projection Points ...'
410      DO 40 I=1,NY
411          DO 30 J=1,NX
412              K = (I-1)*NX + J
413  Comt      CALL PROGSS(' Calculating Projection Points ... Point No',
414                  IF(IPF.EQ.2) CALL PROGSS(PPCS,IT,K,NXY,20)
415                  IF(IPF.EQ.3) CALL PROGSS(PPCS,IT,K,NXY, 5)
416                  IF(MSK.GT.0 .AND. ZM(K).EQ.0) GO TO 30
417                  CALL CALXYC(K,GS,X,Y)
418                  PP(1,J) = X
419                  PP(2,J) = Y
420      30      CONTINUE
421      WRITE(UNIT=IU,REC=I) ((PP(K,J),K=1,2),J=1,NX)
422  40      CONTINUE
423  C      WRITE(IT,*)
424
425      RETURN
426  END
427
428
429
430      SUBROUTINE COMENT(ID,CMT,NC)
431  C-----
432  --
433  C      RETURN COMMENT FOR THE <NAME>.INP FILE
434
435  C      TUBA CREATES A CARD FILE "ON THE FLY" (ie. WHILE IT IS BEING RUN
436  C      INTERACTIVELY). THE CARD FILE PROVIDES A RECORD OF WHAT OPTIONS AND
437  C      PARAMETERS WERE USED AND LISTS THE SAMPLE STATISTICS OF EACH OUTPUT
438  C      FIELD. THE CARD FILE CAN ALSO BE USED FOR BATCH PROCESSING.
439
440      CHARACTER COMTS(37)*42, CMT*(*)
441      INTEGER NCHRS(37)
442      DATA COMTS( 1) /'1=(x,y) Locations, 2=Even Grid, 3=Uneven  '/
443      DATA COMTS( 2) /'Input Filename for (x,y) Locations      '/
444      DATA COMTS( 3) /'1=Point Centered, 2=Block Centered      '/
445      DATA COMTS( 4) /'Maximum X and Y Field Dimensions        '/
446      DATA COMTS( 5) /'Number of Nodes-X and Nodes-Y          '/
447      DATA COMTS( 6) /'1=Normal, 2=exp(X), 3=10**(X)           '/
448      DATA COMTS( 7) /'0=User,1=Exp,2=Gauss,3=Besl,4=Telis,5=GC  '/
449      DATA COMTS( 8) /'1=Point Process, 2=Areal Average Process '/
450      DATA COMTS( 9) /'X and Y Dimensions of Averaging Area    '/
451      DATA COMTS(10) /'Desired Mean, Nugget and Sill            '/
452      DATA COMTS(11) /'X and Y Direction Correlation Lengths   '/
453      DATA COMTS(12) /'Generalized Covariance Model Coefficients '/
454      DATA COMTS(13) /'Line Process by: 1=Spectral, 2=Moving Avg '/
455      DATA COMTS(14) /'1=Default TBM Parameters, 2=Enter Manually'/
456      DATA COMTS(15) /'Number of Turning Band Lines            '/
457      DATA COMTS(16) /'TBM Line Discretization Distance        '/
458      DATA COMTS(17) /'Nbr of Harmonics for Discretizing Spectrum'/
459      DATA COMTS(18) /'Max Frequency for Truncation of Spectrum '/
460      DATA COMTS(19) /'Discretization Distance for MA Process  '/
461      DATA COMTS(20) /'Discretization Distance for Weiner Process'/
462      DATA COMTS(21) /'Field ORIGIN Relative to TBM Origin     '/
463      DATA COMTS(22) /'Output Data Filename                    '/
464      DATA COMTS(23) /'1=Output Only Z, 2=Output X,Y, and Z    '/
465      DATA COMTS(24) /'1=Unformatted, 2=Formatted Output      '/
466      DATA COMTS(25) /'Output Format for Writing Data to Disk  '/

```

```

467      DATA COMTS(26) /'1=Single Write Statement, 2=Line at a Time'/
468      DATA COMTS(27) /'1=First Row to Last, 2=Last Row to First  '/
469      DATA COMTS(28) /'1=Marsaglia URNG, 2=Machine Indep URNG  '/
470      DATA COMTS(29) /'Seed(s) for Random Number Generator  '/
471      DATA COMTS(30) /'Number of Realizations to be Simulated  '/
472      DATA COMTS(31) /'Maximum Turning Band Line Length  '/
473      DATA COMTS(32) /'Mask Filename  '/
474      DATA COMTS(33) /'Input Filename for grid-block widths  '/
475      DATA COMTS(34) /'1=Single file output, 2=Multiple files  '/
476      DATA COMTS(35) /'1=Minimal, 2=Med, 3=Frequent screen output'/
477      DATA COMTS(36) /'0=do not scale, 1=match T-stats exactly  '/
478      DATA COMTS(37) /'Mean, Nugget, Sill for Gen Cov Model  '/
479
480      DATA NCHRS / 40, 34, 35, 32, 29, 29, 40, 40, 36, 29, 37,
481      1 41, 41, 42, 28, 32, 42, 40, 38, 42, 35, 20,
482      1 36, 33, 38, 42, 40, 38, 35, 38, 32, 13, 36,
483      1 38, 42, 39, 36/
484
485      CMT = COMTS(ID)
486      NC = NCHRS(ID)
487
488      RETURN
489      END
490
491
492
493      SUBROUTINE COVPAR(IN, IT, IL, MODEL)
494      C-----
495      --
496      C QUERY FOR COVARIANCE PARAMETERS OF THE RANDOM FIELD
497
498      INCLUDE 'tuba211d.inc'
499
500      C WRITE(IT,10)
501      C 10 FORMAT(//' ++++++ COVARIANCE PARAMETERS ++++++')
502
503      C WRITE(IT,*) 'Select Type Of Covariance Model:'
504      C WRITE(IT,*) '(0) - User Specified'
505      C WRITE(IT,*) '(1) - Exponential Model'
506      C WRITE(IT,*) '(2) - Gaussian Covariance'
507      C WRITE(IT,*) '(3) - Bessel Type Covariance'
508      C WRITE(IT,*) '(4) - Telis Covariance Function'
509      C WRITE(IT,*) '(5) - Generalized Covariance Model'
510      C WRITE(IT,*)
511      C CALL RDINTG(IN,IT,IL,ICOVF,1,7)
512      ICOVF=2
513      MODEL = ICOVF
514
515      IPAA = 1
516      C AREAL AVERAGE PROCESS DATA FOR USER DEFINED OR EXPONENTIAL MODELS
517      IF(ICOVF.LE.1) THEN
518          WRITE(IT,*) '(1) - Point Process'
519          WRITE(IT,*) '(2) - Areal Average Process'
520          WRITE(IT,*)
521          CALL RDINTG(IN,IT,IL,IPAA,1,8)
522          IF(IPAA.EQ.2) THEN
523              WRITE(IT,*) 'Enter X And Y Dimensions Of Averaging Rectangle'
524              WRITE(IT,*)
525              CALL RDREAL(IN,IT,IL,FX,2,9)
526          END IF
527      END IF
528
529      IF(ICOVF.EQ.5) THEN
530          WRITE(IT,*) 'Enter Gen. Covariance Parameters A1,A3,A5'
531          WRITE(IT,*) ' K(r) = A1*r + A3*r**3 + A5*r**5'
532          WRITE(IT,*) '( A1,A5.GE.0, A3.GE.-(10/3)*SQRT(A1*A5) ) '
533          WRITE(IT,*)
534          CALL RDREAL(IN,IT,IL,A1,3,12)

```

```

535      RETURN
536      END IF
537
538 C      WRITE(IT,*) 'Enter Mean And Variance Parameters: If You Will Have'
539 C      WRITE(IT,*) 'The Field(s) Exponentiated, Enter The Desired Mean &'
540 C      WRITE(IT,*) 'Variance BEFORE Exponentiation (Variance=Nugget+Sill)'
541 C      WRITE(IT,*)
542 C      WRITE(IT,*) 'Enter The Mean, Nugget And Sill For Covariance Model'
543 C      WRITE(IT,*)
544 C      CALL RDREAL(IN,IT,IL,AM,3,10)
545      IF(AN.LT.0 .OR. AV.LT.0) THEN
546          STOP '***** ERR, nugget and sill must be > or = 0'
547      END IF
548
549 C      WRITE(IT,*) 'Enter The X and Y Direction Correlation Lengths'
550 C      WRITE(IT,*) ' ( Make These Equal For Isotropic Fields )'
551 C      WRITE(IT,*)
552 C      CALL RDREAL(IN,IT,IL,CLX,2,11)
553
554      RETURN
555      END
556 C
557 C
558      SUBROUTINE DEFPPAR(NLINE,XY)
559 C-----
560 --
561 C      CALCULATE DEFAULT TURNING BAND PARAMETERS
562
563      PARAMETER (PI=3.141592654D0)
564      REAL      DLK(4),XY(*)
565      INTEGER   NHR(4)
566      INCLUDE 'tuba211d.inc'
567      COMMON /IRSGRD/ GXMIN,GYMIN
568
569      DATA      NHR /2048, 1024, 4096, 0 /
570      DATA      DLK /0.05, 0.10, 0.025, 0./
571
572 C      CALCULATE DEFAULT TBM ORIGIN AND MAXIMUM TBM LINE LENGTH
573      CALL ORGMAX(XY)
574
575 C      SET DEFAULT NUMBER OF TBM LINES (BOTH NEEDED BECAUSE OF COMMON)
576 C      THERE IS NO LONGER A "DEFAULT" NUMBER OF TBM LINES ...
577 Comt LINES = 16
578 Comt NLINE = 16
579
580 C      SPECTRAL AND MOVING AVERAGE METHOD LINE PARAMETERS
581      IF(ICOVF.LE.4) THEN
582          ISAJ = 0
583          NHAR = NHR(ICOVF)
584          UN = 0.0625
585          DS = 0.05*AMIN1(CLX,CLY)
586      END IF
587
588 C      BLOCK OR CELL SPACING FOR GRIDDED OUTPUT
589      IF(KS.EQ.2) THEN
590          K = 2 - IP
591          DX = XMAX / MAX(NX-K,1)
592          DY = YMAX / MAX(NY-K,1)
593      ELSE IF(KS.EQ.3) THEN
594          DX = GXMIN
595          DY = GYMIN
596      END IF
597
598 C      GENERALIZED COVARIANCE MODEL DEFAULT LINE DISCRETIZATION DISTANCE
599 C      DX,DY SET IN ORGMAX FOR THE CASE OF KS=1
600      IF(ICOVF.EQ.5) THEN
601          UN = AMIN1(DX,DY)
602          DT = 0.2*UN

```

```

603      END IF
604
605      C      UN = NORMALIZED LINE DISCRETIZATION DISTANCE = 2*PI/FMAX (FFT METHOD)
606      C      FOR STATIONARY MODELS, UN IS SET EQUAL TO 0.0625 (16 PTS/CORR LGTH)
607      C      IF(UN.GT.DX .OR. UN.GT.DY) THEN UN IS DECREASED APPROPRIATELY.
608      C      ALSO MAKE SURE MA PROCESS PARAMETER DS IS SMALL ENOUGH.
609      C      IF(KS.GT.1 .AND. ICOVF.LE.4) THEN
610          CM = AMAX1(C LX,CLY)
611          DC = AMIN1(C LX/16.,CLY/16.)
612          DN = AMIN1(.99*DX/CLX,.99*DY/CLY,DC/CM)
613          UN = AMIN1(UN,DN)
614          DS = AMIN1(DS,UN*AMIN1(C LX,CLY)/10)
615      C      END IF
616
617      C      IF THE SPECTRAL METHOD IS USED .AND. UN IS DECREASED, THEN THE
618      C      FREQUENCY SPACING DELK MAY BE GREATER THAN THE ALLOWABLE MAXIMUM
619      C      (SEE DLK IN DATA STATEMENT). WHEN THIS HAPPENS, NHAR IS INCREASED
620      C      (BY A FACTOR OF 2 FOR THE FFT) TO OBTAIN A SMALLER DELK.
621
622      C      FMAX = 2.*PI/UN
623      C      IF(UN.LT.0.0625 .AND. ICOVF.LE.3) THEN
624      16      IF(FMAX/FLOAT(NHAR) .GT.DLK(ICOVF)) THEN
625          NHAR = 2*NHAR
626          GO TO 16
627      C      END IF
628      C      END IF
629
630      C      RETURN
631      C      END
632
633
634
635      SUBROUTINE FFT(F,NPT,IFB)
636      C-----
637      --
638      C      ONE DIMENSIONAL FAST FOURIER TRANSFORM ROUTINE (FORWARD AND INVERSE)
639      C
640      C      THIS ROUTINE, MODIFIED BY D. A. (TONY) ZIMMERMAN AT NEW MEXICO TECH
641      C      AND VERIFIED WITH IMSL ROUTINES, WAS TAKEN FROM PAGE 108 OF:
642      C
643      C      RAFAEL .C GONZALEZ AND PAUL WINTZ, 1987.
644      C      ``DIGITAL IMAGE PROCESSING''
645      C      ADDISON-WESLEY PUBLISHING COMPANY
646      C
647      C      F = COMPLEX SEQUENCE TO BE TRANSFORMED (INPUT)
648      C      F = COMPLEX TRANSFORMED ARRAY ON OUTPUT
649      C      NPT = NUMBER POINTS IN F TO BE TRANSFORMED
650      C      IFB = -1 FOR FORWARD TRANSFORM ( EXP(-i*2PIux/NPT) )
651      C      IFB = +1 FOR INVERSE TRANSFORM ( EXP(+i*2PIux/NPT) )
652      C-----
653      --
654      C      NOTE: THE INPUT SEQUENCE MUST BE OF LENGTH EQUAL TO 2**N FOR SOME N
655      C-----
656      --
657      C      PARAMETER (PI=3.141592654D0)
658      C      COMPLEX F(*),U,W,T
659
660      C      IF(IFB.GT.0) THEN
661          DO 10 K=1,NPT
662      10      F(K) = CONJG(F(K))
663      C      END IF
664
665      C      LN = ALOG(FLOAT(NPT))/ALOG(2.0)
666      C      N = 2**LN
667      C      NV2 = N/2
668      C      NM1 = N-1
669
670      C      J = 1

```

```

671      DO 3 I=1,NM1
672          IF(I.GE.J) GO TO 1
673          T = F(J)
674          F(J) = F(I)
675          F(I) = T
676      1      K = NV2
677      2      IF(K.GE.J) GO TO 3
678          J = J-K
679          K = K/2
680          GO TO 2
681      3      J = J+K
682
683      DO 5 L=1, LN
684          LE = 2**L
685          LE1 = LE/2
686          U = CMPLX(1.0,0.0)
687          A = PI/LE1
688          W = CMPLX(COS(A),-SIN(A))
689          DO 5 J=1,LE1
690              DO 4 I=J,N,LE
691                  IP = I+LE1
692                  T = F(IP)*U
693                  F(IP) = F(I)-T
694      4                  F(I) = F(I)+T
695      5                  U = U*W
696
697          IF(IFB.GT.0) THEN
698              DO 20 K=1,NPT
699      20          F(K) = CONJG(F(K))
700          END IF
701
702          RETURN
703          END
704
705
706
707      SUBROUTINE FFTGEN(L,L2,PA,Z1,DZ)
708  C-----
709  --
710  C      GENERATION OF THE LINE PROCESS VIA FAST FOURIER TRANSFORM
711
712      REAL      PA(*),Z1(*)
713      COMPLEX   DZ(*),i
714      INCLUDE 'tuba211d.inc'
715
716  C      THE IMAGINARY PART YIELDS AN INDEPENDENT REALIZATION
717      IF(MOD(L,2).EQ.0) GO TO 30
718
719      i = (0.,1.)
720      IF(IPAA.EQ.2) READ(UNIT=L2,REC=L) (PA(M),M=1,NHAR)
721
722      DO 10 M=1,NHAR
723          DELF = PA(M)
724          SQDF = SQRT(6.*DELF)
725          A = SQDF * URN55()
726          B = SQDF * URN55()
727          DZ(M) = A - i*B
728  10      CONTINUE
729
730          CALL FFT(DZ,NHAR,-1)
731
732          DO 20 M=1,NHAR
733      20      Z1(M) = 2.0*REAL(DZ(M))
734
735          RETURN
736
737      DO 40 M=1,NHAR
738      40      Z1(M) = 2.0*AIMAG(DZ(M))

```

```

739
740      RETURN
741      END
742
743
744
745      SUBROUTINE FILPAR(IN, IT, IL)
746  C-----
747  --
748  C      QUERY FOR OUTPUT FILE PARAMETERS
749
750      CHARACTER          FMT*35, FNAM*35
751      INCLUDE 'tuba211d.inc'
752      COMMON /OTPTS1/ FMT, FNAM
753      COMMON /OTPTS2/ IFO, IMO, IRO, ILN
754
755  C      WRITE(IT, 5)
756  C 5      FORMAT(//' ++++++ OUTPUT FILE PARAMETERS ++++++')
757
758  C      WRITE(IT, *) 'Enter A Filename For The Output File(s) '
759  C      WRITE(IT, *)
760  C      CALL RDCHAR(IN, IT, IL, FNAM, 22)
761      FNAM='TUBA.TXT'
762
763      IF(KS.EQ.1) THEN
764          WRITE(IT, *) '(1) - Output Only The Field Values, Z'
765          WRITE(IT, *) '(2) - Output The (X,Y) Locations And Z'
766          WRITE(IT, *)
767          CALL RDINTG(IN, IT, IL, IOF, 1, 23)
768      END IF
769
770  C      WRITE(IT, *) '(1) - Unformatted Output '
771  C      WRITE(IT, *) '(2) - Formatted Output '
772  C      WRITE(IT, *)
773  C      CALL RDINTG(IN, IT, IL, IFM, 1, 24)
774      IFM=1
775
776      IF(IFM.EQ.2) THEN
777          IF(KS.EQ.1) WRITE(IT, 10) '(2F12.2,1PE12.5)''
778          IF(KS.GT.1) WRITE(IT, 10) '(10F12.5)''
779  10      FORMAT(' Enter Output Format, e.g., ', A)
780          WRITE(IT, *) '(include the parentheses) '
781          WRITE(IT, *)
782          CALL RDCHAR(IN, IT, IL, FMT, 25)
783      END IF
784
785      IF(KS.GT.1) THEN
786  C      WRITE(IT, *) '(1) - Write Out Matrix With One WRITE Statement '
787  C      WRITE(IT, *) '(2) - Write Out Matrix One Line (Row) At A Time '
788  C      WRITE(IT, *)
789  C      CALL RDINTG(IN, IT, IL, IMO, 1, 26)
790      IMO=2
791      IMO = 2 - IMO
792      IRO = 1
793      IF(IMO.EQ.0 .AND. IFM.EQ.2) THEN
794          WRITE(IT, *) ' Output the Rows of the Matrix via ... '
795          WRITE(IT, *) '(1) - First Row --> Last Row '
796          WRITE(IT, *) '(2) - Last Row --> First Row '
797          WRITE(IT, *)
798          CALL RDINTG(IN, IT, IL, IRO, 1, 27)
799      END IF
800      END IF
801
802  C      IOF AND IFO ARE PARAMETERS CONTROLLING OUTPUT FORMAT
803      KSS = MIN(KS, 2)
804      IOF = MAX(IOF*(2-KSS), 1)
805      IFO = IOF*2 - IFM + 1
806

```

```

807      RETURN
808      END
809
810
811
812
813      SUBROUTINE FLDPAR (IN, IT, IL, IU, XY, GS, ZM)
814      C-----
815      --
816      C      QUERY FOR OUTPUT FIELD PARAMETERS
817
818      CHARACTER      FMT*35, FNAM*35, DATAF*35, MASKF*35
819      REAL          XY (2, *), GS (*), ZM (*)
820      INCLUDE 'tuba211d.inc'
821      COMMON /IRSGRD/ GXMIN, GYMIN
822      COMMON /OTPTS1/ FMT, FNAM
823      COMMON /OTPTS2/ IFO, IMO, IRO, ILN
824
825      C      WRITE (IT, 5)
826      C 5      FORMAT (// ' ++++++ OUTPUT FIELD PARAMETERS ++++++' /)
827
828      C      WRITE (IT, *) ' (1) - Simulate Only At Specified (x,y) Locations '
829      C      WRITE (IT, *) ' (2) - Simulate Onto A Regularly Spaced Grid '
830      C      WRITE (IT, *) ' (3) - Simulate Onto An Unevenly Spaced Grid '
831      C      WRITE (IT, *)
832      C      CALL RDINTG (IN, IT, IL, KS, 1, 1)
833
834
835      IF (KS.EQ.1) THEN
836          WRITE (IT, *) 'Enter The Filename For Reading (X,Y) Locations '
837          WRITE (IT, *)
838          CALL RDCHAR (IN, IT, IL, DATAF, 2)
839          OPEN (UNIT=IU, FILE=DATAF, STATUS='OLD')
840          I = 0
841          10      I = I + 1
842          READ (IU, *, END=11) XY (1, I), XY (2, I)
843          GO TO 10
844          11      NXY = I-1
845          WRITE (IT, 20) NXY
846          20      FORMAT (' >>>> ', I8, ' Data Pairs Read' /)
847          CLOSE (UNIT=IU)
848      END IF
849
850      IF (KS.GT.1) THEN
851      C      WRITE (IT, *) ' (1) - Point Centered Grid '
852      C      WRITE (IT, *) ' (2) - Block Centered Grid '
853      C      WRITE (IT, *)
854      C      CALL RDINTG (IN, IT, IL, IP, 1, 3)
855
856
857      C      WRITE (IT, *) 'Enter The Maximum X And Y Field Dimensions '
858      C      WRITE (IT, *)
859      C      CALL RDREAL (IN, IT, IL, XMAX, 2, 4)
860
861      C      WRITE (IT, *) 'Enter The Number Of Nodes In The X And Y Directions '
862      C      WRITE (IT, *)
863      C      CALL RDINTG (IN, IT, IL, NX, 2, 5)
864
865      IF (KS.EQ.3) THEN
866          WRITE (IT, *) 'Enter The Filename For Reading Grid-Block Widths '
867          WRITE (IT, *)
868          CALL RDCHAR (IN, IT, IL, DATAF, 33)
869          OPEN (UNIT=IU, FILE=DATAF, STATUS='OLD')
870          READ (IU, *) (GS (I), I=1, NX-2+IP)
871          READ (IU, *) (GS (NX+I), I=1, NY-2+IP)
872          CLOSE (UNIT=IU)
873          DO 30 I=1, NX
874          30      IF (GS (I) .LT. GXMIN) GXMIN = GS (I)

```

```

875      DO 32 I=1,NY
876 32      IF(GS(NX+I).LT.GYMIN) GYMIN = GS(NX+I)
877      END IF
878
879 C      WRITE(IT,*)'Enter mask filename or type NONE or <cr>'
880 C      WRITE(IT,*)
881 C      CALL RDCHAR(IN,IT,IL,MASKF,32)
882 C      IF(MASKF.EQ.' ') MASKF = 'none'
883      MASKF = 'none'
884      NONE = INDEX(MASKF,'NONE') + INDEX(MASKF,'none')
885      IF(NONE.EQ.0) THEN
886          OPEN(UNIT=IU,FILE=MASKF,STATUS='OLD')
887          READ(IU,*) (ZM(I),I=1,NX*NY)
888          CLOSE(UNIT=IU)
889          DO 40 I=1,NX*NY
890 40      IF(ZM(I).NE.0) MSK = MSK + 1
891      END IF
892      END IF
893
894 C      WRITE(IT,*)'(1) - Generate a Field f(x) Whose pdf is Gaussian'
895 C      WRITE(IT,*)'(2) - Generate a Lognormal Field K(x) = exp(f(x))'
896 C      WRITE(IT,*)'(3) - Generate a Lognormal Field K(x) = 10**(f(x))'
897 C      WRITE(IT,*)
898 C      CALL RDINTG(IN,IT,IL,ILN,1,6)
899      ILN=1
900      RETURN
901      END
902
903
904
905      SUBROUTINE FSCALE(XY,ZZ,ZM,ILN,BAR,VAR,SSQ,PTS)
906 C-----
907 --
908 C      DO FINAL SCALING, ADD IN THE MEAN, NUGGET & CALCULATE MEAN AND
909 VARIANCE
910
911      REAL      ZZ(*), ZM(*), XY(2,*)
912      INCLUDE 'tuba211d.inc'
913
914      SUM = 0.0
915      SSQ = 0.0
916      HNUG = SQRT(3.0*AN)
917      SDEV = SQRT(AV)
918      SQLN = SQRT(FLOAT(LINES))
919      DO 10 K=1,NXY
920          IF(MSK.EQ.0 .OR. (MSK.GT.0 .AND. ZM(K).NE.0)) THEN
921              ZZ(K) = SDEV*ZZ(K)/SQLN
922              ZZ(K) = ZZ(K) + AM
923              IF(AN.GT.0) ZZ(K) = ZZ(K) + URNAB(-HNUG,+HNUG)
924              SUM = SUM + ZZ(K)
925              SSQ = SSQ + ZZ(K)*ZZ(K)
926          END IF
927 10      CONTINUE
928      PTS = FLOAT(MSK)
929      IF(PTS.EQ.0) PTS = FLOAT(NXY)
930      BAR = SUM / PTS
931      VAR = (SSQ-PTS*BAR*BAR) / (PTS-1.)
932
933 C      FROM THIS POINT ON WE CAN SIMPLY CHECK IF ZZ(K).NE.0 (.NE.EXACT ZERO)
934 C      RATHER THAN CHECKING THE MSK FLAG AND ZM ARRAY (IF MASK OPTION USED)
935
936 C      USE THE FORMULA ON PAGE 10 OF THE MANUAL (THE FORMULA THAT'S LABELED
937 C      "DO NOT USE") TO SCALE THE FIELD TO MATCH THE DESIRED MEAN & VARIANCE.
938 C      READ SECTION 2.1.2 OF MANUAL BEFORE INVOKING THIS OPTION.
939 C      BAR LEFT IN FORMULAS BELOW FOR CLARITY. AN=NUGGET, AV=SILL
940      IF(IMSEX.EQ.1) THEN
941          DO 30 I=1,NXY
942 30      IF(ZZ(I).NE.0) ZZ(I) = ZZ(I) - BAR

```

```

943         BAR = 0.
944         SFAC = SQRT(AN+AV) / SQRT(VAR-BAR*BAR)
945         DO 40 I=1,NXY
946 40      IF(ZZ(I).NE.0) ZZ(I) = SFAC * (ZZ(I)-BAR) + AM
947         BAR = AM
948         VAR = AN + AV
949         END IF
950 comt  if you don't believe BAR=AM, VAR=AN+AV, uncomment the following lines
951 comt  SUM = 0.
952 comt  SSQ = 0.
953 comt  DO 50 K=1,NXY
954 comt  IF(ZZ(K).NE.0) THEN
955 comt      SUM = SUM + ZZ(K)
956 comt      SSQ = SSQ + ZZ(K)*ZZ(K)
957 comt  END IF
958 50     CONTINUE
959 comt  BAR = SUM / PTS
960 comt  VAR = (SSQ-PTS*BAR*BAR) / (PTS-1.)
961
962 comt  EXPONENTIATE THE FIELD if REQUESTED ...
963      IF(ILN.EQ.2) THEN
964          DO 60 K=1,NXY
965 60      IF(ZZ(K).NE.0) ZZ(K) = EXP(ZZ(K))
966      ELSE IF(ILN.EQ.3) THEN
967          DO 70 K=1,NXY
968 70      IF(ZZ(K).NE.0) ZZ(K) = 10.**ZZ(K)
969      END IF
970
971      RETURN
972      END
973
974
975
976
977      SUBROUTINE INTPAR(XY)
978  C-----
979  --
980  C      CALCULATE INTERNAL PARAMETERS
981
982      PARAMETER (PI=3.141592654)
983      REAL      XY(*)
984      INCLUDE 'tuba211d.inc'
985 comt  SEE BLOCK DATA MODULE
986 comt  DATA    FM,FA,AM,AV,CLX,CLY /1.0, 0.0, 0.0, 1.0, 1.0, 1.0/
987
988  C      NORMALIZE DISTANCE FROM TBM ORIGIN TO OUTPUT FIELD ORIGIN
989      XO = XO / CLX
990      YO = YO / CLY
991
992  C      DX AND DY DEPEND ON WHETHER GRID IS POINT OR BLOCK CENTERED
993      IF(KS.EQ.2) THEN
994          K = 2 - IP
995          DX = XMAX / MAX(NX-K,1)
996          DY = YMAX / MAX(NY-K,1)
997      END IF
998
999  C      NORMALIZE LINE DISCRETIZATION DISTANCE (UN) FOR STATIONARY MODELS
1000     IF(IDFP.NE.1 .AND. ICOVF.LE.4) UN = UN / AMAX1(CLX,CLY)
1001
1002  C      NORMALIZE MAX DISCRETIZATION DISTANCE ALONG ANY TBM LINE, THEN
1003  C      ESTIMATE NMAX = THE NUMBER OF POINTS ALONG THE LONGEST TBM LINE
1004     IF(ICOVF.LE.4) THEN
1005         TBMX = TBMX / AMIN1(CLX,CLY)
1006         NMAX = TBMX / UN + 1
1007     END IF
1008
1009  C      FOR FFT GENERATION ALGORITHM, LINE PROCESS LENGTH = UN*NHAR/2.
1010  C      IF THAT IS LESS THAN TBMX, NHAR MUST BE INCREASED.

```

```

1011      IF(ICOVF.LE.3 .AND. ISAJ.EQ.0) THEN
1012 16      IF(UN*NHAR/2.0 .LT. TBMX) THEN
1013          NHAR = 2*NHAR
1014          GO TO 16
1015      END IF
1016  END IF
1017
1018  C      CALCULATE PARAMETERS NEEDED FOR THE MOVING AVERAGE PROCESS
1019      IF(ICOVF.EQ.4 .OR. IULP.EQ.2) THEN
1020          DS = DS/AMIN1(C LX,CLY)
1021          UD = UN/DS
1022  C      FOR USER DEFINED MA PROCESS, CLN MUST BE REPLACED WITH A NUMBER
1023  C      REPRESENTING THE NBR CORR LGTHS THE MA WEIGHTING FCN IS NON-ZERO
1024  Comt   IF(ICOVF.EQ.0) KD = CLN/DS + 1
1025      IF(ICOVF.EQ.4) KD = 5.0/DS + 1
1026          NR = NMAX*UD + KD
1027          IF(DS.GT.UN) FM = UD
1028          IF(DS.GT.UN) FA = 0.5
1029      END IF
1030
1031  C      GENERALIZED COVARIANCE PARAMETERS
1032      IF(ICOVF.EQ.5) THEN
1033          NMAX = TBMX/UN + 1
1034          KT = AMAX1(UN/DT,1.)
1035          DT = UN / FLOAT(KT)
1036          SG = SQRT( 24.*DT )
1037          B0 = SQRT(A1*PI/2.)
1038          B2 = SQRT(A5*PI*15./16.)
1039          B1 =      A3*PI* 3./4.
1040          B1 = SQRT(B1*B1 + 2.*B0*B2)
1041      END IF
1042
1043      RETURN
1044      END
1045
1046
1047
1048
1049      SUBROUTINE LSTINP(IL)
1050  C-----
1051  --
1052  C      LIST INPUT VALUES & INTERNAL PARAMETERS USED IN LINE PROCESS
1053  C      GENERATION
1054  C
1055  C      AS INPUT IS READ, IT IS WRITTEN (AND ANNOTATED) ON UNIT IL.  NOW
1056  C      REWIND
1057  C      IL, REREAD THOSE LINES AND STORE THEM IN THE "INTERNAL FILE" BUF.
1058  C      THEN
1059  C      OPEN IL WITH THE DATA FILENAME AND EXTENSION ".INP" & DUMP BUF INTO
1060  C      IT.
1061  C-----
1062  --
1063      INTEGER          NC(32)
1064      CHARACTER      FMT*35, FNAM*35, LSTF*35, REC*80, BUF(32)*80
1065      INCLUDE 'tuba211d.inc'
1066      COMMON /OTPTS1/ FMT, FNAM
1067      COMMON /OTPTS2/ IFO, IMO, IRO, ILN
1068
1069  C      READ THE ANNOTATED INPUT PARAMETERS FROM SCRATCH FILE (UNIT IL)
1070  C      AND WRITE THEM TO THE INTERNAL FILE "BUF"
1071      REWIND IL
1072      DO 10 K=1,32
1073          READ(IL,5,END=11) REC
1074  5      FORMAT(A)
1075          WRITE(BUF(K),5) REC
1076          NC(K) = NCHR(REC)
1077  10      CONTINUE
1078  11      NREC = K-1

```

```

1079
1080 C OPEN THE <NAME>.INP LISTING FILE; REUSE LOGICAL UNIT IL AND
1081 C WRITE THE ANNOTATED INPUT PARAMETERS TO THIS LIST FILE
1082 CLOSE(UNIT=IL,STATUS='DELETE')
1083 IDOT = INDEX(FNAM, '.')
1084 IF(IDOT.EQ.0) IDOT = NCHR(FNAM) + 1
1085 LSTF = FNAM(1:IDOT-1) // '.inp'
1086 OPEN(UNIT=IL,FILE=LSTF,STATUS='UNKNOWN',FORM='FORMATTED')
1087 DO 15 K=1,NREC
1088 15 WRITE(IL,5) BUF(K) (1:NC(K))
1089
1090 C LIST OTHER INTERNAL PARAMETERS ...
1091 TBMXX = TBMX * AMIN1(C LX,CLY)
1092 UNLAST = UN * AMAX1(C LX,CLY)
1093 WRITE(IL,20) XO*CLX,YO*CLY,LINES,TBMXX,UNLAST
1094 20 FORMAT(' FIELD ORIGIN relative to the TBM origin =',2G13.6,
1095 1 /' The Number of Turning Band Lines Equals =',I9,
1096 1 /' The Maximum Turning Band Line Length =',G13.6,
1097 1 /' Turning Band Line Discretization Length =',G13.4)
1098
1099 IF(ICOVF.LE.3 .AND. IULP.NE.2 .AND. ISAJ.EQ.0) NMAX = NHAR
1100 IF(ICOVF.EQ.4 .OR. IULP.EQ.2) WRITE(IL,30) DS*AMIN1(C LX,CLY)
1101 30 FORMAT(' Discretization Distance for MA Process =',G13.4)
1102 IF(ICOVF.GE.4 .OR. IULP.EQ.2) WRITE(IL,32) NMAX
1103 32 FORMAT(' Number of Output Points Along each Line =',I9)
1104
1105 IF(ICOVF.EQ.5 .AND. (A3.NE.0 .OR. A5.NE.0) ) WRITE(IL,35) DT
1106 35 FORMAT(' Discretization Distance for WL Process =',G13.4)
1107
1108 IF(ICOVF.LE.3 .AND. IULP.LE.1) WRITE(IL,40) FMAX,NHAR,FMAX/NHAR
1109 40 FORMAT(' The Maximum Frequency for the Spectrum =',G13.6,
1110 1 /' Number of Harmonics for the Spectrum =',I9,
1111 1 /' Frequency Spacing in Spectral Domain =',G13.5)
1112
1113 IF(KS.EQ.1) WRITE(IL,*)
1114 IF(KS.EQ.2) THEN
1115 WRITE(IL,45) DX,DY
1116 45 FORMAT(' The Spatial Discretizations, DELX, DELY =',2G13.4)
1117 SMPLS = (XMAX/CLX)/2.0*(YMAX/CLY)/2.0
1118 IF(ICOVF.LE.4) WRITE(IL,50) CLX/DX,CLY/DY,SMPLS
1119 50 FORMAT(' No Points/correlation Length in X,Y Dir =',F9.1,
1120 1 3X,F9.1/' Approximate No. of Independent Samples =',F9.1)
1121 END IF
1122
1123 RETURN
1124 END
1125
1126
1127
1128
1129 SUBROUTINE MOVAVG(TT,Z1,FF)
1130 C-----
1131 --
1132 C MOVING AVERAGE SIMULATION OF THE LINE PROCESS (FOR TELIS COVARIANCE)
1133
1134 REAL TT(*), Z1(*), FF(*)
1135 INCLUDE 'tuba211d.inc'
1136
1137 C FM, FA, NR, UD AND KD ARE ALL CALCULATED IN SUBROUTINE INTPAR.
1138 C CK IS FOR MOVING AVERAGE PROCESS ASSOCIATED WITH TELIS COV FCN.
1139 C CK IS SET TO 1.0 IN SUBROUTINE CALINP FOR USER-DEFINED MOVING
1140 AVERAGES.
1141
1142 DO 10 K=1,NR
1143 10 TT(K) = URN55()
1144
1145 DO 30 N=1,NMAX
1146 Z1(N) = 0.0

```

```

1147         IOFF = (N-1)*UD + 0.5
1148         DO 20 K=1,KD
1149             IADR = IOFF + FLOAT(K)*FM + FA
1150             Z1(N) = Z1(N) + FF(K)*TT(IADR)
1151 20         CONTINUE
1152             Z1(N) = CK*Z1(N)
1153 30         CONTINUE
1154
1155         RETURN
1156         END
1157
1158
1159
1160
1161         FUNCTION NCHR(BUF)
1162 C-----
1163 --
1164 C     DETERMINE THE NUMBER OF CHARACTERS IN THE CHARACTER ARRAY BUF
1165
1166         CHARACTER BUF*(*)
1167
1168         LGTH = LEN(BUF)
1169         DO 10 K=LGTH,1,-1
1170 10         IF(BUF(K:K).NE.' ') GO TO 20
1171 20         NCHR = K
1172
1173         RETURN
1174         END
1175
1176
1177
1178
1179         SUBROUTINE OPNFIL(IT,IL,IO,LREC,ISIM,NSIM,BAR,VAR,SSQ,PTS,
1180 1          MODEL,ISEED)
1181 C-----
1182 --
1183 C     OPEN DATA OUTPUT FILE AND LIST THE RANDOM FIELD STATISTICS
1184
1185         CHARACTER FMT*35,FNAM*35
1186         CHARACTER FNAME*25,EXT*5,IFM*5,FRM*11
1187         INCLUDE 'tuba211d.inc'
1188         COMMON /OTPTS1/ FMT,FNAM
1189         COMMON /OTPTS2/ IFO,IMO,IRO,ILN
1190         DATA SMBAR,SMSSQ,SMPTS /0.0,0.0,0.0/
1191
1192         NC = NCHR(FNAM)
1193         FNAME(1:NC) = FNAM(1:NC)
1194         FNAME(NC+1:25) = ' '
1195
1196 C     APPEND SIMULATION NUMBER TO FILENAME IF MULTIPLE FILES REQUESTED
1197         IF(NF.GT.1) THEN
1198             IDOT = INDEX(FNAM, '.')
1199             IF(IDOT.EQ.0) IDOT = NC + 1
1200             NDIG = ALOG10( FLOAT(NSIM) ) + 1
1201             WRITE(IFM,10) NDIG
1202 10         FORMAT(2H(I,I1,1H))
1203             WRITE(EXT,IFM) ISIM
1204             DO 15 I=1,NDIG-1
1205 15         IF(EXT(I:I).EQ.' ') EXT(I:I) = '0'
1206             FNAME = FNAM(1:IDOT-1) // '.' // EXT(1:NDIG)
1207             NC = IDOT + NDIG
1208         END IF
1209
1210         IF(NF.GT.1 .OR. ISIM.EQ.1) THEN
1211             CLOSE(UNIT=IO)
1212             IF(MOD(IFO,2).EQ.0) FRM = 'UNFORMATTED'
1213             IF(MOD(IFO,2).NE.0) FRM = 'FORMATTED'
1214 Comt RECL cannot be used for unformatted files with Lahey Fortran

```

```

1215 Comt      OPEN (UNIT=IO, FILE=FNAME, STATUS='UNKNOWN', FORM=FRM, RECL=LREC)
1216          OPEN (UNIT=IO, FILE=FNAME, STATUS='UNKNOWN', FORM=FRM)
1217          END IF
1218
1219 C          LIST NEW RANDOM SEED FOR MULTIPLE SIMULATION RUN
1220          IF (NSIM.GT.1) WRITE (IL,18) ISIM, FNAME(1:NC), ISEED
1221 18        FORMAT (/24X, ' Simulation Nmbr =', I9,
1222 1          /24X, ' Output Filename =', 1X, A,
1223 1          /24X, ' New Random Seed =', I12)
1224
1225 C          LIST THE STATISTICS FOR THE SAMPLE DATA TO LIST FILE AND TERMINAL
1226          WRITE (IL,20) BAR, VAR
1227 20        FORMAT( 24X, ' The Sample Mean =', G13.5,
1228 1          /24X, ' Sample Variance =', G13.5)
1229          IF (IPF.NE.1) WRITE (IT,*)
1230          IF (IPF.NE.1 .AND. NSIM.GT.1) WRITE (IT,28) ISIM
1231 28        FORMAT(' Simulation Nmbr =', I8)
1232          WRITE (IT,30) BAR, VAR
1233 30        FORMAT('          The Sample Mean =', G13.5,
1234 1          /'          Sample Variance =', G13.5/)
1235
1236          SMBAR = SMBAR + BAR
1237          SMSSQ = SMSSQ + SSQ
1238          SMPTS = SMPTS + PTS
1239
1240 C          LIST ENSEMBLE STATISTICS IF THIS IS THE LAST REALIZATION
1241          IF (NSIM.GT.1 .AND. ISIM.EQ.NSIM) THEN
1242              ENBAR = SMBAR/FLOAT(NSIM)
1243              ENVAR = (SMSSQ-SMPTS*ENBAR*ENBAR)/(SMPTS-1.)
1244              WRITE (IL,40) ENBAR, ENVAR
1245 40        FORMAT (/22X, ' THE ENSEMBLE STATISTICS ...' ,
1246 1          /22X, ' The Ensemble Mean =', G13.5,
1247 1          /22X, ' Ensemble Variance =', G13.5)
1248              WRITE (IT,50) ENBAR, ENVAR
1249 50        FORMAT (/' THE ENSEMBLE STATISTICS ...',
1250 1          /'          The Ensemble Mean =', G13.5,
1251 1          /'          Ensemble Variance =', G13.5)
1252          END IF
1253
1254          RETURN
1255          END
1256
1257
1258
1259
1260          SUBROUTINE ORGMAX(XY)
1261 C-----
1262 --
1263 C          CALCULATE DEFAULT TBM ORIGIN AND MAXIMUM DISTANCE ALONG ANY TBM LINE
1264
1265          REAL      XY(2,*)
1266          INCLUDE 'tuba211d.inc'
1267
1268 C          FOR OUTPUT AT ARBITRARY LOCATIONS (KS=1):
1269 C          SET DEFAULT TBM ORIGIN EQUAL TO THE MINIMUM (X,Y) COORDINATE
1270          IF (KS.EQ.1) THEN
1271              X14 = -1.E-15
1272              X23 = +1.E+15
1273              Y12 = -1.E-15
1274              Y34 = +1.E+15
1275              DO 10 I=1,NXY
1276                  X14 = AMAX1 (XY(1,I), X14)
1277                  X23 = AMIN1 (XY(1,I), X23)
1278                  Y12 = AMAX1 (XY(2,I), Y12)
1279                  Y34 = AMIN1 (XY(2,I), Y34)
1280 10          CONTINUE
1281              XO = X23
1282              YO = Y34

```

```

1283      DXX = X14 - XO
1284      DYY = Y12 - YO
1285      TBMX = SQRT(DXX*DXX + DYY*DYY)
1286  C -----
1287  --
1288  C      THE REMAINDER OF THIS IF-BLOCK PERTAINS ONLY TO THE CASE OF GENER-
1289  C      ATING AT ARBITRARY LOCATIONS (KS=1) USING GENERALIZED COVARIANCE.
1290  C      The following is used to calculate DX and DY and ASSUMES a uniform
1291  C      distribution of the "finite element" grid points (i.e., the (x,y)
1292  C      arbitrary locations for generating the field). DX and DY are only
1293  C      needed for this case (KS=1) in subroutine DEFPAR where the DEFAULT
1294  C      TBM line discretization length (UN) is calculated. The calculated
1295  C      value of UN is only APPROXIMATED and should be checked for adequacy
1296  C      (e.g., UN should be .LE. the minimum spacing between any two field
1297  C      generation points). ASSUMPTIONS: (1) NY/NX=DYY/DXX, (2) NX*NY = NXY
1298  C -----
1299  --
1300      NX = SQRT( FLOAT(NXY)*DXX/DYY )
1301      NY = NXY/NX
1302      DX = 0.2*DXX/FLOAT(NX)
1303      DY = 0.2*DYY/FLOAT(NY)
1304  END IF
1305
1306  C      FOR GRIDDED OUTPUT (KS=2,3):
1307  C      SET DEFAULT TBM ORIGIN AND FIND THE MAXIMUM DISTANCE FROM
1308  C      THE TBM ORIGIN TO THE FAR CORNER OF THE GRID
1309  C      IF(KS.GT.1) THEN
1310      XO = 0.0
1311      YO = 0.0
1312      TBMX = SQRT(XMAX*XMAX + YMAX*YMAX)
1313  END IF
1314
1315  RETURN
1316  END
1317
1318
1319
1320
1321  SUBROUTINE OUTPUT(IT,IL,IO,ISIM,NSIM,XY,ZZ,ZM,NEWS)
1322  C-----
1323  --
1324  C      FINISH FIELD GENERATION, THEN WRITE FIELD TO OUTPUT FILE
1325
1326  CHARACTER   FMT*35,FNAM*35
1327  REAL       ZZ(*), ZM(*), XY(2,*),TBKK(1000000)
1328  INCLUDE 'tuba211d.inc'
1329  COMMON /OTPTS1/ FMT,FNAM
1330  COMMON /OTPTS2/ IFO,IMO,IRO,ILN
1331  COMMON /KFIELD/ TBKK
1332
1333  C      DO THE FINAL SCALING, ADD IN THE MEAN, AND CALCULATE STATISTICS
1334  C      CALL FSCALE(XY,ZZ,ZM,ILN,BAR,VAR,SSQ,PTS)
1335
1336  C      OPEN OUTPUT FILE AND LIST RANDOM FIELD SAMPLE STATISTICS
1337  C      LREC = BYTE LENGTH OF UNFORMATTED RECORDS
1338  C      LREC = 256
1339  C      IF(MOD(IFO,2) .EQ.0) THEN
1340      LREC = 4*NX
1341      IF(IMO .EQ.1) LREC = 4*NXY
1342  END IF
1343  C      CALL OPNFIL(IT,IL,IO,LREC,ISIM,NSIM,BAR,VAR,SSQ,PTS,ICOVF,NEWS)
1344
1345  C      IFO,IMO AND IRO ARE INTERNAL PARAMETERS CONTROLLING OUTPUT FORMAT;
1346  C      THESE ARE CALCULATED IN SUBROUTINE FILPAR.
1347  C      IFO EVEN,ODD -> UNFORMATTED,FORMATTED RESPECTIVELY
1348  C      IMO = 0 -> WRITE MATRIX OUT LINE BY LINE
1349  C      IMO = 1 -> WRITE MATRIX OUT WITH ONE WRITE STATEMENT
1350

```

```

1351 C      OPEN(35,FILE='K_TUBA.TXT',STATUS='UNKNOWN')
1352
1353      IF(IMO.EQ.1 .OR. KS.EQ.1) THEN
1354          IF(IFO.EQ.1) WRITE(IO,FMT) (ZZ(K),K=1,NXY)
1355          IF(IFO.EQ.2) WRITE(IO) (ZZ(K),K=1,NXY)
1356          IF(IFO.EQ.3) WRITE(IO,FMT) (XY(1,K),XY(2,K),ZZ(K),K=1,NXY)
1357          IF(IFO.EQ.4) WRITE(IO) (XY(1,K),XY(2,K),ZZ(K),K=1,NXY)
1358      ELSE
1359          JST = (IRO-1)*NY + (2-IRO)
1360          JND = (2-IRO)*NY + (IRO-1)
1361          JNC = 3 - 2*IRO
1362          DO 20 J=JST,JND,JNC
1363              DO 20 I=1,NX
1364                  IP=(J-1)*NX+I
1365                  TBKK(IP)=ZZ(IP)
1366 C                  WRITE(35,*) I,J,1,TBKK(IP)
1367 C                  PRINT*,I,J,ZZ(IP)
1368 20          CONTINUE
1369      END IF
1370
1371      RETURN
1372      END
1373
1374
1375
1376      SUBROUTINE PROGSS(MSG,LU,K,KMAX,INC)
1377 C-----
1378 C      REPORT COMPUTATION PROGRESS
1379
1380      CHARACTER MSG* (*)
1381      COMMON /PGPARS/ PCL,IPG
1382
1383      IF(K.EQ.1) THEN
1384          PCL = 100./FLOAT(KMAX)
1385          WRITE(LU,10) MSG,K,INT(PCL)
1386          IPG = 1
1387          RETURN
1388      END IF
1389
1390      PCT = 100 * FLOAT(K)/FLOAT(KMAX)
1391      IPC = INT(PCT)
1392      DIF = PCT - PCL
1393
1394      IPR = 0
1395      IF(INC.EQ.0) THEN
1396          IPR = 1
1397      ELSE IF(KMAX.LE.99) THEN
1398          IF(DIF.GT.INC) IPR = 1
1399      ELSE
1400          IF(MOD(IPC,INC).EQ.0 .AND. DIF.GE.2) IPR = 1
1401      END IF
1402      IF(K.EQ.KMAX) IPR = 1
1403
1404      IPG = 0
1405      IF(IPR.EQ.1) THEN
1406          IPG = 1
1407          PCT = AMIN1(PCT,99.9)
1408          PCL = PCT
1409          IF(PCT.EQ.99.9) PCL = 0.0
1410          WRITE(LU,10) MSG,K,INT(PCT)
1411 10      FORMAT(A,I8,' ... (',I2,' % ) ')
1412      END IF
1413
1414      RETURN
1415      END
1416
1417
1418

```

```

1419      SUBROUTINE PROJCT(L,IT,IU,XY,PP,SS,CC,ZZ,ZM,Z1)
1420      C-----
1421      --
1422      C      ADD PROJECTIONS FROM THE LTH TBM LINE ONTO OUTPUT FIELD
1423
1424      REAL      XY(2,*), PP(2,*), SS(*), CC(*), ZZ(*), ZM(*), Z1(*)
1425      INTEGER  INC(3)
1426      INCLUDE 'tuba211d.inc'
1427      COMMON   /PGPARS/ PCL,IPG
1428      CHARACTER PLPD*43,TBLIN*22
1429      DATA     INC /20,5,0/
1430      DATA     TBLIN /' Turning Band Line ...'/
1431      DATA     PLPD /' Projecting Line Process Data ... Point No'/
1432
1433      C      ZERO OUT THE OUTPUT FIELD IF ON TURNING BAND LINE NO 1
1434      IF(L.EQ.1) THEN
1435          DO 10 K=1,NXY
1436      10      ZZ(K) = 0.0
1437      END IF
1438
1439      C      FOR OUTPUT AT ARBITRARY (X,Y) LOCATIONS ...
1440      IF(KS.EQ.1) THEN
1441          CALL PROGSS(TBLIN,IT,L,LINES,INC(IPF))
1442          PCLSAV = PCL
1443          IPGSAV = IPG
1444          DO 20 K=1,NXY
1445      Comt      CALL PROGSS(' Projecting Line Process Data ... Point No',
1446          IF(IPF*IPGSAV.GE.2) CALL PROGSS(PLPD,IT,K,NXY,INC(IPF-1))
1447          CALL PROJSB(XY,K,L,K,CC,SS,ZZ,Z1)
1448      20      CONTINUE
1449          PCL = PCLSAV
1450          GO TO 50
1451      END IF
1452
1453      C      FOR OUTPUT ONTO REGULAR OR IRREGULARLY-SPACED GRIDS ...
1454      C      CALL PROGSS(TBLIN,IT,L,LINES,INC(IPF))
1455          PCLSAV = PCL
1456          IPGSAV = IPG
1457          DO 40 I=1,NY
1458          READ(UNIT=IU,REC=I) ((PP(K,J),K=1,2),J=1,NX)
1459          DO 30 J=1,NX
1460          K = (I-1)*NX + J
1461      Comt      CALL PROGSS(' Projecting Line Process Data ... Point No',
1462          IF(IPF*IPGSAV.GE.2) CALL PROGSS(PLPD,IT,K,NXY,INC(IPF-1))
1463          IF(MSK.GT.0 .AND. ZM(K).EQ.0) GO TO 30
1464          CALL PROJSB(PP,J,L,K,CC,SS,ZZ,Z1)
1465      30      CONTINUE
1466      40      CONTINUE
1467          PCL = PCLSAV
1468
1469      50      IF(IPF*IPGSAV.GT.1) WRITE(IT,*)
1470      RETURN
1471      END
1472
1473
1474
1475      SUBROUTINE PROJSB(A2,J,L,K,CC,SS,ZZ,Z1)
1476      C-----
1477      --
1478      C      DO THE PROJECTION FOR BOTH GRIDDED AND NON-GRIDDED FIELDS
1479
1480      REAL      A2(2,*), CC(*), SS(*), ZZ(*), Z1(*)
1481      INCLUDE 'tuba211d.inc'
1482
1483      XP = A2(1,J)/CLX + XO
1484      YP = A2(2,J)/CLY + YO
1485      XD = ABS(XP*CC(L) + YP*SS(L) )
1486      N1 = INT(XD/UN)+1

```

```

1487      ZZ(K) = ZZ(K) + Z1(N1)
1488      RETURN
1489      END
1490
1491
1492
1493      SUBROUTINE RDINPT (IN, IT, IL, IU, XY, ZM, MODEL, NLINE, NSIM)
1494 C-----
1495 --
1496 C      CONTROL MODULE FOR READING INPUT PARAMETERS
1497
1498      REAL      XY(*), ZM(*)
1499      INCLUDE 'tuba211d.inc'
1500
1501 C      WRITE(IT,10)
1502 10  FORMAT(//' ++++++++ Program "TUBA (version 2.11d)" ++++++++',
1503 1      //'          A Code For Simulating 2D Random Fields',
1504 1      '/'          Via The Turning Bands Method'/)
1505
1506 C      OPEN TEMPORARY FILE (LATER DELETED)
1507      OPEN(UNIT=IL, STATUS='SCRATCH')
1508
1509 C      QUERY FOR OUTPUT FIELD PARAMETERS
1510      CALL FLDPAR (IN, IT, IL, IU, XY, XY, ZM)
1511
1512 C      QUERY FOR COVARIANCE PARAMETERS
1513      CALL COVPAR (IN, IT, IL, MODEL)
1514
1515 C      QUERY FOR TURNING BANDS PARAMETERS
1516      CALL TBMPAR (IN, IT, IL, NLINE, XY)
1517
1518 C      MODEL REFERS TO THE LINE PROCESS GENERATION METHOD
1519 C      WHEREAS ICOVF REFERS THE THE COVARIANCE MODEL TYPE
1520 C      NEXT LINE IS NEEDED IN THE MAIN MODULE (FOR A USER-DEFINED MA PROCESS)
1521      IF (IULP.EQ.2) MODEL = 4
1522
1523 C      QUERY FOR OUTPUT FILE PARAMETERS
1524      CALL FILPAR (IN, IT, IL)
1525
1526 C      QUERY FOR SIMULATION PARAMETERS
1527      CALL SIMPAR (IN, IT, IL, NSIM)
1528
1529      RETURN
1530      END
1531
1532
1533
1534      SUBROUTINE RDINTG (IN, IT, IL, IV, NV, ID)
1535 C-----
1536 --
1537 C      READ AND REFLECT INTEGER INPUT DATA
1538
1539      CHARACTER CMT*42, BUF* (*)
1540      INTEGER   IV (*)
1541      REAL      RV (*)
1542
1543      READ (IN, *) (IV(I), I=1, NV)
1544      WRITE (IT, *) '>>>>>' , (IV(I), I=1, NV)
1545      WRITE (IT, *) ' '
1546
1547      CALL COMENT (ID, CMT, NC)
1548      IF (NV.EQ.1) WRITE (IL, 11) IV(1), CMT(1:NC)
1549      IF (NV.EQ.2) WRITE (IL, 12) IV(1), IV(2), CMT(1:NC)
1550 11  FORMAT(2X, I12, T36, A)
1551 12  FORMAT(2X, 2I12, T36, A)
1552
1553      RETURN
1554

```

```

1555      ENTRY RDREAL (IN, IT, IL, RV, NV, ID)
1556      C-----
1557      C      READ AND REFLECT REAL INPUT DATA
1558
1559      READ (IN, *) (RV(I), I=1, NV)
1560      WRITE(IT, *) '>>>>' , (RV(I), I=1, NV)
1561      WRITE(IT, *) ' '
1562
1563      CALL COMENT (ID, CMT, NC)
1564      IF(NV.EQ.1) WRITE(IL, 21) RV(1), CMT(1:NC)
1565      IF(NV.EQ.2) WRITE(IL, 22) RV(1), RV(2), CMT(1:NC)
1566      IF(NV.EQ.3) WRITE(IL, 23) RV(1), RV(2), RV(3), CMT(1:NC)
1567      21 FORMAT(2X, G13.5, T36, A)
1568      22 FORMAT(2X, 2G13.5, T36, A)
1569      23 FORMAT(1PE11.3, 2E11.3, T36, A)
1570
1571      RETURN
1572
1573      ENTRY RDCHAR (IN, IT, IL, BUF, ID)
1574      C-----
1575      C      READ AND REFLECT CHARACTER VARIABLES
1576
1577      READ(IN, 30) BUF
1578      30 FORMAT(A)
1579      NB = NCHR (BUF)
1580      IF(NB.EQ.0) BUF = ' '
1581      IF(NB.EQ.0) NB = 1
1582      WRITE(IT, *) '>>>>' , BUF(1:NB)
1583      WRITE(IT, *) ' '
1584
1585      CALL COMENT (ID, CMT, NC)
1586      WRITE(IL, 35) BUF(1:NB), CMT(1:NC)
1587      35 FORMAT(A, T36, A)
1588
1589      RETURN
1590      END
1591
1592
1593
1594      SUBROUTINE SIMPAR (IN, IT, IL, NSIM)
1595      C-----
1596      --
1597      C      READ SIMULATION PARAMETERS
1598
1599      SAVE ISEED, JSEED
1600      CHARACTER BUF*32
1601      INCLUDE 'tuba211d.inc'
1602
1603      C      WRITE(IT, 10)
1604      C 10 FORMAT(/' ++++++ SIMULATION PARAMETERS ++++++')
1605
1606      C      WRITE(IT, *) '(1) - Marsaglia and Bray Random Number Generator'
1607      C      WRITE(IT, *) '(2) - Machine Independent Random Number Generator'
1608      C      WRITE(IT, *)
1609      C      CALL RDINTG (IN, IT, IL, IURN, 1, 28)
1610      IURN=1
1611
1612      C      WRITE(IT, *) 'Enter Integer Seed(s) To Initialize The Generator'
1613      IF(IURN.EQ.2) WRITE(IT, 20)
1614      20 FORMAT(' ( Seed For This Generator Must Be 8 Digits Long )')
1615      WRITE(IT, *)
1616      Comt CALL RDINTG (IN, IT, IL, ISEED, 1, 29)
1617      C      CALL RDCHAR (IN, IT, IL, BUF, 29)
1618      C      READ(BUF, *, END=21) ISEED, JSEED
1619      C      GO TO 30
1620      ISEED=1
1621      21 JSEED = ISEED
1622      30 IF(IURN.EQ.1) DUMMY = UNITMB (ISEED)

```

```

1623      IF(IURN.EQ.2)  DUMY = UNITSS(IT,ISEED)
1624
1625      C      WRITE(IT,*)'Enter The Number Of Realizations To Be Simulated'
1626      C      WRITE(IT,*)
1627      C      CALL RDINTG(IN,IT,IL,NSIM,1,30)
1628      NSIM=1
1629
1630      IF(NSIM.GT.1) THEN
1631          WRITE(IT,*)'(1) - All Realizations Written To One File'
1632          WRITE(IT,*)'(2) - A Separate File For Each Realization'
1633          WRITE(IT,*)'      (e.g., file.1, file.2 ... file.99)'
1634          WRITE(IT,*)
1635          CALL RDINTG(IN,IT,IL,NF,1,34)
1636      END IF
1637
1638      C      WRITE(IT,*)'(0) - Do NOT Artificially Scale The Realizations'
1639      C      WRITE(IT,*)'(1) - Scale Data To Match Mean and Variance Exactly'
1640      C      WRITE(IT,*)'      Please Read Section 2.1.2 Of The Manual'
1641      C      WRITE(IT,*)'      Before Choosing This Option'
1642      C      WRITE(IT,*)
1643      C      CALL RDINTG(IN,IT,IL,IMSEX,1,36)
1644      IMSEX=0
1645
1646      IF(IMSEX.EQ.1 .AND. ICOVF.EQ.5) THEN
1647          WRITE(*,*)'GC Model: Enter Desired Mean, Nugget and Sill'
1648          WRITE(IT,*)
1649          CALL RDREAL(IN,IT,IL,AM,3,37)
1650      END IF
1651
1652      C      WRITE(IT,*)'Specify The Level Of Status Reporting To The Screen'
1653      C      WRITE(IT,*)'(1) - Minimal (e.g., For Many Realizations)'
1654      C      WRITE(IT,*)'(2) - More Frequent (e.g., For Many TBM Lines)'
1655      C      WRITE(IT,*)'(3) - Very Frequent (e.g., For Very Large Fields)'
1656      C      WRITE(IT,*)
1657      C      CALL RDINTG(IN,IT,IL,IPF,1,35)
1658      IPF=1
1659
1660      RETURN
1661
1662      ENTRY RESEED(ISIM,NUSEED)
1663      C-----
1664      C      RESEED THE RANDOM NUMBER GENERATOR
1665
1666      IF(ISIM.EQ.1) THEN
1667          NUSEED = ISEED
1668          IF(JSEED.EQ.ISEED) RETURN
1669          IF(IURN.EQ.1) DUMY = UNITMB(JSEED)
1670          IF(IURN.EQ.2) DUMY = UNITSS(IT,JSEED)
1671          RETURN
1672      END IF
1673
1674      NUSEED = 1.E+08*(URN55()+0.5)
1675      IF(IURN.EQ.1) DUMY = UNITMB(NUSEED)
1676      IF(IURN.EQ.2) THEN
1677          36      IF(ALOG10(FLOAT(NUSEED)) .LT. 7) THEN
1678              NUSEED = 10*NUSEED
1679              GO TO 36
1680          END IF
1681          DUMY = UNITSS(IT,NUSEED)
1682      END IF
1683
1684      RETURN
1685      END
1686
1687
1688
1689      SUBROUTINE SPCTRL(L,L2,PA,Z1,DZ,S1,C1,S2,C2)
1690      C-----

```

```

1691  --
1692  C   SPECTRAL SIMULATION OF THE LINE PROCESSES
1693
1694  PARAMETER (TUPI=6.2831853)
1695  COMPLEX   DZ(*)
1696  REAL      PA(*),Z1(*),S1(*),C1(*),S2(*),C2(*)
1697  INCLUDE 'tuba211d.inc'
1698
1699  C   GENERATE LINE PROCESS USING THE FFT METHOD
1700  IF(ISAJ.EQ.0) CALL FFTGEN(L,L2,PA,Z1,DZ)
1701  IF(ISAJ.EQ.0) RETURN
1702
1703  C   GENERATE LINE PROCESS USING THE METHOD OF SHINOZUKA AND JAN
1704  DO 10 M=1,NHAR
1705      THETA = URN55() * TUPI
1706      C2(M) = COS(THETA)
1707      S2(M) = SIN(THETA)
1708  10  CONTINUE
1709  IF(IPAA.EQ.2) READ(UNIT=L2,REC=L) (PA(M),M=1,NHAR)
1710
1711  C   PA(M) = 2.0 * SQRT(SPECTRL DENSITY * DELTA OMEGA)
1712  C   C2SAV ETC IS FOR TRIG IDENTITIES - THE COS(OMEGA'*ZETA+PHI) TERM IS
1713  C   CALCULATED BY CONSIDERING ZETA = N*DELTA-ZETA AND TRIG IDENTITIES
1714  DO 30 N=1,NMAX
1715      Z1(N) = 0.0
1716      DO 20 M=1,NHAR
1717          Z1(N) = Z1(N) + PA(M) * C2(M)
1718          C2SAV = C2(M)
1719          S2SAV = S2(M)
1720          C2(M) = C2SAV*C1(M) - S2SAV*S1(M)
1721          S2(M) = S2SAV*C1(M) + C2SAV*S1(M)
1722  20  CONTINUE
1723  30  CONTINUE
1724
1725  RETURN
1726  END
1727
1728
1729
1730  FUNCTION SPDF(FRQ,ICOVF)
1731  C-----
1732  --
1733  C   CALCULATE NORMALIZED 1D SPECTRAL DENSITY FUNCTION FOR POINT PROCESSES
1734  C   HAVING 2D COVARIANCE FUNCTIONS OF: USER-SPECIFIED (ICOVF=0),
1735  C   EXPONENTIAL (ICOVF=1), GAUSSIAN (ICOVF=2), BESSEL (ICOVF=3)
1736
1737  DATA   SOME,THING /0.,1./
1738
1739  IF(ICOVF.EQ.0) THEN
1740  C   USER DEFINED SPECTRUM GOES HERE
1741      SPDF = SOME + THING
1742  RETURN
1743  END IF
1744
1745  C   EXPLANATION OF ANCIENT FORTRAN: (COMPUTED GO TO)
1746  C   IF(ICOVF.EQ. 1,2,3) THEN GO TO (10,20,30)
1747
1748  GO TO (10,20,30) ICOVF
1749
1750  10  DENOM = (1.+FRQ*FRQ)**1.5
1751      SPDF = 0.5*FRQ/DENOM
1752  RETURN
1753
1754  20  XARG = 0.25*FRQ*FRQ
1755      SPDF = 0.25*FRQ*EXP(-XARG)
1756  RETURN
1757
1758  30  DENOM = (1.+FRQ*FRQ)**2.0

```

```

1759     SPDF = 1.0*FRQ/DENOM
1760     RETURN
1761     END
1762
1763
1764
1765     SUBROUTINE TBMPAR(IN, IT, IL, NLINE, XY)
1766 C-----
1767 --
1768 C     QUERY FOR TURNING BANDS LINE PARAMETERS
1769
1770     PARAMETER (PI=3.1415926)
1771     REAL      XY(*)
1772     INCLUDE 'tuba211d.inc'
1773
1774 C     WRITE(IT,10)
1775 C 10     FORMAT(//' ++++++      TURNING BANDS PARAMETERS      ++++++')
1776
1777 C     WRITE(IT,*) 'Enter The Number Of Turning Band Lines'
1778 C     WRITE(IT,*) '          ( Use At Least 16 )'
1779 C     WRITE(IT,*)
1780 C     CALL RDINTG(IN, IT, IL, LINES, 1, 15)
1781     NLINE = LINES
1782
1783     IF (ICOVF.EQ.0) THEN
1784         WRITE(IT,*) '(1) - Line Process By A Spectral Method'
1785         WRITE(IT,*) '(2) - Line Process By A Moving Average Method'
1786         WRITE(IT,*)
1787         CALL RDINTG(IN, IT, IL, IULP, 1, 13)
1788     ELSE
1789 C     WRITE(IT,*) 'For The Remaining Turning Band Parameters:'
1790 C     WRITE(IT,*) '(1) - Use Default Turning Band Parameters'
1791 C     WRITE(IT,*) '(2) - Enter The TBM Parameters Manually'
1792 C     WRITE(IT,*)
1793 C     CALL RDINTG(IN, IT, IL, IDFP, 1, 14)
1794         IDFP=1
1795         IF (IDFP.EQ.1) CALL DEFPPAR(NLINE, XY)
1796         IF (IDFP.EQ.1) RETURN
1797     END IF
1798
1799     WRITE(IT,*) 'Enter The TBM Line Discretization Distance'
1800     WRITE(IT,*) ' (e.g., Smaller Than The Grid Spacing)'
1801     IF (ICOVF.NE.5) THEN
1802         WRITE(IT,*) '(e.g., 1/16th the Correlation Length)'
1803     END IF
1804     WRITE(IT,*)
1805     CALL RDREAL(IN, IT, IL, UN, 1, 16)
1806
1807     IF (ICOVF.LE.3 .AND. IULP.NE.2) THEN
1808         WRITE(IT,*) 'Enter NBR Of Harmonics For Discretizing Spectrum'
1809         WRITE(IT,*)
1810         CALL RDINTG(IN, IT, IL, NHAR, 1, 17)
1811 C     SAJ METHOD BY DEFAULT, FFT METHOD IF NHAR=2*N FOR SOME N
1812         ISAJ = 1
1813         HMCS = NHAR
1814 C 16     IF (HMCS/2 .GT. 1) THEN
1815             HMCS = HMCS/2
1816             GO TO 16
1817         END IF
1818         IF (HMCS.EQ.2) THEN
1819             FMAX = 2.*PI/(UN/AMAX1(C LX, CLY))
1820             ISAJ = 0
1821         END IF
1822         IF (ISAJ.EQ.1) THEN
1823             WRITE(IT,*) 'Enter Max Frequency For Truncation Of Spectrum'
1824             WRITE(IT,*)
1825             CALL RDREAL(IN, IT, IL, FMAX, 1, 18)
1826         END IF

```

```

1827     END IF
1828
1829     IF(ICOVF.EQ.4 .OR. IULP.EQ.2) THEN
1830         WRITE(IT,*) 'Enter Discretization Distance for the MA Process'
1831         WRITE(IT,*) '    (Suggest 1/20th Of The Correlation Length)'
1832         WRITE(IT,*) '(and No Larger Than 1/10th TBM Line Disc. Dist.)'
1833         WRITE(IT,*)
1834         CALL RDREAL(IN,IT,IL,DS,1,19)
1835     END IF
1836
1837     DT = UN
1838     IF(ICOVF.EQ.5 .AND. (A3.NE.0 .OR. A5.NE.0) ) THEN
1839         WRITE(IT,*) 'Enter Discretization Distance for Weiner Process'
1840         WRITE(IT,*) '(Suggest 1/5th Of The TBM Discretized Distance)'
1841         WRITE(IT,*)
1842         CALL RDREAL(IN,IT,IL,DT,1,20)
1843     END IF
1844
1845     WRITE(IT,*) 'Enter (Xo,Yo) Field Origin Relative To TBM Origin'
1846     WRITE(IT,*)
1847     CALL RDREAL(IN,IT,IL,XO,2,21)
1848
1849     WRITE(IT,*) 'Enter the Maximum Turning Band Line Length'
1850     WRITE(IT,*)
1851     CALL RDREAL(IN,IT,IL,TBMX,1,31)
1852
1853     RETURN
1854     END
1855
1856
1857
1858     FUNCTION UNITMB(ISEED)
1859     C-----
1860     --
1861     C    URN01 generates UNIFORM RANDOM NUMBERS on the interval [0,1] using the
1862     C    algorithm of Marsaglia and Bray presented in (pages 567 & 597) of:
1863     C
1864     C           "The Handbook of Random Number Generation and Testing
1865     C                with TESTRAND computer code"
1866     C                E. J. Dudewicz and T. G. Rally
1867     C                American Sciences Press, Inc. 1981.
1868     C
1869     C    This generator was "recommended for practical use" (page 134) by the
1870     C    above authors. This generator passed the very sensitive and
1871     C    exhaustive
1872     C    tests described in the above reference.
1873     C-----
1874     --
1875     C    NOTE !!! Compile with "integer overflow check" turned OFF
1876     C-----
1877     --
1878     C    This version of Marsaglia's code was arranged by D. A. Zimmerman
1879     C    at New Mexico Tech, Geoscience Dept., Hydrology Program, August, 1987.
1880     C-----
1881     --
1882     C    DUMY = URNIT(ISEED)                ! Initialize Random Number
1883     C    Generator
1884     C    DO 10 I=1,N                          ! Generate N Uniformly Distributed
1885     C    10 X(I) = URN01()                    ! Random Numbers On Interval [0,1]
1886     C-----
1887     --
1888     INTEGER      N1(64), N2(64), N(128), MS(6)
1889     EQUIVALENCE (N(1),N1), (N(65),N2), (MS(1),ML)
1890     COMMON      /SEEDS/ ML,MM,MK,L,M,K
1891     C*** SEE BLOCK DATA MODULE
1892     C*** DATA      L, M, K /089347405, 301467177, 240420681/
1893     C*** DATA      ML,MM,MK /65539, 33554433, 36243609/
1894

```

```

1895      DATA          N1/  880431333,  845941495,  233211304, 1989552121,
1896      1      465185814,  280672924,  294923811,  969688974,  798989604,
1897      1      379880543,  130022074, 1958997525, 1074191695,  680854387,
1898      1      751282651, 1208899767,  695831691, 1667008051, 1682546364,
1899      1      1984522335,  287570376, 1137852001, 1597983496, 2015817872,
1900      1      1479672206, 1468443024, 1657203843,  326324124,  680973716,
1901      1      1451006002, 1251441372,  241092947, 1815086916, 1807193097,
1902      1      770906592,  725422944, 1822111098,  470585328,  939566271,
1903      1      1084841038, 1988336409,  229735215, 1763201387, 2072973152,
1904      1      1143606610,  548108569,  544252510, 1980873641, 1195919839,
1905      1      2089487851, 1406149582, 1839198022, 2106705200, 189238196,
1906      1      1170370207, 1304402631, 1936129483,  810953177,  706509560,
1907      1      476957499, 1307077413,  824336639, 1487297852, 1591453718/
1908
1909      DATA          N2/ 1348888685,  155452792,  265840413, 1440038626,
1910      1      770186799, 1152058296, 1726999383, 1389732859, 1838014251,
1911      1      1751063044, 102451305,  212848938, 1046489181,  976388856,
1912      1      1797117421,  461971124,  259337424,  492056652, 1152625277,
1913      1      1087711027,  344810019, 1477716555,  809152324, 1766452264,
1914      1      1687482934, 1077592551, 1906112218,  328744821, 1380339247,
1915      1      339750038, 1993648985, 1054008271, 2006727977, 1618648061,
1916      1      1300903972,  168650429, 1734500183,  906733794,  614096451,
1917      1      1092917209, 1180334545,  577024776, 1406305431,  648073629,
1918      1      973807028,  883884075, 1562357277, 1705648154, 1377603620,
1919      1      1845151798,  220566094,  768813055,  571717967, 218994012,
1920      1      212872559, 1824677815, 1573937649,  450149130, 284847256,
1921      1      2062965934,  47834840, 1766553923, 1580332201, 182920702/
1922
1923      I = MOD(ISEED,6) + 1
1924      MS(I) = ISEED
1925      RETURN
1926
1927      C      ENTRY URN01 ()
1928      ENTRY URNMB ()
1929      C-----
1930      C      URN01 RETURNS UNIFORMLY DISTRIBUTED RANDOM NUMBERS ON [0.,1.]
1931
1932      L = ML * L
1933      M = MM * M
1934      K = MK * K
1935      J = 1.0 + IABS(L) / 16777216
1936      C      URN01 = 0.5 + FLOAT( N(J)+L+M ) * 0.23283064E-09
1937      URNMB =          FLOAT( N(J)+L+M ) * 0.23283064E-09
1938      N(J) = K
1939
1940      RETURN
1941      END
1942
1943
1944
1945      FUNCTION UNITSS(LU, ISEED)
1946      C-----
1947      --
1948      C      URN01 generates UNIFORM RANDOM NUMBERS on the interval [0,1]
1949      C
1950      C      Reference: C. G. Swain and M. S. Swain 1980. "A Uniform
1951      C      Random Number Generator That Is Reproducible,
1952      C      HARDWARE-INDEPENDENT, And Fast" J. Chem. Inf.
1953      C      Comput. Sci. Vol 20. pp 56-58.
1954      C
1955      C      According to E. J. Dudewicz, Dept. Statistics, Ohio State University,
1956      C      in "Modern and Easy Generation of Random Numbers / Testing of Random
1957      C      Number Generators with TESTRAND", 10th IMACS World Congress On System
1958      C      Simulation and Scientific Computation, August 8-13, 1982, Montreal,
1959      C      Canada, Proceedings, Volume 2, page 133, this generator failed the
1960      C      sensitive Chi-square on Chi-square test performed by the TESTRAND
1961      C      code.
1962      C-----

```

```

1963  --
1964  C   This version of Swain & Swain's code was arranged by D. A. Zimmerman
1965  C   at New Mexico Tech, Geoscience Dept., Hydrology Program, June, 1986.
1966  C-----
1967  --
1968  C   DUMY = URNIT(12345678)                ! INITIALIZE URNG: ISEED=12345678
1969  C   DO 10 K=1,N                            ! GENERATE N UNIFORMLY DISTRIBUTED
1970  C 10 X(K) = URN01()                       ! RANDOM NUMBERS ON INTERVAL [0,1]
1971  C-----
1972  --
1973      PARAMETER (K1=35260417, K2=72619094, K3=86952743)
1974      INTEGER   M(0:3)
1975      DATA      M /0,K1,K2,K3 /
1976
1977      SEED = FLOAT(ISEED)
1978      IPWR = ALOG10(SEED)
1979
1980      IF(IPWR.NE.7) THEN
1981          WRITE(LU,*) ' ***** URN GENERATOR SEED MUST BE 8 DIGITS LONG'
1982          WRITE(LU,*) '          PROGRAM EXECUTION HALTED'
1983          STOP
1984      END IF
1985
1986      M(1) = K1
1987      M(2) = K2
1988      M(3) = K3
1989
1990      I = MOD(ISEED,3) + 1
1991      M(I) = ISEED
1992
1993      RETURN
1994
1995  C   ENTRY URN01()
1996  C   ENTRY URNSS()
1997  C-----
1998  C   URN01 RETURNS UNIFORMLY DISTRIBUTED RANDOM NUMBERS ON [0.,1.]
1999
2000      M(0) = M(1) + M(2) + M(3)
2001
2002      IF(M(2) .LT. 50000000) M(0) = M(0) + 1357
2003      IF(M(0) .GE. 100000000) M(0) = M(0) - 100000000
2004      IF(M(0) .GE. 100000000) M(0) = M(0) - 100000000
2005
2006      M(1) = M(2)
2007      M(2) = M(3)
2008      M(3) = M(0)
2009
2010  C   URN01 = 1.0E-08 * M(0)
2011  C   URNSS = 1.0E-08 * M(0) - 0.5
2012
2013      RETURN
2014      END
2015
2016
2017
2018
2019      FUNCTION URNAB(A,B)
2020  C-----
2021  C   URNAB returns uniformly distributed random numbers on [A,B]
2022
2023  comt URNAB = A + (B-A) * URN01()
2024      URNAB = A + (B-A) * ( URN55() + 0.5 )
2025
2026      RETURN
2027      END
2028
2029
2030

```

```

2031
2032      FUNCTION URN55 ()
2033 C-----
2034 --
2035 C      RETURN UNIFORMLY DISTRIBUTED RANDOM NUMBER ON INTERVAL [-.5,+.5]
2036
2037      INCLUDE 'tuba211d.inc'
2038
2039 C      IURN = 1  MARSAGLIA AND BRAY RANDOM NUMBER GENERATOR  (RECOMMENDED)
2040 C      IURN = 2  SWAIN AND SWAIN MACHINE INDEPENDENT RANDOM NUMBER GENERATOR
2041
2042      IF(IURN.EQ.1) URN55 = URNMB ()
2043      IF(IURN.EQ.2) URN55 = URNSS ()
2044
2045      RETURN
2046      END
2047
2048
2049
2050
2051      SUBROUTINE WNRLVY (Z1)
2052 C-----
2053 --
2054 C      NON STATIONARY CASE: WIENER-LEVY SIMULATION OF LINE PROCESS
2055
2056      REAL      Z1 (*)
2057      INCLUDE 'tuba211d.inc'
2058
2059      Z1 (1) = 0.0
2060      W1 = 0.0
2061      AI1 = 0.0
2062      BI1 = 0.0
2063      TT = 0.0
2064      DO 20 N=2, NMAX
2065          DO 10 K=1, KT
2066              TT = TT+DT
2067              W2 = W1 + SG * URN55 ()
2068              AI1 = AI1 + 0.5*(W2+W1)*DT
2069              BI1 = BI1 + 0.5*(W1*(TT-DT)+TT*W2)*DT
2070              W1 = W2
2071      10      CONTINUE
2072              Z1 (N) = B0*W1 + (B1+B2*TT)*AI1 - B2*BI1
2073      20      CONTINUE
2074
2075      RETURN
2076      END
2077
2078
2079
2080
2081      FUNCTION WTEXP (OM, ACL, ASL, AL1, AL2)
2082 C-----
2083 --
2084 C      CALCULATE SPECTRAL DENSITY WEIGHTS FOR EXPONENTIAL AREAL AVERAGE
2085 PROCESS
2086
2087      AS = SIN (AL1*OM*ACL/2.)
2088      BS = SIN (AL2*OM*ASL/2.)
2089
2090      IF(ACL.NE.0. .AND. ASL.NE.0.) THEN
2091          AL12 = AL1*AL1*AL2*AL2
2092          OMOM = OM*OM*OM*OM
2093          A1B1 = ACL*ACL*ASL*ASL
2094          ASBS = AS*AS*BS*BS
2095          ALOA = AL12*OMOM*A1B1
2096          WTEXP = ASBS*(16./ALOA)
2097      END IF
2098

```

```

2099      IF(ACL.EQ.0.) WTEXP = BS*BS*(4./(AL2*AL2*ASL*ASL*OM*OM))
2100      IF(ASL.EQ.0.) WTEXP = AS*AS*(4./(AL1*AL1*ACL*ACL*OM*OM))
2101
2102      RETURN
2103      END
2104
2105
2106
2107
2108      FUNCTION WTUSR(OM,ACL,ASL,AL1,AL2)
2109  C-----
2110  --
2111  C      RETURN SPECTRAL DENSITY WEIGHTS FOR USER-DEFINED AREAL AVERAGE PROCESS
2112
2113      DATA      SOME,THING /0.,1./
2114
2115  C      SEE CHAPTERS 2 AND 5 OF THE DOCUMENTATION
2116      WTUSR = SOME + THING
2117
2118      RETURN
2119

```

# APPENDIX B

## Tables of Simulation Results

---

In this Appendix all simulation results are presented. There are two subsections. At the first numerical results of detection probability of an instantaneous groundwater pollution originating from a point source are presented. At the second subsection results of detection probability of a precipitation triggered pollution originating from a point source are presented. Results presented concern different field heterogeneities ( $\sigma_{\ln K}^2$ ), transverse dispersion coefficients ( $a_T$ ), sampling frequencies and remedial action delay times. Abbreviations referred into Tables are reading as:

<i>nws</i> :	normalized wells space
<i>ndfs</i> :	normalized distance from source
<i>ndfs(max)</i> :	normalized distance from source where detection probability is maximum
$P_d(ED)$ :	Detection probability if sampling is performed Every Day
$P_d(1M)$ :	Detection probability if sampling is performed Monthly
$P_d(2M)$ :	Detection probability if sampling is performed Bimonthly
$P_d(3M)$ :	Detection probability if sampling is performed Quarterly
$P_d(4M)$ :	Detection probability if sampling is performed Every 4Months
$P_d(6M)$ :	Detection probability if sampling is performed Biannually
$P_d(12M)$ :	Detection probability if sampling is performed Annually
<i>RADTi</i> :	<i>Remedial Action Delay Times</i>
<i>NAV</i> :	<i>Not Applicable Value (a computational problem during simulation returned a non valid number)</i>

## B.1 Instantaneous Pollution

**Table B.1:** Detection probability in case of  $\sigma_{\ln K}^2 = 0.0$  and  $\sigma_{\ln K}^2 = 0.5$ , for different sampling frequencies

		$\sigma_{\ln K}^2$																
		0.00								0.50								
$\alpha$ (m)	rms	No Wells	rdfs(max)	$P_d$ (ED)	$P_d$ (1M)	$P_d$ (2M)	$P_d$ (3M)	$P_d$ (4M)	$P_d$ (6M)	$P_d$ (12M)	rdfs(max)	$P_d$ (ED)	$P_d$ (1M)	$P_d$ (2M)	$P_d$ (3M)	$P_d$ (4M)	$P_d$ (6M)	$P_d$ (12M)
0.001	1.00	1	3.00	4.2	4.2	4.2	4.2	4.1	3.9	3.0	1.75	4.5	4.5	4.4	4.5	4.3	4.2	3.1
	0.50	2	3.00	8.5	8.2	8.2	8.0	7.9	7.6	6.1	1.75	8.1	8.1	8.0	7.8	7.8	7.4	5.6
	0.33	3	3.00	13.3	13.2	13.1	13.1	12.8	12.4	10.1	1.75	11.5	11.4	11.3	11.3	11.0	10.6	7.8
	0.25	4	3.00	16.9	16.8	16.5	16.4	16.1	16.0	12.4	1.75	14.5	14.2	14.1	14.0	13.8	13.2	9.2
	0.17	6	3.00	25.3	24.8	24.6	24.3	24.0	23.3	18.3	1.75	21.0	20.7	20.6	20.3	20.2	19.3	14.1
	0.12	8	3.00	33.0	32.6	32.3	32.2	31.8	31.5	24.4	1.75	28.1	27.7	27.5	27.2	26.6	25.7	18.2
	0.08	12	3.00	49.1	48.8	48.4	48.0	47.4	46.6	36.3	1.75	42.0	41.5	41.1	40.8	40.3	38.3	28.1
	0.05	20	3.00	82.7	81.8	81.0	80.4	79.6	77.8	61.0	1.75	64.2	63.7	63.2	62.7	62.0	59.8	44.4
0.010	1.00	1	2.25	6.0	5.7	5.6	5.5	5.4	5.4	4.9	1.50	5.4	5.2	5.2	5.2	5.1	5.0	4.5
	0.50	2	2.25	12.0	11.6	11.3	11.3	10.8	10.8	10.2	1.50	10.9	10.6	10.5	10.3	10.2	10.0	8.9
	0.33	3	2.25	18.9	18.2	17.8	17.5	17.1	16.9	15.9	1.50	15.1	14.5	14.3	14.1	13.9	13.6	11.8
	0.25	4	2.25	23.9	23.3	23.0	22.8	22.5	22.1	20.4	1.50	20.7	20.2	19.9	19.6	19.3	18.9	16.6
	0.17	6	2.25	35.4	34.3	33.6	33.4	32.7	32.3	29.8	1.50	30.7	29.5	29.0	28.6	28.2	27.5	24.1
	0.12	8	2.25	47.2	45.5	44.8	44.2	43.3	42.8	39.9	1.50	41.5	39.7	38.9	38.3	37.9	37.1	32.7
	0.08	12	2.25	70.5	68.5	67.4	66.7	65.8	64.8	59.5	1.50	57.0	55.5	54.5	53.5	53.1	51.8	46.7
	0.05	20	2.25	99.6	99.5	99.4	99.4	99.3	99.3	95.1	1.50	77.2	75.9	75.0	74.2	73.5	72.7	66.8
0.02	1.00	1	1.50	5.8	5.6	5.5	5.4	5.3	5.2	4.5	0.50	5.9	5.9	5.9	5.7	5.7	5.6	4.5
	0.50	2	1.50	11.7	11.1	10.7	10.4	10.3	10.0	8.8	0.50	11.6	11.2	11.1	11.0	10.9	10.8	8.8
	0.33	3	1.50	18.2	17.5	17.0	16.7	16.3	15.9	14.0	0.50	16.9	16.6	16.4	15.9	16.0	15.5	12.8
	0.25	4	1.50	23.5	22.2	21.9	21.5	21.2	20.8	19.2	0.50	22.1	21.2	20.9	20.7	20.4	20.1	17.0
	0.17	6	1.50	34.6	32.9	31.8	31.2	31.0	30.2	27.4	0.50	33.2	32.4	32.0	31.7	31.2	30.8	25.8
	0.12	8	1.50	46.3	43.9	43.0	42.1	41.5	40.2	36.5	0.50	43.6	42.0	41.5	40.9	40.7	39.5	33.8
	0.08	12	1.50	69.0	65.6	64.5	63.2	62.4	60.3	55.0	0.50	61.9	60.0	59.2	58.7	58.0	57.0	48.6
	0.05	20	1.50	99.4	99.3	99.0	98.7	98.5	97.1	89.4	0.50	84.4	83.0	82.2	81.9	81.6	80.8	71.8
0.05	1.00	1	0.50	5.8	5.5	5.2	5.3	5.1	4.9	4.4	0.50	5.6	5.0	4.7	4.5	4.2	4.0	3.0
	0.50	2	0.50	11.6	10.8	10.4	10.4	10.2	9.7	8.2	0.50	10.8	9.6	9.2	8.8	8.6	8.2	5.9
	0.33	3	0.50	18.2	17.3	16.7	16.3	16.3	15.6	13.9	0.50	14.9	13.6	12.9	12.6	12.0	11.5	8.9
	0.25	4	0.50	23.5	22.3	21.3	21.2	20.8	20.0	17.6	0.50	19.8	17.8	17.1	16.4	15.8	14.7	11.5
	0.17	6	0.50	34.1	31.9	31.0	30.6	30.2	29.0	25.3	0.50	29.9	27.0	25.5	24.7	24.0	22.8	17.0
	0.12	8	0.50	45.8	43.2	42.2	41.3	40.5	39.4	34.7	0.50	39.1	35.1	33.7	33.0	31.5	29.7	23.4
	0.08	12	0.50	69.0	65.1	63.0	61.9	60.7	59.0	52.3	0.50	55.7	50.2	48.0	46.2	44.4	41.8	33.2
	0.05	20	0.50	99.4	98.9	98.1	97.4	96.5	94.9	84.7	0.50	78.2	73.4	70.9	69.2	67.4	64.5	51.7
0.10	1.00	1	0.125	5.7	5.3	5.1	4.9	5.0	4.7	4.4	0.125	6.4	5.9	5.6	5.3	5.2	4.8	4.0
	0.50	2	0.125	11.3	10.4	10.1	9.8	9.7	9.5	8.2	0.125	10.3	9.2	9.0	8.5	8.7	8.1	6.7
	0.33	3	0.125	18.1	16.9	16.4	15.9	16.0	15.3	13.9	0.125	16.2	14.9	14.4	13.9	13.5	12.9	10.3
	0.25	4	0.125	23.2	21.7	21.1	20.8	20.4	19.8	17.2	0.125	20.0	18.0	17.2	16.5	16.4	15.3	12.7
	0.17	6	0.125	33.9	31.8	30.9	30.0	29.5	28.6	25.1	0.125	30.3	28.0	27.1	26.0	25.7	24.3	19.9
	0.12	8	0.125	45.8	42.6	41.4	40.7	39.9	38.8	34.1	0.125	42.2	38.4	37.1	35.9	36.0	33.8	27.6
	0.08	12	0.125	67.9	63.7	62.0	60.5	59.8	57.5	51.1	0.125	62.2	56.4	54.6	52.3	51.8	48.7	39.8
	0.05	20	0.125	99.1	97.3	96.0	95.1	93.9	92.3	83.6	0.125	87.0	81.9	79.9	77.9	76.5	73.2	60.7
0.20	1.00	1	0.030	4.7	4.1	3.8	3.6	3.6	3.3	2.7	0.030	4.8	4.2	4.1	4.0	3.9	3.7	2.7
	0.50	2	0.030	8.4	7.4	7.0	6.7	6.5	6.3	4.8	0.030	7.9	6.8	6.4	6.1	5.9	5.4	3.9
	0.33	3	0.030	14.3	12.3	11.6	10.9	11.0	10.1	8.1	0.030	12.9	11.2	10.9	10.6	10.4	9.8	7.2
	0.25	4	0.030	18.0	15.2	14.4	13.7	13.6	12.5	9.4	0.030	15.3	13.5	12.9	12.3	12.0	11.5	8.0
	0.17	6	0.030	26.1	22.5	21.2	20.5	19.5	19.2	14.6	0.030	24.1	20.2	19.2	18.6	17.9	16.7	11.7
	0.12	8	0.030	36.1	30.7	29.1	27.9	27.5	26.1	20.0	0.030	32.5	28.5	27.1	25.9	25.4	23.2	16.2
	0.08	12	0.030	53.9	46.0	44.3	42.1	42.0	39.1	30.2	0.030	48.3	42.3	40.5	39.2	37.9	35.9	25.3
	0.05	20	0.030	80.8	70.9	68.2	65.9	64.8	62.1	47.7	0.030	69.6	61.7	59.7	58.0	56.6	53.3	37.4
0.50	1.00	1	0.015	2.4	2.2	1.9	1.9	1.9	1.7	0.1	0.015	3.0	2.6	2.4	2.2	2.1	1.8	0.9
	0.50	2	0.015	4.9	4.1	3.9	3.7	3.7	3.4	0.3	0.015	4.5	3.7	3.4	3.3	3.2	2.5	1.0
	0.33	3	0.015	7.3	6.2	5.8	5.6	5.5	5.0	0.4	0.015	7.8	6.9	6.6	6.2	5.9	4.9	1.8
	0.25	4	0.015	8.6	7.2	6.8	6.7	6.5	6.0	0.8	0.015	7.8	6.6	6.1	6.0	5.7	4.9	1.5
	0.17	6	0.015	13.7	11.5	11.1	10.7	10.5	9.8	0.8	0.015	13.5	10.9	10.5	10.0	9.3	7.8	2.8
	0.12	8	0.015	18.2	15.1	14.4	13.7	13.5	12.5	1.3	0.015	18.0	15.1	14.4	13.7	13.0	10.6	3.4
	0.08	12	0.015	27.6	23.9	22.5	22.2	21.3	19.8	2.4	0.015	27.5	22.6	21.3	20.5	19.5	16.1	5.6
	0.05	20	0.015	40.5	36.7	35.0	34.2	33.4	31.0	3.1	0.015	38.2	34.0	32.8	31.7	30.0	25.4	8.7

**Table B.2:** Detection probability in case of  $\sigma_{\ln K}^2 = 1.0$  and  $\sigma_{\ln K}^2 = 1.5$ , for different sampling frequencies

		$\sigma_{\ln K}^2$																									
		<b>1.00</b>										<b>1.50</b>															
err(m)	nws	$\sigma_{\ln K}^2$		1M		2M		3M		4M		6M		12M		1M		2M		3M		4M		6M		12M	
		No Wells	nfds(max)	Pd (ED)	Pd (1M)	Pd (2M)	Pd (3M)	Pd (4M)	Pd (6M)	Pd (12M)	nfds(max)	Pd (ED)	Pd (1M)	Pd (2M)	Pd (3M)	Pd (4M)	Pd (6M)	Pd (12M)									
<b>0.001</b>	<b>1.00</b>	<b>1</b>	1.75	3.8	3.8	3.8	3.7	3.7	3.6	2.7	1.25	3.9	3.8	3.8	3.7	3.3	2.5										
	<b>0.50</b>	<b>2</b>	1.75	7.1	7.0	6.9	6.8	6.8	6.5	5.0	1.25	7.2	7.2	7.1	7.0	6.7	6.4	4.8									
	<b>0.33</b>	<b>3</b>	1.75	9.8	9.7	9.6	9.5	9.4	9.1	6.9	1.25	9.4	9.3	9.2	9.1	8.8	8.0	6.1									
	<b>0.25</b>	<b>4</b>	1.75	14.0	13.8	13.5	13.4	13.0	12.4	9.5	1.25	13.3	13.2	13.1	12.7	11.5	8.2										
	<b>0.17</b>	<b>6</b>	1.75	20.6	20.3	20.1	19.8	19.6	18.5	14.2	1.25	20.9	20.7	20.4	19.9	18.1	13.7										
	<b>0.12</b>	<b>8</b>	1.75	26.5	26.1	25.9	25.5	25.4	24.1	17.6	1.25	25.7	25.3	24.8	24.4	23.5	21.9	16.2									
	<b>0.08</b>	<b>12</b>	1.75	39.9	39.3	38.8	38.5	37.6	36.2	27.8	1.25	35.6	35.2	34.9	34.3	33.8	31.0	23.0									
	<b>0.05</b>	<b>20</b>	1.75	57.2	56.4	55.9	55.2	54.8	52.5	41.5	1.25	54.9	54.4	54.0	52.8	52.3	48.1	36.0									
<b>0.010</b>	<b>1.00</b>	<b>1</b>	1.25	5.7	5.3	5.2	5.2	5.1	5.0	4.0	1.00	5.0	4.7	4.7	4.6	4.6	4.3	3.4									
	<b>0.50</b>	<b>2</b>	1.25	9.5	9.1	8.8	8.7	8.5	8.2	6.9	1.00	9.0	8.6	8.3	8.2	7.9	7.8	6.1									
	<b>0.33</b>	<b>3</b>	1.25	14.7	14.0	13.6	13.4	13.2	12.8	10.4	1.00	13.5	12.9	12.7	12.4	12.2	11.4	9.1									
	<b>0.25</b>	<b>4</b>	1.25	18.1	17.5	17.1	16.7	16.5	16.0	13.1	1.00	16.9	16.3	15.8	15.7	15.4	14.6	11.6									
	<b>0.17</b>	<b>6</b>	1.25	27.4	26.3	25.6	25.0	24.5	23.8	19.9	1.00	24.2	23.0	22.4	21.9	21.4	20.7	16.1									
	<b>0.12</b>	<b>8</b>	1.25	35.7	34.4	33.6	32.9	32.6	31.3	25.6	1.00	33.2	31.8	30.9	30.7	30.0	28.7	22.4									
	<b>0.08</b>	<b>12</b>	1.25	50.4	48.4	47.8	46.7	46.2	45.2	37.5	1.00	45.8	44.4	43.4	43.0	42.3	40.1	32.5									
	<b>0.05</b>	<b>20</b>	1.25	68.8	66.7	65.7	64.7	64.3	62.4	53.6	1.00	61.6	59.9	59.0	58.8	57.7	56.2	46.7									
<b>0.02</b>	<b>1.00</b>	<b>1</b>	0.50	6.3	5.9	5.7	5.7	5.6	5.3	4.5	0.50	5.7	5.4	5.4	5.3	5.2	4.6	3.9									
	<b>0.50</b>	<b>2</b>	0.50	10.1	9.7	9.6	9.5	9.3	8.9	7.3	0.50	9.7	9.3	9.2	9.0	8.9	8.3	6.8									
	<b>0.33</b>	<b>3</b>	0.50	17.0	16.2	15.9	15.7	15.5	14.8	12.0	0.50	14.8	14.0	13.6	13.5	13.0	12.2	10.0									
	<b>0.25</b>	<b>4</b>	0.50	20.5	19.7	19.3	19.2	18.9	18.6	15.4	0.50	18.9	18.2	17.8	17.4	17.2	16.2	12.7									
	<b>0.17</b>	<b>6</b>	0.50	28.5	27.5	26.9	26.6	26.0	25.0	20.7	0.50	28.1	26.9	26.6	26.3	25.8	24.5	20.0									
	<b>0.12</b>	<b>8</b>	0.50	42.1	40.8	39.9	39.3	38.6	37.0	29.9	0.50	36.7	35.3	34.3	33.8	33.2	31.6	25.2									
	<b>0.08</b>	<b>12</b>	0.50	57.5	55.6	54.7	53.9	53.5	52.2	44.1	0.50	50.0	48.4	47.5	46.8	46.2	43.6	35.5									
	<b>0.05</b>	<b>20</b>	0.50	77.0	75.5	74.6	74.2	73.5	72.0	61.9	0.50	69.1	67.1	66.2	65.5	64.8	62.7	52.8									
<b>0.05</b>	<b>1.00</b>	<b>1</b>	0.13	5.7	5.6	5.5	5.4	5.1	5.0	3.7	0.13	5.5	5.2	5.1	4.9	4.8	4.6	3.8									
	<b>0.50</b>	<b>2</b>	0.13	11.6	11.2	11.1	10.9	10.7	10.4	8.4	0.13	11.3	10.7	10.4	10.4	10.0	9.7	8.1									
	<b>0.33</b>	<b>3</b>	0.13	17.0	16.5	16.2	16.0	15.4	14.8	11.9	0.13	14.9	14.5	14.2	13.9	13.8	13.2	11.2									
	<b>0.25</b>	<b>4</b>	0.13	22.0	21.3	21.0	20.7	20.4	19.6	16.9	0.13	19.3	18.4	17.9	17.6	17.4	16.5	13.6									
	<b>0.17</b>	<b>6</b>	0.13	33.3	31.9	31.2	30.8	30.2	29.2	23.7	0.13	31.8	30.4	29.5	29.6	28.3	27.4	22.8									
	<b>0.12</b>	<b>8</b>	0.13	43.5	42.1	41.5	40.9	40.3	39.0	32.7	0.13	40.1	38.6	37.8	37.4	36.9	35.1	29.2									
	<b>0.08</b>	<b>12</b>	0.13	61.8	59.7	59.1	58.3	57.5	55.8	47.1	0.13	57.6	55.4	54.4	53.7	52.7	50.5	41.7									
	<b>0.05</b>	<b>20</b>	0.13	86.3	84.7	84.2	83.1	82.9	80.6	68.7	0.13	81.6	79.6	78.3	78.0	76.8	74.0	63.3									
<b>0.10</b>	<b>1.00</b>	<b>1</b>	0.063	5.4	5.1	5.1	4.8	4.8	4.6	3.7	0.063	6.1	5.6	5.4	5.3	5.1	4.8	3.8									
	<b>0.50</b>	<b>2</b>	0.063	11.1	10.2	9.9	9.7	9.5	9.0	7.3	0.063	10.3	9.5	9.1	8.8	8.5	8.1	6.3									
	<b>0.33</b>	<b>3</b>	0.063	17.1	15.9	15.8	15.2	14.9	14.1	10.9	0.063	15.8	14.3	13.9	13.6	13.2	12.4	9.9									
	<b>0.25</b>	<b>4</b>	0.063	21.6	20.4	19.9	19.6	19.0	18.1	14.3	0.063	19.9	18.6	18.1	17.5	17.1	16.0	11.9									
	<b>0.17</b>	<b>6</b>	0.063	31.6	29.4	28.5	27.6	27.1	25.5	19.7	0.063	29.7	27.1	26.3	25.2	24.6	23.0	18.1									
	<b>0.12</b>	<b>8</b>	0.063	43.2	40.0	38.6	37.8	36.8	34.8	27.6	0.063	40.0	36.5	35.3	34.0	33.4	31.5	25.0									
	<b>0.08</b>	<b>12</b>	0.063	60.8	56.5	54.8	53.7	52.5	49.5	38.8	0.063	57.6	54.2	52.4	51.0	49.8	46.2	35.5									
	<b>0.05</b>	<b>20</b>	0.063	86.2	82.7	81.0	79.5	78.5	74.9	59.3	0.063	80.8	76.9	75.5	73.8	72.4	68.7	53.2									
<b>0.20</b>	<b>1.00</b>	<b>1</b>	0.030	4.0	3.4	3.2	3.0	3.0	2.7	1.7	0.015	4.1	3.4	3.1	2.9	2.8	2.5	1.5									
	<b>0.50</b>	<b>2</b>	0.030	7.7	6.5	6.2	6.1	5.6	5.2	3.5	0.015	8.4	7.3	7.0	6.8	6.4	5.8	4.0									
	<b>0.33</b>	<b>3</b>	0.030	12.8	11.2	10.6	10.3	10.0	9.2	5.9	0.015	12.1	10.6	9.8	9.4	8.8	8.2	5.3									
	<b>0.25</b>	<b>4</b>	0.030	16.6	14.5	13.9	13.2	13.1	11.8	8.2	0.015	15.2	13.3	12.7	12.1	11.5	10.4	7.2									
	<b>0.17</b>	<b>6</b>	0.030	22.0	19.2	18.0	17.8	16.7	15.6	10.0	0.015	23.3	20.1	19.2	18.1	17.1	15.6	10.5									
	<b>0.12</b>	<b>8</b>	0.030	31.1	26.6	25.3	24.5	23.2	21.3	14.7	0.015	31.3	27.7	25.9	25.4	23.7	21.6	14.4									
	<b>0.08</b>	<b>12</b>	0.030	44.7	38.6	37.0	35.8	34.3	31.7	21.0	0.015	46.2	40.4	38.4	37.3	35.0	31.7	21.5									
	<b>0.05</b>	<b>20</b>	0.030	64.6	57.8	55.6	53.6	52.7	48.0	32.8	0.015	65.3	58.8	56.8	54.8	52.1	47.6	32.9									
<b>0.50</b>	<b>1.00</b>	<b>1</b>	0.015	2.2	2.0	1.9	1.6	1.5	1.2	0.4	0.015	1.9	1.4	1.4	1.3	1.2	0.9	0.4									
	<b>0.50</b>	<b>2</b>	0.015	4.2	3.6	3.4	3.2	3.0	2.4	0.7	0.015	4.4	3.7	3.4	3.2	2.9	2.1	1.2									
	<b>0.33</b>	<b>3</b>	0.015	7.7	6.7	6.4	5.8	5.4	4.1	1.6	0.015	6.4	5.4	5.1	4.7	4.4	3.3	1.7									
	<b>0.25</b>	<b>4</b>	0.015	9.0	7.5	7.0	6.5	6.1	4.8	2.1	0.015	8.2	7.1	6.8	6.3	5.6	4.6	2.4									
	<b>0.17</b>	<b>6</b>	0.015	12.7	10.9	10.4	9.7	9.3	7.2	2.7	0.015	12.5	10.6	9.9	9.1	8.4	6.2	3.3									
	<b>0.12</b>	<b>8</b>	0.015	18.1	15.6	14.4	13.4	12.2	9.5	4.0	0.015	16.5	14.3	13.2	12.2	11.0	8.6	4.2									
	<b>0.08</b>	<b>12</b>	0.015	25.3	21.6	20.5	19.0	17.8	14.0	5.7	0.015	24.9	21.0	19.9	18.0	16.3	13.0	6.4									
	<b>0.05</b>	<b>20</b>	0.015	36.9	32.9	31.5	29.8	28.0	22.3	9.2	0.015	34.6	30.8	29.6	27.4	24.9	20.4	9.9									

**Table B.3** Detection probability in case of  $\sigma_{\ln K}^2 = 2.0$ , for different sampling frequencies

		$\sigma_{\ln K}^2$		2.00							
$\alpha$ (m)	nws	No Wells	nfds(max)	P <sub>d</sub> (ED)	P <sub>d</sub> (1M)	P <sub>d</sub> (2M)	P <sub>d</sub> (3M)	P <sub>d</sub> (4M)	P <sub>d</sub> (6M)	P <sub>d</sub> (12M)	
0.001	1.00	1	0.75	3.4	3.4	3.3	3.3	3.1	2.8	1.7	
	0.50	2	0.75	6.8	6.7	6.7	6.4	6.0	5.6	3.9	
	0.33	3	0.75	9.2	9.1	8.8	8.5	8.2	7.2	5.1	
	0.25	4	0.75	11.9	11.8	11.5	11.0	10.6	9.7	6.7	
	0.17	6	0.75	19.3	18.9	18.6	18.1	17.3	15.6	11.1	
	0.12	8	0.75	24.3	23.9	23.4	22.6	21.6	19.6	14.3	
	0.08	12	0.75	34.2	33.6	32.8	31.8	30.4	27.6	19.5	
	0.05	20	0.75	53.1	52.3	51.6	49.9	47.6	43.4	30.6	
0.010	1.00	1	0.50	5.3	5.1	5.1	5.1	4.8	4.7	3.3	
	0.50	2	0.50	8.0	7.9	7.8	7.7	7.6	7.1	5.8	
	0.33	3	0.50	14.2	13.9	13.8	13.6	13.1	12.4	9.7	
	0.25	4	0.50	16.8	16.5	16.2	16.0	15.8	14.9	12.0	
	0.17	6	0.50	23.8	23.2	22.7	22.5	22.1	20.9	16.9	
	0.12	8	0.50	32.3	31.6	31.1	30.7	30.0	28.4	22.8	
	0.08	12	0.50	46.8	45.8	45.2	44.4	43.6	40.9	33.6	
	0.05	20	0.50	64.7	63.4	62.7	62.1	61.1	58.2	47.5	
0.02	1.00	1	0.25	5.0	4.9	4.8	4.7	4.7	4.6	3.8	
	0.50	2	0.25	10.4	10.0	9.7	9.5	9.4	8.9	7.1	
	0.33	3	0.25	13.5	13.0	12.9	12.7	12.4	12.0	9.7	
	0.25	4	0.25	17.7	17.2	16.7	16.7	16.2	15.4	12.3	
	0.17	6	0.25	28.0	27.1	26.7	26.0	25.7	24.4	19.8	
	0.12	8	0.25	36.7	35.3	34.5	34.3	33.3	31.6	25.4	
	0.08	12	0.25	50.6	49.1	48.1	47.6	46.2	44.0	35.5	
	0.05	20	0.25	71.7	70.2	69.0	68.6	67.0	64.6	54.4	
0.05	1.00	1	0.13	5.1	4.9	4.7	4.6	4.4	4.1	3.0	
	0.50	2	0.13	10.6	9.9	9.6	9.4	9.1	8.4	7.0	
	0.33	3	0.13	14.0	13.4	13.0	12.6	12.4	11.5	9.0	
	0.25	4	0.13	19.9	19.2	18.9	18.7	18.1	17.6	13.9	
	0.17	6	0.13	29.8	28.3	27.8	27.0	26.5	24.7	20.3	
	0.12	8	0.13	40.4	38.3	37.5	37.1	36.1	34.3	27.0	
	0.08	12	0.13	56.4	54.2	53.1	52.2	51.2	48.2	39.1	
	0.05	20	0.13	76.9	74.8	73.9	73.1	71.7	68.9	56.9	
0.10	1.00	1	0.063	4.9	4.6	4.4	4.1	4.1	3.9	3.1	
	0.50	2	0.063	10.3	9.6	9.3	9.0	8.6	8.1	6.4	
	0.33	3	0.063	14.7	13.7	13.0	12.4	12.2	11.5	8.4	
	0.25	4	0.063	19.2	17.9	17.3	16.6	15.8	14.6	10.5	
	0.17	6	0.063	28.9	26.6	25.7	25.0	24.0	22.7	17.2	
	0.12	8	0.063	37.5	34.7	33.2	32.4	31.2	29.2	22.7	
	0.08	12	0.063	54.5	50.4	48.9	47.1	45.6	42.7	32.5	
	0.05	20	0.063	74.7	71.1	69.4	67.8	65.9	61.9	47.9	
0.20	1.00	1	0.015	3.8	3.5	3.4	3.2	3.0	2.7	1.9	
	0.50	2	0.015	7.8	6.8	6.3	6.0	5.6	5.2	3.8	
	0.33	3	0.015	12.2	10.4	10.0	9.4	8.9	7.9	5.1	
	0.25	4	0.015	15.5	13.2	12.4	11.8	11.0	9.6	6.0	
	0.17	6	0.015	22.0	19.0	17.8	16.6	15.8	14.3	9.7	
	0.12	8	0.015	29.2	24.8	23.4	22.2	21.2	18.6	12.6	
	0.08	12	0.015	44.0	38.2	36.2	34.8	33.0	29.4	18.6	
	0.05	20	0.015	62.3	55.6	53.0	50.9	48.6	43.4	29.9	
0.50	1.00	1	0.015	2.1	1.8	1.7	1.5	1.4	1.0	0.7	
	0.50	2	0.015	4.6	3.8	3.2	2.9	2.7	2.2	1.4	
	0.33	3	0.015	6.8	5.4	4.9	4.4	4.0	3.1	1.8	
	0.25	4	0.015	8.9	7.8	7.3	6.5	6.0	4.3	1.7	
	0.17	6	0.015	12.0	10.0	8.9	8.0	7.3	5.6	3.4	
	0.12	8	0.015	16.6	13.9	12.5	11.8	10.6	8.4	4.6	
	0.08	12	0.015	25.4	22.1	20.5	19.2	17.5	13.5	6.0	
	0.05	20	0.015	34.7	30.6	28.9	26.8	24.6	19.3	9.9	

**Table B.4:** Detection probability, average detection time, contaminated area in case of detection failure and relative contaminated area to control area  $L$  for various RADTi in case of  $\sigma_{InK}^2 = 0.0$  assuming daily (ED) and monthly (1M) sampling frequencies

$\sigma_{InK}^2$		0.00																				
$\alpha_1(m)$	now	Infs(max)	$P_d$ (ED)	$\langle T_{(DET.)} \rangle$ (DAYS)	AREA ON FAILURE	(AREA ON DET.)/L	(3M. RADTi)/L	(6M. RADTi)/L	(12M. RADTi)/L	(24M. RADTi)/L	(36M. RADTi)/L	$P_d$ (1M)	$\langle T_{(DET.)} \rangle$ (DAYS)	AREA ON FAILURE	(AREA ON DET.)/L	(3M. RADTi)/L	(6M. RADTi)/L	(12M. RADTi)/L	(24M. RADTi)/L	(36M. RADTi)/L		
0.001	1	3.00	4.2	9495	0.03	0.02	0.02	0.03	0.03	0.03	0.02	4.2	9513	0.03	0.02	0.02	0.03	0.03	0.03	0.03	0.02	
	2	3.00	8.5	9529	0.03	0.03	0.03	0.03	0.03	0.03	0.02	8.2	9542	0.03	0.03	0.03	0.03	0.03	0.03	0.03	0.02	
	3	3.00	13.3	9524	0.03	0.02	0.03	0.03	0.03	0.03	0.02	13.2	9540	0.03	0.03	0.03	0.03	0.03	0.03	0.03	0.02	
	4	3.00	16.9	9562	0.03	0.03	0.03	0.03	0.03	0.03	0.02	16.8	9578	0.03	0.03	0.03	0.03	0.03	0.03	0.03	0.02	
	6	3.00	25.3	9530	0.03	0.03	0.03	0.03	0.03	0.03	0.02	24.8	9541	0.03	0.03	0.03	0.03	0.03	0.03	0.03	0.02	
	8	3.00	33.0	9520	0.03	0.03	0.03	0.03	0.03	0.03	0.02	32.6	9534	0.03	0.03	0.03	0.03	0.03	0.03	0.03	0.02	
	12	3.00	49.1	9524	0.03	0.03	0.03	0.03	0.03	0.03	0.02	48.8	9538	0.03	0.03	0.03	0.03	0.03	0.03	0.03	0.02	
	20	3.00	82.7	9524	0.03	0.03	0.03	0.03	0.03	0.03	0.02	81.8	9539	0.03	0.03	0.03	0.03	0.03	0.03	0.03	0.02	
	0.01	1	2.25	6.0	7173	0.18	0.13	0.13	0.13	0.13	0.14	0.14	5.7	7187	0.18	0.13	0.13	0.13	0.13	0.13	0.14	0.14
		2	2.25	12.0	7196	0.18	0.13	0.13	0.13	0.13	0.14	0.14	11.6	7214	0.18	0.13	0.13	0.13	0.13	0.13	0.14	0.14
3		2.25	18.9	7196	0.18	0.13	0.13	0.13	0.13	0.14	0.14	18.2	7213	0.18	0.13	0.13	0.13	0.13	0.13	0.14	0.14	
4		2.25	23.9	7222	0.18	0.13	0.13	0.13	0.13	0.14	0.14	23.3	7238	0.18	0.13	0.13	0.13	0.13	0.13	0.14	0.14	
6		2.25	35.4	7201	0.18	0.13	0.13	0.13	0.13	0.14	0.14	34.3	7218	0.18	0.13	0.13	0.13	0.13	0.13	0.14	0.14	
8		2.25	47.2	7196	0.18	0.13	0.13	0.13	0.13	0.14	0.14	45.5	7211	0.18	0.13	0.13	0.13	0.13	0.13	0.14	0.14	
12		2.25	70.5	7193	0.18	0.13	0.13	0.13	0.13	0.14	0.14	68.5	7209	0.18	0.13	0.13	0.13	0.13	0.13	0.14	0.14	
20		2.25	99.6	7176	0.18	0.13	0.13	0.13	0.13	0.14	0.14	99.5	7195	0.18	0.13	0.13	0.13	0.13	0.13	0.14	0.14	
0.02		1	1.50	5.8	4929	0.31	0.16	0.17	0.17	0.17	0.18	0.19	5.6	4940	0.31	0.16	0.17	0.17	0.17	0.17	0.18	0.19
		2	1.50	11.7	4938	0.31	0.16	0.17	0.17	0.17	0.18	0.19	11.1	4959	0.31	0.16	0.17	0.17	0.17	0.17	0.18	0.19
	3	1.50	18.2	4942	0.31	0.16	0.17	0.17	0.17	0.18	0.19	17.5	4962	0.31	0.16	0.17	0.17	0.17	0.17	0.18	0.19	
	4	1.50	23.5	4969	0.31	0.16	0.17	0.17	0.17	0.18	0.19	22.2	4988	0.31	0.16	0.17	0.17	0.17	0.17	0.18	0.19	
	6	1.50	34.6	4948	0.31	0.16	0.17	0.17	0.17	0.18	0.19	32.9	4965	0.31	0.16	0.17	0.17	0.17	0.17	0.18	0.19	
	8	1.50	46.3	4941	0.31	0.16	0.17	0.17	0.17	0.18	0.19	43.9	4961	0.31	0.16	0.17	0.17	0.17	0.17	0.18	0.19	
	12	1.50	69.0	4939	0.31	0.16	0.17	0.17	0.17	0.18	0.19	65.6	4955	0.31	0.16	0.17	0.17	0.17	0.17	0.18	0.19	
	20	1.50	99.4	4929	0.31	0.16	0.17	0.17	0.17	0.18	0.19	99.3	4954	0.31	0.16	0.17	0.17	0.17	0.17	0.18	0.19	
	0.05	1	0.50	5.8	1898	0.63	0.16	0.16	0.17	0.18	0.21	0.23	5.5	1909	0.63	0.16	0.16	0.17	0.18	0.21	0.23	
		2	0.50	11.6	1919	0.63	0.16	0.17	0.17	0.18	0.21	0.23	10.8	1937	0.63	0.16	0.17	0.17	0.18	0.21	0.23	
3		0.50	18.2	1929	0.63	0.16	0.17	0.17	0.18	0.21	0.23	17.3	1943	0.63	0.16	0.17	0.17	0.19	0.21	0.23		
4		0.50	23.5	1959	0.63	0.16	0.17	0.17	0.19	0.21	0.23	22.3	1975	0.63	0.16	0.17	0.18	0.19	0.21	0.23		
6		0.50	34.1	1929	0.63	0.16	0.17	0.17	0.18	0.21	0.23	31.9	1943	0.63	0.16	0.17	0.17	0.19	0.21	0.23		
8		0.50	45.8	1924	0.63	0.16	0.17	0.17	0.18	0.21	0.23	43.2	1941	0.63	0.16	0.17	0.17	0.19	0.21	0.23		
12		0.50	69.0	1923	0.63	0.16	0.17	0.17	0.18	0.21	0.23	65.1	1941	0.63	0.16	0.17	0.17	0.19	0.21	0.23		
20		0.50	99.4	1920	0.64	0.16	0.17	0.17	0.18	0.21	0.23	98.9	1947	0.64	0.16	0.17	0.17	0.19	0.21	0.23		
0.10		1	0.125	5.7	739	1.06	0.13	0.14	0.15	0.18	0.22	0.27	5.3	760	1.06	0.13	0.14	0.16	0.18	0.23	0.27	
		2	0.125	11.3	778	1.06	0.13	0.15	0.16	0.18	0.23	0.27	10.4	786	1.06	0.13	0.15	0.16	0.18	0.23	0.27	
	3	0.125	18.1	772	1.06	0.13	0.14	0.16	0.18	0.23	0.27	16.9	781	1.06	0.13	0.15	0.16	0.18	0.23	0.27		
	4	0.125	23.2	803	1.06	0.14	0.15	0.16	0.19	0.23	0.28	21.7	813	1.06	0.14	0.15	0.16	0.19	0.23	0.28		
	6	0.125	33.9	784	1.06	0.13	0.15	0.16	0.18	0.23	0.27	31.8	793	1.06	0.13	0.15	0.16	0.18	0.23	0.28		
	8	0.125	45.8	776	1.06	0.13	0.15	0.16	0.18	0.23	0.27	42.6	787	1.06	0.13	0.15	0.16	0.18	0.23	0.27		
	12	0.125	67.9	772	1.06	0.13	0.14	0.16	0.18	0.23	0.27	63.7	784	1.06	0.13	0.15	0.16	0.18	0.23	0.27		
	20	0.125	99.1	772	1.06	0.13	0.14	0.16	0.18	0.23	0.27	97.3	788	1.06	0.13	0.15	0.16	0.18	0.23	0.27		
	0.20	1	0.030	4.7	374	1.70	0.13	0.15	0.18	0.22	0.31	0.39	4.1	356	1.70	0.12	0.15	0.17	0.22	0.31	0.39	
		2	0.030	8.4	356	1.70	0.12	0.15	0.17	0.22	0.31	0.39	7.4	331	1.70	0.11	0.14	0.17	0.21	0.30	0.38	
3		0.030	14.3	378	1.70	0.13	0.15	0.18	0.23	0.31	0.39	12.3	353	1.70	0.12	0.15	0.17	0.22	0.31	0.39		
4		0.030	18.0	414	1.70	0.14	0.16	0.19	0.23	0.32	0.40	15.2	380	1.70	0.13	0.15	0.18	0.23	0.31	0.39		
6		0.030	26.1	386	1.70	0.13	0.15	0.18	0.23	0.31	0.39	22.5	355	1.70	0.12	0.15	0.17	0.22	0.31	0.39		
8		0.030	36.1	394	1.70	0.13	0.16	0.18	0.23	0.32	0.39	30.7	362	1.70	0.12	0.15	0.17	0.22	0.31	0.39		
12		0.030	53.9	385	1.70	0.13	0.15	0.18	0.23	0.31	0.39	46.0	352	1.70	0.12	0.15	0.17	0.22	0.31	0.39		
20		0.030	80.8	394	1.71	0.13	0.16	0.18	0.23	0.32	0.39	70.9	355	1.71	0.12	0.15	0.17	0.22	0.31	0.39		
0.50		1	0.015	2.4	93	2.94	0.08	0.15	0.21	0.32	0.51	0.68	2.2	104	2.94	0.09	0.16	0.22	0.33	0.52	0.68	
		2	0.015	4.9	96	2.94	0.08	0.15	0.21	0.32	0.51	0.68	4.1	94	2.94	0.09	0.15	0.21	0.32	0.51	0.68	
	3	0.015	7.3	104	2.94	0.09	0.16	0.22	0.33	0.51	0.68	6.2	102	2.94	0.09	0.16	0.22	0.33	0.51	0.68		
	4	0.015	8.6	102	2.95	0.09	0.16	0.22	0.33	0.51	0.68	7.2	104	2.94	0.09	0.16	0.22	0.33	0.51	0.68		
	6	0.015	13.7	97	2.95	0.09	0.15	0.21	0.32	0.51	0.68	11.5	94	2.95	0.09	0.15	0.21	0.32	0.51	0.68		
	8	0.015	18.2	107	2.96	0.09	0.16	0.22	0.33	0.52	0.68	15.1	99	2.95	0.09	0.16	0.22	0.32	0.51	0.68		
	12	0.015	27.6	98	2.97	0.09	0.15	0.21	0.32	0.51	0.68	23.9	100	2.96	0.09	0.16	0.22	0.33	0.51	0.68		
	20	0.015	40.5	94	2.99	0.08	0.15	0.21	0.32	0.51	0.67	36.7	98	2.98	0.09	0.16	0.21	0.32	0.51	0.68		

**Table B.5:** Detection probability, average detection time, contaminated area in case of detection failure and relative contaminated area to control area  $L$  for various RADTi in case of  $\sigma_{lnK}^2 = 0.0$  assuming bimonthly (2M) and quarterly (3M) sampling frequencies

$\sigma_{lnK}^2$		0.00																				
$\alpha_1(m)$	now	infds(max)	$P_d$ (2M)	$\langle T_{(DET.)} \rangle$ (DAYS)	AREA ON FAILURE	(AREA ON DET.)/L	(3M. RADTi)/L	(6M. RADTi)/L	(12M. RADTi)/L	(24M. RADTi)/L	(36M. RADTi)/L	$P_d$ (3M)	$\langle T_{(DET.)} \rangle$ (DAYS)	AREA ON FAILURE	(AREA ON DET.)/L	(3M. RADTi)/L	(6M. RADTi)/L	(12M. RADTi)/L	(24M. RADTi)/L	(36M. RADTi)/L		
0.001	1	3.00	4.2	9528	0.03	0.02	0.02	0.03	0.03	0.03	0.02	4.2	9544	0.03	0.02	0.02	0.03	0.03	0.03	0.03	0.02	
	2	3.00	8.2	9558	0.03	0.03	0.03	0.03	0.03	0.03	0.02	8.0	9572	0.03	0.03	0.03	0.03	0.03	0.03	0.03	0.02	
	3	3.00	13.1	9555	0.03	0.03	0.03	0.03	0.03	0.03	0.02	13.1	9573	0.03	0.03	0.03	0.03	0.03	0.03	0.03	0.02	
	4	3.00	16.5	9596	0.03	0.03	0.03	0.03	0.03	0.03	0.02	16.4	9610	0.03	0.03	0.03	0.03	0.03	0.03	0.03	0.02	
	6	3.00	24.6	9554	0.03	0.03	0.03	0.03	0.03	0.03	0.02	24.3	9571	0.03	0.03	0.03	0.03	0.03	0.03	0.03	0.02	
	8	3.00	32.3	9549	0.03	0.03	0.03	0.03	0.03	0.03	0.02	32.2	9563	0.03	0.03	0.03	0.03	0.03	0.03	0.03	0.02	
	12	3.00	48.4	9553	0.03	0.03	0.03	0.03	0.03	0.03	0.02	48.0	9568	0.03	0.03	0.03	0.03	0.03	0.03	0.03	0.02	
	20	3.00	81.0	9554	0.03	0.03	0.03	0.03	0.03	0.03	0.02	80.4	9568	0.03	0.03	0.03	0.03	0.03	0.03	0.03	0.02	
	0.01	1	2.25	5.6	7200	0.18	0.13	0.13	0.13	0.13	0.14	0.14	5.5	7204	0.18	0.13	0.13	0.13	0.13	0.13	0.14	0.14
		2	2.25	11.3	7227	0.18	0.13	0.13	0.13	0.13	0.14	0.14	11.3	7243	0.18	0.13	0.13	0.13	0.13	0.13	0.14	0.14
3		2.25	17.8	7225	0.18	0.13	0.13	0.13	0.13	0.14	0.14	17.5	7240	0.18	0.13	0.13	0.13	0.13	0.13	0.14	0.14	
4		2.25	23.0	7252	0.18	0.13	0.13	0.13	0.13	0.14	0.14	22.8	7268	0.18	0.13	0.13	0.13	0.13	0.13	0.14	0.14	
6		2.25	33.6	7231	0.18	0.13	0.13	0.13	0.13	0.14	0.14	33.4	7246	0.18	0.13	0.13	0.13	0.13	0.13	0.14	0.14	
8		2.25	44.8	7222	0.18	0.13	0.13	0.13	0.13	0.14	0.14	44.2	7237	0.18	0.13	0.13	0.13	0.13	0.13	0.14	0.14	
12		2.25	67.4	7221	0.18	0.13	0.13	0.13	0.13	0.14	0.14	66.7	7234	0.18	0.13	0.13	0.13	0.13	0.13	0.14	0.14	
20		2.25	99.4	7210	0.18	0.13	0.13	0.13	0.13	0.14	0.14	99.4	7225	0.18	0.13	0.13	0.13	0.13	0.13	0.14	0.14	
0.02		1	1.50	5.5	4953	0.31	0.16	0.17	0.17	0.17	0.18	0.19	5.4	4975	0.31	0.16	0.17	0.17	0.17	0.17	0.18	0.19
		2	1.50	10.7	4974	0.31	0.16	0.17	0.17	0.17	0.18	0.19	10.4	4983	0.31	0.17	0.17	0.17	0.17	0.17	0.18	0.19
	3	1.50	17.0	4973	0.31	0.16	0.17	0.17	0.17	0.18	0.19	16.7	4989	0.31	0.16	0.17	0.17	0.17	0.17	0.18	0.19	
	4	1.50	21.9	5000	0.31	0.17	0.17	0.17	0.17	0.18	0.19	21.5	5010	0.31	0.17	0.17	0.17	0.17	0.18	0.18	0.19	
	6	1.50	31.8	4977	0.31	0.16	0.17	0.17	0.17	0.18	0.19	31.2	4987	0.31	0.17	0.17	0.17	0.17	0.17	0.18	0.19	
	8	1.50	43.0	4974	0.31	0.16	0.17	0.17	0.17	0.18	0.19	42.1	4983	0.31	0.16	0.17	0.17	0.17	0.17	0.18	0.19	
	12	1.50	64.5	4968	0.31	0.16	0.17	0.17	0.17	0.18	0.19	63.2	4979	0.31	0.16	0.17	0.17	0.17	0.17	0.18	0.19	
	20	1.50	99.0	4970	0.31	0.16	0.17	0.17	0.17	0.18	0.19	98.7	4985	0.31	0.16	0.17	0.17	0.17	0.17	0.18	0.19	
	0.05	1	0.50	5.2	1919	0.63	0.16	0.17	0.17	0.18	0.21	0.23	5.3	1929	0.63	0.16	0.17	0.17	0.17	0.18	0.21	0.23
		2	0.50	10.4	1948	0.63	0.16	0.17	0.17	0.19	0.21	0.23	10.4	1959	0.63	0.16	0.17	0.17	0.17	0.19	0.21	0.23
3		0.50	16.7	1957	0.63	0.16	0.17	0.17	0.19	0.21	0.23	16.3	1957	0.63	0.16	0.17	0.17	0.17	0.19	0.21	0.23	
4		0.50	21.3	1979	0.63	0.16	0.17	0.18	0.19	0.21	0.23	21.2	1999	0.63	0.17	0.17	0.17	0.18	0.19	0.21	0.24	
6		0.50	31.0	1954	0.63	0.16	0.17	0.17	0.19	0.21	0.23	30.6	1969	0.63	0.16	0.17	0.17	0.17	0.19	0.21	0.23	
8		0.50	42.2	1954	0.63	0.16	0.17	0.17	0.19	0.21	0.23	41.3	1965	0.63	0.16	0.17	0.17	0.17	0.19	0.21	0.23	
12		0.50	63.0	1949	0.63	0.16	0.17	0.17	0.19	0.21	0.23	61.9	1963	0.63	0.16	0.17	0.17	0.17	0.19	0.21	0.23	
20		0.50	98.1	1959	0.64	0.16	0.17	0.17	0.19	0.21	0.23	97.4	1971	0.64	0.16	0.17	0.17	0.17	0.19	0.21	0.23	
0.10		1	0.125	5.1	771	1.06	0.13	0.14	0.16	0.18	0.23	0.27	4.9	768	1.06	0.13	0.14	0.16	0.18	0.23	0.27	
		2	0.125	10.1	792	1.06	0.13	0.15	0.16	0.18	0.23	0.27	9.8	798	1.06	0.14	0.15	0.16	0.19	0.23	0.28	
	3	0.125	16.4	791	1.06	0.13	0.15	0.16	0.18	0.23	0.27	15.9	792	1.06	0.13	0.15	0.16	0.18	0.23	0.28		
	4	0.125	21.1	822	1.06	0.14	0.15	0.16	0.19	0.23	0.28	20.8	831	1.06	0.14	0.15	0.17	0.19	0.24	0.28		
	6	0.125	30.9	801	1.06	0.14	0.15	0.16	0.19	0.23	0.28	30.0	810	1.06	0.14	0.15	0.16	0.19	0.23	0.28		
	8	0.125	41.4	797	1.06	0.14	0.15	0.16	0.19	0.23	0.28	40.7	803	1.06	0.14	0.15	0.16	0.19	0.23	0.28		
	12	0.125	62.0	793	1.06	0.13	0.15	0.16	0.18	0.23	0.28	60.5	802	1.06	0.14	0.15	0.16	0.19	0.23	0.28		
	20	0.125	96.0	797	1.06	0.14	0.15	0.16	0.19	0.23	0.28	95.1	808	1.06	0.14	0.15	0.16	0.19	0.23	0.28		
	0.20	1	0.030	3.8	352	1.70	0.12	0.15	0.17	0.22	0.31	0.39	3.6	360	1.70	0.12	0.15	0.17	0.22	0.31	0.39	
		2	0.030	7.0	328	1.70	0.11	0.14	0.16	0.21	0.30	0.38	6.7	328	1.70	0.11	0.14	0.17	0.21	0.30	0.38	
3		0.030	11.6	350	1.70	0.12	0.15	0.17	0.22	0.31	0.39	10.9	348	1.70	0.12	0.15	0.17	0.22	0.31	0.39		
4		0.030	14.4	375	1.70	0.13	0.15	0.18	0.22	0.31	0.39	13.7	373	1.70	0.13	0.15	0.18	0.22	0.31	0.39		
6		0.030	21.2	348	1.70	0.12	0.14	0.17	0.22	0.31	0.39	20.5	355	1.70	0.12	0.15	0.17	0.22	0.31	0.39		
8		0.030	29.1	360	1.70	0.12	0.15	0.17	0.22	0.31	0.39	27.9	359	1.70	0.12	0.15	0.17	0.22	0.31	0.39		
12		0.030	44.3	355	1.70	0.12	0.15	0.17	0.22	0.31	0.39	42.1	353	1.70	0.12	0.15	0.17	0.22	0.31	0.39		
20		0.030	68.2	354	1.71	0.12	0.15	0.17	0.22	0.31	0.39	65.9	357	1.70	0.12	0.15	0.17	0.22	0.31	0.39		
0.50		1	0.015	1.9	107	2.94	0.10	0.16	0.22	0.33	0.52	0.68	1.9	124	2.94	0.11	0.17	0.23	0.34	0.52	0.69	
		2	0.015	3.9	110	2.94	0.10	0.16	0.22	0.33	0.52	0.68	3.7	124	2.94	0.11	0.17	0.23	0.34	0.52	0.69	
	3	0.015	5.8	111	2.94	0.10	0.16	0.22	0.33	0.52	0.68	5.6	124	2.94	0.11	0.17	0.23	0.34	0.52	0.69		
	4	0.015	6.8	109	2.94	0.10	0.16	0.22	0.33	0.52	0.68	6.7	129	2.94	0.11	0.18	0.23	0.34	0.53	0.69		
	6	0.015	11.1	110	2.95	0.10	0.16	0.22	0.33	0.52	0.68	10.7	124	2.95	0.11	0.17	0.23	0.34	0.52	0.69		
	8	0.015	14.4	111	2.95	0.10	0.16	0.22	0.33	0.52	0.68	13.7	124	2.95	0.11	0.17	0.23	0.34	0.52	0.69		
	12	0.015	22.5	109	2.96	0.10	0.16	0.22	0.33	0.52	0.68	22.2	127	2.96	0.11	0.18	0.23	0.34	0.53	0.69		
	20	0.015	35.0	109	2.98	0.10	0.16	0.22	0.33	0.52	0.68	34.2	126	2.98	0.11	0.17	0.23	0.34	0.53	0.69		

**Table B.6:** Detection probability, average detection time, contaminated area in case of detection failure and relative contaminated area to control area  $L$  for various RADTi in case of  $\sigma_{InK}^2 = 0.0$  assuming every 4 months (4M) and biannually (6M) sampling frequencies

$\sigma_{InK}^2$		0.00																				
$\alpha_T(m)$	now	nfsd(max)	$P_d$ (4M)	$\langle T_{det.} \rangle$ (DAYS)	AREA ON FAILURE	(AREA ON DET.)/L	(3M. RADTi)/L	(6M. RADTi)/L	(12M. RADTi)/L	(24M. RADTi)/L	(36M. RADTi)/L	$P_d$ (6M)	$\langle T_{det.} \rangle$ (DAYS)	AREA ON FAILURE	(AREA ON DET.)/L	(3M. RADTi)/L	(6M. RADTi)/L	(12M. RADTi)/L	(24M. RADTi)/L	(36M. RADTi)/L		
0.001	1	3.00	4.1	9562	0.03	0.02	0.03	0.03	0.03	0.03	0.02	3.9	9573	0.03	0.02	0.03	0.03	0.03	0.03	0.02	0.02	
	2	3.00	7.9	9578	0.03	0.03	0.03	0.03	0.03	0.03	0.02	7.6	9595	0.03	0.03	0.03	0.03	0.03	0.03	0.03	0.02	
	3	3.00	12.8	9588	0.03	0.03	0.03	0.03	0.03	0.03	0.02	12.4	9615	0.03	0.03	0.03	0.03	0.03	0.03	0.03	0.02	
	4	3.00	16.1	9628	0.03	0.03	0.03	0.03	0.03	0.03	0.02	16.0	9654	0.03	0.03	0.03	0.03	0.03	0.03	0.03	0.02	
	6	3.00	24.0	9579	0.03	0.03	0.03	0.03	0.03	0.03	0.02	23.3	9604	0.03	0.03	0.03	0.03	0.03	0.03	0.03	0.02	
	8	3.00	31.8	9576	0.03	0.03	0.03	0.03	0.03	0.03	0.02	31.5	9602	0.03	0.03	0.03	0.03	0.03	0.03	0.03	0.02	
	12	3.00	47.4	9582	0.03	0.03	0.03	0.03	0.03	0.03	0.02	46.6	9610	0.03	0.03	0.03	0.03	0.03	0.03	0.03	0.02	
	20	3.00	79.6	9582	0.03	0.03	0.03	0.03	0.03	0.03	0.02	77.8	9609	0.03	0.03	0.03	0.03	0.03	0.03	0.03	0.02	
	0.01	1	2.25	5.4	7222	0.18	0.13	0.13	0.13	0.13	0.14	0.14	5.4	7240	0.18	0.13	0.13	0.13	0.13	0.13	0.14	0.14
		2	2.25	10.8	7247	0.18	0.13	0.13	0.13	0.13	0.14	0.14	10.8	7277	0.18	0.13	0.13	0.13	0.13	0.13	0.14	0.14
3		2.25	17.1	7251	0.18	0.13	0.13	0.13	0.13	0.14	0.14	16.9	7277	0.18	0.13	0.13	0.13	0.13	0.13	0.14	0.14	
4		2.25	22.5	7279	0.18	0.13	0.13	0.13	0.13	0.14	0.14	22.1	7306	0.18	0.13	0.13	0.13	0.13	0.13	0.14	0.14	
6		2.25	32.7	7255	0.18	0.13	0.13	0.13	0.13	0.14	0.14	32.3	7284	0.18	0.13	0.13	0.13	0.13	0.13	0.14	0.14	
8		2.25	43.3	7245	0.18	0.13	0.13	0.13	0.13	0.14	0.14	42.8	7274	0.18	0.13	0.13	0.13	0.13	0.13	0.14	0.14	
12		2.25	65.8	7248	0.18	0.13	0.13	0.13	0.13	0.14	0.14	64.8	7274	0.18	0.13	0.13	0.13	0.13	0.13	0.14	0.14	
20		2.25	99.3	7240	0.18	0.13	0.13	0.13	0.13	0.14	0.14	99.3	7271	0.18	0.13	0.13	0.13	0.13	0.13	0.14	0.14	
0.02		1	1.50	5.3	4974	0.31	0.16	0.17	0.17	0.17	0.18	0.19	5.2	5008	0.31	0.17	0.17	0.17	0.17	0.18	0.18	0.19
		2	1.50	10.3	4996	0.31	0.17	0.17	0.17	0.17	0.18	0.19	10.0	5025	0.31	0.17	0.17	0.17	0.17	0.18	0.19	0.19
	3	1.50	16.3	4998	0.31	0.17	0.17	0.17	0.18	0.18	0.19	15.9	5026	0.31	0.17	0.17	0.17	0.17	0.18	0.19	0.19	
	4	1.50	21.2	5024	0.31	0.17	0.17	0.17	0.18	0.18	0.19	20.8	5049	0.31	0.17	0.17	0.17	0.17	0.18	0.19	0.20	
	6	1.50	31.0	5002	0.31	0.17	0.17	0.17	0.18	0.18	0.19	30.2	5029	0.31	0.17	0.17	0.17	0.17	0.18	0.19	0.19	
	8	1.50	41.5	4998	0.31	0.17	0.17	0.17	0.17	0.18	0.19	40.2	5023	0.31	0.17	0.17	0.17	0.17	0.18	0.19	0.19	
	12	1.50	62.4	4992	0.31	0.17	0.17	0.17	0.17	0.18	0.19	60.3	5016	0.31	0.17	0.17	0.17	0.17	0.18	0.18	0.19	
	20	1.50	98.5	4999	0.31	0.17	0.17	0.17	0.17	0.18	0.19	97.1	5024	0.31	0.17	0.17	0.17	0.17	0.18	0.19	0.19	
	0.05	1	0.50	5.1	1937	0.63	0.16	0.17	0.17	0.18	0.21	0.23	4.9	1971	0.63	0.16	0.17	0.17	0.17	0.19	0.21	0.23
		2	0.50	10.2	1974	0.63	0.16	0.17	0.17	0.19	0.21	0.23	9.7	1991	0.63	0.16	0.17	0.18	0.19	0.21	0.23	
3		0.50	16.3	1978	0.63	0.16	0.17	0.18	0.19	0.21	0.23	15.6	1997	0.63	0.16	0.17	0.18	0.19	0.21	0.23		
4		0.50	20.8	2004	0.63	0.17	0.17	0.18	0.19	0.21	0.24	20.0	2033	0.63	0.17	0.17	0.18	0.19	0.21	0.24		
6		0.50	30.2	1981	0.63	0.16	0.17	0.18	0.19	0.21	0.23	29.0	2002	0.63	0.16	0.17	0.18	0.19	0.21	0.24		
8		0.50	40.5	1975	0.63	0.16	0.17	0.18	0.19	0.21	0.23	39.4	1998	0.63	0.16	0.17	0.18	0.19	0.21	0.23		
12		0.50	60.7	1971	0.63	0.16	0.17	0.17	0.19	0.21	0.23	59.0	1998	0.63	0.16	0.17	0.18	0.19	0.21	0.23		
20		0.50	96.5	1981	0.63	0.16	0.17	0.18	0.19	0.21	0.23	94.9	2004	0.63	0.17	0.17	0.18	0.19	0.21	0.24		
0.10		1	0.125	5.0	790	1.06	0.13	0.15	0.16	0.18	0.23	0.27	4.7	799	1.06	0.14	0.15	0.16	0.19	0.23	0.28	
		2	0.125	9.7	815	1.06	0.14	0.15	0.16	0.19	0.23	0.28	9.5	828	1.06	0.14	0.15	0.16	0.19	0.24	0.28	
	3	0.125	16.0	813	1.06	0.14	0.15	0.16	0.19	0.23	0.28	15.3	830	1.06	0.14	0.15	0.17	0.19	0.24	0.28		
	4	0.125	20.4	836	1.06	0.14	0.15	0.17	0.19	0.24	0.28	19.8	862	1.06	0.14	0.16	0.17	0.19	0.24	0.28		
	6	0.125	29.5	818	1.06	0.14	0.15	0.16	0.19	0.23	0.28	28.6	840	1.06	0.14	0.15	0.17	0.19	0.24	0.28		
	8	0.125	39.9	815	1.06	0.14	0.15	0.16	0.19	0.23	0.28	38.8	834	1.06	0.14	0.15	0.17	0.19	0.24	0.28		
	12	0.125	59.8	808	1.06	0.14	0.15	0.16	0.19	0.23	0.28	57.5	832	1.06	0.14	0.15	0.17	0.19	0.24	0.28		
	20	0.125	93.9	816	1.06	0.14	0.15	0.16	0.19	0.23	0.28	92.3	837	1.06	0.14	0.15	0.17	0.19	0.24	0.28		
	0.20	1	0.030	3.6	361	1.70	0.12	0.15	0.17	0.22	0.31	0.39	3.3	378	1.70	0.13	0.15	0.18	0.23	0.31	0.39	
		2	0.030	6.5	334	1.70	0.12	0.14	0.17	0.21	0.30	0.38	6.3	368	1.70	0.13	0.15	0.18	0.22	0.31	0.39	
3		0.030	11.0	366	1.70	0.12	0.15	0.18	0.22	0.31	0.39	10.1	377	1.70	0.13	0.15	0.18	0.23	0.31	0.39		
4		0.030	13.6	383	1.70	0.13	0.16	0.18	0.23	0.31	0.39	12.5	390	1.70	0.13	0.16	0.18	0.23	0.32	0.39		
6		0.030	19.5	349	1.70	0.12	0.15	0.17	0.22	0.31	0.39	19.2	383	1.70	0.13	0.16	0.18	0.23	0.31	0.39		
8		0.030	27.5	371	1.70	0.13	0.15	0.18	0.22	0.31	0.39	26.1	385	1.70	0.13	0.16	0.18	0.23	0.31	0.39		
12		0.030	42.0	370	1.70	0.13	0.15	0.18	0.22	0.31	0.39	39.1	376	1.70	0.13	0.15	0.18	0.23	0.31	0.39		
20		0.030	64.8	366	1.70	0.12	0.15	0.17	0.22	0.31	0.39	62.1	383	1.70	0.13	0.16	0.18	0.23	0.31	0.39		
0.50		1	0.015	1.9	141	2.94	0.12	0.19	0.24	0.35	0.53	0.69	1.7	180	2.94	0.15	0.21	0.27	0.37	0.55	0.71	
		2	0.015	3.7	145	2.94	0.13	0.19	0.24	0.35	0.53	0.70	3.4	188	2.94	0.16	0.22	0.27	0.37	0.56	0.72	
	3	0.015	5.5	143	2.94	0.13	0.19	0.24	0.35	0.53	0.70	5.0	182	2.94	0.15	0.21	0.27	0.37	0.55	0.71		
	4	0.015	6.5	142	2.94	0.12	0.19	0.24	0.35	0.53	0.70	6.0	185	2.94	0.15	0.21	0.27	0.37	0.55	0.71		
	6	0.015	10.5	146	2.95	0.13	0.19	0.24	0.35	0.54	0.70	9.8	186	2.95	0.16	0.21	0.27	0.37	0.55	0.72		
	8	0.015	13.5	145	2.95	0.13	0.19	0.24	0.35	0.53	0.70	12.5	186	2.95	0.16	0.21	0.27	0.37	0.55	0.71		
	12	0.015	21.3	142	2.96	0.12	0.19	0.24	0.35	0.53	0.70	19.8	185	2.96	0.16	0.21	0.27	0.37	0.55	0.71		
	20	0.015	33.4	145	2.98	0.13	0.19	0.24	0.35	0.53	0.70	31.0	184	2.97	0.15	0.21	0.27	0.37	0.55	0.71		

**Table B.7:** Detection probability, average detection time, contaminated area in case of detection failure and relative contaminated area to control area  $L$  for various RADTi in case of  $\sigma_{lnK}^2 = 0.0$  assuming annually (12M) sampling frequency

		$\sigma_{lnK}^2$		0.00							
$\alpha_1(m)$	now	ntds(max)	Pd (12M)	$<T_{(DET.)}>$ (DAYS)	AREA ON FAILURE	(AREA ON DET.)/L	(3M. RADTi)/L	(6M. RADTi)/L	(12M. RADTi)/L	(24M. RADTi)/L	(36M. RADTi)/L
0.001	1	3.00	3.0	9636	0.03	0.03	0.03	0.03	0.03	0.03	0.02
	2	3.00	6.1	9640	0.03	0.03	0.03	0.03	0.03	0.03	0.02
	3	3.00	10.1	9662	0.03	0.03	0.03	0.03	0.03	0.03	0.02
	4	3.00	12.4	9708	0.03	0.03	0.03	0.03	0.03	0.03	0.02
	6	3.00	18.3	9649	0.03	0.03	0.03	0.03	0.03	0.03	0.02
	8	3.00	24.4	9643	0.03	0.03	0.03	0.03	0.03	0.03	0.02
	12	3.00	36.3	9668	0.03	0.03	0.03	0.03	0.03	0.03	0.02
	20	3.00	61.0	9654	0.03	0.03	0.03	0.03	0.03	0.03	0.02
0.01	1	2.25	4.9	7344	0.18	0.13	0.13	0.13	0.13	0.14	0.14
	2	2.25	10.2	7374	0.18	0.13	0.13	0.13	0.13	0.14	0.14
	3	2.25	15.9	7367	0.18	0.13	0.13	0.13	0.13	0.14	0.14
	4	2.25	20.4	7392	0.18	0.13	0.13	0.13	0.13	0.14	0.14
	6	2.25	29.8	7367	0.18	0.13	0.13	0.13	0.13	0.14	0.14
	8	2.25	39.9	7366	0.18	0.13	0.13	0.13	0.13	0.14	0.14
	12	2.25	59.5	7354	0.18	0.13	0.13	0.13	0.13	0.14	0.14
	20	2.25	95.1	7360	0.18	0.13	0.13	0.13	0.13	0.14	0.14
0.02	1	1.50	4.5	5055	0.31	0.17	0.17	0.17	0.18	0.19	0.20
	2	1.50	8.8	5090	0.31	0.17	0.17	0.17	0.18	0.19	0.20
	3	1.50	14.0	5080	0.31	0.17	0.17	0.17	0.18	0.19	0.20
	4	1.50	19.2	5136	0.31	0.17	0.17	0.17	0.18	0.19	0.20
	6	1.50	27.4	5098	0.31	0.17	0.17	0.17	0.18	0.19	0.20
	8	1.50	36.5	5085	0.31	0.17	0.17	0.17	0.18	0.19	0.20
	12	1.50	55.0	5095	0.31	0.17	0.17	0.17	0.18	0.19	0.20
	20	1.50	89.4	5093	0.31	0.17	0.17	0.17	0.18	0.19	0.20
0.05	1	0.50	4.4	2028	0.63	0.17	0.17	0.18	0.19	0.21	0.24
	2	0.50	8.2	2035	0.63	0.17	0.17	0.18	0.19	0.21	0.24
	3	0.50	13.9	2047	0.63	0.17	0.17	0.18	0.19	0.22	0.24
	4	0.50	17.6	2079	0.63	0.17	0.18	0.18	0.19	0.22	0.24
	6	0.50	25.3	2047	0.63	0.17	0.17	0.18	0.19	0.22	0.24
	8	0.50	34.7	2048	0.63	0.17	0.17	0.18	0.19	0.22	0.24
	12	0.50	52.3	2042	0.63	0.17	0.17	0.18	0.19	0.21	0.24
	20	0.50	84.7	2050	0.63	0.17	0.17	0.18	0.19	0.22	0.24
0.10	1	0.125	4.4	863	1.06	0.14	0.16	0.17	0.19	0.24	0.28
	2	0.125	8.2	862	1.06	0.14	0.16	0.17	0.19	0.24	0.28
	3	0.125	13.9	886	1.06	0.15	0.16	0.17	0.20	0.24	0.29
	4	0.125	17.2	904	1.06	0.15	0.16	0.18	0.20	0.24	0.29
	6	0.125	25.1	878	1.06	0.15	0.16	0.17	0.20	0.24	0.28
	8	0.125	34.1	875	1.06	0.15	0.16	0.17	0.20	0.24	0.28
	12	0.125	51.1	881	1.06	0.15	0.16	0.17	0.20	0.24	0.29
	20	0.125	83.6	886	1.06	0.15	0.16	0.17	0.20	0.24	0.29
0.20	1	0.030	2.7	492	1.70	0.16	0.19	0.21	0.25	0.34	0.42
	2	0.030	4.8	456	1.70	0.15	0.18	0.20	0.25	0.33	0.41
	3	0.030	8.1	493	1.70	0.16	0.19	0.21	0.25	0.34	0.42
	4	0.030	9.4	478	1.70	0.16	0.18	0.21	0.25	0.33	0.41
	6	0.030	14.6	479	1.70	0.16	0.18	0.21	0.25	0.34	0.41
	8	0.030	20.0	475	1.70	0.16	0.18	0.20	0.25	0.33	0.41
	12	0.030	30.2	478	1.70	0.16	0.18	0.21	0.25	0.34	0.41
	20	0.030	47.7	485	1.70	0.16	0.18	0.21	0.25	0.34	0.41
0.50	1	0.015	0.1	365	2.94	0.27	0.32	0.37	0.46	0.64	0.79
	2	0.015	0.3	365	2.94	0.27	0.32	0.37	0.46	0.63	0.79
	3	0.015	0.4	365	2.94	0.27	0.32	0.37	0.47	0.64	0.79
	4	0.015	0.8	365	2.94	0.27	0.32	0.37	0.46	0.63	0.79
	6	0.015	0.8	365	2.94	0.27	0.32	0.37	0.46	0.63	0.79
	8	0.015	1.3	365	2.94	0.27	0.32	0.37	0.46	0.64	0.79
	12	0.015	2.4	365	2.94	0.27	0.32	0.37	0.46	0.63	0.79
	20	0.015	3.1	365	2.94	0.27	0.32	0.37	0.46	0.63	0.79

**Table B.8:** Detection probability, average detection time, contaminated area in case of detection failure and relative contaminated area to control area for various RARDTi in case of  $\sigma_{InK}^2 = 0.5$  assuming daily (ED) and monthly (1M) sampling frequencies

$\sigma_{InK}^2$		0.50																			
$\alpha_1(m)$	now	infd(max)	$P_d$ (ED)	$\langle T_{(DET.)} \rangle$ (DAYS)	AREA ON FAILURE	(AREA ON DET.)/L	(3M. RADTi)/L	(6M. RADTi)/L	(12M. RADTi)/L	(24M. RADTi)/L	(36M. RADTi)/L	$P_d$ (1M)	$\langle T_{(DET.)} \rangle$ (DAYS)	AREA ON FAILURE	(AREA ON DET.)/L	(3M. RADTi)/L	(6M. RADTi)/L	(12M. RADTi)/L	(24M. RADTi)/L	(36M. RADTi)/L	
0.001	1	1.75	4.5	5722	0.06	0.03	0.03	0.03	0.03	0.03	0.03	4.5	5747	0.06	0.03	0.03	0.03	0.03	0.03	0.03	0.03
	2	1.75	8.1	5678	0.06	0.03	0.03	0.03	0.03	0.03	0.03	8.1	5693	0.06	0.03	0.03	0.03	0.03	0.03	0.03	0.03
	3	1.75	11.5	5674	0.06	0.03	0.03	0.03	0.03	0.03	0.03	11.4	5684	0.06	0.03	0.03	0.03	0.03	0.03	0.03	0.03
	4	1.75	14.5	5650	0.06	0.03	0.03	0.03	0.03	0.03	0.03	14.2	5669	0.06	0.03	0.03	0.03	0.03	0.03	0.03	0.03
	6	1.75	21.0	5617	0.06	0.03	0.03	0.03	0.03	0.03	0.03	20.7	5629	0.06	0.03	0.03	0.03	0.03	0.03	0.03	0.03
	8	1.75	28.1	5649	0.06	0.03	0.03	0.03	0.03	0.03	0.03	27.7	5661	0.06	0.03	0.03	0.03	0.03	0.03	0.03	0.03
	12	1.75	42.0	5668	0.06	0.03	0.03	0.03	0.03	0.03	0.03	41.5	5685	0.06	0.03	0.03	0.03	0.03	0.03	0.03	0.03
	20	1.75	64.2	5652	0.06	0.03	0.03	0.03	0.03	0.03	0.03	63.7	5666	0.06	0.03	0.03	0.03	0.03	0.03	0.03	0.03
0.01	1	1.50	5.4	4830	0.34	0.13	0.13	0.14	0.14	0.15	0.16	5.2	4838	0.34	0.13	0.13	0.13	0.14	0.15	0.16	0.16
	2	1.50	10.9	4990	0.34	0.13	0.14	0.14	0.14	0.15	0.17	10.6	5019	0.34	0.13	0.14	0.14	0.14	0.15	0.17	0.17
	3	1.50	15.1	4788	0.34	0.13	0.13	0.14	0.14	0.15	0.16	14.5	4803	0.34	0.13	0.13	0.14	0.14	0.15	0.16	0.16
	4	1.50	20.7	4802	0.34	0.13	0.13	0.14	0.14	0.15	0.16	20.2	4822	0.34	0.13	0.13	0.14	0.14	0.15	0.16	0.16
	6	1.50	30.7	4937	0.34	0.13	0.14	0.14	0.14	0.15	0.17	29.5	4950	0.34	0.13	0.14	0.14	0.14	0.15	0.17	0.17
	8	1.50	41.5	4870	0.34	0.13	0.13	0.14	0.14	0.15	0.16	39.7	4879	0.34	0.13	0.13	0.14	0.14	0.15	0.16	0.16
	12	1.50	57.0	4843	0.34	0.13	0.13	0.14	0.14	0.15	0.16	55.5	4853	0.34	0.13	0.13	0.14	0.14	0.15	0.16	0.16
	20	1.50	77.2	4869	0.35	0.13	0.13	0.14	0.14	0.15	0.16	75.9	4885	0.35	0.13	0.13	0.14	0.14	0.15	0.16	0.16
0.02	1	0.50	5.9	1936	0.57	0.09	0.10	0.10	0.11	0.13	0.15	5.9	1956	0.57	0.09	0.10	0.10	0.11	0.13	0.15	0.15
	2	0.50	11.6	1956	0.57	0.09	0.09	0.10	0.11	0.13	0.14	11.2	1982	0.57	0.09	0.10	0.10	0.11	0.13	0.14	0.14
	3	0.50	16.9	2011	0.57	0.09	0.10	0.10	0.11	0.13	0.14	16.6	2021	0.57	0.09	0.10	0.10	0.11	0.13	0.14	0.14
	4	0.50	22.1	2022	0.57	0.09	0.10	0.10	0.11	0.13	0.14	21.2	2043	0.57	0.09	0.10	0.10	0.11	0.13	0.14	0.14
	6	0.50	33.2	1979	0.57	0.09	0.10	0.10	0.11	0.13	0.14	32.4	1993	0.57	0.09	0.10	0.10	0.11	0.13	0.14	0.14
	8	0.50	43.6	2021	0.57	0.09	0.10	0.10	0.11	0.13	0.14	42.0	2037	0.57	0.09	0.10	0.10	0.11	0.13	0.14	0.14
	12	0.50	61.9	2030	0.57	0.09	0.10	0.10	0.11	0.13	0.14	60.0	2050	0.57	0.09	0.10	0.10	0.11	0.13	0.14	0.14
	20	0.50	84.4	2017	0.58	0.09	0.09	0.10	0.11	0.13	0.14	83.0	2030	0.58	0.09	0.10	0.10	0.11	0.13	0.14	0.14
0.05	1	0.50	5.6	1890	1.08	0.19	0.20	0.21	0.23	0.26	0.30	5.0	1879	1.08	0.19	0.20	0.21	0.23	0.26	0.30	0.30
	2	0.50	10.8	1891	1.08	0.18	0.19	0.20	0.22	0.25	0.29	9.6	1910	1.08	0.18	0.19	0.20	0.22	0.25	0.29	0.29
	3	0.50	14.9	1934	1.09	0.18	0.19	0.20	0.22	0.25	0.29	13.6	1921	1.08	0.19	0.19	0.20	0.22	0.26	0.29	0.29
	4	0.50	19.8	1936	1.09	0.18	0.19	0.20	0.22	0.25	0.29	17.8	1948	1.09	0.18	0.19	0.20	0.22	0.25	0.29	0.29
	6	0.50	29.9	1904	1.08	0.18	0.19	0.20	0.22	0.25	0.29	27.0	1910	1.08	0.18	0.19	0.20	0.22	0.26	0.29	0.29
	8	0.50	39.1	1934	1.08	0.18	0.19	0.20	0.22	0.26	0.29	35.1	1935	1.08	0.18	0.19	0.20	0.22	0.26	0.29	0.29
	12	0.50	55.7	1953	1.09	0.19	0.19	0.20	0.22	0.26	0.29	50.2	1965	1.09	0.18	0.19	0.20	0.22	0.26	0.29	0.29
	20	0.50	78.2	1964	1.09	0.18	0.19	0.20	0.22	0.26	0.32	73.4	1971	1.09	0.18	0.19	0.20	0.22	0.26	0.29	0.29
0.10	1	0.125	6.4	870	1.68	0.14	0.16	0.17	0.20	0.26	0.32	5.9	881	1.68	0.14	0.16	0.17	0.21	0.27	0.32	0.32
	2	0.125	10.3	883	1.68	0.15	0.16	0.18	0.21	0.27	0.33	9.2	870	1.68	0.15	0.16	0.18	0.21	0.27	0.33	0.33
	3	0.125	16.2	829	1.68	0.14	0.16	0.17	0.20	0.26	0.32	14.9	844	1.68	0.14	0.16	0.17	0.20	0.26	0.32	0.32
	4	0.125	20.0	828	1.68	0.14	0.16	0.18	0.21	0.27	0.33	18.0	816	1.68	0.14	0.16	0.17	0.21	0.26	0.32	0.32
	6	0.125	30.3	828	1.68	0.14	0.16	0.17	0.20	0.26	0.32	28.0	831	1.68	0.14	0.16	0.17	0.21	0.27	0.32	0.32
	8	0.125	42.2	814	1.68	0.14	0.16	0.17	0.20	0.27	0.33	38.4	806	1.68	0.14	0.16	0.17	0.20	0.26	0.32	0.32
	12	0.125	62.2	819	1.67	0.14	0.16	0.17	0.21	0.27	0.33	56.4	813	1.68	0.14	0.16	0.17	0.20	0.26	0.32	0.32
	20	0.125	87.0	828	1.72	0.14	0.16	0.17	0.20	0.26	0.32	81.9	821	1.71	0.14	0.16	0.17	0.20	0.26	0.32	0.32
0.20	1	0.030	4.8	375	2.45	0.12	0.15	0.18	0.23	0.33	0.43	4.2	373	2.45	0.12	0.15	0.17	0.23	0.33	0.42	0.42
	2	0.030	7.9	375	2.45	0.12	0.15	0.18	0.24	0.35	0.45	6.8	338	2.45	0.12	0.15	0.18	0.23	0.34	0.44	0.44
	3	0.030	12.9	356	2.46	0.12	0.15	0.18	0.23	0.33	0.43	11.2	339	2.46	0.11	0.14	0.17	0.22	0.33	0.42	0.42
	4	0.030	15.3	372	2.45	0.13	0.16	0.19	0.24	0.35	0.45	13.5	355	2.45	0.12	0.15	0.18	0.24	0.34	0.44	0.44
	6	0.030	24.1	375	2.45	0.12	0.16	0.18	0.24	0.35	0.45	20.2	329	2.45	0.11	0.15	0.17	0.23	0.34	0.44	0.44
	8	0.030	32.5	369	2.46	0.12	0.15	0.18	0.24	0.34	0.44	28.5	358	2.46	0.12	0.15	0.18	0.23	0.34	0.44	0.44
	12	0.030	48.3	369	2.46	0.12	0.15	0.18	0.24	0.34	0.44	42.3	349	2.46	0.12	0.15	0.18	0.23	0.34	0.44	0.44
	20	0.030	69.6	378	2.47	0.12	0.15	0.18	0.24	0.35	0.45	61.7	349	2.47	0.12	0.15	0.18	0.23	0.34	0.44	0.44
0.50	1	0.015	3.0	113	3.63	0.10	0.17	0.24	0.36	0.57	0.76	2.6	111	3.63	0.10	0.17	0.24	0.36	0.57	0.76	0.76
	2	0.015	4.5	119	3.63	0.09	0.17	0.23	0.35	0.56	0.76	3.7	113	3.63	0.09	0.16	0.22	0.34	0.56	0.75	0.75
	3	0.015	7.8	101	3.64	0.08	0.16	0.22	0.34	0.56	0.75	6.9	107	3.63	0.09	0.16	0.23	0.35	0.55	0.74	0.74
	4	0.015	7.8	120	3.63	0.10	0.17	0.24	0.36	0.57	0.76	6.6	120	3.63	0.10	0.17	0.24	0.35	0.56	0.76	0.76
	6	0.015	13.5	110	3.64	0.09	0.17	0.23	0.35	0.57	0.77	10.9	104	3.64	0.09	0.16	0.23	0.35	0.56	0.76	0.76
	8	0.015	18.0	110	3.64	0.09	0.17	0.23	0.36	0.57	0.77	15.1	106	3.64	0.09	0.17	0.23	0.35	0.57	0.76	0.76
	12	0.015	27.5	121	3.65	0.10	0.17	0.23	0.35	0.57	0.76	22.6	111	3.65	0.09	0.17	0.23	0.35	0.56	0.76	0.76
	20	0.015	38.2	104	3.67	0.09	0.16	0.23	0.35	0.57	0.77	34.0	105	3.66	0.09	0.16	0.23	0.35	0.57	0.77	0.77

**Table B.9:** Detection probability, average detection time, contaminated area in case of detection failure and relative contaminated area to control area for various RADTi in case of  $\sigma_{InK}^2 = 0.5$  assuming bimonthly (2M) and quarterly (3M) sampling frequencies

$\sigma_{InK}^2$		0.50																			
$\alpha_1(m)$	now	infd(max)	$P_d$ (2M)	$\langle T_{(DET.)} \rangle$ (DAYS)	AREA ON FAILURE	(AREA ON DET.)/L	(3M. RADTi)/L	(6M. RADTi)/L	(12M. RADTi)/L	(24M. RADTi)/L	(36M. RADTi)/L	$P_d$ (3M)	$\langle T_{(DET.)} \rangle$ (DAYS)	AREA ON FAILURE	(AREA ON DET.)/L	(3M. RADTi)/L	(6M. RADTi)/L	(12M. RADTi)/L	(24M. RADTi)/L	(36M. RADTi)/L	
0.001	1	1.75	4.4	5749	0.06	0.03	0.03	0.03	0.03	0.03	0.03	4.5	5776	0.06	0.03	0.03	0.03	0.03	0.03	0.03	0.03
	2	1.75	8.0	5692	0.06	0.03	0.03	0.03	0.03	0.03	0.03	7.8	5751	0.06	0.03	0.03	0.03	0.03	0.03	0.03	0.03
	3	1.75	11.3	5703	0.06	0.03	0.03	0.03	0.03	0.03	0.03	11.3	5720	0.06	0.03	0.03	0.03	0.03	0.03	0.03	0.03
	4	1.75	14.1	5680	0.06	0.03	0.03	0.03	0.03	0.03	0.03	14.0	5711	0.06	0.03	0.03	0.03	0.03	0.03	0.03	0.03
	6	1.75	20.6	5639	0.06	0.03	0.03	0.03	0.03	0.03	0.03	20.3	5678	0.06	0.03	0.03	0.03	0.03	0.03	0.03	0.03
	8	1.75	27.5	5678	0.06	0.03	0.03	0.03	0.03	0.03	0.03	27.2	5705	0.06	0.03	0.03	0.03	0.03	0.03	0.03	0.03
	12	1.75	41.1	5699	0.06	0.03	0.03	0.03	0.03	0.03	0.03	40.8	5723	0.06	0.03	0.03	0.03	0.03	0.03	0.03	0.03
	20	1.75	63.2	5677	0.06	0.03	0.03	0.03	0.03	0.03	0.03	62.7	5700	0.06	0.03	0.03	0.03	0.03	0.03	0.03	0.03
0.01	1	1.50	5.2	4863	0.34	0.13	0.13	0.14	0.14	0.15	0.16	5.2	4868	0.34	0.13	0.13	0.14	0.14	0.14	0.15	0.16
	2	1.50	10.5	5029	0.34	0.13	0.14	0.14	0.14	0.16	0.17	10.3	5041	0.34	0.13	0.14	0.14	0.14	0.14	0.16	0.17
	3	1.50	14.3	4815	0.34	0.13	0.13	0.14	0.14	0.15	0.16	14.1	4821	0.34	0.13	0.13	0.14	0.14	0.15	0.16	
	4	1.50	19.9	4812	0.34	0.13	0.13	0.14	0.14	0.15	0.16	19.6	4814	0.34	0.13	0.13	0.14	0.14	0.15	0.16	
	6	1.50	29.0	4966	0.34	0.13	0.14	0.14	0.14	0.16	0.17	28.6	4967	0.34	0.13	0.14	0.14	0.14	0.15	0.17	
	8	1.50	38.9	4878	0.34	0.13	0.13	0.14	0.14	0.15	0.16	38.3	4897	0.34	0.13	0.13	0.14	0.14	0.15	0.16	
	12	1.50	54.5	4863	0.34	0.13	0.13	0.14	0.14	0.15	0.16	53.5	4857	0.34	0.13	0.13	0.14	0.14	0.15	0.16	
	20	1.50	75.0	4890	0.35	0.13	0.13	0.14	0.14	0.15	0.16	74.2	4907	0.35	0.13	0.13	0.14	0.14	0.15	0.16	
0.02	1	0.50	5.9	1967	0.57	0.09	0.10	0.10	0.11	0.13	0.15	5.7	1977	0.57	0.09	0.10	0.10	0.11	0.13	0.15	
	2	0.50	11.1	1988	0.57	0.09	0.10	0.10	0.11	0.13	0.14	11.0	2001	0.57	0.09	0.10	0.10	0.11	0.13	0.15	
	3	0.50	16.4	2036	0.57	0.09	0.10	0.10	0.11	0.13	0.15	15.9	2044	0.57	0.09	0.10	0.10	0.11	0.13	0.15	
	4	0.50	20.9	2051	0.57	0.09	0.10	0.10	0.11	0.13	0.15	20.7	2078	0.57	0.09	0.10	0.10	0.11	0.13	0.15	
	6	0.50	32.0	2002	0.57	0.09	0.10	0.10	0.11	0.13	0.15	31.7	2019	0.57	0.09	0.10	0.10	0.11	0.13	0.15	
	8	0.50	41.5	2051	0.57	0.09	0.10	0.10	0.11	0.13	0.15	40.9	2063	0.57	0.09	0.10	0.10	0.11	0.13	0.15	
	12	0.50	59.2	2065	0.57	0.09	0.10	0.10	0.11	0.13	0.15	58.7	2078	0.57	0.09	0.10	0.10	0.11	0.13	0.15	
	20	0.50	82.2	2041	0.58	0.09	0.10	0.10	0.11	0.13	0.14	81.9	2050	0.58	0.09	0.10	0.10	0.11	0.13	0.14	
0.05	1	0.50	4.7	1879	1.08	0.19	0.20	0.21	0.23	0.26	0.30	4.5	1871	1.08	0.19	0.20	0.21	0.22	0.26	0.29	
	2	0.50	9.2	1919	1.08	0.18	0.19	0.20	0.22	0.25	0.29	8.8	1935	1.08	0.18	0.19	0.20	0.22	0.26	0.29	
	3	0.50	12.9	1936	1.08	0.19	0.19	0.20	0.22	0.25	0.29	12.6	1935	1.08	0.19	0.19	0.20	0.22	0.26	0.29	
	4	0.50	17.1	1955	1.09	0.18	0.19	0.20	0.22	0.25	0.29	16.4	1976	1.09	0.18	0.19	0.20	0.22	0.25	0.29	
	6	0.50	25.5	1919	1.08	0.18	0.19	0.20	0.22	0.25	0.29	24.7	1930	1.08	0.18	0.19	0.20	0.22	0.26	0.29	
	8	0.50	33.7	1939	1.08	0.18	0.19	0.20	0.22	0.26	0.29	33.0	1946	1.08	0.19	0.19	0.20	0.22	0.26	0.29	
	12	0.50	48.0	1970	1.09	0.18	0.19	0.20	0.22	0.25	0.29	46.2	1982	1.09	0.19	0.19	0.20	0.22	0.25	0.29	
	20	0.50	70.9	1978	1.09	0.19	0.19	0.20	0.22	0.26	0.29	69.2	1988	1.09	0.19	0.19	0.20	0.22	0.26	0.29	
0.10	1	0.125	5.6	877	1.68	0.14	0.16	0.18	0.21	0.27	0.32	5.3	893	1.68	0.15	0.16	0.18	0.21	0.27	0.32	
	2	0.125	9.0	888	1.68	0.15	0.16	0.18	0.21	0.27	0.33	8.5	877	1.68	0.15	0.16	0.18	0.21	0.27	0.33	
	3	0.125	14.4	845	1.68	0.14	0.16	0.17	0.20	0.26	0.32	13.9	849	1.68	0.14	0.16	0.17	0.20	0.26	0.32	
	4	0.125	17.2	818	1.68	0.14	0.16	0.17	0.21	0.26	0.32	16.5	818	1.68	0.14	0.16	0.17	0.20	0.26	0.32	
	6	0.125	27.1	832	1.68	0.14	0.16	0.18	0.21	0.27	0.33	26.0	827	1.68	0.14	0.16	0.17	0.21	0.27	0.32	
	8	0.125	37.1	813	1.68	0.14	0.16	0.17	0.20	0.26	0.32	35.9	817	1.69	0.14	0.16	0.17	0.20	0.26	0.32	
	12	0.125	54.6	818	1.68	0.14	0.16	0.17	0.20	0.26	0.32	52.3	813	1.68	0.14	0.16	0.17	0.20	0.26	0.32	
	20	0.125	79.9	829	1.71	0.14	0.16	0.17	0.20	0.26	0.32	77.9	824	1.71	0.14	0.16	0.17	0.20	0.26	0.32	
0.20	1	0.030	4.1	382	2.45	0.12	0.15	0.18	0.23	0.33	0.43	4.0	394	2.45	0.13	0.15	0.18	0.23	0.34	0.43	
	2	0.030	6.4	339	2.45	0.12	0.15	0.17	0.23	0.34	0.44	6.1	346	2.45	0.12	0.15	0.18	0.24	0.34	0.45	
	3	0.030	10.9	344	2.46	0.11	0.14	0.17	0.23	0.33	0.42	10.6	355	2.46	0.12	0.15	0.17	0.23	0.33	0.43	
	4	0.030	12.9	366	2.45	0.13	0.16	0.18	0.24	0.34	0.45	12.3	380	2.45	0.13	0.16	0.19	0.24	0.34	0.44	
	6	0.030	19.2	335	2.45	0.12	0.15	0.18	0.23	0.34	0.44	18.6	340	2.45	0.12	0.15	0.18	0.23	0.34	0.44	
	8	0.030	27.1	360	2.46	0.12	0.15	0.18	0.23	0.34	0.44	25.9	369	2.46	0.12	0.15	0.18	0.24	0.34	0.44	
	12	0.030	40.5	355	2.46	0.12	0.15	0.18	0.23	0.34	0.44	39.2	368	2.46	0.12	0.15	0.18	0.24	0.34	0.44	
	20	0.030	59.7	354	2.47	0.12	0.15	0.18	0.23	0.34	0.44	58.0	358	2.47	0.12	0.15	0.18	0.23	0.34	0.44	
0.50	1	0.015	2.4	125	3.63	0.11	0.18	0.24	0.36	0.57	0.76	2.2	132	3.63	0.12	0.19	0.25	0.36	0.57	0.76	
	2	0.015	3.4	131	3.63	0.10	0.17	0.23	0.35	0.56	0.75	3.3	136	3.63	0.11	0.18	0.24	0.35	0.56	0.76	
	3	0.015	6.6	120	3.63	0.10	0.17	0.24	0.35	0.56	0.75	6.2	135	3.63	0.12	0.18	0.25	0.36	0.56	0.75	
	4	0.015	6.1	126	3.63	0.11	0.18	0.24	0.36	0.56	0.76	6.0	148	3.63	0.13	0.19	0.25	0.37	0.57	0.76	
	6	0.015	10.5	121	3.64	0.10	0.17	0.24	0.36	0.57	0.76	10.0	135	3.64	0.11	0.18	0.24	0.36	0.57	0.76	
	8	0.015	14.4	122	3.64	0.11	0.18	0.24	0.36	0.58	0.77	13.7	138	3.64	0.12	0.19	0.25	0.37	0.58	0.77	
	12	0.015	21.3	122	3.65	0.11	0.17	0.24	0.36	0.57	0.76	20.5	140	3.65	0.12	0.19	0.25	0.37	0.58	0.77	
	20	0.015	32.8	118	3.66	0.10	0.18	0.24	0.36	0.58	0.77	31.7	137	3.66	0.12	0.19	0.25	0.37	0.58	0.78	

**Table B.10:** Detection probability, average detection time, contaminated area in case of detection failure and relative contaminated area to control area  $L$  for various RADTi in case of  $\sigma_{lnk}^2 = 0.5$  assuming every 4 months (4M) and biannually (6M) sampling frequencies

$\sigma_{lnk}^2$		0.50																			
$\alpha_r(m)$	now	nfds(max)	$P_d$ (4M)	$\langle T_{(DET.)} \rangle$ (DAYS)	AREA ON FAILURE	(AREA ON DET.)/L	(3M. RADTi)/L	(6M. RADTi)/L	(12M. RADTi)/L	(24M. RADTi)/L	(36M. RADTi)/L	$P_d$ (6M)	$\langle T_{(DET.)} \rangle$ (DAYS)	AREA ON FAILURE	(AREA ON DET.)/L	(3M. RADTi)/L	(6M. RADTi)/L	(12M. RADTi)/L	(24M. RADTi)/L	(36M. RADTi)/L	
0.001	1	1.75	4.3	5774	0.06	0.03	0.03	0.03	0.03	0.03	0.03	4.2	5784	0.06	0.03	0.03	0.03	0.03	0.03	0.03	0.03
	2	1.75	7.8	5736	0.06	0.03	0.03	0.03	0.03	0.03	0.03	7.4	5833	0.06	0.03	0.03	0.03	0.03	0.03	0.03	0.03
	3	1.75	11.0	5750	0.06	0.03	0.03	0.03	0.03	0.03	0.03	10.6	5771	0.06	0.03	0.03	0.03	0.03	0.03	0.03	0.03
	4	1.75	13.8	5713	0.06	0.03	0.03	0.03	0.03	0.03	0.03	13.2	5786	0.06	0.03	0.03	0.03	0.03	0.03	0.03	0.03
	6	1.75	20.2	5685	0.06	0.03	0.03	0.03	0.03	0.03	0.03	19.3	5759	0.06	0.03	0.03	0.03	0.03	0.03	0.03	0.03
	8	1.75	26.6	5725	0.06	0.03	0.03	0.03	0.03	0.03	0.03	25.7	5798	0.06	0.03	0.03	0.03	0.03	0.03	0.03	0.03
	12	1.75	40.3	5740	0.06	0.03	0.03	0.03	0.03	0.03	0.03	38.3	5819	0.06	0.03	0.03	0.03	0.03	0.03	0.03	0.03
	20	1.75	62.0	5717	0.06	0.03	0.03	0.03	0.03	0.03	0.03	59.8	5776	0.06	0.03	0.03	0.03	0.03	0.03	0.03	0.03
	0.01	1	1.50	5.1	4887	0.34	0.13	0.13	0.14	0.14	0.15	0.16	5.0	4882	0.34	0.13	0.13	0.14	0.14	0.15	0.16
		2	1.50	10.2	5057	0.34	0.13	0.14	0.14	0.15	0.16	0.17	10.0	5095	0.34	0.14	0.14	0.14	0.15	0.16	0.17
3		1.50	13.9	4859	0.34	0.13	0.13	0.14	0.14	0.15	0.16	13.6	4858	0.34	0.13	0.13	0.14	0.14	0.15	0.16	
4		1.50	19.3	4835	0.34	0.13	0.13	0.14	0.14	0.15	0.16	18.9	4840	0.34	0.13	0.13	0.14	0.14	0.15	0.16	
6		1.50	28.2	4992	0.34	0.13	0.14	0.14	0.14	0.15	0.17	27.5	5001	0.34	0.13	0.14	0.14	0.14	0.16	0.17	
8		1.50	37.9	4921	0.34	0.13	0.14	0.14	0.14	0.15	0.16	37.1	4949	0.34	0.13	0.14	0.14	0.14	0.15	0.17	
12		1.50	53.1	4884	0.34	0.13	0.13	0.14	0.14	0.15	0.16	51.8	4903	0.34	0.13	0.13	0.14	0.14	0.15	0.16	
20		1.50	73.5	4924	0.35	0.13	0.13	0.14	0.14	0.15	0.17	72.7	4948	0.35	0.13	0.14	0.14	0.14	0.15	0.17	
0.02		1	0.50	5.7	2009	0.57	0.10	0.10	0.10	0.11	0.13	0.15	5.6	2016	0.57	0.10	0.10	0.10	0.11	0.13	0.15
		2	0.50	10.9	2009	0.57	0.09	0.10	0.10	0.11	0.13	0.15	10.8	2033	0.57	0.09	0.10	0.10	0.11	0.13	0.15
	3	0.50	16.0	2072	0.57	0.09	0.10	0.10	0.11	0.13	0.15	15.5	2087	0.57	0.10	0.10	0.10	0.11	0.13	0.15	
	4	0.50	20.4	2090	0.57	0.09	0.10	0.10	0.11	0.13	0.15	20.1	2114	0.57	0.10	0.10	0.10	0.11	0.13	0.15	
	6	0.50	31.2	2034	0.57	0.09	0.10	0.10	0.11	0.13	0.15	30.8	2062	0.57	0.09	0.10	0.10	0.11	0.13	0.15	
	8	0.50	40.7	2070	0.57	0.09	0.10	0.10	0.11	0.13	0.15	39.5	2104	0.57	0.09	0.10	0.10	0.11	0.13	0.15	
	12	0.50	58.0	2093	0.57	0.09	0.10	0.10	0.11	0.13	0.15	57.0	2123	0.57	0.10	0.10	0.10	0.11	0.13	0.15	
	20	0.50	81.6	2069	0.58	0.09	0.10	0.10	0.11	0.13	0.15	80.8	2092	0.58	0.09	0.10	0.10	0.11	0.13	0.15	
	0.05	1	0.50	4.2	1885	1.08	0.19	0.20	0.21	0.22	0.26	0.29	4.0	1892	1.08	0.19	0.20	0.21	0.22	0.26	0.29
		2	0.50	8.6	1917	1.08	0.18	0.19	0.20	0.22	0.26	0.29	8.2	1969	1.08	0.19	0.20	0.20	0.22	0.26	0.29
3		0.50	12.0	1959	1.09	0.19	0.19	0.20	0.22	0.25	0.29	11.5	1963	1.09	0.19	0.20	0.20	0.22	0.26	0.29	
4		0.50	15.8	1970	1.09	0.18	0.19	0.20	0.22	0.25	0.29	14.7	2009	1.09	0.18	0.19	0.20	0.22	0.25	0.29	
6		0.50	24.0	1934	1.08	0.18	0.19	0.20	0.22	0.25	0.29	22.8	1973	1.08	0.19	0.19	0.20	0.22	0.26	0.29	
8		0.50	31.5	1940	1.08	0.19	0.19	0.20	0.22	0.26	0.29	29.7	1985	1.08	0.19	0.20	0.20	0.22	0.26	0.29	
12		0.50	44.4	1981	1.09	0.19	0.19	0.20	0.22	0.26	0.29	41.8	2017	1.09	0.19	0.19	0.20	0.22	0.25	0.29	
20		0.50	67.4	1986	1.09	0.19	0.19	0.20	0.22	0.26	0.29	64.5	2021	1.10	0.19	0.20	0.20	0.22	0.26	0.29	
0.10		1	0.125	5.2	901	1.68	0.15	0.16	0.18	0.21	0.26	0.32	4.8	903	1.68	0.15	0.16	0.18	0.21	0.27	0.32
		2	0.125	8.7	912	1.68	0.15	0.17	0.18	0.21	0.27	0.33	8.1	910	1.68	0.15	0.17	0.18	0.21	0.27	0.33
	3	0.125	13.5	866	1.68	0.14	0.16	0.17	0.20	0.26	0.32	12.9	873	1.69	0.14	0.16	0.18	0.21	0.26	0.32	
	4	0.125	16.4	837	1.68	0.15	0.16	0.18	0.21	0.27	0.32	15.3	835	1.68	0.14	0.16	0.18	0.21	0.26	0.32	
	6	0.125	25.7	851	1.68	0.15	0.16	0.18	0.21	0.27	0.33	24.3	858	1.69	0.15	0.16	0.18	0.21	0.27	0.33	
	8	0.125	36.0	837	1.69	0.14	0.16	0.18	0.21	0.27	0.33	33.8	848	1.69	0.15	0.16	0.18	0.21	0.27	0.33	
	12	0.125	51.8	834	1.68	0.14	0.16	0.17	0.21	0.27	0.32	48.7	842	1.68	0.14	0.16	0.18	0.21	0.27	0.32	
	20	0.125	76.5	838	1.71	0.14	0.16	0.17	0.21	0.27	0.32	73.2	847	1.71	0.14	0.16	0.18	0.21	0.27	0.32	
	0.20	1	0.030	3.9	403	2.45	0.13	0.15	0.18	0.23	0.33	0.43	3.7	445	2.45	0.14	0.16	0.19	0.24	0.34	0.43
		2	0.030	5.9	355	2.45	0.12	0.15	0.18	0.23	0.34	0.44	5.4	376	2.45	0.13	0.15	0.18	0.24	0.34	0.44
3		0.030	10.4	366	2.46	0.12	0.15	0.18	0.23	0.33	0.43	9.8	403	2.46	0.13	0.16	0.18	0.23	0.33	0.43	
4		0.030	12.0	381	2.45	0.13	0.16	0.19	0.24	0.34	0.44	11.5	419	2.45	0.14	0.17	0.19	0.25	0.35	0.45	
6		0.030	17.9	351	2.46	0.12	0.15	0.18	0.23	0.34	0.44	16.7	379	2.46	0.13	0.16	0.18	0.24	0.34	0.44	
8		0.030	25.4	376	2.46	0.12	0.15	0.18	0.24	0.34	0.44	23.2	407	2.46	0.13	0.16	0.19	0.24	0.34	0.44	
12		0.030	37.9	371	2.46	0.12	0.15	0.18	0.24	0.34	0.44	35.9	406	2.47	0.13	0.16	0.19	0.24	0.34	0.44	
20		0.030	56.6	362	2.47	0.12	0.15	0.18	0.24	0.34	0.44	53.3	394	2.48	0.13	0.16	0.19	0.24	0.34	0.44	
0.50		1	0.015	2.1	156	3.63	0.13	0.19	0.25	0.37	0.56	0.75	1.8	196	3.63	0.15	0.21	0.27	0.37	0.57	0.75
		2	0.015	3.2	161	3.63	0.13	0.19	0.25	0.37	0.58	0.77	2.5	201	3.63	0.15	0.20	0.26	0.36	0.57	0.75
	3	0.015	5.9	156	3.63	0.13	0.20	0.25	0.37	0.57	0.75	4.9	203	3.63	0.16	0.21	0.27	0.38	0.57	0.76	
	4	0.015	5.7	159	3.63	0.14	0.20	0.26	0.38	0.58	0.77	4.9	196	3.63	0.16	0.22	0.28	0.39	0.59	0.78	
	6	0.015	9.3	157	3.64	0.13	0.19	0.25	0.37	0.57	0.76	7.8	204	3.64	0.15	0.21	0.26	0.37	0.57	0.75	
	8	0.015	13.0	158	3.64	0.14	0.20	0.26	0.38	0.59	0.78	10.6	203	3.64	0.16	0.22	0.27	0.38	0.58	0.77	
	12	0.015	19.5	158	3.65	0.13	0.20	0.26	0.38	0.58	0.78	16.1	200	3.65	0.16	0.22	0.27	0.38	0.58	0.77	
	20	0.015	30.0	155	3.66	0.13	0.20	0.26	0.38	0.58	0.78	25.4	202	3.66	0.16	0.22	0.27	0.38	0.58	0.77	

**Table B.11:** Detection probability, average detection time, contaminated area in case of detection failure and relative contaminated area to control area  $L$  for various RADTi in case of  $\sigma_{lnK}^2 = 0.5$  assuming annually sampling frequency

		$\sigma_{lnK}^2$										
		0.50										
$\alpha_i(m)$	now	infd5(max)	$P_d$ (12M)	$\langle T_{(DET)} \rangle$ (DAYS)	AREA ON FAILURE	(AREA ON DET.)/L	(3M. RADTi)/L	(6M. RADTi)/L	(12M. RADTi)/L	(24M. RADTi)/L	(36M. RADTi)/L	
0.001	1	1.75	3.1	6150	0.06	0.03	0.03	0.03	0.03	0.03	0.04	
	2	1.75	5.6	6046	0.06	0.03	0.03	0.03	0.03	0.03	0.03	
	3	1.75	7.8	6125	0.06	0.03	0.03	0.03	0.03	0.03	0.03	
	4	1.75	9.2	6107	0.06	0.03	0.03	0.03	0.03	0.03	0.04	
	6	1.75	14.1	5975	0.06	0.03	0.03	0.03	0.03	0.03	0.03	
	8	1.75	18.2	6130	0.06	0.03	0.03	0.03	0.03	0.03	0.03	
	12	1.75	28.1	6133	0.06	0.03	0.03	0.03	0.03	0.03	0.04	
	20	1.75	44.4	6089	0.06	0.03	0.03	0.03	0.03	0.03	0.03	
	0.01	1	1.50	4.5	4988	0.34	0.13	0.13	0.14	0.14	0.15	0.16
		2	1.50	8.9	5266	0.34	0.14	0.14	0.14	0.15	0.16	0.17
3		1.50	11.8	5027	0.34	0.13	0.14	0.14	0.14	0.15	0.17	
4		1.50	16.6	5000	0.34	0.13	0.14	0.14	0.14	0.16	0.17	
6		1.50	24.1	5217	0.34	0.14	0.14	0.14	0.15	0.16	0.17	
8		1.50	32.7	5111	0.35	0.14	0.14	0.14	0.15	0.16	0.17	
12		1.50	46.7	5051	0.35	0.13	0.14	0.14	0.15	0.16	0.17	
20		1.50	66.8	5082	0.35	0.13	0.14	0.14	0.15	0.16	0.17	
0.02		1	0.50	4.5	2171	0.57	0.10	0.11	0.11	0.12	0.14	0.15
		2	0.50	8.8	2202	0.57	0.10	0.10	0.11	0.12	0.13	0.15
	3	0.50	12.8	2214	0.57	0.10	0.10	0.11	0.11	0.13	0.15	
	4	0.50	17.0	2273	0.57	0.10	0.10	0.11	0.12	0.13	0.15	
	6	0.50	25.8	2216	0.57	0.10	0.10	0.11	0.12	0.13	0.15	
	8	0.50	33.8	2240	0.57	0.10	0.10	0.11	0.12	0.13	0.15	
	12	0.50	48.6	2271	0.58	0.10	0.10	0.11	0.12	0.13	0.15	
	20	0.50	71.8	2246	0.60	0.10	0.10	0.11	0.11	0.13	0.15	
	0.05	1	0.50	3.0	2046	1.09	0.19	0.20	0.21	0.23	0.26	0.29
		2	0.50	5.9	2085	1.09	0.19	0.20	0.21	0.22	0.26	0.29
3		0.50	8.9	2078	1.09	0.19	0.20	0.21	0.22	0.26	0.29	
4		0.50	11.5	2118	1.09	0.19	0.20	0.20	0.22	0.25	0.29	
6		0.50	17.0	2082	1.09	0.19	0.20	0.20	0.22	0.26	0.29	
8		0.50	23.4	2112	1.09	0.19	0.20	0.21	0.22	0.26	0.29	
12		0.50	33.2	2137	1.10	0.19	0.20	0.21	0.22	0.26	0.29	
20		0.50	51.7	2124	1.11	0.19	0.20	0.21	0.22	0.26	0.29	
0.10		1	0.125	4.0	917	1.68	0.15	0.16	0.18	0.21	0.26	0.32
		2	0.125	6.7	943	1.68	0.15	0.17	0.18	0.21	0.27	0.33
	3	0.125	10.3	917	1.69	0.15	0.16	0.18	0.21	0.26	0.32	
	4	0.125	12.7	910	1.68	0.15	0.16	0.18	0.21	0.27	0.32	
	6	0.125	19.9	913	1.69	0.15	0.17	0.18	0.21	0.27	0.33	
	8	0.125	27.6	913	1.69	0.15	0.16	0.18	0.21	0.27	0.32	
	12	0.125	39.8	913	1.69	0.15	0.16	0.18	0.21	0.27	0.32	
	20	0.125	60.7	916	1.73	0.15	0.16	0.18	0.21	0.27	0.32	
	0.20	1	0.030	2.7	547	2.45	0.15	0.17	0.20	0.24	0.34	0.43
		2	0.030	3.9	488	2.45	0.15	0.17	0.20	0.25	0.35	0.45
3		0.030	7.2	507	2.46	0.15	0.17	0.20	0.24	0.34	0.43	
4		0.030	8.0	502	2.46	0.16	0.18	0.21	0.26	0.35	0.45	
6		0.030	11.7	496	2.46	0.15	0.17	0.20	0.25	0.34	0.44	
8		0.030	16.2	511	2.47	0.15	0.18	0.20	0.25	0.35	0.44	
12		0.030	25.3	501	2.47	0.15	0.18	0.20	0.25	0.35	0.44	
20		0.030	37.4	501	2.49	0.15	0.18	0.20	0.25	0.35	0.44	
0.50		1	0.015	0.9	365	3.63	0.21	0.26	0.31	0.40	0.58	0.76
		2	0.015	1.0	389	3.63	0.20	0.24	0.28	0.37	0.54	0.71
	3	0.015	1.8	378	3.63	0.21	0.25	0.30	0.38	0.56	0.73	
	4	0.015	1.5	365	3.63	0.20	0.24	0.28	0.36	0.52	0.68	
	6	0.015	2.8	378	3.63	0.20	0.24	0.28	0.37	0.54	0.71	
	8	0.015	3.4	372	3.63	0.20	0.24	0.29	0.37	0.54	0.71	
	12	0.015	5.6	371	3.64	0.20	0.24	0.28	0.36	0.53	0.69	
	20	0.015	8.7	371	3.64	0.20	0.24	0.29	0.37	0.54	0.71	

**Table B.12:** Detection probability, average detection time, contaminated area in case of detection failure and relative contaminated area to control area for various RADTi in case of  $\sigma_{\ln K}^2 = 1.0$  assuming daily (ED) and monthly (1M) sampling frequencies

$\sigma_{\ln K}^2$		1.00																			
$\alpha_i(m)$	now	nfds(max)	$P_d$ (ED)	$\langle T_{(DET.)} \rangle$ (DAYS)	AREA ON FAILURE	(AREA ON DET.)/L	(3M. RADTi)/L	(6M. RADTi)/L	(12M. RADTi)/L	(24M. RADTi)/L	(36M. RADTi)/L	$P_d$ (1M)	$\langle T_{(DET.)} \rangle$ (DAYS)	AREA ON FAILURE	(AREA ON DET.)/L	(3M. RADTi)/L	(6M. RADTi)/L	(12M. RADTi)/L	(24M. RADTi)/L	(36M. RADTi)/L	
0.001	1	1.75	3.8	5629	0.12	0.04	0.04	0.04	0.04	0.05	0.05	3.8	5605	0.12	0.04	0.04	0.04	0.04	0.05	0.05	
	2	1.75	7.1	5373	0.12	0.04	0.04	0.04	0.04	0.05	0.05	7.0	5388	0.12	0.04	0.04	0.04	0.04	0.05	0.05	
	3	1.75	9.8	5606	0.12	0.04	0.04	0.04	0.04	0.05	0.05	9.7	5597	0.12	0.04	0.04	0.04	0.04	0.05	0.05	
	4	1.75	14.0	5509	0.12	0.04	0.04	0.04	0.04	0.04	0.05	13.8	5510	0.12	0.04	0.04	0.04	0.04	0.04	0.05	
	6	1.75	20.6	5397	0.12	0.04	0.04	0.04	0.04	0.04	0.05	20.3	5415	0.12	0.04	0.04	0.04	0.04	0.04	0.05	
	8	1.75	26.5	5439	0.12	0.04	0.04	0.04	0.04	0.04	0.05	26.1	5446	0.12	0.04	0.04	0.04	0.04	0.04	0.05	
	12	1.75	39.9	5455	0.12	0.04	0.04	0.04	0.04	0.04	0.05	39.3	5471	0.12	0.04	0.04	0.04	0.04	0.04	0.05	
	20	1.75	57.2	5407	0.11	0.04	0.04	0.04	0.04	0.04	0.05	56.4	5423	0.11	0.04	0.04	0.04	0.04	0.04	0.05	
	0.01	1	1.25	5.7	3950	0.55	0.14	0.14	0.15	0.15	0.17	0.19	5.3	3916	0.55	0.14	0.14	0.14	0.15	0.17	0.19
		2	1.25	9.5	3961	0.55	0.14	0.14	0.15	0.15	0.17	0.19	9.1	3962	0.55	0.14	0.14	0.15	0.15	0.17	0.19
3		1.25	14.7	4008	0.55	0.14	0.14	0.15	0.16	0.17	0.19	14.0	4005	0.56	0.14	0.14	0.15	0.16	0.17	0.19	
4		1.25	18.1	4005	0.55	0.14	0.14	0.15	0.15	0.17	0.19	17.5	4014	0.55	0.14	0.14	0.14	0.15	0.17	0.18	
6		1.25	27.4	4020	0.55	0.14	0.14	0.15	0.15	0.17	0.19	26.3	4015	0.55	0.14	0.14	0.15	0.15	0.17	0.19	
8		1.25	35.7	3983	0.55	0.14	0.14	0.14	0.15	0.17	0.19	34.4	3995	0.55	0.14	0.14	0.14	0.15	0.17	0.19	
12		1.25	50.4	3980	0.54	0.14	0.14	0.14	0.15	0.17	0.19	48.4	4000	0.55	0.14	0.14	0.14	0.15	0.17	0.19	
20		1.25	68.8	4028	0.55	0.14	0.14	0.14	0.15	0.17	0.19	66.7	4022	0.55	0.14	0.14	0.14	0.15	0.17	0.19	
0.02		1	0.50	6.3	1940	0.88	0.10	0.11	0.12	0.13	0.15	0.18	5.9	1957	0.88	0.10	0.11	0.12	0.13	0.15	0.18
		2	0.50	10.1	2100	0.88	0.10	0.11	0.11	0.13	0.15	0.17	9.7	2110	0.88	0.10	0.11	0.12	0.13	0.15	0.17
	3	0.50	17.0	1938	0.88	0.10	0.11	0.11	0.13	0.15	0.17	16.2	1949	0.88	0.10	0.11	0.11	0.13	0.15	0.17	
	4	0.50	20.5	2046	0.88	0.11	0.11	0.12	0.13	0.15	0.18	19.7	2066	0.88	0.11	0.11	0.12	0.13	0.15	0.18	
	6	0.50	28.5	2055	0.88	0.10	0.11	0.12	0.13	0.15	0.18	27.5	2071	0.88	0.10	0.11	0.12	0.13	0.15	0.18	
	8	0.50	42.1	2082	0.87	0.11	0.11	0.12	0.13	0.15	0.18	40.8	2088	0.87	0.11	0.11	0.12	0.13	0.15	0.18	
	12	0.50	57.5	2073	0.87	0.10	0.11	0.12	0.13	0.15	0.18	55.6	2086	0.88	0.10	0.11	0.12	0.13	0.15	0.18	
	20	0.50	77.0	2046	0.86	0.10	0.11	0.11	0.13	0.15	0.18	75.5	2056	0.86	0.10	0.11	0.11	0.13	0.15	0.18	
	0.05	1	0.13	5.7	874	1.54	0.10	0.11	0.12	0.15	0.19	0.24	5.6	887	1.54	0.10	0.11	0.12	0.15	0.20	0.25
		2	0.13	11.6	1033	1.55	0.09	0.10	0.11	0.13	0.18	0.22	11.2	1037	1.55	0.09	0.10	0.11	0.14	0.18	0.22
3		0.13	17.0	906	1.54	0.09	0.10	0.11	0.14	0.18	0.23	16.5	925	1.55	0.09	0.11	0.12	0.14	0.19	0.23	
4		0.13	22.0	968	1.55	0.09	0.10	0.11	0.13	0.18	0.22	21.3	985	1.55	0.09	0.10	0.11	0.13	0.18	0.22	
6		0.13	33.3	985	1.56	0.09	0.10	0.11	0.14	0.18	0.22	31.9	999	1.56	0.09	0.10	0.12	0.14	0.18	0.22	
8		0.13	43.5	963	1.55	0.09	0.10	0.11	0.14	0.18	0.22	42.1	985	1.56	0.09	0.10	0.12	0.14	0.18	0.23	
12		0.13	61.8	965	1.56	0.09	0.10	0.11	0.13	0.18	0.22	59.7	983	1.57	0.09	0.10	0.11	0.14	0.18	0.22	
20		0.13	86.3	931	1.54	0.09	0.10	0.11	0.13	0.18	0.22	84.7	942	1.54	0.09	0.10	0.11	0.13	0.18	0.22	
0.10		1	0.063	5.4	668	2.23	0.12	0.14	0.16	0.20	0.28	0.36	5.1	697	2.24	0.12	0.14	0.16	0.20	0.28	0.36
		2	0.063	11.1	804	2.24	0.12	0.14	0.16	0.19	0.26	0.34	10.2	779	2.24	0.12	0.14	0.16	0.19	0.26	0.34
	3	0.063	17.1	654	2.24	0.12	0.13	0.15	0.19	0.27	0.34	15.9	663	2.24	0.11	0.13	0.15	0.19	0.26	0.34	
	4	0.063	21.6	686	2.25	0.11	0.13	0.15	0.19	0.26	0.33	20.4	681	2.24	0.12	0.13	0.15	0.19	0.26	0.33	
	6	0.063	31.6	740	2.25	0.12	0.14	0.16	0.19	0.27	0.34	29.4	733	2.24	0.12	0.14	0.16	0.19	0.27	0.34	
	8	0.063	43.2	705	2.25	0.12	0.14	0.16	0.19	0.26	0.34	40.0	703	2.24	0.12	0.14	0.15	0.19	0.26	0.34	
	12	0.063	60.8	689	2.25	0.12	0.14	0.15	0.19	0.26	0.34	56.5	686	2.24	0.12	0.14	0.15	0.19	0.26	0.34	
	20	0.063	86.2	691	2.24	0.11	0.13	0.15	0.19	0.26	0.34	82.7	695	2.24	0.12	0.13	0.15	0.19	0.27	0.34	
	0.20	1	0.030	4.0	435	3.03	0.13	0.17	0.20	0.26	0.39	0.51	3.4	403	3.03	0.13	0.16	0.19	0.26	0.38	0.51
		2	0.030	7.7	407	3.03	0.13	0.16	0.20	0.26	0.38	0.50	6.5	398	3.03	0.12	0.15	0.19	0.25	0.37	0.48
3		0.030	12.8	373	3.03	0.12	0.16	0.19	0.25	0.38	0.50	11.2	355	3.03	0.12	0.15	0.18	0.25	0.37	0.49	
4		0.030	16.6	401	3.03	0.12	0.16	0.19	0.25	0.37	0.49	14.5	383	3.03	0.12	0.15	0.18	0.25	0.36	0.48	
6		0.030	22.0	395	3.03	0.12	0.16	0.19	0.25	0.38	0.50	19.2	390	3.03	0.12	0.15	0.18	0.25	0.37	0.49	
8		0.030	31.1	382	3.03	0.12	0.16	0.19	0.26	0.38	0.50	26.6	359	3.03	0.12	0.15	0.18	0.25	0.37	0.49	
12		0.030	44.7	398	3.03	0.12	0.16	0.19	0.25	0.38	0.50	38.6	380	3.04	0.12	0.15	0.18	0.24	0.36	0.48	
20		0.030	64.6	390	3.02	0.12	0.16	0.19	0.25	0.38	0.50	57.8	362	3.02	0.12	0.15	0.18	0.25	0.37	0.49	
0.50		1	0.015	2.2	124	4.02	0.10	0.18	0.25	0.38	0.63	0.86	2.0	131	4.02	0.11	0.19	0.26	0.40	0.65	0.88
		2	0.015	4.2	112	4.03	0.09	0.17	0.24	0.38	0.62	0.84	3.6	112	4.03	0.09	0.17	0.25	0.38	0.62	0.85
	3	0.015	7.7	117	4.03	0.10	0.18	0.26	0.39	0.64	0.87	6.7	118	4.03	0.10	0.19	0.26	0.40	0.64	0.87	
	4	0.015	9.0	127	4.02	0.10	0.18	0.25	0.38	0.63	0.86	7.5	127	4.02	0.10	0.18	0.24	0.38	0.62	0.85	
	6	0.015	12.7	131	4.03	0.09	0.17	0.25	0.38	0.62	0.84	10.9	124	4.03	0.09	0.17	0.25	0.38	0.62	0.84	
	8	0.015	18.1	125	4.03	0.10	0.18	0.25	0.38	0.63	0.85	15.6	121	4.03	0.10	0.18	0.25	0.39	0.63	0.86	
	12	0.015	25.3	119	4.03	0.09	0.17	0.25	0.38	0.62	0.85	21.6	117	4.03	0.09	0.17	0.24	0.38	0.62	0.84	
	20	0.015	36.9	114	4.04	0.09	0.17	0.24	0.38	0.62	0.85	32.9	119	4.04	0.09	0.17	0.25	0.38	0.62	0.84	

**Table B.13:** Detection probability, average detection time, contaminated area in case of detection failure and relative contaminated area to control area for various RADTi in case of  $\sigma_{\ln K}^2 = 1.0$  assuming bimonthly (2M) and quarterly (3M) sampling frequencies

$\sigma_{\ln K}^2$		1.00																				
$\alpha_i(m)$	now	nfds(max)	$P_d$ (2M)	$\langle T_{(DET)} \rangle$ (DAYS)	AREA ON FAILURE	(AREA ON DET.)/L	(3M. RADTi)/L	(6M. RADTi)/L	(12M. RADTi)/L	(24M. RADTi)/L	(36M. RADTi)/L	$P_d$ (3M)	$\langle T_{(DET)} \rangle$ (DAYS)	AREA ON FAILURE	(AREA ON DET.)/L	(3M. RADTi)/L	(6M. RADTi)/L	(12M. RADTi)/L	(24M. RADTi)/L	(36M. RADTi)/L		
0.001	1	1.75	3.8	5620	0.12	0.04	0.04	0.04	0.04	0.05	0.05	3.7	5645	0.12	0.04	0.04	0.04	0.04	0.04	0.05	0.05	
	2	1.75	6.9	5395	0.12	0.04	0.04	0.04	0.05	0.05	0.05	6.8	5446	0.12	0.04	0.04	0.04	0.05	0.05	0.05	0.05	
	3	1.75	9.6	5617	0.12	0.04	0.04	0.04	0.04	0.05	0.05	9.5	5643	0.12	0.04	0.04	0.04	0.04	0.05	0.05	0.05	
	4	1.75	13.5	5513	0.12	0.04	0.04	0.04	0.04	0.04	0.05	13.4	5518	0.12	0.04	0.04	0.04	0.04	0.04	0.04	0.05	0.05
	6	1.75	20.1	5435	0.12	0.04	0.04	0.04	0.04	0.05	0.05	19.8	5456	0.12	0.04	0.04	0.04	0.04	0.04	0.05	0.05	0.05
	8	1.75	25.9	5458	0.12	0.04	0.04	0.04	0.04	0.05	0.05	25.5	5456	0.12	0.04	0.04	0.04	0.04	0.04	0.05	0.05	0.05
	12	1.75	38.8	5486	0.12	0.04	0.04	0.04	0.04	0.04	0.05	38.5	5500	0.12	0.04	0.04	0.04	0.04	0.04	0.04	0.04	0.05
	20	1.75	55.9	5434	0.11	0.04	0.04	0.04	0.04	0.04	0.05	55.2	5451	0.12	0.04	0.04	0.04	0.04	0.04	0.04	0.04	0.05
	0.01	1	1.25	5.2	3872	0.55	0.14	0.14	0.14	0.15	0.17	0.19	5.2	3893	0.55	0.14	0.14	0.15	0.15	0.17	0.19	0.19
2		1.25	8.8	4008	0.55	0.14	0.14	0.15	0.16	0.17	0.19	8.7	3992	0.55	0.14	0.14	0.15	0.16	0.17	0.19	0.19	
3		1.25	13.6	3982	0.56	0.14	0.14	0.15	0.16	0.17	0.19	13.4	4003	0.56	0.14	0.14	0.15	0.16	0.17	0.19	0.19	
4		1.25	17.1	4025	0.55	0.14	0.14	0.14	0.15	0.17	0.18	16.7	4022	0.55	0.14	0.14	0.14	0.15	0.17	0.18	0.18	
6		1.25	25.6	4041	0.55	0.14	0.14	0.15	0.15	0.17	0.19	25.0	4042	0.55	0.14	0.14	0.15	0.15	0.17	0.19	0.19	0.19
8		1.25	33.6	4004	0.55	0.14	0.14	0.14	0.15	0.17	0.19	32.9	4022	0.55	0.14	0.14	0.14	0.15	0.17	0.19	0.19	0.19
12		1.25	47.8	4019	0.55	0.14	0.14	0.14	0.15	0.17	0.19	46.7	4028	0.55	0.14	0.14	0.14	0.15	0.17	0.19	0.19	0.19
20		1.25	65.7	4030	0.55	0.14	0.14	0.14	0.15	0.17	0.19	64.7	4047	0.55	0.14	0.14	0.14	0.15	0.17	0.19	0.19	0.19
0.02		1	0.50	5.7	1926	0.88	0.10	0.11	0.12	0.13	0.15	0.18	5.7	1971	0.88	0.10	0.11	0.12	0.13	0.16	0.18	0.18
	2	0.50	9.6	2141	0.88	0.10	0.11	0.12	0.13	0.15	0.17	9.5	2167	0.88	0.11	0.11	0.12	0.13	0.15	0.18	0.18	
	3	0.50	15.9	1943	0.88	0.10	0.11	0.11	0.13	0.15	0.17	15.7	1974	0.88	0.10	0.11	0.12	0.13	0.15	0.18	0.18	
	4	0.50	19.3	2078	0.88	0.11	0.11	0.12	0.13	0.16	0.18	19.2	2098	0.88	0.11	0.11	0.12	0.13	0.16	0.18	0.18	
	6	0.50	26.9	2076	0.88	0.11	0.11	0.12	0.13	0.15	0.18	26.6	2098	0.88	0.11	0.11	0.12	0.13	0.15	0.18	0.18	0.18
	8	0.50	39.9	2101	0.88	0.11	0.11	0.12	0.13	0.15	0.18	39.3	2120	0.88	0.11	0.11	0.12	0.13	0.16	0.18	0.18	0.18
	12	0.50	54.7	2097	0.88	0.11	0.11	0.12	0.13	0.15	0.18	53.9	2115	0.88	0.11	0.11	0.12	0.13	0.15	0.18	0.18	0.18
	20	0.50	74.6	2064	0.87	0.10	0.11	0.11	0.13	0.15	0.18	74.2	2077	0.87	0.10	0.11	0.12	0.13	0.15	0.18	0.18	0.18
	0.05	1	0.13	5.5	894	1.54	0.10	0.11	0.12	0.15	0.20	0.25	5.4	904	1.54	0.10	0.11	0.13	0.15	0.20	0.25	0.25
2		0.13	11.1	1049	1.55	0.10	0.11	0.12	0.14	0.18	0.22	10.9	1052	1.55	0.10	0.11	0.12	0.14	0.18	0.22	0.22	
3		0.13	16.2	926	1.54	0.09	0.11	0.12	0.14	0.19	0.23	16.0	959	1.55	0.10	0.11	0.12	0.14	0.19	0.23	0.23	
4		0.13	21.0	999	1.55	0.09	0.10	0.11	0.13	0.18	0.22	20.7	1017	1.56	0.09	0.10	0.11	0.14	0.18	0.22	0.22	
6		0.13	31.2	1013	1.56	0.09	0.11	0.12	0.14	0.18	0.22	30.8	1022	1.56	0.10	0.11	0.12	0.14	0.18	0.23	0.23	0.23
8		0.13	41.5	999	1.56	0.10	0.11	0.12	0.14	0.18	0.23	40.9	1015	1.56	0.10	0.11	0.12	0.14	0.18	0.23	0.23	0.23
12		0.13	59.1	998	1.57	0.09	0.10	0.11	0.14	0.18	0.23	58.3	1014	1.57	0.10	0.11	0.12	0.14	0.18	0.23	0.23	0.23
20		0.13	84.2	957	1.55	0.09	0.10	0.11	0.14	0.18	0.23	83.1	972	1.57	0.09	0.10	0.11	0.14	0.18	0.23	0.23	0.23
0.10		1	0.063	5.1	715	2.24	0.13	0.14	0.16	0.20	0.28	0.36	4.8	717	2.24	0.13	0.14	0.16	0.20	0.28	0.36	0.36
	2	0.063	9.9	787	2.24	0.12	0.14	0.16	0.19	0.26	0.34	9.7	785	2.24	0.12	0.14	0.16	0.19	0.27	0.34	0.34	
	3	0.063	15.8	678	2.24	0.12	0.14	0.15	0.19	0.27	0.34	15.2	683	2.24	0.12	0.14	0.15	0.19	0.26	0.34	0.34	
	4	0.063	19.9	687	2.24	0.12	0.14	0.15	0.19	0.26	0.34	19.6	710	2.24	0.12	0.14	0.15	0.19	0.26	0.33	0.33	
	6	0.063	28.5	731	2.24	0.12	0.14	0.16	0.19	0.27	0.34	27.6	745	2.25	0.12	0.14	0.16	0.19	0.27	0.34	0.34	0.34
	8	0.063	38.6	709	2.25	0.12	0.14	0.16	0.19	0.26	0.34	37.8	725	2.25	0.12	0.14	0.16	0.19	0.27	0.34	0.34	0.34
	12	0.063	54.8	696	2.24	0.12	0.14	0.16	0.19	0.26	0.34	53.7	714	2.25	0.12	0.14	0.16	0.19	0.27	0.34	0.34	0.34
	20	0.063	81.0	703	2.25	0.12	0.14	0.15	0.19	0.27	0.34	79.5	712	2.25	0.12	0.14	0.16	0.19	0.27	0.34	0.34	0.34
	0.20	1	0.030	3.2	399	3.03	0.13	0.16	0.19	0.26	0.38	0.51	3.0	392	3.03	0.13	0.16	0.19	0.26	0.38	0.50	0.50
2		0.030	6.2	405	3.03	0.12	0.16	0.19	0.25	0.37	0.48	6.1	409	3.03	0.13	0.16	0.19	0.25	0.37	0.48	0.48	
3		0.030	10.6	359	3.03	0.12	0.15	0.19	0.25	0.37	0.49	10.3	361	3.03	0.12	0.16	0.19	0.25	0.38	0.50	0.50	
4		0.030	13.9	392	3.03	0.12	0.15	0.18	0.25	0.36	0.48	13.2	401	3.03	0.12	0.16	0.19	0.25	0.36	0.48	0.48	0.48
6		0.030	18.0	385	3.03	0.12	0.15	0.18	0.25	0.37	0.49	17.8	394	3.03	0.12	0.16	0.19	0.25	0.37	0.49	0.49	0.49
8		0.030	25.3	362	3.03	0.12	0.15	0.18	0.25	0.37	0.49	24.5	373	3.03	0.12	0.16	0.19	0.25	0.37	0.49	0.49	0.49
12		0.030	37.0	388	3.04	0.12	0.15	0.18	0.25	0.37	0.48	35.8	397	3.04	0.12	0.15	0.19	0.25	0.37	0.49	0.49	0.49
20		0.030	55.6	367	3.03	0.12	0.15	0.18	0.25	0.37	0.49	53.6	372	3.03	0.12	0.15	0.19	0.25	0.37	0.49	0.49	0.49
0.50		1	0.015	1.9	152	4.02	0.13	0.20	0.27	0.41	0.65	0.88	1.6	170	4.02	0.14	0.21	0.28	0.41	0.65	0.88	0.88
	2	0.015	3.4	127	4.03	0.11	0.18	0.25	0.39	0.62	0.85	3.2	134	4.03	0.12	0.19	0.26	0.39	0.63	0.86	0.86	
	3	0.015	6.4	131	4.03	0.12	0.20	0.27	0.41	0.65	0.88	5.8	153	4.03	0.13	0.21	0.28	0.41	0.65	0.87	0.87	
	4	0.015	7.0	136	4.02	0.11	0.18	0.25	0.38	0.62	0.85	6.5	162	4.03	0.12	0.19	0.25	0.38	0.62	0.84	0.84	0.84
	6	0.015	10.4	133	4.03	0.11	0.18	0.25	0.38	0.62	0.84	9.7	152	4.03	0.12	0.19	0.26	0.39	0.62	0.83	0.83	0.83
	8	0.015	14.4	132	4.03	0.11	0.19	0.26	0.39	0.63	0.86	13.4	150	4.03	0.12	0.20	0.26	0.39	0.63	0.85	0.85	0.85
	12	0.015	20.5	126	4.03	0.11	0.18	0.25	0.38	0.62	0.85	19.0	143	4.03	0.12	0.19	0.26	0.39	0.62	0.85	0.85	0.85
	20	0.015	31.5	132	4.04	0.11	0.19	0.26	0.39	0.63	0.85	29.8	151	4.04	0.12	0.20	0.26	0.39	0.63	0.85	0.85	0.85

**Table B.14:** Detection probability, average detection time, contaminated area in case of detection failure and relative contaminated area to control area  $L$  for various RADTi in case of  $\sigma_{InK}^2 = 1.0$  assuming every 4 months (4M) and biannually (6M) sampling frequencies

$\sigma_{InK}^2$		1.00																				
$\alpha_1(m)$	now	ntds(max)	$P_d$ (4M)	$\langle T_{(DET.)} \rangle$ (DAYS)	AREA ON FAILURE	(AREA ON DET.)/L	(3M. RADTi)/L	(6M. RADTi)/L	(12M. RADTi)/L	(24M. RADTi)/L	(36M. RADTi)/L	$P_d$ (6M)	$\langle T_{(DET.)} \rangle$ (DAYS)	AREA ON FAILURE	(AREA ON DET.)/L	(3M. RADTi)/L	(6M. RADTi)/L	(12M. RADTi)/L	(24M. RADTi)/L	(36M. RADTi)/L		
0.001	1	1.75	3.7	5682	0.12	0.04	0.04	0.04	0.04	0.05	0.05	3.6	5643	0.12	0.04	0.04	0.04	0.04	0.04	0.05	0.05	
	2	1.75	6.8	5413	0.12	0.04	0.04	0.04	0.05	0.05	0.05	6.5	5535	0.12	0.04	0.04	0.04	0.04	0.04	0.05	0.05	
	3	1.75	9.4	5660	0.12	0.04	0.04	0.04	0.04	0.05	0.05	9.1	5709	0.12	0.04	0.04	0.04	0.04	0.04	0.05	0.05	
	4	1.75	13.0	5554	0.12	0.04	0.04	0.04	0.04	0.04	0.05	12.4	5646	0.12	0.04	0.04	0.04	0.04	0.04	0.04	0.05	
	6	1.75	19.6	5480	0.12	0.04	0.04	0.04	0.04	0.05	0.05	18.5	5579	0.12	0.04	0.04	0.04	0.04	0.04	0.05	0.05	
	8	1.75	25.4	5484	0.12	0.04	0.04	0.04	0.04	0.05	0.05	24.1	5581	0.12	0.04	0.04	0.04	0.04	0.04	0.05	0.05	
	12	1.75	37.6	5539	0.12	0.04	0.04	0.04	0.04	0.04	0.05	36.2	5607	0.12	0.04	0.04	0.04	0.04	0.04	0.04	0.05	
	20	1.75	54.8	5471	0.11	0.04	0.04	0.04	0.04	0.04	0.05	52.5	5542	0.12	0.04	0.04	0.04	0.04	0.04	0.05	0.05	
	0.01	1	1.25	5.1	3878	0.55	0.14	0.14	0.14	0.15	0.17	0.19	5.0	3926	0.55	0.14	0.14	0.15	0.15	0.15	0.17	0.19
		2	1.25	8.5	4046	0.55	0.14	0.14	0.15	0.16	0.17	0.19	8.2	4058	0.55	0.14	0.14	0.15	0.16	0.17	0.19	
3		1.25	13.2	4005	0.56	0.14	0.14	0.15	0.16	0.17	0.19	12.8	4038	0.56	0.14	0.14	0.15	0.16	0.17	0.19		
4		1.25	16.5	4043	0.55	0.14	0.14	0.14	0.15	0.17	0.18	16.0	4054	0.55	0.14	0.14	0.15	0.15	0.17	0.19		
6		1.25	24.5	4085	0.55	0.14	0.14	0.15	0.15	0.17	0.19	23.8	4100	0.55	0.14	0.14	0.15	0.15	0.17	0.19		
8		1.25	32.6	4029	0.55	0.14	0.14	0.14	0.15	0.17	0.19	31.3	4074	0.55	0.14	0.14	0.15	0.15	0.17	0.19		
12		1.25	46.2	4041	0.55	0.14	0.14	0.14	0.15	0.17	0.19	45.2	4075	0.55	0.14	0.14	0.14	0.15	0.17	0.19		
20		1.25	64.3	4064	0.55	0.14	0.14	0.14	0.15	0.17	0.19	62.4	4085	0.55	0.14	0.14	0.15	0.15	0.17	0.19		
0.02		1	0.50	5.6	1955	0.88	0.10	0.11	0.12	0.13	0.15	0.18	5.3	2002	0.88	0.11	0.11	0.12	0.13	0.16	0.18	
		2	0.50	9.3	2200	0.88	0.11	0.11	0.12	0.13	0.15	0.18	8.9	2242	0.88	0.11	0.11	0.12	0.13	0.15	0.18	
	3	0.50	15.5	1968	0.88	0.10	0.11	0.12	0.13	0.15	0.18	14.8	2024	0.88	0.11	0.11	0.12	0.13	0.15	0.18		
	4	0.50	18.9	2115	0.88	0.11	0.11	0.12	0.13	0.16	0.18	18.6	2153	0.88	0.11	0.12	0.12	0.13	0.16	0.18		
	6	0.50	26.0	2123	0.88	0.11	0.11	0.12	0.13	0.15	0.18	25.0	2167	0.88	0.11	0.11	0.12	0.13	0.16	0.18		
	8	0.50	38.6	2141	0.88	0.11	0.11	0.12	0.13	0.16	0.18	37.0	2188	0.88	0.11	0.11	0.12	0.13	0.16	0.18		
	12	0.50	53.5	2134	0.88	0.11	0.11	0.12	0.13	0.16	0.18	52.2	2172	0.88	0.11	0.11	0.12	0.13	0.16	0.18		
	20	0.50	73.5	2092	0.87	0.10	0.11	0.12	0.13	0.15	0.18	72.0	2135	0.89	0.11	0.11	0.12	0.13	0.15	0.18		
	0.05	1	0.13	5.1	927	1.54	0.10	0.11	0.13	0.15	0.20	0.25	5.0	950	1.54	0.11	0.12	0.13	0.15	0.20	0.25	
		2	0.13	10.7	1083	1.55	0.10	0.11	0.12	0.14	0.18	0.23	10.4	1112	1.55	0.10	0.11	0.12	0.14	0.19	0.23	
3		0.13	15.4	964	1.55	0.10	0.11	0.12	0.14	0.19	0.23	14.8	1005	1.55	0.10	0.11	0.12	0.15	0.19	0.24		
4		0.13	20.4	1028	1.56	0.10	0.11	0.12	0.14	0.18	0.23	19.6	1076	1.56	0.10	0.11	0.12	0.14	0.18	0.23		
6		0.13	30.2	1044	1.56	0.10	0.11	0.12	0.14	0.18	0.23	29.2	1083	1.56	0.10	0.11	0.12	0.14	0.19	0.23		
8		0.13	40.3	1027	1.56	0.10	0.11	0.12	0.14	0.18	0.23	39.0	1070	1.57	0.10	0.11	0.12	0.14	0.19	0.23		
12		0.13	57.5	1031	1.57	0.10	0.11	0.12	0.14	0.18	0.23	55.8	1071	1.58	0.10	0.11	0.12	0.14	0.19	0.23		
20		0.13	82.9	985	1.56	0.09	0.10	0.12	0.14	0.18	0.23	80.6	1026	1.61	0.10	0.11	0.12	0.14	0.19	0.23		
0.10		1	0.063	4.8	725	2.24	0.13	0.14	0.16	0.20	0.28	0.36	4.6	765	2.24	0.13	0.15	0.17	0.21	0.28	0.36	
		2	0.063	9.5	804	2.24	0.13	0.15	0.16	0.20	0.27	0.34	9.0	822	2.24	0.13	0.15	0.16	0.20	0.27	0.34	
	3	0.063	14.9	687	2.24	0.12	0.14	0.16	0.19	0.27	0.34	14.1	729	2.25	0.12	0.14	0.16	0.19	0.27	0.34		
	4	0.063	19.0	702	2.24	0.12	0.14	0.15	0.19	0.26	0.34	18.1	741	2.24	0.12	0.14	0.16	0.19	0.26	0.34		
	6	0.063	27.1	755	2.24	0.13	0.14	0.16	0.20	0.27	0.34	25.5	776	2.25	0.13	0.15	0.16	0.20	0.27	0.34		
	8	0.063	36.8	735	2.25	0.12	0.14	0.16	0.19	0.27	0.34	34.8	767	2.26	0.13	0.14	0.16	0.20	0.27	0.34		
	12	0.063	52.5	717	2.25	0.12	0.14	0.16	0.19	0.27	0.34	49.5	756	2.26	0.13	0.14	0.16	0.20	0.27	0.34		
	20	0.063	78.5	722	2.26	0.12	0.14	0.16	0.20	0.27	0.34	74.9	754	2.29	0.13	0.14	0.16	0.20	0.27	0.34		
	0.20	1	0.030	3.0	396	3.03	0.13	0.17	0.20	0.26	0.39	0.51	2.7	418	3.03	0.14	0.17	0.20	0.26	0.38	0.50	
		2	0.030	5.6	393	3.03	0.12	0.16	0.19	0.25	0.36	0.48	5.2	456	3.03	0.13	0.16	0.19	0.25	0.36	0.47	
3		0.030	10.0	368	3.03	0.13	0.16	0.19	0.26	0.38	0.50	9.2	401	3.03	0.13	0.17	0.20	0.26	0.38	0.49		
4		0.030	13.1	421	3.03	0.13	0.16	0.19	0.25	0.37	0.49	11.8	435	3.03	0.13	0.16	0.19	0.25	0.37	0.48		
6		0.030	16.7	400	3.03	0.12	0.16	0.19	0.25	0.37	0.49	15.6	428	3.03	0.13	0.16	0.19	0.25	0.37	0.48		
8		0.030	23.2	387	3.04	0.12	0.16	0.19	0.25	0.37	0.49	21.3	419	3.04	0.13	0.16	0.19	0.25	0.37	0.49		
12		0.030	34.3	406	3.05	0.13	0.16	0.19	0.25	0.37	0.48	31.7	433	3.05	0.13	0.16	0.19	0.25	0.37	0.48		
20		0.030	52.7	391	3.04	0.13	0.16	0.19	0.25	0.37	0.49	48.0	413	3.05	0.13	0.16	0.19	0.25	0.37	0.49		
0.50		1	0.015	1.5	189	4.03	0.14	0.21	0.27	0.40	0.63	0.84	1.2	260	4.03	0.18	0.24	0.30	0.41	0.63	0.84	
		2	0.015	3.0	170	4.03	0.14	0.21	0.27	0.40	0.63	0.84	2.4	215	4.03	0.16	0.23	0.29	0.41	0.63	0.85	
	3	0.015	5.4	171	4.03	0.15	0.22	0.28	0.41	0.64	0.86	4.1	226	4.03	0.17	0.23	0.28	0.40	0.62	0.83		
	4	0.015	6.1	176	4.03	0.14	0.20	0.27	0.39	0.62	0.84	4.8	231	4.03	0.15	0.20	0.26	0.37	0.59	0.80		
	6	0.015	9.3	166	4.03	0.14	0.21	0.27	0.39	0.62	0.83	7.2	230	4.03	0.16	0.22	0.28	0.39	0.60	0.81		
	8	0.015	12.2	171	4.03	0.14	0.21	0.27	0.40	0.63	0.85	9.5	219	4.03	0.16	0.21	0.27	0.38	0.60	0.81		
	12	0.015	17.8	167	4.04	0.14	0.20	0.27	0.39	0.62	0.84	14.0	214	4.04	0.15	0.21	0.27	0.38	0.59	0.80		
	20	0.015	28.0	171	4.04	0.14	0.21	0.27	0.39	0.62	0.84	22.3	229	4.05	0.16	0.22	0.27	0.39	0.60	0.81		

**Table B.15:** Detection probability, average detection time, contaminated area in case of detection failure and relative contaminated area to control area  $L$  for various RADTi in case of  $\sigma_{\ln K}^2 = 1.0$  assuming annually sampling frequency

		$\sigma_{\ln K}^2$									
		1.00									
$\alpha_i(m)$	now	nfds(max)	$P_d$ (12M)	$\langle T_{(DET)} \rangle$ (DAYS)	AREA ON FAILURE	(AREA ON DET.)/L	(3M. RADTi)/L	(6M. RADTi)/L	(12M. RADTi)/L	(24M. RADTi)/L	(36M. RADTi)/L
0.001	1	1.75	2.7	6049	0.12	0.04	0.04	0.04	0.04	0.05	0.05
	2	1.75	5.0	5808	0.12	0.04	0.04	0.04	0.05	0.05	0.05
	3	1.75	6.9	6106	0.12	0.04	0.04	0.04	0.05	0.05	0.05
	4	1.75	9.5	5992	0.12	0.04	0.04	0.04	0.04	0.05	0.05
	6	1.75	14.2	5914	0.12	0.04	0.04	0.04	0.05	0.05	0.05
	8	1.75	17.6	5935	0.12	0.04	0.04	0.04	0.05	0.05	0.05
	12	1.75	27.8	5964	0.12	0.04	0.04	0.04	0.04	0.05	0.05
	20	1.75	41.5	5907	0.12	0.04	0.04	0.04	0.04	0.05	0.05
0.01	1	1.25	4.0	4257	0.56	0.14	0.14	0.14	0.15	0.17	0.18
	2	1.25	6.9	4378	0.55	0.15	0.15	0.15	0.16	0.18	0.20
	3	1.25	10.4	4303	0.56	0.14	0.14	0.15	0.16	0.17	0.19
	4	1.25	13.1	4334	0.56	0.14	0.14	0.14	0.15	0.17	0.18
	6	1.25	19.9	4377	0.56	0.14	0.15	0.15	0.16	0.17	0.19
	8	1.25	25.6	4350	0.56	0.14	0.14	0.15	0.16	0.17	0.19
	12	1.25	37.5	4343	0.57	0.14	0.14	0.15	0.15	0.17	0.19
	20	1.25	53.6	4313	0.57	0.14	0.14	0.15	0.16	0.17	0.19
0.02	1	0.50	4.5	2138	0.88	0.11	0.11	0.12	0.13	0.15	0.18
	2	0.50	7.3	2498	0.89	0.11	0.12	0.12	0.13	0.15	0.18
	3	0.50	12.0	2182	0.88	0.11	0.11	0.12	0.13	0.15	0.18
	4	0.50	15.4	2335	0.89	0.11	0.12	0.13	0.14	0.16	0.19
	6	0.50	20.7	2399	0.89	0.11	0.12	0.12	0.13	0.16	0.18
	8	0.50	29.9	2379	0.90	0.11	0.12	0.12	0.13	0.16	0.18
	12	0.50	44.1	2363	0.90	0.11	0.12	0.12	0.14	0.16	0.19
	20	0.50	61.9	2308	0.93	0.11	0.12	0.12	0.13	0.16	0.18
0.05	1	0.13	3.7	1023	1.54	0.11	0.12	0.13	0.15	0.20	0.25
	2	0.13	8.4	1246	1.55	0.11	0.12	0.13	0.15	0.19	0.23
	3	0.13	11.9	1110	1.55	0.10	0.11	0.12	0.15	0.19	0.23
	4	0.13	16.9	1186	1.56	0.10	0.11	0.12	0.14	0.19	0.23
	6	0.13	23.7	1214	1.57	0.11	0.12	0.13	0.15	0.19	0.23
	8	0.13	32.7	1195	1.58	0.11	0.12	0.13	0.15	0.19	0.23
	12	0.13	47.1	1205	1.61	0.11	0.12	0.13	0.15	0.19	0.23
	20	0.13	68.7	1159	1.65	0.10	0.11	0.12	0.15	0.19	0.23
0.10	1	0.063	3.7	889	2.24	0.14	0.16	0.17	0.21	0.28	0.36
	2	0.063	7.3	977	2.25	0.14	0.16	0.17	0.20	0.27	0.34
	3	0.063	10.9	858	2.25	0.13	0.15	0.16	0.20	0.27	0.33
	4	0.063	14.3	883	2.25	0.13	0.15	0.17	0.20	0.27	0.33
	6	0.063	19.7	932	2.26	0.14	0.15	0.17	0.20	0.27	0.34
	8	0.063	27.6	904	2.27	0.14	0.15	0.17	0.20	0.27	0.34
	12	0.063	38.8	897	2.29	0.14	0.15	0.17	0.20	0.27	0.34
	20	0.063	59.3	895	2.35	0.14	0.15	0.17	0.20	0.27	0.34
0.20	1	0.030	1.7	558	3.03	0.16	0.18	0.20	0.26	0.36	0.46
	2	0.030	3.5	543	3.03	0.15	0.18	0.21	0.26	0.37	0.47
	3	0.030	5.9	519	3.04	0.15	0.18	0.20	0.25	0.36	0.46
	4	0.030	8.2	592	3.04	0.15	0.18	0.20	0.25	0.36	0.47
	6	0.030	10.0	592	3.04	0.15	0.18	0.20	0.25	0.36	0.46
	8	0.030	14.7	556	3.05	0.15	0.18	0.20	0.26	0.36	0.47
	12	0.030	21.0	583	3.06	0.15	0.18	0.20	0.25	0.36	0.46
	20	0.030	32.8	578	3.09	0.15	0.18	0.20	0.26	0.36	0.47
0.50	1	0.015	0.4	365	4.03	0.19	0.22	0.26	0.35	0.51	0.68
	2	0.015	0.7	417	4.03	0.20	0.24	0.27	0.35	0.52	0.69
	3	0.015	1.6	387	4.03	0.20	0.25	0.29	0.38	0.57	0.75
	4	0.015	2.1	410	4.03	0.18	0.22	0.26	0.34	0.51	0.69
	6	0.015	2.7	409	4.03	0.19	0.23	0.27	0.35	0.52	0.69
	8	0.015	4.0	428	4.03	0.20	0.24	0.28	0.36	0.54	0.71
	12	0.015	5.7	401	4.04	0.19	0.23	0.27	0.36	0.54	0.72
	20	0.015	9.2	402	4.04	0.19	0.24	0.28	0.37	0.54	0.72

**Table B.16:** Detection probability, average detection time, contaminated area in case of detection failure and relative contaminated area to control area for various RADTi in case of  $\sigma_{lnK}^2 = 1.5$  assuming daily (ED) and monthly (1M) sampling frequencies

$\sigma_{lnK}^2$		1.50																			
$\alpha_i(m)$	now	nfds(max)	$P_d$ (ED)	$\langle T_{(DET)} \rangle$ (DAYS)	AREA ON FAILURE	(AREA ON DET.)/L	(3M. RADTi)/L	(6M. RADTi)/L	(12M. RADTi)/L	(24M. RADTi)/L	(36M. RADTi)/L	$P_d$ (1M)	$\langle T_{(DET)} \rangle$ (DAYS)	AREA ON FAILURE	(AREA ON DET.)/L	(3M. RADTi)/L	(6M. RADTi)/L	(12M. RADTi)/L	(24M. RADTi)/L	(36M. RADTi)/L	
0.001	1	1.25	3.9	3790	0.21	0.03	0.03	0.03	0.04	0.04	0.05	3.8	3826	0.21	0.03	0.03	0.03	0.04	0.04	0.05	
	2	1.25	7.2	4296	0.20	0.04	0.04	0.04	0.04	0.05	7.2	4319	0.20	0.04	0.04	0.04	0.04	0.04	0.04	0.05	
	3	1.25	9.4	3999	0.21	0.03	0.03	0.04	0.04	0.04	0.05	9.3	4028	0.21	0.03	0.03	0.04	0.04	0.04	0.05	
	4	1.25	13.3	3962	0.21	0.03	0.04	0.04	0.04	0.04	0.05	13.2	3986	0.21	0.03	0.04	0.04	0.04	0.04	0.05	
	6	1.25	20.9	4164	0.20	0.03	0.03	0.04	0.04	0.04	0.05	20.7	4180	0.20	0.03	0.04	0.04	0.04	0.04	0.05	
	8	1.25	25.7	4176	0.21	0.03	0.03	0.04	0.04	0.04	0.05	25.3	4189	0.21	0.03	0.03	0.04	0.04	0.04	0.05	
	12	1.25	35.6	4093	0.20	0.03	0.03	0.04	0.04	0.04	0.05	35.2	4109	0.20	0.03	0.03	0.04	0.04	0.04	0.05	
	20	1.25	54.9	4095	0.22	0.03	0.03	0.03	0.04	0.04	0.05	54.4	4116	0.22	0.03	0.03	0.03	0.04	0.04	0.05	
	0.01	1	1.00	5.0	3389	0.80	0.13	0.13	0.14	0.15	0.17	1.9	4.7	3373	0.80	0.13	0.13	0.14	0.15	0.17	0.19
		2	1.00	9.0	3282	0.79	0.13	0.13	0.14	0.15	0.17	2.0	8.6	3293	0.79	0.13	0.13	0.14	0.15	0.17	0.19
3		1.00	13.5	3355	0.80	0.13	0.13	0.14	0.15	0.17	1.9	12.9	3356	0.80	0.13	0.13	0.14	0.15	0.17	0.19	
4		1.00	16.9	3359	0.80	0.13	0.13	0.14	0.15	0.17	1.9	16.3	3349	0.80	0.13	0.13	0.14	0.15	0.17	0.19	
6		1.00	24.2	3261	0.78	0.13	0.13	0.14	0.15	0.17	2.0	23.0	3241	0.78	0.13	0.13	0.14	0.15	0.17	0.19	
8		1.00	33.2	3288	0.79	0.13	0.13	0.14	0.15	0.17	1.9	31.8	3269	0.79	0.12	0.13	0.13	0.14	0.17	0.19	
12		1.00	45.8	3325	0.79	0.12	0.13	0.13	0.15	0.17	1.9	44.4	3337	0.79	0.12	0.13	0.13	0.15	0.17	0.19	
20		1.00	61.6	3308	0.79	0.12	0.13	0.13	0.15	0.17	1.9	59.9	3301	0.79	0.12	0.13	0.13	0.14	0.17	0.19	
0.02		1	0.50	5.7	1974	1.20	0.11	0.12	0.13	0.14	0.18	2.1	5.4	1997	1.20	0.11	0.12	0.13	0.14	0.18	0.21
		2	0.50	9.7	2045	1.20	0.11	0.12	0.13	0.14	0.17	2.1	9.3	2062	1.20	0.11	0.12	0.13	0.14	0.17	0.20
	3	0.50	14.8	2089	1.20	0.12	0.12	0.13	0.15	0.18	2.1	14.0	2095	1.20	0.12	0.12	0.13	0.15	0.18	0.21	
	4	0.50	18.9	1982	1.20	0.11	0.12	0.13	0.14	0.17	2.1	18.2	1991	1.19	0.11	0.12	0.13	0.14	0.17	0.21	
	6	0.50	28.1	2046	1.18	0.11	0.12	0.13	0.14	0.18	2.1	26.9	2057	1.19	0.11	0.12	0.13	0.14	0.17	0.21	
	8	0.50	36.7	2003	1.20	0.11	0.12	0.13	0.14	0.17	2.1	35.3	2014	1.20	0.11	0.12	0.13	0.14	0.17	0.21	
	12	0.50	50.0	2040	1.20	0.11	0.12	0.13	0.14	0.17	2.0	48.4	2055	1.20	0.11	0.12	0.13	0.14	0.17	0.20	
	20	0.50	69.1	2055	1.17	0.11	0.12	0.12	0.14	0.17	2.1	67.1	2056	1.17	0.11	0.12	0.13	0.14	0.17	0.21	
	0.05	1	0.13	5.5	927	1.96	0.09	0.11	0.12	0.15	0.20	0.26	5.2	938	1.96	0.09	0.11	0.12	0.14	0.20	0.25
		2	0.13	11.3	1023	1.96	0.10	0.11	0.12	0.15	0.20	0.26	10.7	1046	1.96	0.10	0.11	0.13	0.15	0.21	0.26
3		0.13	14.9	1029	1.96	0.10	0.11	0.12	0.15	0.20	0.25	14.5	1052	1.96	0.10	0.11	0.12	0.15	0.20	0.25	
4		0.13	19.3	1057	1.97	0.10	0.11	0.12	0.15	0.20	0.26	18.4	1051	1.97	0.10	0.11	0.12	0.15	0.20	0.26	
6		0.13	31.8	1093	1.97	0.10	0.11	0.12	0.15	0.20	0.26	30.4	1115	1.96	0.10	0.11	0.13	0.15	0.20	0.26	
8		0.13	40.1	1018	1.97	0.10	0.11	0.12	0.15	0.20	0.25	38.6	1039	1.97	0.10	0.11	0.12	0.15	0.20	0.25	
12		0.13	57.6	1030	1.95	0.10	0.11	0.12	0.15	0.20	0.26	55.4	1034	1.95	0.10	0.11	0.12	0.15	0.20	0.26	
20		0.13	81.6	1054	1.98	0.09	0.11	0.12	0.14	0.20	0.25	79.6	1054	1.98	0.09	0.11	0.12	0.15	0.20	0.26	
0.10		1	0.063	6.1	763	2.68	0.12	0.15	0.17	0.21	0.30	0.39	5.6	760	2.68	0.12	0.14	0.17	0.21	0.30	0.39
		2	0.063	10.3	726	2.68	0.12	0.14	0.16	0.20	0.28	0.36	9.5	735	2.68	0.12	0.14	0.16	0.20	0.28	0.36
	3	0.063	15.8	735	2.68	0.12	0.14	0.16	0.20	0.28	0.37	14.3	724	2.68	0.12	0.14	0.16	0.20	0.28	0.37	
	4	0.063	19.9	766	2.69	0.12	0.14	0.16	0.20	0.29	0.37	18.6	795	2.69	0.12	0.14	0.16	0.20	0.29	0.37	
	6	0.063	29.7	737	2.67	0.12	0.14	0.16	0.20	0.29	0.37	27.1	748	2.68	0.12	0.14	0.16	0.20	0.29	0.37	
	8	0.063	40.0	754	2.70	0.12	0.14	0.16	0.20	0.29	0.37	36.5	758	2.70	0.12	0.14	0.16	0.20	0.28	0.37	
	12	0.063	57.6	742	2.70	0.12	0.14	0.16	0.20	0.29	0.37	54.2	759	2.71	0.12	0.14	0.16	0.20	0.29	0.37	
	20	0.063	80.8	736	2.65	0.12	0.14	0.16	0.20	0.29	0.37	76.9	738	2.67	0.12	0.14	0.16	0.20	0.29	0.37	
	0.20	1	0.015	4.1	435	3.41	0.14	0.18	0.22	0.29	0.43	0.57	3.4	411	3.41	0.13	0.17	0.21	0.28	0.42	0.55
		2	0.015	8.4	399	3.41	0.12	0.16	0.20	0.27	0.40	0.53	7.3	398	3.41	0.12	0.15	0.19	0.26	0.39	0.53
3		0.015	12.1	401	3.41	0.12	0.16	0.20	0.27	0.40	0.54	10.6	388	3.41	0.12	0.15	0.19	0.26	0.39	0.53	
4		0.015	15.2	433	3.42	0.12	0.16	0.19	0.26	0.40	0.53	13.3	410	3.42	0.11	0.15	0.18	0.25	0.39	0.53	
6		0.015	23.3	411	3.41	0.12	0.16	0.19	0.26	0.40	0.54	20.1	408	3.42	0.11	0.15	0.19	0.26	0.39	0.53	
8		0.015	31.3	400	3.42	0.12	0.16	0.19	0.26	0.40	0.53	27.7	387	3.42	0.12	0.15	0.19	0.26	0.39	0.52	
12		0.015	46.2	413	3.43	0.12	0.16	0.19	0.26	0.40	0.53	40.4	399	3.44	0.11	0.15	0.18	0.25	0.39	0.52	
20		0.015	65.3	410	3.43	0.12	0.15	0.19	0.26	0.40	0.53	58.8	393	3.43	0.11	0.15	0.18	0.25	0.39	0.52	
0.50		1	0.015	1.9	195	4.25	0.13	0.21	0.29	0.42	0.67	0.90	1.4	158	4.25	0.11	0.19	0.26	0.39	0.63	0.86
		2	0.015	4.4	137	4.25	0.10	0.19	0.26	0.40	0.65	0.90	3.7	132	4.25	0.10	0.19	0.26	0.40	0.65	0.90
	3	0.015	6.4	135	4.25	0.10	0.18	0.25	0.39	0.63	0.86	5.4	125	4.25	0.09	0.17	0.24	0.38	0.62	0.85	
	4	0.015	8.2	145	4.25	0.08	0.17	0.25	0.39	0.64	0.88	7.1	150	4.26	0.09	0.17	0.24	0.38	0.63	0.87	
	6	0.015	12.5	135	4.25	0.10	0.18	0.26	0.40	0.65	0.89	10.6	145	4.26	0.10	0.18	0.26	0.40	0.64	0.88	
	8	0.015	16.5	139	4.26	0.10	0.18	0.25	0.39	0.63	0.87	14.3	148	4.26	0.10	0.18	0.25	0.39	0.62	0.85	
	12	0.015	24.9	151	4.27	0.10	0.18	0.26	0.40	0.65	0.88	21.0	148	4.26	0.10	0.18	0.25	0.39	0.64	0.87	
	20	0.015	34.6	135	4.27	0.09	0.18	0.25	0.39	0.64	0.88	30.8	145	4.27	0.10	0.18	0.25	0.39	0.64	0.88	

**Table B.17:** Detection probability, average detection time, contaminated area in case of detection failure and relative contaminated area to control area for various RADTi in case of  $\sigma_{\ln K}^2 = 1.5$  assuming bimonthly (2M) and quarterly (3M) sampling frequencies

$\sigma_{\ln K}^2$		1.50																				
$\alpha_f(m)$	now	nfds(max)	$P_d$ (2M)	$\langle T_{(DET)} \rangle$ (DAYS)	AREA ON FAILURE	(AREA ON DET.)/L	(3M. RADTi)/L	(6M. RADTi)/L	(12M. RADTi)/L	(24M. RADTi)/L	(36M. RADTi)/L	$P_d$ (3M)	$\langle T_{(DET)} \rangle$ (DAYS)	AREA ON FAILURE	(AREA ON DET.)/L	(3M. RADTi)/L	(6M. RADTi)/L	(12M. RADTi)/L	(24M. RADTi)/L	(36M. RADTi)/L		
0.001	1	1.25	3.8	3851	0.21	0.03	0.03	0.03	0.04	0.04	0.05	3.8	3864	0.21	0.03	0.03	0.03	0.04	0.04	0.05	0.05	
	2	1.25	7.1	4356	0.21	0.04	0.04	0.04	0.04	0.04	0.05	7.0	4416	0.21	0.04	0.04	0.04	0.04	0.05	0.05	0.05	
	3	1.25	9.2	4048	0.21	0.03	0.03	0.04	0.04	0.04	0.05	9.1	4044	0.21	0.03	0.03	0.04	0.04	0.04	0.04	0.05	
	4	1.25	13.1	4009	0.21	0.03	0.04	0.04	0.04	0.04	0.05	12.7	4082	0.21	0.03	0.04	0.04	0.04	0.04	0.04	0.05	
	6	1.25	20.4	4218	0.21	0.03	0.04	0.04	0.04	0.04	0.05	19.9	4270	0.21	0.03	0.04	0.04	0.04	0.04	0.04	0.05	
	8	1.25	24.8	4222	0.21	0.03	0.03	0.04	0.04	0.04	0.05	24.4	4256	0.21	0.03	0.03	0.04	0.04	0.04	0.04	0.05	
	12	1.25	34.9	4136	0.21	0.03	0.03	0.04	0.04	0.04	0.05	34.3	4165	0.21	0.03	0.04	0.04	0.04	0.04	0.04	0.05	
	20	1.25	54.0	4137	0.22	0.03	0.03	0.04	0.04	0.04	0.05	52.8	4179	0.23	0.03	0.03	0.04	0.04	0.04	0.04	0.05	
	0.01	1	1.00	4.7	3384	0.80	0.13	0.13	0.14	0.15	0.17	0.19	4.6	3420	0.80	0.13	0.13	0.14	0.15	0.17	0.19	0.20
		2	1.00	8.3	3326	0.79	0.13	0.13	0.14	0.15	0.17	0.19	8.2	3369	0.79	0.13	0.13	0.14	0.15	0.17	0.19	0.20
3		1.00	12.7	3355	0.80	0.13	0.13	0.14	0.15	0.17	0.19	12.4	3409	0.80	0.13	0.13	0.14	0.15	0.17	0.19	0.20	
4		1.00	15.8	3366	0.80	0.13	0.13	0.14	0.14	0.17	0.19	15.7	3376	0.79	0.13	0.13	0.14	0.15	0.17	0.19	0.20	
6		1.00	22.4	3265	0.79	0.13	0.13	0.14	0.15	0.17	0.19	21.9	3285	0.79	0.13	0.13	0.14	0.15	0.17	0.19	0.20	
8		1.00	30.9	3290	0.79	0.12	0.13	0.13	0.14	0.17	0.19	30.7	3306	0.79	0.13	0.13	0.14	0.15	0.17	0.19	0.20	
12		1.00	43.4	3353	0.79	0.12	0.13	0.13	0.15	0.17	0.19	43.0	3366	0.79	0.13	0.13	0.14	0.15	0.17	0.19	0.20	
20		1.00	59.0	3315	0.79	0.12	0.13	0.13	0.14	0.17	0.19	58.8	3326	0.79	0.12	0.13	0.13	0.15	0.17	0.19	0.20	
0.02		1	0.50	5.4	2016	1.20	0.12	0.12	0.13	0.15	0.18	0.21	5.3	2003	1.20	0.12	0.12	0.13	0.15	0.18	0.21	0.21
		2	0.50	9.2	2072	1.20	0.11	0.12	0.13	0.14	0.17	0.21	9.0	2098	1.20	0.11	0.12	0.13	0.14	0.17	0.21	0.21
	3	0.50	13.6	2097	1.20	0.12	0.13	0.13	0.15	0.18	0.21	13.5	2110	1.20	0.12	0.13	0.13	0.15	0.18	0.21	0.21	
	4	0.50	17.8	2023	1.20	0.11	0.12	0.13	0.14	0.17	0.21	17.4	2038	1.20	0.11	0.12	0.13	0.14	0.17	0.21	0.21	
	6	0.50	26.6	2071	1.19	0.11	0.12	0.13	0.14	0.18	0.21	26.3	2098	1.19	0.11	0.12	0.13	0.15	0.18	0.21	0.21	
	8	0.50	34.3	2031	1.20	0.11	0.12	0.13	0.14	0.17	0.21	33.8	2045	1.20	0.11	0.12	0.13	0.14	0.17	0.21	0.21	
	12	0.50	47.5	2067	1.20	0.11	0.12	0.13	0.14	0.17	0.21	46.8	2086	1.20	0.11	0.12	0.13	0.14	0.17	0.21	0.21	
	20	0.50	66.2	2073	1.17	0.11	0.12	0.13	0.14	0.17	0.21	65.5	2084	1.18	0.11	0.12	0.13	0.14	0.17	0.21	0.21	
	0.05	1	0.13	5.1	946	1.96	0.09	0.11	0.12	0.15	0.20	0.26	4.9	982	1.96	0.10	0.11	0.12	0.15	0.20	0.25	0.25
		2	0.13	10.4	1059	1.96	0.10	0.12	0.13	0.16	0.21	0.27	10.4	1059	1.96	0.10	0.12	0.13	0.16	0.21	0.27	0.27
3		0.13	14.2	1060	1.96	0.10	0.11	0.12	0.15	0.20	0.25	13.9	1092	1.97	0.10	0.11	0.12	0.15	0.20	0.25	0.25	
4		0.13	17.9	1054	1.97	0.10	0.11	0.12	0.15	0.20	0.26	17.6	1080	1.97	0.10	0.11	0.13	0.15	0.21	0.26	0.26	
6		0.13	29.5	1135	1.96	0.10	0.11	0.13	0.15	0.20	0.26	29.6	1145	1.96	0.10	0.12	0.13	0.16	0.21	0.26	0.26	
8		0.13	37.8	1047	1.97	0.10	0.11	0.12	0.15	0.20	0.26	37.4	1071	1.97	0.10	0.11	0.13	0.15	0.20	0.26	0.26	
12		0.13	54.4	1040	1.96	0.10	0.11	0.12	0.15	0.20	0.26	53.7	1064	1.96	0.10	0.11	0.13	0.15	0.20	0.26	0.26	
20		0.13	78.3	1067	1.99	0.10	0.11	0.12	0.15	0.20	0.26	78.0	1078	1.98	0.10	0.11	0.12	0.15	0.20	0.26	0.26	
0.10		1	0.063	5.4	779	2.68	0.13	0.15	0.17	0.21	0.30	0.39	5.3	774	2.68	0.13	0.15	0.17	0.21	0.30	0.39	0.39
		2	0.063	9.1	735	2.68	0.12	0.14	0.16	0.20	0.28	0.36	8.8	773	2.68	0.12	0.14	0.16	0.20	0.27	0.36	0.36
	3	0.063	13.9	734	2.68	0.12	0.14	0.16	0.20	0.28	0.37	13.6	739	2.68	0.12	0.14	0.16	0.20	0.29	0.37	0.37	
	4	0.063	18.1	797	2.69	0.12	0.14	0.17	0.21	0.29	0.37	17.5	809	2.69	0.12	0.14	0.16	0.20	0.29	0.37	0.37	
	6	0.063	26.3	761	2.68	0.12	0.14	0.16	0.20	0.29	0.37	25.2	777	2.68	0.12	0.14	0.16	0.20	0.28	0.37	0.37	
	8	0.063	35.3	760	2.70	0.12	0.14	0.16	0.20	0.29	0.37	34.0	761	2.70	0.12	0.14	0.16	0.20	0.28	0.37	0.37	
	12	0.063	52.4	770	2.71	0.12	0.14	0.16	0.20	0.29	0.37	51.0	782	2.72	0.12	0.14	0.16	0.20	0.29	0.37	0.37	
	20	0.063	75.5	743	2.68	0.12	0.14	0.16	0.20	0.29	0.38	73.8	756	2.70	0.12	0.14	0.16	0.20	0.29	0.37	0.37	
	0.20	1	0.015	3.1	403	3.41	0.13	0.17	0.20	0.27	0.41	0.55	2.9	414	3.41	0.13	0.17	0.21	0.28	0.41	0.55	0.55
		2	0.015	7.0	413	3.41	0.12	0.16	0.19	0.26	0.39	0.52	6.8	405	3.41	0.12	0.16	0.19	0.26	0.39	0.53	0.53
3		0.015	9.8	392	3.41	0.12	0.15	0.19	0.26	0.39	0.52	9.4	412	3.41	0.12	0.16	0.19	0.26	0.39	0.52	0.52	
4		0.015	12.7	407	3.42	0.12	0.15	0.19	0.25	0.39	0.53	12.1	424	3.42	0.12	0.15	0.19	0.26	0.39	0.52	0.52	
6		0.015	19.2	424	3.42	0.12	0.15	0.19	0.26	0.39	0.52	18.1	422	3.42	0.12	0.15	0.19	0.26	0.39	0.52	0.52	
8		0.015	25.9	392	3.42	0.12	0.15	0.19	0.25	0.38	0.52	25.4	411	3.42	0.12	0.16	0.19	0.26	0.39	0.52	0.52	
12		0.015	38.4	400	3.44	0.12	0.15	0.18	0.25	0.38	0.52	37.3	415	3.44	0.12	0.16	0.19	0.26	0.39	0.52	0.52	
20		0.015	56.8	397	3.44	0.11	0.15	0.18	0.25	0.39	0.52	54.8	414	3.45	0.12	0.15	0.19	0.25	0.39	0.52	0.52	
0.50		1	0.015	1.4	180	4.25	0.13	0.20	0.27	0.40	0.63	0.86	1.3	203	4.25	0.14	0.22	0.28	0.41	0.65	0.88	0.88
		2	0.015	3.4	137	4.25	0.12	0.20	0.27	0.41	0.66	0.90	3.2	153	4.25	0.13	0.20	0.27	0.41	0.65	0.89	0.89
	3	0.015	5.1	142	4.25	0.11	0.18	0.25	0.38	0.61	0.84	4.7	160	4.25	0.12	0.19	0.25	0.38	0.60	0.83	0.83	
	4	0.015	6.8	173	4.26	0.11	0.18	0.25	0.39	0.63	0.86	6.3	194	4.26	0.12	0.19	0.26	0.38	0.62	0.85	0.85	
	6	0.015	9.9	160	4.26	0.12	0.19	0.26	0.40	0.64	0.88	9.1	161	4.26	0.13	0.20	0.27	0.40	0.64	0.87	0.87	
	8	0.015	13.2	161	4.26	0.12	0.19	0.26	0.39	0.62	0.85	12.2	175	4.26	0.12	0.20	0.26	0.39	0.62	0.84	0.84	
	12	0.015	19.9	166	4.27	0.11	0.19	0.26	0.39	0.64	0.87	18.0	189	4.27	0.13	0.20	0.26	0.39	0.63	0.86	0.86	
	20	0.015	29.6	160	4.27	0.11	0.19	0.26	0.40	0.64	0.88	27.4	174	4.28	0.12	0.20	0.26	0.39	0.63	0.87	0.87	

**Table B.18:** Detection probability, average detection time, contaminated area in case of detection failure and relative contaminated area to control area  $L$  for various RADTi in case of  $\sigma_{lnK}^2 = 1.5$  assuming every 4 months (4M) and biannually (6M) sampling frequencies

$\sigma_{lnK}^2$		1.50																				
$\alpha_r(m)$	now	nfds(max)	$P_d$ (4M)	$\langle T_{(DET)} \rangle$ (DAYS)	AREA ON FAILURE	(AREA ON DET.)/L	(3M. RADTi)/L	(6M. RADTi)/L	(12M. RADTi)/L	(24M. RADTi)/L	(36M. RADTi)/L	$P_d$ (6M)	$\langle T_{(DET)} \rangle$ (DAYS)	AREA ON FAILURE	(AREA ON DET.)/L	(3M. RADTi)/L	(6M. RADTi)/L	(12M. RADTi)/L	(24M. RADTi)/L	(36M. RADTi)/L		
0.001	1	1.25	3.7	3926	0.21	0.03	0.03	0.04	0.04	0.04	0.05	3.3	4062	0.21	0.03	0.04	0.04	0.04	0.04	0.04	0.05	
	2	1.25	6.7	4484	0.21	0.04	0.04	0.04	0.04	0.05	0.05	6.4	4522	0.21	0.04	0.04	0.04	0.04	0.04	0.04	0.05	
	3	1.25	8.8	4101	0.21	0.03	0.03	0.04	0.04	0.04	0.05	8.0	4226	0.21	0.03	0.04	0.04	0.04	0.04	0.04	0.05	
	4	1.25	12.7	4094	0.21	0.04	0.04	0.04	0.04	0.04	0.05	11.5	4274	0.21	0.04	0.04	0.04	0.04	0.04	0.04	0.05	
	6	1.25	19.5	4326	0.21	0.04	0.04	0.04	0.04	0.04	0.05	18.1	4419	0.21	0.04	0.04	0.04	0.04	0.04	0.04	0.05	
	8	1.25	23.5	4326	0.22	0.03	0.04	0.04	0.04	0.04	0.05	21.9	4416	0.21	0.03	0.04	0.04	0.04	0.04	0.04	0.05	
	12	1.25	33.8	4214	0.21	0.03	0.04	0.04	0.04	0.04	0.05	31.0	4370	0.22	0.04	0.04	0.04	0.04	0.04	0.04	0.05	
	20	1.25	52.3	4217	0.23	0.03	0.03	0.04	0.04	0.04	0.05	48.1	4351	0.23	0.03	0.04	0.04	0.04	0.04	0.04	0.05	
	0.01	1	1.00	4.6	3411	0.80	0.13	0.13	0.14	0.15	0.17	0.19	4.3	3558	0.80	0.13	0.13	0.14	0.14	0.15	0.17	0.19
		2	1.00	7.9	3397	0.79	0.13	0.13	0.14	0.15	0.17	0.19	7.8	3433	0.79	0.13	0.13	0.14	0.14	0.15	0.17	0.20
3		1.00	12.2	3425	0.80	0.13	0.13	0.14	0.15	0.17	0.19	11.4	3497	0.80	0.13	0.13	0.14	0.15	0.17	0.19		
4		1.00	15.4	3409	0.80	0.13	0.13	0.14	0.15	0.17	0.19	14.6	3459	0.80	0.13	0.13	0.14	0.15	0.17	0.19		
6		1.00	21.4	3319	0.79	0.13	0.13	0.14	0.15	0.17	0.19	20.7	3345	0.79	0.13	0.13	0.14	0.15	0.17	0.19		
8		1.00	30.0	3348	0.80	0.13	0.13	0.14	0.15	0.17	0.19	28.7	3374	0.80	0.13	0.13	0.14	0.15	0.17	0.19		
12		1.00	42.3	3392	0.79	0.13	0.13	0.14	0.15	0.17	0.19	40.1	3437	0.80	0.13	0.13	0.14	0.15	0.17	0.19		
20		1.00	57.7	3345	0.79	0.12	0.13	0.13	0.15	0.17	0.19	56.2	3402	0.80	0.13	0.13	0.14	0.15	0.17	0.19		
0.02		1	0.50	5.2	2023	1.20	0.12	0.12	0.13	0.15	0.18	0.22	4.6	2160	1.20	0.12	0.12	0.13	0.15	0.18	0.21	
		2	0.50	8.9	2133	1.20	0.11	0.12	0.13	0.15	0.18	0.21	8.3	2202	1.20	0.12	0.12	0.13	0.15	0.18	0.21	
	3	0.50	13.0	2123	1.20	0.12	0.13	0.13	0.15	0.18	0.21	12.2	2197	1.20	0.12	0.13	0.13	0.15	0.18	0.21		
	4	0.50	17.2	2082	1.20	0.12	0.12	0.13	0.14	0.18	0.21	16.2	2138	1.20	0.12	0.12	0.13	0.15	0.18	0.21		
	6	0.50	25.8	2109	1.19	0.12	0.12	0.13	0.15	0.18	0.21	24.5	2195	1.20	0.12	0.13	0.13	0.15	0.18	0.21		
	8	0.50	33.2	2066	1.21	0.11	0.12	0.13	0.14	0.17	0.21	31.6	2120	1.21	0.12	0.12	0.13	0.15	0.18	0.21		
	12	0.50	46.2	2109	1.21	0.11	0.12	0.13	0.14	0.17	0.21	43.6	2177	1.22	0.12	0.12	0.13	0.15	0.18	0.21		
	20	0.50	64.8	2100	1.18	0.11	0.12	0.13	0.14	0.18	0.21	62.7	2157	1.21	0.11	0.12	0.13	0.15	0.18	0.21		
	0.05	1	0.13	4.8	990	1.96	0.10	0.11	0.12	0.15	0.20	0.25	4.6	1056	1.96	0.10	0.11	0.12	0.15	0.20	0.25	
		2	0.13	10.0	1104	1.96	0.11	0.12	0.13	0.16	0.21	0.27	9.7	1128	1.96	0.11	0.12	0.13	0.16	0.21	0.27	
3		0.13	13.8	1097	1.97	0.10	0.11	0.12	0.15	0.20	0.25	13.2	1143	1.97	0.10	0.11	0.13	0.15	0.20	0.25		
4		0.13	17.4	1097	1.97	0.10	0.12	0.13	0.15	0.20	0.26	16.5	1134	1.97	0.10	0.12	0.13	0.15	0.21	0.26		
6		0.13	28.3	1178	1.97	0.11	0.12	0.13	0.16	0.21	0.26	27.4	1223	1.97	0.11	0.12	0.13	0.16	0.21	0.26		
8		0.13	36.9	1084	1.97	0.10	0.11	0.13	0.15	0.20	0.26	35.1	1118	1.98	0.10	0.12	0.13	0.15	0.21	0.26		
12		0.13	52.7	1085	1.97	0.10	0.11	0.13	0.15	0.20	0.26	50.5	1124	1.98	0.11	0.12	0.13	0.15	0.21	0.26		
20		0.13	76.8	1103	2.02	0.10	0.11	0.12	0.15	0.20	0.26	74.0	1135	2.03	0.10	0.11	0.13	0.15	0.20	0.26		
0.10		1	0.063	5.1	809	2.68	0.13	0.15	0.17	0.21	0.30	0.39	4.8	853	2.68	0.13	0.15	0.17	0.21	0.30	0.39	
		2	0.063	8.5	777	2.68	0.12	0.14	0.16	0.20	0.28	0.36	8.1	830	2.68	0.13	0.15	0.16	0.20	0.28	0.36	
	3	0.063	13.2	761	2.68	0.12	0.14	0.16	0.20	0.28	0.37	12.4	811	2.68	0.13	0.15	0.16	0.20	0.29	0.37		
	4	0.063	17.1	838	2.69	0.13	0.15	0.17	0.21	0.29	0.37	16.0	870	2.70	0.13	0.15	0.17	0.21	0.28	0.37		
	6	0.063	24.6	797	2.68	0.13	0.14	0.16	0.20	0.29	0.37	23.0	842	2.69	0.13	0.15	0.16	0.20	0.28	0.37		
	8	0.063	33.4	784	2.70	0.13	0.14	0.16	0.20	0.29	0.37	31.5	813	2.71	0.13	0.15	0.17	0.20	0.28	0.37		
	12	0.063	49.8	804	2.72	0.13	0.15	0.17	0.21	0.29	0.37	46.2	839	2.74	0.13	0.15	0.17	0.20	0.28	0.37		
	20	0.063	72.4	773	2.71	0.12	0.14	0.16	0.21	0.29	0.38	68.7	808	2.77	0.13	0.15	0.17	0.21	0.29	0.37		
	0.20	1	0.015	2.8	422	3.41	0.14	0.17	0.21	0.27	0.41	0.55	2.5	423	3.41	0.14	0.17	0.21	0.27	0.41	0.55	
		2	0.015	6.4	419	3.41	0.13	0.16	0.19	0.26	0.39	0.52	5.8	468	3.42	0.13	0.16	0.19	0.26	0.38	0.51	
3		0.015	8.8	433	3.42	0.12	0.16	0.19	0.25	0.38	0.51	8.2	465	3.42	0.13	0.17	0.20	0.26	0.39	0.52		
4		0.015	11.5	442	3.43	0.12	0.16	0.19	0.25	0.39	0.52	10.4	480	3.43	0.13	0.17	0.20	0.26	0.39	0.52		
6		0.015	17.1	451	3.42	0.12	0.16	0.19	0.25	0.38	0.52	15.6	493	3.43	0.13	0.16	0.19	0.26	0.38	0.51		
8		0.015	23.7	430	3.43	0.13	0.16	0.19	0.26	0.38	0.51	21.6	465	3.43	0.13	0.17	0.20	0.26	0.38	0.51		
12		0.015	35.0	436	3.45	0.12	0.16	0.19	0.25	0.38	0.51	31.7	473	3.45	0.13	0.17	0.20	0.26	0.38	0.51		
20		0.015	52.1	430	3.46	0.12	0.16	0.19	0.26	0.39	0.52	47.6	475	3.47	0.13	0.16	0.19	0.26	0.38	0.51		
0.50		1	0.015	1.2	216	4.25	0.15	0.21	0.28	0.40	0.62	0.85	0.9	282	4.25	0.17	0.23	0.28	0.39	0.62	0.84	
		2	0.015	2.9	182	4.25	0.14	0.21	0.28	0.40	0.64	0.88	2.1	217	4.25	0.15	0.21	0.26	0.37	0.58	0.80	
	3	0.015	4.4	185	4.25	0.13	0.20	0.26	0.38	0.60	0.82	3.3	243	4.25	0.15	0.20	0.25	0.36	0.56	0.76		
	4	0.015	5.6	229	4.26	0.13	0.19	0.25	0.37	0.60	0.82	4.6	290	4.26	0.15	0.20	0.26	0.36	0.57	0.78		
	6	0.015	8.4	209	4.26	0.14	0.21	0.27	0.39	0.62	0.84	6.2	241	4.26	0.15	0.20	0.26	0.36	0.57	0.77		
	8	0.015	11.0	193	4.26	0.14	0.20	0.26	0.39	0.61	0.82	8.6	259	4.26	0.15	0.21	0.26	0.37	0.58	0.78		
	12	0.015	16.3	207	4.27	0.14	0.20	0.26	0.39	0.62	0.84	13.0	270	4.27	0.15	0.21	0.26	0.37	0.59	0.80		
	20	0.015	24.9	205	4.28	0.14	0.20	0.27	0.39	0.63	0.85	20.4	255	4.28	0.15	0.21	0.27	0.38	0.60	0.81		

**Table B.19:** Detection probability, average detection time, contaminated area in case of detection failure and relative contaminated area to control area  $L$  for various RADTi in case of  $\sigma_{\ln K}^2 = 1.5$  assuming annually sampling frequency

		$\sigma_{\ln K}^2$									
		1.50									
$\alpha_i(m)$	now	nfd5(max)	$P_d$ (12M)	$\langle T_{(DET)} \rangle$ (DAYS)	AREA ON FAILURE	(AREA ON DET.)/L	(3M. RADTi)/L	(6M. RADTi)/L	(12M. RADTi)/L	(24M. RADTi)/L	(36M. RADTi)/L
0.001	1	1.25	2.5	4365	0.21	0.04	0.04	0.04	0.04	0.05	0.05
	2	1.25	4.8	5115	0.21	0.04	0.04	0.04	0.04	0.05	0.05
	3	1.25	6.1	4566	0.21	0.04	0.04	0.04	0.04	0.05	0.05
	4	1.25	8.2	4677	0.21	0.04	0.04	0.04	0.05	0.05	0.05
	6	1.25	13.7	4879	0.21	0.04	0.04	0.04	0.04	0.05	0.05
	8	1.25	16.2	4945	0.21	0.04	0.04	0.04	0.04	0.05	0.05
	12	1.25	23.0	4770	0.22	0.04	0.04	0.04	0.04	0.05	0.05
	20	1.25	36.0	4742	0.22	0.04	0.04	0.04	0.04	0.05	0.05
0.01	1	1.00	3.4	3896	0.80	0.13	0.14	0.14	0.15	0.18	0.20
	2	1.00	6.1	3702	0.79	0.14	0.14	0.14	0.16	0.18	0.20
	3	1.00	9.1	3902	0.80	0.14	0.14	0.14	0.15	0.17	0.20
	4	1.00	11.6	3817	0.80	0.13	0.14	0.14	0.15	0.17	0.19
	6	1.00	16.1	3662	0.80	0.13	0.14	0.14	0.15	0.18	0.20
	8	1.00	22.4	3776	0.81	0.13	0.14	0.14	0.15	0.17	0.19
	12	1.00	32.5	3769	0.82	0.13	0.13	0.14	0.15	0.17	0.19
	20	1.00	46.7	3693	0.84	0.13	0.14	0.14	0.15	0.17	0.19
0.02	1	0.50	3.9	2397	1.20	0.12	0.13	0.13	0.15	0.18	0.21
	2	0.50	6.8	2403	1.21	0.12	0.13	0.13	0.15	0.18	0.21
	3	0.50	10.0	2411	1.20	0.12	0.13	0.14	0.15	0.18	0.21
	4	0.50	12.7	2383	1.21	0.12	0.13	0.14	0.15	0.18	0.21
	6	0.50	20.0	2385	1.21	0.12	0.13	0.14	0.15	0.18	0.21
	8	0.50	25.2	2352	1.23	0.12	0.13	0.14	0.15	0.18	0.21
	12	0.50	35.5	2414	1.24	0.12	0.13	0.14	0.15	0.18	0.21
	20	0.50	52.8	2357	1.25	0.12	0.13	0.13	0.15	0.18	0.21
0.05	1	0.13	3.8	1197	1.96	0.10	0.11	0.12	0.15	0.20	0.25
	2	0.13	8.1	1284	1.97	0.12	0.13	0.14	0.16	0.21	0.27
	3	0.13	11.2	1285	1.97	0.11	0.12	0.13	0.15	0.20	0.25
	4	0.13	13.6	1327	1.98	0.11	0.12	0.14	0.16	0.21	0.26
	6	0.13	22.8	1386	1.99	0.12	0.13	0.14	0.16	0.21	0.26
	8	0.13	29.2	1286	2.00	0.11	0.12	0.13	0.16	0.21	0.26
	12	0.13	41.7	1297	2.02	0.11	0.12	0.13	0.16	0.21	0.26
	20	0.13	63.3	1317	2.12	0.11	0.12	0.13	0.16	0.21	0.26
0.10	1	0.063	3.8	1020	2.68	0.15	0.16	0.18	0.22	0.30	0.38
	2	0.063	6.3	973	2.69	0.14	0.15	0.17	0.21	0.28	0.35
	3	0.063	9.9	970	2.68	0.14	0.16	0.17	0.21	0.29	0.37
	4	0.063	11.9	1040	2.70	0.14	0.15	0.17	0.21	0.28	0.35
	6	0.063	18.1	1003	2.70	0.14	0.15	0.17	0.21	0.28	0.36
	8	0.063	25.0	972	2.72	0.14	0.16	0.17	0.21	0.28	0.36
	12	0.063	35.5	996	2.76	0.14	0.16	0.17	0.21	0.28	0.36
	20	0.063	53.2	959	2.81	0.14	0.15	0.17	0.21	0.28	0.36
0.20	1	0.015	1.5	650	3.42	0.16	0.19	0.21	0.26	0.37	0.47
	2	0.015	4.0	619	3.42	0.15	0.17	0.20	0.25	0.36	0.48
	3	0.015	5.3	647	3.43	0.15	0.17	0.20	0.25	0.35	0.46
	4	0.015	7.2	648	3.43	0.15	0.17	0.20	0.25	0.36	0.48
	6	0.015	10.5	670	3.43	0.15	0.17	0.20	0.25	0.36	0.47
	8	0.015	14.4	616	3.44	0.15	0.18	0.20	0.25	0.36	0.48
	12	0.015	21.5	657	3.47	0.15	0.18	0.20	0.26	0.36	0.48
	20	0.015	32.9	641	3.50	0.15	0.18	0.20	0.26	0.37	0.49
0.50	1	0.015	0.4	486	4.25	0.17	0.21	0.25	0.33	0.49	0.67
	2	0.015	1.2	375	4.25	0.19	0.23	0.28	0.37	0.56	0.75
	3	0.015	1.7	416	4.25	0.17	0.21	0.25	0.33	0.49	0.67
	4	0.015	2.4	496	4.26	0.18	0.22	0.26	0.34	0.51	0.69
	6	0.015	3.3	409	4.26	0.18	0.22	0.26	0.35	0.52	0.69
	8	0.015	4.2	414	4.26	0.18	0.22	0.26	0.34	0.51	0.69
	12	0.015	6.4	468	4.27	0.19	0.23	0.27	0.35	0.52	0.69
	20	0.015	9.9	432	4.28	0.18	0.22	0.26	0.35	0.52	0.70

**TableB.20:** Detection probability, average detection time, contaminated area in case of detection failure and relative contaminated area to control area for various RADTi in case of  $\sigma_{\ln K}^2 = 2.0$  assuming daily (ED) and monthly (1M) sampling frequencies

$\sigma_{\ln K}^2$		2.00																		
$\alpha_i(m)$	now	nfds(max)	$P_d$ (ED)	$\langle T_{(DET)} \rangle$ (DAYS)	AREA ON FAILURE	(AREA ON DET.)/L	(3M. RADTi)/L	(6M. RADTi)/L	(12M. RADTi)/L	(24M. RADTi)/L	(36M. RADTi)/L	$P_d$ (1M)	$\langle T_{(DET)} \rangle$ (DAYS)	AREA ON FAILURE	(AREA ON DET.)/L	(3M. RADTi)/L	(6M. RADTi)/L	(12M. RADTi)/L	(24M. RADTi)/L	(36M. RADTi)/L
0.001	1	0.75	3.4	3075	0.37	0.02	0.03	0.03	0.03	0.04	0.04	3.4	3089	0.37	0.03	0.03	0.03	0.03	0.04	0.04
	2	0.75	6.8	2996	0.36	0.02	0.02	0.02	0.03	0.03	0.04	6.7	2999	0.36	0.02	0.02	0.03	0.03	0.03	0.04
	3	0.75	9.2	3015	0.36	0.02	0.02	0.03	0.03	0.03	0.04	9.1	3040	0.36	0.02	0.02	0.03	0.03	0.03	0.04
	4	0.75	11.9	3002	0.37	0.03	0.03	0.03	0.03	0.04	0.04	11.8	3016	0.37	0.03	0.03	0.03	0.03	0.04	0.04
	6	0.75	19.3	3114	0.37	0.02	0.03	0.03	0.03	0.03	0.04	18.9	3144	0.37	0.03	0.03	0.03	0.03	0.03	0.04
	8	0.75	24.3	3020	0.38	0.02	0.03	0.03	0.03	0.03	0.04	23.9	3052	0.38	0.02	0.03	0.03	0.03	0.03	0.04
	12	0.75	34.2	3028	0.35	0.02	0.03	0.03	0.03	0.03	0.04	33.6	3059	0.36	0.02	0.03	0.03	0.03	0.04	0.04
	20	0.75	53.1	3008	0.35	0.02	0.03	0.03	0.03	0.03	0.04	52.3	3019	0.35	0.02	0.03	0.03	0.03	0.03	0.04
0.01	1	0.50	5.3	2322	1.07	0.08	0.09	0.09	0.10	0.13	0.15	5.1	2327	1.07	0.08	0.09	0.09	0.10	0.13	0.15
	2	0.50	8.0	2188	1.07	0.08	0.08	0.09	0.10	0.12	0.15	7.9	2211	1.07	0.08	0.08	0.09	0.10	0.12	0.15
	3	0.50	14.2	2294	1.07	0.08	0.08	0.09	0.10	0.12	0.15	13.9	2309	1.07	0.08	0.08	0.09	0.10	0.12	0.15
	4	0.50	16.8	2382	1.07	0.08	0.08	0.09	0.10	0.12	0.15	16.5	2396	1.07	0.08	0.08	0.09	0.10	0.12	0.15
	6	0.50	23.8	2317	1.07	0.08	0.08	0.09	0.10	0.12	0.15	23.2	2331	1.07	0.08	0.08	0.09	0.10	0.12	0.15
	8	0.50	32.3	2265	1.07	0.08	0.08	0.09	0.10	0.12	0.15	31.6	2296	1.08	0.08	0.08	0.09	0.10	0.12	0.15
	12	0.50	46.8	2308	1.05	0.08	0.08	0.09	0.10	0.12	0.15	45.8	2331	1.05	0.08	0.08	0.09	0.10	0.12	0.15
	20	0.50	64.7	2297	1.04	0.07	0.08	0.09	0.10	0.12	0.14	63.4	2303	1.03	0.07	0.08	0.09	0.10	0.12	0.14
0.02	1	0.25	5.0	1642	1.52	0.08	0.08	0.09	0.11	0.14	0.17	4.9	1666	1.52	0.08	0.08	0.09	0.11	0.14	0.17
	2	0.25	10.4	1514	1.51	0.08	0.09	0.10	0.11	0.15	0.19	10.0	1544	1.52	0.08	0.09	0.10	0.11	0.15	0.19
	3	0.25	13.5	1609	1.52	0.08	0.08	0.09	0.11	0.14	0.17	13.0	1621	1.52	0.08	0.08	0.09	0.11	0.14	0.17
	4	0.25	17.7	1585	1.53	0.08	0.09	0.09	0.11	0.14	0.18	17.2	1619	1.53	0.08	0.09	0.10	0.11	0.15	0.18
	6	0.25	28.0	1585	1.53	0.08	0.09	0.10	0.11	0.15	0.18	27.1	1607	1.53	0.08	0.09	0.10	0.11	0.15	0.18
	8	0.25	36.7	1593	1.53	0.08	0.09	0.09	0.11	0.14	0.18	35.3	1607	1.53	0.08	0.09	0.09	0.11	0.14	0.18
	12	0.25	50.6	1566	1.51	0.08	0.08	0.09	0.11	0.14	0.18	49.1	1585	1.52	0.08	0.09	0.09	0.11	0.15	0.18
	20	0.25	71.7	1550	1.49	0.07	0.08	0.09	0.11	0.14	0.18	70.2	1562	1.49	0.07	0.08	0.09	0.11	0.14	0.18
0.05	1	0.13	5.1	1084	2.32	0.11	0.12	0.14	0.17	0.23	0.29	4.9	1076	2.32	0.11	0.13	0.14	0.17	0.23	0.29
	2	0.13	10.6	1139	2.31	0.11	0.12	0.14	0.17	0.23	0.30	9.9	1155	2.31	0.11	0.12	0.13	0.16	0.23	0.29
	3	0.13	14.0	1034	2.32	0.10	0.12	0.13	0.16	0.22	0.28	13.4	1045	2.32	0.10	0.12	0.13	0.16	0.22	0.29
	4	0.13	19.9	1133	2.32	0.10	0.12	0.13	0.16	0.22	0.28	19.2	1138	2.32	0.10	0.12	0.13	0.16	0.22	0.28
	6	0.13	29.8	1168	2.32	0.11	0.12	0.14	0.17	0.23	0.29	28.3	1171	2.32	0.11	0.12	0.13	0.16	0.22	0.29
	8	0.13	40.4	1065	2.30	0.10	0.12	0.13	0.16	0.22	0.29	38.3	1087	2.31	0.10	0.12	0.13	0.16	0.22	0.29
	12	0.13	56.4	1066	2.29	0.10	0.11	0.13	0.16	0.22	0.28	54.2	1076	2.30	0.10	0.12	0.13	0.16	0.22	0.28
	20	0.13	76.9	1079	2.22	0.10	0.11	0.13	0.16	0.22	0.28	74.8	1096	2.25	0.10	0.11	0.13	0.16	0.22	0.28
0.10	1	0.063	4.9	818	3.02	0.12	0.14	0.16	0.21	0.30	0.39	4.6	861	3.02	0.12	0.14	0.16	0.20	0.29	0.39
	2	0.063	10.3	801	3.02	0.13	0.16	0.18	0.23	0.32	0.42	9.6	762	3.02	0.13	0.15	0.17	0.22	0.32	0.42
	3	0.063	14.7	799	3.02	0.12	0.15	0.17	0.22	0.31	0.41	13.7	793	3.02	0.12	0.14	0.17	0.21	0.31	0.41
	4	0.063	19.2	751	3.01	0.12	0.15	0.17	0.22	0.32	0.42	17.9	773	3.01	0.12	0.15	0.17	0.22	0.31	0.42
	6	0.063	28.9	781	3.03	0.13	0.15	0.17	0.22	0.32	0.42	26.6	758	3.02	0.12	0.15	0.17	0.22	0.31	0.41
	8	0.063	37.5	791	3.02	0.12	0.15	0.17	0.22	0.31	0.42	34.7	802	3.02	0.13	0.15	0.17	0.22	0.31	0.42
	12	0.063	54.5	763	3.00	0.12	0.14	0.17	0.21	0.31	0.41	50.4	767	3.01	0.12	0.14	0.17	0.21	0.31	0.41
	20	0.063	74.7	737	2.96	0.12	0.14	0.16	0.21	0.31	0.41	71.1	743	2.98	0.12	0.14	0.16	0.21	0.31	0.41
0.20	1	0.015	3.8	505	3.69	0.12	0.16	0.19	0.26	0.40	0.54	3.5	499	3.69	0.12	0.15	0.19	0.26	0.39	0.53
	2	0.015	7.8	438	3.69	0.12	0.16	0.20	0.27	0.41	0.55	6.8	420	3.69	0.12	0.16	0.19	0.26	0.40	0.53
	3	0.015	12.2	457	3.68	0.12	0.16	0.20	0.28	0.43	0.59	10.4	459	3.68	0.12	0.16	0.20	0.27	0.42	0.57
	4	0.015	15.5	414	3.67	0.12	0.16	0.20	0.28	0.44	0.60	13.2	399	3.68	0.11	0.15	0.19	0.27	0.42	0.58
	6	0.015	22.0	419	3.68	0.12	0.16	0.20	0.28	0.42	0.58	19.0	408	3.69	0.12	0.16	0.20	0.27	0.42	0.56
	8	0.015	29.2	432	3.68	0.12	0.16	0.20	0.28	0.43	0.58	24.8	418	3.68	0.11	0.15	0.19	0.26	0.41	0.56
	12	0.015	44.0	391	3.65	0.12	0.16	0.19	0.27	0.42	0.57	38.2	385	3.67	0.11	0.15	0.19	0.26	0.41	0.56
	20	0.015	62.3	402	3.63	0.11	0.16	0.19	0.27	0.42	0.58	55.6	388	3.66	0.11	0.15	0.19	0.26	0.41	0.56
0.50	1	0.015	2.1	140	4.37	0.10	0.19	0.27	0.42	0.68	0.95	1.8	135	4.37	0.10	0.18	0.26	0.40	0.66	0.92
	2	0.015	4.6	188	4.38	0.12	0.20	0.26	0.40	0.63	0.86	3.8	182	4.38	0.11	0.19	0.26	0.39	0.64	0.86
	3	0.015	6.8	158	4.37	0.11	0.20	0.28	0.43	0.70	0.96	5.4	163	4.38	0.11	0.19	0.27	0.41	0.67	0.92
	4	0.015	8.9	134	4.38	0.10	0.19	0.28	0.43	0.71	0.98	7.8	152	4.38	0.11	0.20	0.28	0.43	0.70	0.97
	6	0.015	12.0	160	4.38	0.10	0.19	0.27	0.41	0.67	0.91	10.0	167	4.38	0.11	0.19	0.26	0.40	0.66	0.90
	8	0.015	16.6	143	4.38	0.10	0.19	0.27	0.41	0.68	0.94	13.9	137	4.38	0.10	0.18	0.26	0.40	0.67	0.92
	12	0.015	25.4	147	4.38	0.09	0.18	0.26	0.41	0.68	0.93	22.1	157	4.38	0.10	0.19	0.26	0.41	0.67	0.92
	20	0.015	34.7	129	4.38	0.09	0.18	0.26	0.41	0.68	0.94	30.6	136	4.39	0.10	0.18	0.26	0.40	0.67	0.92

**Table B.21:** Detection probability, average detection time, contaminated area in case of detection failure and relative contaminated area to control area for various RADTi in case of  $\sigma_{\ln K}^2 = 2.0$  assuming bimonthly (2M) and quarterly (3M) sampling frequencies

$\sigma_{\ln K}^2$		2.00																			
$\alpha_f(m)$	now	nfds(max)	$P_d$ (2M)	$\langle T_{(DET)} \rangle$ (DAYS)	AREA ON FAILURE	(AREA ON DET.)/L	(3M. RADTi)/L	(6M. RADTi)/L	(12M. RADTi)/L	(24M. RADTi)/L	(36M. RADTi)/L	$P_d$ (3M)	$\langle T_{(DET)} \rangle$ (DAYS)	AREA ON FAILURE	(AREA ON DET.)/L	(3M. RADTi)/L	(6M. RADTi)/L	(12M. RADTi)/L	(24M. RADTi)/L	(36M. RADTi)/L	
0.001	1	0.75	3.3	3114	0.37	0.03	0.03	0.03	0.03	0.04	0.04	3.3	3103	0.37	0.03	0.03	0.03	0.03	0.03	0.04	0.04
	2	0.75	6.7	3035	0.36	0.02	0.02	0.03	0.03	0.03	0.04	6.4	3130	0.36	0.02	0.02	0.03	0.03	0.03	0.03	0.04
	3	0.75	8.8	3081	0.36	0.02	0.02	0.03	0.03	0.03	0.04	8.5	3162	0.36	0.02	0.02	0.03	0.03	0.03	0.03	0.04
	4	0.75	11.5	3068	0.37	0.03	0.03	0.03	0.03	0.04	0.04	11.0	3119	0.37	0.03	0.03	0.03	0.03	0.03	0.04	0.04
	6	0.75	18.6	3192	0.37	0.03	0.03	0.03	0.03	0.03	0.04	18.1	3244	0.37	0.03	0.03	0.03	0.03	0.03	0.03	0.04
	8	0.75	23.4	3090	0.38	0.02	0.03	0.03	0.03	0.03	0.04	22.6	3151	0.38	0.02	0.03	0.03	0.03	0.03	0.03	0.04
	12	0.75	32.8	3107	0.36	0.02	0.03	0.03	0.03	0.04	0.04	31.8	3152	0.36	0.02	0.03	0.03	0.03	0.03	0.04	0.04
	20	0.75	51.6	3053	0.35	0.02	0.03	0.03	0.03	0.03	0.04	49.9	3110	0.36	0.02	0.03	0.03	0.03	0.03	0.03	0.04
	0.01	1	0.50	5.1	2340	1.07	0.08	0.09	0.09	0.10	0.13	0.15	5.1	2368	1.07	0.08	0.09	0.09	0.10	0.13	0.15
		2	0.50	7.8	2245	1.08	0.08	0.08	0.09	0.10	0.12	0.15	7.7	2280	1.08	0.08	0.08	0.09	0.10	0.12	0.15
3		0.50	13.8	2323	1.07	0.08	0.08	0.09	0.10	0.12	0.15	13.6	2345	1.07	0.08	0.09	0.09	0.10	0.13	0.15	
4		0.50	16.2	2422	1.07	0.08	0.08	0.09	0.10	0.12	0.15	16.0	2453	1.07	0.08	0.08	0.09	0.10	0.12	0.15	
6		0.50	22.7	2359	1.08	0.08	0.08	0.09	0.10	0.12	0.15	22.5	2387	1.08	0.08	0.09	0.09	0.10	0.12	0.15	
8		0.50	31.1	2311	1.08	0.08	0.08	0.09	0.10	0.12	0.15	30.7	2337	1.08	0.08	0.08	0.09	0.10	0.12	0.15	
12		0.50	45.2	2346	1.06	0.08	0.08	0.09	0.10	0.12	0.15	44.4	2367	1.07	0.08	0.08	0.09	0.10	0.12	0.15	
20		0.50	62.7	2314	1.04	0.08	0.08	0.09	0.10	0.12	0.14	62.1	2327	1.04	0.08	0.08	0.09	0.10	0.12	0.15	
0.02		1	0.25	4.8	1694	1.52	0.08	0.09	0.09	0.11	0.14	0.17	4.7	1732	1.52	0.08	0.09	0.09	0.11	0.14	0.17
		2	0.25	9.7	1573	1.52	0.08	0.09	0.10	0.11	0.15	0.19	9.5	1579	1.52	0.08	0.09	0.10	0.11	0.15	0.19
	3	0.25	12.9	1645	1.52	0.08	0.09	0.09	0.11	0.14	0.17	12.7	1669	1.52	0.08	0.09	0.09	0.11	0.14	0.17	
	4	0.25	16.7	1604	1.53	0.08	0.09	0.10	0.11	0.14	0.18	16.7	1665	1.53	0.08	0.09	0.10	0.11	0.15	0.18	
	6	0.25	26.7	1630	1.54	0.08	0.09	0.10	0.11	0.15	0.18	26.0	1642	1.54	0.08	0.09	0.10	0.11	0.15	0.18	
	8	0.25	34.5	1634	1.54	0.08	0.09	0.09	0.11	0.14	0.18	34.3	1642	1.54	0.08	0.09	0.10	0.11	0.15	0.18	
	12	0.25	48.1	1592	1.53	0.08	0.09	0.09	0.11	0.15	0.18	47.6	1629	1.54	0.08	0.09	0.10	0.11	0.15	0.18	
	20	0.25	69.0	1580	1.50	0.08	0.08	0.09	0.11	0.14	0.18	68.6	1600	1.51	0.08	0.08	0.09	0.11	0.14	0.18	
	0.05	1	0.13	4.7	1108	2.32	0.11	0.13	0.14	0.17	0.23	0.29	4.6	1114	2.32	0.11	0.13	0.14	0.17	0.23	0.29
		2	0.13	9.6	1163	2.31	0.11	0.12	0.14	0.17	0.23	0.29	9.4	1165	2.31	0.11	0.12	0.14	0.17	0.23	0.29
3		0.13	13.0	1069	2.32	0.11	0.12	0.13	0.16	0.22	0.29	12.6	1081	2.32	0.11	0.12	0.14	0.17	0.23	0.29	
4		0.13	18.9	1148	2.32	0.11	0.12	0.13	0.16	0.22	0.28	18.7	1171	2.32	0.11	0.12	0.13	0.16	0.22	0.28	
6		0.13	27.8	1187	2.33	0.11	0.12	0.14	0.16	0.22	0.29	27.0	1200	2.33	0.11	0.12	0.14	0.16	0.22	0.29	
8		0.13	37.5	1103	2.32	0.11	0.12	0.13	0.16	0.22	0.29	37.1	1115	2.32	0.11	0.12	0.13	0.16	0.22	0.29	
12		0.13	53.1	1093	2.31	0.10	0.12	0.13	0.16	0.22	0.28	52.2	1105	2.31	0.10	0.12	0.13	0.16	0.22	0.28	
20		0.13	73.9	1113	2.28	0.10	0.11	0.13	0.16	0.22	0.29	73.1	1123	2.29	0.10	0.12	0.13	0.16	0.22	0.29	
0.10		1	0.063	4.4	875	3.02	0.12	0.14	0.16	0.20	0.29	0.38	4.1	924	3.02	0.12	0.14	0.16	0.20	0.28	0.37
		2	0.063	9.3	773	3.02	0.13	0.15	0.17	0.22	0.32	0.41	9.0	790	3.02	0.13	0.15	0.17	0.22	0.31	0.41
	3	0.063	13.0	803	3.02	0.12	0.14	0.17	0.21	0.31	0.41	12.4	822	3.02	0.12	0.15	0.17	0.21	0.30	0.40	
	4	0.063	17.3	788	3.01	0.13	0.15	0.17	0.22	0.32	0.42	16.6	795	3.01	0.13	0.15	0.17	0.22	0.32	0.42	
	6	0.063	25.7	767	3.03	0.12	0.15	0.17	0.22	0.32	0.41	25.0	785	3.03	0.13	0.15	0.17	0.22	0.31	0.41	
	8	0.063	33.2	811	3.03	0.13	0.15	0.17	0.22	0.31	0.41	32.4	817	3.03	0.13	0.15	0.17	0.22	0.31	0.41	
	12	0.063	48.9	779	3.01	0.12	0.15	0.17	0.21	0.31	0.41	47.1	791	3.02	0.12	0.15	0.17	0.21	0.31	0.41	
	20	0.063	69.4	751	3.00	0.12	0.14	0.16	0.21	0.31	0.41	67.8	763	3.01	0.12	0.14	0.17	0.21	0.31	0.41	
	0.20	1	0.015	3.4	525	3.69	0.12	0.16	0.19	0.26	0.39	0.53	3.2	542	3.69	0.13	0.16	0.20	0.26	0.40	0.54
		2	0.015	6.3	417	3.69	0.12	0.15	0.19	0.26	0.39	0.52	6.0	439	3.69	0.12	0.16	0.19	0.25	0.38	0.51
3		0.015	10.0	480	3.68	0.12	0.16	0.20	0.27	0.42	0.57	9.4	496	3.68	0.13	0.16	0.20	0.27	0.42	0.57	
4		0.015	12.4	405	3.68	0.12	0.16	0.19	0.27	0.42	0.58	11.8	418	3.68	0.12	0.16	0.19	0.27	0.42	0.57	
6		0.015	17.8	411	3.69	0.12	0.16	0.20	0.27	0.41	0.56	16.6	427	3.69	0.13	0.16	0.20	0.27	0.41	0.55	
8		0.015	23.4	423	3.69	0.12	0.15	0.19	0.26	0.41	0.56	22.2	439	3.69	0.12	0.15	0.19	0.26	0.41	0.55	
12		0.015	36.2	400	3.67	0.11	0.15	0.19	0.26	0.41	0.56	34.8	407	3.68	0.12	0.15	0.19	0.26	0.41	0.55	
20		0.015	53.0	393	3.68	0.11	0.15	0.19	0.26	0.41	0.56	50.9	407	3.69	0.12	0.15	0.19	0.26	0.41	0.56	
0.50		1	0.015	1.7	153	4.37	0.12	0.20	0.28	0.42	0.68	0.93	1.5	183	4.37	0.13	0.20	0.27	0.40	0.66	0.91
		2	0.015	3.2	189	4.38	0.12	0.19	0.25	0.38	0.60	0.82	2.9	219	4.38	0.13	0.19	0.25	0.36	0.58	0.79
	3	0.015	4.9	171	4.37	0.12	0.20	0.27	0.41	0.67	0.92	4.4	199	4.38	0.13	0.20	0.27	0.39	0.64	0.88	
	4	0.015	7.3	176	4.38	0.13	0.21	0.28	0.43	0.70	0.96	6.5	180	4.38	0.14	0.21	0.29	0.43	0.69	0.95	
	6	0.015	8.9	177	4.38	0.11	0.19	0.26	0.40	0.65	0.89	8.0	207	4.38	0.12	0.19	0.26	0.39	0.63	0.86	
	8	0.015	12.5	150	4.38	0.11	0.19	0.26	0.40	0.66	0.91	11.8	171	4.38	0.12	0.20	0.27	0.40	0.66	0.90	
	12	0.015	20.5	171	4.38	0.11	0.20	0.27	0.41	0.67	0.92	19.2	191	4.38	0.13	0.20	0.27	0.41	0.66	0.91	
	20	0.015	28.9	151	4.39	0.11	0.19	0.27	0.41	0.67	0.92	26.8	168	4.39	0.13	0.20	0.27	0.41	0.66	0.91	

**Table B.22:** Detection probability, average detection time, contaminated area in case of detection failure and relative contaminated area to control area  $L$  for various RADTi in case of  $\sigma_{\ln K}^2 = 2.0$  assuming every 4 months (4M) and biannually (6M) sampling frequencies

$\sigma_{\ln K}^2$		2.00																			
$\alpha_r(m)$	now	nfds(max)	$P_d$ (4M)	$\langle T_{(DET)} \rangle$ (DAYS)	AREA ON FAILURE	(AREA ON DET.)/L	(3M. RADTi)/L	(6M. RADTi)/L	(12M. RADTi)/L	(24M. RADTi)/L	(36M. RADTi)/L	$P_d$ (6M)	$\langle T_{(DET)} \rangle$ (DAYS)	AREA ON FAILURE	(AREA ON DET.)/L	(3M. RADTi)/L	(6M. RADTi)/L	(12M. RADTi)/L	(24M. RADTi)/L	(36M. RADTi)/L	
0.001	1	0.75	3.1	3254	0.37	0.03	0.03	0.03	0.03	0.04	0.04	2.8	3381	0.37	0.03	0.03	0.03	0.03	0.03	0.04	0.04
	2	0.75	6.0	3240	0.37	0.02	0.03	0.03	0.03	0.03	0.04	5.6	3326	0.37	0.02	0.03	0.03	0.03	0.03	0.03	0.04
	3	0.75	8.2	3247	0.36	0.02	0.03	0.03	0.03	0.03	0.04	7.2	3420	0.36	0.03	0.03	0.03	0.03	0.03	0.03	0.04
	4	0.75	10.6	3211	0.37	0.03	0.03	0.03	0.03	0.04	0.04	9.7	3343	0.37	0.03	0.03	0.03	0.03	0.03	0.04	0.04
	6	0.75	17.3	3357	0.37	0.03	0.03	0.03	0.03	0.04	0.04	15.6	3503	0.38	0.03	0.03	0.03	0.03	0.03	0.04	0.04
	8	0.75	21.6	3252	0.39	0.03	0.03	0.03	0.03	0.04	0.04	19.6	3380	0.39	0.03	0.03	0.03	0.03	0.03	0.04	0.04
	12	0.75	30.4	3244	0.37	0.03	0.03	0.03	0.03	0.04	0.04	27.6	3404	0.37	0.03	0.03	0.03	0.03	0.03	0.04	0.04
	20	0.75	47.6	3201	0.37	0.03	0.03	0.03	0.03	0.04	0.04	43.4	3348	0.39	0.03	0.03	0.03	0.03	0.03	0.04	0.04
	0.01	1	0.50	4.8	2414	1.07	0.08	0.09	0.09	0.11	0.13	0.15	4.7	2473	1.07	0.08	0.09	0.09	0.10	0.13	0.15
		2	0.50	7.6	2304	1.08	0.08	0.08	0.09	0.10	0.12	0.15	7.1	2362	1.08	0.08	0.08	0.09	0.10	0.12	0.15
3		0.50	13.1	2398	1.07	0.08	0.09	0.09	0.10	0.13	0.15	12.4	2477	1.07	0.08	0.09	0.09	0.10	0.13	0.15	
4		0.50	15.8	2496	1.08	0.08	0.09	0.09	0.10	0.12	0.15	14.9	2585	1.08	0.08	0.09	0.09	0.10	0.12	0.15	
6		0.50	22.1	2418	1.08	0.08	0.09	0.09	0.10	0.12	0.15	20.9	2496	1.09	0.08	0.09	0.09	0.10	0.12	0.15	
8		0.50	30.0	2365	1.08	0.08	0.08	0.09	0.10	0.12	0.15	28.4	2451	1.09	0.08	0.09	0.09	0.10	0.12	0.15	
12		0.50	43.6	2413	1.07	0.08	0.08	0.09	0.10	0.12	0.15	40.9	2496	1.09	0.08	0.08	0.09	0.10	0.12	0.15	
20		0.50	61.1	2365	1.07	0.08	0.08	0.09	0.10	0.12	0.15	58.2	2437	1.09	0.08	0.08	0.09	0.10	0.12	0.15	
0.02		1	0.25	4.7	1743	1.52	0.08	0.09	0.10	0.11	0.14	0.17	4.6	1784	1.52	0.08	0.09	0.10	0.11	0.14	0.17
		2	0.25	9.4	1638	1.52	0.08	0.09	0.10	0.12	0.15	0.19	8.9	1671	1.52	0.09	0.09	0.10	0.12	0.15	0.19
	3	0.25	12.4	1704	1.52	0.08	0.09	0.10	0.11	0.14	0.17	12.0	1758	1.52	0.08	0.09	0.10	0.11	0.14	0.17	
	4	0.25	16.2	1662	1.53	0.08	0.09	0.10	0.11	0.15	0.18	15.4	1740	1.53	0.09	0.09	0.10	0.12	0.15	0.18	
	6	0.25	25.7	1688	1.55	0.08	0.09	0.10	0.11	0.15	0.18	24.4	1732	1.55	0.09	0.09	0.10	0.12	0.15	0.18	
	8	0.25	33.3	1685	1.54	0.08	0.09	0.10	0.11	0.15	0.18	31.6	1746	1.55	0.08	0.09	0.10	0.11	0.15	0.18	
	12	0.25	46.2	1649	1.54	0.08	0.09	0.10	0.11	0.15	0.18	44.0	1726	1.56	0.08	0.09	0.10	0.12	0.15	0.19	
	20	0.25	67.0	1632	1.55	0.08	0.09	0.09	0.11	0.14	0.18	64.6	1696	1.57	0.08	0.09	0.10	0.11	0.15	0.18	
	0.05	1	0.13	4.4	1114	2.32	0.12	0.13	0.14	0.17	0.23	0.29	4.1	1183	2.32	0.12	0.13	0.14	0.17	0.23	0.29
		2	0.13	9.1	1203	2.32	0.11	0.12	0.14	0.16	0.22	0.28	8.4	1272	2.32	0.11	0.12	0.14	0.17	0.22	0.28
3		0.13	12.4	1096	2.32	0.11	0.12	0.14	0.17	0.23	0.29	11.5	1165	2.33	0.11	0.12	0.14	0.17	0.22	0.29	
4		0.13	18.1	1189	2.32	0.11	0.12	0.13	0.16	0.22	0.28	17.6	1245	2.33	0.11	0.12	0.14	0.16	0.22	0.29	
6		0.13	26.5	1237	2.34	0.11	0.12	0.14	0.16	0.22	0.29	24.7	1301	2.34	0.11	0.13	0.14	0.17	0.22	0.29	
8		0.13	36.1	1138	2.33	0.11	0.12	0.13	0.16	0.22	0.29	34.3	1195	2.33	0.11	0.12	0.14	0.16	0.22	0.29	
12		0.13	51.2	1128	2.32	0.11	0.12	0.13	0.16	0.22	0.29	48.2	1178	2.35	0.11	0.12	0.13	0.16	0.22	0.28	
20		0.13	71.7	1144	2.32	0.10	0.12	0.13	0.16	0.22	0.29	68.9	1197	2.37	0.11	0.12	0.13	0.16	0.22	0.29	
0.10		1	0.063	4.1	934	3.02	0.12	0.14	0.16	0.20	0.29	0.38	3.9	981	3.02	0.13	0.14	0.16	0.20	0.29	0.37
		2	0.063	8.6	819	3.03	0.13	0.15	0.17	0.22	0.31	0.40	8.1	837	3.03	0.13	0.15	0.17	0.22	0.31	0.40
	3	0.063	12.2	840	3.02	0.13	0.15	0.17	0.21	0.31	0.40	11.5	882	3.02	0.13	0.15	0.17	0.21	0.30	0.40	
	4	0.063	15.8	827	3.02	0.13	0.15	0.17	0.22	0.32	0.42	14.6	883	3.02	0.13	0.16	0.18	0.22	0.32	0.42	
	6	0.063	24.0	811	3.04	0.13	0.15	0.17	0.22	0.31	0.41	22.7	831	3.04	0.13	0.15	0.17	0.22	0.31	0.41	
	8	0.063	31.2	832	3.03	0.13	0.15	0.17	0.22	0.31	0.41	29.2	872	3.05	0.13	0.15	0.17	0.22	0.31	0.41	
	12	0.063	45.6	817	3.03	0.13	0.15	0.17	0.21	0.31	0.41	42.7	860	3.05	0.13	0.15	0.17	0.22	0.31	0.41	
	20	0.063	65.9	774	3.03	0.12	0.14	0.17	0.21	0.31	0.41	61.9	820	3.08	0.13	0.15	0.17	0.21	0.31	0.40	
	0.20	1	0.015	3.0	572	3.69	0.13	0.17	0.20	0.26	0.39	0.52	2.7	632	3.69	0.13	0.16	0.19	0.25	0.37	0.50
		2	0.015	5.6	460	3.69	0.13	0.16	0.19	0.25	0.38	0.50	5.2	506	3.69	0.13	0.16	0.19	0.25	0.37	0.50
3		0.015	8.9	519	3.69	0.13	0.16	0.20	0.27	0.41	0.55	7.9	586	3.69	0.13	0.17	0.20	0.26	0.39	0.52	
4		0.015	11.0	423	3.68	0.12	0.16	0.20	0.27	0.42	0.57	9.6	491	3.69	0.13	0.16	0.20	0.26	0.41	0.56	
6		0.015	15.8	450	3.70	0.13	0.16	0.20	0.27	0.40	0.54	14.3	492	3.70	0.14	0.17	0.20	0.27	0.40	0.54	
8		0.015	21.2	459	3.70	0.12	0.16	0.19	0.26	0.40	0.55	18.6	513	3.70	0.13	0.16	0.19	0.26	0.39	0.53	
12		0.015	33.0	424	3.68	0.12	0.16	0.19	0.26	0.41	0.55	29.4	479	3.70	0.13	0.16	0.19	0.26	0.40	0.54	
20		0.015	48.6	425	3.70	0.12	0.16	0.19	0.26	0.41	0.55	43.4	485	3.73	0.13	0.16	0.19	0.26	0.40	0.54	
0.50		1	0.015	1.4	196	4.37	0.14	0.20	0.27	0.39	0.65	0.89	1.0	261	4.38	0.14	0.19	0.24	0.34	0.56	0.77
		2	0.015	2.7	219	4.38	0.13	0.19	0.25	0.36	0.57	0.78	2.2	271	4.38	0.15	0.20	0.25	0.35	0.55	0.75
	3	0.015	4.0	208	4.38	0.13	0.20	0.26	0.39	0.63	0.87	3.1	286	4.38	0.15	0.20	0.25	0.35	0.56	0.77	
	4	0.015	6.0	208	4.38	0.15	0.22	0.29	0.43	0.69	0.95	4.3	275	4.38	0.17	0.23	0.28	0.40	0.64	0.88	
	6	0.015	7.3	224	4.38	0.13	0.20	0.26	0.38	0.61	0.84	5.6	290	4.39	0.15	0.21	0.26	0.37	0.58	0.80	
	8	0.015	10.6	188	4.38	0.13	0.20	0.27	0.40	0.65	0.88	8.4	240	4.39	0.15	0.21	0.26	0.38	0.60	0.83	
	12	0.015	17.5	215	4.39	0.14	0.21	0.28	0.41	0.65	0.89	13.5	277	4.40	0.16	0.22	0.27	0.39	0.61	0.84	
	20	0.015	24.6	193	4.40	0.14	0.21	0.27	0.40	0.65	0.88	19.3	250	4.41	0.15	0.21	0.27	0.38	0.61	0.83	

**Table B.23:** Detection probability, average detection time, contaminated area in case of detection failure and relative contaminated area to control area  $L$  for various RADTi in case of  $\sigma_{lnK}^2 = 2.0$  assuming annually sampling frequency

$\sigma_{lnK}^2$		2.00										
$\alpha_1(m)$	now	nfd5(max)	$P_d$ (12M)	$\langle T_{(DET)} \rangle$ (DAYS)	AREA ON FAILURE	(AREA ON DET.)/L	(3M. RADTi)/L	(6M. RADTi)/L	(12M. RADTi)/L	(24M. RADTi)/L	(36M. RADTi)/L	
0.001	1	0.75	1.7	4085	0.37	0.03	0.03	0.03	0.04	0.04	0.05	
	2	0.75	3.9	3826	0.37	0.03	0.03	0.03	0.03	0.04	0.04	
	3	0.75	5.1	3930	0.37	0.03	0.03	0.03	0.03	0.04	0.04	
	4	0.75	6.7	3849	0.37	0.03	0.03	0.03	0.04	0.04	0.05	
	6	0.75	11.1	4009	0.37	0.03	0.03	0.03	0.03	0.04	0.04	
	8	0.75	14.3	3842	0.39	0.03	0.03	0.03	0.03	0.04	0.05	
	12	0.75	19.5	3851	0.37	0.03	0.03	0.03	0.03	0.04	0.05	
	20	0.75	30.6	3811	0.40	0.03	0.03	0.03	0.03	0.04	0.04	
	0.01	1	0.50	3.3	2872	1.07	0.09	0.09	0.10	0.11	0.13	0.15
		2	0.50	5.8	2649	1.08	0.08	0.09	0.09	0.10	0.13	0.15
3		0.50	9.7	2792	1.08	0.09	0.09	0.10	0.11	0.13	0.16	
4		0.50	12.0	2952	1.09	0.09	0.09	0.10	0.11	0.13	0.15	
6		0.50	16.9	2811	1.10	0.09	0.09	0.10	0.11	0.13	0.15	
8		0.50	22.8	2763	1.10	0.08	0.09	0.09	0.11	0.13	0.15	
12		0.50	33.6	2833	1.12	0.09	0.09	0.10	0.11	0.13	0.15	
20		0.50	47.5	2750	1.16	0.08	0.09	0.09	0.11	0.13	0.15	
0.02		1	0.25	3.8	1994	1.52	0.09	0.09	0.10	0.11	0.14	0.17
		2	0.25	7.1	1913	1.53	0.09	0.10	0.11	0.12	0.16	0.19
	3	0.25	9.7	2007	1.53	0.09	0.09	0.10	0.11	0.14	0.17	
	4	0.25	12.3	1973	1.54	0.09	0.10	0.11	0.12	0.15	0.18	
	6	0.25	19.8	1975	1.56	0.09	0.10	0.10	0.12	0.15	0.18	
	8	0.25	25.4	1995	1.57	0.09	0.10	0.10	0.12	0.15	0.19	
	12	0.25	35.5	1975	1.59	0.09	0.10	0.10	0.12	0.15	0.19	
	20	0.25	54.4	1929	1.64	0.09	0.09	0.10	0.12	0.15	0.19	
	0.05	1	0.13	3.0	1391	2.32	0.12	0.14	0.15	0.17	0.22	0.28
		2	0.13	7.0	1472	2.33	0.12	0.13	0.14	0.17	0.23	0.28
3		0.13	9.0	1325	2.33	0.12	0.13	0.14	0.17	0.22	0.28	
4		0.13	13.9	1421	2.34	0.12	0.13	0.14	0.17	0.22	0.29	
6		0.13	20.3	1514	2.36	0.12	0.13	0.14	0.17	0.22	0.28	
8		0.13	27.0	1389	2.36	0.12	0.13	0.14	0.17	0.22	0.28	
12		0.13	39.1	1363	2.40	0.12	0.13	0.14	0.17	0.22	0.28	
20		0.13	56.9	1388	2.47	0.11	0.13	0.14	0.17	0.22	0.28	
0.10		1	0.063	3.1	1126	3.02	0.13	0.15	0.17	0.20	0.28	0.36
		2	0.063	6.4	1007	3.03	0.14	0.16	0.18	0.22	0.29	0.38
	3	0.063	8.4	1105	3.03	0.14	0.16	0.17	0.21	0.29	0.37	
	4	0.063	10.5	1070	3.03	0.14	0.16	0.18	0.22	0.31	0.40	
	6	0.063	17.2	1026	3.06	0.14	0.16	0.18	0.22	0.30	0.39	
	8	0.063	22.7	1068	3.07	0.14	0.16	0.18	0.22	0.30	0.39	
	12	0.063	32.5	1032	3.09	0.14	0.16	0.18	0.22	0.30	0.39	
	20	0.063	47.9	1001	3.16	0.14	0.16	0.18	0.22	0.30	0.39	
	0.20	1	0.015	1.9	703	3.69	0.14	0.16	0.18	0.23	0.33	0.44
		2	0.015	3.8	614	3.70	0.14	0.17	0.19	0.24	0.35	0.46
3		0.015	5.1	737	3.70	0.14	0.17	0.19	0.25	0.36	0.48	
4		0.015	6.0	677	3.69	0.15	0.18	0.21	0.26	0.39	0.53	
6		0.015	9.7	670	3.71	0.15	0.18	0.20	0.26	0.37	0.49	
8		0.015	12.6	718	3.72	0.15	0.18	0.20	0.26	0.37	0.50	
12		0.015	18.6	661	3.73	0.15	0.18	0.20	0.26	0.37	0.50	
20		0.015	29.9	656	3.76	0.15	0.18	0.20	0.26	0.38	0.51	
0.50		1	0.015	0.7	434	4.38	0.19	0.23	0.27	0.36	0.55	0.74
		2	0.015	1.4	415	4.38	0.17	0.21	0.25	0.33	0.49	0.65
	3	0.015	1.8	461	4.38	0.18	0.22	0.26	0.35	0.53	0.72	
	4	0.015	1.7	512	4.38	0.18	0.21	0.25	0.33	0.51	0.70	
	6	0.015	3.4	487	4.39	0.18	0.22	0.26	0.35	0.52	0.70	
	8	0.015	4.6	423	4.39	0.18	0.22	0.26	0.34	0.52	0.70	
	12	0.015	6.0	451	4.40	0.18	0.22	0.26	0.34	0.52	0.70	
	20	0.015	9.9	427	4.41	0.18	0.22	0.26	0.35	0.53	0.72	



**Table B.25:** Precipitation triggered pollution detection probability, average detection time, contaminated area in case of detection failure and relative contaminated area to control area for various RADTi in case of  $\sigma_{lnK}^2 = 0.0$  assuming daily (ED) and monthly (1M) sampling frequencies

$\sigma_{lnK}^2$		0.00																		
$\alpha_T(m)$	now	nfd(s(max)	$P_d$ (ED)	$\langle T_{(DET)} \rangle$ (DAYS)	AREA ON FAILURE	(AREA ON DET.)/L	(3M. RADTi)/L	(6M. RADTi)/L	(12M. RADTi)/L	(24M. RADTi)/L	(36M. RADTi)/L	$P_d$ (1M)	$\langle T_{(DET)} \rangle$ (DAYS)	AREA ON FAILURE	(AREA ON DET.)/L	(3M. RADTi)/L	(6M. RADTi)/L	(12M. RADTi)/L	(24M. RADTi)/L	(36M. RADTi)/L
0.001	1	3.00	7.5	9405	0.36	0.29	0.30	0.29	0.30	0.29	0.21	7.4	9402	0.36	0.29	0.30	0.30	0.30	0.29	0.19
	2	3.00	16.3	9586	0.36	0.30	0.30	0.31	0.31	0.31	0.23	16.1	9598	0.36	0.30	0.30	0.31	0.31	0.31	0.23
	3	3.00	24.3	9556	0.36	0.30	0.30	0.30	0.31	0.31	0.25	24.1	9569	0.36	0.30	0.30	0.31	0.31	0.31	0.25
	4	3.00	31.5	9555	0.36	0.30	0.30	0.31	0.31	0.31	0.24	31.2	9569	0.36	0.30	0.31	0.31	0.31	0.31	0.24
	6	3.00	48.8	9587	0.36	0.30	0.30	0.31	0.31	0.31	0.24	48.5	9601	0.36	0.30	0.30	0.31	0.31	0.31	0.23
	8	3.00	62.3	9560	0.35	0.30	0.31	0.31	0.31	0.31	0.25	62.0	9576	0.35	0.30	0.31	0.31	0.31	0.31	0.24
	12	3.00	92.5	9579	NAV	0.30	0.31	0.31	0.31	0.31	0.24	91.8	9593	NAV	0.30	0.31	0.31	0.31	0.31	0.24
	20	3.00	100.0	9457	NAV	0.30	0.30	0.30	0.31	0.33	0.27	100.0	9472	NAV	0.30	0.30	0.30	0.31	0.33	0.27
	0.01	1	2.25	19.9	7254	0.80	0.46	0.46	0.47	0.49	0.52	0.54	19.8	7296	0.80	0.46	0.47	0.47	0.49	0.52
2		2.25	40.0	7242	0.80	0.46	0.47	0.47	0.49	0.51	0.54	39.5	7265	0.80	0.46	0.47	0.47	0.49	0.51	0.54
3		2.25	59.9	7251	0.80	0.46	0.47	0.47	0.48	0.51	0.54	59.2	7268	0.80	0.46	0.47	0.47	0.49	0.52	0.54
4		2.25	79.5	7215	0.80	0.46	0.46	0.47	0.48	0.51	0.54	79.1	7238	0.80	0.46	0.46	0.47	0.48	0.51	0.54
6		2.25	100.0	7007	NAV	0.44	0.44	0.45	0.47	0.50	0.53	100.0	7032	NAV	0.44	0.45	0.45	0.47	0.50	0.53
8		2.25	97.4	6935	NAV	0.43	0.44	0.45	0.46	0.49	0.52	97.3	6955	NAV	0.43	0.44	0.45	0.46	0.49	0.53
12		2.25	100.0	6854	NAV	0.42	0.43	0.44	0.46	0.49	0.52	100.0	6874	NAV	0.43	0.43	0.44	0.46	0.49	0.52
20		2.25	100.0	6823	NAV	0.42	0.43	0.44	0.45	0.48	0.52	100.0	6842	NAV	0.42	0.43	0.44	0.45	0.49	0.52
0.05		1	0.50	26.1	2397	1.52	0.22	0.22	0.23	0.25	0.29	0.32	25.5	2430	1.52	0.22	0.23	0.24	0.25	0.29
	2	0.50	50.3	2183	1.52	0.19	0.20	0.20	0.22	0.26	0.31	49.4	2252	1.52	0.19	0.20	0.21	0.23	0.27	0.31
	3	0.50	76.4	2285	1.52	0.20	0.21	0.22	0.24	0.28	0.31	74.8	2329	1.52	0.21	0.22	0.22	0.24	0.28	0.32
	4	0.50	96.7	2086	NAV	0.17	0.18	0.19	0.21	0.25	0.29	95.6	2137	NAV	0.18	0.19	0.20	0.22	0.25	0.29
	6	0.50	100.0	1669	NAV	0.12	0.13	0.14	0.16	0.20	0.24	100.0	1705	NAV	0.13	0.14	0.15	0.16	0.20	0.25
	8	0.50	99.3	1649	NAV	0.12	0.13	0.14	0.16	0.20	0.24	99.1	1683	NAV	0.13	0.14	0.14	0.16	0.20	0.24
	12	0.50	100.0	1553	NAV	0.11	0.12	0.13	0.15	0.19	0.23	100.0	1584	NAV	0.12	0.12	0.13	0.15	0.19	0.23
	20	0.50	100.0	1526	NAV	0.11	0.12	0.13	0.15	0.18	0.22	100.0	1556	NAV	0.11	0.12	0.13	0.15	0.19	0.23
	0.10	1	0.13	27.2	1383	1.97	0.16	0.17	0.18	0.19	0.23	0.29	26.3	1412	1.97	0.16	0.17	0.18	0.20	0.24
2		0.13	53.6	1377	1.97	0.16	0.17	0.17	0.20	0.24	0.29	52.0	1375	1.97	0.16	0.16	0.17	0.19	0.23	0.28
3		0.13	79.5	1289	1.97	0.14	0.15	0.16	0.18	0.22	0.27	77.3	1340	1.97	0.15	0.16	0.17	0.19	0.23	0.28
4		0.13	96.0	1064	1.97	0.11	0.12	0.13	0.15	0.19	0.24	94.6	1138	1.97	0.12	0.13	0.14	0.16	0.20	0.25
6		0.13	100.0	657	NAV	0.05	0.06	0.07	0.09	0.13	0.18	100.0	702	NAV	0.06	0.07	0.08	0.10	0.14	0.19
8		0.13	99.5	634	NAV	0.05	0.06	0.07	0.09	0.13	0.18	99.4	676	NAV	0.06	0.07	0.08	0.10	0.14	0.18
12		0.13	100.0	535	NAV	0.04	0.05	0.06	0.08	0.12	0.16	100.0	566	NAV	0.05	0.05	0.06	0.08	0.12	0.17
20		0.13	100.0	510	NAV	0.04	0.05	0.06	0.08	0.12	0.16	100.0	540	NAV	0.04	0.05	0.06	0.08	0.12	0.16
0.50		1	0.015	72.4	1843	NAV	1.13	1.17	1.23	1.36	1.60	1.85	67.4	1856	6.78	1.21	1.26	1.33	1.46	1.68
	2	0.015	100.0	743	NAV	0.39	0.45	0.51	0.63	0.88	1.14	100.0	908	NAV	0.48	0.54	0.60	0.73	0.98	1.23
	3	0.015	100.0	390	NAV	0.17	0.22	0.28	0.41	0.66	0.91	100.0	463	NAV	0.21	0.27	0.34	0.46	0.71	0.96
	4	0.015	100.0	278	NAV	0.11	0.16	0.22	0.35	0.60	0.86	100.0	334	NAV	0.15	0.21	0.27	0.40	0.64	0.89
	6	0.015	100.0	202	NAV	0.07	0.11	0.17	0.30	0.54	0.81	100.0	244	NAV	0.09	0.14	0.21	0.34	0.58	0.84
	8	0.015	100.0	186	NAV	0.07	0.11	0.16	0.30	0.54	0.81	100.0	226	NAV	0.09	0.14	0.20	0.33	0.57	0.84
	12	0.015	100.0	156	NAV	0.05	0.09	0.14	0.28	0.52	0.79	100.0	189	NAV	0.07	0.12	0.18	0.31	0.55	0.82
	20	0.015	100.0	144	NAV	0.05	0.08	0.13	0.26	0.51	0.78	100.0	174	NAV	0.06	0.10	0.16	0.30	0.54	0.80

**Table B.26:** Precipitation triggered pollution detection probability, average detection time, contaminated area in case of detection failure and relative contaminated area to control area for various RADTi in case of  $\sigma_{Ink}^2 = 0.0$  assuming bimonthly (2M) and quarterly (3M) sampling frequencies

$\sigma_{Ink}^2$		0.00																		
$\alpha_T(m)$	now	nfd <sub>s</sub> (max)	$P_d$ (2M)	$\langle T_{(DET)} \rangle$ (DAYS)	AREA ON FAILURE	(AREA ON DET.)/L	(3M. RADTi)/L	(6M. RADTi)/L	(12M. RADTi)/L	(24M. RADTi)/L	(36M. RADTi)/L	$P_d$ (3M)	$\langle T_{(DET)} \rangle$ (DAYS)	AREA ON FAILURE	(AREA ON DET.)/L	(3M. RADTi)/L	(6M. RADTi)/L	(12M. RADTi)/L	(24M. RADTi)/L	(36M. RADTi)/L
0.001	1	3.00	7.3	9408	0.36	0.29	0.30	0.29	0.30	0.29	0.20	7.1	9399	0.36	0.29	0.30	0.30	0.31	0.30	0.20
	2	3.00	15.9	9610	0.36	0.30	0.31	0.31	0.32	0.31	0.23	15.7	9632	0.36	0.30	0.30	0.31	0.31	0.31	0.22
	3	3.00	24.0	9583	0.36	0.30	0.30	0.30	0.31	0.31	0.25	23.6	9586	0.36	0.30	0.31	0.31	0.31	0.31	0.25
	4	3.00	30.7	9577	0.36	0.30	0.31	0.31	0.31	0.31	0.24	30.6	9602	0.36	0.30	0.31	0.31	0.31	0.31	0.23
	6	3.00	47.6	9612	0.36	0.30	0.31	0.31	0.31	0.31	0.23	46.8	9627	0.36	0.30	0.31	0.31	0.31	0.31	0.23
	8	3.00	61.4	9588	0.35	0.30	0.31	0.31	0.31	0.32	0.25	60.6	9604	0.35	0.30	0.31	0.31	0.31	0.31	0.24
	12	3.00	90.4	9603	NAV	0.30	0.31	0.31	0.31	0.31	0.24	89.2	9620	NAV	0.30	0.31	0.31	0.31	0.31	0.23
	20	3.00	100.0	9488	NAV	0.30	0.30	0.30	0.31	0.33	0.27	100.0	9503	NAV	0.30	0.30	0.31	0.31	0.33	0.26
	0.01	1	2.25	19.7	7340	0.80	0.47	0.47	0.48	0.49	0.52	0.54	19.2	7324	0.80	0.47	0.47	0.48	0.49	0.52
2		2.25	38.9	7293	0.80	0.46	0.47	0.48	0.49	0.51	0.54	38.1	7314	0.80	0.46	0.47	0.48	0.49	0.52	0.54
3		2.25	58.6	7303	0.80	0.46	0.47	0.47	0.49	0.52	0.54	57.1	7290	0.80	0.46	0.47	0.48	0.49	0.52	0.55
4		2.25	77.8	7250	0.80	0.46	0.47	0.47	0.49	0.51	0.54	76.8	7288	0.80	0.46	0.47	0.48	0.49	0.51	0.54
6		2.25	100.0	7062	NAV	0.44	0.45	0.46	0.47	0.50	0.54	100.0	7101	NAV	0.45	0.45	0.46	0.48	0.51	0.54
8		2.25	97.1	6978	NAV	0.43	0.44	0.45	0.47	0.50	0.53	96.9	7001	NAV	0.44	0.44	0.45	0.47	0.50	0.53
12		2.25	100.0	6898	NAV	0.43	0.44	0.44	0.46	0.49	0.52	100.0	6922	NAV	0.43	0.44	0.45	0.46	0.49	0.52
20		2.25	100.0	6866	NAV	0.43	0.43	0.44	0.46	0.49	0.52	100.0	6889	NAV	0.43	0.43	0.44	0.46	0.49	0.52
0.05		1	0.50	25.1	2449	1.52	0.22	0.23	0.24	0.26	0.30	0.34	24.3	2355	1.52	0.21	0.22	0.22	0.24	0.28
	2	0.50	48.6	2314	1.52	0.20	0.21	0.22	0.24	0.28	0.32	47.9	2336	1.52	0.21	0.21	0.22	0.24	0.28	0.32
	3	0.50	73.7	2373	1.52	0.21	0.22	0.23	0.25	0.29	0.32	71.9	2343	1.52	0.21	0.21	0.22	0.24	0.28	0.32
	4	0.50	94.8	2211	1.52	0.19	0.20	0.21	0.23	0.27	0.31	93.8	2225	NAV	0.19	0.20	0.21	0.23	0.27	0.31
	6	0.50	100.0	1741	NAV	0.13	0.14	0.15	0.17	0.21	0.25	100.0	1764	NAV	0.13	0.14	0.15	0.17	0.21	0.25
	8	0.50	99.0	1720	NAV	0.13	0.14	0.15	0.17	0.21	0.25	98.7	1736	NAV	0.13	0.14	0.15	0.17	0.21	0.25
	12	0.50	100.0	1610	NAV	0.12	0.13	0.14	0.15	0.19	0.23	100.0	1632	NAV	0.12	0.13	0.14	0.16	0.20	0.24
	20	0.50	100.0	1581	NAV	0.12	0.12	0.13	0.15	0.19	0.23	100.0	1601	NAV	0.12	0.13	0.14	0.15	0.19	0.23
	0.10	1	0.13	25.8	1483	1.97	0.17	0.18	0.19	0.21	0.25	0.29	25.2	1534	1.97	0.18	0.19	0.20	0.21	0.25
2		0.13	50.9	1421	1.97	0.16	0.17	0.18	0.20	0.24	0.29	49.6	1424	1.97	0.16	0.17	0.18	0.20	0.24	0.29
3		0.13	75.9	1398	1.97	0.16	0.17	0.18	0.20	0.24	0.29	74.8	1441	1.97	0.16	0.17	0.18	0.20	0.24	0.29
4		0.13	93.7	1187	1.97	0.13	0.14	0.14	0.16	0.21	0.26	93.0	1235	1.97	0.13	0.14	0.15	0.17	0.22	0.26
6		0.13	100.0	737	NAV	0.06	0.07	0.08	0.10	0.14	0.19	100.0	764	NAV	0.06	0.07	0.08	0.10	0.15	0.19
8		0.13	99.3	704	NAV	0.06	0.07	0.08	0.10	0.14	0.19	99.3	735	NAV	0.07	0.07	0.08	0.10	0.14	0.19
12		0.13	100.0	587	NAV	0.05	0.06	0.06	0.08	0.12	0.17	100.0	607	NAV	0.05	0.06	0.07	0.09	0.13	0.17
20		0.13	100.0	561	NAV	0.04	0.05	0.06	0.08	0.12	0.17	100.0	578	NAV	0.05	0.05	0.06	0.08	0.12	0.17
0.50		1	0.015	64.9	1878	6.71	1.31	1.36	1.40	1.50	1.72	1.99	63.1	1871	6.77	1.26	1.33	1.40	1.53	1.78
	2	0.015	99.7	985	NAV	0.54	0.59	0.66	0.78	1.03	1.29	99.5	1059	NAV	0.58	0.64	0.70	0.83	1.08	1.33
	3	0.015	100.0	508	NAV	0.25	0.31	0.37	0.50	0.74	0.99	100.0	540	NAV	0.27	0.33	0.39	0.52	0.76	1.01
	4	0.015	100.0	366	NAV	0.17	0.23	0.29	0.42	0.67	0.92	100.0	391	NAV	0.19	0.25	0.31	0.44	0.69	0.93
	6	0.015	100.0	269	NAV	0.11	0.17	0.23	0.36	0.60	0.86	100.0	288	NAV	0.12	0.18	0.25	0.37	0.62	0.88
	8	0.015	100.0	250	NAV	0.11	0.16	0.22	0.35	0.60	0.85	100.0	267	NAV	0.12	0.18	0.24	0.37	0.61	0.87
	12	0.015	100.0	210	NAV	0.08	0.13	0.19	0.33	0.56	0.83	100.0	228	NAV	0.09	0.15	0.21	0.34	0.58	0.84
	20	0.015	100.0	195	NAV	0.07	0.12	0.18	0.31	0.55	0.82	100.0	214	NAV	0.08	0.13	0.19	0.33	0.56	0.83

**Table B.27:** Precipitation triggered pollution detection probability, average detection time, contaminated area in case of detection failure and relative contaminated area to control area for various RADTi in case of  $\sigma_{lnK}^2 = 0.0$  assuming every 4 months (4M) and biannually (6M) sampling frequencies

$\sigma_{lnK}^2$		0.00																		
$\alpha_T(m)$	now	nfd(s(max)	Pd (4M)	$\langle T_{DET} \rangle$ (DAYS)	AREA ON FAILURE	(AREA ON DET.)/L	(3M. RADTi)/L	(6M. RADTi)/L	(12M. RADTi)/L	(24M. RADTi)/L	(36M. RADTi)/L	Pd (6M)	$\langle T_{DET} \rangle$ (DAYS)	AREA ON FAILURE	(AREA ON DET.)/L	(3M. RADTi)/L	(6M. RADTi)/L	(12M. RADTi)/L	(24M. RADTi)/L	(36M. RADTi)/L
0.001	1	3.00	6.9	9390	0.36	0.29	0.30	0.30	0.31	0.31	0.21	6.8	9415	0.36	0.29	0.30	0.30	0.30	0.29	0.18
	2	3.00	15.6	9650	0.36	0.31	0.31	0.31	0.31	0.31	0.23	14.7	9645	0.36	0.30	0.31	0.31	0.32	0.31	0.20
	3	3.00	23.3	9608	0.36	0.30	0.30	0.31	0.31	0.31	0.25	22.7	9614	0.36	0.30	0.31	0.31	0.31	0.31	0.23
	4	3.00	29.8	9601	0.36	0.30	0.31	0.31	0.32	0.31	0.24	29.3	9627	0.36	0.30	0.31	0.31	0.31	0.30	0.22
	6	3.00	46.3	9645	0.36	0.30	0.31	0.31	0.31	0.31	0.23	44.8	9660	0.36	0.31	0.31	0.31	0.31	0.30	0.21
	8	3.00	60.0	9617	0.35	0.30	0.31	0.31	0.32	0.32	0.25	58.3	9632	0.36	0.31	0.31	0.31	0.31	0.30	0.22
	12	3.00	87.5	9628	0.35	0.30	0.31	0.31	0.32	0.31	0.24	86.0	9649	0.35	0.31	0.31	0.31	0.31	0.30	0.21
	20	3.00	100.0	9520	NAV	0.30	0.30	0.31	0.31	0.33	0.27	100.0	9549	NAV	0.30	0.30	0.31	0.31	0.32	0.24
	0.01	1	2.25	19.1	7379	0.80	0.47	0.47	0.48	0.50	0.52	18.5	7369	0.80	0.47	0.48	0.48	0.50	0.53	0.55
2		2.25	38.0	7350	0.80	0.47	0.47	0.48	0.49	0.51	36.5	7344	0.80	0.47	0.47	0.48	0.49	0.52	0.54	
3		2.25	56.6	7332	0.80	0.47	0.47	0.48	0.49	0.52	55.0	7347	0.80	0.47	0.47	0.48	0.49	0.52	0.54	
4		2.25	75.8	7299	0.80	0.46	0.47	0.47	0.49	0.51	74.2	7322	0.80	0.46	0.47	0.48	0.49	0.52	0.54	
6		2.25	100.0	7125	NAV	0.45	0.45	0.46	0.48	0.51	99.9	7178	NAV	0.45	0.46	0.47	0.48	0.51	0.55	
8		2.25	96.8	7022	NAV	0.44	0.45	0.45	0.47	0.50	96.6	7054	NAV	0.44	0.45	0.46	0.47	0.50	0.53	
12		2.25	100.0	6944	NAV	0.43	0.44	0.45	0.46	0.49	100.0	6976	NAV	0.43	0.44	0.45	0.47	0.50	0.53	
20		2.25	100.0	6907	NAV	0.43	0.44	0.44	0.46	0.49	100.0	6940	NAV	0.43	0.44	0.45	0.46	0.49	0.53	
0.05		1	0.50	24.5	2481	1.52	0.22	0.23	0.24	0.26	0.30	23.8	2457	1.52	0.22	0.23	0.24	0.26	0.30	0.33
	2	0.50	47.0	2327	1.52	0.20	0.21	0.22	0.24	0.28	46.6	2403	1.52	0.21	0.22	0.23	0.25	0.29	0.33	
	3	0.50	71.6	2402	1.52	0.21	0.22	0.23	0.25	0.29	70.0	2410	1.52	0.21	0.22	0.23	0.25	0.29	0.33	
	4	0.50	93.0	2271	1.51	0.20	0.20	0.21	0.23	0.27	92.0	2327	1.51	0.20	0.21	0.22	0.24	0.28	0.32	
	6	0.50	100.0	1791	NAV	0.14	0.15	0.15	0.17	0.21	100.0	1829	NAV	0.14	0.15	0.16	0.18	0.22	0.26	
	8	0.50	98.8	1755	NAV	0.13	0.14	0.15	0.17	0.21	98.6	1791	NAV	0.14	0.15	0.16	0.17	0.21	0.25	
	12	0.50	100.0	1651	NAV	0.12	0.13	0.14	0.16	0.20	100.0	1687	NAV	0.13	0.13	0.14	0.16	0.20	0.24	
	20	0.50	100.0	1619	NAV	0.12	0.13	0.14	0.16	0.19	100.0	1652	NAV	0.12	0.13	0.14	0.16	0.20	0.24	
	0.10	1	0.13	25.0	1560	1.97	0.18	0.19	0.20	0.22	0.26	24.7	1624	1.97	0.19	0.20	0.21	0.22	0.26	0.31
2		0.13	49.6	1509	1.97	0.18	0.18	0.19	0.21	0.25	48.3	1512	1.97	0.17	0.18	0.19	0.21	0.25	0.29	
3		0.13	74.2	1481	1.97	0.17	0.18	0.19	0.21	0.26	72.4	1502	1.97	0.17	0.18	0.19	0.21	0.25	0.30	
4		0.13	92.2	1244	1.97	0.13	0.14	0.15	0.17	0.22	91.4	1288	1.97	0.14	0.15	0.16	0.18	0.22	0.27	
6		0.13	100.0	791	NAV	0.07	0.08	0.09	0.11	0.15	100.0	834	NAV	0.07	0.08	0.09	0.11	0.16	0.20	
8		0.13	99.2	747	NAV	0.07	0.07	0.08	0.10	0.15	99.0	779	NAV	0.07	0.08	0.09	0.11	0.15	0.20	
12		0.13	100.0	622	NAV	0.05	0.06	0.07	0.09	0.13	100.0	654	NAV	0.05	0.06	0.07	0.09	0.13	0.18	
20		0.13	100.0	596	NAV	0.05	0.06	0.07	0.08	0.13	100.0	627	NAV	0.05	0.06	0.07	0.09	0.13	0.18	
0.50		1	0.015	61.5	1838	NAV	1.26	1.31	1.38	1.51	1.76	2.01	59.8	1863	NAV	1.30	1.37	1.43	1.57	1.81
	2	0.015	99.5	1117	NAV	0.62	0.68	0.74	0.87	1.12	1.37	99.0	1200	NAV	0.67	0.73	0.79	0.92	1.17	1.43
	3	0.015	100.0	567	NAV	0.29	0.35	0.42	0.54	0.79	1.03	100.0	613	NAV	0.31	0.38	0.44	0.56	0.81	1.05
	4	0.015	100.0	411	NAV	0.21	0.27	0.33	0.46	0.71	0.95	100.0	450	NAV	0.23	0.29	0.35	0.47	0.73	0.96
	6	0.015	100.0	308	NAV	0.14	0.20	0.26	0.39	0.63	0.89	100.0	337	NAV	0.16	0.22	0.28	0.41	0.66	0.90
	8	0.015	100.0	287	NAV	0.14	0.19	0.25	0.38	0.63	0.88	100.0	320	NAV	0.15	0.21	0.27	0.40	0.65	0.90
	12	0.015	100.0	246	NAV	0.10	0.16	0.22	0.35	0.59	0.86	100.0	284	NAV	0.13	0.19	0.25	0.38	0.62	0.88
	20	0.015	100.0	232	NAV	0.09	0.15	0.21	0.34	0.58	0.84	100.0	272	NAV	0.12	0.17	0.23	0.36	0.61	0.86

**Table B.28:** Precipitation triggered pollution detection probability, average detection time, contaminated area in case of detection failure and relative contaminated area to control area for various RADTi in case of  $\sigma_{lnK}^2 = 0.0$  assuming annually sampling frequency

		$\sigma_{lnK}^2$				0.00					
$\alpha_T(m)$	now	nfdS(max)	$P_d$ (12M)	$\langle T_{(DET)} \rangle$ (DAYS)	AREA ON FAILURE	(AREA ON DET.)/L	(3M. RADTi)/L	(6M. RADTi)/L	(12M. RADTi)/L	(24M. RADTi)/L	(36M. RADTi)/L
0.001	1	3.00	6.6	9488	0.36	0.30	0.30	0.30	0.31	0.32	0.23
	2	3.00	14.6	9735	0.36	0.31	0.31	0.31	0.32	0.32	0.24
	3	3.00	22.4	9719	0.36	0.31	0.31	0.31	0.32	0.32	0.27
	4	3.00	28.2	9716	0.36	0.31	0.31	0.31	0.32	0.32	0.26
	6	3.00	44.0	9759	0.36	0.31	0.31	0.31	0.32	0.32	0.25
	8	3.00	57.8	9741	0.36	0.31	0.31	0.31	0.32	0.32	0.25
	12	3.00	84.0	9750	0.35	0.31	0.31	0.31	0.32	0.32	0.25
	20	3.00	100.0	9652	NAV	0.30	0.31	0.31	0.32	0.33	0.28
0.01	1	2.25	18.1	7477	0.80	0.48	0.48	0.49	0.50	0.53	0.55
	2	2.25	35.3	7453	0.80	0.48	0.47	0.48	0.50	0.53	0.55
	3	2.25	53.4	7435	0.80	0.47	0.48	0.48	0.50	0.53	0.55
	4	2.25	72.1	7422	0.80	0.47	0.48	0.48	0.50	0.53	0.56
	6	2.25	99.7	7316	NAV	0.46	0.47	0.48	0.49	0.53	0.56
	8	2.25	96.2	7152	NAV	0.45	0.46	0.46	0.48	0.51	0.54
	12	2.25	100.0	7074	NAV	0.44	0.45	0.46	0.47	0.51	0.54
	20	2.25	100.0	7042	NAV	0.44	0.45	0.46	0.47	0.50	0.54
0.05	1	0.50	22.7	2582	1.52	0.23	0.24	0.25	0.27	0.31	0.34
	2	0.50	45.2	2513	1.52	0.23	0.23	0.24	0.26	0.30	0.34
	3	0.50	67.2	2494	1.52	0.22	0.23	0.24	0.26	0.30	0.34
	4	0.50	89.7	2426	1.51	0.21	0.22	0.23	0.25	0.29	0.33
	6	0.50	100.0	1931	NAV	0.15	0.16	0.17	0.19	0.23	0.27
	8	0.50	98.4	1887	NAV	0.15	0.16	0.17	0.18	0.22	0.27
	12	0.50	100.0	1778	NAV	0.13	0.14	0.15	0.17	0.21	0.25
	20	0.50	100.0	1742	NAV	0.13	0.14	0.15	0.17	0.21	0.25
0.10	1	0.13	23.3	1574	1.97	0.18	0.19	0.20	0.22	0.27	0.31
	2	0.13	47.0	1656	1.97	0.20	0.20	0.21	0.24	0.28	0.33
	3	0.13	69.0	1584	1.97	0.18	0.19	0.20	0.22	0.27	0.31
	4	0.13	89.4	1446	1.97	0.16	0.17	0.18	0.20	0.25	0.30
	6	0.13	99.9	945	NAV	0.09	0.09	0.11	0.13	0.17	0.22
	8	0.13	98.7	878	NAV	0.08	0.09	0.10	0.12	0.16	0.21
	12	0.13	100.0	741	NAV	0.06	0.07	0.08	0.10	0.14	0.19
	20	0.13	100.0	715	NAV	0.06	0.07	0.08	0.10	0.14	0.19
0.50	1	0.015	57.2	2063	6.79	1.50	1.50	1.57	1.70	1.93	2.18
	2	0.015	97.9	1439	NAV	0.83	0.89	0.95	1.07	1.33	1.58
	3	0.015	100.0	739	NAV	0.40	0.46	0.52	0.64	0.90	1.13
	4	0.015	100.0	561	NAV	0.31	0.37	0.43	0.55	0.80	1.03
	6	0.015	100.0	445	NAV	0.25	0.30	0.36	0.48	0.75	0.96
	8	0.015	100.0	435	NAV	0.24	0.29	0.35	0.47	0.73	0.96
	12	0.015	100.0	406	NAV	0.21	0.26	0.32	0.44	0.70	0.93
	20	0.015	100.0	395	NAV	0.18	0.23	0.29	0.42	0.68	0.92

**Table B.29:** Precipitation triggered pollution detection probability, average detection time, contaminated area in case of detection failure and relative contaminated area to control area for various RADTi in case of  $\sigma_{Ink}^2 = 1.0$  assuming daily (ED) and monthly (1M) sampling frequencies

$\sigma_{Ink}^2$		1.00																		
$\alpha_T(m)$	now	nfd <sub>s</sub> (max)	$P_d$ (ED)	$\langle T_{(DET)} \rangle$ (DAYS)	AREA ON FAILURE	(AREA ON DET.)/L	(3M. RADTi)/L	(6M. RADTi)/L	(12M. RADTi)/L	(24M. RADTi)/L	(36M. RADTi)/L	$P_d$ (1M)	$\langle T_{(DET)} \rangle$ (DAYS)	AREA ON FAILURE	(AREA ON DET.)/L	(3M. RADTi)/L	(6M. RADTi)/L	(12M. RADTi)/L	(24M. RADTi)/L	(36M. RADTi)/L
0.001	1	1.75	8.4	5827	0.61	0.22	0.23	0.23	0.24	0.25	0.26	8.2	5824	0.61	0.22	0.23	0.23	0.24	0.25	0.26
	2	1.75	18.2	5770	0.59	0.23	0.23	0.24	0.24	0.26	0.27	17.8	5805	0.59	0.23	0.23	0.24	0.24	0.26	0.27
	3	1.75	24.9	5686	0.61	0.22	0.23	0.23	0.24	0.25	0.27	24.4	5699	0.61	0.22	0.23	0.23	0.24	0.26	0.27
	4	1.75	31.4	5688	0.57	0.22	0.22	0.23	0.24	0.25	0.27	30.4	5685	0.57	0.22	0.22	0.23	0.23	0.26	0.27
	6	1.75	46.4	5614	0.59	0.21	0.22	0.22	0.23	0.25	0.27	45.2	5614	0.59	0.21	0.22	0.22	0.23	0.25	0.27
	8	1.75	56.7	5557	0.65	0.20	0.21	0.21	0.22	0.24	0.26	55.3	5585	0.65	0.21	0.21	0.22	0.22	0.24	0.26
	12	1.75	71.8	5496	0.54	0.20	0.20	0.20	0.21	0.23	0.26	70.3	5496	0.59	0.20	0.20	0.20	0.21	0.23	0.25
	20	1.75	83.0	5340	NAV	0.18	0.19	0.19	0.20	0.22	0.24	82.7	5384	NAV	0.19	0.19	0.20	0.20	0.22	0.24
	1	1.25	22.2	4430	1.32	0.32	0.33	0.34	0.36	0.39	0.43	21.9	4505	1.32	0.33	0.34	0.35	0.37	0.40	0.44
2	1.25	41.1	4237	1.26	0.31	0.32	0.33	0.35	0.39	0.43	40.5	4266	1.26	0.31	0.32	0.33	0.35	0.39	0.43	
3	1.25	55.8	4211	1.29	0.30	0.31	0.32	0.34	0.38	0.42	54.7	4263	1.29	0.31	0.32	0.33	0.35	0.38	0.43	
4	1.25	67.3	4123	1.23	0.28	0.29	0.30	0.32	0.36	0.40	66.2	4139	1.22	0.29	0.30	0.31	0.33	0.37	0.41	
6	1.25	80.7	3955	1.25	0.26	0.27	0.27	0.29	0.33	0.37	80.2	3996	1.25	0.26	0.27	0.28	0.30	0.34	0.38	
8	1.25	82.8	3848	1.29	0.24	0.24	0.25	0.27	0.31	0.35	82.3	3892	1.29	0.24	0.25	0.26	0.28	0.32	0.36	
12	1.25	90.9	3751	1.30	0.22	0.23	0.24	0.26	0.30	0.34	90.6	3793	1.29	0.23	0.24	0.25	0.27	0.31	0.35	
20	1.25	92.6	3676	1.26	0.22	0.23	0.23	0.25	0.29	0.33	92.5	3714	NAV	0.22	0.23	0.24	0.26	0.29	0.34	
0.05	1	0.13	21.3	1420	2.20	0.14	0.15	0.16	0.18	0.23	0.28	20.8	1514	2.20	0.16	0.17	0.18	0.20	0.25	0.30
	2	0.13	42.0	1401	2.21	0.13	0.13	0.14	0.16	0.20	0.25	41.0	1501	2.21	0.15	0.16	0.17	0.18	0.22	0.27
	3	0.13	58.4	1412	2.22	0.13	0.14	0.15	0.17	0.21	0.26	56.7	1510	2.24	0.14	0.15	0.16	0.18	0.23	0.28
	4	0.13	71.6	1355	2.24	0.13	0.14	0.15	0.16	0.21	0.26	70.0	1389	2.26	0.13	0.14	0.15	0.17	0.21	0.27
	6	0.13	91.0	1108	2.22	0.08	0.09	0.10	0.12	0.17	0.21	89.2	1143	2.23	0.09	0.10	0.11	0.13	0.17	0.22
	8	0.13	92.3	898	NAV	0.06	0.06	0.07	0.09	0.13	0.18	91.9	947	2.21	0.06	0.07	0.08	0.10	0.14	0.19
	12	0.13	97.1	771	NAV	0.04	0.05	0.06	0.08	0.12	0.16	97.1	807	NAV	0.05	0.05	0.06	0.08	0.12	0.17
	20	0.13	97.9	741	NAV	0.04	0.05	0.06	0.07	0.11	0.16	97.7	768	NAV	0.04	0.05	0.06	0.08	0.12	0.16
	0.10	1	0.06	28.5	1343	2.60	0.18	0.19	0.20	0.23	0.29	0.35	27.4	1459	2.60	0.20	0.21	0.23	0.26	0.31
2		0.06	56.3	1320	2.61	0.17	0.18	0.19	0.22	0.27	0.33	54.4	1328	2.61	0.17	0.18	0.19	0.22	0.27	0.33
3		0.06	76.5	1205	2.60	0.15	0.16	0.17	0.20	0.25	0.31	74.1	1259	2.61	0.15	0.16	0.18	0.20	0.26	0.32
4		0.06	88.4	1086	NAV	0.12	0.13	0.15	0.17	0.23	0.28	86.6	1190	2.71	0.14	0.15	0.16	0.19	0.25	0.30
6		0.06	98.0	720	NAV	0.06	0.07	0.08	0.10	0.16	0.22	97.8	786	2.22	0.07	0.08	0.09	0.12	0.17	0.23
8		0.06	96.2	612	NAV	0.05	0.06	0.07	0.09	0.14	0.20	95.9	651	2.48	0.05	0.06	0.07	0.09	0.15	0.20
12		0.06	99.6	521	NAV	0.04	0.05	0.06	0.08	0.13	0.18	99.3	556	NAV	0.04	0.05	0.06	0.08	0.13	0.19
20		0.06	99.8	477	NAV	0.03	0.04	0.05	0.07	0.12	0.18	99.7	511	NAV	0.04	0.05	0.06	0.08	0.13	0.18
0.50		1	0.015	90.9	1872	NAV	1.10	1.15	1.20	1.30	1.53	1.77	86.9	2006	NAV	1.19	1.25	1.30	1.43	1.65
	2	0.015	99.9	662	NAV	0.29	0.34	0.40	0.52	0.77	1.02	99.8	777	NAV	0.36	0.41	0.47	0.60	0.84	1.10
	3	0.015	100.0	424	NAV	0.17	0.21	0.27	0.39	0.64	0.89	100.0	498	NAV	0.22	0.27	0.32	0.45	0.69	0.95
	4	0.015	100.0	322	NAV	0.12	0.16	0.20	0.33	0.58	0.83	100.0	383	NAV	0.15	0.20	0.25	0.38	0.62	0.88
	6	0.015	100.0	241	NAV	0.08	0.11	0.16	0.28	0.52	0.78	100.0	289	NAV	0.10	0.14	0.19	0.32	0.56	0.82
	8	0.015	100.0	230	NAV	0.08	0.11	0.16	0.27	0.52	0.78	100.0	275	NAV	0.10	0.14	0.19	0.31	0.56	0.82
	12	0.015	100.0	188	NAV	0.06	0.09	0.13	0.25	0.49	0.75	100.0	226	NAV	0.08	0.12	0.16	0.28	0.53	0.79
	20	0.015	100.0	174	NAV	0.05	0.08	0.12	0.24	0.48	0.74	100.0	208	NAV	0.07	0.11	0.15	0.27	0.51	0.77

**Table B.30:** Precipitation triggered pollution detection probability, average detection time, contaminated area in case of detection failure and relative contaminated area to control area for various RADTi in case of  $\sigma_{lnK}^2 = 1.0$  assuming bimonthly (2M) and quarterly (3M) sampling frequencies

$\sigma_{lnK}^2$		1.00																		
$\alpha_T$ (m)	now	nfds(max)	$P_d$ (2M)	$\langle T_{(DET)} \rangle$ (DAYS)	AREA ON FAILURE	(AREA ON DET.)/L	(3M. RADTi)/L	(6M. RADTi)/L	(12M. RADTi)/L	(24M. RADTi)/L	(36M. RADTi)/L	$P_d$ (3M)	$\langle T_{(DET)} \rangle$ (DAYS)	AREA ON FAILURE	(AREA ON DET.)/L	(3M. RADTi)/L	(6M. RADTi)/L	(12M. RADTi)/L	(24M. RADTi)/L	(36M. RADTi)/L
0.001	1	1.75	8.1	5788	0.61	0.22	0.22	0.22	0.23	0.25	0.26	8.0	5800	0.61	0.22	0.22	0.23	0.24	0.25	0.26
	2	1.75	17.2	5781	0.59	0.23	0.23	0.24	0.24	0.26	0.27	17.2	5850	0.59	0.23	0.24	0.24	0.25	0.26	0.27
	3	1.75	23.8	5690	0.61	0.22	0.23	0.23	0.24	0.26	0.27	23.5	5704	0.61	0.22	0.23	0.23	0.24	0.26	0.27
	4	1.75	29.9	5725	0.57	0.22	0.22	0.23	0.24	0.26	0.28	29.7	5746	0.57	0.22	0.23	0.23	0.24	0.26	0.28
	6	1.75	44.2	5631	0.59	0.21	0.22	0.22	0.23	0.25	0.27	43.9	5685	0.59	0.22	0.22	0.23	0.23	0.25	0.27
	8	1.75	54.6	5630	0.65	0.21	0.21	0.22	0.23	0.24	0.26	54.3	5651	0.65	0.21	0.22	0.22	0.23	0.25	0.27
	12	1.75	69.8	5531	0.59	0.20	0.20	0.21	0.22	0.24	0.26	69.1	5554	0.59	0.20	0.20	0.21	0.22	0.24	0.26
	20	1.75	82.4	5411	NAV	0.19	0.19	0.20	0.21	0.23	0.25	82.1	5432	NAV	0.19	0.19	0.20	0.21	0.23	0.25
	1	1.25	21.7	4558	1.32	0.34	0.35	0.36	0.37	0.41	0.45	21.3	4577	1.32	0.34	0.35	0.36	0.37	0.41	0.45
2	1.25	40.0	4331	1.28	0.32	0.33	0.34	0.36	0.40	0.43	39.2	4351	1.26	0.33	0.33	0.34	0.36	0.40	0.44	
3	1.25	54.2	4321	1.29	0.32	0.33	0.34	0.36	0.39	0.43	53.1	4308	1.29	0.31	0.32	0.33	0.35	0.39	0.44	
4	1.25	65.3	4161	1.22	0.29	0.30	0.31	0.33	0.37	0.42	64.7	4212	1.23	0.30	0.31	0.32	0.34	0.38	0.42	
6	1.25	79.5	4042	1.31	0.27	0.27	0.28	0.30	0.34	0.38	78.9	4055	1.25	0.27	0.28	0.29	0.31	0.35	0.39	
8	1.25	81.8	3925	1.28	0.25	0.25	0.26	0.28	0.32	0.36	81.6	3963	1.29	0.25	0.26	0.27	0.29	0.33	0.37	
12	1.25	90.3	3826	1.28	0.23	0.24	0.25	0.27	0.31	0.35	90.2	3850	1.28	0.23	0.24	0.25	0.27	0.31	0.35	
20	1.25	92.3	3747	NAV	0.22	0.23	0.24	0.26	0.30	0.34	92.1	3770	NAV	0.22	0.23	0.24	0.26	0.30	0.34	
0.05	1	0.13	20.3	1503	2.21	0.15	0.16	0.17	0.19	0.24	0.30	19.9	1522	2.21	0.15	0.16	0.17	0.19	0.24	0.30
	2	0.13	40.3	1592	2.21	0.16	0.17	0.18	0.20	0.24	0.29	39.9	1592	2.21	0.16	0.17	0.17	0.19	0.23	0.28
	3	0.13	55.8	1562	2.24	0.15	0.16	0.17	0.19	0.24	0.29	54.9	1573	2.23	0.16	0.16	0.17	0.20	0.24	0.29
	4	0.13	69.1	1467	2.26	0.14	0.15	0.16	0.18	0.23	0.28	67.6	1432	2.26	0.13	0.14	0.15	0.17	0.22	0.27
	6	0.13	88.4	1186	2.21	0.10	0.11	0.11	0.13	0.18	0.23	87.9	1202	2.22	0.10	0.10	0.11	0.14	0.18	0.23
	8	0.13	91.6	978	2.21	0.06	0.07	0.08	0.10	0.14	0.19	91.4	1003	2.25	0.07	0.08	0.08	0.10	0.15	0.20
	12	0.13	97.0	834	NAV	0.05	0.06	0.06	0.08	0.12	0.17	97.0	853	NAV	0.05	0.06	0.07	0.08	0.13	0.17
	20	0.13	97.7	793	NAV	0.05	0.05	0.06	0.08	0.12	0.17	97.7	810	NAV	0.05	0.06	0.06	0.08	0.12	0.17
	0.10	1	0.06	27.0	1505	2.60	0.21	0.22	0.24	0.26	0.31	0.38	26.5	1531	2.60	0.21	0.22	0.24	0.27	0.32
2		0.06	53.4	1369	2.61	0.18	0.19	0.20	0.22	0.28	0.34	53.0	1436	2.61	0.19	0.20	0.22	0.24	0.29	0.35
3		0.06	73.0	1317	2.61	0.16	0.18	0.19	0.21	0.26	0.32	71.8	1344	2.62	0.17	0.18	0.19	0.22	0.27	0.33
4		0.06	85.7	1261	2.70	0.16	0.17	0.18	0.21	0.27	0.32	84.3	1276	2.70	0.16	0.17	0.18	0.21	0.25	0.31
6		0.06	97.4	824	2.29	0.08	0.09	0.10	0.12	0.18	0.24	97.0	844	NAV	0.08	0.09	0.10	0.12	0.18	0.24
8		0.06	95.8	698	2.48	0.06	0.07	0.08	0.10	0.15	0.21	95.6	718	NAV	0.06	0.07	0.08	0.11	0.16	0.21
12		0.06	99.3	581	NAV	0.04	0.05	0.06	0.08	0.13	0.19	99.3	597	NAV	0.05	0.05	0.06	0.09	0.14	0.20
20		0.06	99.7	529	NAV	0.04	0.05	0.06	0.08	0.13	0.18	99.6	545	NAV	0.04	0.05	0.06	0.08	0.13	0.19
0.50		1	0.015	84.6	2087	NAV	1.25	1.31	1.36	1.49	1.73	1.97	82.4	2056	NAV	1.25	1.31	1.37	1.50	1.76
	2	0.015	99.7	839	NAV	0.40	0.46	0.52	0.64	0.89	1.14	99.7	894	NAV	0.43	0.49	0.55	0.68	0.93	1.18
	3	0.015	100.0	541	NAV	0.24	0.29	0.35	0.48	0.72	0.98	100.0	573	NAV	0.27	0.32	0.38	0.50	0.75	1.00
	4	0.015	100.0	417	NAV	0.17	0.22	0.27	0.40	0.65	0.90	100.0	445	NAV	0.19	0.24	0.30	0.42	0.67	0.93
	6	0.015	100.0	316	NAV	0.12	0.16	0.21	0.34	0.58	0.84	100.0	338	NAV	0.13	0.18	0.23	0.36	0.60	0.86
	8	0.015	100.0	302	NAV	0.12	0.16	0.21	0.33	0.58	0.84	100.0	322	NAV	0.13	0.17	0.23	0.35	0.59	0.85
	12	0.015	100.0	249	NAV	0.09	0.13	0.18	0.30	0.55	0.81	100.0	269	NAV	0.10	0.14	0.19	0.32	0.56	0.82
	20	0.015	100.0	230	NAV	0.08	0.12	0.16	0.29	0.53	0.79	100.0	248	NAV	0.09	0.13	0.18	0.30	0.54	0.80

**Table B.31:** Precipitation triggered pollution detection probability, average detection time, contaminated area in case of detection failure and relative contaminated area to control area for various RADTi in case of  $\sigma_{lnK}^2 = 1.0$  assuming every 4 months (4M) and biannually (6M) sampling frequencies

$\sigma_{lnK}^2$		1.00																		
$\alpha_T(m)$	now	nfd(s(max)	Pd (4M)	$\langle T_{(DET)} \rangle$ (DAYS)	AREA ON FAILURE	(AREA ON DET.)/L	(3M. RADTi)/L	(6M. RADTi)/L	(12M. RADTi)/L	(24M. RADTi)/L	(36M. RADTi)/L	Pd (6M)	$\langle T_{(DET)} \rangle$ (DAYS)	AREA ON FAILURE	(AREA ON DET.)/L	(3M. RADTi)/L	(6M. RADTi)/L	(12M. RADTi)/L	(24M. RADTi)/L	(36M. RADTi)/L
0.001	1	1.75	8.0	5845	0.61	0.22	0.23	0.23	0.24	0.25	0.27	7.8	5808	0.61	0.22	0.23	0.23	0.24	0.25	0.27
	2	1.75	16.8	5805	0.59	0.23	0.24	0.24	0.25	0.27	0.28	16.7	5883	0.59	0.24	0.24	0.24	0.25	0.27	0.28
	3	1.75	23.5	5726	0.61	0.22	0.23	0.23	0.24	0.26	0.28	22.9	5749	0.61	0.23	0.23	0.23	0.24	0.26	0.28
	4	1.75	29.4	5762	0.57	0.22	0.23	0.23	0.24	0.26	0.28	28.8	5794	0.57	0.23	0.23	0.23	0.24	0.27	0.28
	6	1.75	43.6	5702	0.59	0.22	0.22	0.23	0.24	0.26	0.27	42.8	5719	0.59	0.22	0.23	0.23	0.24	0.26	0.28
	8	1.75	53.6	5667	0.65	0.21	0.22	0.22	0.23	0.25	0.27	53.0	5691	0.65	0.21	0.22	0.22	0.23	0.25	0.27
	12	1.75	68.9	5577	0.59	0.20	0.20	0.21	0.22	0.24	0.26	68.4	5626	0.59	0.21	0.21	0.21	0.22	0.24	0.26
	20	1.75	82.0	5446	NAV	0.19	0.20	0.20	0.21	0.23	0.25	81.6	5472	NAV	0.19	0.20	0.20	0.21	0.23	0.25
	0.01	1	1.25	21.3	4591	1.32	0.34	0.35	0.36	0.38	0.42	0.45	20.8	4580	1.32	0.34	0.35	0.36	0.38	0.42
2		1.25	39.0	4369	1.28	0.32	0.33	0.34	0.36	0.39	0.44	38.4	4421	1.28	0.33	0.34	0.35	0.37	0.41	0.44
3		1.25	52.6	4325	1.29	0.32	0.33	0.34	0.36	0.40	0.44	51.6	4355	1.29	0.32	0.33	0.34	0.36	0.40	0.45
4		1.25	64.5	4247	1.23	0.30	0.31	0.32	0.34	0.38	0.43	63.6	4280	1.23	0.31	0.32	0.33	0.35	0.39	0.43
6		1.25	78.5	4106	1.31	0.27	0.28	0.29	0.31	0.35	0.39	77.8	4134	1.31	0.28	0.29	0.30	0.32	0.36	0.40
8		1.25	81.2	3975	1.28	0.25	0.26	0.27	0.29	0.33	0.37	81.1	4036	1.28	0.26	0.27	0.28	0.30	0.34	0.38
12		1.25	90.1	3882	1.28	0.24	0.25	0.26	0.28	0.32	0.36	89.9	3914	1.27	0.24	0.25	0.26	0.28	0.32	0.36
20		1.25	92.1	3803	NAV	0.23	0.24	0.25	0.27	0.30	0.35	91.9	3835	NAV	0.23	0.24	0.25	0.27	0.31	0.35
0.05		1	0.13	19.9	1608	2.21	0.17	0.18	0.19	0.21	0.26	0.31	19.4	1535	2.20	0.15	0.16	0.17	0.19	0.24
	2	0.13	39.6	1609	2.21	0.16	0.17	0.18	0.20	0.25	0.30	38.9	1669	2.21	0.17	0.18	0.19	0.21	0.26	0.30
	3	0.13	54.6	1614	2.23	0.16	0.17	0.18	0.20	0.25	0.30	53.6	1644	2.23	0.16	0.17	0.18	0.20	0.25	0.30
	4	0.13	67.4	1479	2.26	0.14	0.15	0.16	0.18	0.23	0.28	66.2	1546	2.25	0.15	0.16	0.17	0.19	0.24	0.28
	6	0.13	88.0	1265	2.20	0.11	0.12	0.13	0.15	0.19	0.24	86.6	1277	2.23	0.11	0.12	0.12	0.15	0.19	0.24
	8	0.13	91.3	1031	2.21	0.07	0.08	0.09	0.11	0.15	0.20	90.9	1077	2.24	0.08	0.09	0.10	0.12	0.16	0.21
	12	0.13	97.0	878	NAV	0.05	0.06	0.07	0.09	0.13	0.18	96.8	907	NAV	0.05	0.06	0.07	0.09	0.13	0.18
	20	0.13	97.7	829	NAV	0.05	0.06	0.07	0.08	0.13	0.17	97.5	850	NAV	0.05	0.06	0.07	0.08	0.13	0.17
	0.10	1	0.06	26.1	1546	2.60	0.22	0.24	0.25	0.27	0.33	0.39	25.6	1552	2.60	0.22	0.23	0.24	0.27	0.33
2		0.06	52.6	1504	2.61	0.20	0.21	0.23	0.25	0.30	0.36	50.8	1420	2.62	0.18	0.19	0.20	0.23	0.29	0.35
3		0.06	71.3	1372	2.62	0.17	0.19	0.20	0.22	0.27	0.34	70.0	1390	2.61	0.17	0.19	0.20	0.23	0.28	0.35
4		0.06	83.8	1283	2.68	0.16	0.17	0.18	0.20	0.26	0.32	82.6	1345	2.68	0.17	0.18	0.19	0.22	0.27	0.33
6		0.06	97.0	894	2.51	0.09	0.10	0.11	0.13	0.19	0.25	96.4	930	2.51	0.09	0.10	0.11	0.14	0.19	0.25
8		0.06	95.4	733	2.54	0.06	0.07	0.08	0.11	0.16	0.22	95.3	756	2.54	0.07	0.08	0.09	0.11	0.16	0.22
12		0.06	99.2	616	NAV	0.05	0.06	0.07	0.09	0.14	0.20	99.2	655	NAV	0.05	0.06	0.07	0.10	0.15	0.21
20		0.06	99.7	565	NAV	0.04	0.05	0.06	0.08	0.13	0.19	99.6	600	NAV	0.05	0.05	0.06	0.09	0.14	0.20
0.50		1	0.015	81.4	2147	NAV	1.33	1.39	1.45	1.58	1.82	2.06	78.8	2138	NAV	1.35	1.42	1.47	1.60	1.83
	2	0.015	99.5	941	NAV	0.46	0.52	0.58	0.71	0.95	1.21	99.6	1018	NAV	0.51	0.57	0.63	0.75	1.00	1.26
	3	0.015	99.9	597	NAV	0.28	0.33	0.39	0.52	0.77	1.02	99.9	647	NAV	0.31	0.36	0.42	0.55	0.80	1.05
	4	0.015	100.0	467	NAV	0.20	0.25	0.31	0.43	0.68	0.94	100.0	511	NAV	0.23	0.28	0.34	0.47	0.72	0.97
	6	0.015	100.0	357	NAV	0.14	0.19	0.24	0.37	0.61	0.87	100.0	393	NAV	0.16	0.21	0.27	0.39	0.64	0.90
	8	0.015	100.0	343	NAV	0.14	0.18	0.24	0.36	0.61	0.87	100.0	381	NAV	0.16	0.21	0.26	0.39	0.63	0.89
	12	0.015	100.0	286	NAV	0.11	0.15	0.21	0.33	0.57	0.83	100.0	326	NAV	0.13	0.18	0.23	0.36	0.60	0.86
	20	0.015	100.0	268	NAV	0.10	0.14	0.19	0.31	0.56	0.82	100.0	307	NAV	0.11	0.16	0.21	0.34	0.58	0.84

**Table B.32:** Precipitation triggered pollution detection probability, average detection time, contaminated area in case of detection failure and relative contaminated area to control area for various RADTi in case of  $\sigma_{\ln K}^2 = 1.0$  assuming annually sampling frequency

		$\sigma_{\ln K}^2$				1.00					
$\alpha_T(m)$	now	nfdS(max)	$P_d$ (12M)	$\langle T_{(DET)} \rangle$ (DAYS)	AREA ON FAILURE	(AREA ON DET.)/L	(3M. RADTi)/L	(6M. RADTi)/L	(12M. RADTi)/L	(24M. RADTi)/L	(36M. RADTi)/L
0.001	1	1.75	7.8	5968	0.61	0.23	0.23	0.24	0.25	0.26	0.28
	2	1.75	16.3	6003	0.59	0.24	0.24	0.25	0.26	0.27	0.28
	3	1.75	22.2	5823	0.61	0.23	0.23	0.24	0.25	0.26	0.28
	4	1.75	28.3	5927	0.57	0.23	0.24	0.24	0.25	0.27	0.29
	6	1.75	41.8	5840	0.59	0.23	0.23	0.23	0.25	0.26	0.28
	8	1.75	51.9	5806	0.64	0.22	0.22	0.23	0.24	0.26	0.28
	12	1.75	67.6	5748	0.58	0.21	0.21	0.22	0.23	0.25	0.27
	20	1.75	81.0	5550	NAV	0.20	0.20	0.21	0.22	0.24	0.26
0.01	1	1.25	20.1	4720	1.32	0.35	0.36	0.37	0.39	0.43	0.47
	2	1.25	36.6	4451	1.29	0.33	0.34	0.35	0.37	0.41	0.45
	3	1.25	50.3	4502	1.29	0.34	0.34	0.35	0.37	0.41	0.45
	4	1.25	62.6	4400	1.29	0.32	0.33	0.34	0.36	0.40	0.44
	6	1.25	76.9	4256	1.35	0.29	0.30	0.31	0.33	0.37	0.42
	8	1.25	80.4	4130	1.29	0.27	0.27	0.28	0.30	0.34	0.39
	12	1.25	89.3	4022	1.28	0.25	0.26	0.27	0.29	0.33	0.38
	20	1.25	91.7	3934	1.32	0.24	0.25	0.26	0.28	0.32	0.36
0.05	1	0.13	18.5	1616	2.21	0.16	0.17	0.18	0.21	0.26	0.31
	2	0.13	37.6	1710	2.21	0.17	0.18	0.19	0.21	0.26	0.31
	3	0.13	51.1	1695	2.23	0.17	0.17	0.19	0.21	0.26	0.31
	4	0.13	63.5	1628	2.25	0.16	0.17	0.18	0.20	0.24	0.29
	6	0.13	85.5	1412	2.22	0.12	0.13	0.14	0.16	0.21	0.26
	8	0.13	90.3	1193	2.24	0.09	0.10	0.11	0.13	0.18	0.23
	12	0.13	96.8	1008	NAV	0.07	0.07	0.08	0.10	0.15	0.19
	20	0.13	97.6	951	NAV	0.06	0.07	0.08	0.10	0.14	0.19
0.10	1	0.06	24.3	1718	2.60	0.26	0.26	0.27	0.30	0.36	0.43
	2	0.06	49.2	1550	2.62	0.20	0.20	0.21	0.24	0.30	0.36
	3	0.06	67.6	1586	2.60	0.22	0.23	0.24	0.27	0.32	0.39
	4	0.06	79.9	1397	2.68	0.17	0.18	0.19	0.22	0.28	0.34
	6	0.06	95.9	1064	2.43	0.11	0.12	0.13	0.16	0.22	0.28
	8	0.06	94.7	846	2.55	0.07	0.08	0.09	0.12	0.17	0.23
	12	0.06	99.0	747	NAV	0.06	0.07	0.08	0.11	0.16	0.22
	20	0.06	99.4	701	NAV	0.06	0.07	0.08	0.10	0.15	0.21
0.50	1	0.015	75.3	2321	NAV	1.46	1.50	1.57	1.70	1.94	2.19
	2	0.015	99.0	1203	NAV	0.62	0.67	0.74	0.86	1.11	1.36
	3	0.015	99.9	775	NAV	0.39	0.45	0.51	0.64	0.89	1.13
	4	0.015	100.0	625	NAV	0.29	0.35	0.41	0.54	0.79	1.03
	6	0.015	100.0	502	NAV	0.21	0.27	0.33	0.46	0.71	0.95
	8	0.015	100.0	501	NAV	0.21	0.27	0.33	0.46	0.70	0.95
	12	0.015	100.0	453	NAV	0.18	0.23	0.29	0.42	0.67	0.92
	20	0.015	100.0	433	NAV	0.16	0.21	0.28	0.41	0.65	0.90

**Table B.33:** Precipitation triggered pollution detection probability, average detection time, contaminated area in case of detection failure and relative contaminated area to control area for various RADTi in case of  $\sigma_{lnK}^2 = 2.0$  assuming daily (ED) and monthly (1M) sampling frequencies

$\sigma_{lnK}^2$		2.00																		
$\alpha_r(m)$	now	infds(max)	$P_d$ (ED)	$\langle T_{(DET)} \rangle$ (DAYS)	AREA ON FAILURE	(AREA ON DET.)/L	(3M. RADTi)/L	(6M. RADTi)/L	(12M. RADTi)/L	(24M. RADTi)/L	(36M. RADTi)/L	$P_d$ (1M)	$\langle T_{(DET)} \rangle$ (DAYS)	AREA ON FAILURE	(AREA ON DET.)/L	(3M. RADTi)/L	(6M. RADTi)/L	(12M. RADTi)/L	(24M. RADTi)/L	(36M. RADTi)/L
0.001	1	0.75	6.6	3315	1.50	0.12	0.12	0.13	0.14	0.16	0.17	6.6	3225	1.49	0.11	0.12	0.12	0.13	0.15	0.18
	2	0.75	16.5	3220	1.47	0.11	0.11	0.12	0.13	0.15	0.17	16.1	3229	1.46	0.11	0.11	0.12	0.13	0.15	0.17
	3	0.75	18.6	3293	1.53	0.13	0.14	0.15	0.17	0.22	0.26	18.0	3279	1.55	0.11	0.12	0.12	0.13	0.15	0.17
	4	0.75	23.8	3113	1.35	0.11	0.11	0.12	0.13	0.15	0.17	23.3	3100	1.35	0.11	0.11	0.12	0.13	0.15	0.17
	6	0.75	39.0	3185	1.56	0.10	0.11	0.11	0.12	0.14	0.16	37.9	3162	1.55	0.10	0.11	0.11	0.12	0.14	0.16
	8	0.75	44.7	3197	1.54	0.11	0.12	0.13	0.14	0.17	0.21	42.9	3175	1.55	0.10	0.11	0.11	0.12	0.14	0.16
	12	0.75	61.5	3025	1.56	0.09	0.09	0.10	0.11	0.13	0.15	60.0	3065	1.55	0.09	0.10	0.10	0.11	0.13	0.16
	20	0.75	76.9	2956	1.61	0.08	0.09	0.09	0.10	0.12	0.15	75.8	2981	1.62	0.08	0.09	0.09	0.10	0.12	0.14
0.01	1	0.50	16.2	2820	2.31	0.18	0.19	0.20	0.22	0.26	0.31	15.8	2952	2.31	0.20	0.21	0.22	0.23	0.28	0.32
	2	0.50	29.1	2460	2.36	0.16	0.17	0.18	0.20	0.25	0.29	28.3	2493	2.35	0.17	0.17	0.18	0.20	0.25	0.29
	3	0.50	43.5	2598	2.29	0.16	0.17	0.18	0.20	0.24	0.29	42.5	2701	2.27	0.19	0.20	0.21	0.23	0.27	0.32
	4	0.50	50.6	2475	2.12	0.15	0.16	0.17	0.19	0.22	0.27	49.3	2570	2.11	0.17	0.17	0.18	0.20	0.24	0.28
	6	0.50	65.3	2327	2.64	0.13	0.14	0.14	0.16	0.20	0.24	64.1	2386	2.60	0.13	0.14	0.15	0.17	0.21	0.25
	8	0.50	74.8	2240	2.11	0.11	0.11	0.12	0.14	0.18	0.22	73.8	2324	2.13	0.12	0.13	0.14	0.16	0.20	0.24
	12	0.50	84.9	2136	2.30	0.10	0.10	0.11	0.13	0.17	0.21	83.9	2172	2.31	0.10	0.11	0.12	0.13	0.17	0.21
	20	0.50	87.9	2063	2.26	0.08	0.09	0.10	0.11	0.15	0.19	87.7	2102	2.26	0.09	0.09	0.10	0.12	0.15	0.19
0.05	1	0.13	21.8	1652	3.03	0.16	0.17	0.18	0.21	0.26	0.33	21.1	1759	3.03	0.17	0.18	0.20	0.22	0.28	0.32
	2	0.13	45.1	1514	3.05	0.16	0.17	0.18	0.20	0.25	0.31	43.7	1655	3.06	0.18	0.19	0.20	0.22	0.28	0.34
	3	0.13	61.3	1461	3.02	0.14	0.15	0.16	0.19	0.24	0.30	59.7	1563	3.02	0.16	0.17	0.18	0.21	0.25	0.30
	4	0.13	72.4	1442	3.00	0.13	0.14	0.16	0.18	0.24	0.30	70.8	1535	2.99	0.18	0.19	0.17	0.20	0.25	0.31
	6	0.13	88.5	1199	3.32	0.09	0.10	0.11	0.13	0.18	0.24	87.2	1281	3.26	0.10	0.11	0.12	0.14	0.19	0.25
	8	0.13	90.7	1053	3.73	0.06	0.07	0.08	0.10	0.15	0.21	90.3	1138	3.70	0.08	0.09	0.09	0.12	0.17	0.22
	12	0.13	95.9	933	3.03	0.05	0.06	0.07	0.09	0.14	0.19	95.8	976	3.04	0.06	0.06	0.07	0.09	0.14	0.20
	20	0.13	97.3	881	0.00	0.05	0.05	0.06	0.08	0.13	0.18	97.0	910	0.00	0.05	0.06	0.06	0.09	0.13	0.19
0.10	1	0.06	29.9	1672	3.26	0.24	0.25	0.27	0.30	0.36	0.43	28.5	1706	3.25	0.25	0.26	0.28	0.32	0.37	0.45
	2	0.06	60.4	1484	3.46	0.19	0.21	0.22	0.25	0.31	0.38	57.9	1499	3.44	0.20	0.21	0.22	0.25	0.31	0.37
	3	0.06	78.5	1316	3.44	0.16	0.18	0.19	0.22	0.28	0.35	76.2	1407	3.42	0.19	0.20	0.21	0.24	0.30	0.38
	4	0.06	88.0	1104	3.50	0.12	0.13	0.14	0.17	0.23	0.30	86.7	1236	3.51	0.15	0.16	0.17	0.20	0.26	0.33
	6	0.06	96.7	853	NAV	0.07	0.08	0.10	0.12	0.18	0.25	95.9	920	NAV	0.08	0.09	0.11	0.13	0.19	0.26
	8	0.06	95.0	696	NAV	0.05	0.06	0.07	0.10	0.15	0.22	94.9	762	NAV	0.06	0.07	0.08	0.11	0.17	0.24
	12	0.06	98.9	620	NAV	0.05	0.05	0.06	0.09	0.14	0.21	98.6	654	NAV	0.05	0.06	0.07	0.09	0.15	0.21
	20	0.06	99.3	565	NAV	0.04	0.05	0.06	0.08	0.13	0.19	99.2	607	NAV	0.04	0.05	0.06	0.08	0.14	0.20
0.50	1	0.015	92.5	1750	NAV	0.99	1.05	1.11	1.24	1.49	1.75	89.7	1986	NAV	1.16	1.19	1.26	1.40	1.66	1.93
	2	0.015	100.0	704	NAV	0.31	0.36	0.42	0.55	0.80	1.06	99.8	804	NAV	0.37	0.43	0.48	0.62	0.87	1.13
	3	0.015	100.0	469	NAV	0.17	0.21	0.26	0.39	0.65	0.91	100.0	552	NAV	0.22	0.26	0.32	0.46	0.71	0.97
	4	0.015	100.0	361	NAV	0.12	0.15	0.20	0.33	0.58	0.84	100.0	423	NAV	0.15	0.19	0.24	0.38	0.63	0.89
	6	0.015	100.0	286	NAV	0.09	0.12	0.16	0.28	0.54	0.80	100.0	339	NAV	0.11	0.15	0.19	0.33	0.58	0.84
	8	0.015	100.0	273	NAV	0.08	0.12	0.16	0.28	0.53	0.79	100.0	322	NAV	0.11	0.14	0.19	0.32	0.57	0.83
	12	0.015	100.0	221	NAV	0.06	0.09	0.13	0.24	0.50	0.76	100.0	263	NAV	0.08	0.11	0.16	0.28	0.54	0.80
	20	0.015	100.0	203	NAV	0.06	0.09	0.12	0.23	0.49	0.75	100.0	243	NAV	0.07	0.11	0.15	0.27	0.52	0.78

**Table B.34:** Precipitation triggered pollution detection probability, average detection time, contaminated area in case of detection failure and relative contaminated area to control area for various RADTi in case of  $\sigma_{lnK}^2 = 2.0$  assuming bimonthly (2M) and quarterly (3M) sampling frequencies

$\sigma_{lnK}^2$		2.00																		
$\alpha_{tr}(m)$	row	nfds(max)	$P_d$ (2M)	$\langle T_{(DET)} \rangle$ (DAYS)	AREA ON FAILURE	(AREA ON DET.)/L	(3M. RADTi)/L	(6M. RADTi)/L	(12M. RADTi)/L	(24M. RADTi)/L	(36M. RADTi)/L	$P_d$ (3M)	$\langle T_{(DET)} \rangle$ (DAYS)	AREA ON FAILURE	(AREA ON DET.)/L	(3M. RADTi)/L	(6M. RADTi)/L	(12M. RADTi)/L	(24M. RADTi)/L	(36M. RADTi)/L
0.001	1	0.75	6.5	3334	1.50	0.12	0.12	0.13	0.14	0.16	0.18	6.3	3171	1.49	0.11	0.11	0.12	0.13	0.15	0.17
	2	0.75	16.0	3331	1.48	0.12	0.12	0.12	0.14	0.16	0.18	15.7	3376	1.46	0.12	0.12	0.13	0.14	0.16	0.18
	3	0.75	17.8	3343	1.55	0.12	0.12	0.13	0.14	0.16	0.18	17.3	3298	1.55	0.11	0.12	0.12	0.13	0.15	0.17
	4	0.75	22.9	3121	1.34	0.11	0.12	0.12	0.13	0.15	0.18	22.6	3105	1.34	0.11	0.11	0.12	0.13	0.15	0.17
	6	0.75	37.7	3219	1.57	0.10	0.11	0.11	0.12	0.14	0.17	37.0	3232	1.54	0.11	0.11	0.12	0.13	0.15	0.17
	8	0.75	42.3	3178	1.55	0.10	0.11	0.11	0.12	0.14	0.16	41.6	3168	1.53	0.10	0.11	0.11	0.12	0.14	0.16
	12	0.75	59.2	3086	1.54	0.00	0.10	0.10	0.11	0.13	0.16	58.3	3078	1.53	0.09	0.10	0.10	0.11	0.13	0.15
	20	0.75	75.4	3011	1.58	0.00	0.09	0.09	0.10	0.12	0.15	74.9	3008	1.56	0.09	0.09	0.09	0.10	0.12	0.15
	0.01	1	0.50	15.5	2997	2.31	0.20	0.21	0.22	0.23	0.28	0.32	15.3	3019	2.31	0.20	0.21	0.22	0.24	0.28
2		0.50	27.9	2578	2.35	0.18	0.19	0.20	0.22	0.27	0.31	27.4	2610	2.35	0.19	0.20	0.21	0.23	0.27	0.31
3		0.50	41.6	2717	2.27	0.19	0.20	0.21	0.23	0.27	0.32	41.3	2713	2.29	0.17	0.18	0.19	0.21	0.25	0.30
4		0.50	48.4	2591	2.14	0.00	0.18	0.19	0.21	0.24	0.28	48.0	2608	2.10	0.17	0.18	0.19	0.21	0.25	0.30
6		0.50	63.4	2462	2.59	0.00	0.16	0.17	0.18	0.22	0.26	62.9	2488	2.57	0.15	0.16	0.17	0.19	0.22	0.26
8		0.50	73.1	2342	2.22	0.00	0.13	0.14	0.16	0.20	0.24	72.6	2379	2.30	0.13	0.13	0.14	0.16	0.20	0.24
12		0.50	83.4	2197	2.42	0.00	0.11	0.12	0.14	0.17	0.21	83.1	2224	2.28	0.11	0.11	0.12	0.14	0.18	0.22
20		0.50	87.6	2124	2.32	0.00	0.10	0.10	0.12	0.16	0.20	87.6	2145	2.25	0.09	0.10	0.10	0.12	0.16	0.20
0.05		1	0.13	20.5	1747	3.03	0.16	0.18	0.19	0.20	0.26	0.32	20.3	1793	3.04	0.17	0.18	0.19	0.21	0.26
	2	0.13	42.7	1689	3.08	0.18	0.19	0.20	0.23	0.28	0.34	42.2	1782	3.08	0.21	0.22	0.23	0.26	0.29	0.35
	3	0.13	58.8	1606	3.01	0.16	0.18	0.19	0.21	0.25	0.31	57.9	1604	3.02	0.16	0.17	0.18	0.20	0.25	0.31
	4	0.13	70.2	1608	2.97	0.20	0.22	0.20	0.21	0.27	0.33	69.0	1617	3.04	0.16	0.18	0.19	0.21	0.27	0.33
	6	0.13	86.3	1307	3.24	0.00	0.11	0.12	0.14	0.20	0.25	85.9	1357	3.22	0.11	0.12	0.13	0.15	0.20	0.26
	8	0.13	89.7	1173	3.64	0.00	0.09	0.10	0.12	0.17	0.22	89.6	1219	3.62	0.09	0.10	0.11	0.13	0.18	0.24
	12	0.13	95.7	1007	2.99	0.00	0.07	0.08	0.10	0.15	0.20	95.4	1012	3.15	0.06	0.07	0.07	0.10	0.15	0.20
	20	0.13	97.0	938	0.00	0.00	0.06	0.07	0.09	0.14	0.19	96.8	957	0.00	0.05	0.06	0.07	0.09	0.14	0.19
	0.10	1	0.06	28.0	1781	3.25	0.26	0.28	0.29	0.32	0.38	0.47	27.3	1760	3.26	0.24	0.25	0.27	0.30	0.36
2		0.06	56.6	1534	3.44	0.20	0.21	0.22	0.25	0.32	0.38	55.4	1533	3.45	0.20	0.21	0.22	0.26	0.32	0.38
3		0.06	74.9	1454	3.38	0.20	0.21	0.22	0.25	0.31	0.39	73.8	1465	3.43	0.19	0.21	0.22	0.25	0.31	0.38
4		0.06	85.4	1267	3.52	0.00	0.16	0.17	0.20	0.27	0.33	85.3	1335	3.47	0.16	0.17	0.19	0.22	0.28	0.35
6		0.06	95.6	981	NAV	0.00	0.11	0.12	0.14	0.20	0.27	95.3	1014	NAV	0.10	0.11	0.12	0.15	0.21	0.28
8		0.06	94.6	791	NAV	0.00	0.07	0.08	0.11	0.17	0.24	94.5	825	NAV	0.07	0.08	0.09	0.12	0.18	0.25
12		0.06	98.5	681	NAV	0.00	0.06	0.07	0.09	0.15	0.22	98.4	697	NAV	0.05	0.06	0.07	0.09	0.15	0.22
20		0.06	99.1	622	NAV	0.00	0.05	0.06	0.08	0.14	0.21	99.1	650	NAV	0.05	0.06	0.07	0.09	0.15	0.21
0.50		1	0.015	87.9	2078	NAV	1.27	1.34	1.40	1.52	1.79	2.03	86.0	2099	NAV	1.23	1.29	1.36	1.49	1.75
	2	0.015	99.6	879	NAV	0.00	0.48	0.54	0.67	0.93	1.19	99.6	939	NAV	0.46	0.52	0.58	0.72	0.97	1.23
	3	0.015	100.0	594	NAV	0.24	0.29	0.35	0.49	0.74	1.01	100.0	627	NAV	0.26	0.32	0.38	0.51	0.77	1.03
	4	0.015	100.0	458	NAV	0.17	0.21	0.27	0.40	0.65	0.92	100.0	490	NAV	0.19	0.24	0.29	0.43	0.68	0.95
	6	0.015	100.0	369	NAV	0.12	0.16	0.21	0.35	0.60	0.87	100.0	393	NAV	0.14	0.18	0.23	0.37	0.62	0.89
	8	0.015	100.0	348	NAV	0.12	0.16	0.21	0.34	0.59	0.85	100.0	376	NAV	0.13	0.18	0.23	0.36	0.61	0.88
	12	0.015	100.0	289	NAV	0.09	0.13	0.17	0.30	0.56	0.82	100.0	309	NAV	0.10	0.14	0.19	0.32	0.57	0.84
	20	0.015	100.0	266	NAV	0.08	0.12	0.16	0.29	0.54	0.81	100.0	288	NAV	0.09	0.13	0.18	0.30	0.56	0.82

**Table B.35:** Precipitation triggered pollution detection probability, average detection time, contaminated area in case of detection failure and relative contaminated area to control area for various RADTi in case of  $\sigma_{\ln K}^2 = 2.0$  assuming every 4 months (4M) and biannually (6M) sampling frequencies

$\sigma_{\ln K}^2$		2.00																		
$\alpha_{T_i}(m)$	now	nfds(max)	$P_d$ (4M)	$\langle T_{(DET)} \rangle$ (DAYS)	AREA ON FAILURE	(AREA ON DET.)/L	(3M. RADTi)/L	(6M. RADTi)/L	(12M. RADTi)/L	(24M. RADTi)/L	(36M. RADTi)/L	$P_d$ (6M)	$\langle T_{(DET)} \rangle$ (DAYS)	AREA ON FAILURE	(AREA ON DET.)/L	(3M. RADTi)/L	(6M. RADTi)/L	(12M. RADTi)/L	(24M. RADTi)/L	(36M. RADTi)/L
0.001	1	0.75	6.3	3334	1.49	0.12	0.12	0.13	0.14	0.16	0.18	6.2	3325	1.49	0.12	0.12	0.13	0.14	0.16	0.18
	2	0.75	15.5	3337	1.48	0.12	0.12	0.13	0.14	0.16	0.18	15.2	3430	1.48	0.12	0.12	0.13	0.14	0.16	0.18
	3	0.75	17.4	3389	1.55	0.12	0.13	0.13	0.14	0.16	0.18	17.0	3413	1.54	0.12	0.13	0.13	0.14	0.16	0.18
	4	0.75	22.7	3171	1.34	0.11	0.12	0.12	0.13	0.16	0.18	22.1	3178	1.36	0.11	0.12	0.12	0.13	0.16	0.18
	6	0.75	36.9	3229	1.56	0.11	0.11	0.12	0.13	0.15	0.17	36.2	3307	1.56	0.11	0.12	0.12	0.13	0.15	0.17
	8	0.75	41.5	3227	1.54	0.10	0.11	0.11	0.12	0.14	0.17	41.0	3217	1.53	0.10	0.11	0.11	0.12	0.14	0.17
	12	0.75	58.4	3139	1.53	0.10	0.10	0.11	0.12	0.14	0.16	57.7	3157	1.54	0.10	0.10	0.11	0.12	0.14	0.16
	20	0.75	74.7	3036	1.55	0.09	0.09	0.10	0.11	0.13	0.15	74.5	3072	1.54	0.10	0.11	0.11	0.11	0.13	0.15
	0.01	1	0.50	14.9	2992	2.30	0.19	0.20	0.21	0.23	0.27	0.32	14.9	3076	2.31	0.21	0.22	0.23	0.25	0.28
2		0.50	27.3	2645	2.35	0.19	0.20	0.21	0.23	0.27	0.31	26.6	2708	2.34	0.20	0.21	0.22	0.24	0.28	0.32
3		0.50	40.6	2747	2.28	0.18	0.19	0.20	0.22	0.26	0.30	40.0	2759	2.28	0.18	0.19	0.20	0.22	0.26	0.30
4		0.50	47.0	2629	2.14	0.17	0.18	0.19	0.21	0.25	0.29	46.7	2675	2.20	0.18	0.19	0.20	0.22	0.26	0.30
6		0.50	62.2	2515	2.56	0.15	0.16	0.17	0.19	0.23	0.27	61.5	2552	2.56	0.16	0.17	0.18	0.20	0.24	0.28
8		0.50	72.3	2424	2.20	0.13	0.14	0.15	0.17	0.21	0.25	71.8	2457	2.35	0.13	0.14	0.15	0.17	0.21	0.25
12		0.50	83.0	2266	2.40	0.11	0.12	0.13	0.14	0.18	0.22	82.7	2296	2.39	0.11	0.12	0.13	0.15	0.19	0.23
20		0.50	87.4	2155	2.29	0.09	0.10	0.11	0.12	0.16	0.20	87.3	2186	2.30	0.09	0.10	0.11	0.13	0.16	0.21
0.05		1	0.13	19.7	1768	3.03	0.17	0.18	0.19	0.22	0.28	0.34	19.4	1868	3.03	0.18	0.19	0.21	0.23	0.28
	2	0.13	41.2	1715	3.07	0.18	0.19	0.20	0.23	0.27	0.33	40.8	1779	3.07	0.21	0.22	0.23	0.25	0.29	0.35
	3	0.13	57.3	1662	3.00	0.18	0.19	0.20	0.23	0.27	0.34	56.5	1705	3.01	0.18	0.19	0.20	0.22	0.27	0.33
	4	0.13	68.7	1657	3.07	0.17	0.18	0.19	0.22	0.27	0.33	67.9	1734	3.02	0.20	0.22	0.23	0.24	0.29	0.36
	6	0.13	85.3	1373	3.27	0.11	0.12	0.13	0.15	0.20	0.26	84.1	1390	3.28	0.11	0.12	0.14	0.16	0.20	0.26
	8	0.13	88.9	1213	3.57	0.08	0.09	0.10	0.13	0.18	0.24	88.7	1282	3.55	0.10	0.11	0.12	0.14	0.19	0.25
	12	0.13	95.4	1045	3.09	0.06	0.07	0.08	0.10	0.15	0.21	95.3	1073	3.14	0.06	0.07	0.08	0.11	0.16	0.21
	20	0.13	96.7	981	0.00	0.06	0.06	0.07	0.09	0.14	0.20	96.6	1007	0.00	0.06	0.07	0.08	0.10	0.15	0.20
	0.10	1	0.06	27.3	1875	3.25	0.29	0.30	0.31	0.35	0.41	0.49	26.0	1832	3.26	0.25	0.26	0.27	0.30	0.36
2		0.06	54.9	1554	3.47	0.20	0.21	0.22	0.26	0.32	0.39	54.0	1584	3.45	0.20	0.22	0.23	0.26	0.32	0.38
3		0.06	73.6	1526	3.39	0.21	0.23	0.24	0.27	0.33	0.41	72.0	1591	3.39	0.22	0.23	0.24	0.27	0.33	0.40
4		0.06	83.8	1308	3.50	0.16	0.17	0.18	0.21	0.27	0.34	83.0	1393	3.44	0.17	0.18	0.20	0.23	0.29	0.37
6		0.06	95.0	1047	NAV	0.10	0.12	0.13	0.16	0.22	0.29	94.3	1088	NAV	0.11	0.12	0.14	0.16	0.22	0.29
8		0.06	94.2	827	NAV	0.06	0.07	0.08	0.11	0.17	0.24	94.0	869	NAV	0.07	0.08	0.10	0.12	0.18	0.25
12		0.06	98.5	719	NAV	0.05	0.06	0.07	0.10	0.16	0.22	98.2	748	NAV	0.05	0.06	0.08	0.10	0.16	0.23
20		0.06	98.9	659	NAV	0.05	0.06	0.07	0.09	0.15	0.21	99.0	701	NAV	0.05	0.06	0.07	0.10	0.16	0.22
0.50		1	0.015	85.3	2200	NAV	1.31	1.38	1.44	1.59	1.86	2.08	82.6	2200	NAV	1.33	1.40	1.46	1.60	1.86
	2	0.015	99.6	988	NAV	0.49	0.54	0.61	0.74	1.00	1.26	99.3	1052	NAV	0.52	0.58	0.65	0.78	1.03	1.29
	3	0.015	99.9	654	NAV	0.28	0.34	0.40	0.54	0.79	1.05	100.0	710	NAV	0.32	0.37	0.43	0.57	0.82	1.09
	4	0.015	100.0	513	NAV	0.20	0.25	0.31	0.44	0.70	0.96	100.0	558	NAV	0.22	0.28	0.34	0.47	0.73	0.99
	6	0.015	100.0	413	NAV	0.15	0.19	0.25	0.38	0.63	0.90	100.0	453	NAV	0.17	0.22	0.28	0.41	0.66	0.93
	8	0.015	100.0	396	NAV	0.14	0.19	0.24	0.37	0.63	0.89	100.0	438	NAV	0.16	0.21	0.27	0.40	0.65	0.92
	12	0.015	100.0	332	NAV	0.11	0.15	0.20	0.34	0.59	0.85	100.0	372	NAV	0.13	0.18	0.23	0.37	0.62	0.88
	20	0.015	100.0	307	NAV	0.10	0.14	0.18	0.32	0.57	0.83	100.0	347	NAV	0.12	0.16	0.21	0.35	0.59	0.86

**Table B.36:** Precipitation triggered pollution detection probability, average detection time, contaminated area in case of detection failure and relative contaminated area to control area for various RADTi in case of  $\sigma_{lnK}^2 = 2.0$  assuming annually sampling frequency

		$\sigma_{lnK}^2$										
		2.00										
$\alpha_T(m)$	now	nfdS(max)	$P_d$ (12M)	$\langle T_{(DET)} \rangle$ (DAYS)	AREA ON FAILURE	(AREA ON DET.)/L	(3M. RADTi)/L	(6M. RADTi)/L	(12M. RADTi)/L	(24M. RADTi)/L	(36M. RADTi)/L	
0.001	1	0.75	6.1	3409	1.49	0.12	0.12	0.13	0.14	0.16	0.19	
	2	0.75	15.1	3607	1.46	0.17	0.18	0.19	0.22	0.27	0.19	
	3	0.75	17.0	3438	1.54	0.12	0.13	0.13	0.14	0.17	0.19	
	4	0.75	21.7	3387	1.34	0.13	0.13	0.14	0.15	0.17	0.20	
	6	0.75	35.9	3515	1.53	0.14	0.15	0.16	0.18	0.22	0.18	
	8	0.75	40.8	3403	1.53	0.12	0.12	0.12	0.14	0.16	0.18	
	12	0.75	57.3	3303	1.50	0.11	0.11	0.12	0.13	0.15	0.17	
	20	0.75	74.0	3207	1.64	0.10	0.10	0.11	0.12	0.14	0.16	
0.01	1	0.50	14.4	3203	2.30	0.25	0.26	0.27	0.30	0.36	0.43	
	2	0.50	26.0	2800	2.35	0.21	0.21	0.22	0.24	0.28	0.33	
	3	0.50	39.0	2940	2.27	0.21	0.22	0.23	0.26	0.30	0.36	
	4	0.50	45.3	2741	2.17	0.18	0.19	0.20	0.22	0.26	0.31	
	6	0.50	59.9	2689	2.53	0.18	0.19	0.20	0.22	0.26	0.31	
	8	0.50	70.5	2602	2.29	0.15	0.16	0.17	0.19	0.22	0.27	
	12	0.50	82.0	2404	2.36	0.12	0.13	0.14	0.16	0.20	0.24	
	20	0.50	86.9	2294	2.29	0.10	0.11	0.12	0.14	0.18	0.22	
0.05	1	0.13	18.9	1984	3.02	0.22	0.23	0.24	0.27	0.33	0.40	
	2	0.13	38.9	1779	3.04	0.19	0.20	0.21	0.24	0.30	0.36	
	3	0.13	55.1	1863	3.01	0.20	0.22	0.23	0.26	0.30	0.37	
	4	0.13	65.1	1740	3.06	0.17	0.18	0.19	0.22	0.28	0.34	
	6	0.13	83.0	1497	3.23	0.13	0.14	0.15	0.18	0.23	0.29	
	8	0.13	87.7	1396	3.60	0.11	0.12	0.13	0.15	0.21	0.27	
	12	0.13	95.0	1171	3.31	0.07	0.08	0.09	0.12	0.17	0.23	
	20	0.13	96.1	1090	0.00	0.07	0.07	0.09	0.11	0.16	0.21	
0.10	1	0.06	25.3	1975	3.26	0.28	0.29	0.30	0.34	0.40	0.47	
	2	0.06	52.8	1771	3.40	0.25	0.25	0.27	0.30	0.37	0.43	
	3	0.06	69.5	1607	3.34	0.24	0.22	0.24	0.27	0.34	0.41	
	4	0.06	81.6	1536	3.59	0.20	0.20	0.22	0.25	0.32	0.39	
	6	0.06	93.3	1218	NAV	0.13	0.14	0.16	0.19	0.25	0.32	
	8	0.06	93.9	989	NAV	0.09	0.10	0.11	0.14	0.20	0.27	
	12	0.06	98.0	854	NAV	0.07	0.08	0.09	0.12	0.18	0.25	
	20	0.06	98.6	797	NAV	0.06	0.07	0.08	0.11	0.17	0.24	
0.50	1	0.015	79.6	2391	NAV	1.59	1.54	1.61	1.76	1.95	2.21	
	2	0.015	99.1	1224	NAV	0.65	0.71	0.78	0.91	1.16	1.42	
	3	0.015	99.8	837	NAV	0.40	0.46	0.53	0.66	0.92	1.18	
	4	0.015	100.0	679	NAV	0.30	0.36	0.43	0.56	0.81	1.07	
	6	0.015	100.0	570	NAV	0.22	0.28	0.35	0.49	0.73	0.99	
	8	0.015	100.0	567	NAV	0.23	0.29	0.36	0.49	0.74	1.00	
	12	0.015	100.0	501	NAV	0.19	0.24	0.31	0.45	0.69	0.95	
	20	0.015	100.0	481	NAV	0.17	0.22	0.29	0.43	0.67	0.94	

(This page was left intentionally blank)

# References

---

- Ababou, R., McLaughlin, D., Gelhar, L., & Tompson, A. B. (1989). Numerical simulation of three-dimensional saturated flow in randomly heterogeneous porous media. *Transport in Porous Media*, 4(6), 549-565. doi: 10.1007/bf00223627
- Academies, N. (1994). *Alternatives for Groundwater Cleanup*. Washington D.C.: National Academies Press.
- Adams, E. E., & Gelhar, L. W. (1992). Field study of dispersion in a heterogeneous aquifer: 2. Spatial moments analysis. *Water Resources Research*, 28(12), 3293-3307. doi: 10.1029/92wr01757
- Ahlstrom, S. W., Foote, H. P., Arnett, R. C., Cole, C. R., & Serne, R. J. (1977). Multicomponent mass transport model: theory and numerical implementation (discrete-parcel-random-walk version) (pp. Medium: ED; Size: Pages: 128).
- Allen, A. (2001). Containment landfills: the myth of sustainability. *Engineering Geology*, 60(1-4), 3-19. doi: [http://dx.doi.org/10.1016/S0013-7952\(00\)00084-3](http://dx.doi.org/10.1016/S0013-7952(00)00084-3)
- Apgar, M. A., & Langmuir, D. (1971). Ground-Water Pollution Potential of a Landfill Above the Water Table. *Ground Water*, 9(6), 76-96. doi: 10.1111/j.1745-6584.1971.tb03582.x
- Baccini, P., Henseler, G., Figi, R., & Belevi, H. (1987). Water and element balances of municipal solid waste landfills. *Waste Management & Research*, 5(4), 483-499. doi: <http://dx.doi.org/>
- Bear, J. (1988). *Dynamics of fluids in porous media*: Dover.
- Bear, J., & Buchlin, J.-M. (1987). *Modeling and applications of transport phenomena in porous media*. Netherlands: Kluwer Academic Publishers.
- Bedford, D., & Cooke, R. (2003). *Probabilistic Risk Analysis: Foundations and Methods*. New York: Cambridge University Press.
- Bierkens, M. F. P. (2006). Designing a monitoring network for detecting groundwater pollution with stochastic simulation and a cost model. *Stochastic Environmental Research and Risk Assessment*, 20(5), 335-351. doi: 10.1007/s00477-005-0025-2
- Boggs, J. M., Young, S. C., Beard, L. M., Gelhar, L. W., Rehfeldt, K. R., & Adams, E. E. (1992). Field study of dispersion in a heterogeneous aquifer: 1. Overview and site description. *Water Resources Research*, 28(12), 3281-3291. doi: 10.1029/92wr01756
- Bolster, D., Barahona, M., Dentz, M., Fernandez-Garcia, D., Sanchez-Vila, X., Trinchero, P., . . . Tartakovsky, D. M. (2009). Probabilistic risk analysis of groundwater remediation strategies. *Water Resources Research*, 45(6), W06413. doi: 10.1029/2008wr007551

- Brooker, P. (1985). Two-dimensional simulation by turning bands. *Journal of the International Association for Mathematical Geology*, 17(1), 81-90. doi: 10.1007/bf01030369
- Çelik, B., Rowe, R. K., & Ünlü, K. (2009). Effect of vadose zone on the steady-state leakage rates from landfill barrier systems. *Waste Management*, 29(1), 103-109. doi: <http://dx.doi.org/10.1016/j.wasman.2008.02.012>
- Cirpka, O. A., & Kitanidis, P. K. (2001). Theoretical basis for the measurement of local transverse dispersion in isotropic porous media. *Water Resources Research*, 37(2), 243-252. doi: 10.1029/2000wr900314
- Collucci, P., Darilek, G. T., Laine, D. L., & Binley, A. (1999). *Locating landfill leaks covered with waste*. Paper presented at the Seventh International Waste Management and Landfill Symposium, Sardinia
- Dagan, G. (1984). Solute transport in heterogeneous porous formations. *Journal of Fluid Mechanics*, 145, 27.
- Dagan, G. (1986). Statistical theory of groundwater flow and transport: Pore to laboratory, laboratory to formation, and formation to regional scale. *Water Resources Research*, 22(9S), 120S-134S. doi: 10.1029/WR022i09Sp0120S
- Dagan, G. (1989). *Flow and transport in porous formations*.
- Dagan, G. (1994). The significance of heterogeneity of evolving scales to transport in porous formations. *Water Resources Research*, 30(12), 3327-3336. doi: 10.1029/94wr01798
- Dagan, G., Lesoff, S. C., & Fiori, A. (2009). Is transmissivity a meaningful property of natural formations? Conceptual issues and model development. *Water Resources Research*, 45(3), W03425. doi: 10.1029/2008wr007410
- De Cortázar, A. L. G., Lantarón, J. H., Fernández, O. M., Monzón, I. T., & Lamia, M. F. (2002). Modelling for environmental assessment of municipal solid waste landfills (Part 1: Hydrology). *Waste Management & Research*, 20(2), 198-210. doi: 10.1177/0734242x0202000211
- Delay, F., Ackerer, P., & Danquigny, C. (2005a). Simulating Solute Transport in Porous or Fractured Formations Using Random Walk Particle Tracking. *Vadose Zone J.*, 4(2), 360-379. doi: 10.2136/vzj2004.0125
- Delay, F., Ackerer, P., & Danquigny, C. (2005b). Simulating Solute Transport in Porous or Fractured Formations Using Random Walk Particle Tracking: A Review *Vadose Zone Journal*, 4(2). doi: 10.2136/vzj2004.0125
- Desbarats, A. J. (1992). Spatial averaging of hydraulic conductivity in three-dimensional heterogeneous porous media. *Mathematical Geology*, 24(3), 249-267. doi: 10.1007/bf00893749
- Dimitrakopoulos, R., & Luo, X. (2004). Generalized Sequential Gaussian Simulation on Group Size  $v$  and Screen-Effect Approximations for Large Field Simulations.

*Mathematical Geology*, 36(5), 567-591. doi:  
10.1023/B:MATG.0000037737.11615.df

- El-Zein, A. (2008). A general approach to the modelling of contaminant transport through composite landfill liners with intact or leaking geomembranes. *International Journal for Numerical and Analytical Methods in Geomechanics*, 32(3), 265-287. doi: 10.1002/nag.626
- Elfeki, A. M. M. (1996). *Stochastic characterization of geological heterogeneity and its impact on groundwater contaminant transport*. PhD, Delft University, Balkema Publisher, Rotterdam.
- Emery, X. (2008). A turning bands program for conditional co-simulation of cross-correlated Gaussian random fields. *Computers & Geosciences*, 34(12), 1850-1862. doi: <http://dx.doi.org/10.1016/j.cageo.2007.10.007>
- European Council Directive 99/31/EC on the Landfill of Waste (1999/31/EC).
- Groundwater Protection in Europe - The New Groundwater Directive (2008).
- Farrell, D. A., Woodbury, A. D., & Sudicky, E. A. (1994). The 1978 Borden tracer experiment: Analysis of the spatial moments. *Water Resources Research*, 30(11), 3213-3223. doi: 10.1029/94wr00622
- Fatta, D., Papadopoulos, A., & Loizidou, M. (1999). A study on the landfill leachate and its impact on the groundwater quality of the greater area. *Environmental Geochemistry and Health*, 21(2), 175-190. doi: 10.1023/a:1006613530137
- Fernández-García, D., Rajaram, H., & Illangasekare, T. H. (2005). Assessment of the predictive capabilities of stochastic theories in a three-dimensional laboratory test aquifer: Effective hydraulic conductivity and temporal moments of breakthrough curves. *Water Resources Research*, 41(4), W04002. doi: 10.1029/2004wr003523
- Feyen, J., Jacques, D., Timmerman, A., & Vanderborght, J. (1998). Modelling Water Flow and Solute Transport in Heterogeneous Soils: A Review of Recent Approaches. *Journal of Agricultural Engineering Research*, 70(3), 231-256. doi: <http://dx.doi.org/10.1006/jaer.1998.0272>
- Fiori, A., Janković, I., & Dagan, G. (2006). Modeling flow and transport in highly heterogeneous three-dimensional aquifers: Ergodicity, Gaussianity, and anomalous behavior—2. Approximate semianalytical solution. *Water Resources Research*, 42(6), W06D13. doi: 10.1029/2005wr004752
- Freeze, R. A. (1975). A stochastic-conceptual analysis of one-dimensional groundwater flow in nonuniform homogeneous media. *Water Resources Research*, 11(5), 725-741. doi: 10.1029/WR011i005p00725
- Freeze, R. A., Massmann, J., Smith, L., Sperling, T., & James, B. (1990). Hydrogeological Decision Analysis: 1. A Framework. *Ground Water*, 28(5), 738-766. doi: 10.1111/j.1745-6584.1990.tb01989.x

- Freyberg, D. L. (1986). A natural gradient experiment on solute transport in a sand aquifer: 2. Spatial moments and the advection and dispersion of nonreactive tracers. *Water Resources Research*, 22(13), 2031-2046. doi: 10.1029/WR022i013p02031
- Gardiner, C. W. (1990). *Handbook of Stochastic Methods for Physics, Chemistry, and the Natural Sciences*. New York: Springer Verlag.
- Gau, S.-H., & Chow, J.-D. (1998). Landfill leachate characteristics and modeling of municipal solid wastes combined with incinerated residuals. *Journal of Hazardous Materials*, 58(1-3), 249-259. doi: [http://dx.doi.org/10.1016/S0304-3894\(97\)00136-2](http://dx.doi.org/10.1016/S0304-3894(97)00136-2)
- Gelhar, L. W. (1986). Stochastic subsurface hydrology from theory to applications. *Water Resources Research*, 22(9S), 135S-145S. doi: 10.1029/WR022i09Sp0135S
- Gelhar, L. W., Welty, C., & Rehfeldt, K. R. (1992). A critical review of data on field-scale dispersion in aquifers. *Water Resources Research*, 28(7), 1955-1974. doi: 10.1029/92wr00607
- Giroud, J. P., & Bonaparte, R. (1989). Leakage through liners constructed with geomembranes—part I. Geomembrane liners. *Geotextiles and Geomembranes*, 8(1), 27-67. doi: [http://dx.doi.org/10.1016/0266-1144\(89\)90009-5](http://dx.doi.org/10.1016/0266-1144(89)90009-5)
- Gleick, P. H. (1993). *Water in Crisis*. New York, USA: Oxford University Press.
- Godfrey, K. A., Kurtovich, M., & Daniel, D. (1987). Monitoring for Hazardous Waste Leaks. *Civil Engineering*, 57(2), 4.
- Gómez-Hernández, J. J., & Gorelick, S. M. (1989). Effective groundwater model parameter values: Influence of spatial variability of hydraulic conductivity, leakage, and recharge. *Water Resources Research*, 25(3), 405-419. doi: 10.1029/WR025i003p00405
- Gutjahr, A. L., Gelhar, L. W., Bakr, A. A., & MacMillan, J. R. (1978). Stochastic analysis of spatial variability in subsurface flows: 2. Evaluation and application. *Water Resources Research*, 14(5), 953-959. doi: 10.1029/WR014i005p00953
- Harr, M. E. (1962). *Groundwater and Seepage*. New York: McGraw-Hill Book Company.
- Harvey, C. F., & Gorelick, S. M. (1995). Mapping Hydraulic Conductivity: Sequential Conditioning with Measurements of Solute Arrival Time, Hydraulic Head, and Local Conductivity. *Water Resources Research*, 31(7), 1615-1626. doi: 10.1029/95wr00547
- Hassan, A. E., & Mohamed, M. M. (2003). On using particle tracking methods to simulate transport in single-continuum and dual continua porous media. *Journal of Hydrology*, 275(3-4), 242-260. doi: [http://dx.doi.org/10.1016/S0022-1694\(03\)00046-5](http://dx.doi.org/10.1016/S0022-1694(03)00046-5)
- Hess, K. M., Wolf, S. H., & Celia, M. A. (1992). Large-scale natural gradient tracer test in sand and gravel, Cape Cod, Massachusetts: 3. Hydraulic conductivity variability and calculated macrodispersivities. *Water Resources Research*, 28(8), 2011-2027. doi: 10.1029/92wr00668

- Hoeksema, R. J., & Kitanidis, P. K. (1985). Comparison of Gaussian Conditional Mean and Kriging Estimation in the Geostatistical Solution of the Inverse Problem. *Water Resources Research*, 21(6), 825-836. doi: 10.1029/WR021i006p00825
- Højberg, A., Refsgaard, J., Geer, F., Jørgensen, L., & Zsuffa, I. (2007). Use of Models to Support the Monitoring Requirements in the Water Framework Directive. *Water Resources Management*, 21(10), 1649-1672. doi: 10.1007/s11269-006-9119-y
- Hudak, P. F. (1998). Configuring Detection Wells Near Landfills. *Ground Water Monitoring & Remediation*, 18(2), 93-96. doi: 10.1111/j.1745-6592.1998.tb00619.x
- Hudak, P. F. (2001). Effective contaminant detection networks in uncertain groundwater flow fields. *Waste Management*, 21(4), 309-312. doi: [http://dx.doi.org/10.1016/S0956-053X\(00\)00079-9](http://dx.doi.org/10.1016/S0956-053X(00)00079-9)
- Hudak, P. F. (2005). Sensitivity of groundwater monitoring networks to contaminant source width for various seepage velocities. *Water Resources Research*, 41(8), W08501. doi: 10.1029/2005wr003968
- Hudak, P. F., & Loaiciga, H. A. (1992). A location modeling approach for groundwater monitoring network augmentation. *Water Resources Research*, 28(3), 643-649. doi: 10.1029/91wr02851
- ISWA. (1992). *1000 Terms in Solid Waste Management*. Copenhagen: International Solid Waste Association.
- ITRC. (2003). *Technical and Regulatory Guidance for Design, Installation, and Monitoring of Alternative Landfill Covers*: Interstate Technology Regulatory Council.
- Izbicki, J. A., Ball, J. W., Bullen, T. D., & Sutley, S. J. (2008). Chromium, chromium isotopes and selected trace elements, western Mojave Desert, USA. *Applied Geochemistry*, 23(5), 1325-1352. doi: <http://dx.doi.org/10.1016/j.apgeochem.2007.11.015>
- Journel, A. G. (1974). Geostatistics for Conditional Simulation of Ore Bodies. *Economic Geology*, 69(5), 673-687. doi: 10.2113/gsecongeo.69.5.673
- Kaczmarek, M., Hueckel, T., Chawla, V., & Imperiali, P. (1997). Transport Through a Clay Barrier with the Contaminant Concentration Dependent Permeability. *Transport in Porous Media*, 29(2), 159-178. doi: 10.1023/a:1006565417159
- Kim, K.-H., & Lee, K.-K. (2007). Optimization of groundwater-monitoring networks for identification of the distribution of a contaminant plume. *Stochastic Environmental Research and Risk Assessment*, 21(6), 785-794. doi: 10.1007/s00477-006-0094-x
- Kinzelbach, W. (1987). *Simulation of pollutant transport in groundwater with the random walk method*. Paper presented at the Groundwater Monitoring and Management, Dresden Symposium.
- Kjeldsen, P. (1993). Groundwater pollution source characterization of an old landfill. *Journal of Hydrology*, 142(1-4), 349-371. doi: [http://dx.doi.org/10.1016/0022-1694\(93\)90018-5](http://dx.doi.org/10.1016/0022-1694(93)90018-5)

- Koerner, G. R., & Koerner, G. R. (1995). Leachate Clogging Assessment of Geotextile and Soil Landfill Filters. Cincinnati OH 45268: National Risk Management Research Laboratory.
- Koerner, R. M., & Soong, T. Y. (2000). Leachate in landfills: the stability issues. *Geotextiles and Geomembranes*, 18(5), 293-309. doi: [http://dx.doi.org/10.1016/S0266-1144\(99\)00034-5](http://dx.doi.org/10.1016/S0266-1144(99)00034-5)
- Kulikowska, D., & Klimiuk, E. (2008). The effect of landfill age on municipal leachate composition. *Bioresource Technology*, 99(13), 5981-5985. doi: <http://dx.doi.org/10.1016/j.biortech.2007.10.015>
- Laine, D. L., Binley, A. M., & Darilek, G. T. (1997). Locating geomembrane liner leaks under waste in a landfill. *Geosynthetics*, 5.
- LeBlanc, D. R., Garabedian, S. P., Hess, K. M., Gelhar, L. W., Quadri, R. D., Stollenwerk, K. G., & Wood, W. W. (1991). Large-scale natural gradient tracer test in sand and gravel, Cape Cod, Massachusetts: 1. Experimental design and observed tracer movement. *Water Resources Research*, 27(5), 895-910. doi: 10.1029/91wr00241
- Lee, G. F., & Jones-Lee, A. (1994). A Groundwater Protection Strategy for Lined Landfills. *Environmental Science & Technology*, 28(13), 584A-585A. doi: 10.1021/es00062a718
- Lema, J. M., Mendez, R., & Blazquez, R. (1988). Characteristics of landfill leachates and alternatives for their treatment: A review. *Water, Air, and Soil Pollution*, 40(3-4), 223-250. doi: 10.1007/bf00163730
- LENNTech. (2013). Sources of groundwater pollution, from [www.lenntech.com](http://www.lenntech.com)
- Loaiciga, H., Charbeneau, R., Everett, L., Fogg, G., Hobbs, B., & Rouhani, S. (1992). Review of Ground - Water Quality Monitoring Network Design. *Journal of Hydraulic Engineering*, 118(1), 11-37. doi: doi:10.1061/(ASCE)0733-9429(1992)118:1(11)
- Loaiciga, H. A. (1989). An optimization approach for groundwater quality monitoring network design. *Water Resources Research*, 25(8), 1771-1782. doi: 10.1029/WR025i008p01771
- Lund, J. R. (2008). A risk analysis of risk analysis. *Contemporary water research and education*(140), 53-60.
- Mackay, D. M., Freyberg, D. L., Roberts, P. V., & Cherry, J. A. (1986). A natural gradient experiment on solute transport in a sand aquifer: 1. Approach and overview of plume movement. *Water Resources Research*, 22(13), 2017-2029. doi: 10.1029/WR022i013p02017
- Mahar, P., & Datta, B. (2000). Identification of Pollution Sources in Transient Groundwater Systems. *Water Resources Management*, 14(3), 209-227. doi: 10.1023/a:1026527901213

- Mantoglou, A. (1987). Digital simulation of multivariate two- and three-dimensional stochastic processes with a spectral turning bands method. *Mathematical Geology*, 19(2), 129-149. doi: 10.1007/bf00898192
- Mantoglou, A., & Wilson, J. L. (1982). The Turning Bands Method for simulation of random fields using line generation by a spectral method. *Water Resources Research*, 18(5), 1379-1394. doi: 10.1029/WR018i005p01379
- McLaughlin, D., Reid, L. B., Li, S.-G., & Hyman, J. (1993). A Stochastic Method for Characterizing Ground-Water Contamination. *Ground Water*, 31(2), 237-249. doi: 10.1111/j.1745-6584.1993.tb01816.x
- Meyer, P. D., Valocchi, A. J., & Eheart, J. W. (1994). Monitoring network design to provide initial detection of groundwater contamination. *Water Resources Research*, 30(9), 2647-2659. doi: 10.1029/94wr00872
- Miller, C. J., & Mishra, M. (1989a). MODELING OF LEAKAGE THROUGH CRACKED CLAY LINERS - II: A NEW PERSPECTIVE1. *JAWRA Journal of the American Water Resources Association*, 25(3), 557-563. doi: 10.1111/j.1752-1688.1989.tb03092.x
- Miller, C. J., & Mishra, M. (1989b). MODELING OF LEAKAGE THROUGH CRACKED CLAY LINERS -I: STATE OF THE ART1. *JAWRA Journal of the American Water Resources Association*, 25(3), 551-556. doi: 10.1111/j.1752-1688.1989.tb03091.x
- Morisawa, S., & Inoue, Y. (1991). Optimum allocation of monitoring wells around a solid-waste landfill site using precursor indicators and fuzzy utility functions. *Journal of Contaminant Hydrology*, 7(4), 337-370. doi: [http://dx.doi.org/10.1016/0169-7722\(91\)90002-I](http://dx.doi.org/10.1016/0169-7722(91)90002-I)
- Moustris, K., Larissi, I., Nastos, P., & Paliatsos, A. (2011). Precipitation Forecast Using Artificial Neural Networks in Specific Regions of Greece. *Water Resources Management*, 25(8), 1979-1993. doi: 10.1007/s11269-011-9790-5
- Munawar, E., & Fellner, J. (2013). Guidelines for Design and Operation of Municipal Solid Waste Landfills in Tropical Climates. In ISWA (Ed.).
- Nunes, L. M., Cunha, M. d. C., Ribeiro, L., & Azevedo, J. (2007). A new method for groundwater plume detection under uncertainty. In J. P. L. Ferreira & J. M. P. Vieira (Eds.), *Water in Celtic countries: quantity, quality and climate variability* (pp. 191-198). Wallingford, UK.
- Paleologos, E., & Sarris, T. (2011). Stochastic analysis of flux and head moments in a heterogeneous aquifer system. *Stochastic Environmental Research and Risk Assessment*, 25(6), 747-759. doi: 10.1007/s00477-011-0459-7
- Paleologos, E. K. (2008). The lost value of groundwater and its influence on environmental decision making. *Risk Anal*, 28(4), 939-950. doi: 10.1111/j.1539-6924.2008.01073.x
- Papapetridis, K., & Paleologos, E. K. (2010). *Stochastic Modeling of Subsurface Pollution in 2-D Heterogeneous Aquifers and Detection Probability for Linear Configuration of*

- Monitoring Wells*. Paper presented at the Hazardous and Industrial Waste Management, Crete, Greece.
- Papapetridis, K., & Paleologos, E. K. (2011a). Contaminant detection probability in heterogeneous aquifers and corrected risk analysis for remedial response delay. *Water Resources Research*, 47(10). doi: 10.1029/2011wr010652
- Papapetridis, K., & Paleologos, E. K. (2011b). Stochastic Modeling of Plume Evolution and Monitoring into Heterogeneous Aquifers. In N. Lambrakis, G. Stournaras & K. Katsanou (Eds.), *Advances in the Research of Aquatic Environment* (pp. 349-356): Springer Berlin Heidelberg.
- Papapetridis, K., & Paleologos, E. K. (2012). Sampling Frequency of Groundwater Monitoring and Remediation Delay at Contaminated Sites. *Water Resources Management*, 26(9), 2673-2688. doi: 10.1007/s11269-012-0039-8
- Prickett, T. A., Naymik, T. G., & Lonquist, C. G. (1981). A Random Walk Solute Transport Model for Selected Groundwater Quality Evaluations: State of Illinois, Department of Energy and Natural Resources.
- Ptak, T., Piepenbrink, M., & Martac, E. (2004). Tracer tests for the investigation of heterogeneous porous media and stochastic modelling of flow and transport—a review of some recent developments. *Journal of Hydrology*, 294(1–3), 122-163. doi: <http://dx.doi.org/10.1016/j.jhydrol.2004.01.020>
- Reed, P., Minsker, B., & Valocchi, A. J. (2000). Cost-effective long-term groundwater monitoring design using a genetic algorithm and global mass interpolation. *Water Resour. Res.*, 12(36), 10.
- Rehfeldt, K. R., Boggs, J. M., & Gelhar, L. W. (1992). Field study of dispersion in a heterogeneous aquifer: 3. Geostatistical analysis of hydraulic conductivity. *Water Resources Research*, 28(12), 3309-3324. doi: 10.1029/92wr01758
- Renou, S., Givaudan, J. G., Poulain, S., Dirassouyan, F., & Moulin, P. (2008). Landfill leachate treatment: Review and opportunity. *Journal of Hazardous Materials*, 150(3), 468-493. doi: <http://dx.doi.org/10.1016/j.jhazmat.2007.09.077>
- Riediker, S. S., MJF; Giger, W; . (2000). Benzene- and naphthalenesulfonates in leachates and plumes of landfills. *WATER RESEARCH* 34(7), 10.
- Rowe, R. K. (1995). Leachate Characteristics for MSW Landfills (D. o. C. Engineering, Trans.). London, Canada: Geotechnical Research Centre, University of Western Ontario.
- Rumer, R. R., & Mitchell, J. K. (1995). Assessment of barrier containment technologies: A comprehensive treatment for environmental remedial application *International Containment Technology Workshop*: National Technical Information Service.

- Salamon, P., Fernández-García, D., & Gómez-Hernández, J. J. (2006a). Modeling mass transfer processes using random walk particle tracking. *Water Resources Research*, 42(11), W11417. doi: 10.1029/2006wr004927
- Salamon, P., Fernández-García, D., & Gómez-Hernández, J. J. (2006b). A review and numerical assessment of the random walk particle tracking method. *Journal of Contaminant Hydrology*, 87(3-4), 277-305. doi: <http://dx.doi.org/10.1016/j.jconhyd.2006.05.005>
- Sarris, T. S. (1999). Effective Hydraulic Properties of Heterogeneous Bounded Aquifers *MSc Thesis*. South Carolina USA: University of South Carolina.
- Sarris, T. S., & Paleologos, E. K. (2004). Numerical investigation of the anisotropic hydraulic conductivity behavior in heterogeneous porous media. *Stochastic Environmental Research and Risk Assessment*, 18(3), 188-197. doi: 10.1007/s00477-003-0171-3
- Selker, J. S., Steenhuis, T. S., & Parlange, J.-Y. (1996). An engineering approach to fingered vadose pollutant transport. *Geoderma*, 70(2-4), 197-206. doi: [http://dx.doi.org/10.1016/0016-7061\(95\)00085-2](http://dx.doi.org/10.1016/0016-7061(95)00085-2)
- Shafer, J. M., & Varljen, M. D. (1990). Approximation of confidence limits on sample semivariograms from single realizations of spatially correlated random fields. *Water Resources Research*, 26(8), 1787-1802. doi: 10.1029/WR026i008p01787
- Shinozuka, M., & Jan, C. M. (1972). Digital simulation of random processes and its applications. *Journal of Sound and Vibration*, 25(1), 111-128. doi: [http://dx.doi.org/10.1016/0022-460X\(72\)90600-1](http://dx.doi.org/10.1016/0022-460X(72)90600-1)
- Slack, R. J., Gronow, J. R., Hall, D. H., & Voulvoulis, N. (2007). Household hazardous waste disposal to landfill: Using LandSim to model leachate migration. *Environmental Pollution*, 146(2), 501-509. doi: <http://dx.doi.org/10.1016/j.envpol.2006.07.011>
- Solomon, U. (2010). A detailed look at the three disciplines, environmental ethics, law and education to determine which plays the most critical role in environmental enhancement and protection. *Environment, Development and Sustainability*, 12(6), 1069-1080. doi: 10.1007/s10668-010-9242-z
- Spitz, K., & Moreno, J. (1996). *A Practical Guide to Groundwater and Solute Transport Modeling* (1st ed.). New York: Wiley-Interscience Publication.
- Storck, P., Eheart, J. W., & Valocchi, A. J. (1997). A method for the optimal location of monitoring wells for detection of groundwater contamination in three-dimensional heterogeneous aquifers. *Water Resources Research*, 33(9), 2081-2088. doi: 10.1029/97wr01704
- Sudicky, E. A. (1986). A natural gradient experiment on solute transport in a sand aquifer: Spatial variability of hydraulic conductivity and its role in the dispersion process. *Water Resources Research*, 22(13), 2069-2082. doi: 10.1029/WR022i013p02069
- Tartakovsky, D. M. (2007). Probabilistic risk analysis in subsurface hydrology. *Geophysical Research Letters*, 34(5), L05404. doi: 10.1029/2007gl029245

- Tatsi, A. A., & Zouboulis, A. I. (2002). A field investigation of the quantity and quality of leachate from a municipal solid waste landfill in a Mediterranean climate (Thessaloniki, Greece). *Advances in Environmental Research*, 6(3), 207-219. doi: [http://dx.doi.org/10.1016/S1093-0191\(01\)00052-1](http://dx.doi.org/10.1016/S1093-0191(01)00052-1)
- Tompson, A. F. B., Ababou, R., & Gelhar, L. W. (1989). Implementation of the three-dimensional turning bands random field generator. *Water Resources Research*, 25(10), 2227-2243. doi: 10.1029/WR025i010p02227
- Tompson, A. F. B., & Gelhar, L. W. (1990a). Numerical simulation of solute transport in three-dimensional, randomly heterogeneous porous media. *Water Resour. Res.*, 26(10), 2541-2562. doi: 10.1029/WR026i010p02541
- Tompson, A. F. B., & Gelhar, L. W. (1990b). Numerical simulation of solute transport in three-dimensional, randomly heterogeneous porous media. *Water Resources Research*, 26(10), 2541-2562. doi: 10.1029/WR026i010p02541
- Tompson, A. F. B., Vomvoris, G., & Gelhar, L. G. (1987a). Numerical Simulation of Solute Transport in Randomly Heterogeneous Porous Media: Motivation, Model Development, and Application *Lawrence Livermore National Laboratory*. Livermore, California: Law.
- Tompson, A. F. B., Vomvoris, G., & Gelhar, L. W. (1987b). Numerical Simulation of Solute Transport in Randomly Heterogeneous Porous Media: Motivation, Model Development, and Application: Lawrence Livermore National Laboratory, Livermore, California.
- Tsanis, I. K. (2006). Modeling Leachate Contamination and Remediation of Groundwater at a Landfill Site. *Water Resources Management*, 20(1), 109-132. doi: 10.1007/s11269-006-4634-4
- U.S.N.R.C. (2012). Alternatives for Managing the Nation's Complex Contaminated Groundwater Sites. In C. o. F. O. f. M. i. t. N. s. S. R. Effort (Ed.). Washington, D.C.: THE NATIONAL ACADEMIES PRESS.
- Uffink, G. J. (1990). *Analysis of dispersion by the random walk method*. PhD, Delft University of Technology, The Netherlands.
- Warrick, A. W., Younga, M. H., & Wierenga, P. J. (1998). Probabilistic Analysis of Monitoring Systems for Detecting Subsurface Contaminant Plumes. *Ground Water*, 36(6), 894-900. doi: 10.1111/j.1745-6584.1998.tb02096.x
- Woodbury, A. D., & Sudicky, E. A. (1991). The geostatistical characteristics of the borden aquifer. *Water Resources Research*, 27(4), 533-546. doi: 10.1029/90wr02545
- Wu, J., Zheng, C., & Chien, C. C. (2005). Cost-effective sampling network design for contaminant plume monitoring under general hydrogeological conditions. *Journal of Contaminant Hydrology*, 77(1-2), 41-65. doi: <http://dx.doi.org/10.1016/j.jconhyd.2004.11.006>
- Yenigül, N. B., Elfeki, A. M. M., Gehrels, J. C., van den Akker, C., Hensbergen, A. T., & Dekking, F. M. (2005). Reliability assessment of groundwater monitoring networks at

- landfill sites. *Journal of Hydrology*, 308(1–4), 1-17. doi: <http://dx.doi.org/10.1016/j.jhydrol.2004.10.017>
- Yenigül, N. B., Hensbergen, A., Elfeki, A. M., & Dekking, F. M. (2011). Detection of contaminant plumes released from landfills: numerical versus analytical solutions. *Environmental Earth Sciences*, 64(8), 2127-2140. doi: 10.1007/s12665-011-1039-3
- Yenigül, N. B., Elfeki, A. M. M., Van Den Akker, C., & Dekking, F. M. (2006). A decision analysis approach for optimal groundwater monitoring system design under uncertainty. [Journal Article]. *Hydrology and Earth System Sciences Discussions Discussions*, 3( 1), 27-68.
- Young, D. (1954). Iterative methods for solving partial difference equations of elliptic type. *Transactions of the American Mathematical Society*(76), 20.
- Zacarias-Farah, A., & Geyer-Allely, E. (2003). Household consumption patterns in OECD countries: trends and figures. *Journal of Cleaner Production*(11), 9.
- Zhao, X.-c., Zhang, Y.-d., Yang, P., & Nai, C.-x. (2007). High voltage DC leakage detection for double-lined hazardous waste landfill based on finite element method. *Journal of Shanghai University (English Edition)*, 11(6), 585-590. doi: 10.1007/s11741-007-0612-1
- Zimmermann, S., Koumoutsakos, P., & Kinzelbach, W. (2001). Simulation of Pollutant Transport Using a Particle Method. *Journal of Computational Physics*, 173(1), 322-347. doi: <http://dx.doi.org/10.1006/jcph.2001.6879>